

INTERNAL RESEARCH REPORT

2020-2021

Programme Leader

Dr. Md. Anower Hossain
Chief Scientific Officer (In-charge & Head)



Irrigation and Water Management Division
Bangladesh Agricultural Research Institute
Joydebpur, Gazipur-1701

August 2021

INTERNAL RESEARCH REPORT

2020-2021

Programme Leader

Dr. Md. Anower Hossain
Chief Scientific Officer (In-charge & Head)

Edited by

Dr. Md. Anower Hossain, CSO (Incharge)
Dr. Sujit Kumar Biswas, SSO
Dr. Dilip Kumar Roy, SSO
Farzana Akter, SO
Khandakar Faisal Ibn Murad, SO
Shamsul Alam Kamar, SO



IRRIGATION AND WATER MANAGEMENT DIVISION
BARI, GAZIPUR-1701

Citation

M. A. Hossain, S. K. Biswas, D. K. Roy, F. Akther, K. F. I. Murad, S. S. A. Kamer, M. P. Haque, 2021. Internal Research Report 2020-21. Irrigation and Water Management Division. Bangladesh Agricultural Research Institute (BARI), Joydebpur, Gazipur-1701.

Editorial Committee

Dr. Md. Anower Hossain, CSO (In-charge)

Dr. Sujit Kumar Biswas, SSO

Dr. Dilip Kumar Roy, SSO

Compilation

Khandakar Faisal Ibn Murad, SO

Farzana Akter, SO

Sk. Shamsul Alam Kamar, SO

Word Processing

Md. Samim Miah, Office Assistant

Published by

Irrigation and Water Management Division

Bangladesh Agricultural Research Institute

Gazipur-1701

Phone: +88 0249270175, Cell: +8801711249767

E-mail: cso.iwm.bari.gov.bd

Published on

August 2021

List of Contributors

Dr. Md. Anower Hossain, CSO (In-charge)

Dr. Sujit Kumar Biswas, SSO

Dr. Dilip Kumar Roy, SSO

Farzana Akter, SO

Khandakar Faisal Ibn Murad, SO

Shamsul Alam Kamar, SO

Md. Panjarul Haque, SO

PREFACE

The principal objective of irrigation and water management research is to determine how best the water resources, be it from underground, surface or rainfall can be utilized for crop production and how to minimize the harmful effect of this water. This inevitably demands research on how to exploit available sources of water, convey and distribute them to farms and apply the same to the individual crop field. The next important aim is to increase the crop water use efficiency in order to obtain maximum production per unit drop of water thereby increasing economic return and improving livelihood of the farmers. To achieve this goal, research need to be conducted on when and how much water should be applied, and when irrigation is not necessary at all.

The general objectives of the division are to conduct research on: a) proper irrigation scheduling and rain water management of the upland crops and drainage thereof, b) finding appropriate technologies for conveyance, distribution, application and utilization of water resources for crop production, c) assessment of ground water reserves and its development for agricultural use, d) water management in saline and drought prone areas e) wastewater management f) micro irrigation, and g) impact of climate change on irrigated agriculture.

There are great potentialities that need to be developed in the management of ground and surface water resources. In many crops improved irrigation system has the potential to double the production. Rice crop, on average, require 1000 mm of water for the growing season whereas most upland crops require 200 to 500 mm water when applied efficiently. All these indicate that there remains tremendous possibility of increasing crop production by bringing more upland crops under irrigation and by properly controlling and managing the available water resources.

The task requires, amidst others, research in larger scale and in diversified crops. However, the division has got a very limited number of scientists and facilities to address the aforementioned research problems. With this manpower and facilities, we are trying our best to the benefit of our agricultural concerns.

Research and development activities of Irrigation and Water Management Division are directed towards the economic development of the country. The division is working to help the nation becoming self-sufficient in food, to generate employment in agriculture and to increase income of farmers through the development of appropriate water management practices and techniques widely acceptable to all categories of farmers. This report presents the findings of both on-station and on-farm studies conducted during 2020-21. This year, the division carried out researches in the areas of crop water requirement and irrigation scheduling, water application and distribution methods, on-farm water management, saline and wastewater management, groundwater management and dissemination of developed water saving technologies at the farmer's level and improvement of farmers' traditional irrigation practices.

Finally, I like to express my sincere thanks to the scientists/staffs concerned with these studies and to all who helped in bringing out this report.

Dr. Md. Anower Hossain
Chief Scientific Officer (in-charge) and Head

CONTENTS

EXPT. NO.	TITLE OF CONTENTS	PAGE NO.
<i>Research Area: Crop Water Requirement and Irrigation Scheduling</i>		
1	Optimize Fertigation Management to Minimize Nitrate Leaching from Drip Irrigated Brinjal Field	1-7
2	Multi-Step Ahead Forecasting of Potential Evapotranspiration using Bidirectional Long Short-Term Memory (Bi-Lstm)	8-21
3	Daily and Multi-Step Ahead Forecasting of Potential Evapotranspiration using Machine Learning Algorithms with Limited Climatic Data	22-35
<i>Research Area: Water Application and Distribution Methods</i>		
4	Effect of Drip Irrigation and Mulching on Growth and Flowering of Chrysanthemum as Cut Flower	36-45
5	Effect of Irrigation on Mango Fruit Cracking in Chattogram Region	46-50
6	Performance of Fertigation System on Pumpkin Cultivation	51-56
7	Yield and Water Productivity Indices of Different Onion Varieties under Sprinkler Irrigation	57-68
8	Effect of Fertilizer and Irrigation Frequency on the Yield and Quality of Export and Processing Potato	69-78
<i>Research Area: Saline and Waste Water Management</i>		
9	Effect of Saline Water Irrigation with Different Doses of Potassium on Crop Growth and Yield of Mung bean	79-88
10	<i>Project (ACIAR-KGF):</i> Mitigation Risk and Scaling-Out Profitable Cropping system Intensification Practices in the Salt Affected Coastal Zones of the Ganges Delta	89-106
10.1	Conjunctive Use of Fresh- and Saline Water for Maize and Sunflower Cultivation in Coastal Areas of Bangladesh	89-94
10.2	Low Cost Drip Irrigation for Tomato and Chili Cultivation in Saline Coastal Areas of Bangladesh	95-98
10.3	Growth and Yield of Spinach as Affected by Different Levels of Irrigation in Coastal Saline Area of Bangladesh	99-103
10.4	Crop Cafeteria with Some Promising Crops in Salt-affected Coastal Areas of Bangladesh	104-106
<i>Research Area: Groundwater Management</i>		
11	Multi-Step Ahead Prediction of Groundwater Level Fluctuations using Coupled Wavelet Transform and Long Short-Term Memory Networks	107-118
12	Coastal Groundwater Management Using an Uncertainty-Based Coupled Simulation-Optimization Approach	119-141
13	Prediction of Salt Water Intrusion for Different Scenarios of Aquifer Recharge and Groundwater Extraction Under Changing Climate	142-149
14	Monitoring of Ground Water Level at Different Research Station of BARI	150-155
15	<i>Project (NATP-2, PBRG):</i> Groundwater Resources Management for Sustainable Crop Production in Northwest Hydrological Region of Bangladesh	156-211
<i>Research Area: Water Quality Monitoring and Assessment</i>		
16	Effects of Floating Agriculture Practice on the Water Body of Pond	212-218
<i>Research Area: Transfer of Technology</i>		
17	<i>Project (SACP-IWM part):</i> Dissemination of Water Saving Irrigation Technologies For Non-rice Crops in Saline Prone Areas of Bangladesh	219-231

OPTIMIZE FERTIGATION MANAGEMENT TO MINIMIZE NITRATE LEACHING FROM DRIP IRRIGATED BRINJAL FIELD

D.K. ROY¹, S.K. BISWAS¹, K.F.I. MURAD² AND K.K. SARKAR³

Abstract

This research was carried out at the research field of Irrigation and Water Management Division (IWM) of Bangladesh Agricultural Research Institute (BARI), Gazipur during 2019-2020 and 2020-2021 to optimize fertigation management for minimizing nitrate leaching from drip irrigated brinjal field. BARI Bt. Brinjal 4 cultivar was used for the experiment. There were four different irrigation treatments comprising two levels of irrigation intervals and two irrigation timings [Drip irrigation at 4-day interval with fertigation at the beginning of the irrigation cycle (T₁), Drip irrigation at 3-day interval with fertigation at the beginning of the irrigation cycle (T₂), Drip irrigation at 4-day interval with fertigation at the end of the irrigation cycle (T₃), and Drip irrigation at 3-day interval with fertigation at the end of the irrigation cycle (T₄)]. It was observed that yield and yield contributing characters varied significantly among the irrigation treatments for both growing seasons and that yield components followed the similar trend. It was also observed that treatment T₄ received highest amount of irrigation (270 mm) followed by the treatments T₂, T₃, and T₁ in 2019-2020 growing season. Although the treatments received different amounts of irrigation water in the growing season 2020-2021, the trend of water application remained the same. Modelling results for optimizing fertigation management will be conducted and presented after obtaining the results of third year.

Introduction

Groundwater pollution from use of nitrogenous fertilizer in intensive agriculture is becoming one of the major concerns in recent years. Appropriate management of nutrient and water in agricultural activities is the key to minimizing groundwater pollution and maximizing crop productivity (Abdelkhalik et al., 2019; Ajdary et al., 2007; Azad et al., 2018). Optimized management practices aiming at reducing the amount of water and nitrogen application without compromising with the yield reduction are able to reduce the extent of groundwater pollution through nitrate leaching (Shrestha et al., 2010). Based on the crop nitrogen requirement, this management strategy should incorporate soil moisture regulation for nitrate transport as well as managing the amount and timing of application of nitrogen fertilizers (Shrestha et al., 2010). Drip fertigation is a promising irrigation technology, which improves water and nutrient use efficiency to enhance crop productivity. If designed and managed properly, drip fertigation is likely to maximize nutrients uptake by plants and minimize water and solute losses beyond the root zone of the plants. However, optimization strategy of fertigation management plays an important role in the implementation of drip fertigation in order to obtain better crop yields and reduced soil and groundwater contamination. Therefore, the main objective of this study is to develop a drip fertigation management strategy that includes supplying adequate nitrogen to brinjal crop, minimizing nitrate leaching to groundwater, and avoiding nitrogen accumulation in the soil at the end of the crop growing season.

Development of any management strategy requires evaluation of several scenarios through optimization approach. These scenarios are very difficult, if not impossible to obtain from the field experimental setup. A simulation model is often employed to generate different scenarios using a particular set of data obtained from the field. Many simulation models have been implemented to simulate water flow and solute transport in soil, among which HYDRUS-1D and HYDRUS (2D/3D) (Simunek et al. 2011) has been extensively used because of its ability to incorporate root distribution as well as water and nutrient uptake by the crop. Present study intended to utilize HYDRUS (2D/3D) simulation to generate various scenarios of drip fertigation management and the corresponding nitrate

¹ SSO, IWM Division, BARI, Gazipur

² SO, IWM Division, BARI, Gazipur

³ SSO, HRC, BARI, Gazipur

concentration in the root zone water and beyond the root zone. Therefore, the objective of this study was to optimize drip fertigation management to minimize nitrate leaching.

Materials and Methods

The field experiment was conducted during the rabi season of 2019-2020 (Year-1) and 2020-2021 (Year-2), between the months of December and April, at the research field of Irrigation and Water Management Division (IWM), Bangladesh Agricultural Research Institute (BARI), Gazipur. The experimental field was located between 24.00° N latitude and 90.25°E longitude with an altitude of 8.40 m above MSL. The sand, silt and clay proportions of the soil in the experimental field were 36.5, 35.4 and 28.1, respectively. Top 30 cm of the soil layer had a field capacity, wilting point and bulk density values of 28.5%, 13.72% and 1.46 g cm⁻³, respectively. The nutrient content of the experimental soil in the form of N, P₂O₅ and K₂O were 51.1, 12.5 and 265.6 kg ha⁻¹, respectively while the organic matter content of the top soil was recorded as 1.04%.

BARI Bt. Brinjal 4 cultivar was used for the study. The experiment was laid out in a randomized complete block design with four drip fertigation treatments replicated thrice. The treatments were as follows:

T₁ = Drip irrigation at 4-day interval with fertigation at the beginning of the irrigation cycle

T₂ = Drip irrigation at 3-day interval with fertigation at the beginning of the irrigation cycle

T₃ = Drip irrigation at 4-day interval with fertigation at the end of the irrigation cycle

T₄ = Drip irrigation at 3-day interval with fertigation at the end of the irrigation cycle

The unit plot size was 5 m × 4 m. The experimental blocks were separated by 2 m and the plots within each block were separated by 1 m wide buffer strips in order to prevent lateral seepage of applied irrigation water into the adjacent plots. Brinjal plants of 28 days old were transplanted on 08 December 2019 with a plant spacing of 100 × 75 cm. Farm yard manure at the rate of 10 t ha⁻¹ was properly mixed with the soil during the land preparation. Fertilizers were applied at the rate of 375 kg N, 250 kg P, 250 kg K, and 100 kg gypsum per hectare. Half of the nitrogen and phosphorus, and the full doses of potassium and gypsum were applied during the land preparation while the remaining half of the nitrogen and phosphorus was applied with drip fertigation.

Estimation of irrigation water

The irrigation water was applied to bring the soil moisture at field capacity considering effective root zone depth. Soil moisture was determined before each irrigation by gravimetric method. Irrigation was applied up to the field capacity of the soil. Measured amount water was applied to all treatments in ring basin method.

The normal depth of water needed to apply was determined using the following equation:

$$d = \frac{FC - MC_i}{100} \times A_s \times D \quad (1)$$

where, d = depth of irrigation, mm; FC = field capacity of the soil, %; MC_i = moisture content of the soil at the time of irrigation, %; A_s = apparent specific gravity of the soil; D = root zone depth, mm.

Rainfall data were collected from the weather station, Joydebpur, Gazipur. Effective rainfall was calculated on daily basis during the growing period.

Water Productivity Index (WPI)

Water productivity index was calculated using the following equation:

$$WPI = Y/q \quad (2)$$

where, WPI = Water Productivity Index, kg/m³; Y = the yield (kg/ha) for the season in the specific area; q = total supply of water including rainfall per ha for the season in the specific area, m³/ha.

Statistical analysis

Statistical analysis was carried out to obtain the variance for different parameters. Treatment effects were analyzed using a one-way ANOVA using MATLAB.

Results and Discussion

Yield and yield contributing characters of brinjal during 2019-2020 (Year-1) and 2020-2021 (Year-2) growing seasons were analyzed statistically and are presented in Table-1. It is observed from Table-1 that irrigation treatments had significant effects on all the yield and yield contributing characters of brinjal. In 2019-2020 (Year-1), the highest marketable yield was obtained from treatment T₄ (32.91 t/ha) followed by the treatments T₂ (32.64 t/ha), T₃ (31.84 t/ha), and T₁ (31.29 t/ha). Similarly, the highest (37.24 t/ha) and lowest (31.41 t/ha) marketable yields were obtained from treatments T₄ and T₁, respectively. Therefore, it is perceived from the results of two growing seasons that despite varied in magnitude, the marketable yield of brinjal followed the similar trend.

Table 1. Yield and yield contributing characters of brinjal during 2019-2020 growing season

Treatments	Length of fruit, cm	Diameter of fruit, cm	Unit weight of fruit, g	Cull yield, t/ha	Marketable yield, t/ha
Year-1 (2019-2020)					
T ₁	7.92	6.45	425	8.71	31.29
T ₂	8.54	7.25	450	7.36	32.64
T ₃	8.01	5.92	432	8.16	31.84
T ₄	8.85	7.93	438	7.09	32.91
F	6.74	27.35	141.14	17.18	47.08
Prob.>F	0.014	0.0001	2.88×10 ⁻⁷	0.0008	1.98×10 ⁻⁵
Year-2 (2020-2021)					
T ₁	7.87	6.52	428	8.69	31.41
T ₂	8.56	7.21	455	7.42	32.71
T ₃	8.02	5.87	437	8.11	31.97
T ₄	8.85	7.97	442	7.08	33.01
F	5.49	25.79	44.48	83.89	37.24
Prob.>F	0.0241	0.0002	2.46×10 ⁻⁵	2.19×10 ⁻⁶	4.77×10 ⁻⁵

Multiple comparison tests were performed to determine which treatments were different than the others in terms of yield and yield attributing characters of brinjal. Multiple comparison test for the treatments in terms of the length of fruit of brinjal is presented in Figure 1.

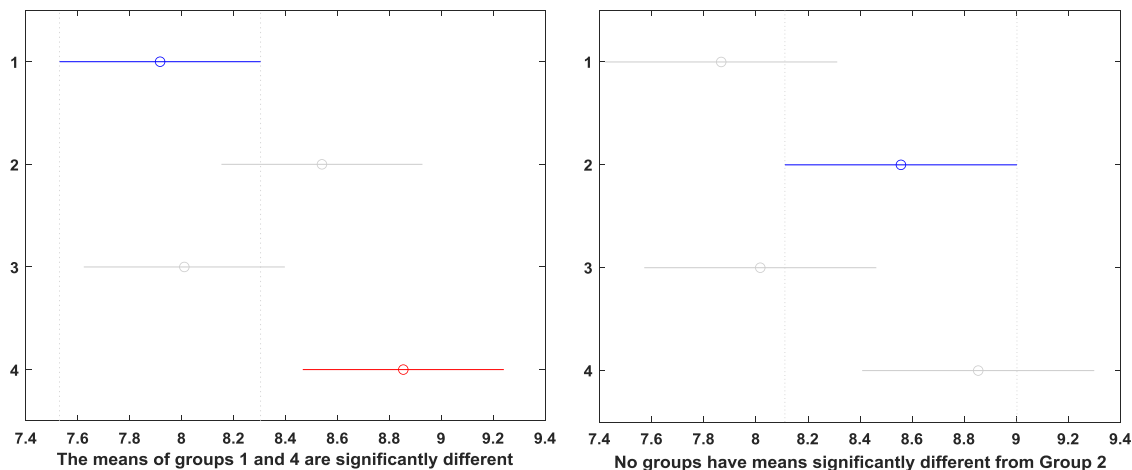


Figure 1. Multiple comparison test for the treatments in terms of the length of fruit: (a) 2019-2020, and (b) 2020-2021.

The multiple comparison test for the two growing seasons (2019-2020 and 2020-2021) suggested that the means of groups 1 and 4 were significantly different; no groups had means significantly different from group 2; the means of groups 3 and 4 were significantly different; and two groups (group 1 and group 3) had means significantly different from group 4. For the diameter of fruit, the multiple comparison test showed the similar trends for both the growing seasons. The multiple comparison test for different treatments (presented in Figure 2) revealed that two groups (group 2 and 4) had means significantly different from group 1; two groups (group 1 and 3) had means significantly different from group 2; two groups (group 2 and 4) had means significantly different from group 3; and two groups (group 1 and 3) had means significantly different from group 4.

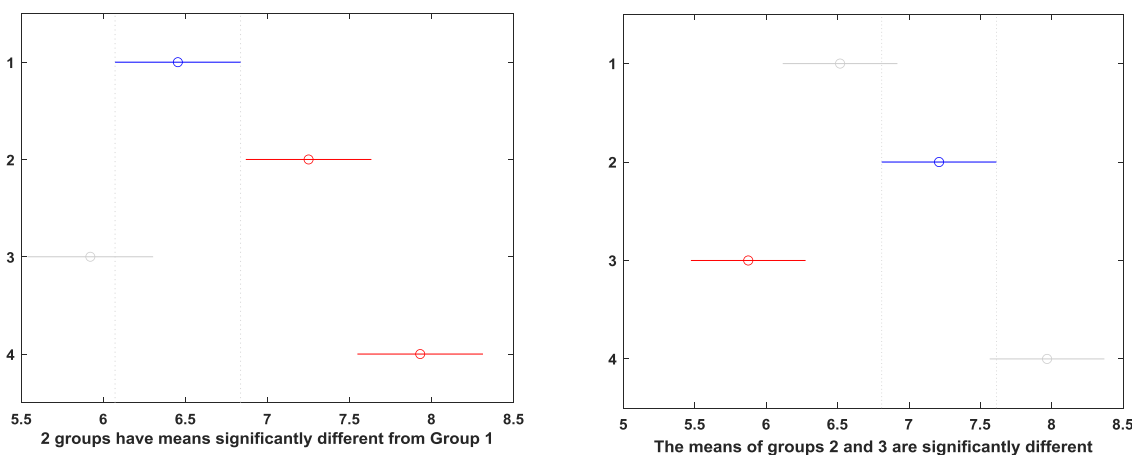


Figure 2. Multiple comparison test for the treatments in terms of the diameter of fruit: (a) 2019-2020, and (b) 2020-2021.

Multiple comparison test for the treatments in terms of the unit weight of fruit of brinjal for the growing season 2019-2020 is presented in Figure 3 (a), which suggested that three groups (groups 2, 3, 4) had means significantly different from group 1; three groups (groups 1, 3, 4) had means significantly different from group 2; three groups (groups 1, 2, 4) had means significantly different from group 3; and three groups (groups 1, 2, 3) had means significantly different from group 4. Results for the growing season 2020-2021 are presented in Figure 3 (b), which indicates that two groups (groups 2 and 4) have means significantly different from group 1; two groups (group 1 and 3) have means significantly different from group 2; two groups (groups (2 and 4) have means significantly different from group 3; and two groups (group 1 and 3) have means significantly different from group 4.

(a)

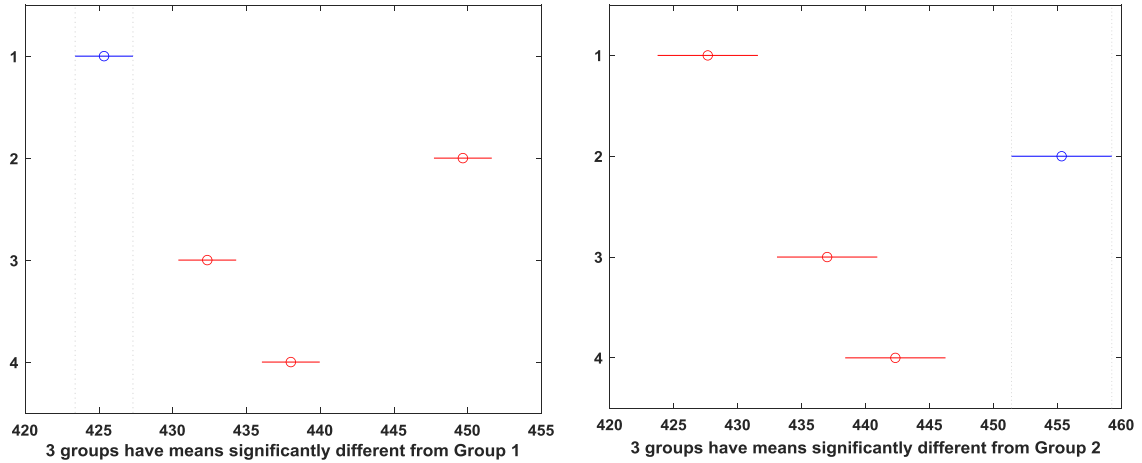


Figure 3. Multiple comparison test for the treatments in terms of the unit weight of fruit: (a) 2019-2020, and (b) 2020-2021.

Treatment variations for the marketable yield obtained from the multiple comparison test for the growing season 2019-2020 are presented in Figure 4 (a). It was observed from Figure 4 (a) that two groups (groups 2 and 4) had means significantly different from group 1; the means of groups 2 and 1 were significantly different; the means of groups 3 and 4 were significantly different; two groups (groups 1 and 3) had means significantly different from group 4. Results of multiple comparison test for the growing season 2020-2021 is illustrated in Figure 4 (b), which revealed the similar trend as in case of multiple comparison tests for the growing season 2019-2020.

(a)

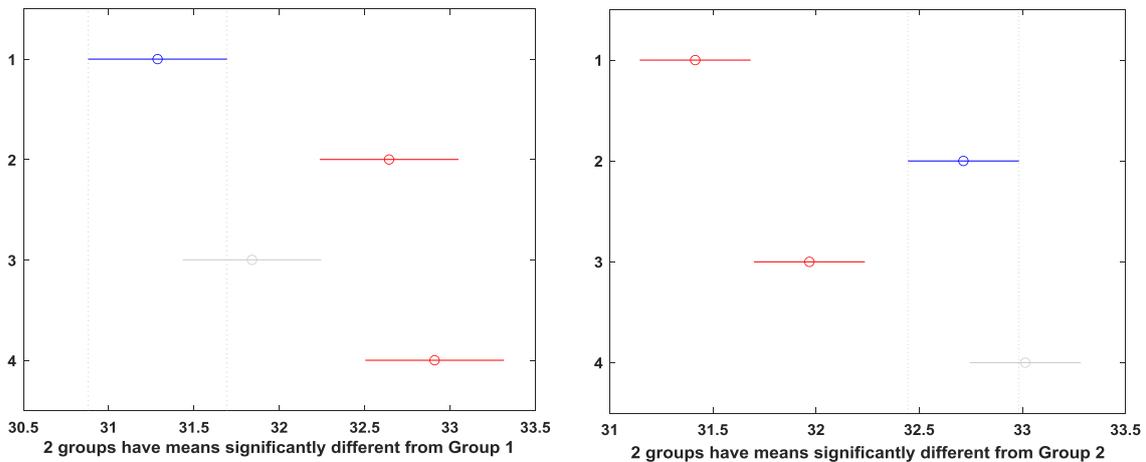


Figure 4. Multiple comparison test for the treatments in terms of marketable yield: (a) 2019-2020, and (b) 2020-2021.

Multiple comparison test for the treatments in terms of the cull yield of brinjal for the two growing seasons is presented in Figure 5, which suggested that, for both growing seasons, three groups (groups 1, 2, 3) had means significantly different from group 1; two groups (groups 1 and 3) had means significantly different from group 2; three groups (groups 1, 2, 4) had means significantly different from group 3; and two groups (groups 1 and 3) had means significantly different from group 4.

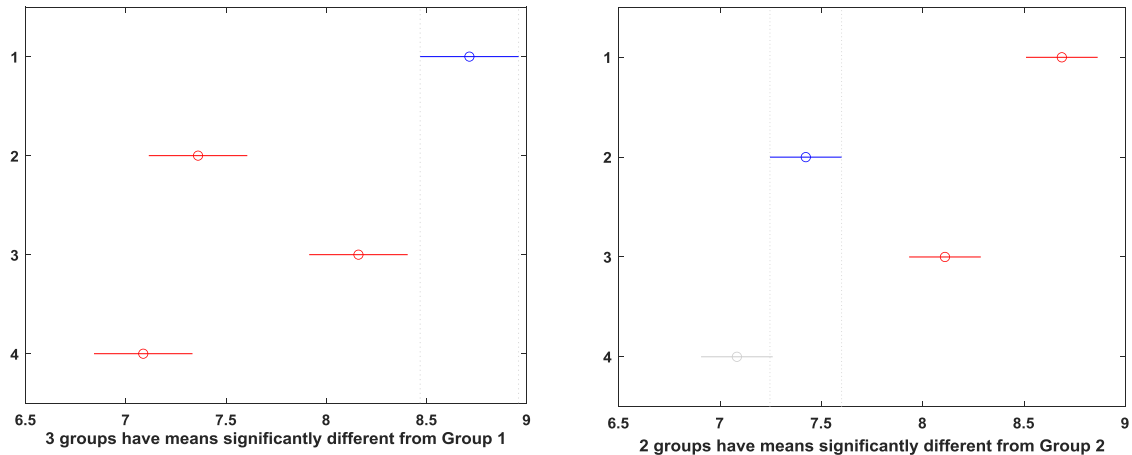


Figure 5. Multiple comparison test for the treatments in terms of cull yield: (a) 2019-2020, and (b) 2020-2021

Seasonal water use and water productivity

In growing season 2019-2020, treatments T_1 and T_3 received 23 numbers of irrigation events whereas treatments T_2 and T_4 received a total number of 31 irrigations. On the other hand, treatments T_1 and T_3 received 26 numbers of irrigation events whereas treatments T_2 and T_4 received a total number of 32 irrigations in the growing season 2020-2021. The irrigation events were accomplished based on the design of the experiment. In 2019-2020, treatment T_4 received highest amount of irrigation (270 mm) followed by the treatments T_2 , T_3 , and T_1 . Effective rainfall for the crop growing period was calculated as 223 mm (80% of total rainfall). Likewise in 2019-2020, the highest (276 mm) and lowest (202 mm) amounts of irrigation water was received by treatments T_4 and T_1 , respectively. The effective rainfall during the crop growing period of 2020-2021 was estimated to be 112 mm. Water used by the plants in different treatments during growing season is shown in Table-2.

Table-2. Water use and water productivity of brinjal in different treatments

Treatments	Amount of irrigation water, mm	Effective rainfall, mm	Soil water contribution, mm	Seasonal water use, mm	Yield, t/ha	Water productivity, kg/m ³
Year-1 (2019-2020)						
T_1	195	223	18.92	436.92	31.29	7.16
T_2	260	223	12.55	495.55	32.64	6.59
T_3	202	223	24.33	449.33	31.84	7.09
T_4	270	223	28.18	521.18	32.91	6.31
Year -2 (2020-2021)						
T_1	202	112	16.83	330.83	31.41	9.49
T_2	268	112	11.41	391.41	32.71	8.36
T_3	208	112	20.34	340.34	31.97	9.39
T_4	276	112	24.13	412.13	33.01	8.01

Conclusion

The findings of the growing seasons 2019-2020 and 2020-2021 revealed a similar pattern of yield response, yield attributing characters, and seasonal crop water use. At least three years' data will be required to develop modelling of nitrate leaching. Therefore, for obtaining a definite conclusion regarding the yield response and nitrate leaching, the experiment will be conducted during the growing season of 2021-2022.

References

- Abdelkhalik, A., Pascual-Seva, N., Nájera, I., Giner, A., Baixauli, C., Pascual, B., 2019. Yield response of seedless watermelon to different drip irrigation strategies under Mediterranean conditions. *Agric. Water Manag.* 212, 99–110. <https://doi.org/https://doi.org/10.1016/j.agwat.2018.08.044>
- Ajdary, K., Singh, D.K., Singh, A.K., Khanna, M., 2007. Modelling of nitrogen leaching from experimental onion field under drip fertigation. *Agric. Water Manag.* 89, 15–28. <https://doi.org/https://doi.org/10.1016/j.agwat.2006.12.014>
- Azad, N., Behmanesh, J., Rezaverdinejad, V., Abbasi, F., Navabian, M., 2018. Developing an optimization model in drip fertigation management to consider environmental issues and supply plant requirements. *Agric. Water Manag.* 208, 344–356. <https://doi.org/https://doi.org/10.1016/j.agwat.2018.06.030>
- Shrestha, R.K., Cooperband, L.R., MacGuidwin, A.E., 2010. Strategies to reduce nitrate leaching into groundwater in potato grown in sandy soils: Case study from north central USA. *Am. J. Potato Res.* 87, 229–244. <https://doi.org/10.1007/s12230-010-9131-x>
- Šimůnek, J., van Genuchten, M.Th., Sejna, M., 2011. The HYDRUS software package for simulating two- and three-dimensional movement of water, heat, and multiple solutes in variably-saturated media. Technical Manual, Version 2. PC Progress, Prague, Czech Republic.

MULTI-STEP AHEAD FORECASTING OF POTENTIAL EVAPOTRANSPIRATION USING BIDIRECTIONAL LONG SHORT-TERM MEMORY (BI-LSTM) NETWORKS

D.K. ROY¹, S.K. BISWAS¹ AND M.A. HOSSAIN²

Abstract

Precise estimation and forecast of reference evapotranspiration (ET_0) stand crucial for developing an efficient irrigation scheduling that helps better utilization of scanty water resources. One of the tools to predict ET_0 is to employ machine learning algorithms that predict near future ET_0 values based on past values from the ET_0 timeseries. The aim of this research is to provide multi-step ahead predictions of ET_0 with a deep and machine learning algorithm using calculated past values of ET_0 . In this context, daily values of ET_0 were computed via the FAO-56 Penman-Monteith approach that employ five climatic variables. For predicting multi-step ahead ET_0 , this study evaluates the prediction accuracy and estimation capability of a bi-directional LSTM (Bi-LSTM) network. According to the findings, the Bi-LSTM produced multi-step ahead ET_0 amounts in satisfactory precision and error levels as indicated by different statistical performance evaluation indices. The overall results indicate that the Bi-LSTM model could be successfully employed to predict multi-step (5-day) ahead ET_0 values quite precisely.

Introduction

Agriculture is considered to be the largest consumer of global freshwater reserves. Therefore, a careful and judicious management of irrigation practices would allow significant water savings. To achieve this water saving, an accurate estimation of the evapotranspiration (ET) is required, which is regarded as one of the major components of water balance. ET plays an important role in surface energy and water budgets, and is an important parameter in the interactions between vegetation, soil, and the atmosphere (Liu et al., 2013). Accordingly, proper management of water resources in irrigated agriculture is largely dependent on an accurate estimation of this vital component of the hydrologic cycle. In general, precise quantification of ET aids in the design and management of efficient irrigation systems, simulation of crop yields, determination of the hydrologic water balance, along with the planning and allocation of water resources (Kisi, 2016). ET can be measured directly by experimental techniques such as the Bowen ratio energy balance method, lysimeter approaches, or eddy covariance systems (Kool et al., 2014; Martí et al., 2015; Zhang et al., 2013) or estimated by computing potential or reference evapotranspiration (ET_0) from meteorological variables. As direct methods of ET measurement are costly, complex and largely unavailable in many regions (Allen et al., 1998; Ding et al., 2013), indirect methods based on ET_0 estimation have become popular in many regions where direct experimental techniques are not available. The FAO-56 Penman-Monteith (FAO-56 PM) model is recommended by the United Nations' Food and Agriculture Organization (FAO) as the standard reference method for estimating ET_0 and validating other methods (Allen et al., 1998). The FAO-56 PM method having been recognized as a universal approach to ET_0 estimation, this method can be used in a wide range of environmental and climatic conditions without the requirement of any local calibration. This well-established method has been validated using lysimeters under a range of different climatic conditions (Landeras et al., 2008). Since ET_0 is solely affected by meteorological conditions, it can be calculated using the FAO-56 PM method by drawing upon several meteorological variables (e.g., relative humidity, wind speed, solar radiation, and minimum/maximum air temperatures). Once the ET_0 is estimated, the actual evapotranspiration (ET_a) can be calculated by means of the ET_0 and crop coefficients.

In recent years, Artificial Intelligence (AI) models have been successfully applied to the modelling of ET_0 in different hydrologic regions. Artificial Neural Networks (ANN) were the first AI models implemented to estimate ET_0 (Kumar et al., 2002). Other applications of AI models in estimating ET_0 includes the use of Random Forests (RF) (Feng et al., 2017a; Huang et al., 2019), Generalized Regression Neural Networks (GRNN) (Feng et al., 2017a, 2017b), Extreme Learning

¹ SSO, IWM Division, BARI, Gazipur 1701

² CSO(in-charge), IWM Division, BARI, Gazipur 1701

Machine (ELM) (Abdullah et al., 2015; Dou and Yang, 2018; Feng et al., 2017b, 2016), Support Vector Machine (SVM) (Ferreira et al., 2019; Huang et al., 2019; Tabari et al., 2012), Genetic Programming (GP) (Gocić et al., 2015), Gaussian Process Regression (GPR) (Karbasi, 2018), Multivariate Adaptive Regression Splines (MARS) (Kisi, 2016), M5 Model Tree (M5Tree) (Kisi, 2016), Multivariate Relevance Vector Machine (MVRVM) (Torres et al., 2011), Gene-Expression Programming (GEP) (Gavili et al., 2018; Shiri et al., 2014b, 2012, Wang et al., 2019, 2016), and Adaptive Neuro Fuzzy Inference System (ANFIS) (Doğan, 2009; Dou and Yang, 2018; Gavili et al., 2018; Shiri et al., 2013; Tabari et al., 2012).

Deep learning (DL) has recently been recognized as a developed and sophisticated sub-domain of machine learning techniques in the arena of artificial intelligence. The DL-based modelling has gained popularity in the successful application to various domain of science including language processing (Plappert et al., 2018), image classification (Fan et al., 2019), computer vision (Fang et al., 2019), speech recognition (Cummins et al., 2018), and time series prediction (Tien Bui et al., 2020; Xu et al., 2019; Yang and Chen, 2019). The usage of DL has also been observed in developing prediction models in the research niche of groundwater level forecasting (Bowes et al., 2019; Supreetha et al., 2020), and prediction of short-term water quality variable (Barzegar et al., 2020). Recurrent Neural Network (RNN) models are able to preserve a memory of previous network states and are better suited for predicting groundwater levels through modelling time series of groundwater table data observed at an observation well. For this reason, numerous recent studies related to groundwater modelling (Chang et al., 2016; Daliakopoulos et al., 2005; Guzman et al., 2017) have focused on the successful application of the RNNs. However, the standard RNN architectures cannot properly grab hold of the long-term reliance between variables (Bengio et al., 1994) due mainly to the occurrences of two problems: vanishing and exploding gradients. These are situations where the network weights either reach to zero or turn out to be enormously large during training of the network.

Long Short-Term Memory (LSTM) networks, a variant of typical RNN architectures, is capable of overcoming the training drawbacks (vanishing and exploding gradient problems) of RNNs through retaining valuable information for model development while avoiding unnecessary or redundant information being passed to the subsequent states in the model development process. LSTM has successfully been applied to the research arena of natural language processing, and financial time series prediction (Fischer and Krauss, 2018), traffic congestion and travelling period predictions (Zhao et al., 2017). In spite of wide applicability in various research domains, LSTM models has only recently been utilized for the forecast of hydrologic time series (Hu et al., 2018; Liang et al., 2018; Tian et al., 2018; Zhang et al., 2018). Recently, Jeong et al., (2020) applied LSTM-based modelling to estimate groundwater level using the corrupted data (with outliers and noise) and found that robust training of an LSTM model using a developed cost function (“least trimmed squares with asymmetric weighting and the Whittaker smoother”) can adequately model noisy groundwater level data. The prediction ability of an LSTM network was found superior than that of a RNN in predicting hourly groundwater level values in a coastal city (susceptible to periodic flooding) of Norfolk, Virginia, USA (Bowes et al., 2019). Mouatadid et al., (2019) used a coupled “maximum overlap discrete wavelet transformation” and LSTM for achieving precision and robustness in the forecasting of irrigation flow. Zhang et al., (2018) proposed an LSTM network for predicting depths in water table in agrarian areas and obtained an acceptable prediction result by utilizing simply an uncomplicated data pre-processing technique. Based on their findings, one can argue that an LSTM network does not require a massive data smoothing or pre-processing in producing an acceptable prediction accuracy. The integrated use of Gated Recurrent Unit and Convolutional Neural Network (CNN-GRU) can also be found in recent literature (Pan et al., 2020) for developing water level prediction models in which CNN-GRU outperformed an LSTM model with regard to Nash-Sutcliffe (NS) Efficiency Coefficient, Average Relative Error, and Root Mean Squared Error. The prediction accuracy of a lion algorithm optimized LSTM network was found superior than an ordinary LSTM network for the prediction of groundwater level using the historical groundwater level data obtained from an observation well and rainfall data collected from a weather station located in the Udupi district, India (Supreetha et al., 2020). To the best of the author’s

understanding, an LSTM network has not previously been used to predict daily and multi-step ahead ET_0 predictions especially in the Gazipur district of Bangladesh.

The key motivation and focus of this study were to: (1) delve into the potential of Bi-LSTM model in forecasting multi-step (5-day ahead) ahead ET_0 predictions using data obtained from a weather station located in Gazipur Sadar Upazilla

Materials and Methods

Study area and the data

The study area is situated in the Gazipur Sadar Upazilla having an aerial extent of 446.38 km². It is located between 23.88°N and 24.18°N latitudes and between 90.33°E and 92.50°E longitudes. Meteorological data including daily maximum and minimum temperatures, wind speed, relative humidity and sunshine duration) for a period of 15.5 years (1 January 2004 to 30 June 2019) were obtained from a weather station located in the Gazipur Sadar upazilla (lat. 24.00°N, long. 90.43°E, elevation of 8.4 m above mean sea level) of Gazipur District, Bangladesh. The study area receives an average annual rainfall of 2036 mm, of which roughly 80% occurs during the monsoon season (May to August). In general, the study area has a subtropical climate, with heavier rainfall events in the summer and lighter rainfall events in winter. Descriptive statistics of the input variables are presented in Table-1. The mean values of minimum and maximum temperatures range between 21.2 °C and 30.9 °C, while the mean relative humidity across the year is approximately 80%. The wind speed in the study area ranges between 59 km/d and 437 km/d with a mean value of 242 km/d and a standard deviation of 90.69 km/d. The sunshine duration peaks at 11 h on a sunny day, while its minimum value is 0 on a cloudy day with the mean and standard deviations of 5.54 h and 3.09 h, respectively. All meteorological variables showed negative (left) skewness (Table-1), indicating the data have a longer left tail than right tail in their distribution. The kurtosis values of maximum temperature and relative humidity showed positive values indicating these datasets had “heavy tails” or outliers. The negative kurtosis values of minimum temperatures, wind speed, and sunshine durations indicate “light-tailed” distributions of these variables.

Table-1. Statistics of meteorological variables acquired from a weather station in Gazipur Sadar Upazilla, Bangladesh

Variables	Min	Max	Mean	Standard deviation	Skewness	Kurtosis
Minimum temperature, °C	4.40	34.50	21.17	5.64	-0.63	-0.88
Maximum temperature, °C	12.00	53.00	30.93	3.92	-1.10	2.11
Relative humidity, %	38.00	89.00	80.22	8.20	-0.63	0.75
Wind speed, km/d	59.00	437.00	241.15	90.69	-0.06	-1.32
Sunshine duration, h	0.00	11.40	5.54	3.09	-0.40	-1.04

The study area with the location of the weather station is presented in Figure 1.

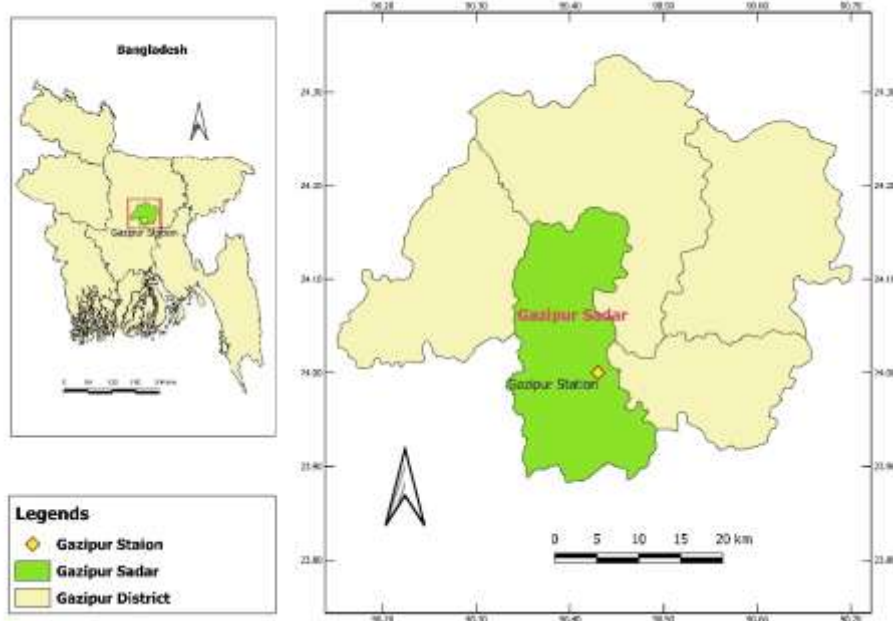


Figure 1. Map of the study area.

The ET_0 values for the study area across the study period were computed from the climatic variables using the FAO-56 PM model. These computed ET_0 values form the ET_0 time series, which was used to provide one-step ahead prediction using. This method is widely accepted and has become a common practice in situations where ET_0 values are difficult to obtain experimentally (Allen et al., 1998; Feng et al., 2017b; Shiri et al., 2014a). The FAO-56 PM model is given as:

$$ET_0 = \frac{0.408\Delta(R_n - G) + \gamma \frac{900}{T_{\text{mean}} + 273} u_2 (e_s - e_a)}{\Delta + \gamma(1 + 0.34u_2)} \quad (1)$$

where, ET_0 is the reference evapotranspiration, mm/d; R_n is the net radiation at the crop surface, $MJ/m^2/d$ is the heat flux density of soil, $MJ/m^2/d$; Δ is the slope of the saturation vapor pressure curve, $kPa/^\circ C$; γ is the psychrometric constant; e_s is saturation vapor pressure, kPa ; e_a is the actual vapor pressure, kPa ; u_2 is the wind speed at a height of 2 m, m/s ; and T_{mean} is the mean air temperature at 2.0 m height, $^\circ C$. Computed ET_0 values range between 0.92 mm/d and 8.02 mm/d with a mean and standard deviation of 3.80 mm/d and 1.32 mm/d, respectively. Moreover, the skewness and kurtosis values varied between 0.30 and -0.67. The climatic variables and the computed ET_0 constituted the input-output training patterns for the machine learning algorithms. The resulting time-series of ET_0 values are presented in Figure 2.

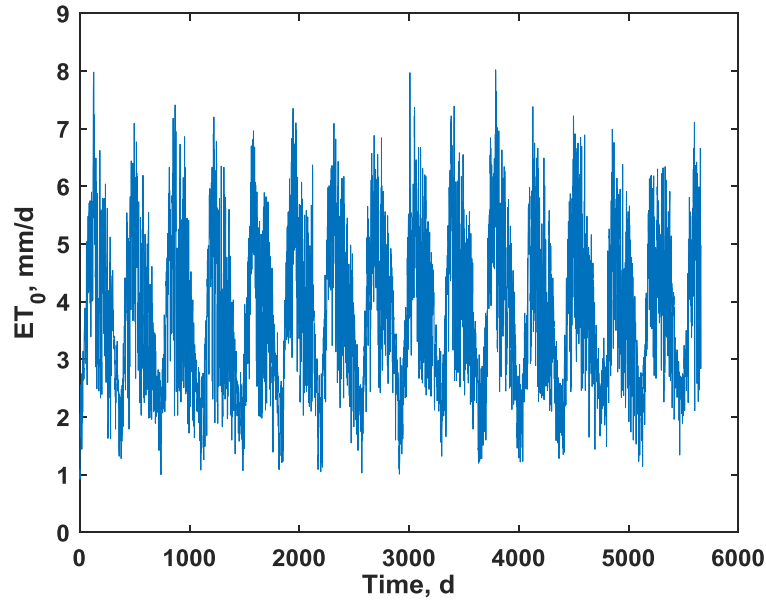


Figure 2. ET_0 time series.

The dataset contains 5660 daily entries (from 01 January 2004 to 30 June 2019) of climatological variables and the computed daily ET_0 . Several previous studies of ET_0 modelling utilized climatic variables as inputs to the developed models. However, little research is devoted to developing ET_0 models based solely on the ET_0 timeseries. Present study utilized calculated ET_0 timeseries in developing models through extracting time-lagged information from the timeseries data. Another reason of using timeseries data instead of using climatic variables as inputs to the models is to observe whether the proposed models can predict future ET_0 values without learning from the climatic variables – ET_0 relationships. Therefore, only the past values of the estimated daily ET_0 timeseries were used for the 5-day ahead prediction. The entire dataset was portioned into sets (training and testing): 80% of the total samples (4528 entries – from 01 January 2004 to 24 May 2016) was used to train the DL based models whereas the remaining 20% (1132 entries – from 25 May 2016 to 30 June 2019) was used to test the models (LSTM, Bi-LSTM, and SSR-LSTM). The performance evaluation indices calculated and presented in this study were based on the test dataset.

A Bi-LSTM learns bidirectional long-term dependencies between time steps of time series or sequence data. These dependencies can be useful when we want the network to learn from the complete time series at each time step. For the Bi-LSTM models, network architectures with three hidden layers were employed. Each of the hidden layers were followed by a dropout layer to prevent model overfitting. The numbers of hidden neurons for the first, second, and third hidden layers were 100, 50, and 20, respectively whereas the dropout rates assigned for the associated dropout layers were chosen as 0.4, 0.3, and 0.2, respectively. These optimum values were obtained upon conducting several trials. Various training options for the Bi-LSTM model were obtained through trials, and the best options were used for model training. Optimum combinations of different training options are presented in Table 2.

Table 2. Optimum combinations of different training options

Options	Corresponding parameters or values
Optimization solver	'adam'
Maximum epochs	1000
Gradient threshold	1
Initial learning rate	0.01
Minimum batch size	150
Sequence length	1000

Four layers were used for the training purpose: a sequence input layer equivalent to the number of input variables or features, a LSTM layer corresponding to the number of hidden units, fully connected layer associated with the number of output variables or the responses, and a regression layer.

Variable selection for the Bi-LSTM model

Partial Autocorrelation Functions (PACF) were determined to acquire time-lagged statistics from the daily timeseries data of ET_0 . This time-lagged information was used to evaluate the temporal dependencies between ET_0 for a current week (ET_t) and the ET_0 values at a certain point in an earlier period (i.e., a time lag of ET_{t-1} , ET_{t-2} , ET_{t-3} , ET_{t-4} , and ET_{t-5} , etc.). These temporal reliance in the ET_0 timeseries were evaluated for 50 lags (i.e., from ET_{t-1} to ET_{t-50}) as depicted in Figure 3. In Figure 3, the 95% confidence band is indicated by the blue lines. Daily lag times of ET_0 values were specified as inputs or predictors to the prediction models while the output from the models was the one-day ahead ET_0 values. The selection of optimal combination of inputs for the models was executed through careful examination of the PACF functions.

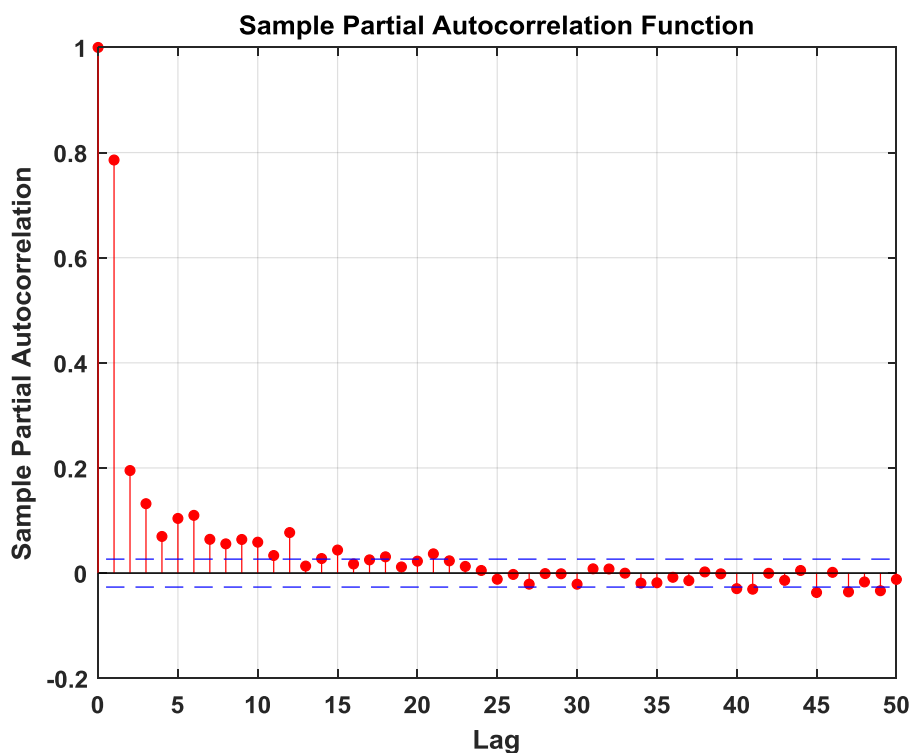


Figure 3. Plot of partial autocorrelation functions for 50 lags

Results and Discussion

The performance of the developed ET_0 prediction model using Bi-LSTM is assessed quantitatively for both the training and the testing phases to ensure that no over- or under-fitting occurs during the model development. Statistical performance evaluation indices were then computed on test dataset using the adequately trained and tested models.

Five Bi-LSTM models were developed to forecast 1-, 2-, 3-, 4-, and 5-day ahead ET_0 forecasting. For all models, the selected time lagged variables were served as inputs to the Bi-LSTM models. Table 3 presents the training and validation performances of the developed Bi-LSTM models. It is observed from Table 3 that the differences between the training and validation performances increased with the increase in the forecasting horizon. Overall, the training performances were satisfactory for all forecasting horizons.

Table 3. Training and validation performances of the developed Bi-LSTM models

Forecasting horizon	Training RMSE	Validation RMSE
1-day	0.08	0.11
2-days	0.12	0.17
3-days	0.09	0.18
4-days	0.10	0.22
5-days	0.10	0.28

The trained and validated Bi-LSTM models were then used to forecast ET_0 values on the test dataset, which were selected from the entire dataset. Testing performances were evaluated using several statistical performance evaluation indices as presented in Table 4. It is observed from Table 4 that forecasting horizon greatly influenced the forecasting accuracies, and that the accuracy decreased with the increase in the forecasting horizon as in the case of the training and validation performances. However, the overall performances of the B-LSTM model for all forecasting horizons showed particularly good performance as indicated by the computed statistical performance evaluation indices.

Table 4. Performance of the bi-LSTM model on the test dataset

Indices	Forecasting horizon				
	1-day	2-days	3-days	4-days	5-days
RMSE	0.11	0.17	0.18	0.22	0.28
NRMSE	0.03	0.04	0.05	0.06	0.07
R	1.00	0.99	0.99	0.98	0.97
MAD	0.03	0.04	0.04	0.06	0.08
MAE	0.07	0.08	0.10	0.13	0.17
NS	0.99	0.98	0.98	0.97	0.95
IOA	1.00	0.99	0.99	0.99	0.99

Performance of the developed models was also evaluated by means of line graph and error plots as shown in Figures 4, 5, 6, 7, and 8.

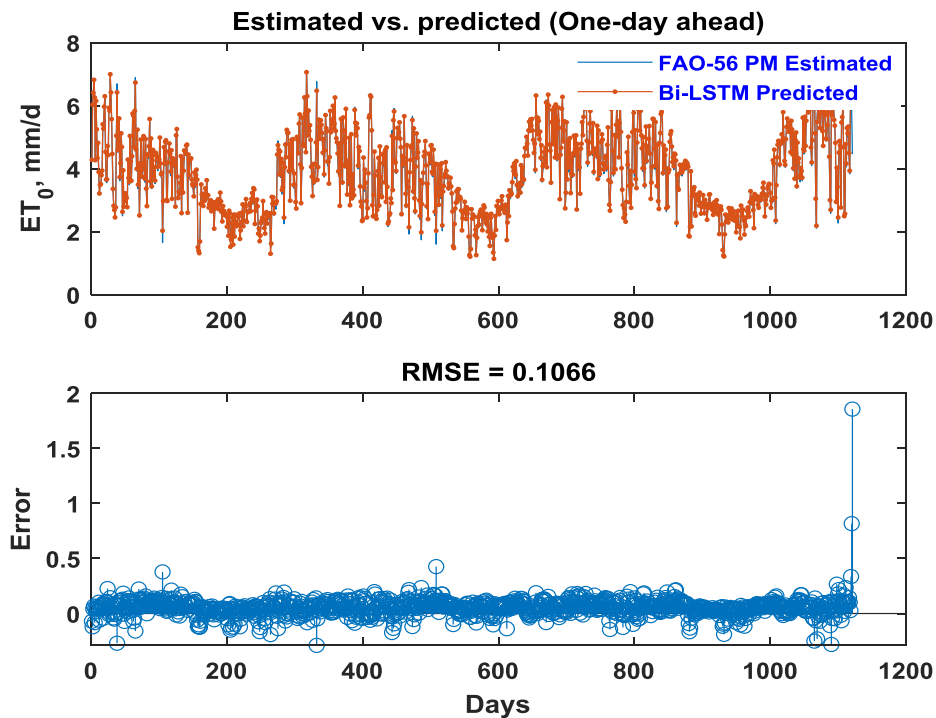


Figure 4. Line graph and error plots for 1-day ahead forecasting.

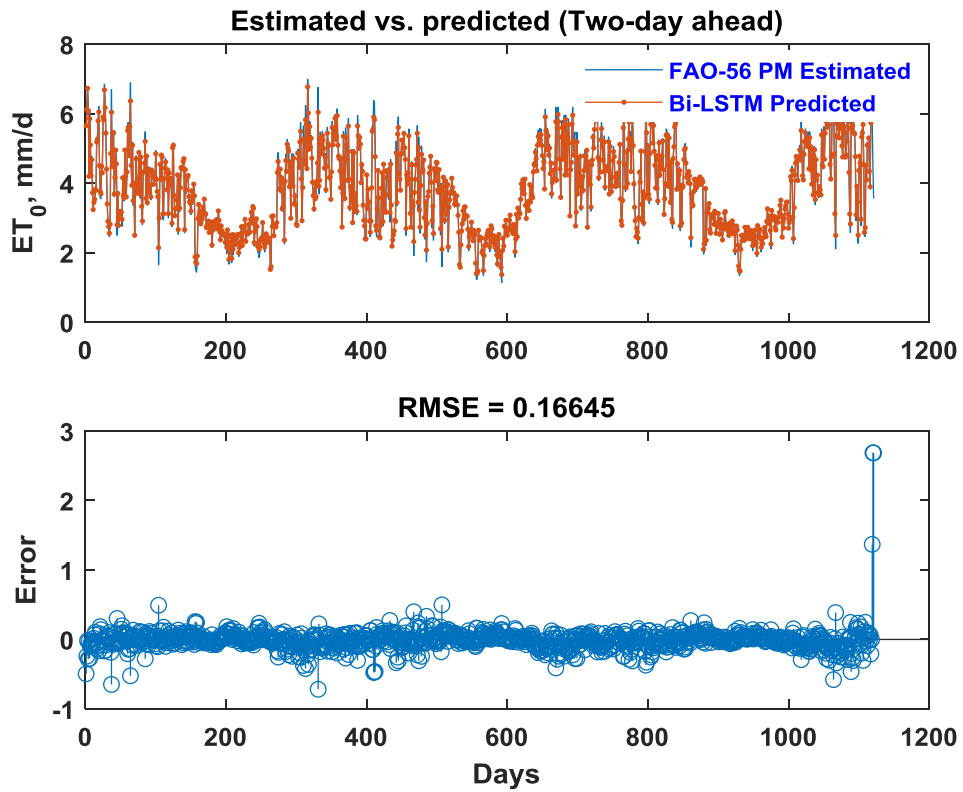


Figure 5. Line graph and error plots for 2-day ahead forecasting.

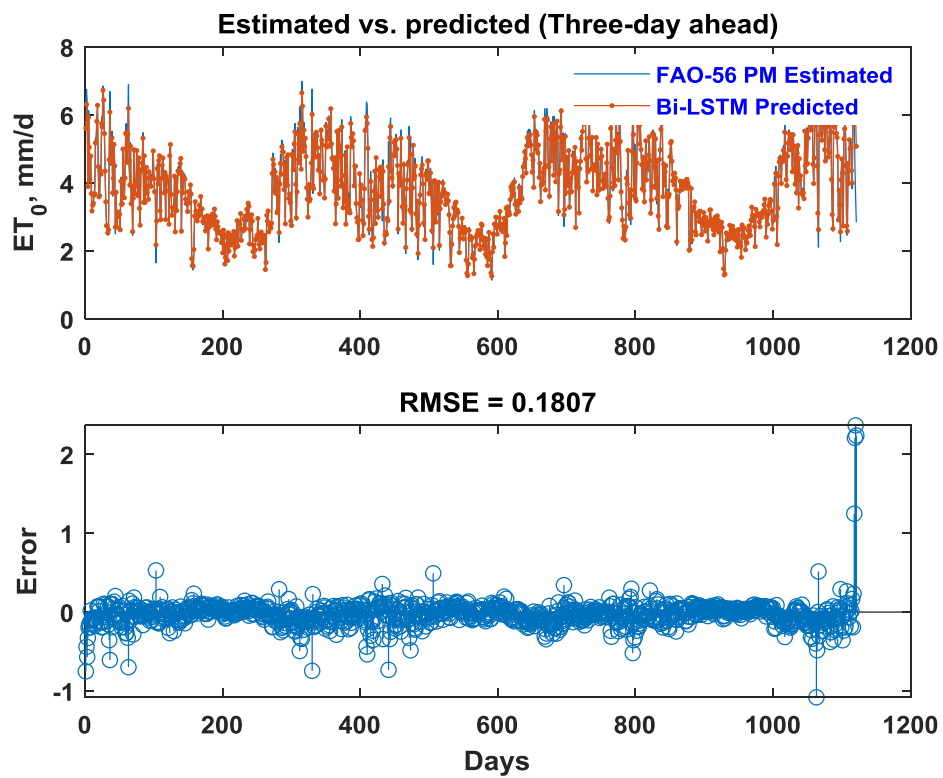


Figure 6. Line graph and error plots for 3-day ahead forecasting.

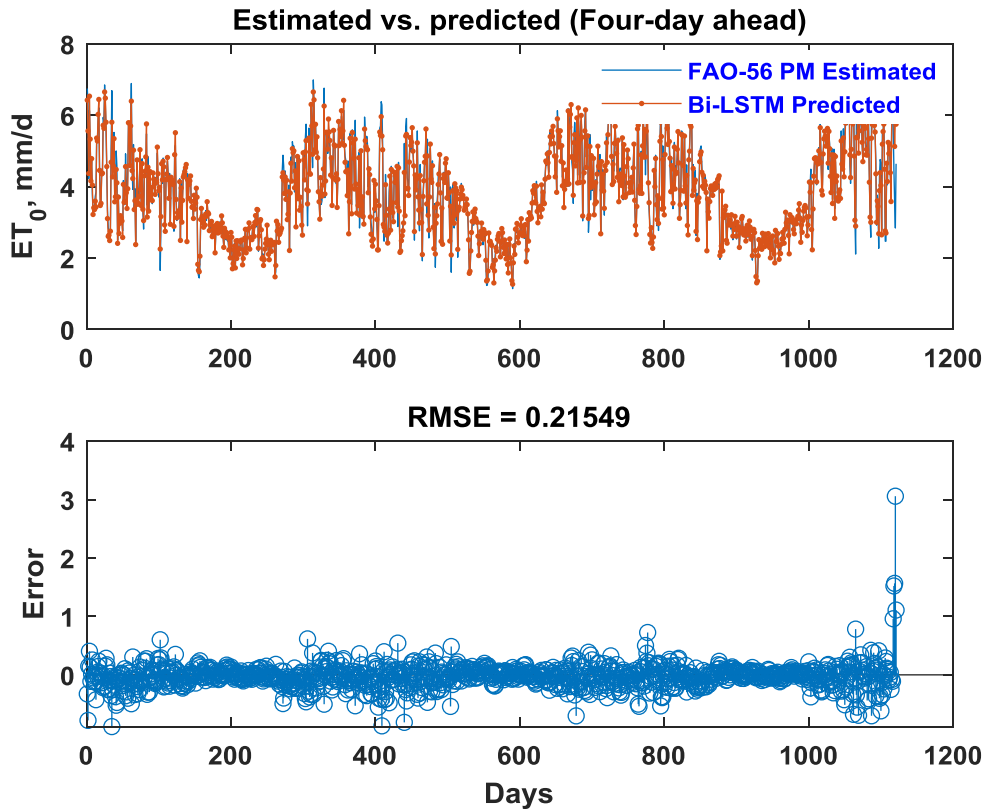


Figure 7. Line graph and error plots for 4-day ahead forecasting.

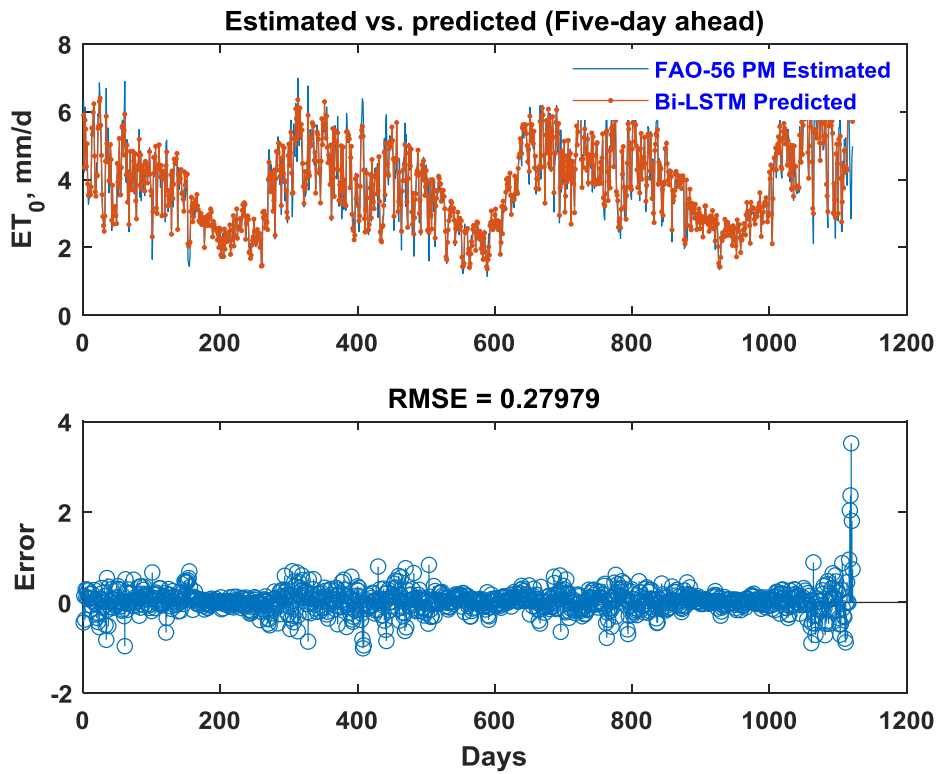


Figure 8. Line graph and error plots for 5-day ahead forecasting.

Conclusion

Precise and reliable prediction of reference evapotranspiration can effectively be employed in developing a sustainable and efficient agricultural water management strategy. This study developed a robust prediction and forecasting tool for daily and multi-step ahead ET_0 values through a deep learning algorithm, bidirectional LSTM (Bi-LSTM) network, which was developed to forecast 1-, 2-, 3-, 4-, and 5-day ahead ET_0 forecasting. Results revealed the suitability of the Bi-LSTM model in forecasting multi-step ahead ET_0 values.

References

- Abdullah, S.S., Malek, M.A., Abdullah, N.S., Kisi, O., Yap, K.S., 2015. Extreme Learning Machines: A new approach for prediction of reference evapotranspiration. *J. Hydrol.* 527, 184–195. <https://doi.org/https://doi.org/10.1016/j.jhydrol.2015.04.073>
- Allen, R.G., Pereira, L.S., Raes, D., Smith, M., 1998. Crop evapotranspiration – Guidelines for computing crop water requirements. FAO Irrigation and Drainage Paper 56. Rome: FAO
- Basak, D., Pal, S., Patranabis, D.C., 2007. Support vector regression. *Neural Inf. Process.* 11, 203–224.
- Bera, P., Prasher, S.O., Patel, R.M., Madani, A., Lacroix, R., Gaynor, J.D., Tan, C.S., Kim, S.H., 2006. Application of MARS in simulating pesticide concentrations in soil. *Trans. Asabe* 49, 297–307.
- Barzegar, R., Aalami, M.T., Adamowski, J., 2020. Short-term water quality variable prediction using a hybrid CNN–LSTM deep learning model. *Stoch. Environ. Res. Risk Assess.* 34, 415–433. <https://doi.org/10.1007/s00477-020-01776-2>
- Bengio, Y., Simard, P., Frasconi, P., 1994. Learning long-term dependencies with gradient descent is difficult. *IEEE Trans. Neural Networks Learn. Syst.* 5, 157–166.
- Bezdek, J.C., Ehrlich, R., Full, W., 1984. FCM: The fuzzy c-means clustering algorithm. *Comput. Geosci.* 10, 191–203. [https://doi.org/https://doi.org/10.1016/0098-3004\(84\)90020-7](https://doi.org/https://doi.org/10.1016/0098-3004(84)90020-7)
- Bhattacharya, B., Solomatine, D. P., 2005. Neural networks and M5model trees in modelling water level–discharge relationship. *Neuro Comput.* 63, 381–396.
- Bishop, C., 2006. Pattern recognition and machine learning. Springer-Verlag, New York.
- Bowes, B.D., Sadler, J.M., Morsy, M.M., Behl, M., Goodal, J.L., 2019. Forecasting groundwater table in a flood prone coastal city with long short-term memory and recurrent neural networks. *Water* 11, 1–38.
- Chang, F.-J., Chang, L.-C., Huang, C.-W., Kao, I.-F., 2016. Prediction of monthly regional groundwater levels through hybrid soft-computing techniques. *J. Hydrol.* 541, 965–976. <https://doi.org/https://doi.org/10.1016/j.jhydrol.2016.08.006>
- Chevalier, R.F., Hoogenboom, G., McClendon, R.W., Paz, J.A., 2011. Support vector regression with reduced training sets for air temperature prediction: a comparison with artificial neural networks. *Neural Comput. Appl.* 20, 151–159. <https://doi.org/10.1007/s00521-010-0363-y>
- Cummins, N., Baird, A., Schuller, B.W., 2018. Speech analysis for health: Current state-of-the-art and the increasing impact of deep learning. *Methods* 151, 41–54. <https://doi.org/https://doi.org/10.1016/j.ymeth.2018.07.007>
- Daliakopoulos, I.N., Coulibaly, P., Tsanis, I.K., 2005. Groundwater level forecasting using artificial neural networks. *J. Hydrol.* 309, 229–240. <https://doi.org/https://doi.org/10.1016/j.jhydrol.2004.12.001>
- Dempster, A.P., Laird, N.M., Rubin, D.B., 1977. Maximum likelihood from incomplete data via the EM algorithm. *J. R. Stat. Soc. Ser. B* 39.
- Ding, R., Kang, S., Zhang, Y., Hao, X., Tong, L., Du, T., 2013. Partitioning evapotranspiration into soil evaporation and transpiration using a modified dual crop coefficient model in irrigated maize field with ground-mulching. *Agric. Water Manag.* 127, 85–96. <https://doi.org/https://doi.org/10.1016/j.agwat.2013.05.018>
- Doğan, E., 2009. Reference evapotranspiration estimation using adaptive neuro-fuzzy inference systems. *Irrig. Drain.* 58, 617–628. <https://doi.org/10.1002/ird.445>
- Dou, X., Yang, Y., 2018. Evapotranspiration estimation using four different machine learning approaches in different terrestrial ecosystems. *Comput. Electron. Agric.* 148, 95–106.

- <https://doi.org/https://doi.org/10.1016/j.compag.2018.03.010>
- Fan, L., Zhang, T., Zhao, X., Wang, H., Zheng, M., 2019. Deep topology network: A framework based on feedback adjustment learning rate for image classification. *Adv. Eng. Informatics* 42, 100935. <https://doi.org/https://doi.org/10.1016/j.aei.2019.100935>
- Fang, W., Zhong, B., Zhao, N., Love, P.E.D., Luo, H., Xue, J., Xu, S., 2019. A deep learning-based approach for mitigating falls from height with computer vision: Convolutional neural network. *Adv. Eng. Informatics* 39, 170–177. <https://doi.org/https://doi.org/10.1016/j.aei.2018.12.005>
- Feng, Y., Cui, N., Gong, D., Zhang, Q., Zhao, L., 2017a. Evaluation of random forests and generalized regression neural networks for daily reference evapotranspiration modelling. *Agric. Water Manag.* 193, 163–173. <https://doi.org/https://doi.org/10.1016/j.agwat.2017.08.003>
- Feng, Y., Cui, N., Zhao, L., Hu, X., Gong, D., 2016. Comparison of ELM, GANN, WNN and empirical models for estimating reference evapotranspiration in humid region of Southwest China. *J. Hydrol.* 536, 376–383. <https://doi.org/https://doi.org/10.1016/j.jhydrol.2016.02.053>
- Feng, Y., Peng, Y., Cui, N., Gong, D., Zhang, K., 2017b. Modeling reference evapotranspiration using extreme learning machine and generalized regression neural network only with temperature data. *Comput. Electron. Agric.* 136, 71–78. <https://doi.org/https://doi.org/10.1016/j.compag.2017.01.027>
- Ferreira, L.B., da Cunha, F.F., de Oliveira, R.A., Fernandes Filho, E.I., 2019. Estimation of reference evapotranspiration in Brazil with limited meteorological data using ANN and SVM – A new approach. *J. Hydrol.* 572, 556–570. <https://doi.org/https://doi.org/10.1016/j.jhydrol.2019.03.028>
- Fischer, T., Krauss, C., 2018. Deep learning with long short-term memory networks for financial market predictions. *Eur. J. Oper. Res.* 270, 654–669. <https://doi.org/https://doi.org/10.1016/j.ejor.2017.11.054>
- Friedman, J.H., 1991. Multivariate adaptive regression splines (with discussion). *Ann. Stat.* 19, 1–67. <https://doi.org/doi:10.1214/aos/1176347963>
- Gavili, S., Sanikhani, H., Kisi, O., Mahmoudi, M.H., 2018. Evaluation of several soft computing methods in monthly evapotranspiration modelling. *Meteorol. Appl.* 25, 128–138. <https://doi.org/10.1002/met.1676>
- Gocić, M., Motamedi, S., Shamshirband, S., Petković, D., Ch, S., Hashim, R., Arif, M., 2015. Soft computing approaches for forecasting reference evapotranspiration. *Comput. Electron. Agric.* 113, 164–173. <https://doi.org/https://doi.org/10.1016/j.compag.2015.02.010>
- Guzman, S.M., Paz, J.O., Tagert, M.L.M., 2017. The use of NARX neural networks to forecast daily groundwater levels. *Water Resour. Manag.* 31, 1591–1603. <https://doi.org/10.1007/s11269-017-1598-5>
- Hochreiter, S., Schmidhuber, J., 1997. Long short-term memory. *Neural Comput.* 9, 1735–1780. <https://doi.org/https://doi.org/10.1162/neco.1997.9.8.1735>
- Hu, C., Wu, Q., Li, H., Jian, S., Li, N., Lou, Z., 2018. Deep learning with a long short-term memory networks approach for rainfall-runoff simulation. *Water* 10, 1543.
- Huang, G., Wu, L., Ma, X., Zhang, W., Fan, J., Yu, X., Zeng, W., Zhou, H., 2019. Evaluation of CatBoost method for prediction of reference evapotranspiration in humid regions. *J. Hydrol.* 574, 1029–1041. <https://doi.org/https://doi.org/10.1016/j.jhydrol.2019.04.085>
- Jang, J.-S.R., 1993. ANFIS: adaptive-network-based fuzzy inference system. *IEEE Trans. Syst. Man. Cybern.* 23, 665–685. <https://doi.org/10.1109/21.256541>
- Jang, J.-S.R., Sun, C.T., Mizutani, E., 1997. *Neuro-fuzzy and soft computing: a computational approach to learning and machine intelligence*. Prentice Hall, Upper Saddle River, New Jersey.
- Jekabsons G., M5PrimeLab: M5' regression tree, model tree, and tree ensemble toolbox for Matlab/Octave, 2016, available at <http://www.cs.rtu.lv/jekabsons/>
- Jekabsons G., ARESLab: Adaptive Regression Splines toolbox for Matlab/Octave, 2016, available at <http://www.cs.rtu.lv/jekabsons/>
- Jeong, J., Park, E., Chen, H., Kim, K.-Y., Shik Han, W., Suk, H., 2020. Estimation of groundwater level based on the robust training of recurrent neural networks using corrupted data. *J. Hydrol.* 582, 124512. <https://doi.org/https://doi.org/10.1016/j.jhydrol.2019.124512>
- Karbasi, M., 2018. Forecasting of Multi-Step Ahead Reference Evapotranspiration Using Wavelet-Gaussian Process Regression Model. *Water Resour. Manag.* 32, 1035–1052. <https://doi.org/10.1007/s11269-017-1853-9>

- Kisi, O., 2016. Modeling reference evapotranspiration using three different heuristic regression approaches. *Agric. Water Manag.* 169, 162–172. <https://doi.org/https://doi.org/10.1016/j.agwat.2016.02.026>
- Kool, D., Agam, N., Lazarovitch, N., Heitman, J.L., Sauer, T.J., Ben-Gal, A., 2014. A review of approaches for evapotranspiration partitioning. *Agric. For. Meteorol.* 184, 56–70. <https://doi.org/https://doi.org/10.1016/j.agrformet.2013.09.003>
- Kumar, M., Raghuvanshi, N.S., Singh, R., Wallender, W.W., Pruitt, W.O., 2002. Estimating evapotranspiration using artificial neural network. *J. Irrig. Drain. Eng.* 128, 224–233. [https://doi.org/10.1061/\(ASCE\)0733-9437\(2002\)128:4\(224\)](https://doi.org/10.1061/(ASCE)0733-9437(2002)128:4(224))
- Landeras, G., Ortiz-Barredo, A., López, J.J., 2008. Comparison of artificial neural network models and empirical and semi-empirical equations for daily reference evapotranspiration estimation in the Basque Country (Northern Spain). *Agric. Water Manag.* 95, 553–565. <https://doi.org/https://doi.org/10.1016/j.agwat.2007.12.011>
- Li, X., Wang, K., Liu, L., Xin, J., Yang, H., Gao, C., 2011. Application of the entropy weight and TOPSIS method in safety evaluation of coal mines. *Procedia Eng.* 26, 2085–2091. <https://doi.org/https://doi.org/10.1016/j.proeng.2011.11.2410>
- Liang, C., Li, H., Lei, M., Du, Q., 2018. Dongting lake water level forecast and its relationship with the three Gorges dam based on a long short-term memory network. *Water* 10, 1389.
- Liu, S.M., Xu, Z.W., Zhu, Z.L., Jia, Z.Z., Zhu, M.J., 2013. Measurements of evapotranspiration from eddy-covariance systems and large aperture scintillometers in the Hai River Basin, China. *J. Hydrol.* 487, 24–38. <https://doi.org/https://doi.org/10.1016/j.jhydrol.2013.02.025>
- MacKay, D.J.C., 1992. The evidence framework applied to classification networks. *Neural Comput.* 4, 720–736. <https://doi.org/10.1162/neco.1992.4.5.720>
- Martí, P., González-Altozano, P., López-Urrea, R., Mancha, L.A., Shiri, J., 2015. Modeling reference evapotranspiration with calculated targets. Assessment and implications. *Agric. Water Manag.* 149, 81–90. <https://doi.org/https://doi.org/10.1016/j.agwat.2014.10.028>
- Mathworks, 2019a. MATLAB Version R2019b.
- Mathworks, 2019b. Technical documentation: zscore [WWW Document]. Stand. z-scores. URL <https://au.mathworks.com/help/stats/zscore.html> (accessed 5.2.20).
- Mathworks, 2019c. Long short-term memory networks [WWW Document]. LSTM Netw. Archit. URL <https://au.mathworks.com/help/deeplearning/ug/long-short-term-memory-networks.html> (accessed 5.2.20).
- Mouatadid, S., Adamowski, J., Tiwari, M.K., Quilty, J.M., 2019. Coupling the maximum overlap discrete wavelet transform and long short-term memory networks for irrigation flow forecasting. *Agric. Water Manag.* 219, 72–85. <https://doi.org/https://doi.org/10.1016/j.agwat.2019.03.045>
- Pan, M., Zhou, H., Cao, J., Liu, Y., Hao, J., Li, S., Chen, C.-H., 2020. Water level prediction model based on GRU and CNN. *IEEE Access* 8, 60090–60100.
- Plappert, M., Mandery, C., Asfour, T., 2018. Learning a bidirectional mapping between human whole-body motion and natural language using deep recurrent neural networks. *Rob. Auton. Syst.* 109, 13–26. <https://doi.org/https://doi.org/10.1016/j.robot.2018.07.006>
- Quinlan J. R., 1992. Learning with continuous classes. *Proceedings of 5th Australian Joint Conference on Artificial Intelligence*, World Scientific, Singapore, pp. 343-348.
- Rasmussen, C.E., Williams, C.K., 2006. Gaussian process for machine learning. The MIT Press, Cambridge, Massachusetts.
- Roy, D.K., Datta, B., 2017. Multivariate Adaptive Regression Spline Ensembles for Management of Multilayered Coastal Aquifers. *J. Hydrol. Eng.* 22, 4017031. [https://doi.org/10.1061/\(ASCE\)HE.1943-5584.0001550](https://doi.org/10.1061/(ASCE)HE.1943-5584.0001550)
- Shiri, J., Kişi, Ö., Landeras, G., López, J.J., Nazemi, A.H., Stuyt, L.C.P.M., 2012. Daily reference evapotranspiration modeling by using genetic programming approach in the Basque Country (Northern Spain). *J. Hydrol.* 414–415, 302–316. <https://doi.org/https://doi.org/10.1016/j.jhydrol.2011.11.004>
- Shiri, J., Marti, P., Nazemi, A.H., Sadraddini, A.A., Kisi, O., Landeras, G., Fakheri Fard, A., 2013. Local vs. external training of neuro-fuzzy and neural networks models for estimating reference evapotranspiration assessed through k-fold testing. *Hydrol. Res.* 46, 72–88. <https://doi.org/10.2166/nh.2013.112>

- Shiri, J., Nazemi, A.H., Sadraddini, A.A., Landaras, G., Kisi, O., Fakheri Fard, A., Marti, P., 2014a. Comparison of heuristic and empirical approaches for estimating reference evapotranspiration from limited inputs in Iran. *Comput. Electron. Agric.* 108, 230–241. <https://doi.org/https://doi.org/10.1016/j.compag.2014.08.007>
- Shiri, J., Sadraddini, A.A., Nazemi, A.H., Kisi, O., Landaras, G., Fakheri Fard, A., Marti, P., 2014b. Generalizability of Gene Expression Programming-based approaches for estimating daily reference evapotranspiration in coastal stations of Iran. *J. Hydrol.* 508, 1–11. Solomatine, D.P., Dulal, K.N., 2003. Model trees as an alternative to neural networks in rainfall-runoff modelling. *J. Hydro Sci.* 48(3), 399–411.
- Solomatine, D. and Yunpeng, X. 2004. M5 model trees and neural networks: application to flood forecasting in the upper reach of the Huai River in China. *J. Hydrol. Eng.*, 9(6), 491-501. 2004.
- Solomatine, D.P., Siek, M.B., 2006. Modular learning models in forecasting natural phenomena. *Neural Netw. J.* 19(2), 215–224. <https://doi.org/https://doi.org/10.1016/j.jhydrol.2013.10.034>
- Sugeno, M., Yasukawa, T., 1993. A fuzzy-logic-based approach to qualitative modeling. *IEEE Trans. Fuzzy Syst.* 1, 7. <https://doi.org/10.1109/TFUZZ.1993.390281>
- Supreetha, B.S., Shenoy, N., Nayak, P., 2020. Lion algorithm-optimized long short-term memory network for groundwater level forecasting in Udupi District, India. *Appl. Comput. Intell. Soft Comput.* 2020, 8685724. <https://doi.org/10.1155/2020/8685724>
- Tabari, H., Kisi, O., Ezani, A., Hosseinzadeh, T.P., 2012. SVM, ANFIS, regression and climate based models for reference evapotranspiration modeling using limited climatic data in a semi-arid highland environment. *J. Hydrol.* 444–445, 78–89. <https://doi.org/https://doi.org/10.1016/j.jhydrol.2012.04.007>
- Takagi, T., Sugeno, M., 1985. Fuzzy identification of systems and its applications to modeling and control. *IEEE Trans. Syst. Man. Cybern.* SMC-15, 116–132. <https://doi.org/10.1109/TSMC.1985.6313399>
- Tian, Y., Xu, Y.-P., Yang, Z., Wang, G., Zhu, Q., 2018. Integration of a parsimonious hydrological model with recurrent neural networks for improved streamflow forecasting. *Water* 10, 1655.
- Tien Bui, D., Hoang, N.-D., Martínez-Álvarez, F., Ngo, P.-T.T., Hoa, P.V., Pham, T.D., Samui, P., Costache, R., 2020. A novel deep learning neural network approach for predicting flash flood susceptibility: A case study at a high frequency tropical storm area. *Sci. Total Environ.* 701, 134413. <https://doi.org/https://doi.org/10.1016/j.scitotenv.2019.134413>
- Wang Y., Witten I. H., 1997. Induction of model trees for predicting continuous classes. *Proceedings of the 9th European Conference on Machine Learning Poster Papers, Prague*, 128-137.
- Wang, S., Fu, Z.-Y., Chen, H.-S., Nie, Y.-P., Wang, K.L., 2016. Modeling daily reference ET in the karst area of northwest Guangxi (China) using gene expression programming (GEP) and artificial neural network (ANN). *Theor. Appl. Climatol.* 126, 493–504. <https://doi.org/10.1007/s00704-015-1602-z>
- Wang, S., Lian, J., Peng, Y., Hu, B., Chen, H., 2019. Generalized reference evapotranspiration models with limited climatic data based on random forest and gene expression programming in Guangxi, China. *Agric. Water Manag.* 221, 220–230. <https://doi.org/https://doi.org/10.1016/j.agwat.2019.03.027>
- Wu, J., Sun, J., Liang, L., Zha, Y., 2011. Determination of weights for ultimate cross efficiency using Shannon entropy. *Expert Syst. Appl.* 38(5), 5162–5165. <https://doi.org/10.1016/j.eswa.2010.10.046>
- Xu, H., Zhou, J., Asteris, P.G., Jahed Armaghani, D., Tahir, M.M., 2019. Supervised machine learning techniques to the prediction of tunnel boring machine penetration rate. *Appl. Sci.* <https://doi.org/10.3390/app9183715>
- Yang, H.-F., Chen, Y.-P.P., 2019. Hybrid deep learning and empirical mode decomposition model for time series applications. *Expert Syst. Appl.* 120, 128–138. <https://doi.org/https://doi.org/10.1016/j.eswa.2018.11.019>
- Yoon, H., Jun, S.-C., Hyun, Y., Bae, G.-O., Lee, K.-K., 2011. A comparative study of artificial neural networks and support vector machines for predicting groundwater levels in a coastal aquifer. *J. Hydrol.* 396, 128–138. <https://doi.org/https://doi.org/10.1016/j.jhydrol.2010.11.002>
- Yu, P.-S., Chen, S.-T., Chang, I.-F., 2006. Support vector regression for real-time flood stage forecasting. *J. Hydrol.* 328, 704–716.

- <https://doi.org/https://doi.org/10.1016/j.jhydrol.2006.01.021>
- Yuan, X., Chen, C., Lei, X., Yuan, Y., Muhammad Adnan, R., 2018. Monthly runoff forecasting based on LSTM–ALO model. *Stoch. Environ. Res. Risk Assess.* 32, 2199–2212. <https://doi.org/10.1007/s00477-018-1560-y>
- Zhang, J., Zhu, Y., Zhang, X., Ye, M., Yang, J., 2018. Developing a long short-term memory (LSTM) based model for predicting water table depth in agricultural areas. *J. Hydrol.* 561, 918–929. <https://doi.org/https://doi.org/10.1016/j.jhydrol.2018.04.065>
- Zhang, B., Liu, Y., Xu, D., Zhao, N., Lei, B., Rosa, R.D., Paredes, P., Paço, T.A., Pereira, L.S., 2013. The dual crop coefficient approach to estimate and partitioning evapotranspiration of the winter wheat–summer maize crop sequence in North China Plain. *Irrig. Sci.* 31, 1303–1316. <https://doi.org/10.1007/s00271-013-0405-1>
- Zhao, Z., Chen, W., Wu, X., Chen, P.C.Y., Liu, J., 2017. LSTM network: a deep learning approach for short-term traffic forecast. *IET Intell. Transp. Syst.* 11, 68–75. <https://doi.org/10.1049/iet-its.2016.0208>

DAILY AND MULTI-STEP AHEAD FORECASTING OF POTENTIAL EVAPOTRANSPIRATION USING MACHINE LEARNING ALGORITHMS WITH LIMITED CLIMATIC DATA

D.K. ROY¹, S.K. BISWAS¹ AND M.A. HOSSAIN²

Abstract

Accurate prediction of potential evapotranspiration (ET_0) is essential for efficient planning and management of limited water resources through judicial irrigation scheduling. The FAO-56 Penman-Monteith approach to ET_0 estimation was adopted to compute ET_0 from data obtained during the period 2004–2019 from a weather station located in Gazipur Sadar Upazilla, Bangladesh. The obtained meteorological variables (e.g., daily maximum and minimum temperatures, wind speed, relative humidity, and sunshine duration) and computed ET_0 values were used as inputs and outputs, respectively, for modelling daily and multi-step ahead ET_0 predictions. These input-output training dataset were used to develop several machine learning based prediction models. Based on the previous years' finding, LSTM and Bi-LSTM models were found to be the best performer over others for daily and one-step ahead ET_0 predictions, respectively. In this effort, the generalization capability of the developed best models was evaluated on a new unseen data obtained from a test station, Ishurdi. The model performance was evaluated on three distinct datasets (entire dataset, first half of the entire dataset, and second half of the entire dataset) obtained from the test dataset spanning over 01 January 2015 to 31 December 2020. Results revealed that the deep learning models performed equally well as with the training station dataset, for which the models were developed. Both models showed very good performance for both daily and multi-step (5-day ahead) predictions as indicated by the computed performance evaluation indices. The findings of this research demonstrated the ability of the developed deep learning models to generalize the prediction capabilities outside the training station.

Introduction

Agriculture is considered to be the largest consumer of global freshwater reserves. Therefore, a careful and judicious management of irrigation practices would allow significant water savings. To achieve this water saving, an accurate estimation of the evapotranspiration (ET) is required, which is regarded as one of the major components of water balance. ET plays an important role in surface energy and water budgets, and is an important parameter in the interactions between vegetation, soil, and the atmosphere (Liu et al., 2013). Accordingly, proper management of water resources in irrigated agriculture is largely dependent on an accurate estimation of this vital component of the hydrologic cycle. In general, precise quantification of ET aids in the design and management of efficient irrigation systems, simulation of crop yields, determination of the hydrologic water balance, along with the planning and allocation of water resources (Kisi, 2016). ET can be measured directly by experimental techniques such as the Bowen ratio energy balance method, lysimeter approaches, or eddy covariance systems (Kool et al., 2014; Martí et al., 2015; Zhang et al., 2013) or estimated by computing potential or reference evapotranspiration (ET_0) from meteorological variables. As direct methods of ET measurement are costly, complex and largely unavailable in many regions (Allen et al., 1998; Ding et al., 2013), indirect methods based on ET_0 estimation have become popular in many regions where direct experimental techniques are not available. The FAO-56 Penman-Monteith (FAO-56 PM) model is recommended by the United Nations' Food and Agriculture Organization (FAO) as the standard reference method for estimating ET_0 and validating other methods (Allen et al., 1998). The FAO-56 PM method having been recognized as a universal approach to ET_0 estimation, this method can be used in a wide range of environmental and climatic conditions without the requirement of any local calibration. This well-established method has been validated using lysimeters under a range of different climatic conditions (Landeras et al., 2008). Since ET_0 is solely affected by meteorological conditions, it can be calculated using the FAO-56 PM method by drawing upon several meteorological variables (e.g., relative humidity, wind speed, solar radiation, and minimum/maximum air temperatures). Once the ET_0 is estimated, the actual evapotranspiration (ET_a) can be calculated by means of the ET_0 and crop coefficients.

¹ Senior Scientific Officer, IWM Division, BARI, Gazipur

² CSO(in-charge), IWM Division, BARI, Gazipur

In recent years, Artificial Intelligence (AI) models have been successfully applied to the modelling of ET_0 in different hydrologic regions. Artificial Neural Networks (ANN) were the first AI models implemented to estimate ET_0 (Kumar et al., 2002). Other applications of AI models in estimating ET_0 includes the use of Random Forests (RF) (Feng et al., 2017a; Huang et al., 2019), Generalized Regression Neural Networks (GRNN) (Feng et al., 2017a, 2017b), Extreme Learning Machine (ELM) (Abdullah et al., 2015; Dou and Yang, 2018; Feng et al., 2017b, 2016), Support Vector Machine (SVM) (Ferreira et al., 2019; Huang et al., 2019; Tabari et al., 2012), Genetic Programming (GP) (Gocić et al., 2015), Gaussian Process Regression (GPR) (Karbasi, 2018), Multivariate Adaptive Regression Splines (MARS) (Kisi, 2016), M5 Model Tree (M5Tree) (Kisi, 2016), Multivariate Relevance Vector Machine (MVRVM) (Torres et al., 2011), Gene-Expression Programming (GEP) (Gavili et al., 2018; Shiri et al., 2014b, 2012, Wang et al., 2019, 2016), and Adaptive Neuro Fuzzy Inference System (ANFIS) (Doğan, 2009; Dou and Yang, 2018; Gavili et al., 2018; Shiri et al., 2013; Tabari et al., 2012).

Deep learning (DL) has recently been recognized as a developed and sophisticated sub-domain of machine learning techniques in the arena of artificial intelligence. The DL-based modelling has gained popularity in the successful application to various domain of science including language processing (Plappert et al., 2018), image classification (Fan et al., 2019), computer vision (Fang et al., 2019), speech recognition (Cummins et al., 2018), and time series prediction (Tien Bui et al., 2020; Xu et al., 2019; Yang and Chen, 2019). The usage of DL has also been observed in developing prediction models in the research niche of groundwater level forecasting (Bowes et al., 2019; Supreetha et al., 2020), and prediction of short-term water quality variable (Barzegar et al., 2020). Recurrent Neural Network (RNN) models are able to preserve a memory of previous network states and are better suited for predicting groundwater levels through modelling time series of groundwater table data observed at an observation well. For this reason, numerous recent studies related to groundwater modelling (Chang et al., 2016; Daliakopoulos et al., 2005; Guzman et al., 2017) have focused on the successful application of the RNNs. However, the standard RNN architectures cannot properly grab hold of the long-term reliance between variables (Bengio et al., 1994) due mainly to the occurrences of two problems: vanishing and exploding gradients. These are situations where the network weights either reach to zero or turn out to be enormously large during training of the network.

Long Short-Term Memory (LSTM) networks, a variant of typical RNN architectures, is capable of overcoming the training drawbacks (vanishing and exploding gradient problems) of RNNs through retaining valuable information for model development while avoiding unnecessary or redundant information being passed to the subsequent states in the model development process. LSTM has successfully been applied to the research arena of natural language processing, and financial time series prediction (Fischer and Krauss, 2018), traffic congestion and travelling period predictions (Zhao et al., 2017). In spite of wide applicability in various research domains, LSTM models has only recently been utilized for the forecast of hydrologic time series (Hu et al., 2018; Liang et al., 2018; Tian et al., 2018; Zhang et al., 2018). Recently, Jeong et al., (2020) applied LSTM-based modelling to estimate groundwater level using the corrupted data (with outliers and noise) and found that robust training of an LSTM model using a developed cost function (“least trimmed squares with asymmetric weighting and the Whittaker smoother”) can adequately model noisy groundwater level data. The prediction ability of an LSTM network was found superior than that of a RNN in predicting hourly groundwater level values in a coastal city (susceptible to periodic flooding) of Norfolk, Virginia, USA (Bowes et al., 2019). Mouatadid et al., (2019) used a coupled “maximum overlap discrete wavelet transformation” and LSTM for achieving precision and robustness in the forecasting of irrigation flow. Zhang et al., (2018) proposed an LSTM network for predicting depths in water table in agrarian areas and obtained an acceptable prediction result by utilizing simply an uncomplicated data pre-processing technique. Based on their findings, one can argue that an LSTM network does not require a massive data smoothing or pre-processing in producing an acceptable prediction accuracy. The integrated use of Gated Recurrent Unit and Convolutional Neural Network (CNN-GRU) can also be found in recent literature (Pan et al., 2020) for developing water level prediction models in which CNN-GRU outperformed an LSTM model with regard to Nash-Sutcliffe (NS) Efficiency Coefficient, Average Relative Error, and Root Mean

Squared Error. The prediction accuracy of a lion algorithm optimized LSTM network was found superior than an ordinary LSTM network for the prediction of groundwater level using the historical groundwater level data obtained from an observation well and rainfall data collected from a weather station located in the Udupi district, India (Supreetha et al., 2020). To the best of the author’s understanding, an LSTM network has not previously been used to predict daily and multi-step ahead ET_0 predictions especially in the Gazipur district of Bangladesh.

The key motivation and focus of this study were to: (1) assess the generalization capability of the proposed deep learning models (LSTM and Bi-LSTM) to predict ET_0 at a nearby station, at which the models were neither trained or validated; and (2) provide both daily predictions and multi-step (5-day ahead) ahead forecasting of ET_0 values.

Materials and Methods

Meteorological variables were acquired from two weather stations located in the Gazipur Sadar Upazila of the Gazipur district and Ishurdi Upazilla of the Pabna district in Bangladesh. The weather station in Gazipur is situated between $24.00^{\circ}N$ latitude and $90.43^{\circ}S$ longitude with an altitude of 8.4 m above the mean sea level. Meteorological variables including solar radiation, relative humidity, minimum and maximum temperatures, and wind speed were obtained for 15.5 years (from 01 January 2004 to 30 June 2019). Descriptive statistics of the meteorological variables for the training station are given in Table 1. It is perceived from Table 1 that the climatological variables demonstrated left (negative) skewness which indicates that the distribution of data for all variables had an extended left tail than the right tail. Kurtosis, on the other hand, had both positive and negative values indicating that the datasets had both “heavy-tailed” (positive values of kurtosis) and “light-tailed” (negative values of kurtosis) distributions.

Table 1. Statistical metrics of climatological variables obtained from an automatic weather station located in Gazipur Sadar Upazilla, Bangladesh

Variables	Mean	Standard deviation	Skewness	Kurtosis
Minimum temperature, °C	21.17	5.64	-0.63	-0.88
Maximum temperature, °C	30.93	3.92	-1.10	2.11
Relative humidity, %	80.22	8.20	-0.63	0.75
Wind speed, km/d	241.15	90.69	-0.06	-1.32
Sunshine duration, h	5.54	3.09	-0.40	-1.04

The data for the test station were acquired from 01 June 2015 to 31 December 2020 (2021 daily entries of meteorological variables and computed daily ET_0). The performance evaluation indices were calculated for the entire (2021 entries: from 01 June 2015 to 31 December 2020), first half (1021 entries: from 01 June 2015 to 17 March 2018), and the second half (1020 entries: from 18 March 2018 to 31 December 2020) of the dataset for the test station. The selection of three sets of data allows investigating a better generalization capability of the model. Descriptive statistics of the meteorological variables of the test station are presented in Table 2. The locations of the weather stations in the study areas are presented in Fig. 1.

Table 2. Descriptive statistics of meteorological variables for the test station (Ishurdi station), Bangladesh

Variables	Mean	Standard deviation	Skewness	Kurtosis
Entire dataset				
Minimum temperature, °C	21.37	5.98	-0.73	-0.76
Maximum temperature, °C	31.46	4.16	-0.83	0.28
Relative humidity, %	78.89	12.18	-1.23	1.93
Wind speed, m s^{-1}	1.43	0.23	0.07	0.22
Sunshine duration, h	5.90	3.19	-0.41	-0.71
First half data				
Minimum temperature, °C	21.06	6.08	-0.65	-0.92
Maximum temperature, °C	31.27	4.21	-0.71	0.26
Relative humidity, %	80.06	11.30	-1.24	2.25
Wind speed, m s^{-1}	1.43	0.23	0.06	0.35
Sunshine duration, h	5.75	3.18	-0.42	-0.98
Second half data				
Minimum temperature, °C	21.69	5.87	-0.83	-0.56
Maximum temperature, °C	31.66	4.11	-0.95	0.35
Relative humidity, %	77.71	12.89	-1.18	1.54
Wind speed, m s^{-1}	1.44	0.23	0.09	0.08
Sunshine duration, h	6.05	3.19	-0.39	-0.44

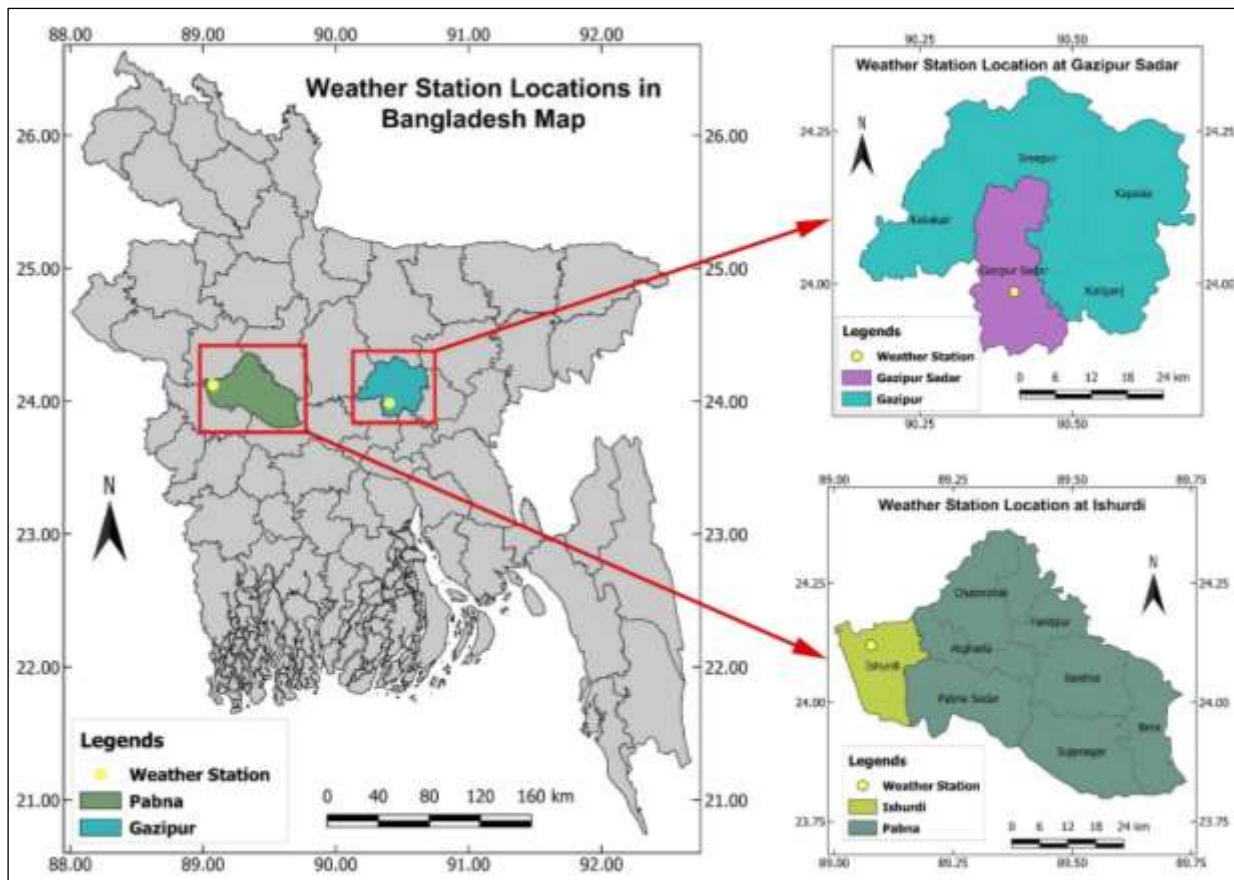


Figure 1. Locations of the weather stations within the study areas.

Meteorological variables obtained from the study areas across the period of study were utilized to estimate daily ET_0 by employing the FAO 56 PM equation. These computed daily values of

ET_0 and the meteorological variables were used as outputs and inputs, respectively for the proposed HFS and other models. This indirect approach of ET_0 estimation from meteorological variables has been widely accepted in circumstances when ET_0 values are extremely hard to acquire directly (Allen et al. 1998; Shiri et al. 2014; Feng et al. 2017b). The FAO 56 PM equation is represented by:

$$ET_0 = \frac{0.408\Delta(R_n - G) + \gamma \frac{900}{T_{\text{mean}} + 273} u_2 (e_s - e_a)}{\Delta + \gamma(1 + 0.34u_2)} \quad (1)$$

where, ET_0 represents reference evapotranspiration, mm d^{-1} ; R_n is the net radiation at the crop surface, $\text{MJ m}^{-2}\text{d}^{-1}$; G is the heat flux density of soil, $\text{MJ m}^{-2}\text{d}^{-1}$; Δ is the slope of the saturation vapor pressure curve, $\text{kPa}^\circ\text{C}^{-1}$; γ is the psychrometric constant, $\text{kPa}^\circ\text{C}^{-1}$; e_s is the saturation vapor pressure, kPa ; e_a is the actual vapor pressure, kPa ; u_2 is the wind speed at a height of 2 m, m s^{-1} ; and T_{mean} is the mean air temperature at 2.0 m height, $^\circ\text{C}$.

For the training station (Gazipur Sadar), computed ET_0 values ranged between 0.92 and 8.02 mm d^{-1} with the mean and standard deviation values of 3.80 and 1.32 mm d^{-1} , respectively. The distribution of ET_0 time-series had an extended right tail compared to the left tail as indicated by a positive skewness value of 0.30. The negative kurtosis value of -0.67 indicates a “light-tailed” distribution for the computed ET_0 values of the train station. On the other hand, the mean, standard deviation, skewness, and kurtosis values of the computed ET_0 for the entire dataset of the test station were 3.67 mm d^{-1} , 1.24 mm d^{-1} , 0.28, and -0.62, respectively. For the first half of the dataset, the values were 3.57 mm d^{-1} , 1.25 mm d^{-1} , 0.35, and -0.62, respectively. The second half of the dataset comprised the following values of ET_0 : mean = 3.76 mm d^{-1} , standard deviation = 1.23 mm d^{-1} , skewness = 0.22, kurtosis = -0.59.

Results and discussion

The LSTM and Bi-LSTM models developed at the training station (Gazipur Sadar) were validated using meteorological data obtained from a test station (Ishurdi station). Three distinct sets of data of the test station were inputted to the developed models for predicting daily ET_0 , which were then compared with the estimated ET_0 and different performance evaluation indices were computed using the model predicted and FAO 56 PM estimated ET_0 values.

Generalization of developed models for a new unseen test dataset: Daily prediction

The performance evaluation results in terms of various statistical indices are shown in Table 3. As the results indicate, the models performed equally well when compared to the results of the training station. The model performances were satisfactory concerning the computed statistical indices: the model produced higher values of accuracy, NS, IOA, and R as well as lower values of RMSE, NRMSE, MAE, and MAD for all three datasets. It is also observed that the first half of the dataset produced relatively better performance when compared to that of the second half and the entire dataset. Overall, the performance is satisfactory, and based on that it can be concluded that the developed LSTM model at Gazipur station is able to predict daily ET_0 values at Ishurdi station without the need to develop model at Ishurdi station.

Table 3. Performance of the LSTM model for predicting daily ET_0 values

Performance indices	Ishurdi dataset		
	Entire dataset	First half data	Second half data
RMSE	0.65	0.49	0.84
NRMSE	0.18	0.13	0.23
R	0.87	0.92	0.83
MAD	0.18	0.18	0.20
MAE	0.44	0.39	0.52
NS	0.72	0.84	0.57
IOA	0.97	0.98	0.96

Performance results are also presented in the form of scatter and error plots as shown in Figure 2, which indicate the distribution of errors at individual datapoints.

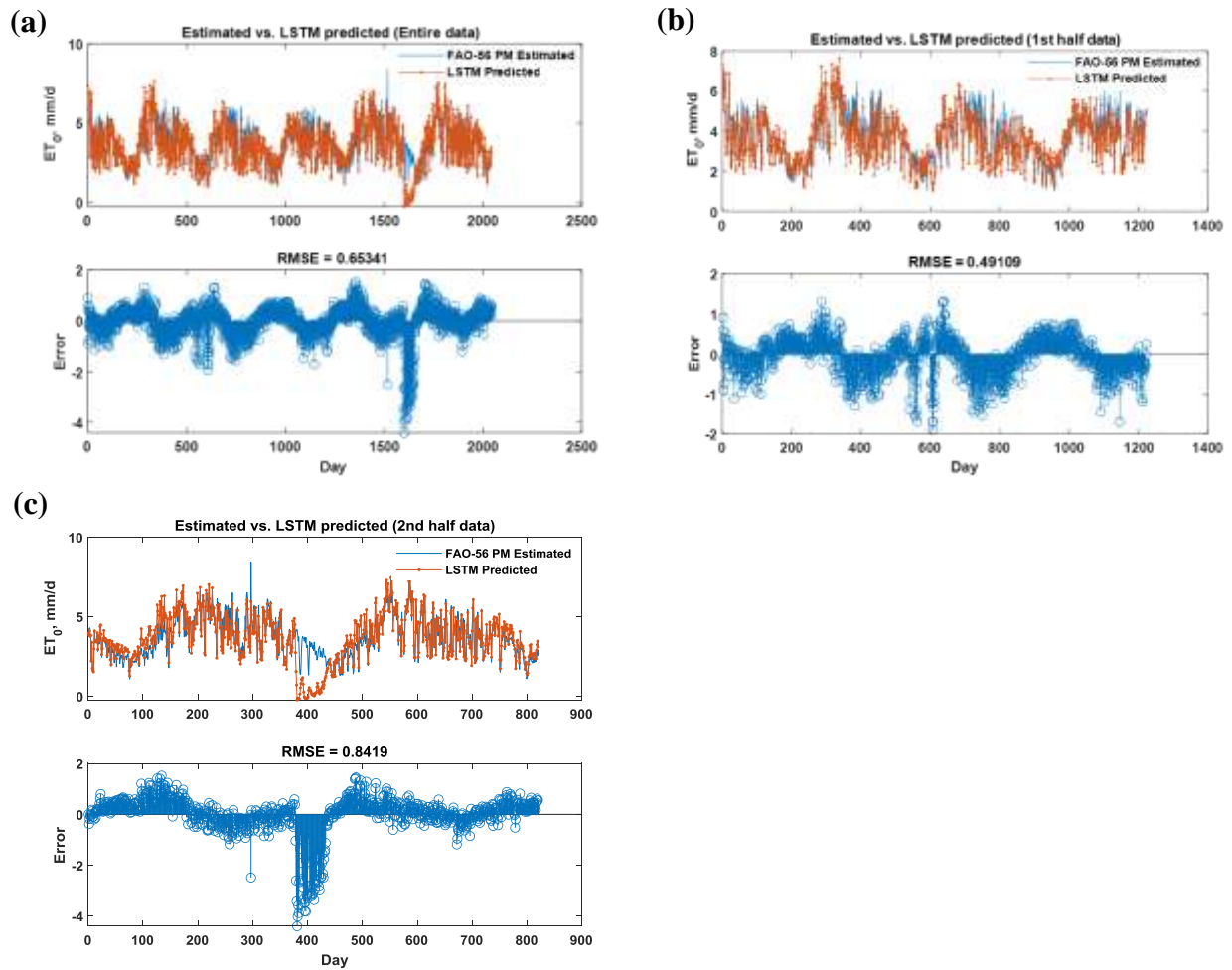


Figure 2. Scatter and error plots of FAO-56 PM estimated, and LSTM predicted daily ET_0 values at Ishudi station: (a) Entire dataset, (b) first half of the dataset, and (c) second half of the dataset.

Generalization of developed models for a new unseen test dataset: multi-step ahead forecasting

For multi-step ahead forecasting, new Bi-LSTM models was developed because the nature of data was different. However, the similar model structure and parameters as in the case of Gazipur station was used. As a Bi-LSTM model performed better for one-step ahead prediction at Gazipur station, Bi-LSTM model was used to develop models for forecasting 1-, 2-, 3-, and 5-day ahead ET_0 values at the Ishurdi station. For this, time-lagged information from the ET_0 timeseries was collected for 50 lags. The most significant input variables were determined by observing partial autocorrelation functions of the lagged timeseries as shown in Figure 3.

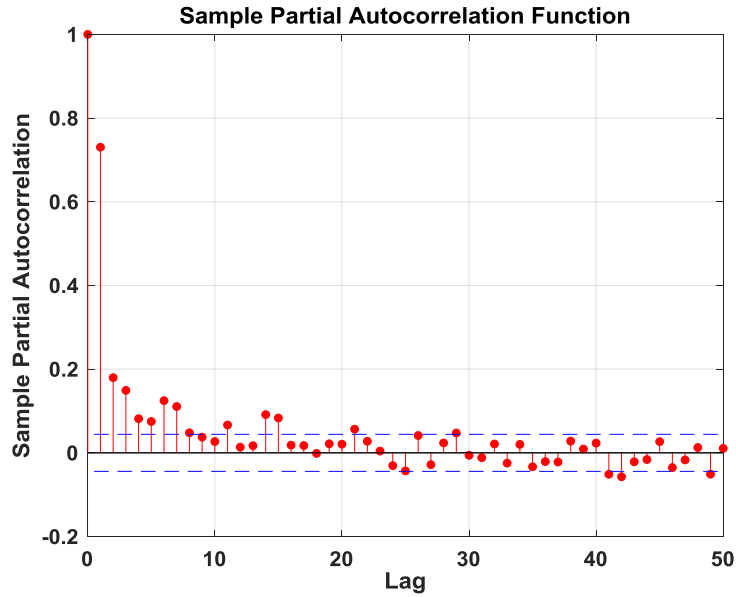


Figure 3. Sample partial autocorrelation functions of the lagged ET_0 timeseries.

Five Bi-LSTM models were developed to forecast 1-, 2-, 3-, 4-, and 5-day ahead ET_0 forecasting. For all models, the selected time lagged variables were served as inputs to the Bi-LSTM models. Table 4 presents the training and validation performances of the developed Bi-LSTM models. It is observed from Table 4 that the differences between the training and validation performances increased with the increase in the forecasting horizon. Overall, the training performances were satisfactory for all forecasting horizons.

Table 4. Training and validation performances of the developed Bi-LSTM models

Forecasting horizon	Training RMSE	Validation RMSE
1-day	0.09	0.12
2-days	0.10	0.17
3-days	0.11	0.29
4-days	0.12	0.56
5-days	0.10	0.73

The trained and validated Bi-LSTM models were then used to forecast ET_0 values on the test dataset, which were selected from the entire dataset. Testing performances were evaluated using several statistical performance evaluation indices as presented in Table 5. It is observed from Table 5 that forecasting horizon greatly influenced the forecasting accuracies, and that the accuracy decreased with the increase in the forecasting horizon as in the case of the training and validation performances. However, the overall performances of the B-LSTM model for all forecasting horizons showed particularly good performance as indicated by the computed statistical performance evaluation indices.

Table 5. Performance of the bi-LSTM model on the test dataset

Indices	Forecasting horizon				
	1-day	2-days	3-days	4-days	5-days
RMSE	0.12	0.17	0.29	0.56	0.73
NRMSE	0.03	0.05	0.08	0.16	0.20
R	1.00	0.99	0.98	0.90	0.86
MAD	0.04	0.05	0.08	0.14	0.24
MAE	0.09	0.12	0.19	0.37	0.56
NS	0.99	0.98	0.95	0.81	0.69
IOA	1.00	1.00	0.99	0.95	0.91

Performance of the developed models was also evaluated by means of line graph and error plots as shown in Figures 4, 5, 6, 7, and 8.

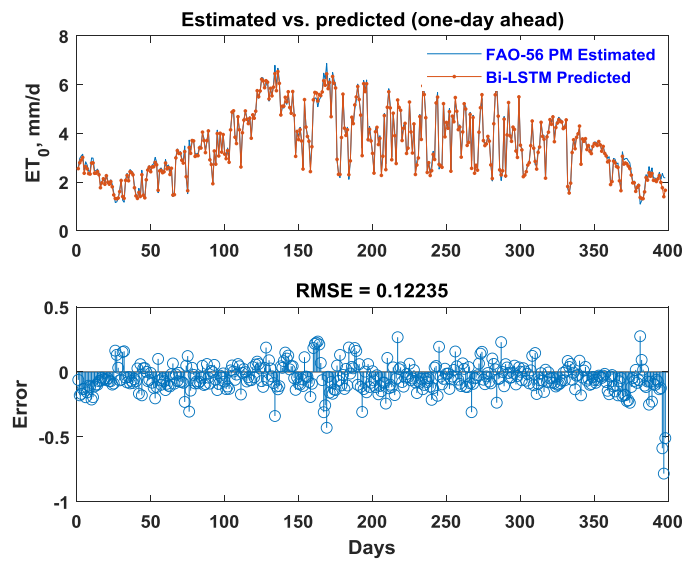


Figure 4. Line graph and error plots for 1-day ahead forecasting.

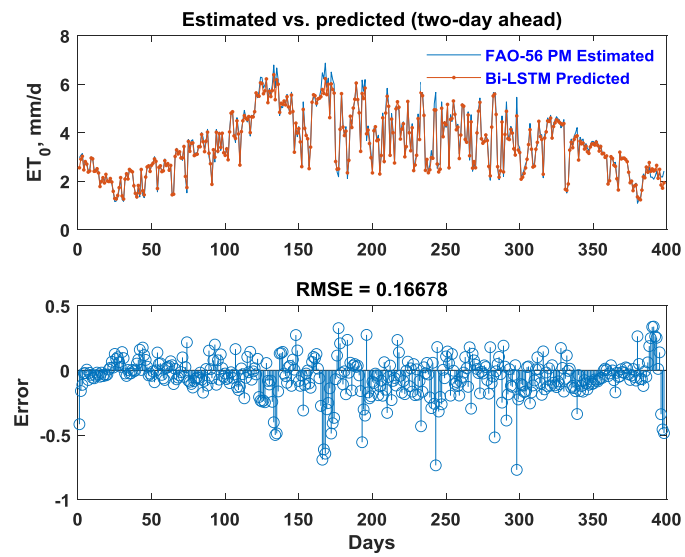


Figure 5. Line graph and error plots for 2-day ahead forecasting.

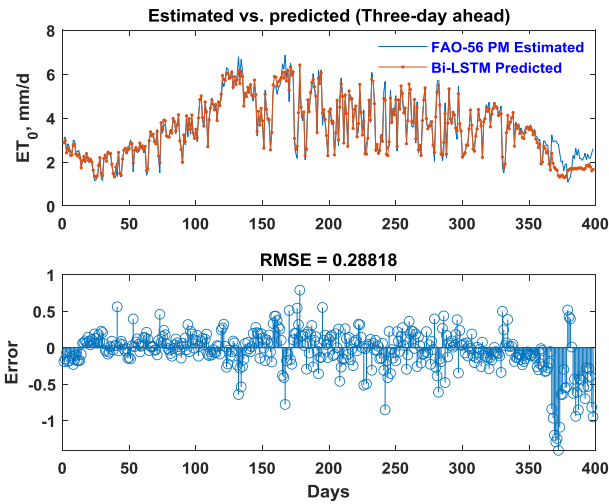


Figure 6. Line graph and error plots for 3-day ahead forecasting.

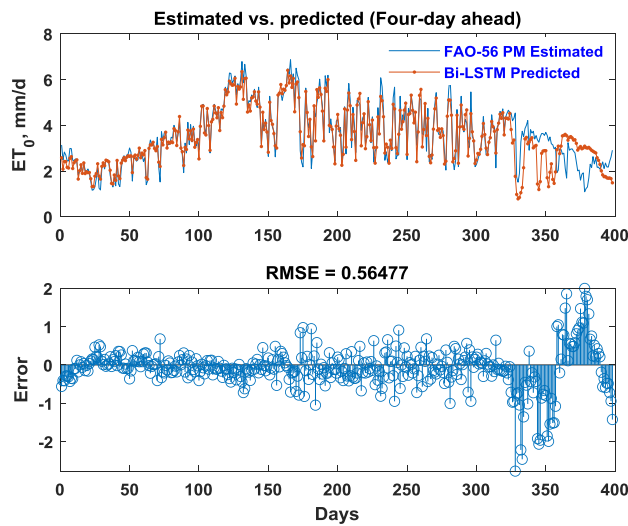


Figure 7. Line graph and error plots for 4-day ahead forecasting.

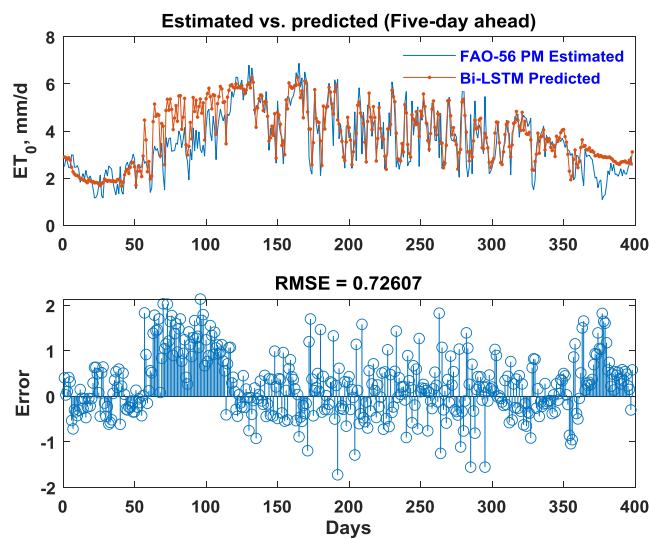


Figure 8. Line graph and error plots for 5-day ahead forecasting.

Conclusions

Precise and reliable prediction of reference evapotranspiration can effectively be employed in developing a sustainable and efficient agricultural water management strategy. This study developed a robust prediction and forecasting tool for daily and multi-step ahead ET_0 values through deep learning algorithms: Long Short Term Memory (LSTM) networks and bidirectional LSTM (Bi-LSTM) networks. LSTM network was used to generalize the daily ET_0 predictions in a nearby meteorological station without developing model for that station. On the other hand, Bi-LSTM model was developed for the Ishurdi station to forecast 1-, 2-, 3-, 4-, and 5-day ahead ET_0 forecasting. Results revealed the suitability of the models in prediction daily ET_0 values and forecasting multi-step ahead ET_0 values. The study will be continued to evaluate the generalization capability of the developed LSTM model at a meteorological station other than the Ishurdi station. In addition, multi-step ahead ET_0 forecasting for a new station needs also to be performed.

References

- Abdullah, S.S., Malek, M.A., Abdullah, N.S., Kisi, O., Yap, K.S., 2015. Extreme Learning Machines: A new approach for prediction of reference evapotranspiration. *J. Hydrol.* 527, 184–195. <https://doi.org/https://doi.org/10.1016/j.jhydrol.2015.04.073>
- Allen, R.G., Pereira, L.S., Raes, D., Smith, M., 1998. Crop evapotranspiration – Guidelines for computing crop water requirements. FAO Irrigation and Drainage Paper 56. Rome: FAO
- Basak, D., Pal, S., Patranabis, D.C., 2007. Support vector regression. *Neural Inf. Process.* 11, 203–224.
- Bera, P., Prasher, S.O., Patel, R.M., Madani, A., Lacroix, R., Gaynor, J.D., Tan, C.S., Kim, S.H., 2006. Application of MARS in simulating pesticide concentrations in soil. *Trans. Asabe* 49, 297–307.
- Barzegar, R., Aalami, M.T., Adamowski, J., 2020. Short-term water quality variable prediction using a hybrid CNN–LSTM deep learning model. *Stoch. Environ. Res. Risk Assess.* 34, 415–433. <https://doi.org/10.1007/s00477-020-01776-2>
- Bengio, Y., Simard, P., Frasconi, P., 1994. Learning long-term dependencies with gradient descent is difficult. *IEEE Trans. Neural Networks Learn. Syst.* 5, 157–166.
- Bezdek, J.C., Ehrlich, R., Full, W., 1984. FCM: The fuzzy c-means clustering algorithm. *Comput. Geosci.* 10, 191–203. [https://doi.org/https://doi.org/10.1016/0098-3004\(84\)90020-7](https://doi.org/https://doi.org/10.1016/0098-3004(84)90020-7)
- Bhattacharya, B., Solomatine, D. P., 2005. Neural networks and M5model trees in modelling water level–discharge relationship. *Neuro Comput.* 63, 381–396.
- Bishop, C., 2006. Pattern recognition and machine learning. Springer-Verlag, New York.
- Bowes, B.D., Sadler, J.M., Morsy, M.M., Behl, M., Goodal, J.L., 2019. Forecasting groundwater table in a flood prone coastal city with long short-term memory and recurrent neural networks. *Water* 11, 1–38.
- Chang, F.-J., Chang, L.-C., Huang, C.-W., Kao, I.-F., 2016. Prediction of monthly regional groundwater levels through hybrid soft-computing techniques. *J. Hydrol.* 541, 965–976. <https://doi.org/https://doi.org/10.1016/j.jhydrol.2016.08.006>
- Chevalier, R.F., Hoogenboom, G., McClendon, R.W., Paz, J.A., 2011. Support vector regression with reduced training sets for air temperature prediction: a comparison with artificial neural networks. *Neural Comput. Appl.* 20, 151–159. <https://doi.org/10.1007/s00521-010-0363-y>
- Cummins, N., Baird, A., Schuller, B.W., 2018. Speech analysis for health: Current state-of-the-art and the increasing impact of deep learning. *Methods* 151, 41–54. <https://doi.org/https://doi.org/10.1016/j.ymeth.2018.07.007>
- Daliakopoulos, I.N., Coulibaly, P., Tsanis, I.K., 2005. Groundwater level forecasting using artificial neural networks. *J. Hydrol.* 309, 229–240. <https://doi.org/https://doi.org/10.1016/j.jhydrol.2004.12.001>
- Dempster, A.P., Laird, N.M., Rubin, D.B., 1977. Maximum likelihood from incomplete data via the EM algorithm. *J. R. Stat. Soc. Ser. B* 39.
- Ding, R., Kang, S., Zhang, Y., Hao, X., Tong, L., Du, T., 2013. Partitioning evapotranspiration into soil evaporation and transpiration using a modified dual crop coefficient model in irrigated maize field with ground-mulching. *Agric. Water Manag.* 127, 85–96.

- <https://doi.org/https://doi.org/10.1016/j.agwat.2013.05.018>
- Doğan, E., 2009. Reference evapotranspiration estimation using adaptive neuro-fuzzy inference systems. *Irrig. Drain.* 58, 617–628. <https://doi.org/10.1002/ird.445>
- Dou, X., Yang, Y., 2018. Evapotranspiration estimation using four different machine learning approaches in different terrestrial ecosystems. *Comput. Electron. Agric.* 148, 95–106. <https://doi.org/https://doi.org/10.1016/j.compag.2018.03.010>
- Fan, L., Zhang, T., Zhao, X., Wang, H., Zheng, M., 2019. Deep topology network: A framework based on feedback adjustment learning rate for image classification. *Adv. Eng. Informatics* 42, 100935. <https://doi.org/https://doi.org/10.1016/j.aei.2019.100935>
- Fang, W., Zhong, B., Zhao, N., Love, P.E.D., Luo, H., Xue, J., Xu, S., 2019. A deep learning-based approach for mitigating falls from height with computer vision: Convolutional neural network. *Adv. Eng. Informatics* 39, 170–177. <https://doi.org/https://doi.org/10.1016/j.aei.2018.12.005>
- Feng, Y., Cui, N., Gong, D., Zhang, Q., Zhao, L., 2017a. Evaluation of random forests and generalized regression neural networks for daily reference evapotranspiration modelling. *Agric. Water Manag.* 193, 163–173. <https://doi.org/https://doi.org/10.1016/j.agwat.2017.08.003>
- Feng, Y., Cui, N., Zhao, L., Hu, X., Gong, D., 2016. Comparison of ELM, GANN, WNN and empirical models for estimating reference evapotranspiration in humid region of Southwest China. *J. Hydrol.* 536, 376–383. <https://doi.org/https://doi.org/10.1016/j.jhydrol.2016.02.053>
- Feng, Y., Peng, Y., Cui, N., Gong, D., Zhang, K., 2017b. Modeling reference evapotranspiration using extreme learning machine and generalized regression neural network only with temperature data. *Comput. Electron. Agric.* 136, 71–78. <https://doi.org/https://doi.org/10.1016/j.compag.2017.01.027>
- Ferreira, L.B., da Cunha, F.F., de Oliveira, R.A., Fernandes Filho, E.I., 2019. Estimation of reference evapotranspiration in Brazil with limited meteorological data using ANN and SVM – A new approach. *J. Hydrol.* 572, 556–570. <https://doi.org/https://doi.org/10.1016/j.jhydrol.2019.03.028>
- Fischer, T., Krauss, C., 2018. Deep learning with long short-term memory networks for financial market predictions. *Eur. J. Oper. Res.* 270, 654–669. <https://doi.org/https://doi.org/10.1016/j.ejor.2017.11.054>
- Friedman, J.H., 1991. Multivariate adaptive regression splines (with discussion). *Ann. Stat.* 19, 1–67. <https://doi.org/doi:10.1214/aos/1176347963>
- Gavili, S., Sanikhani, H., Kisi, O., Mahmoudi, M.H., 2018. Evaluation of several soft computing methods in monthly evapotranspiration modelling. *Meteorol. Appl.* 25, 128–138. <https://doi.org/10.1002/met.1676>
- Gocić, M., Motamedi, S., Shamshirband, S., Petković, D., Ch, S., Hashim, R., Arif, M., 2015. Soft computing approaches for forecasting reference evapotranspiration. *Comput. Electron. Agric.* 113, 164–173. <https://doi.org/https://doi.org/10.1016/j.compag.2015.02.010>
- Guzman, S.M., Paz, J.O., Tagert, M.L.M., 2017. The use of NARX neural networks to forecast daily groundwater levels. *Water Resour. Manag.* 31, 1591–1603. <https://doi.org/10.1007/s11269-017-1598-5>
- Hochreiter, S., Schmidhuber, J., 1997. Long short-term memory. *Neural Comput.* 9, 1735–1780. <https://doi.org/https://doi.org/10.1162/neco.1997.9.8.1735>
- Hu, C., Wu, Q., Li, H., Jian, S., Li, N., Lou, Z., 2018. Deep learning with a long short-term memory networks approach for rainfall-runoff simulation. *Water* 10, 1543.
- Huang, G., Wu, L., Ma, X., Zhang, W., Fan, J., Yu, X., Zeng, W., Zhou, H., 2019. Evaluation of CatBoost method for prediction of reference evapotranspiration in humid regions. *J. Hydrol.* 574, 1029–1041. <https://doi.org/https://doi.org/10.1016/j.jhydrol.2019.04.085>
- Jang, J.-S.R., 1993. ANFIS: adaptive-network-based fuzzy inference system. *IEEE Trans. Syst. Man. Cybern.* 23, 665–685. <https://doi.org/10.1109/21.256541>
- Jang, J.-S.R., Sun, C.T., Mizutani, E., 1997. *Neuro-fuzzy and soft computing: a computational approach to learning and machine intelligence*. Prentice Hall, Upper Saddle River, New Jersey.
- Jekabsons G., M5PrimeLab: M5' regression tree, model tree, and tree ensemble toolbox for Matlab/Octave, 2016, available at <http://www.cs.rtu.lv/jekabsons/>
- Jekabsons G., ARESLab: Adaptive Regression Splines toolbox for Matlab/Octave, 2016, available at <http://www.cs.rtu.lv/jekabsons/>
- Jeong, J., Park, E., Chen, H., Kim, K.-Y., Shik Han, W., Suk, H., 2020. Estimation of groundwater

- level based on the robust training of recurrent neural networks using corrupted data. *J. Hydrol.* 582, 124512. <https://doi.org/https://doi.org/10.1016/j.jhydrol.2019.124512>
- Karbasi, M., 2018. Forecasting of Multi-Step Ahead Reference Evapotranspiration Using Wavelet-Gaussian Process Regression Model. *Water Resour. Manag.* 32, 1035–1052. <https://doi.org/10.1007/s11269-017-1853-9>
- Kisi, O., 2016. Modeling reference evapotranspiration using three different heuristic regression approaches. *Agric. Water Manag.* 169, 162–172. <https://doi.org/https://doi.org/10.1016/j.agwat.2016.02.026>
- Kool, D., Agam, N., Lazarovitch, N., Heitman, J.L., Sauer, T.J., Ben-Gal, A., 2014. A review of approaches for evapotranspiration partitioning. *Agric. For. Meteorol.* 184, 56–70. <https://doi.org/https://doi.org/10.1016/j.agrformet.2013.09.003>
- Kumar, M., Raghuvanshi, N.S., Singh, R., Wallender, W.W., Pruitt, W.O., 2002. Estimating evapotranspiration using artificial neural network. *J. Irrig. Drain. Eng.* 128, 224–233. [https://doi.org/10.1061/\(ASCE\)0733-9437\(2002\)128:4\(224\)](https://doi.org/10.1061/(ASCE)0733-9437(2002)128:4(224))
- Landeras, G., Ortiz-Barredo, A., López, J.J., 2008. Comparison of artificial neural network models and empirical and semi-empirical equations for daily reference evapotranspiration estimation in the Basque Country (Northern Spain). *Agric. Water Manag.* 95, 553–565. <https://doi.org/https://doi.org/10.1016/j.agwat.2007.12.011>
- Li, X., Wang, K., Liu, L., Xin, J., Yang, H., Gao, C., 2011. Application of the entropy weight and TOPSIS method in safety evaluation of coal mines. *Procedia Eng.* 26, 2085–2091. <https://doi.org/https://doi.org/10.1016/j.proeng.2011.11.2410>
- Liang, C., Li, H., Lei, M., Du, Q., 2018. Dongting lake water level forecast and its relationship with the three Gorges dam based on a long short-term memory network. *Water* 10, 1389.
- Liu, S.M., Xu, Z.W., Zhu, Z.L., Jia, Z.Z., Zhu, M.J., 2013. Measurements of evapotranspiration from eddy-covariance systems and large aperture scintillometers in the Hai River Basin, China. *J. Hydrol.* 487, 24–38. <https://doi.org/https://doi.org/10.1016/j.jhydrol.2013.02.025>
- MacKay, D.J.C., 1992. The evidence framework applied to classification networks. *Neural Comput.* 4, 720–736. <https://doi.org/10.1162/neco.1992.4.5.720>
- Martí, P., González-Altozano, P., López-Urrea, R., Mancha, L.A., Shiri, J., 2015. Modeling reference evapotranspiration with calculated targets. Assessment and implications. *Agric. Water Manag.* 149, 81–90. <https://doi.org/https://doi.org/10.1016/j.agwat.2014.10.028>
- Mathworks, 2019a. MATLAB Version R2019b.
- Mathworks, 2019b. Technical documentation: zscore [WWW Document]. Stand. z-scores. URL <https://au.mathworks.com/help/stats/zscore.html> (accessed 5.2.20).
- Mathworks, 2019c. Long short-term memory networks [WWW Document]. LSTM Netw. Archit. URL <https://au.mathworks.com/help/deeplearning/ug/long-short-term-memory-networks.html> (accessed 5.2.20).
- Mouatadid, S., Adamowski, J., Tiwari, M.K., Quilty, J.M., 2019. Coupling the maximum overlap discrete wavelet transform and long short-term memory networks for irrigation flow forecasting. *Agric. Water Manag.* 219, 72–85. <https://doi.org/https://doi.org/10.1016/j.agwat.2019.03.045>
- Pan, M., Zhou, H., Cao, J., Liu, Y., Hao, J., Li, S., Chen, C.-H., 2020. Water level prediction model based on GRU and CNN. *IEEE Access* 8, 60090–60100.
- Plappert, M., Mandery, C., Asfour, T., 2018. Learning a bidirectional mapping between human whole-body motion and natural language using deep recurrent neural networks. *Rob. Auton. Syst.* 109, 13–26. <https://doi.org/https://doi.org/10.1016/j.robot.2018.07.006>
- Quinlan J. R., 1992. Learning with continuous classes. *Proceedings of 5th Australian Joint Conference on Artificial Intelligence*, World Scientific, Singapore, pp. 343-348.
- Rasmussen, C.E., Williams, C.K., 2006. Gaussian process for machine learning. The MIT Press, Cambridge, Massachusetts.
- Roy, D.K., Datta, B., 2017. Multivariate Adaptive Regression Spline Ensembles for Management of Multilayered Coastal Aquifers. *J. Hydrol. Eng.* 22, 4017031. [https://doi.org/10.1061/\(ASCE\)HE.1943-5584.0001550](https://doi.org/10.1061/(ASCE)HE.1943-5584.0001550)
- Shiri, J., Kişi, Ö., Landeras, G., López, J.J., Nazemi, A.H., Stuyt, L.C.P.M., 2012. Daily reference evapotranspiration modeling by using genetic programming approach in the Basque Country (Northern Spain). *J. Hydrol.* 414–415, 302–316.

- <https://doi.org/https://doi.org/10.1016/j.jhydrol.2011.11.004>
- Shiri, J., Marti, P., Nazemi, A.H., Sadraddini, A.A., Kisi, O., Landeras, G., Fakheri Fard, A., 2013. Local vs. external training of neuro-fuzzy and neural networks models for estimating reference evapotranspiration assessed through k-fold testing. *Hydrol. Res.* 46, 72–88. <https://doi.org/10.2166/nh.2013.112>
- Shiri, J., Nazemi, A.H., Sadraddini, A.A., Landeras, G., Kisi, O., Fakheri Fard, A., Marti, P., 2014a. Comparison of heuristic and empirical approaches for estimating reference evapotranspiration from limited inputs in Iran. *Comput. Electron. Agric.* 108, 230–241. <https://doi.org/https://doi.org/10.1016/j.compag.2014.08.007>
- Shiri, J., Sadraddini, A.A., Nazemi, A.H., Kisi, O., Landeras, G., Fakheri Fard, A., Marti, P., 2014b. Generalizability of Gene Expression Programming-based approaches for estimating daily reference evapotranspiration in coastal stations of Iran. *J. Hydrol.* 508, 1–11. Solomatine, D.P., Dulal, K.N., 2003. Model trees as an alternative to neural networks in rainfall-runoff modelling. *J. Hydro Sci.* 48(3), 399–411.
- Solomatine, D. and Yunpeng, X. 2004. M5 model trees and neural networks: application to flood forecasting in the upper reach of the Huai River in China. *J. Hydrol. Eng.*, 9(6), 491-501. 2004.
- Solomatine, D.P., Siek, M.B., 2006. Modular learning models in forecasting natural phenomena. *Neural Netw. J.* 19(2), 215–224. <https://doi.org/https://doi.org/10.1016/j.jhydrol.2013.10.034>
- Sugeno, M., Yasukawa, T., 1993. A fuzzy-logic-based approach to qualitative modeling. *IEEE Trans. Fuzzy Syst.* 1, 7. <https://doi.org/10.1109/TFUZZ.1993.390281>
- Supreetha, B.S., Shenoy, N., Nayak, P., 2020. Lion algorithm-optimized long short-term memory network for groundwater level forecasting in Udipi District, India. *Appl. Comput. Intell. Soft Comput.* 2020, 8685724. <https://doi.org/10.1155/2020/8685724>
- Tabari, H., Kisi, O., Ezani, A., Hosseinzadeh, T.P., 2012. SVM, ANFIS, regression and climate based models for reference evapotranspiration modeling using limited climatic data in a semi-arid highland environment. *J. Hydrol.* 444–445, 78–89. <https://doi.org/https://doi.org/10.1016/j.jhydrol.2012.04.007>
- Takagi, T., Sugeno, M., 1985. Fuzzy identification of systems and its applications to modeling and control. *IEEE Trans. Syst. Man. Cybern.* SMC-15, 116–132. <https://doi.org/10.1109/TSMC.1985.6313399>
- Tian, Y., Xu, Y.-P., Yang, Z., Wang, G., Zhu, Q., 2018. Integration of a parsimonious hydrological model with recurrent neural networks for improved streamflow forecasting. *Water* 10, 1655.
- Tien Bui, D., Hoang, N.-D., Martínez-Álvarez, F., Ngo, P.-T.T., Hoa, P.V., Pham, T.D., Samui, P., Costache, R., 2020. A novel deep learning neural network approach for predicting flash flood susceptibility: A case study at a high frequency tropical storm area. *Sci. Total Environ.* 701, 134413. <https://doi.org/https://doi.org/10.1016/j.scitotenv.2019.134413>
- Wang Y., Witten I. H., 1997. Induction of model trees for predicting continuous classes. *Proceedings of the 9th European Conference on Machine Learning Poster Papers, Prague*, 128-137.
- Wang, S., Fu, Z.-Y., Chen, H.-S., Nie, Y.-P., Wang, K.L., 2016. Modeling daily reference ET in the karst area of northwest Guangxi (China) using gene expression programming (GEP) and artificial neural network (ANN). *Theor. Appl. Climatol.* 126, 493–504. <https://doi.org/10.1007/s00704-015-1602-z>
- Wang, S., Lian, J., Peng, Y., Hu, B., Chen, H., 2019. Generalized reference evapotranspiration models with limited climatic data based on random forest and gene expression programming in Guangxi, China. *Agric. Water Manag.* 221, 220–230. <https://doi.org/https://doi.org/10.1016/j.agwat.2019.03.027>
- Wu, J., Sun, J., Liang, L., Zha, Y., 2011. Determination of weights for ultimate cross efficiency using Shannon entropy. *Expert Syst. Appl.* 38(5), 5162–5165. <https://doi.org/10.1016/j.eswa.2010.10.046>
- Xu, H., Zhou, J., Asteris, P.G., Jahed Armaghani, D., Tahir, M.M., 2019. Supervised machine learning techniques to the prediction of tunnel boring machine penetration rate. *Appl. Sci.* <https://doi.org/10.3390/app9183715>
- Yang, H.-F., Chen, Y.-P.P., 2019. Hybrid deep learning and empirical mode decomposition model for time series applications. *Expert Syst. Appl.* 120, 128–138. <https://doi.org/https://doi.org/10.1016/j.eswa.2018.11.019>

- Yoon, H., Jun, S.-C., Hyun, Y., Bae, G.-O., Lee, K.-K., 2011. A comparative study of artificial neural networks and support vector machines for predicting groundwater levels in a coastal aquifer. *J. Hydrol.* 396, 128–138. <https://doi.org/https://doi.org/10.1016/j.jhydrol.2010.11.002>
- Yu, P.-S., Chen, S.-T., Chang, I.-F., 2006. Support vector regression for real-time flood stage forecasting. *J. Hydrol.* 328, 704–716. <https://doi.org/https://doi.org/10.1016/j.jhydrol.2006.01.021>
- Yuan, X., Chen, C., Lei, X., Yuan, Y., Muhammad Adnan, R., 2018. Monthly runoff forecasting based on LSTM–ALO model. *Stoch. Environ. Res. Risk Assess.* 32, 2199–2212. <https://doi.org/10.1007/s00477-018-1560-y>
- Zhang, J., Zhu, Y., Zhang, X., Ye, M., Yang, J., 2018. Developing a long short-term memory (LSTM) based model for predicting water table depth in agricultural areas. *J. Hydrol.* 561, 918–929. <https://doi.org/https://doi.org/10.1016/j.jhydrol.2018.04.065>
- Zhang, B., Liu, Y., Xu, D., Zhao, N., Lei, B., Rosa, R.D., Paredes, P., Paço, T.A., Pereira, L.S., 2013. The dual crop coefficient approach to estimate and partitioning evapotranspiration of the winter wheat–summer maize crop sequence in North China Plain. *Irrig. Sci.* 31, 1303–1316. <https://doi.org/10.1007/s00271-013-0405-1>
- Zhao, Z., Chen, W., Wu, X., Chen, P.C.Y., Liu, J., 2017. LSTM network: a deep learning approach for short-term traffic forecast. *IET Intell. Transp. Syst.* 11, 68–75. <https://doi.org/10.1049/iet-its.2016.0208>

EFFECT OF DRIP IRRIGATION AND MULCHING ON GROWTH AND FLOWERING OF CHRYSANTHEMUM AS CUT FLOWER

F. AKTER¹, M.A. HOSSAIN², S.K. BISWAS³, S.S.A. KAMAR¹, AND F.N. KHAN⁴

Abstract

The experiment was conducted in the experimental field of IWM Division, BARI, Gazipur during 2020-2021 to evaluate the effect of different irrigation amount with different mulching systems. Nine treatments were designed in randomized complete block for the experiment with three replications. The treatments comprised different combinations of three drip irrigation levels (100, 80 and 60% of ET_0) and three mulching systems (no mulch, black plastic and straw mulch). Stem length (33.03 cm), flower diameter (11.11 cm), number of branches/plant (35.87), number of flower/branches (5.10), number of flowers/plant (38.33), marketable branches/plant (8.33), flowers/marketable branch (5.10) and marketable branches/plot (249.9) were found to be maximum with drip irrigation at 100% ET_0 with black plastic mulch. The highest plant height (70.73 cm) was obtained from drip irrigation at 100% ET_0 with paddy straw mulch followed by drip irrigation at 100% ET_0 with black plastic mulch. And the highest number of plant leaves was obtained from drip irrigation at 80% ET_0 with black plastic mulch followed by drip irrigation at 80% ET_0 with paddy straw mulch. Results of this study revealed that the drip system of irrigation at 100% ET_0 with black plastic mulch showed better performance followed by drip irrigation at 100% ET_0 with paddy straw mulch and drip irrigation at 80% ET_0 with black plastic mulch over drip irrigation at 60% ET_0 with no mulch and drip irrigation at 80% ET_0 with no mulch. The highest BCR of 4.69 was found for treatment T_2 followed by treatment T_3 .

Introduction

Floriculture has been identified as an emerging sector of agriculture in Bangladesh due to divergence of farmers towards high value floriculture and utilization of flowers in social occasion. Chrysanthemum is one of the most important flower crop of commercial importance grown in different parts of the world as cut flower and potted plant. In International flower trade, it ranks next to rose. Preferred particularly for its range of shapes and size of flower, brilliant color tones and long lasting flower life. As in all plants, irrigation is an essential practice for chrysanthemum growing, but its adequate handling has been neglected by growers, resulting in growing loss and consequent productivity and quality decreases in the final product (Farias et al., 2009). In order to irrigate more extensive areas with the available water resources, such factors as soil, plant, and water resource must be taken into consideration. In addition, the values of plant water consumption under either sufficient or deficient water conditions should be known throughout the growing season of plants and water-yield relationships should be formed accordingly. These data can be obtained by making a large number of investigations for each plant (Doorenbos and Kassam, 1979). To generate the data concerned, Conover (1969), Parnell (1989), Kiehl et al. (1992), Schuch et al. (1998), Rego et al. (2004), Fernandes et al. (2006), Budiarto et al. (2007), Farisa et al. (2009), Waterland et al. (2010) and Villalabos (2014) made investigations on irrigation and flower quality in the chrysanthemum plant. The majority of the investigations concerned are in the form of pot studies, and they are studies in which the plant quality was determined in different soil moisture tensions. Unlike the above-mentioned studies, this study aimed to determine the effects of different irrigation intervals and water amounts on yield and quality parameters in the chrysanthemum plant under greenhouse conditions in the Mediterranean climatic zone.

Among the water management practices for increasing WUE, there are several practices, one of them being mulching. Different types of materials such as straw, plastic film, grass, hyacinth, gravel, sand etc. are used as mulches. Mulching contributed to the crop production by influencing soil productivity; weed control, etc., depending upon the type of mulches (Asiegbu 1991). In addition, drip irrigation increases the yield of crops even at reduced irrigation water application (Yohannes and

¹ SO, IWM Division, BARI, Gazipur

² CSO (in-charge), IWM Division, BARI, Gazipur

³ SSO, IWM Division, BARI, Gazipur

⁴ PSO, Floriculture Division, BARI, Gazipur

Tadesse 1998). The use of polyethylene mulch with drip irrigation in chrysanthemum production was reported to high yield and net income (Jawaharlal *et al.*, 2017). In Bangladesh, chrysanthemum is gaining importance day by day for its demand and commercial value. But still there is a lack of standard research work on water management and use of mulches to produce quality chrysanthemum. Hence, an attempt was made to investigate the performance of drip irrigation in conjunction with mulches for growth and flowering of chrysanthemum as cut flower.

Objectives:

- To find out the optimum irrigation scheduling and mulches for Chrysanthemum production.
- To evaluate the feasibility of drip irrigation with different mulches for Chrysanthemum cultivation in terms of growth and flowering of Chrysanthemum.

Materials and Methods

The experiment was conducted during the winter season of 2020-2021 at the experimental field of IWM Division, BARI, Gazipur. The soils were silty clay loam with field capacity (28.5-29%), and bulk density (1.44-1.48) gm/cc. The experiment was laid out in a RCBD design with four replications. Nine treatments were designed for the experiment as stated below:

T₁ = Drip irrigation at 100% ET₀ with no mulch

T₂ = Drip irrigation at 100% ET₀ with black plastic mulch

T₃ = Drip irrigation at 100% ET₀ with paddy straw mulch

T₄ = Drip irrigation at 80% ET₀ with no mulch

T₅ = Drip irrigation at 80% ET₀ with black plastic mulch

T₆ = Drip irrigation at 80% ET₀ with paddy straw mulch

T₇ = Drip irrigation at 60% ET₀ with no mulch

T₈ = Drip irrigation at 60% ET₀ with black plastic mulch

T₉ = Drip irrigation at 60% ET₀ with paddy straw mulch

The unit plot size was 1.8 m × 1.5 m, with 1.5m wide buffer strip between plots to restrict seepage from neighboring plots. Recommended dose of fertilizers were applied @ 500 kg TSP, 160 kg MoP and cow-dung 8 t/ha. After one month of planting, urea @ 300kg and MoP @ 160kg were applied as top dressed. Besides, urea @ 100kg/ha was applied just after 1st pinching for better results. Seedling of chrysanthemum were used as the plant material in the research. Uniform rooted cuttings were planted on 02 December 2021 into plots with five rows 30×30 cm spacing and each plot contained 30 plants. Standard cultivation practices for flower bud removal, supporting system, disease and pest control as used for commercial chrysanthemum production were employed for growing the crops during the experiment. The practice of pinching was not applied to the plants in the study.

Soil moisture and temperature at every 10days interval was measured. Three plants were selected randomly and tagged in each plot for analysis of growth and flower yield characters viz. plant height, number of branches, number of bud, number of flower, date of bud initiation, date of bud burst, date of full blooming, stem length, flower diameter and various other similar characters. Data of the investigation is presented in the Table 1.

Irrigations were done in drip irrigation method with three mulches as per treatments. The drippers having a discharge of 4 l h⁻¹ at a pressure of 0.1 MPa on laterals were located 30 cm apart. The dripper were arranged in such a way that every lateral had six drippers with 30 cm intervals. The amount of irrigation water applied in the treatments was controlled by using a gauge on the main pipeline and valves located on each lateral. The irrigation water to be applied was calculated by the equation given below.

$$I = P_c \times E_{pan} \times A \times P \quad (1)$$

where, I is the irrigation water (mm), P_c is the pan coefficient, E_{pan} is the cumulative pan evaporation (mm), A is the plot area (m^2) and P is the wetted area percentage (%). The wetted area was taken as 100% assuming that lateral interval is equal to the spaces between drippers.

All the water which evaporated from Class A Pan (CAP) for 25 days after planting (DAP) was applied equally to all the treatments as irrigation water to ensure the root development and full survival of seedlings. The application of different irrigation water amounts was initiated 25 days after planting (DAP).

For mulching, 10 t/ha paddy straw was used after 7 days of transplanting. For black polyethylene mulch, 10 μ m black polyethylene sheet having holes of 50 mm diameter at a distance of 30 cm \times 30 cm was spread over the beds and chrysanthemum seedlings were transplanted in the holes. Undesirable plants were rouged out. The flowers were harvested from February 06, 2021 to February 30, 2021 when the flower in the middle opened completely and the surrounding flowers displayed full development.

Results and discussions

Effect of irrigation on plant growth of chrysanthemum

The bar charts (Fig. 1a, 1b and 1c) illustrate changes in root length, root fresh weight and dry weight resulted from applying different amount of irrigation with different mulching practices. It is shown from the charts root length varied at different dates with different treatments.

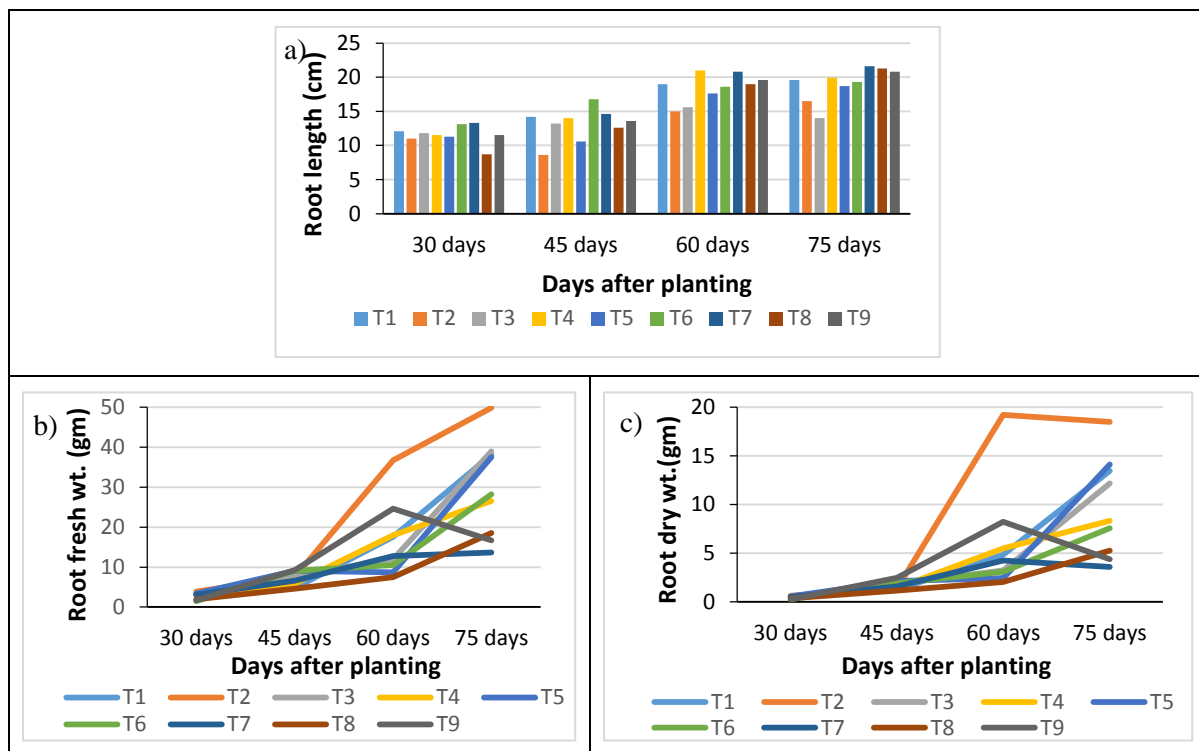


Fig. 1. Effect of different irrigation treatments with different mulching on root length, root fresh weight and root dry weight at different days after sowing.

The highest root length was found in low irrigation applied treatments T_4 and T_7 where mulching was absent. Lower root length was found in mulching treatments T_2 , T_3 , T_5 , T_6 , T_8 and T_9 , might be due to higher moisture content. However, the highest root fresh weight and dry weight was found in treatment T_2 (irrigation was given at 100% ET_0 with black plastic mulch) followed by treatment T_3 (irrigation was given at 100% ET_0 with paddy straw mulch) and the lowest root fresh weight and dry weight was found in treatment T_2 (irrigation was given at 100% ET_0 with black plastic mulch) followed by treatment T_3 (irrigation was given at 100% ET_0 with paddy straw mulch). Both higher value and lower value of root fresh weight and dry weight was due to moisture content of soil. Moisture content of black plastic mulch and paddy straw mulch was higher than no mulch treatments.

It is seen in the (fig. 2a), at 70 days after planting, the highest plant height was found of about 70.73 cm in treatment T₃ followed by treatments T₂, while the lowest plant height (58.53 cm) was found in treatment T₇, followed by treatments T₄, T₈ and T₉. The highest number of bud was obtained from treatment T₂ followed by treatment T₃ and T₇, whereas the lowest number of bud was obtained from treatment T₇ which was significantly par with treatment T₄. Similarly, the highest plant fresh weight and dry weight was recorded in treatment T₂ which was very close to treatment T₃ and the lowest was recorded from no mulch treatment of T₇(Fig. 2c, 2d) followed by treatment T₄ and T₉.

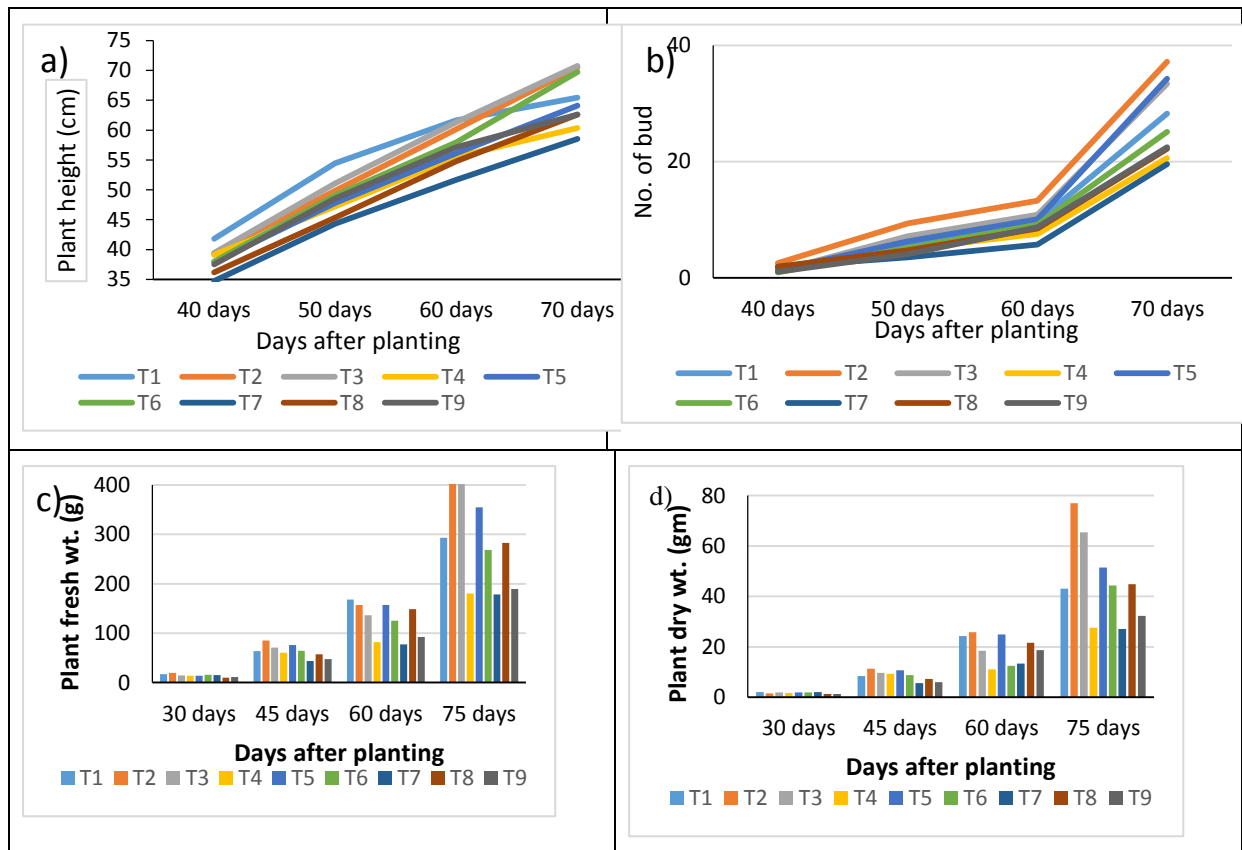


Fig. 2. Effect of different irrigation treatments with different mulching on plant height, plant fresh weight and plant dry weight at different days after sowing.

Plant growth and floral characters

The growth and flower quality characteristics of chrysanthemum such as Plant height (cm), no. of leaves, no. of branches/plant, days to bud initiation, days to bud burst, burst bud diameter, days to flower blooming, flower diameter, stem length, no. of flower/branch, no. of flowers/plant, marketable branches/plant, flowers/marketable branch and marketable branches/plot were significantly ($p < 0.01$) influenced by the drip irrigation with different amount of water along with different type of mulching. Table 1.a. revealed that The treatment T₂ and Treatment T₃ exhibited better performance for all parameters followed by treatment T₅. However, the lowest results were determined in treatment (T₇) for all parameters that was statistically significant with the highest one. Floral characters like days to bud initiation, bud burst, flower blooming and flower destroy were greatly influenced by the treatments (table 1.b). It is evident that the days taken to bud initiation to bud burst and bud burst to flower blooming were significantly varied with different treatments. But there was no significant effect on days to plant sowing to bud initiation and days to flower blooming to flower destroy. Bud burst time needed maximum for treatment T₇ and T₉ followed by treatment T₄ and minimum time needed treatment was treatment T₂. Bud burst to flower blooming time was maximum for treatment T₇ followed by treatment T₄ and minimum for the treatment T₂. The maximum marketable branches/plot (249.90) was achieved with the treatment T₂ (drip irrigation at 100% ET₀ with black plastic mulch) which was significantly par with the treatment T₃ (drip irrigation at 100% ET₀ with paddy straw

mulch) (table 1.b). And the minimum marketable branches/plot (73.2) was achieved with the treatment (T₇) (drip irrigation at 60% ET₀ with no mulch)

Table 1.a. Effect of drip irrigation levels and mulching on growth and flowering parameters of chrysanthemum plant and flower

Treatments	No. of leaves	No. of branches/ plant	Days to bud initiation	Days to bud burst	Burst bud diameter (cm)	Days to flower blooming	Flower diameter (cm)	Stem length (cm)
T1	205	34.07	36.32	17.09	0.18	12.16	10.56	27.92
T2	209.78	35.87	36.2	15.78	0.19	11.89	11.11	33.03
T3	210.89	33.27	36.47	16.55	0.19	12.1	10.89	32.67
T4	160.44	25.93	37.6	18.07	0.18	14.96	10.22	25.77
T5	251.78	35.33	36.44	17.09	0.19	12.4	10.44	30.23
T6	248.45	28.8	37.11	17.21	0.19	12.62	10.33	29.39
T7	166.11	24.6	36.42	18.49	0.17	15.34	9.33	25.36
T8	171.22	27.4	36.9	17.21	0.18	13.51	9.78	26.85
T9	204.56	26.6	37.67	18.46	0.19	13.3	9.67	28.47
CV (%)	16.98	5.81	NS	2.37	NS	8.88	3.09	7.36
LSD (0.05)	59.69	3.05	-	0.71	-	2.02	0.55	3.68

The highest number of flower per branch (5.10) or marketable branch both were same and obtained from treatment T₂ followed by treatment T₃. And the lowest number of flower/branch (2.72) and number of flower/ marketable branch (4.00) were obtained from treatment T₇ and T₈ respectively and they were significantly par with each other for both the parameters. Maximum number of branches/plant (35.87) and marketable branches/plant (8.33) were recorded for treatment T₂, was almost significantly equal to the treatment (T₃), treatment (T₁) and treatment (T₅), while the minimum number of branches/plant (24.60) and marketable branches/plant (2.44) were recorded for the treatment (T₇) (drip irrigation at 60% ET₀ with no mulch).

Table 1.b. Effect of drip irrigation levels and mulching on growth and flowering parameters of chrysanthemum plant and flower

Treatments	No. of flower/ branch	No. of flowers/ plant	Marketable branch/ plant	Flowers/ marketable branch	Marketable branch/ 10m ²	Days to flower destroy (in field)
T ₁	3.38	28.22	6.67	4.55	741	14.03
T ₂	5.10	38.33	8.33	5.10	926	15.17
T ₃	4.03	33.02	7.50	4.87	833	14.14
T ₄	3.07	20.74	4.33	4.33	481	13.00
T ₅	3.69	34.05	6.11	4.55	679	14.03
T ₆	3.30	26.78	5.87	4.45	652	13.64
T ₇	2.72	19.11	2.44	4.11	271	11.14
T ₈	3.16	21.56	3.56	4.00	396	12.61
T ₉	3.23	21.56	3.67	4.22	408	12.39
CV (%)	13.41	9.45	4.43	8.37	4.45	-
LSD (0.05)	0.78	4.43	3.66	0.86	3.52	0.55

The treatment T₂ exhibited better performance for number of flowers/plant (38.33), flower diameter (11.11 cm), and stem length (33.03 cm) was statistically comparable with the treatment (T₃) and treatment (T₅). However, the lowest number of flowers/plant (19.11), flower diameter (9.33 cm), and stem length (25.36 cm) were determined in treatment (T₇) followed by treatments (T₄). The bud diameter was non-significant (p=0.05) and the highest number of leaves (251) was resulted from treatment T₅ (drip irrigation at 80% ET₀ with black plastic mulch) followed by treatment (T₆). Whereas, the lowest number of leaves (160.44) was obtained from treatment T₄ (drip irrigation at 80% ET₀ with no mulch) that was statistically significant with the highest one.

Table 2. revealed that black plastic mulch hampered weed growth effectively. But paddy straw mulch was more vulnerable for weed growth than no mulch treatments. No of weeds, weed fresh weight (gm) and dry weight (gm) were significantly varied with the treatments. Maximum no of weeds, weed fresh weight (gm) and dry weight (gm) were obtained from treatment T3 followed by treatment T6. And minimum no of weeds, weed fresh weight (gm) and dry weight (gm) were obtained from treatment T7 followed by treatment T4. There was negligible weed in black plastic mulch treatments. Among the paddy straw mulch treatments, lower no of weeds and their fresh weight (gm) and dry weight (gm) were found in treatment T9 than others. It might be also moisture content effect.

Table 2. Effect of irrigation levels and mulching on weed growth

Treatments	No of weeds	Fresh weight (gm)	Dry weight (gm)
T ₁	132.67	254.21	39.78
T ₂	13.00	26.6	4.33
T ₃	221.00	712.86	116.01
T ₄	90.33	220.5	37.88
T ₅	9.00	11.97	2.46
T ₆	169.33	504.55	80.60
T ₇	86.67	187.74	36.53
T ₈	7.67	15.32	2.32
T ₉	114.00	227.44	36.58
CV(%)	12.00	13.4	10.03
LSD(0.05)	19.48	14.26	6.88

Amount of irrigation water and water use

At the start of the experiment, 33 mm irrigation water was applied for about 20 days to all experimental plots to avoid any problems in the plant establishment. After the completion of plant establishment, irrigation water was applied to the experimental plots according to the designed treatments. The amount of irrigation water based on the treatments was initiated on 22 December 2020 and ended on 27 February 2021. The amount of water applied to the crop ranged from 181.51 mm and 219.94 mm with minimum in the 60% ET₀ treatment and maximum in the wettest treatment of 100% ET₀ (Table 3). Among the all treatments, the highest water productivity was 39.34 kg/m³ obtained from treatment T₂, as this treatment produced the highest yield than other treatments. Similar observation was found by Maheria et al. (2013). Total water used for no mulch treatments were ranged from 183.77 to 219.94 mm, for black plastic mulch from 181.51 to 214.27 mm and for paddy

straw mulch from 182.4 to 214.78 mm at 60% ET₀, 80% ET₀ and 100% ET₀ treatments, respectively. The lowest water productivity was achieved with treatment T7 as this treatment yielded minimum.

Table 3. Irrigation water applied in different treatments

Treatment	Number of Irrigation applied	Dripper discharge (l/h)	Water for plant establishment (mm)	Irrigation water applied (mm)	Effective rainfall (mm)	Soil moisture contribution (mm)	Total water Use (mm)	Water productivity (kg/m ³)
T ₁	25	4	33	93	95.6	-1.66	219.94	20.63
T ₂	25	4	33	93	95.6	-7.33	214.27	39.34
T ₃	25	4	33	93	95.6	-6.82	214.78	30.67
T ₄	25	4	33	74.4	95.6	-0.78	202.22	13.33
T ₅	25	4	33	74.4	95.6	-4.38	198.62	28.15
T ₆	25	4	33	74.4	95.6	-3.53	199.47	17.88
T ₇	25	4	33	55.8	95.6	-0.63	183.77	12.55
T ₈	25	4	33	55.8	95.6	-2.89	181.51	15.69
T ₉	25	4	33	55.8	95.6	-2	182.4	15.32

Soil moisture and temperature

The figure 3 revealed that soil temperature was increased in black plastic mulch to some extent (fig:3b). But whenever it irrigated properly then temperature became low. Same observation was reported by Tariq et al. and Diaz-Perez et al. Sufficient amount of moisture content and temperature ensure quality chrysanthemum at drip irrigation at 100% ET₀ with black plastic mulch. The figure 3 showed that before sowing, soil moisture was found to be almost similar for all the treatments. But with the passing time, there were great variations among the treatments. The highest moisture content was found from treatment T₂ followed by treatment T₃. The lowest moisture content was found from treatment T₇ followed by treatment T₈ and T₉. It was found that soil temperature of treatment T₈ was higher than other treatment, but soil moisture trend was found comparatively lower. However, the lower soil temperature was recorded in no mulch treatments (T₁, T₄, T₇) during the cropping period.

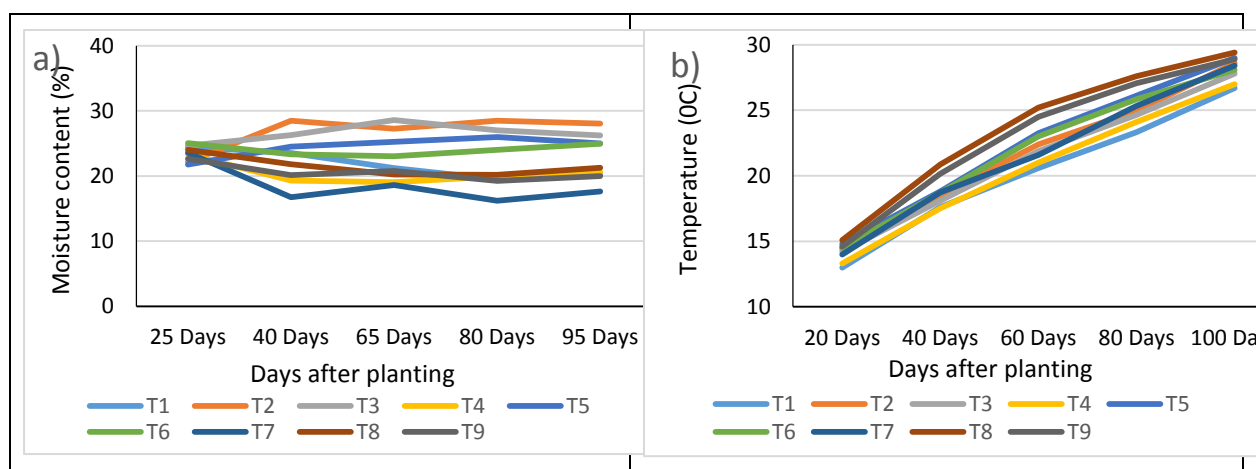


Fig. 3. Effect of different irrigation treatments with different mulching on soil moisture content and temperature.

Table (1 & 2) and fig: (1, 2 & 3) delineated that the performance of the drip irrigation at 100% ET₀ with black plastic mulch was the best treatment for chrysanthemum cultivation. Whereas, the performance of the drip irrigation system with no mulch at 80 % ET₀ and 60% ET₀ was not so good for chrysanthemum production. Drip irrigation at 100% ET₀ with black plastic mulch was the best treatment. Similar observations were found from Jawaharlal et al., (2017) that drip irrigation scheduling at 1.0 E pan with application of black plastic mulch was the best combination for getting higher chrysanthemum flower yield and net income. Treatments T₂, T₃, T₅, T₁ and T₆ did well for all the parameters which were statistically comparable with each other. On the other hand, treatments T₄, T₇, T₈ and T₉ exhibited low performance for all the parameters which were statistically par with each other for lowest values.

These clearly indicate that optimal or, marginal deficit application of irrigation with mulching system on regular basis enhanced the growth and quality promoting characters of chrysanthemum. These also clearly indicate that, both black plastic mulch and paddy straw mulch conserve moisture to the soil. Lack of water delayed bud initiation, bud burst, flower blooming and ultimately flower destroying time. As mulching system enhanced moisture conservation, it increases flower quality with water productivity (fig:3a). Similar observation was found by Maheria et al. (2013). Black plastic mulch hampered weed growth effectively. Pritee Awasthy et al., 2014 also found the same results that the black plastic mulch increased maize yield by controlling weed growth. But paddy straw mulch was more vulnerable for weed growth than no mulch treatments. Sufficient amount of moisture content and temperature ensure quality chrysanthemum at drip irrigation at 100% ET₀ with black plastic mulch. The treatment T₃ (drip irrigation at 100% ET₀ with paddy straw mulch) was also good. But flower quality and initiation to destroy time was little bit less, might be for the increased weed growth.

Economic analysis

Table 4 showed economic analysis of chrysanthemum production with different amount of irrigation and different types of mulching. The highest BCR (4.69) was found in treatment T₂, followed by treatment T₃, and the lowest BCR (1.54) was obtained from treatment T₇ followed by treatment T₈ and treatment T₉.

Table 3. economic analysis of chrysanthemum

Treatments	Marketable branch/ 10 m ²	Selling rate (Tk/branch)	Gross return (tk)	Total fixed cost/year	Total cost/year	Net return	BCR
T ₁	741	20	14822	2135	3777.778	11044	3.92
T ₂	926	20	18511	2135	3944.444	14567	4.69
T ₃	833	20	16667	2135	3934.568	12732	4.24
T ₄	481	20	9622	2135	3654.321	5968	2.63
T ₅	679	20	13578	2135	3820.988	9757	3.55
T ₆	652	20	13044	2135	3811.111	9233	3.42
T ₇	271	20	5422	2135	3530.864	1891	1.54
T ₈	396	20	7911	2135	3697.531	4214	2.14
T ₉	408	20	8156	2135	3687.654	4468	2.21

Conclusion

It was observed that drip irrigation at 100% ET₀ with black plastic mulch was superior over drip irrigation at 100% ET₀ with paddy straw mulch and drip irrigation at 100% ET₀ with no mulch. In terms of marketable production, the optimum irrigation treatment is drip irrigation at 100% ET₀ with black plastic mulch. Where there is a lack of water availability and it is intended to save water, drip

irrigation at 80% ET₀ with black plastic mulch or paddy straw mulch is better than no mulch system. However, this is only a single year data; therefore, no discreet conclusion can be drawn unless the research runs for few more years.

References

- Asiegbu, J.E., 1991. Response of tomato and eggplant to mulching and nitrogen fertilization under tropical conditions. *Scientia Horticulturae*, 46(1-2), pp.33-41.
- Awasthy, P., Bhambri, M.C., Pandey, N., Bajpai, R.K. and Dwivedi, S.K., 2014. Effect of water management and mulches on weed dynamics and yield of maize. *The Ecoscan*, 6, pp.473-478.
- Budiarto, K., Sulyo, Y., SN, E.D. and Maaswinkel, R.H.M., 2007. Effects of irrigation frequency and leaf detachment on chrysanthemum grown in two types of plastic house. *Indonesian Journal of Agricultural Science*, 8(1), pp.39-42.
- Conover, C.A., 1970. Responses of pot-grown *Chrysanthemum morifolium*'Yellow Delaware'to media, watering and fertilizer levels. *Proceedings of the Florida State Horticultural Society*, 1969, 82, pp.425-9.
- de Farias, M.F., Saad, J.C.C., Carnietto, M. and Laschi, D., 2009. Effect of soil-water tension on cut chrysanthemum floral quality and longevity. *Applied Research & Agrotechnology*, 2(1).
- Diaz-Perez, J.C., Granberry, D., Bertrand, D. and Giddings, D., 2002, August. Tomato plant growth during establishment as affected by root zone temperature under colored mulches. In XXVI International Horticultural Congress: Issues and Advances in Transplant Production and Stand Establishment Research 631 (pp. 119-124).
- Doorenbos, J. and Kassam, A.H., 1979. Yield response to water. *Irrigation and drainage paper*, 33, p.257.
- Fernandes, A.L.T., Folegatti, M.V. and Pereira, A.R., 2006. Avaliação de diferentes métodos de estimativa da evapotranspiração da cultura do crisântemo (*Chrysanthemum* spp.) cultivado em estufa plástica. *Irriga*, 11(2), pp.139-149.
- Jawaharlal, D., 2017. Water Use Efficiency of Chrysanthemum Crop for Different Mulches under Drip Irrigation System in Semi Arid Region. *International Journal of Agriculture Sciences*, ISSN, pp.0975-3710.
- Kiehl, P.A., Lieth, J.H. and Burger, D.W., 1992. Growth response of chrysanthemum to various container medium moisture tension levels. *Journal of the American Society for Horticultural Science*, 117(2), pp.224-229.
- Maheria, S.P., Lal, G., Mehta, R.S., Singh, R. and Singh, B., 2013. Mulching to improve water productivity in cumin. In Abstract book of "National seminar on advances in protected cultivation", New Delhi. pp (Vol. 160).
- Parnell, J.R., 1990. Ornamental plant growth responses to different application rates of reclaimed water. In *Proceedings of the... annual meeting of the Florida State Horticulture Society (USA)*.
- Rego, J.L., Viana, T.V.A., Azevedo, B.M., Bastos, F.G.C. and Gondim, R.S., 2004. Effects of irrigation levels on the chrysanthemum. *Agronomic Science Magazine*, 35(2), pp.302-310.
- Schuch, U.K., Redak, R.A. and Bethke, J.A., 1998. Cultivar, fertilizer, and irrigation affect vegetative growth and susceptibility of chrysanthemum to western flower thrips. *Journal of the American Society for Horticultural Science*, 123(4), pp.727-733.
- Tariq, M.S., Bano, A. and Qureshi, K.M., 2016. Response of strawberry (*Fragaria annanasa*) cv. Chandler to different mulching materials. *Science, Technology and Development*, 35(3), pp.117-122.
- Villalobos, R. and America, S., 2014. Reduction of irrigation water consumption in the Colombian Floriculture with the use of tensiometer.

Waterland, N.L., Finer, J.J. and Jones, M.L., 2010. Abscisic acid applications decrease stomatal conductance and delay wilting in drought-stressed chrysanthemums. *HortTechnology*, 20(5), pp.896-901.

Yohannes, F. and Tadesse, T., 1998. Effect of drip and furrow irrigation and plant spacing on yield of tomato at Dire Dawa, Ethiopia. *Agricultural Water Management*, 35(3), pp.201-207.

EFFECT OF IRRIGATION ON MANGO FRUIT CRACKING IN CHATTOGRAM REGION

M.P.HAQUE¹, M.K.R. BHUIYAN², M .A. HOSSAIN³, ANDS.K. BISWAS⁴

Abstract

The study was conducted at existing HRC Mango Orchard of Regional Agricultural Research Station, Hathazari, Chattogram during the Rabi season of 2019-20 and 2020-21 to explore the optimal period of irrigation to mitigate mango fruit cracking. Five treatments were applied: T₁ (rain-fed i.e. local practice), T₂ (irrigation at flowering stage), T₃ (irrigation at fruiting stage), T₄ (irrigation at flowering and fruiting stages T₅ (irrigation at 2-weeks interval,)). It is important to mention the age of the plant or canopy. The highest yield (76.5Kg plant⁻¹ and 74.6 Kg plant⁻¹ in successive years) was found at higher frequency irrigation (T₅). The maximum irrigation (average 1926 litres plant⁻¹) was applied at two-weeks interval irrigation (T₅). In rain-fed condition (T₁), yield was lowest (56.8Kg plant⁻¹ and 55.2Kg plant⁻¹ in first and second years). The lowest number of fruits dropping (21 and 19no.fruits) was occurred in irrigation at flowering and fruiting stages (T₄). The lowest number of cracking (15 and 13no.fruits) as well as the highest sweetness (average TSS=24%) occurred irrigation at fruiting stage (T₃) and the benefit-cost ratio was also higher in this treatment.

Introduction

Mango (*Mangifera indica*) is one of the most popular fruits in Bangladesh. Mango belongs to the familyAnacardiaceae is a tropical to sub-tropical fruit, originated in the Indian sub-continent (Indo-Burma region) in the prehistoric times. Bangladesh is the world's eighth largest mango producing country as it produces about 1,047,850 tons of mangos every year which accounts for 3.9 percent of the world total mango production.

Mango production increases day by day in Chattogram region e.g. 71459 M.ton.in 2015 and 81112 M.ton in 2016 (BBS, 2017). Irrigation is one of parameters besides nutrition management that increases the yields and improves the quality of mango (W. Spreer et al., 2007). In this region, farmers are still empirically applying water based upon experiences, without technical criteria. As a result, chances are that the mango crop cannot uptake enough water for its development and production due to soil water stress or excess. This kind of irrigation management may also lead to an increase in production costs due to excess amount of water applied that affects the sustainability of water resources. Therefore, irrigation management for the mango crop should follow technical criteria, so that water is applied at the right time and at the right amount.

Alam et al. (2017) found that the fruits dropping and cracking of mangoes causes four reasons-diseases, insects, nutrient deficiency, water scarcity in Bangladesh. Mango fruit cracking occurs in Chattogram region during dry season (Nov-March). The cracked fruits lose keeping quality and unsuitable for transportation and consumption. The scarcity of soil moisture and also excess of soil moisture cause fruit cracking (Saran et al., 2008). There is also water scarcity during this period in Chattogram region. So, Optimal stages of irrigation in mango production may save water and boost up quantity and quality (fruit cracking) of mango. The aim of this experiment is to find out the critical stage of irrigation to mitigate mango fruit cracking of mango.

¹SO, RARS, BARI, Hathazari, Khagrachari

²CSO and in-charge, RARS, BARI, Hathazari, Khagrachari

³PSO and Head, IWM, BARI, Gazipur

⁴SSO, IWM, BARI, Gazipur

Materials and Methods

A field experiment was conducted at existing HRC Mango Orchard (BARI Aam-4, Age 5-7 years), Hathazari, Chattogram during the rabi season of 2019-20 and 2020-21. The design of a randomized complete block was performed with three replications and five treatments.

The five irrigation treatments are:

- 1) Rain fed condition i.e. Local practice (T₁)
- 2) Irrigation at flowering stage (T₂)
- 3) Irrigation at fruiting stage (T₃),
- 4) Irrigation at flowering and fruiting stages (T₄)
- 5) Irrigation at 2-weeks intervals (T₅)

Fertilizer dose and methods of application were Manure (35 kg/plant), Urea (875 gm/plant), TSP (437 gm/plant), MOP (350 gm/plant), Zn (350 gm/plant), Zn-SO₄ (17 gm/plant), and Boric acid (35 gm /plant) (FRG, 2012).

Amount of water to be applied, during each irrigation event, was estimated by measuring soil moisture depletion from the field capacity. The water was applied by hose pipe with ring basin method.

Water content was calculated gravimetrically or volumetrically. Gravimetric soil water content is the mass of water divided by the mass of dry soil. It was measured by weighing a mass of wet soil, drying the soil for 24 hours at 105 °C in Oven, and then reweighing the sample (Waller & Yitayew, 2016).

$$\theta_{\text{grav}} (\text{gm/gm}) = \frac{\text{Mass of water (gm)}}{\text{Mass of dry soil (gm)}} = \frac{\text{Mass of wet soil (gm)} - \text{Mass of dry soil (gm)}}{\text{Mass of dry soil}} \quad (1)$$

$$\theta_v (\text{cm}^3/\text{cm}^3) = \theta_{\text{grav}} \times \text{soil bulk density (gm/cm}^3) \quad (2)$$

The depth of irrigation water requirement was estimated with the guideline of Michael (2007) as follows in equation (3).

$$d_{IR} = \frac{(FC - RL) \times A_s \times D}{100} \quad (3)$$

where, d_{IR} = depth of irrigation water requirement (mm), FC= field capacity (%) which measured by ponding water method on the soil surface (Michael, 2007), RL= residual moisture content (%) which measured before irrigation gravimetrically, A_s = apparent specific gravity of soil, D= depth of effective root zone to be irrigated (mm).

The time, required to be irrigation, was calculated following equation (4).

$$t = \frac{d_{IR} \times A}{Q \times 1000} \quad (4)$$

where t = time to be irrigated (min), d_{IR} = depth of irrigation water requirement, A = area of plot (m²), Q= discharge (m³/min).

The data were analyzed with “agricolae” R version 4.0.0 software package (Mendiburu, 2020).

Results and Discussion

The highest yield (76.5Kg plant⁻¹ and 74.6Kg plant⁻¹ in first and second years) was obtained at 2-weeks interval irrigation (T₅) and the lowest yield (56.8 Kg plant⁻¹ and 55.2Kg plant⁻¹ in first and second years) was in rainfed condition (T₁). The fruit weight per plant was also highest (526 gm/plant and 511.7 gm/plant) and lowest (355 gm/plant and 335 gm/plant) in irrigation at 2-weeks interval and rainfed condition respectively. The more frequent irrigation was more response to yield. One irrigation event occurred at both flowering stage and fruiting stage. The fruiting stage irrigation was responsive to yield which was more yield than flowering stage irrigation (Table 1 and Table 2).

Table 1. Irrigation effect on Mango production during 2019-20

Treatment	No of fruits per plant	Weight per fruit (gm)	Yield per plant (kg)	No of fruits drop	No of fruit cracks	TSS (%)
T ₁	160.0	355.0	56.8	38.3	32.7	23.0
T ₂	142.3	410.0	58.4	37.7	25.7	22.3
T ₃	147.0	458.3	67.4	24.7	15.0	24.0
T ₄	145.7	485.0	70.6	21.0	25.0	21.7
T ₅	145.3	526.7	76.5	31.0	39.0	19.3
CV (%)	3.8	2.8	4.3	10.8	11.6	4.3
LSD	10.7	23.8	5.4	6.2	6.0	1.8

*Note:*T₁=Rain fed , T₅= Irrigation at 2 weeks interval, T₂= Irrigation at flowering stage, T₃= Irrigation at fruiting stage, T₄= Irrigation at flowering and fruiting stages

Table 2. Irrigation effect on Mango production during 2020-21

Treatment	No of fruits per plant	Weight per fruit (gm)	Yield per plant (kg)	No of fruits drop	No of fruit cracks	TSS (%)
T ₁	165.0	335.0	55.2	33.3	30.3	23.1
T ₂	145.7	440.0	64.2	32.7	23.7	22.5
T ₃	148.0	456.7	67.6	19.7	13.0	24.0
T ₄	146.3	489.0	71.6	16.0	23.0	21.2
T ₅	145.7	511.7	74.6	26.0	37.0	22.0
CV (%)	4.3	4.8	6.9	12.8	12.7	5.7
LSD (5%)	12.2	40.6	8.7	6.2	6.0	2.4

*Note:*T₁=Rain fed , T₅= Irrigation at 2-weeks interval, T₂= Irrigation at flowering stage, T₃= Irrigation at fruiting stage, T₄= Irrigation at flowering and fruiting stages

The fruits' cracking at 2-weeks interval irrigation (T₅) was also the highest level (39 and 37 no. fruits in successive years) than any other treatments. The lowest number of fruits cracking (15 and 13 no. Fruits in successive years) was occurred at fruiting stage irrigation. The results revealed that the less irrigation and excessive irrigation than a certain level may cause more fruit cracking which was similar findings to Saran et al.(2008) .However, this study was found that irrigation at fruiting stage was more critical stage of irrigation.

The highest number of fruits' dropping (38 and 33 no. Fruits in two years) was obtained at rainfed condition (T₁) which was control treatment in comparison to other treatments. The lowest number of fruit dropping (21 and 16no. Fruits in successive years) was occurred in irrigation at flowering stage plus fruiting stage (T₄). So, irrigation at both flowing stage and fruiting stage were crucial for reduction of fruits dropping. Spreer et al.(2009) also had evidence that fruits dropping without irrigation were higher.

The percentage of TSS at rainfed condition (T₁) was less than irrigation at fruiting stage (T₃). The sweetness (TSS) was the lowest (average 20.5%) in 2-weeks interval irrigation (T₅) and

the highest sweetness (24%) was at fruiting stage irrigation (T₃). Therefore, the more frequent interval irrigation decreased the sweetness of mango. Léchaudel et al. (2005) also showed that the frequent irrigation water supply reduced the sugar or sweetness of mango. This study revealed that irrigation at fruiting stage (T₃) was the optimal stage of irrigation to maintain the level of higher sweetness.

Irrigation at 2-weeks interval was required more water (average 1926 liters/plant) than any other irrigation treatments (Table 3 and Table 4). The cost and benefit of this irrigation treatment (T₅) was higher although the benefit-cost ratio was lowest (average BCR=1.5). The benefit-cost ratio of irrigation at fruiting stage was highest (average BCR about to 3). Rahman et al. (2019) also found that the benefit-cost ratio of mango production at farmer's level in Bangladesh was 3.00.

However, with respect to economic return and fruits cracking, the irrigation at fruiting stage was the more beneficial and suitable stage of irrigation (T₃).

Table 3. Irrigation event, amount of irrigation, and Profitability analysis of mango production during 2019-2020

Treatment	Irrigation no.	Amount of irrigation (Liters/plant)	Effective rainfall (Liters/m ²)	Yield per plant (Kg)	Benefit (Tk/plant)	Cost(Tk/plant)	Benefit/Cost Ratio
T ₁	0	0	28.7	56.8	2272	780	2.91
T ₂	1	1000	28.7	58.4	2336	900	2.60
T ₃	1	1200	28.7	67.4	2696	900	3.00
T ₄	2	1300	28.7	70.6	2824	1300	2.17
T ₅	10	2000	28.7	76.5	3048	2000	1.52

Note: T₁=Rain fed, T₅= Irrigation at 2 weeks interval, T₂= Irrigation at flowering stage, T₃= Irrigation at fruiting stage, T₄= Irrigation at flowering and fruiting stages

Table 4. Irrigation event, amount of irrigation, and Profitability analysis of mango production during 2020-21

Treatment	Irrigation no.	Amount of irrigation (Liters/plant)	Effective rainfall (Liters/m ²)	Yield per plant (Kg)	Benefit (Tk/plant)	Cost(Tk/plant)	Benefit/Cost Ratio
T ₁	0	0	50.2	55.2	2210	800	2.8
T ₂	1	950	50.2	64.2	2568	950	2.7
T ₃	1	1130	50.2	67.6	2702	950	2.8
T ₄	2	1270	50.2	71.6	2862	1400	2.0
T ₅	10	1852	50.2	74.6	2982	2200	1.4

Note: T₁=Rain fed, T₅= Irrigation at 2 weeks interval, T₂= Irrigation at flowering stage, T₃= Irrigation at fruiting stage, T₄= Irrigation at flowering and fruiting stages. Assume labor per day Tk550 and selling price per Kg at farm gate Tk40.

Conclusion

Irrigation at fruiting stage of mango (T₃) was the more profitable, sweetness, and lower fruits cracking although its yield was lower than the highest frequency irrigation (T₅) at two weeks intervals. The more frequent irrigation events was occurred more fruit cracking. The irrigation at fruiting stage mitigated the lower number of fruit cracking.

References

Alam, M. J., Momin, M. A., Ahmed, A., Rahman, R., Alam, K., Islam, A. J., & Ali, M. M. (2017). Production performance of mango in Dinajpur district of Bangladesh (a case study at sadar

- upazilla). *European Journal of Agriculture and Forestry Research*, 5(4), 16–57.
- BBS. (2017). *Yearbook of Agricultural Statistics-2016 28th Series* (Issue May).
- FRG. (2012). *Fertilizer Recommendation Guide*. Bangladesh Agricultural Research Council (BARC).
- Léchaudel, M., Joas, J., Caro, Y., Génard, M., & Jannoyer, M. (2005). Leaf:fruit ratio and irrigation supply affect seasonal changes in minerals, organic acids and sugars of mango fruit. *Journal of the Science of Food and Agriculture*, 85(2), 251–260. <https://doi.org/10.1002/jsfa.1968>
- Mendiburu, F. de. (2020). *Agricolae: Statistical Procedures for Agricultural Research*. <https://cran.r-project.org/package=agricolae>
- Michael, A. M. (2007). *Irrigation Theory and Practice* (Second). Vikas Publishing House Pvt Ltd.
- Rahman, M. S., Khatun, M., & Miah, M. A. (2019). Profitability analysis of mango cultivation and its impact on farmer's livelihood in some areas of Bangladesh. *Bangladesh Journal of Agricultural Research*, 44(1), 139–152.
- Saran, P. L., Kumar, R., & Johari, R. K. (2008). Fruit cracking disorder: An emerging problem of fruit crops. *Indian Farmers' Digest*, 41(7), 30–32.
- Spreer, W., Nagle, M., Neidhart, S., Carle, R., Ongprasert, S., & Müller, J. (2007). Effect of regulated deficit irrigation and partial rootzone drying on the quality of mango fruits (*Mangifera indica* L., cv. 'Chok Anan'). *Agricultural Water Management*, 88(1–3), 173–180. <https://doi.org/10.1016/j.agwat.2006.10.012>
- Spreer, Wolfram, Ongprasert, S., Hegele, M., Wünsche, J. N., & Müller, J. (2009). Yield and fruit development in mango (*Mangifera indica* L. cv. Chok Anan) under different irrigation regimes. *Agricultural Water Management*, 96(4), 574–584. <https://doi.org/10.1016/j.agwat.2008.09.020>
- Waller, P., & Yitayew, M. (2016). *Irrigation and Drainage Engineering*. Springer International Publishing AG Switzerland.

PERFORMANCE OF FERTIGATION SYSTEM ON PUMPKIN CULTIVATION

M.A. HOSSAIN¹, K.F.I. MURAD², S.K. BISWAS³ and M. KAMRUZZAMAN⁴

Abstract

An experiment was conducted at the research field of Irrigation and water Management (IWM) Division, Bangladesh Agricultural Research Institute (BARI), Joydebpur, Gazipur during the rabi season of 2020-21 to determine the performance of pumpkin (var. BARI Hybrid Mistikumra-1) under fertigation systems. Six different irrigation treatments T₁= Ring Basin irrigation at 7 days interval with recommended fertilizer doses, T₂= Fertigation at an alternate day with recommended fertilizer doses, T₃= Fertigation at an alternate day with 20% less N and K than recommended doses, T₄= Fertigation at an alternate day with 35% less N and K than recommended doses, T₅= Fertigation at an alternate day with 50% less N and K than recommended doses were selected. The highest yield of 32.41 t/ha was obtained from treatment T₄ by applying 35% less N and K than recommended doses through drip system followed by treatment T₃ (30.71 t/ha) by applying 20% less N and K than recommended doses through drip system. Ring basin method required 413 mm of water during the season whereas only 241 mm water was needed in drip method. The economic analysis revealed that the highest benefit cost ratio (2.60) was obtained from treatment T₄ by applying 35% less N and K than recommended doses through drip system followed by treatment T₃ (2.48) by applying 20% less N and K than recommended doses through drip system. This is the first year results, so the experiment should be continued for the next year.

Introduction

Global fruit and vegetable production has increased to 1.34 billion MT in 2003, up from 396 million MT in 1961 (FAO, 2005). Vegetable production is usually lucrative compared to staple crops. Therefore, a relatively large body of the literature deals with poverty outcomes for small farmers from opportunities represented through horticultural trade (Dolan and Humphrey, 2000; Henson et al., 2005, Maertens, 2006). Bottle gourd (*Lagenaria siceraria* L.) belongs to Cucurbitaceae family. It is characterized by trailing growth habit, branched tendril, male flowers appear first, fruits are pepo varying greatly in shapes, sizes and colors. It thrives well in hot and humid conditions. Higher temperature, long day length, and sun light render more male flowers. It can grow over a wide range of soils but sandy loam soil with good natural drainage and pH near 6.5 is desirable.

Pumpkin (*Cucurbita moschata*) is an important vegetable crop grown in all over the world. Considering its high nutritional content (vitamin, carbohydrate, mineral, fibre, antioxidant, and phytonutrient) (Aruah et al. 2010) and lucrative market value, this vegetable may be considered as a high value crop (Rahman et al. 2013). Pumpkin is also known as a less water consuming crop. Therefore, its survival ability under water stress condition could be explored to find out opportunities of cultivation in areas where irrigation water is scarce. Currently, pumpkin is widely grown in char areas of Bangladesh, such as Lalmonirhat and Kurigram, where irrigation facility is scarce.

Pumpkin is a winter crop and it takes about five months for the fruits to get matured. Therefore, without proper irrigation management it is difficult to obtain reasonable yield of pumpkin.

Variety is an important characteristic that regulates yield and water requirement of crop. For high yielding variety, irrigation is very much essential during winter season to produce better yield in terms of quality and quantity (Bose et al. 1980). The frequency of irrigation in summer is very important but irrigation may not be necessary at all in summer for the crop if rainfall is well distributed between June and September. The role of irrigation at proper level and stages of plant growth has great significance in improving the yield (Singh et al., 1990). Padem and Alan (1992), Gupta (1990), Bandel et al. (1980), and Thomas et al. (1970) reported that judicious application of fertilizers in conjunction with proper irrigation is the principal factor affecting the crop yield. Modern

¹ CSO (in-charge), IWM Division, BARI, Gazipur

² SO, IWM Division, BARI, Gazipur

³ SSO, IWM Division, BARI, Gazipur

⁴ PSO, HRC, BARI, Gazipur

farming systems have taken advantages of different sophisticated techniques of irrigation that are based either on assessment of soil moisture depletion or moisture tension. Irrigation, once in 5 to 6 days, may be necessary depending upon soil, location, temperature etc, and it is very much essential during winter season to produce better yield in terms of quality and quantity (Bose et al. 1980).

Fertigation is a modern technique and is widely used in many developed countries for horticultural crops. But it is not yet to practice widely in Bangladesh. Furrow and flood irrigation are being widely practiced here for papaya cultivation. The concept of fertigation is to create a continuous method strip along the lines of the plants. It increases the irrigation water and fertilizer use efficiency to a considerable extent and is especially used for high value horticultural crops. This technology saves both water and fertilizer and gives higher yield than any other method (Bresler, 1997). Fertigation in tomato gave encouraging results in terms of yield and economic return (Akanda *et al.*, 2004).

Several studies have been reported on drip irrigation of fruit crop in different countries of the world (Birbal *et al.*, 1998; Birbal *et al.*, 2003; Suresh and Kumar, 2007; Tan *et al.*, 2009). But, Information regarding drip irrigation of bottle gourd in the context of our country is not available. So, it is important to determine the performance of sweet gourd under fertigation systems in the context of our country for higher yield of bottle gourd. That is why; the present study was undertaken in the field of Irrigation and Water Management Division of Bangladesh Agricultural Research Institute, Joydebpur, Gazipur.

Materials and Methods

The experiment was conducted on pumpkin (BARI Hybrid Mistikumra-1) in the field of Irrigation and Water Management Division of Bangladesh Agricultural Research Institute, Joydebpur, Gazipur. during rabi seasons of 2020-2021. Five treatments including a control were designed for the experiment. Each treatment was replicated thrice. The treatments were:

- T₁ = Ring Basin irrigation at 7 days interval with recommended fertilizer doses
- T₂ = Fertigation at an alternate day with recommended fertilizer doses
- T₃ = Fertigation at an alternate day with 20% less N and K than recommended doses
- T₄ = Fertigation at an alternate day with 35% less N and K than recommended doses
- T₅ = Fertigation at an alternate day with 50% less N and K than recommended doses

Each plot size was 4.0m × 4.0m. The soil was silty clay loam with an average bulk density of 1.5 gm/cc and field capacity of 28 percent (by weight basis). The experiment was laid out in a randomized complete block design. Seeds were shown on 14 November 2020 to produce seedlings and these were transplanted in experimental plots on 09 December 2020. Fruits were harvested from 08 April 2020 and continued upto 13 April 2020 depending on maturity. The N and K in the form of urea and MP, respectively, were applied with irrigation water as per design of the treatments. The total P in the form of TSP, Gypsum, Borax Zn and Magnesium were applied as the basal dose in the pit. Cow-dung was applied at the rate of 10 kg/pit. Depleted soil moisture was applied to the soil in ring basin irrigation method (control). Soil moisture was determined before each irrigation by gravimetric method for control treatment. Irrigation was applied upto the field capacity of the soil.

A common irrigation of 14mm was applied from seedling to proper plant establishment. After one month of transplanting, every treatment was mulched by using paddy straw @2.0 t/ha. Sex feromen traps were placed in the field to control fruit fly infestation. Pruning was done continuously up to 8 to 10 nodes on the main branch. To control disease infection and insect infestation Otistin @20g/20L of water, Admire @4ml/15L of water and secure @30g/30L of water were sprayed. Weeding was done according to necessary.

The soil moisture was monitored in each plot by using the gravimetric method at 30 cm intervals down to 60 cm. The amount of applied water was measured by time-volume technique. Soil moisture was collected before sowing, before irrigation and after harvest. Irrigation water was applied by ring basin method to bring the soil moisture up to field capacity considering the effective root zone

depth of 60cm. In case of drip irrigation, two drippers were installed per plant and dripper emission was assumed to be uniform. A 500L water tank was installed between two treatments and irrigated according to the design.

Seasonal water use (SWU) was calculated by adding applied water, effective rainfall (ER), and soil water contribution (SWC). Water productivity (WP) was calculated as the ratio of fruit yield and water use (SWU). Data on number of fresh and damaged fruit, number of fruit per plant, unit fruit weight, yield per plant and fruit yield was recorded. All the data were analyzed statistically by using R software and mean separation was done Duncan multiple range test at 5% level of significant. Financial analysis was also done with considering total operating cost, interest on operating cost, and land use cost.

In drip system, irrigation was applied at every alternate day meeting the demand of crop evapotranspiration. The average dripper discharge was 3.50 litres/hr. Experimental irrigation schedule was started just after plant establishment. In the early stage of crop, the irrigation time was 25 minutes in drip system and in fruiting stage, it was up to 60 minutes depending on crop ET. Data in respect of yield and yield contributing parameters viz. fruit weight, length, breadth, no. of fruits/plant and total yield were recorded.

Fertigation system

Four tank for four fertigation treatments ($T_2 - T_5$) were placed at a height of 1.0 m from the ground surface supported by bamboo structure on one side of the treatments. Each drum had a capacity of 215 litres of water. A water tap was attached to one side of the bottom part of each drum to which fertigation system was connected. The drippers were set according to the plant spacing in the treatments. Each plant received an emitter through which, water was applied to the plant in drips. A schematic diagram of the fertigation system is shown in Fig.1.

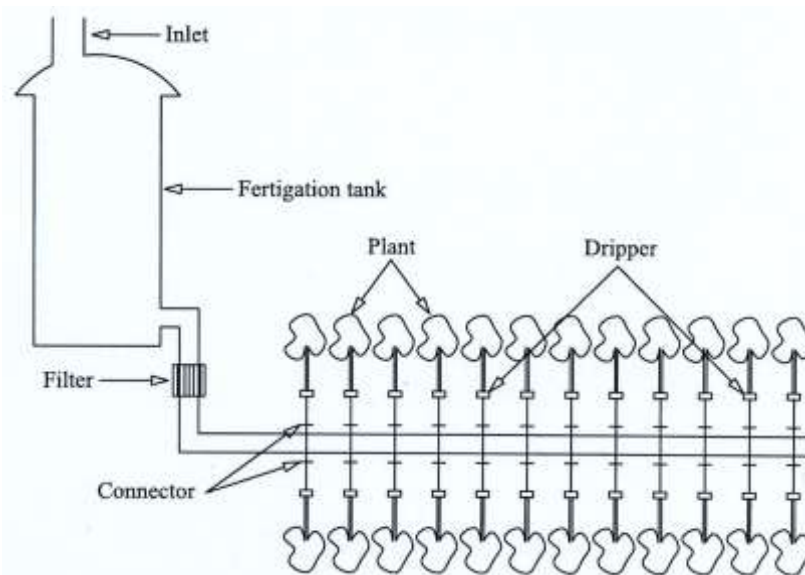


Fig.1 Schematic diagram of fertigation system.

Results and Discussion

Fertigation effect on yield and yield contributing characters of bottle gourd were analyzed statistically and are presented in Table 1. The yield and yield contributing characters like no. of fruit/plant, yield per plot varied significantly. Referring to Table-1, the highest yield of 32.41 t/ha was obtained from treatment T_4 by applying 35% less N and K than recommended doses through drip system followed by treatment T_5 (30.71 t/ha) by applying 20% less N and K than recommended doses through drip system. But yield difference was not statistically significant. The highest yield obtained from T_4 was significantly differ with the yield obtained from ring basin method i.e. farmers practice. The lowest

yield was found 24.09 t/ha by applying irrigation in ring basin method at 7 days interval with recommended fertilizer doses (farmer's practice). Irrigation water applied in different treatments was shown in Table 2. Referring to Table 2, it was seen that 413.64 mm water for ring basin method were needed during the season whereas only 166.33 mm water was needed in drip method. Water can be saved about 70% compared to ring basin method. There was no effective rainfall during the growing season 2020-21.

Table 1. Yield and yield contributing characters of pumpkin during 2020-21

Treatment	Fruit length (cm)	Fruit dia (cm)	Fruits/plant (no.)	Unit weight of fruit (kg)	Weight of fruits/plot (kg)	Yield (t/ha)
T ₁	10.46	18.27	5.33	2.36	38.54	24.09
T ₂	11.13	18.07	5.67	2.42	46.56	29.09
T ₃	10.40	18.20	6.00	2.45	49.14	30.71
T ₄	11.50	18.87	5.50	2.59	51.85	32.41
T ₅	11.30	18.87	5.27	2.48	45.83	28.63
CV (%)	6.37	4.21	13.28	10.88	11.67	11.65
LSD _{0.05}	1.31	1.46	1.38	0.50	10.19	6.36
Tukey's HSD	0.38	0.38	0.22	0.09	0.65	0.65
P-value	0.28	0.59	0.69	0.85	0.12	0.12

Table 2. Irrigation water applied in different treatments during 2020-21

Treatment	Number of Irrigation applied	Dripper discharge (l/h)	Water for plant establishment (mm)	Irrigation water applied (mm)	Soil moisture contribution (mm)	Total water use (mm)	Water productivity (kg/m ³)
T ₁	14	3.75	14	361	38.64	413.64	5.82
T ₂	25	3.75	14	192	35.33	241.33	17.49
T ₃	25	3.75	14	192	35.33	241.33	18.46
T ₄	25	3.75	14	192	35.33	241.33	19.48
T ₅	25	3.75	14	192	35.33	241.33	17.21

Economic analysis for fertigation over traditional system for pumpkin cultivation was done and is presented in Table 3. The economic analysis reveals that the benefit cost ratio is the highest of 2.60 was obtained from treatment T₄ by applying 35% less N and K than recommended doses through drip system followed by treatment T₃ (2.48) by applying 20% less N and K than recommended doses through drip system. The lowest BCR was found 1.88 by applying irrigation in ring basin method at 7 days interval with recommended fertilizer doses (farmer's practice). The higher return is also found (Tk. 29972.00) in fertigation (T₄) system by cultivating pumpkin from only 0.1 ha of land.

Table 3. Economic analysis for fertigation over traditional system for bottle gourd cultivation (for 1000 m² of land)

(a). Fixed cost

Item	Quantity	Rate	Cost (Tk.)		
			T ₁	Fertigation (T ₄)	Fertigation (T ₃)
Fertigation tank	4 nos	1000.00	-	4000.00	4000.00
GI fittings and supporting platform	-	LS	-	1000.00	1000.00
1.25 cm dia PVC pipe	300 m	4.00	-	1200.00	1200.00
0.32 m dia micro-tube	750 m	2.50	-	1875.00	1875.00
Total fixed cost, Tk.				8075.00	8075.00

Expected life of the system = 4 years

Fixed cost/year = 2018.00

(b). Variable cost

Item	Cost (Tk.)		
	Ring basin (T ₁)	Fertigation (T ₄)	Fertigation (T ₃)
Seedlings	160.00	160.00	160.00
Pit making	250.00	250.00	250.00
Fertilizer	1915.00	1600.00	1525.00
Trail	12500.00	12500.00	12500.00
Irrigation cost	2000.00	500.00	500.00
Labour	2400.00	1600.00	1600.00
Total variable cost, Tk.	19225.00	16610.00	16535.00

(c). Return

Item	Return, Tk.		
	Ring basin (T ₁)	Fertigation (T ₄)	Fertigation (T ₃)
Yield/1000m ² (metric ton)	2.41	3.24	3.07
Selling rate (Tk./ton)	15000.00	15000.00	15000.00
Gross return (Tk.)	36150.00	48600.00	46050.00
Total fixed cost/year (Tk.)	-	2018.00	2018.00
Total cost/year (Tk.)	19225.00	18628.00	18553
Net return (Tk./ha)	16925.00	29972.00	27497.00
Benefit cost ratio (BCR)	1.88	2.60	2.48

Conclusion

The highest yield of pumpkin 32.41 t/ha was obtained from treatment T₄ by applying 35% less N and K than recommended doses through drip system followed by treatment T₃ (30.71 t/ha) by applying 20% less N and K than recommended doses through drip system. This is the first year result. No definite conclusion could be made. So, the experiment should be continued for the next year.

References

- Akanda, M. A. R., M. Abdullah, M. A. Bhuiyan, M. A. Hossain and M. A. Rashid. 2004. Comparative performance of fertigation and traditional system of tomato cultivation. *Bangladesh J. Agril. Res.* 29 (3): 387-392, September.
- Aruah, C. B., M. I. Uguru and B.C. Oyiga . 2010. Nutritional evaluation of some Nigerian pumpkins (*Cucurbita* spp.) Fruit, vegetable and Cereal Science and Biotechnology 5 (Special Issue 2): 64-71.
- Bandel V. A., Dziemia S., Standford G. (1980). Comparison of nitrogen fertilizer for no-till corn. *J Agron* 72:334–337.
- Birbal, Malik Y. S. and Khurana S. C. (1998). Effect of irrigation methods, staking and plants per hill on bottle gourd. *Vegetable Science.* 25 (2): 109-112.
- Birbal, Malik Y. S., Khurana S. C. and Nehra B. K. (2003). Effect of irrigation level and maleic hydrazide on the growth of bottle gourd. *Haryana Journal of Horticultural Sciences.* 32 (1/2): 125-127.
- Bose T. K., Som M.G., Kabir J. (1980). Vegetable crops Naya PROKASH 206 Bidhan Sarani, Calcutta 70006 India PP.-85.
- Bresler E.1997. Drip Irrigation: Principles and applications to soil under management. *Adv. Agron.* 29:343-393.
- Dolan C. S., Humphrey J. (2000). Governance and trade in fresh vegetables: the impact of UK supermarkets on the African horticulture industry. *J Dev Stud* 37(2000):147–176.
- FAO (2005). FAOSTAT data. Accessed November 2004, <http://www.fao.org>.
- Gupta A (1990). Response of spring planted okra to varying levels of irrigation and plant spacing. *J Veg Sci*17:16–19.
- Henson S., Masakure O., Boselie D. (2005). Private food safety and quality standards for fresh produce exporters: The case of Hortico Agrisystems, Zimbabwe. *Food Policy* 30(2005):371–384.
- Maertens M. (2006). High value supply chains, food standards and poor farmers in developing countries: The case of vegetable exports from Senegal. In selected paper prepared for presentation at the American Agricultural Economics Association Annual Meeting, Long Beach, California (July 23–26).
- Padem H., Alan R. (1992). The effect of N rates and irrigation levels on growth, yield and nutrient content of cabbage. *J Veg Sci* 19:121–125.
- Rahman, M.A., Miaruddin, M., Khan, M.H.H., Masud, M.A.T. and Begum, M.M., 2013. Effect of storage periods on postharvest quality of pumpkin. *Bangladesh Journal of Agricultural Research*, 38(2):247-255.
- Singh J., Pandey U. C., Kohli V. P. (1990). Response of vegetable pea to irrigation. *Journal Veg. Sci.* 17:11–15
- Suresh R., Kumar A. (2007). Effect of drip irrigation on bottle gourd in calcareous soil of North Bihar. *Environment and Ecology.* 25S (Special 2): 314-317.
- Tan Y. C., Lai J.S., Adhikari K. R., Shakya S. M., Shukla A. K., Sharma K. R. (2009). Efficacy of mulching, irrigation and nitrogen applications on bottle gourd and okra for yield improvement and crop diversification. *Irrig Drainage Syst* (2009) 23:25–41.
- Thomas JR, Mamken LN, Brown RG (1970) Yield of cabbage in relation to nitrogen and water supply. *Journal of American Society of Horticultural Science* 95:732–735.

YIELD AND WATER PRODUCTIVITY INDICES OF DIFFERENT ONION VARIETIES UNDER SPRINKLER IRRIGATION

S.K. BISWAS¹, M.A. HOSSAIN², D.K. ROY¹

Abstract

To evaluate the performance of four onion varieties under sprinkler irrigation and their sensitivity to water stress, a study was conducted at the experimental field of IWM Division, BARI during the winter season of 2020-2021. The experiment comprised of five irrigation treatments with sprinkler system based on 60%, 80%, 100%, 120% and 140% of crop water use (ET_o) laid out in split-plot design with three replications. Irrigation water was applied at a fixed 6-day interval with sprinkler system throughout the crops growing season. Onion sensitivity to water stress was determined using a yield response factor (K_y) that derived from the linear relationship between relative evapotranspiration deficits (1-ET_a/ET_m) and relative yield decrease (1-Y_a/Y_m). Statistical analysis revealed that plant height was not much affected by the level of irrigation while, leaf number, bulb diameter, bulb unit weight and total bulb yield was affected significantly (P<0.05) by the irrigation regimes. Among the four onion varieties, the highest plant height, bulb diameter and unit bulb weight contributed to the highest yield of 31.02 t/ha for BARI Pijaj-4 (V₄) while the lowest yield of 19.03 t/ha was obtained from BARI Pijaj-1 (V₁). Hybrid variety (V₂) produced the second highest yield of 25.93 t/ha which was comparable to the yield (24.72 t/ha) obtained from Taherpuri King (V₃). For varieties, V₁ and V₃, highest yields were obtained under 120% ET_o water regime while the same were obtained under 140% ET_o water regime for V₂ and V₄. Value of K_y determined for the whole growing season was found higher for V₄ (K_y: 1.08), V₂ (1.044) and V₃ (K_y: 1.05) than BARI Pijaj-1 (K_y: 0.93) indicates that the varieties V₄, V₃ and V₂ are more sensitive to water stress. This fact is also evident by the water productivity (WP) with higher value obtained under higher water regimes (120% ET_o) in case of V₄, V₃, and V₂ but for V₁, higher WP was obtained from 100% ET_o water regime. The amounts of water used for evapotranspiration under different irrigation regimes ranged from 149 to 269 mm, 150 to 272 mm, 150 to 270 mm and 150 to 272 mm, respectively, for V₁, V₂, V₃ and V₄ with minimum at 60% ET_o and maximum at 140% ET_o water regime. Though seasonal evapotranspiration was higher under wetter water regimes, yield was lower and consequently WP was the lowest. Considering K_y as a limiting factor, application of irrigation at 100% ET_o was a marginal for V₁ and V₂ and 100-120% ET_o for V₃ and V₄, beyond that yield losses are unacceptable.

Introduction

Onion is considered as one of the most important spice and vegetable crop grown in Bangladesh. It is grown extensively during winter season in Bangladesh, occupying the second position both in area and production (BBS, 2013) next to chilli. Though it is grown more or less in all the districts of the country, the dominant areas are the greater districts of Faridpur, Rajshahi, Jessore, Pabna and Kushtia. Land area under onion cultivation in Bangladesh was 0.33 million ha during 2000-2001 and within a span of 12 years, it has increased four-fold to 1.32 million ha (BBS, 2013). However, the bulb yield of onion (8.6 t ha⁻¹) in Bangladesh is less than many other onion producing countries. It is about half of the world average (17 t ha⁻¹) and four fold lower than those achieved in the European Union (30-35 t ha⁻¹) (FAOSTAT 2010). On an average, the total annual requirement of onion in Bangladesh stands at 2200 thousand metric tons whereas the total production is about 1168 thousand metric tons and thereby, there is a shortage of 1030 thousand metric tons per annum. To meet this shortage, Bangladesh has to import onion every year at the cost of its hard earned foreign currency. The reasons for the lower productivity of onion in Bangladesh are many including inadequate management practices, short day length during the growing season, low organic carbon content of the soil, shorter (3-4 months) growing period, as well as poor water management. However, to increase the productivity, the grower must have prior knowledge of the crop yield responses to deficit irrigation. Many investigations have been carried out worldwide regarding the effects of deficit irrigation on yield of mainly horticultural crops (Olalla et al. 2004; Bazza and Tayaa, 1999; Faberio et al. 2003 and Sezen et al. 2008). Other experiments with onion (Bekle et al., 2007) showed that deficit irrigation

¹ SSO, IWM Division,, BARI, Gazipur

² CSO (in-charge),, IWM, BARI, Gazipur

throughout the growing season of onion as 50 and 75% of ET_c reduced yields from full irrigation and resulted in the highest water saving and crop water use efficiency. Kumar et al. (2007) also investigated the impact of deficit irrigation strategies on onion yield and water savings. They reported that applying 80 and 60% of crop water requirements resulted in yield decreases of 14 and 38% and saved 18 and 33% of irrigation water compared to full irrigation, respectively.

The evaluation of stress associated with the yield due to soil water deficit during the crop growing season can be obtained by the estimation of the yield response factor (K_y) that represents the relationship between a relative yield decrease ($1 - Y_a/Y_m$) and a relative evaporation deficit ($1 - ET_a/ET_m$). Determination of K_y values after adaptive research has been carried out in numerous studies for various crops and under different environments. Results showed a wide range of variations in K_y values and suggest that the within-crop variation in K_y may be as large as that between crops (Stanhill et al., 1985). Moreover, factors other than water such as nutrients, different cultivars, ET_o , also affect the response to water. Vaux and Pruitt (1983) suggest that it is highly important to know not only the K_y values from the literature but also those determined for a particular crop species under specific climatic and soil conditions. In fact, adjustments for site-specific conditions would be needed if greater accuracy is sought. This is because K_y may be affected by other factors besides soil water deficiency, viz. soil properties, climate, growing season length and growing technology. Water deficit effect on crops yield can be presented in two ways, for individual growth periods or for the total growing season. Kobossi and Kaveh (2010) suggested K_y values for the total growing period instead for individual growth stages as the decrease in yield due to water stress during specific periods, such as vegetative and ripening periods, is relatively small compared with the yield formation period, which is relatively large.

Both variety and water management practices play a major role in increasing the productivity of crops. The crops having higher yield potential and higher yield response to water have a wide range of water productivity. Onion crop needs adequate management practices especially proper irrigation management to contribute potential yield. The principle and pervasive reasons of low productivity of onion in our country is due to lack of high yielding varieties and proper irrigation management practices. Improved variety contributes substantially to enhance crop yield (Shaikh *et al.*, 2002). Recently, some private seed companies have released few high yielding winter onion varieties and those are cultivating by farmers with same irrigation practices they follow for BARI onion-1. As water management may vary with the crop varieties and their yield response to water, so farmers are not getting good harvest as expected. However, to increase the productivity, the grower must have prior knowledge of the crop yield responses to deficit irrigation. Hence, it is warranted to test the water requirement of the commercial varieties and its yield potential compared to BARI Paj -1. Therefore, the objective of this study was to find out the proper irrigation scheduling of commercial onion varieties and their yield response to water compared to local variety.

Materials and Methods

The field experiment was conducted during the winter season of 2020- 2021, between the months of December and March, at the research field of Irrigation and Water Management Division, Bangladesh Agricultural Research Institute (BARI) (Latitude 24.00° N, Longitude 90.25° E and altitude 8.40 m msl), Gazipur. The average temperature, relative humidity, wind speed and pan evaporation rate during the crop growing season ranged from 14.5 to 26.4 $^\circ$ C, 56–89%, 0.76 – 10.87 km h^{-1} and 1.6 – 3.5 mm d^{-1} , respectively. Total rainfall occurred during crop growing season was recorded as only 2 mm and the total was considered effective. The percentage of sand, silt and clay in the experimental soil were 36.5, 35.4 and 28.1, respectively. Field capacity, wilting point and bulk density of top 30 cm of the soil were 28.5%, 13.72% and 1.46 g cm^{-3} . The concentrations (kg ha^{-1}) of N, P_2O_5 and K_2O were 51.1, 12.5 and 265.6, respectively. The soil had an organic matter content of 1.04%.

The experiment was set up in a split-plot design with three onion varieties and five different irrigation treatments that were replicated thrice. Sprinkler irrigation with five different water levels were applied compensating crop coefficient (K_c) and potential evapotranspiration (ET_o) based predicted evapotranspiration loss (ET_o). Each of the onion varieties experienced five levels of sprinkler irrigation as follows:

Onion varieties

V₁= BARI Piaj-1

V₂= Hybrid (Lal Teer))

V₃= Taherpuri King (Lal Teer)

V₄= BARI Piaj-4

Irrigation levels

I₁= Sprinkler irrigation at 60% ETo

I₂= Sprinkler irrigation at 80% ETo

I₃= Sprinkler irrigation at 100% ETo

I₄= Sprinkler irrigation at 120% ETo

I₅= Sprinkler irrigation at 140% ETo

Onion varieties were kept in the main plots and irrigation levels in the sub-plots. The treatments with the same irrigation regime were arranged in a line covering all four varieties for better management of irrigation. Since, the characteristics of the experimental land were homogeneous, there was little possibility of variation in results for such arrangements of the treatments. Each plot was of 4 m × 3.75 m size surrounded by 1.5 m wide buffer strip to restrict lateral seepage of water in-between adjoining plots. Forty days old seedlings of onions (cv. BARI Piaj- 1, Taherpuri Super, Taherpuri King and BARI Piaj-4)) were planted at 15 cm × 10 cm spacing on 30 December 2018. During land preparation, farm yard manure @ 5 t/ha was properly mixed with the soil. Fertilizers were applied @ 115 kg N, 60 kg P and 60 kg K per hectare. Half of the nitrogen and potassium and the full dose of phosphorus were applied at planting and the rest half of the nitrogen and potassium was applied in two equal splits at 25 and 50 days after planting.

Just after transplanting, a common irrigation was applied to all plots for establishing the plants. Thereafter, irrigation treatments started at 12 DAT and subsequent applications were applied according to the treatments design. Irrigation was applied through sprinkler system based on reference evapotranspiration (ETo). Reference evapotranspiration (ETo) was calculated on a daily basis from daily meteorological data by Penman–Monteith’s equation using CROPWAT computer programme. Daily meteorological data required for CROPWAT model including maximum and minimum air temperature, relative humidity, wind speed at 2 m height and sun shine hour were collected from a weather station about 1.0 km away from the study site. The daily irrigation requirement for the crop was calculated by subtracting the effective rainfall from the computed ETo. Time of operation of sprinkler system was calculated for different levels of irrigation dividing water requirement of the crop over irrigation intervals (6 d) by discharge of a sprinkler nozzle. The duration of operation was controlled with gate valves provided at the inlet of each lateral. Soil water content measurements were made from 0-15, 15-30 and 30-45 cm depths before and after each irrigation as well as at transplanting and at harvest and after each rainfall event by gravimetric method. Seasonal crop water use (SET) was estimated using the water balance method (Walker and Skogerboe, 1987) as:

$$SET= I + P - D - R \pm \Delta SWS \dots\dots\dots(1)$$

Where P is precipitation (mm), I is irrigation (mm), D is the drainage (mm), R the run-off and ΔSWS is the variation in water content of the soil profile. The change in soil water contents at 30–45 cm soil layer was considered to be deep percolation. Run-off was taken to be zero since it did not occur with the use of micro-sprinkler irrigation system.

The recommended plant protection measures were adopted as and when required. Irrigation was stopped 15 days before harvesting in all treatments. Ten plants from each plot were selected randomly and tagged for recording growth parameters viz., plant height, number of leaves and neck girth at 70 DAT. Leaf area and above ground dry matter were also recorded on 10 plants at different phenological stages. Yield parameters viz., bulb diameter, bulb length, bulb unit weight were recorded

from the plants used for recording observations. The bulbs were harvested at full maturity stage on 27 March 2019. Yield of onions were measured after naturally drying the bulbs for seven days. The bulb yield per hectare was calculated based on the plot yield.

The yield response factor (Ky) of onion was estimated using the following relationship given by Doorenbos and Kassam (1979).

$$\left(1 - \frac{Y_a}{Y_m}\right) = K_y \left(1 - \frac{ET_a}{ET_m}\right) \dots\dots\dots(2)$$

Where,

Y_a = the actual harvested yield (kg ha⁻¹),

Y_m = the maximum harvested yield (kg ha⁻¹),

K_y = the yield response factor,

ET_a = the actual evapotranspiration (mm) corresponding to Y_a,

ET_m = the maximum evapotranspiration (mm) corresponding to Y_m,

(1-ET_a/ET_m) = the relative evapotranspiration deficit, and

(1-Y_a/Y_m) = the relative yield decrease

The data collected during the experimental period were subjected to statistical analysis using MSTAT computer program to interpret the results. Whenever treatment effects were significant, least Significance Differences (LSD) test was done using analysis of variance technique as described by Gomez and Gomez (1984).

Results and Discussion

Plant height

The height of onion plant was not much affected by the variety, but significantly by the irrigation regimes (Table 1). In general, application of water with higher regime produced taller plant, but it was insignificant compared to lower water regime. The plant height, on average, ranged from 51.60 to 63.94 cm with the shortest and tallest plant height was observed from treatment receiving 60% and 120% or 140% ETo, respectively. However, variety V₃ and V₄ produced the taller plant than the varieties V₁ and V₂, with V₁ had the shortest height and V₄ the tallest. Variation in plant height with the changing in irrigation regimes was found greater in the variety V₃ and V₄ than other two varieties. It ranged from 53.87 to 66.40 cm for V₄, 53.13 to 66.10 cm for V₃, 52.07 to 64.73 cm for V₂ and from 47.33 to 59.07 for V₁ with the lowest value for 60% and the highest value for 140% ETo, except for V₁, where highest plant height obtained from 120% ETo water regime. The increasing of plant height with adequate soil moisture application is related to water in maintaining the turgid pressure of the plant cells which is the main reason for the growth (Fabeiro et al., 2002). On the contrary the shortening of plant height under soil moisture stress may be associated with the closure of stomata to reduce crop evapotranspiration, which leads to reduce uptake of CO₂ and nutrient. Therefore, photosynthesis and other biochemical reactions are hindered that eventually affecting plant growth. This finding is in line with the result that has been obtained by Fabeiro et al., 2003, indicated that soil water supply is directly proportional with plant height growth.

Leaf number

The number of leaves per plant ranged from 6.79 to 7.98 with minimum in 60% ETo and maximum in 140% ETo water regime across the varieties. Among the varieties, V₂ had the highest leaf number closely followed by V₄ and V₃ while V₁ had the lowest number of leaves per plant. With the increasing in irrigation regime from 60% to 140% ETo, the leaf number increased from 6.70 to 7.58 for V₁, 6.92 to 8.13 for V₂, 6.87 to 8.17 for V₃ and from 6.67 to 8.04 for V₄, respectively (Table 1). In case of V₁, V₃ and V₄, leaf number showed no significant differences due to variation in water regimes. But variation in water regimes made significant differences (p<0.05) in leaf numbers for V₂

varieties. Treatment receiving 60% ETo had significantly lower number of leaves than treatment receiving 140% ETo. Over the varieties, number of leaves gradually increased with the increased in water regime from 60%ETo to 140%ETo.

Bulb length and diameter

The application of deficit irrigation affected the size of onion bulb. The highest bulb length and diameter was recorded from the wettest treatment 120-140% ETo non-significantly followed by 100% ETo. The least bulb length and diameter was recorded from treatment receiving 60% ETo and this was significantly different to treatment receiving higher irrigation regimes. In general, bulb diameter was greater than bulb length for all varieties studied, except variety V₄. Bulb length and diameter of the variety V₁ and V₂ were identical and significantly lower than variety V₃ and V₄. Like the bulb size, unit bulb weight was found higher for wetter treatments than for drier treatments. Variety V₄ produced the bigger size bulbs with higher unit weight (56.10 g) than other three varieties. The second highest unit weight was recorded as 50.15 g for variety V₃ while the lowest was recorded as 40.63 g for V₁. Like the bulb size, unit weight of V₂ (40.90 g) was comparable to V₁. In general, unit bulb weight gradually increased with the increasing of irrigation regimes. This result is in agreement with that of a study conducted by Sezen et al. (2008), high amount of soil moisture application leads to large photosynthesis area (plant height and large number of leaves), results to large bulb size and weight as well.

Onion bulb and biomass yield

Like yield contributing characters, variation in the amount of the applied water caused a significant ($P \leq 0.05$) variation in bulb and biomass yield of onion (Table 1). Irrespective of variety, bulb yield was found the highest when irrigation was applied on the basis of 120% ETo, while the least amount of applied water (60% ETo) resulted in the lowest bulb yield. Application of increasing amount of water per irrigation from 0.6 ETo to 1.2 ETo resulted in significant increase in bulb yield. The increase in yield per unit of applied water decreased with the increasing amount of applied water. The rate of increment was 24.32% from 0.6ETo to 0.8ETo, 14.23% from 0.8 ETo to 1.0 ETo, and only 11.87% from 1.0ETo to 1.2ETo. Bulb yield increased significantly at each irrigation level from 60% ETo to 100% ETo; however, from 100% to 120% ETo the increase in BY was insignificant, which is consistent with the findings reported by Kang et al. (2002) and further increase in water regime from 120% to 140% failed to increase BY of onion rather yield was decreased. Thus water can be saved without significant reduction in yield by irrigating the crop at the level of 1.0 ETo and 1.2 ETo. In case of 0.8 ETo water regime, plant felt strees between two consecutive irrigations and that was the probable reason for lower BY as compared to 80% ETo and higher water regimes. Onions have been shown to be productive under frequent irrigations that allow little soil water depletion (Shock et al., 1998).

In case of variety, the highest bulb yield was obtained from variety V₄ followed by V₃ while variety V₁ gave the lowest yield that was identical with V₂. Bulb yield of onion ranged from 14.49 to 24.53 t/ha for V₄, from 13.15 to 22.04 t/ha for V₃, 12.03 to 17.73 t/ha for V₂ and from 11.34 to 16.57 t/ha for V₁ with minimum in treatment 60% ETo and maximum value in treatment 120% ETo. In the present study, the increased yield in sprinkler irrigation system was mostly due to the favorable effect of available soil moisture, uniform distribution of irrigation water during entire growth period. Another possible reason is continuous availability of moisture enhanced the availability and uptake of nutrients throughout the cropping period which resulted in better growth and bulb development. However, the yield of onion at 100% and 120% ETo was found to be non-significant which was probably due to the fact that irrigation at 100% ETo was adequate to provide sufficient soil moisture for optimum onion production. Effect of irrigation regimes on above-ground biomass yield followed almost similar trend like that of bulb yield (Table 1). Unlike bulb yield, the highest biomass yield was recorded under wettest treatment of 120% and 140% ETo and the least amount of applied water (0.6ETo) resulted in the lowest above ground biomass yield.

Table 1. Yield and yield contributing parameters of onions under sprinkler irrigation with different water regimes

Treatment	Plant ht, cm	Leaves/plant (no)	Stem dia(mm)	Bulb length(mm)	Bulb dia(mm)	Unit bulb wt,g	Yield, t/ha	DM(kg/ha)
Irrigation levels								
I ₁	51.60	6.79	11.00	52.69	48.13	50.80	14.74	792.83
I ₂	55.67	6.94	12.38	57.26	51.51	60.67	18.19	847.17
I ₃	58.98	7.07	13.08	58.72	52.56	66.57	22.20	1018.75
I ₄	62.35	7.70	14.13	59.14	54.03	70.82	24.87	1112.21
I ₅	63.94	7.98	14.61	60.93	54.81	72.61	24.77	1251.21
LSD _{0.05}	3.35	1.18	1.12	3.18	4.12	3.68	2.85	44.13
CV (%)	6.16	5.26	5.74	4.66	4.55	7.64	6.38	9.27
Onion variety								
V ₁	54.21	7.09	12.74	49.16	50.49	47.92	16.02	958.63
V ₂	58.89	7.48	12.79	58.26	53.08	67.74	21.82	920.73
V ₃	60.35	7.35	13.36	57.75	51.48	62.97	20.74	1069.53
V ₄	60.57	7.26	13.28	65.81	53.78	78.55	25.23	1068.83
LSD _{0.05}	3.78	1.46	1.04	4.72	4.09	3.55	1.86	33.68
CV (%)	5.21	4.68	5.14	6.26	5.82	7.22	5.47	8.38
Irrigation x Variety								
V ₁ I ₁	47.33	6.70	10.80	43.60	45.80	35.59	11.74	720.00
V ₁ I ₂	52.20	6.87	12.33	48.73	50.93	46.31	14.26	854.67
V ₁ I ₃	53.93	6.94	12.40	49.63	51.97	50.97	17.18	1022.00
V ₁ I ₄	59.07	7.38	14.27	51.80	51.37	54.88	19.03	1001.33
V ₁ I ₅	58.53	7.58	13.90	52.03	52.37	51.87	17.92	1195.17
V ₂ I ₁	52.07	6.92	11.20	53.87	47.33	50.74	15.45	699.50
V ₂ I ₂	55.07	7.17	11.67	60.70	55.73	68.11	18.84	859.17
V ₂ I ₃	60.40	7.33	13.20	58.30	53.40	70.70	22.92	980.00
V ₂ I ₄	62.20	7.87	13.53	56.97	52.43	72.05	25.93	909.17
V ₂ I ₅	64.73	8.13	14.33	61.47	56.50	77.10	25.97	1155.83
V ₃ I ₁	53.13	6.87	10.87	52.30	46.47	51.72	14.73	779.50
V ₃ I ₂	58.60	6.93	13.53	57.03	48.23	59.09	18.15	824.00
V ₃ I ₃	60.40	7.13	13.13	59.73	53.10	66.16	21.94	1139.67
V ₃ I ₄	63.53	7.63	13.60	58.20	54.77	70.78	24.72	1229.17
V ₃ I ₅	66.10	8.17	15.67	61.50	54.83	67.09	24.17	1375.33
V ₄ I ₁	53.87	6.67	11.13	61.00	52.90	65.16	17.03	972.33
V ₄ I ₂	56.80	6.80	12.00	62.57	51.13	69.20	21.53	850.83
V ₄ I ₃	61.20	6.87	13.60	67.20	51.77	78.44	26.76	933.33
V ₄ I ₄	64.60	7.93	15.13	69.60	57.57	85.58	29.81	1309.17
V ₄ I ₅	66.40	8.04	14.53	68.70	55.53	94.37	31.02	1278.50
LSD _{0.05}	4.16	1.21	1.16	4.64	4.44	7.64	2.06	65.34
CV (%)	5.21	4.68	5.14	6.26	5.82	7.22	5.47	8.38

Leaf area

Leaf area (LA) was positively affected by increasing level of water regimes. Irrespective of variety, application of water with higher water regimes (120% and 140% ETo) significantly increased the leaf area of onion compared with lower water regime (60% ETo). Application of water at 60% ETo produced the lowest leaf area while water application at 120% or 140% ETo regime produced the highest LA (Figure 1) at different days after transplanting (DAP). Starting from 35 DAP, increment of LA was almost linear up to 60 DAP, thereafter LA started to decrease. After the maximum leaf area was reached at 60 DAP, the following stage lasted around 15 days, thereafter it started to decrease. Increasing rate was faster in early stage than mid stage and at the later stage it decreased as the leaves started to die. Across the variety, about 170% increment in LA was recorded from 35 to 45 DAP and from 45 to 60 DAP, it was only about 29%. Rate of increment in LA was somewhat different in magnitude among the varieties. On average over water regimes, it ranged between 33% and 138% for the variety V₁, between 15% and 184% for the variety V₂, between 31% and 193% for the variety V₃ and between 36% and 162% for the variety V₄ with maximum values at early stage (from 35 to 45 DAP) and minimum values at mid stage (from 45 to 60 DAP). Among the varieties, V₃ and V₄ had the significantly higher LAs at all water regimes than the varieties V₂ and V₁ which had the lowest LA. The differences in LA between V₁ and V₂ were very marginal and insignificant and so as to between V₃ and V₄. The difference in LA among the water regimes was observed to be higher for V₃ and V₄ than other two varieties, indicating that the variety V₃ and V₄ were much sensitive to water.

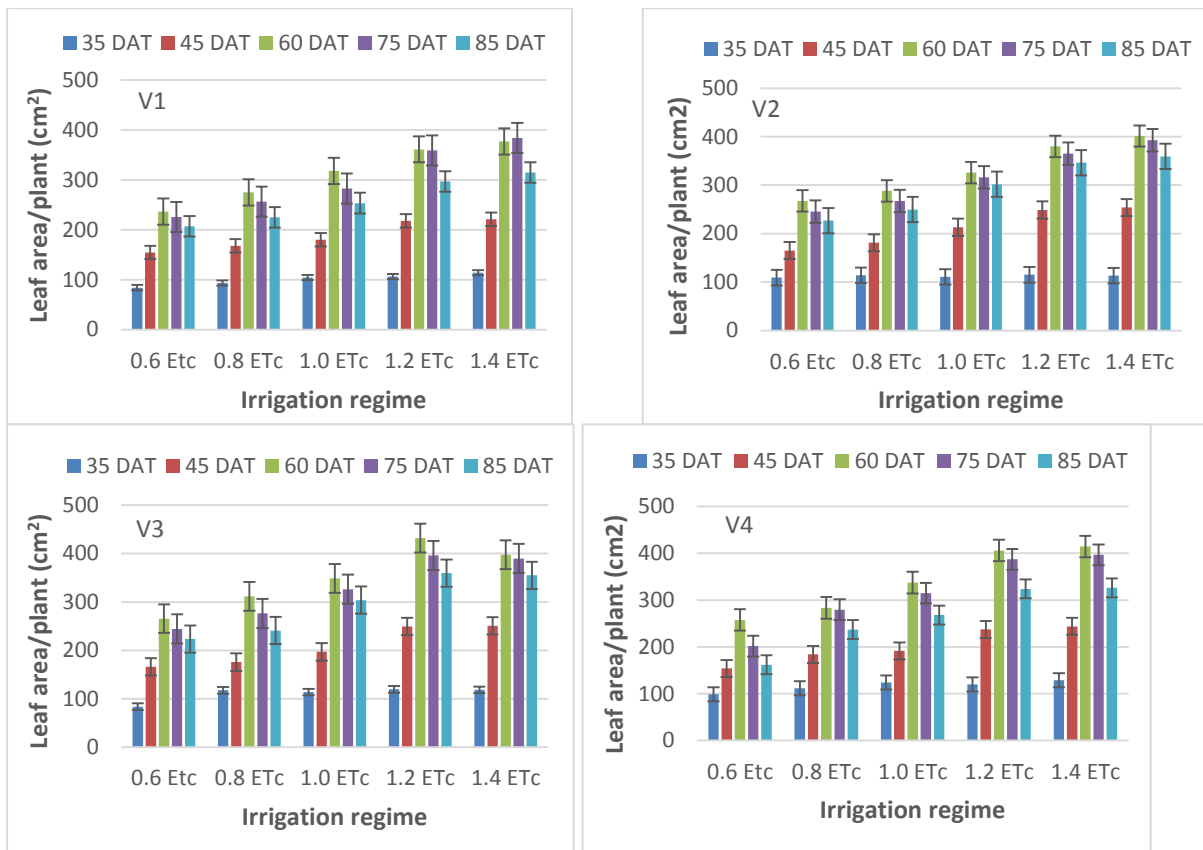


Figure 1. Leaf area of onion varieties affected by water regimes at different days after transplanting (DAT).

Yield response factor (Ky)

The relationship between evapotranspiration deficit ($1 - ET_a/ET_m$) and yield depression ($1 - Y_a/Y_m$) is always linear (Doorenbos and Kassam, 1979), with a slope called the yield response factor (Ky). Crop yield response factor (Ky) for different onion varieties showed statistically significant linear relationship between the decrease in relative evapotranspiration deficit and the decrease in relative yield (Figure 2). The Ky values for total onion growing season ranged between 0.93 to 1.08, the

lowest and the highest being for V_1 and V_4 variety, respectively ((Figure 3). K_y value for V_4 was the highest (1.07) which is comparable to V_2 (1.044) and V_3 (1.05) while K_y value for V_1 was the lowest (0.93). The greater K_y value of V_2 , V_3 and V_4 than the variety V_1 indicates that the variety V_2 , V_3 and V_4 are more responsive to irrigation, that is relative decrease in evapotranspiration resulted in more reduction in yield. The determined K_y values are very close to 1.10 that reported by Doorenbos and Kassam (1986) and Kadayifci et al. (2005). These findings revealed that onion is very sensitive to soil water stress during the total growing season and hence onion should be grown with adequate irrigation for obtaining a good yield. For variety V_1 , K_y value was less than unity indicated that this variety can tolerate a mild stress without a considerable yield loss.

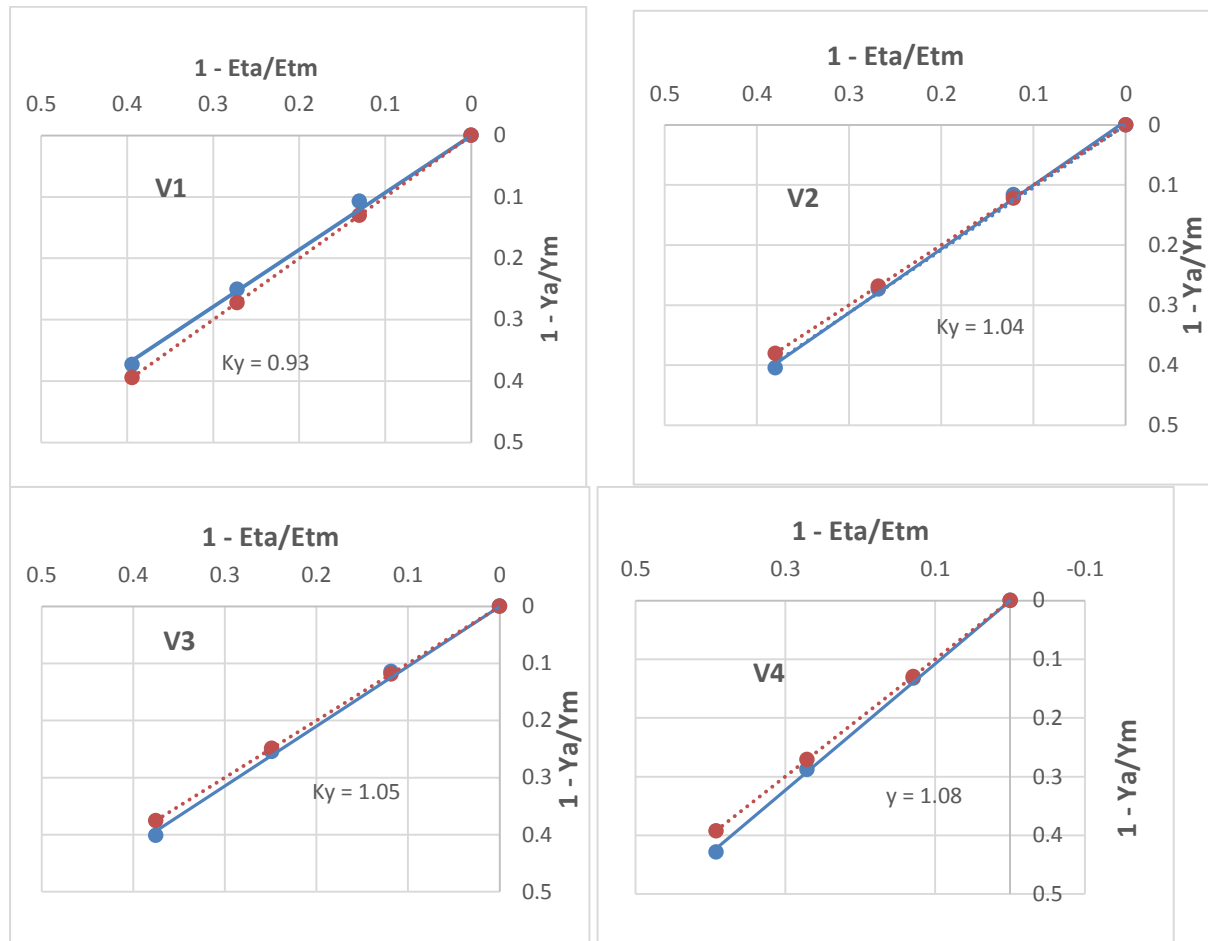


Figure 2. Relationship between relative yield decrease and relative crop evapotranspiration decrease for onion (full line) and reported by Doorenbos and Kassam (dotted line).

The higher K_y values for V_2 , V_3 and V_4 indicate that the crop will have a greater yield loss when the crop water requirements are not met. Therefore, DI practices should be avoided for K_y values that are more than unity. This conclusion is in line with a statement given by Doorenbos and Kassam (1986) who underline that $K_y > 1.0$ indicates the decrease in yield is proportionally greater with increase in water deficit. Considering K_y as a limiting factor, 80% ETo application was a marginal for V_1 and V_2 and 100% ETo for V_3 and V_4 , beyond that yield losses are unbearable. These K_y values for onion could be used for planning, design and operation of irrigation projects which allows quantifications of water supply and water use in terms of crop yield and total production for the project area.

Seasonal water use and water productivity

Total water used by the crop was equal to the applied irrigation water, effective rainfall plus contribution by soil water during the growing season. Irrespective of variety, the amount of water

applied to the crop ranged from 1217 and 269 mm with minimum in the 60% ETo treatment and maximum in the wettest treatment of 140% ETo (Table 2).

Table 2. Water productivity of onion varieties under different irrigation regimes

Treatment	Irrigation for plant estb (mm)	Irrigation after plant estb (mm)	ER (mm)	SMC (mm)	Drainage (mm)	SET (mm)	Yield (t/ha)	WP (kg/m ³)
Variety: V1 (BARI Piaj-1)								
I ₁	20	107	2	20	0	149	11.74	7.89
I ₂	20	142	2	15	0	179	14.26	7.95
I ₃	20	178	2	14	0	214	17.18	8.03
I ₄	20	213	2	11	4	242	19.03	7.86
I ₅	20	249	2	5	7	269	17.92	6.66
Variety: V2 (Lal Teer Hybrid)								
I ₁	20	107	2	21	0	150	15.45	10.32
I ₂	20	142	2	16	0	180	18.84	10.44
I ₃	20	178	2	16	0	216	22.92	10.61
I ₄	20	213	2	11	2	244	25.93	10.63
I ₅	20	249	2	8	7	272	25.97	9.61
Variety: V3 (Taherpuri King)								
I ₁	20	107	2	21	0	150	14.73	9.83
I ₂	20	142	2	17	0	181	18.15	10.00
I ₃	20	178	2	15	0	215	21.44	10.13
I ₄	20	213	2	12	3	244	24.72	10.21
I ₅	20	249	2	7	7	271	24.17	8.94
Variety: V4 (BARI Piaj-1)								
I ₁	20	107	2	21	0	150	17.03	11.37
I ₂	20	142	2	16	0	180	21.53	11.93
I ₃	20	178	2	15	0	215	26.56	12.17
I ₄	20	213	2	12	2	245	29.81	12.45
I ₅	20	249	2	7	6	272	31.02	11.40

Seasonal evapo-transpiration (SET) varied, to a greater extent, with the variation in amount of water application and, to a lesser extent, with the varieties. Though all varieties received same amount of irrigation water, water productivity varied remarkably as variety V₃ and V₄ produced significantly higher yield than other two varieties. Seasonal evapotranspiration was increased with the applied irrigation water and on average it ranged from 149 to 269 mm for V₁, from 150 to 272 mm for V₂, from 150 to 271 mm for V₃ and from 150 to 272 mm at 60% ETo and 120% ETo treatments, respectively.

In the present study, under different sprinkler irrigation regimes, water productivity ranged between 6.66 and 8.03 kg/m³ for V₁ with maximum value in 100% ETo, between 9.61 and 10.61 kg/m³ for V₂, between 8.94 and 10.21 kg/m³ for V₃ and between 11.37 and 12.45 kg/m³ with maximum value in 120% ETo and minimum value in 60% or 140% ETo. Unlike V₁, the highest WP for V₄, V₃ and V₂ were obtained from 120% ETo treatment rather than the treatment 100% ETo. This indicates that variety V₂, V₃ and V₄ are more responsive to irrigation even at higher water regime. In this case, the greater increase in bulb yield than that of SET was responsible for the higher magnitude of WP than other two varieties. In case of V₁, WP increased up to 100% Eto; thereafter it decreased with further increasing of irrigation regime. But for V₂, V₃ and V₄, WP was still increasing with the increasing in irrigation regime and attained the highest level under 120% ETo. This was due to the fact that, for V₁, up to 100% ETo the relative increment of bulb yield was greater than the relative increment of SET. For variety V₂, V₃ and V₄, relative increment in yield was always higher than

relative increment of SET. However, for all levels of irrigation regimes, variety V₄ had the higher water productivity closely followed by V₂ and V₃ while the variety V₁ had the lower WPs due to the greater decrease in bulb yield than that of SET.

Changes in soil moisture storage

Changes in soil moisture storage during the growing period were always higher under lower regime than under higher regime irrigation treatments (Fig. 3).

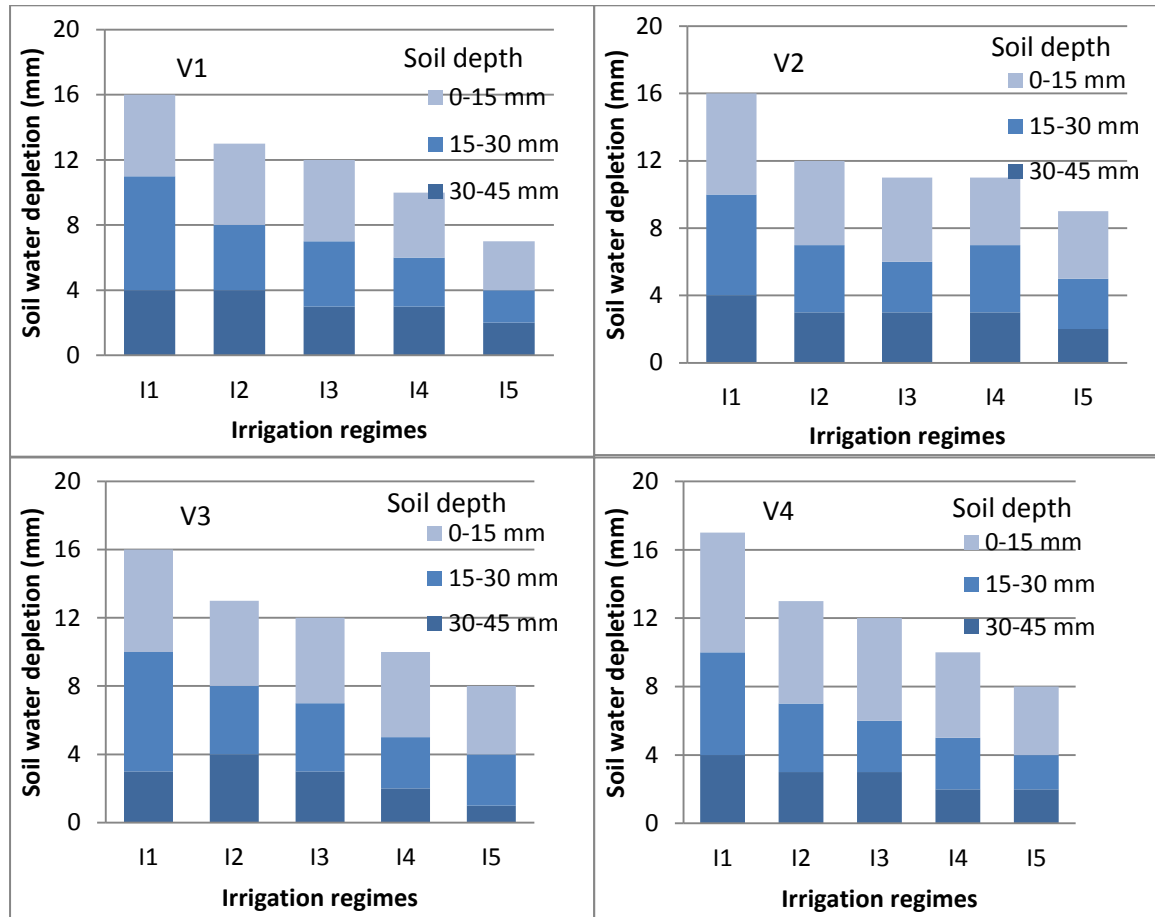


Figure 3. Soil water depletion pattern by soil depth under different water regimes.

The least amount of irrigation applied under lowest irrigation regime of 0.6 ETo may be the reason for the higher changes in soil moisture storage. Under lower irrigation regimes, the water depletion from the first layer (0–15 cm) was maximum (12 mm). When the surface layer (0–15 cm) became dry, the 15–30 cm layer was the primary source of water used by the plant, due either to upward movement of water to the roots, or by direct water uptake by the roots within this depth. In wetter regime treatments, pattern was almost same as of drier regime treatments with difference in magnitude. But under driest irrigation regime (60% ETo), the highest changes occurred in the mid layer (15–30 cm) followed by that obtained in the 0–15 cm layer. This may be due to the fact that under these irrigation treatments a small amount of water was applied at each irrigation, which caused soil wetness down to 15 cm depth, leaving mid layer soil (15–30 cm) drier. As a result, moisture depletion was more in this layer than top layer. Difference in soil water storage between these two layers increased from wetter to drier irrigation regimes (120% ETo to 60% ETo) due to decrease in amount of water applied at each irrigation.

Conclusions

Sprinkler irrigation with different water regimes had a significant effect on the growth and bulb yield of onion. Onion bulb yield under sprinkler irrigation with higher water regimes was significantly higher than the yield recorded under lower irrigation regimes. For all varieties, bulb yield of onion increased significantly with increasing of water regime from 60% to 120% ETo. For V₁, application of water beyond 100% ETo water regime increased the yield insignificantly, but it was significant for the variety V₂, V₃ and V₄. The yield obtained from V₂, V₃ and V₄ was always higher under all levels of irrigation regimes than that obtained from V₁. The variety V₄ produced the highest yield of 31.02 t/ha under 120% ETo regime closely followed by the yield of 25.97 t/ha obtained from V₂ and 24.72 t/ha obtained from V₃. Yield obtained from BARI Paj-1 (V₁) was the lowest (19.03 t/ha). The amounts of water used for evapotranspiration under different irrigation regimes ranged from 149 to 269 mm, 149 to 270 mm, 150 to 270 mm and 150 to 272 mm, respectively, for V₁, V₂, V₃ and V₄ with minimum at 60% ETo and maximum at 140% ETo water regime. In case of V₁, application of water helped to increase the WP up to 100% ETo; thereafter it started to decrease, while for the varieties V₂, V₃ and V₄ it continued to increase even at higher water regime of 140% ETo. Values of Ky determined for the whole growing season was found higher for V₄ (1.08), V₃ (Ky: 1.05) and V₂ (Ky: 1.044) than V₁ (BARI Paj-1). The higher WP and Ky indicate that variety V₂, V₃ and V₄ are highly responsive to irrigation. The values of Ky and WP can be a good basis for onion growers in relation to the optimum irrigation water use and utilization of irrigation systems, and also for improving the production technology of the crop.

References

- Bazza, M. and M. Tayaa, 1999. Contribution to improve sugar beet deficit irrigation, In *Crop Yield Response to Deficit Irrigation, Developments in Plant and Soil Sciences*, C. Kirda, P. Moutonner, C.Hera, and D. R.Nielsen, Eds., vol. 84, pp. 72–97, Kluwer Academic, Dordrecht, The Netherlands.
- BBS 2013. Statistical Year Book of Bangladesh. Bangladesh Bureau of Statistics, Statistics Division, Ministry of Planning, Government of the People's Republic of Bangladesh.
- Bekele S. and K. Tilahun, 2007. Regulated deficit irrigation scheduling of onion in a semiarid region of Ethiopia. *Agricultural Water Management*, vol. 89, no. 1-2, pp. 148–152.
- Doorenbos J, and Kassam AH, 1979. Yield Response to Water. FAO Irrigation and Drainage Paper No. 33, FAO, Rome, Italy. p. 193.
- Fabeiro Cortés, C., F. J. Olalla, and J. A. de Juan, 2002. Production of muskmelon (*Cucumis melo* L.) under controlled deficit irrigation in a semi-arid climate, *Agricultural Water Management*, vol. 54, no. 2, pp. 93–105.
- Fabeiro Cortés, C., F. J. Olalla, R. López Urrea, and A. Domínguez, 2003. Production and quality of the sugar beet (*Betavulgaris* L.) cultivated under controlled deficit irrigation conditions in a semi-arid climate. *Agricultural Water Management*, vol. 62, no. 3, pp. 215–227.
- Fabeiro Cortés, C., F. J. Olalla, and R. López Urrea, 2003. Production of garlic (*Allium sativum* L.) under controlled deficit irrigation in a semi-arid climate. *Agricultural Water Management*, vol. 59, no. 2, pp. 155–167.
- FAOSTAT, 2010. On line statistical database of the Food and Agricultural Organization of the United Nations. <http://apps.fao.org/>.
- Kadayifci, A., Tuylu, G.I., Ucar, Y., Cakmak, B., 2005. Crop water use of onion (*Allium cepa* L.) in Turkey. *Agric. Water Manage.* 72, 59–68.
- Kang, S.Z., Zhang, L., Liang, Y.L., Hu, X.T., Cai, H.J., Gu, B.J., 2002. Effects of limited irrigation on yield and water use efficiency of winter wheat in Loess Plateau of China. *Agric. Water Manage.* 55, 203–216.
- Kobossi, K. and F. Kaveh, 2010. Sensitivity analysis of Doorenbos and Kassam (1979) crop water production function. *African Journal of Agricultural Research*, 5: 2399-2417.
- Kumar S., M. Imtiyaz, A. Kumar, and R. Singh, 2007. Response of onion (*Allium cepa* L.) to different levels of irrigation water. *Agricultural Water Management*, vol. 89, no. 1-2, pp. 161–166, 2007.

- Olalla, F.M., de, S., Padilla, A.D., Lopez, R., 2004. Production and quality of onion crop (*Allium cepa* L.) cultivated under controlled deficit irrigation conditions in a semi-arid climate. *Agric. Water Manage.* 68, 77–89.
- Sezen, S.M., A. Yazar, A. Akyildiz, H. Y. Dasgan, and B. Gencel, 2008. Yield and quality response of drip irrigated green beans under full and deficit irrigation. *Scientia Horticulturae*, vol. 117, no. 2, pp. 95–102.
- Shock, C.C., Feibert, E.B.G., Saunders, L.D., 1998. Onion yield and quality affected by soil water potential as irrigation threshold. *Hort. Sci.* 33, 1188–1191.
- Vaux, H. J. and W. O. Pruitt, 1983. Crop-water production functions. In: D. Hillel, ed. *Advances in Irrigation*. Vol. 2, pp. 61-93. New York, USA, *Academic Press*.

EFFECT OF FERTILIZER AND IRRIGATION FREQUENCY ON THE YIELD AND QUALITY OF EXPORT AND PROCESSING POTATO

S.K. BISWAS¹, M.A. HOSSAIN², D.K. ROY¹, K.F.I. MURAD³, FARZANA³, S.S.A. KAMAR³

Abstract

Despite growing demand in home and abroad, Bangladesh lacks in producing export and processing quality potato due to varietal constraints and to a lesser extent, absence of apposite cultural practices. Proper irrigation and nutrient management can play a vital role in achieving higher productivity and quality of potato. With these perspectives, a field experiment was conducted at the research field of Irrigation and Water Management Division of the Bangladesh Agricultural Research Institute, Gazipur, to evaluate the effects of fertilizer and irrigation on dry matter content, tuber yield and water productivity of an export and processing potato variety (BARI Alu-25). The treatments consisted of nine combinations of three fertilizers levels and three irrigation levels. Three fertilizer levels were F₁: Recommended fertilizer dose, F₂: Recommended dose with 75% MOP + 25% SOP + Vermicompost @2t/ha, F₃: Recommended dose with 50% MOP + 50% SOP. Similarly, three irrigation levels were I₁: 3 irrigations at 30, 45 and 60 days after planting (DAP), I₂: 4 Irrigations at 30, 45, 60 and 75 DAP and I₃: 4 Irrigations at 30, 45, 60 and 80 DAP. The results indicated that fresh tuber yields of potato were not significantly influenced either by the irrigation treatments or by the fertilizer treatments. The fertilizer treatment F₂ produced slightly higher tuber yield and dry matter content compared to F₁ and F₃. While the trivially higher yield was obtained from the irrigation treatment I₂ where last irrigation was applied up to 50% of FC. Thus, the combination of I₂ and F₂ contributed the highest tuber yield, dry matter content and water productivity compared to other combinations of irrigation and fertilizer. Water productivity among the treatments ranged from 11.87 to 12.74 t/ha under I₁, from 11.66 to 13.0 t/ha under I₂, and 11.63 to 11.98 t/ha under I₃ irrigation regimes with minimum values in F₁ and maximum in F₂. These results are of considerable importance to the growers of potato and may be preferred for growing export and processing potato in Bangladesh.

Introduction

Potato is a tuber crop that plays an important role in feeding people of the world and consumed daily by millions of people from diverse cultural backgrounds (Ahmadi et al., 2014). Potatoes are processed into a great variety of products, including cooked products, par-fried, French fries, chips, starch. Worldwide, potato is the most important agricultural food crop after cereals, like wheat, rice and maize is a high yielding crop. It is a cheap source of energy due to its large carbohydrate content (13 to 23%) (Haase, 2003; Ahmadi et al., 2014), as well as containing vitamins B and C and minerals. Moreover, potato is also used in many industries like textile and alcohol production (Abdeldagir et al., 2003). Exporting potato by increasing its yield and quality may keep an important role on economic development of Bangladesh. But potato farmers in Bangladesh often struggle to export their produce as the potato they produce lacks in quality and fails to meet the standard required for export and processing as well. One of the important quality parameters considered for export and processing is dry matter content in tuber. Potato with higher dry matter content, preferred for both export and processing purposes, lacks in Bangladesh due varietal and other constraints like climate, soil, growing duration, irrigation and nutrient management, etc. Potato tubers intended for chips should contain 20-22% of dry matter and 14-17% of starch, and for crisps 20-25% of dry matter and 16-20% of starch (Lisińska 2000, Zgórska and Frydecka-Mazurczyk 2002, Grudzińska et al. 2016). Water is a basic requirement for early plant growth and tuber development. It is also related to dry matter content of the tuber. Potato plants are sensitive to water stress, and soil moisture is one of the important factors affecting the quantity and quality of tubers yield. Bao-Zhong et. al. (2003) noted that tubers yield increased by increasing the amount of irrigation water, while the specific weight of tubers dropped. Harvesting or maturity also directly affects dry matter content. So, it is necessary to find out the optimum irrigation scheduling and harvesting time in order to maximize the economic return from exporting as well as processing. Dry matter content is

¹ SSO, IWM Division, BARI, Gazipur

² CSO (in-charge.) and Head, IWM, BARI, Gazipur

³ SO, IWM Division, BARI, Gazipur

important for both fresh markets and processing. Tubers with dry matter above 18-20% tend to be more susceptible to bruising and tubers disintegrate more readily when cooked. However, for processing high dry matter content is required to achieve a good fry color and often 20-25% is specified. Nitrogen, potassium and magnesium can all have influences on tuber dry matter content (Sarker et al., 2019). Nitrogen is often the limiting nutrient to achieve higher tuber yields (Marshall, 2007) but excessive amounts of N may be detrimental to quality traits (Bucher & Kossmann, 2007). While the optimal rate of N is not detrimental to DM production and content (Stark & Love, 2003). Potassium is essential for synthesis of sugars and starch and for translocation of carbohydrates (Singh et al., 1996). It also plays an important role for maintaining tone and vigor of the plants. The form of potassium has an effect on dry matter. Sulphate of potash - SOP (potassium sulphate) can achieve higher dry matters than muriate of potash - MOP (potassium chloride) and therefore is frequently the preferred form for processing potatoes. This is due to the chloride in the muriate of potash having a negative effect on tuber dry matter content. Other crop management practices influencing dry matter content like selecting the right variety to meet dry matter production needs; selecting quality seed with less risk of disease; avoiding fields, with adverse factors such poor drainage or low water holding capabilities; ensuring blight spray programs are effective; scheduling irrigation to maximize quality characteristics; harvesting early, thereby minimizing late disease ingress or tuber deterioration. With these viewpoints, this study was intended to find out the appropriate irrigation and fertilizer management for higher tuber yield, dry matter content and quality of processing potato.

Materials and Methods

The study was conducted at the research field of Irrigation and Water Management (IWM) Division of Bangladesh Agricultural Research Institute (BARI) in Gazipur during the rabi season (November-February) of 2020-2021. The soil was silt clay loam with an average field capacity (FC) of 28.4% (weight basis) and mean bulk density of 1.47 g cm⁻³ over 0-45 cm soil profile. The experiment was laid out in randomized complete block design (RCBD) with nine treatments replicated three.

The treatments consisted of nine combinations of three fertilizers levels and three irrigation levels. Three fertilizer levels were:

F₁: Recommended fertilizer dose

F₂: Recommended dose with 75% MOP + 25% SOP + Vermicompost @2t/ha

F₃: Recommended dose with 50% MOP + 50% SOP

Three irrigation levels were:

I₁: 3 irrigations at 30, 45 and 60 DAP

I₂: 4 irrigations at 30, 45, 60 and 75 DAP (Last irrigation upto 50%FC) and

I₃: 4 irrigations at 30, 45, 60 and 75 DAP (Last irrigation upto 50%FC) and

At each irrigation event, water was applied up to 100% of field capacity (estimated at weight basis). The unit plot size was 18 square meter (3 m × 6 m). A processing potato variety, 'BARI Alu-25 (cv. 'Asterix') was used in this study.

Seed potatoes were planted on 29 November in 2020, with the row to row spacing of 60 cm and plant to plant 15 cm. After planting of potato, 20 mm of irrigation water was applied in every furrow in all treatments for ensuring proper germination and the irrigation treatments were initiated after plant establishment. The recommended doses of fertilizers were nitrogen (N) at 120, phosphorus (P) at 30, potassium (K) at 100, sulfur (S) at 15, zinc (Zn) at 4, and boron (B) at 1.4 kg ha⁻¹ and applied in the form of urea, triple super phosphate, muriate of potash, gypsum, zinc sulfate and borax, respectively (FRG, 2018). Decomposed cowdung was applied @ 4 t ha⁻¹ before land preparation. Some of fertilizers were applied as basal during land preparation 4 days befo planting. Remaining were applied as side-dressing during earthing up operation followed by irrigation. Adequate plant protection measures were taken whenever required. In order to assess the change in soil water status, soil moisture was measured periodically by gravimetric method in 0–15, 15–30 and 30–45 cm soil profiles, considering the effective root zone of potato as 45 cm. The soils were sampled from both the

center of the raised beds and bottom of the furrows with the depth of 15 cm increment during the time of planting to harvest. The calculated amount of irrigation water was supplied to the experimental plot using a polyethylene hose pipe connected to a water flow meter. Seasonal crop water use (CWU) and the change in soil water contribution before planting and final harvest was estimated by the soil water balance approach (Micheal 1978; Sarker et al., 2019; 2020). Three plants were randomly collected from each treatment periodically to record the data on dry matter partitioning of potato plants. The roots and tubers were collected, cleaned and washed on a nylon net with clean tap water. The dry matter of roots, stems, leaves and tubers were separated and dried in the oven at 60⁰ C until a constant weight was achieved and expressed in g plant⁻¹. Aside from dry matter content per plant, dry matter percentage of potato also determined after harvesting of potato. For this two to three potatoes were collected from each of five places from the pile of harvested potatoes to make a representative sample of potatoes. Then the collected samples were divided into three each of 200-250 g potatoes. Sample potatoes were weighed, sliced and dried in an oven to determine the dry matter percentage. At harvest on 28 February 2021, 10 plants were selected randomly from each plot to record data periodically on plant characters like plant height, stem per hill, and number of tuber per hill, weight of tuber per hill and tuber yield. For determining dry weight of tubers, 500 grams of potatoes were sliced, dried in the sun for two days and then dried in oven at 65 °C for 72 h. Then the samples were cooled and weighed.

Crop water productivity (WP) was calculated as the ratio of tuber yield (t ha⁻¹) and crop water use, and expressed as kg m⁻³. Data on tuber yield and yield attributes and dry matter of potato were statistically analyzed to test the effects of fertilizer and irrigation levels on these parameters using MSTAT-C program. All the treatment means were subjected to analysis of variance (ANOVA) and compared for any significant differences at P < 0.05.

Results and Discussion

Fresh tuber yield of export and processing potato

Yield contributing parameters and tuber yield of potato affected by different irrigation and fertilizer levels are presented in Table 1. Neither of yield contributing parameters, nor the tuber yield were significantly affected by either the irrigation or the fertilizer treatments. But tuber yield was slightly increased in the irrigation treatment I₂, where last irrigation was applied at 75 days after planting. Similarly, fertilization treatment F₂ where SOP and vermicompost were applied produced the slightly higher yield than other treatments. A trivial difference in yield between irrigation levels I₁ and I₃ and also between the fertilizer treatments F₁ and F₃ were observed. Most of the yield contributing parameters like plant height, stem per plant, and number of tuber per plant, weight of tuber per plant showed similar patterns in their variations. The interaction of fertilizer and irrigation also led to insignificant effect on both yield contributing parameters and tuber yield. Under I₁ irrigation level, tuber yield ranged from 29.92 to 32.10 t/ha for I₁, from 31.14 to 34.71 t/ha for I₂ and from 31.51 to 32.47 t/ha for I₃ with minimum vales in F₁ fertilizer level and maximum values in F₂ fertilizer levels. The better plant growth under I₂ irrigation treatment and F₂ fertilizer treatment produced slightly better tuber yield than other treatments.

Table 1. Tuber yield and yield contributing characters of processing potato (BARI Alu-25) under different irrigation and fertilizer levels

Treatment	Plant height (cm)	Stem/plant (no.)	Potato/plant (no.)	Tuber wt/plant (g)	Tuber yield (t/ha)
Irrigation levels					
I ₁	54.22	4.04	7.70	317.51	30.80
I ₂	56.22	3.15	8.30	334.04	32.89
I ₃	55.04	3.19	7.26	320.08	31.74
LSD _{0.05}	ns	ns	ns	ns	ns
CV(%)	9.15	6.29	7.16	10.06	8.24
Fertilizer levels					
F ₁	52.56	3.26	7.81	307.27	30.86
F ₂	59.22	3.85	8.41	335.56	33.09
F ₃	52.89	3.26	7.04	311.81	31.48
LSD _{0.05}	5.82	ns	ns	ns	ns
CV (%)	8.11	6.78	7.48	11.26	9.02
Irrigation x Fertilizer					
I ₁ F ₁	52.67	3.44	7.78	299.21	29.92
I ₁ F ₂	61.00	5.00	8.44	341.40	32.10
I ₁ F ₃	51.00	3.67	6.89	314.91	30.37
I ₂ F ₁	53.67	3.11	7.67	322.96	31.14
I ₂ F ₂	58.00	3.44	9.22	360.96	34.71
I ₂ F ₃	52.33	3.33	6.56	322.98	31.62
I ₃ F ₁	52.33	3.22	8.00	310.63	31.51
I ₃ F ₂	56.67	3.11	7.56	324.31	32.47
I ₃ F ₃	53.33	2.78	7.67	320.54	32.44
LSD _{0.05}	ns	ns	ns	ns	ns
CV(%)	8.11	6.78	7.48	11.26	9.02

Total dry matter of potato

The total dry matter, TDM, of potato plants as influenced by different irrigation and fertilizer treatments recorded at different dates over the growing season showed that it increased slowly up to 45 DAP; thereafter it increased sharply (Fig. 1). As far as crop growth stages are concerned, there was a big difference between early stages (at 45 and 65 DAP) and the differences were minimal at the later growth stages. But no significant differences in total dry matter were found among irrigation treatments for a particular stage. Similarly, among the fertilizer treatments, differences in dry matter content were insignificant. Slightly higher TDM was observed in fertilizer treatment F₂ at all levels of irrigations. The increase in TDM under this fertilizer treatment might be due to the application of vermi-compost, an organic fertilizer, along with a potassium fertilizer, sulphate of potash (SOP). A study from Denmark demonstrates the higher dry matter content achieved with SOP (potassium sulphate) rather than MOP (potassium chloride). This is due to the chloride in the muriate of potash (MOP) having a negative effect on tuber dry matter content of potato.

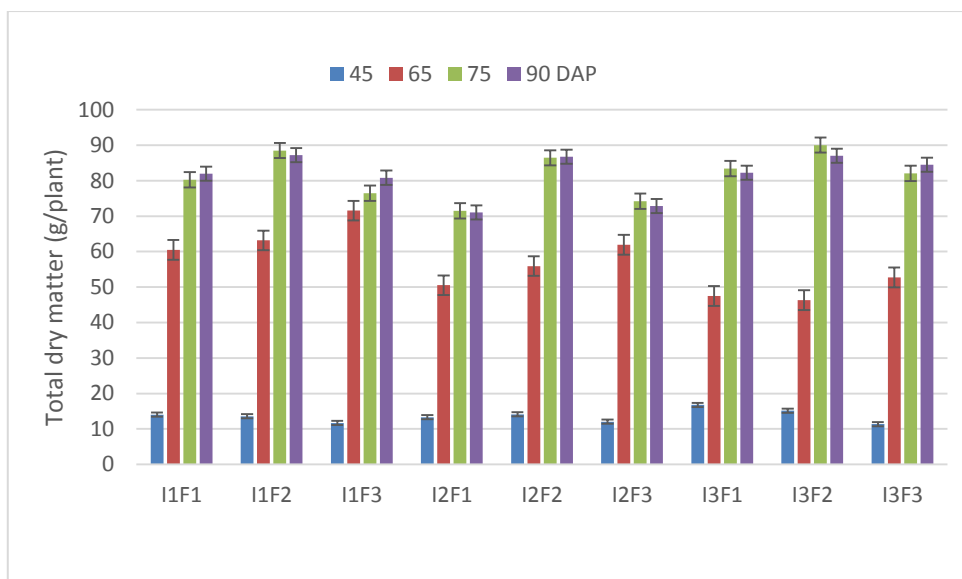


Figure 1. Effect of irrigation and fertilizer on total dry matter content at different growth stages (days after planting, DAP) of potato.

The accumulation of dry matter in different parts (root, stem, leaves and tuber) of potato plants as influenced by irrigation and fertilizer treatments at different growth stages are depicted in Fig. 2. There was no significant effect of irrigation on dry matter partitioning in root, stem, leaves and tuber of potato. The fertilizer treatment also led to an insignificant effect on dry matter partitioning in different organs in potato plant. At the early stage (45 DAP), the share of the leaves was greater than that of the stem, root and tuber thereafter, it decreased, and the share of stems started to increase as the plant grew up. At maturity (90 DAP), the contribution of the share of tuber to the dry matter per plant was greater than the share of stem and leaves. This was due to mobilization of assimilates from leaves and stem to the tuber for bulking. The share of stem was also higher than that of root and tuber at early stage when only vegetative growth happened. At the later stage, tuber formation starts and thereby increased its contribution to the total dry matter content. Tuber dry matter was somewhat affected by fertilizer with higher values in F₂ than F₁ and F₃ under all irrigation treatments. The contribution of tuber to dry matter was found to increase from tuber development at mid stage and reached its maximum at maturity stage.

Dry matter partitioning of potato



Figure 2. Dry matter allocation of potato plant at different growth stages under different irrigation and fertilizer managements during crop growing season.

Dry matter percentage and dry matter yield of potato

Tuber dry matter percentage was not affected by the irrigation schedule, but it was affected significantly by fertilizer treatments with maximum value (21.55%) obtained from F₂ where both SOP and vermicompost were used (Fig. 3a).

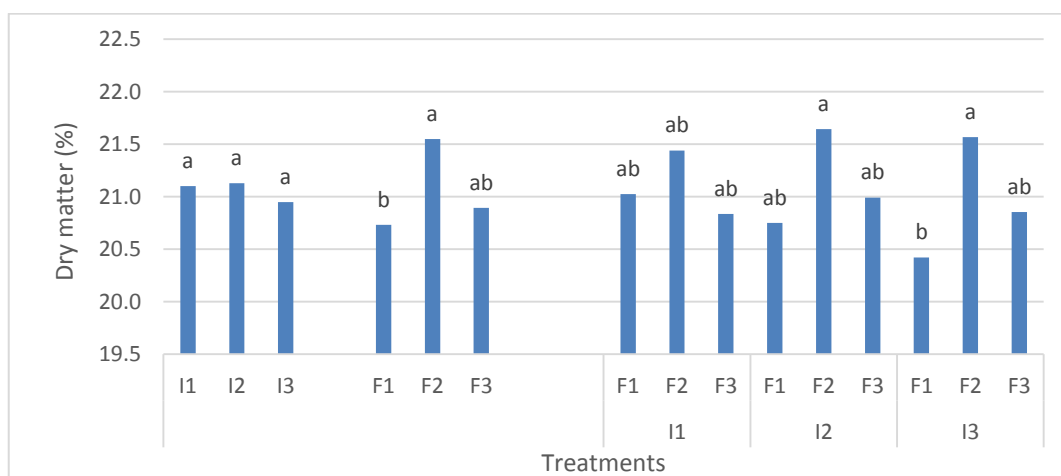


Figure 3a. Dry matter percentage of potato tuber as influenced by different fertilizer and irrigation managements.

In fertilizer treatment F_3 , where only SOP with recommended fertilizers were used, percentage of dry matter retained in tuber was in between that retained under fertilizer treatments F_1 and F_2 . Obviously, the lowest value of dry matter percentage (20.73%) was obtained from recommended fertilizer dose. Combination of irrigation and fertilizer had almost similar effect on accumulation of dry matter in tuber as realized by irrigation and fertilizer separately. Here the highest dry matter retained in F_2 under I_2 irrigation treatment insignificantly followed by I_3F_2 (21.57%) and all other combinations, except the lowest percentage (20.42%) retained in F_1 under I_3 irrigation treatment (I_3F_1). Though variation in dry matter percentage was not significant among irrigation treatments, treatment F_2 under all irrigation treatments contributed to the higher dry matter percentage than both F_1 and F_3 . A significant and positive effect of vermicompost on dry matter accumulation in potato tuber was reported by Ferdous et al. 2019. Kahlel (2015) also noted the highest percentage of dry matter in tubers resulted from the treatment of organic fertilization by irrigation.

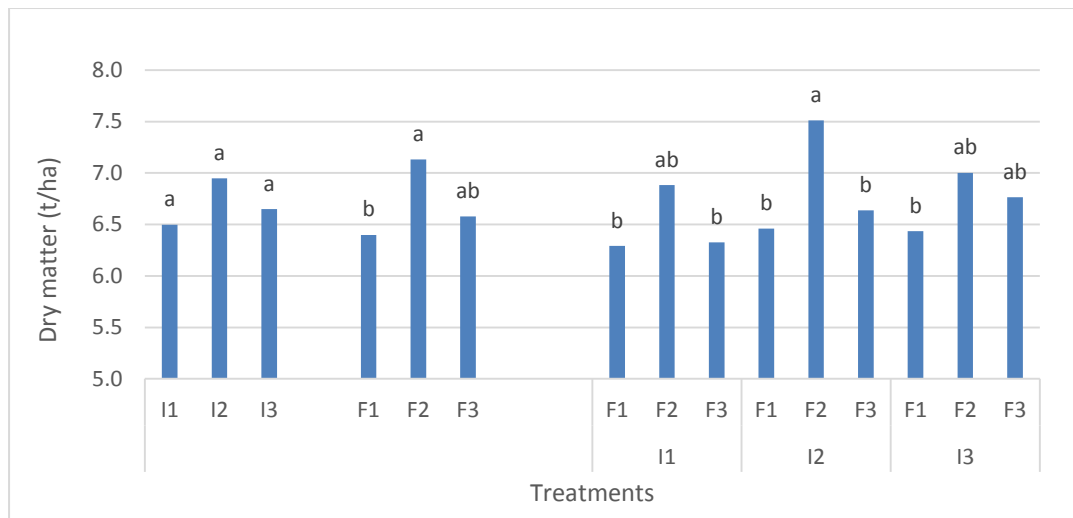


Figure 3b. Dry matter yield of potato as influenced by different fertilizer and irrigation treatments.

Dry matter yield of potato depends on both tuber yield and dry matter percentage as the yield of dry matter is a product of the fresh yield of tubers and the content of dry matter in tubers. According to Gabriel and Świeżyński (1977), the value of dry matter yield is determined in 72-92% by the yield of tubers, and only in 14-15% by the content of this trait in tubers. So, dry matter yield of potato followed the similar trend as that of dry matter percentage and fresh tuber yield (Fig. 3b). In this case, dry matter yield was found the lowest (6.29 t/ha) in F_1 under I_1 irrigation treatment and that of the highest (7.51 t/ha) obtained in F_2 under I_2 irrigation treatment.

Soil water content, crop water use and water productivity

Soil water content at different layer was measured periodically and before each irrigation gravimetrically and demonstrated in Fig.3. Irrespective of irrigation treatments, soil water content varied with soil depth with lower in top 0-15 cm layer and higher in mid-and bottom layer as depletion of soil moisture was more in top layer. In this layer, soil water was progressively decreased with advancement of crop stages. When the top layer became dry, the mid layer was the primary source of water used by the plant, due either to upward movement of water, or by direct water uptake by the roots within this depth. Thus, the pattern of changes in soil water in mid layer (15-30 cm) was almost same as of top layer. In the bottom layer (30-45 cm), changes in soil water with advancement of time were marginal due to less water uptake by potato plants and no or little evaporation took place from this layer. As treatment I_2 and I_3 received irrigation at 75 and 80 DAP, respectively, water content was found higher at the end of crop duration in all layers.

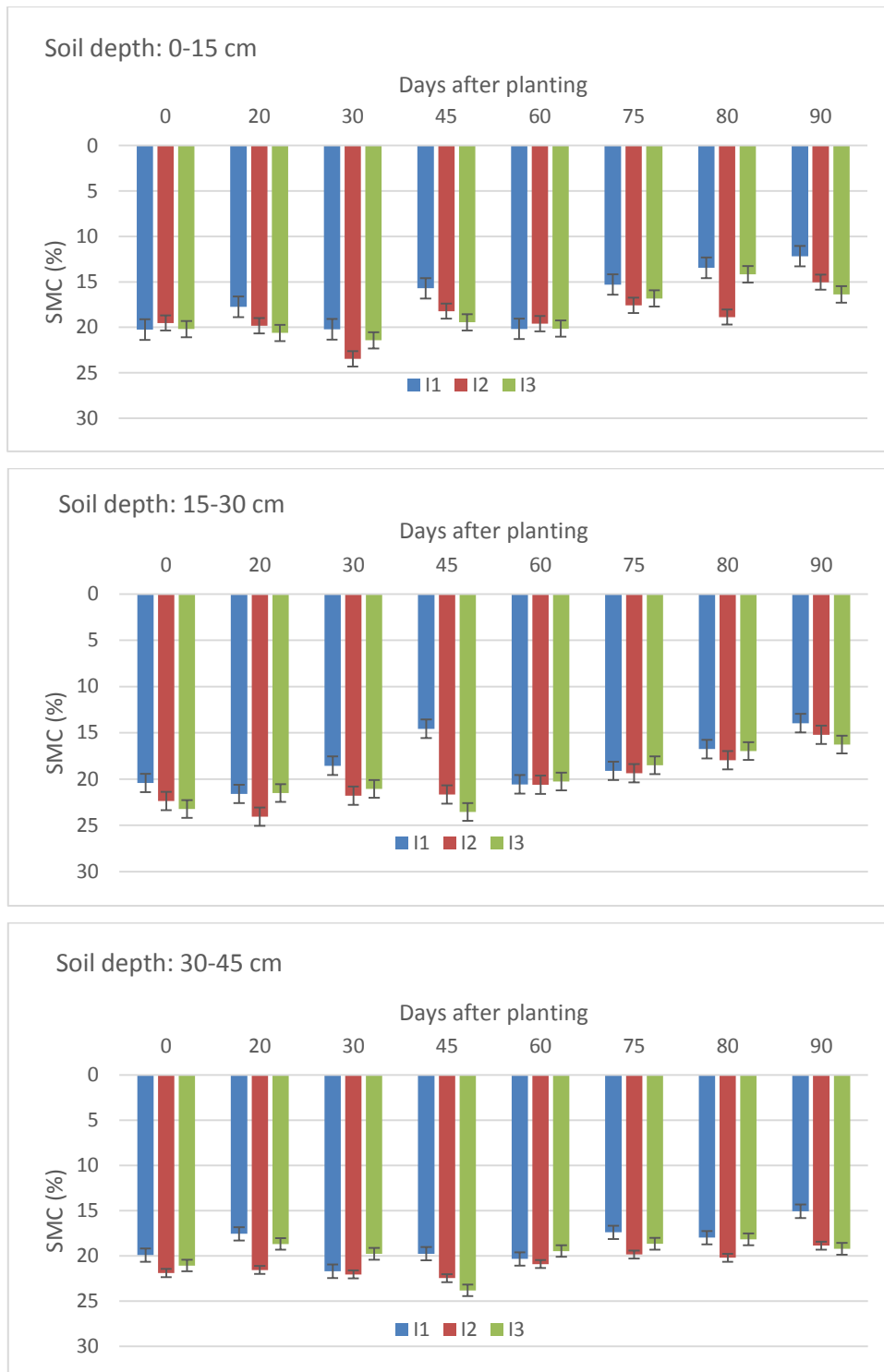


Figure 3. Profile soil moisture (SMC) under different irrigation levels during growing season of potato (Vertical bars indicate the standard error).

Crop water use was equal to the applied irrigation water, effective rainfall plus contribution by soil water during the growing season. Water use by the crop varied with the variation in amount of water applied to the crop and ranged from 252 to 271 mm with minimum in I₁ treatment and maximum in I₃ (Table 2). Though CWU was same across all fertilizer treatments under a particular irrigation treatment, WPs were varied due to difference in tuber yields. WPs ranged from 11.87 to 12.74 t/ha for I₁, from 11.66 to 13.0 t/ha for I₂, and 11.63 to 11.98 t/ha for I₃ with minimum values in F₁ and maximum values in F₂.

Table 2. Irrigation water applied, crop water use (CWU) and water productivity (WP) of potato cultivated under three irrigation and fertilizer levels

Irrigation level	Fertilizer level	IR (mm)	SWC (mm)	ER (mm)	CWU (mm)	Tuber yield (t/ha)	WP (kg/m ³)
I ₁	F ₁	196	56	0	252	29.92	11.87
	F ₂	196	56	0	252	32.10	12.74
	F ₃	196	56	0	252	30.37	12.05
I ₂	F ₁	225	42	0	267	31.14	11.66
	F ₂	225	42	0	267	34.71	13.00
	F ₃	225	42	0	267	31.62	11.84
I ₃	F ₁	232	39	0	271	31.51	11.63
	F ₂	232	39	0	271	32.47	11.98
	F ₃	232	39	0	271	32.44	11.97

WPs obtained in this study were consistent to other studies (Sarker et al., 2019; Jovanovic et al., 2010; Ahmadi et al., 2010). The results indicate that I₂ irrigation strategy produced the greater WP as compared to I₁ and I₃. The combination of F₂ and I₂ produced the highest tuber yield that resulted in the highest WP. The reduced WP in I₁ and I₃ is mainly due to lower fresh tuber yield compared to water use by the crop. This study revealed that proper fertilizer and irrigation strategy could improve water productivity of potato.

Conclusion

Total dry matter and yield of potato were influenced slightly by the combination of fertilizer and irrigation strategies. Fertilizer treatment with SOP and vermicompost (F₂) produced the higher tuber yield and dry matter percentage under all levels of irrigation. Irrigation treatments had insignificant effect on increasing dry matter percentage, though trivially higher dry matter percentage was recorded in I₂ irrigation strategy. Thus, the combination of fertilizer treatment F₂ and irrigation treatment I₂ demonstrated to be the best to increase dry matter, tuber yield and water productivity and may be preferred for growing export and processing potato in Bangladesh. Fertilizer treatment with 50% SOP (F₃) resulted insignificant effect on tuber yield and dry matter content. This study needs to be repeated to understand the fertilizer levels with various irrigation strategies for improving the dry matter, tuber size, yield, water productivity and tuber quality for production of export quality potato which will benefit the growers to have higher price.

References

- Ahmadi, S.H., Andersen, M.N., Plauborg, F., Poulsen, R.T., Jensen, C.R., Sepaskhah, A.R., Hansen, S., 2010. Effects of irrigation strategies and soils on field grown potatoes: yield and water productivity. *Agric. Water Manag.* 97, 1923–1930.
- Ahmadi, S.H., 2009. Agronomic and physiological studies of partial root-zone drying and deficit irrigation on potato in different soil textures. Published Ph.D. Thesis, Department of Basic Sciences and Environment, Faculty of Life Sciences University of Copenhagen, Denmark, 77p.
- Ahmadi, S.H., Andersen, M.N., Plauborg, F., Poulsen, R.T., and Hansen, S., 2009. A quantitative approach to developing more mechanistic gas exchange models for field grown potato: A

- new insight into chemical and hydraulic signalling. *Agri. and Forest Meteorology*, 149: 1541-1551.
- Ahmadi, S.H., Andersen, M.N., Plauborg, F., Poulsen, R.T., Jensen, C.R., Sepaskhah, A.R., Hansen, S., 2010a. effects of irrigation strategies and soils on field grown potatoes: Gas exchange and xylem [ABA]. *Agri. Water Management*, 97: 1486-1494.
- Ahmadi, S.H., Andersen, M.N., Plauborg, F., Poulsen, R.T., Jensen, C.R., Sepaskhah, A.R., Hansen, S., 2010b. Effects of irrigation strategies and soils on field grown potatoes: Yield and water productivity. *Agri. Water Management*. DOI 10.1016/j.agwat.2010.07.007.
- Bao-Zhong Y, Soich M, Kang Y .2003. Effect of different irrigation regimes on the growth and yield of drip- irrigation potato. *Agricultural Water Management*, 63: 153-167.
- Ferdous, J., Roy, T.S., Chakraborty, R., Mostofa, M., Noor, R., Nowroz, F., Kundu, B.C., 2019. Vermicompost influences processing quality of potato tubers. *SAARC J. Agric.*, 17(2): 173-184, DOI: <https://doi.org/10.3329/sja.v17i2.45304>
- Gabriel W., Świeżyński K., 1977. Potato cultivation and seed production (in Polish). PWRiL, Warsaw.
- Jovanovic, Z., Stikic, R., Vucelic-Radovic, B., Paukovic, M., Brocic, Z., Matovic, G., Rovcanin, S., Mojevic, M., 2010. Partial root-zone drying increases WUE, N and antioxidant content in field potatoes. *European J. Agron.* 33 (2), 124–131.
- Kahlel, A.M.S., 2015. Effects of different irrigation and fertilization treatments on growth and yield of potato (*Solanum tuberosum* L.) in Iraq, *International Journal of Horticulture and Ornamental Plants*, 1(1): 2-10.
- M. Zameer Khan, M. Ehsan Akhtar, M. Mahmood-ul-Hassan, M. Masud Mahmood, and M. Naeem Safdar, 2012. POTATO TUBER YIELD AND QUALITY AS AFFECTED BY RATES AND SOURCES OF POTASSIUM FERTILIZER. *Journal of Plant Nutrition*, 35:664–677, 2012
- Mokarroma N, Ahmed IM, Zonayed-Ull-Noor AKM, Rahman KAMM (2017) Effect of harvesting time on growth and tuber formation in processing potato. *Int. J. Sustain. Crop Prod.* 12(2), 17-25. <http://doi.org/10.1016/b978-0-12-802232-0.00015-3>, 2016, pp360-382
- Sarker, K.K., Hossain, A., Timsina, J., Biswas, S.K., Kundu, B.C., Barman, A., Murad, K.F.I. and Akter, F., 2019. Yield and quality of potato tuber and its water productivity are influenced by alternate furrow irrigation in a raised bed system. *Agricultural Water Management*, 224, p.105750. <https://doi.org/10.1016/j.agwat.2019.105750>

EFFECT OF SALINE WATER IRRIGATION WITH DIFFERENT DOSES OF POTASSIUM ON CROP GROWTH AND YIELD OF MUNGBEAN

F. AKTER¹, M.A. HOSSAIN², S.K. BISWAS³, I. M. AHMED, M.K. ALAM⁴, R.P. RANNU¹, AND K.F.I. MURAD¹

Abstract

The experiment was conducted at the shade house of IWM Division, BARI, Gazipur during 2018 - 2019 to evaluate the effect of saline water irrigation with different doses of potassium on crop growth and yield of mung bean. Thirteen treatments were designed for the experiment with four replications. The treatments comprised different combinations of three salinity levels (4 dS/m, 8 dS/m and 12 dS/m) with four potassium levels (0%, 100%, 125% and 150% of recommended dose). Results of experimental findings revealed that salinity seriously affected yield and yield contributing characters of mung bean and potassium can eliminate such type of deleterious effects of salinity to some extent. Application of higher amount of K improved the plant fresh weight and dry weight, and chlorophyll content. Application of different levels of potassium did not influence on plant height, number of leaves and root length. However, different levels of potassium application increased the uptake of Ca, Mg, P and K, while decreased Na uptake several fold. Mg accumulation was unchanged due to salinity. It was concluded that application of higher levels (125% or 150% of recommended dose) of K improves growth and yield of mung bean under saline conditions.

Introduction

Climate change is now one of the biggest problems across the globe as its impacts on human being and the environment are very terrible and prolonged. Bangladesh is exposed to be one of the most vulnerable countries of the world to climate change and sea level rise. There are several environmental issues and problems that are hindering the development of Bangladesh. Salinity is such an environmental problem. Salinity has been a threat to agriculture in some parts of the world for over 3000 years; in recent times, the threat has grown (Tim Flowers, 2006). It is estimated that at least 20% of all irrigated lands are salt affected (Pitman and Läuchli, 2002) in whole world and about 53% of the coastal areas are affected by salinity in Bangladesh (Haque, 2006). Agricultural land use in these areas is very poor, which is much lower than country's average cropping intensity. Salinity causes unfavorable environment and hydrological situation that restrict the normal crop production throughout the year. Excessive soil salinity may adversely affect plant growth by increasing the osmotic pressure in the solution, forming toxicity in the plant tissue and changing the plants mineral nutritional characteristics (Michael, 1978). In the face of high salinity, a plant's ability to control water potential and hydraulic conductivity is essential for the maintenance of water levels in tissue (Negrao et al., 2017).

Among the alternatives employed to minimize the deleterious effects caused by the high salt concentrations on plants, K fertilization stands out. Hence, studies have associated the tolerance of crops to salinity with an adequate K nutrition (Blanco et al., 2008; Gurgel et al., 2010). Potassium is essential to plants because it plays a key role in osmotic regulation and promotes the maintenance of turgor in guard cells. By increasing their osmotic potential, potassium allows this cell to absorb more water, and the adjacent cell acts as a counter cation for anion accumulation and electrogenic transport processes and, consequently, generates higher turgor pressure (Langer et al., 2004; Islam et al., 2015).

Besides being an osmoregulator, K creates an osmotic gradient that allows water movement and regulates stomatal opening and closure, playing an essential role in water saving and cell turgor, transport of carbohydrates and respiration (Shimazaki et al., 2007). Application of higher level of K

¹ SO, IWM Division, BARI, Gazipur

² CSO (in-charge), IWM Division, BARI, Gazipur

³ SSO, IWM Division, BARI, Gazipur

⁴ SSO, Soil Science Division, BARI, Gazipur

improves growth and yield of mungbean under mild level of saline conditions (M. E. Kbir et al.,2004).

The mungbean (*Vigna radiata*), locally known as the *moog*, *sonamoog*, is a plant *species* in the legume family. It has a distinct advantage of being short-duration and can grow in wide range of soils and environments (as mono or relay legume). It has a high nutrient value with protein, carbohydrate, minerals, pro vitamin A and vitamin B-complex.

Material and Methods

An experiment was conducted at IWM shed house of Bangladesh Agricultural Research Institute, Gazipur. BARI Mungbean -5 is used for the experiment. The experimental design was in CRD, with four replicates, and the treatments consisted of four levels of irrigation water electrical conductivity - EC_w (0, 4, 8 and 12 dS/m) and four K doses (0, 100, 125 and 150% of recommendation). The treatments were

- T₁= Irrigation with fresh water with 100% potassium
- T₂= Irrigation with (4 dS/m) saline water with 0% potassium
- T₃= Irrigation with (4 dS/m) saline water with 100% potassium
- T₄= Irrigation with (4 dS/m) saline water with 125% potassium
- T₅= Irrigation with (4 dS/m) saline water with 150% potassium
- T₆= Irrigation with (8 dS/m) saline water with 0% potassium
- T₇= Irrigation with (8 dS/m) saline water with 100% potassium
- T₈= Irrigation with (8 dS/m) saline water with 125% potassium
- T₉= Irrigation with (8 dS/m) saline water with 150% potassium
- T₁₀= Irrigation with (12 dS/m) saline water with 0% potassium
- T₁₁= Irrigation with (12 dS/m) saline water with 100% potassium
- T₁₂= Irrigation with (12 dS/m) saline water with 125% potassium
- T₁₃= Irrigation with (12 dS/m) saline water with 150% potassium

Total fifty-two plastic pots (depth: 34 cm and diameter on an average 30.50 cm) were used. Each pot was filled with 24 kg soil collected from IWM experiment field and contained two plants. The bottom of the pot was perforated and filled with the coarse aggregate to drain the excess of water to a plate, in order to analyzed their chemical composition. Direct soil EC meter was used to measure in situ soil salinity. The salinity data were measured at two depths (0-5 cm) and (5-15 cm) for each treatment. Four levels of K in the form of muriate of potash (MOP) were applied as the potassium source. Recommended dose of fertilizer was applied equally to all treatments.

The irrigation waters with the respective EC_w values were prepared artificially by mixing raw salt into water using trial and error method in the laboratory to get the expected soil salinity. Before using raw salt, salt analysis was done by Flame photometer to compare the amount of percentage of each component (e.g. Na, K, Ca) of salt with the sea salt, and found that raw salt contains desired amount of NaCl as in sea salt.

Before sowing, equal amount of saline water irrigation was used for developing and maintaining soil salinity to some extent in the pots of different treatments. Pre-soaked purified 10 seeds were sown in each pot and irrigated with fresh water for easy germination. At the 2nd trifoliate leaf stage, two uniform and healthy plants were kept at each pot and other plants were picked out. Fresh water was used for plant establishment up to 2nd trifoliate leaf appeared before applying actual treatments. When the first trifoliate appeared, all the treatments were started and continued till maturity. Soil salinity was measured after each irrigation for different treatments. Amount of irrigation water was applied up to field capacity. Plants were grown up to maturity stage and dry matter yield was recorded. Extra 1 replication was included for growth stage wise sampling.

Table- 1. Physical and chemical characteristics of the primary soil

Soil	Texture	pH	Organic Material (%)	Ca	Mg	K	Total N (%)	P	S
				meq/100ml				µg/ml	
Studied soil	silty clay loam	6.4	1.39	5.2	1.8	0.12	0.074	39.0	19.0

Results and Discussion

Yield and yield components of mungbean

The summary of ANOVA suggested that EC of irrigation waters significantly ($p < 0.05$) affected yield and all the other yield components (Table 1) of mungbean. There was significant difference in the relative yield decrease with salinity increase between the lowest and highest K application rates. The mungbean yield decreased to 0.89 and 1.29 t ha⁻¹, respectively with saline irrigation and variable level of potassium doses when compared to 1.47 t ha⁻¹ in pots treated with non-saline irrigation water with recommended potassium dose. The highest yield (1.47 t ha⁻¹) was obtained at treatment T₁ (irrigation with fresh water with 100% potassium) and the lowest yield of 0.89 t ha⁻¹ was recorded at treatment T₁₀ (irrigation with (12 dS/m) saline water with 0% potassium) (Table 1). Table 1. revealed that the highest yield (1.29 t/ha and 1.28 t/ha) among the saline irrigation treatments was achieved with the treatment (T₅) (Irrigation with 4 dS/m saline water with 150% potassium) and treatment (T₃) (irrigation with 4 dS/m saline water with 100% potassium) which was significantly comparable with the treatment (T₄) (Irrigation with 4 dS/m saline water with 125% potassium), treatment (T₉) (Irrigation with (8 dS/m) saline water with 150% potassium). M. Salim and M. G. Pitman showed 60 % and 25% reduction of mungbean yield due to addition of 50 mM NaCl and 100 mM NaCl respectively. But in this study, maximum and minimum yield reduction due to 50 mM NaCl and 90 mM NaCl addition was 40 % and 12 % respectively. These result showed that the harmful effects of salinity on the yield of mungbean were minimized to some extent with potassium fertilization.

The EC_{iw} x K interaction was significant ($p > 0.05$) for all the yield parameters such as number of pod/plant, wt. of seeds/pod, 1000 seed wt. (gm), except pod length and no. of seeds per pod. All the yield parameters decreased with increasing salinity levels, but increased with the increasing potassium level. The highest no. of pods/plant (14.75), pod length (7.54 cm), no. of seeds/pod (9.71), wt. of seeds/pod (0.52 gm), 1000 seed wt. (55.27 gm) was achieved from the fresh water treatment. Among the saline water irrigation treatments, the treatment T₃ (irrigation with (4 dS/m) saline water with 100% potassium) and treatment T₈ (irrigation with (8 dS/m) saline water with 125% potassium) exhibited better performance for no. of pod/plant (12.00). The highest pod length (9.50 cm) was recorded for treatment T₃ along with treatment T₆. While the highest no. of seeds/pod was obtained for the treatment (T₂) irrigation with (4 dS/m) saline water with 0% potassium) along with treatment (T₅) irrigation with (4 dS/m) saline water with 150% potassium) (9.50). Whereas, the highest wt. of seeds/pod (0.49 gm), 1000 seeds wt. (50.79 gm) and seed yield (15.50 gm) was resulted from treatment T₅. However, the lowest no. of pod/plant (09.75), pod length (6.09 cm), wt. of seeds/pod (0.37 gm) and seed yield (8.89gm) was determined in treatment (T₁₀) (irrigation with (12 dS/m) saline water with 0% potassium). Treatment (T₁₀) and treatment (T₁₁) were significantly par with each other for the lowest wt. of seeds/pod and 1000 seed wt. The lowest no. of seeds/pod (8.46) was resulted from treatment T₁₂.

Table 2. Summary of analysis of variance (ANOVA) for yield and yield components of mungbean as affected by the application of saline water and potassium

Treatments	Number of pod/plant	Pod length(cm)	Number of seeds/pod	Wt. of seeds/pod	1000 seed wt. (gm)	Seed yield (gm/plant)
T ₁	14.75	7.54	9.71	0.52	55.27	5.82
T ₂	10.75	7.42	9.50	0.42	47.05	4.38
T ₃	12	7.46	9.34	0.46	48.85	5.07
T ₄	10.75	7.40	9.38	0.47	48.51	5.04
T ₅	11.50	7.00	9.50	0.49	50.79	5.17
T ₆	11.25	7.46	9.33	0.43	43.37	4.36
T ₇	10.50	7.38	9.29	0.43	45.40	4.57
T ₈	12.00	7.44	9.25	0.45	45.46	4.73
T ₉	11.00	7.06	9.33	0.44	46.00	4.86
T ₁₀	9.75	6.09	8.84	0.37	39.38	2.96
T ₁₁	10.00	6.86	9.29	0.38	39.21	3.30
T ₁₂	10.25	6.96	8.46	0.40	40.21	3.56
T ₁₃	10.25	6.88	9.33	0.39	40.75	3.66
CV(0.05)	10.85	8.38	7.76	9.69	6.16	5.40
LSD	1.73	0.86	1.03	0.06	4.04	0.09

Mungbean growth parameters at harvesting stage as affected by the application of saline water and potassium

Plant height, root length, number of leaves, fresh and dry weight of different parts of mungbean were significantly affected by different salinity level (fig:1,2,3 and 4). Potassium can slightly reduce the hazardous effect of salinity on fresh and dry weight of different parts of mungbean. In presence of 150% K application, the fresh and dry weight of mungbean increased significantly for all salinity treatments.

Fig: 1. a. reveals that Salinity affected plant height of mungbean. The plant height decreased with the increase in salinity levels. However, there was no effect of K on plant height. Relative (per cent of control) plant height decreased ranged from 8% to 17% at 4 dS/m salinity level with all potassium doses except 100% potassium application. At 100% potassium with 4 dS/m salinity, there was a plant height increment of about 3.95%. Whereas, at 8 dS/m and 12 dS/m salinity level with all potassium doses, the plant height decreased ranged from 15% to 36% and 34% to 43% respectively. The minimum relative plant height (43%) was obtained at the highest salinity (S2) with no potassium fertilizer.

There was a significant positive plant fresh weight and dry weight response to K application. The plant fresh and dry weights reduction for zero K treatment with increasing salinity became significant (fig: 1. b & c). The fig. showed that the average decrease in plant FW and DW caused by an increase in salinity from 0 to 4 dS/m was approximately 4-42%. As the salinity increases further to 8 dS/m, a further weight reduction of approximately 12-51% for FW and 15-40% for DW, and the reduction continued to increase from 42-53% for FW and 43-61% for DW as the salinity increased from 8 to 12 dS/m. Comparing among the three salinity levels, it was showed for plant FW and DW that 125% potassium application treatments did better performance than 150% K application treatments.

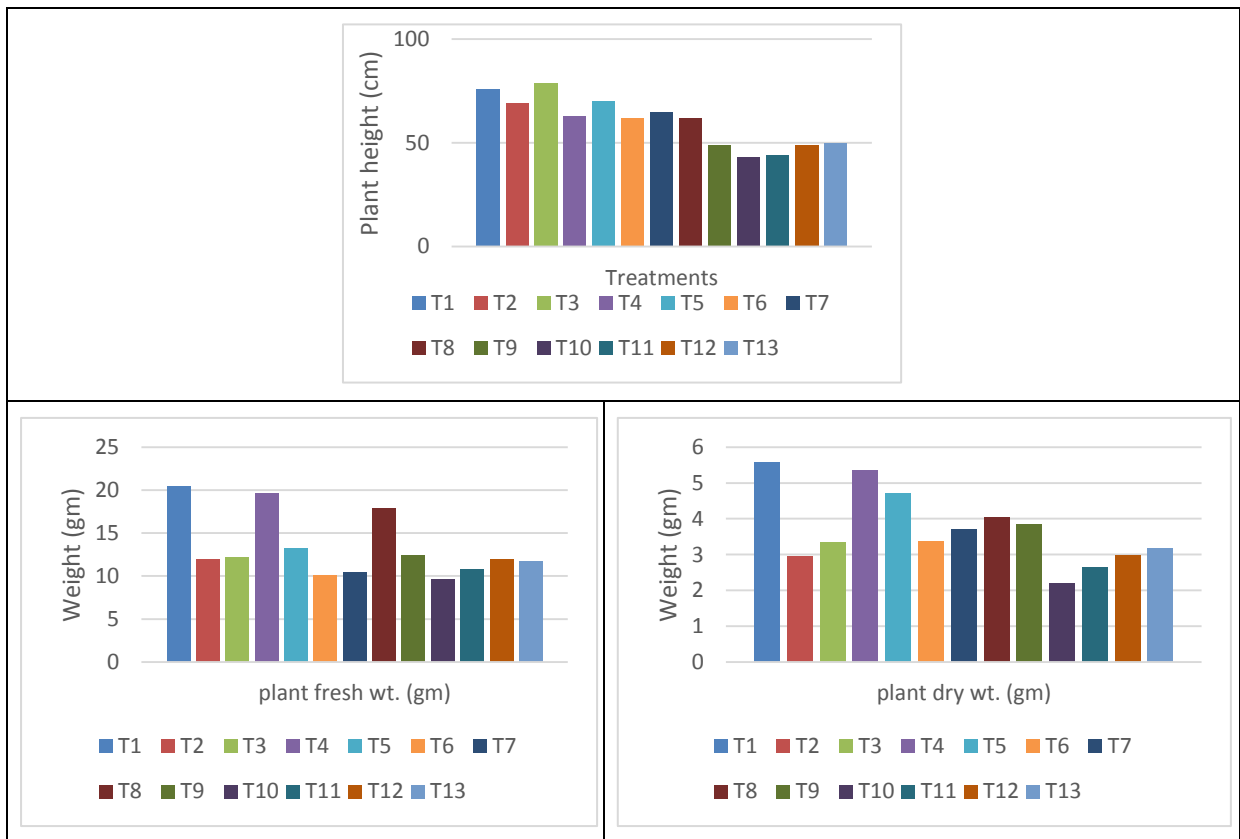


Fig. 1. Effect of salinity and potassium on plant height, plant FW and plant DW at harvesting stage of mungbean.

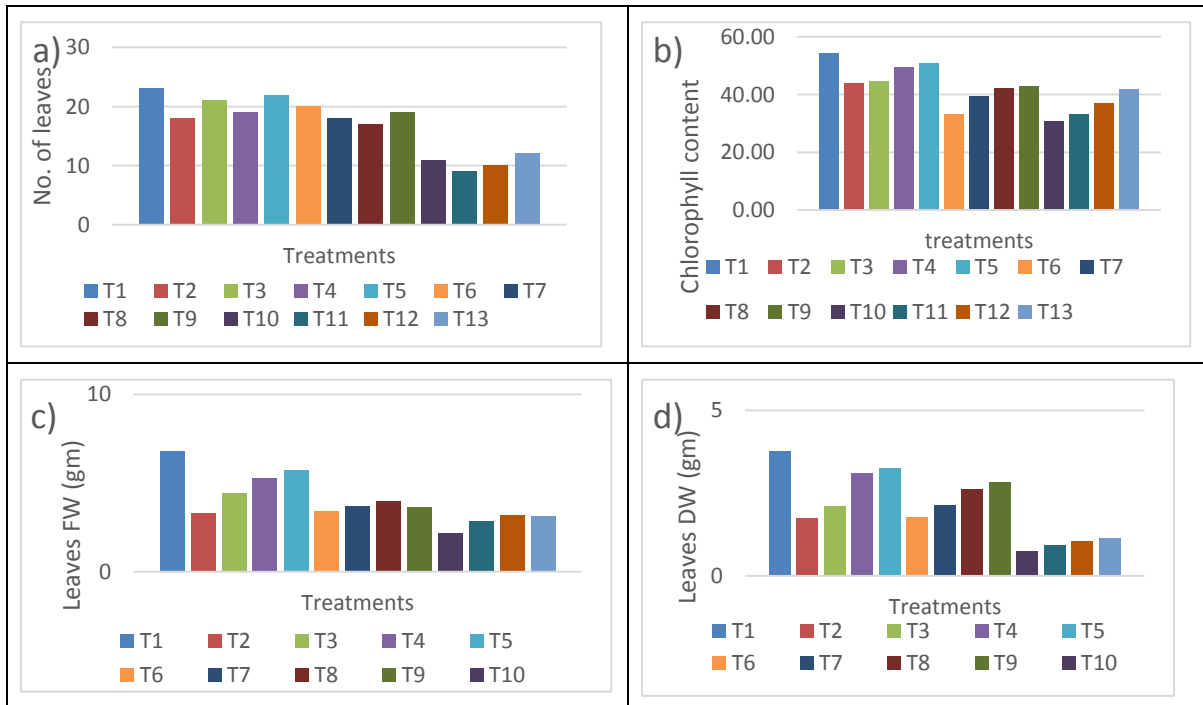


Fig. 2. Effect of salinity and potassium on number of leaves, leaves fresh weight and dry weight at harvesting stage of mungbean.

The results for number of leaves, leaves fresh weight (FW) and dry weight (DW) are given in fig: 2. (a, b, c) and pod fresh weight (FW) and dry weight (DW) are given in fig: 3 (a, b). These parameters were affected by salinity and potassium except number of leaves. No. of leaves did not show any response to potassium fertilizer levels. It was not also affected by low to mild salinity, but at 12 dS/m salinity it decreased markedly. Chlorophyll content at harvesting stage was affected by salinity and potassium (fig: (2.b)). With the increasing level of salinity chlorophyll content was decreased and decreasing level of K chlorophyll content was also decreased Therefore, the percent reduction in chlorophyll level of K chlorophyll was range from 7-18 % in 4 dS/m level of the salinity, 21-39 % in 8 dS/m level of the salinity and 23-43 % in 12 dS/m level of the salinity. The fig: (2.c, d) showed that leaves FW and DW were already reduced at 4 dS/m salinity level and the reduction continued to increase as the salinity increased from 4 to 12 dS/m. The average decrease in leaves FW and DW at 4 dS/m salinity level was approximately 16-51% for FW and 14-54% for DW, at 8 dS/m salinity level was 42-50% for FW and 25-53% for DW and at 12 dS/m salinity level it was 53-68% for FW and 70-81% DW. Leaf chlorosis was observed in plant treated with 12 dS/m salinity. The effect of combination treatments of 12 dS/m salinity with 150 % of disappeared leaf chlorosis in comparison to that treated with saline water with 0%, 100% or 125% of K.

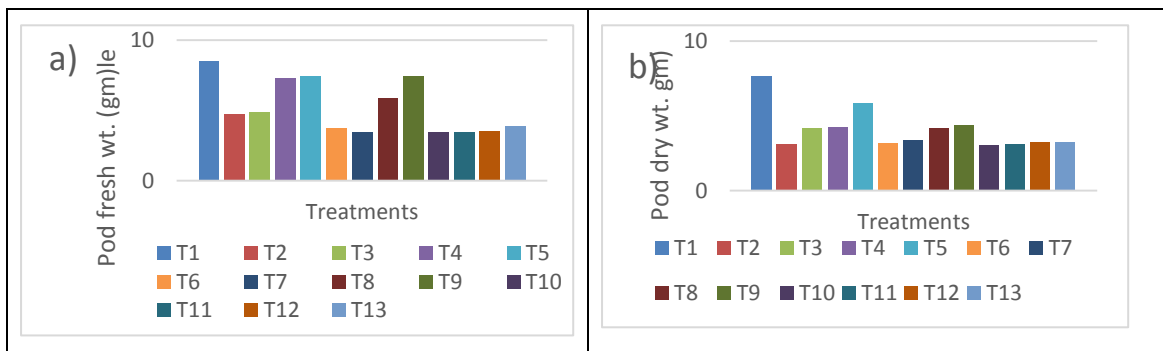


Fig. 3. Effect of salinity and potassium on pod fresh weight and dry weight at harvesting stage of mungbean.

Comparing control plants, pods fresh weight and dry weight reductions in 4 dS/m salinity was 13-44% and 24-60%, in 8 dS/m salinity was 13-60% and 43-58% and in 12 dS/m salinity was 55-60% and 58-61% respectively.

At each salinity level, leaves FW and DW and pods fresh weight and dry weight reduction was decreased as the application of K was increased. Therefore, application of higher level of potassium treatments increased FW and DW of leaves and pods of mungbean. However, the percent reduction in FW and DW of leaves and pods due to salinity was more in 0% K application treatments than others K application treatments.

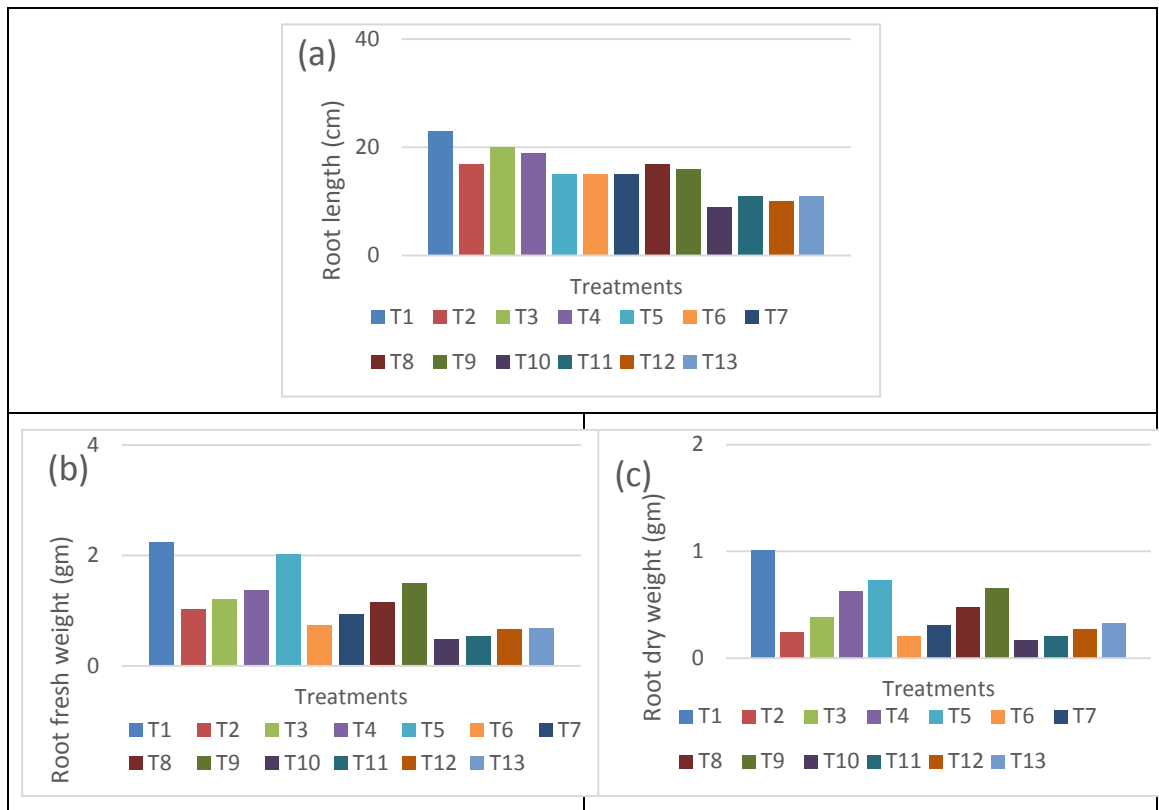


Fig. 4. Effect of salinity and potassium on root height, root FW and root DW at harvesting stage of mungbean.

Fig: 4 shows that Salinity levels, strongly affected the root length, root FW and root DW, and these parameters decreased linearly with increasing salinity levels. Potassium fertilizer levels did not have any effect on root length. Potassium application significantly affected dry and fresh weights of roots for any salinity level with different K doses. There was a significant positive fresh weight and dry weight response to K application. Root FW and DW were reduced with different levels of salinity under different potassium treatments compared to the control. Whereas, application of 150% of K increased the production of relative root fresh weight and dry weight (DW) at every salinity levels compared to the control. At 4 dS/m salinity the relative root FW and DW in ranged from 10 to 55% and 28 -76%, at 8 dS/m salinity from 34-68% and 36-80% and at 12 dS/m salinity from 70-80% and 67-83% respectively. Therefore, the percent reduction in root FW and DW due to salinity was more in 12 dS/m levels of the salinity treatments than others. However, application of increasing rate of potassium increased relative root FW and DW in all salinity levels. And this increasing rate was more in 150% K application treatments than others.

Saline irrigation significantly ($P < 0.001$) decreased mungbean yield, plant height, root length, number of leaves and all fresh and dry weight of different parts of mungbean as compared to control. The K addition improved almost all the parameters except plant height, root length and number of leaves. It has been previously reported that increased soil salinity resulted in reduction of plant growth, yield and in severe case, total crop failure (Qadir et al., 2000). In saline soils, water uptake by roots was limited because of higher osmotic potential which increased Na and Cl toxicity and thus plant production was affected in salt-affected soils (Flowers and Yeo, 1986).

Salinity stress interfere the uptake and accumulation of essential nutrients (Shannon and Grieve, 1999). Generally, Ca^{2+} and K^+ are decreased in plants under saline conditions. These decreases could be due to the antagonism of Na^+ and K^+ at uptake sites in the roots, the effect of Na^+ on K^+ transport into the xylem or the inhibition of uptake processes (Al-Harbi, 1995).

Additional Potassium application affected on the percent amount of calcium, potassium, magnesium, phosphorus and sodium concentration in mungbean plants (Table-3 & 4). Figures 1-4 and table 3-4

showed that calcium, potassium and magnesium content in leaves, stems, seeds and roots of mungbean under salinity treatments, significantly increased and sodium content decreased with increasing potassium levels.

The mungbean plants chemical analysis revealed that applied saline irrigation water affected ionic concentrations (Table 3&4). Salinity stress caused an increase in Na⁺ content and a considerable decrease in K⁺ content, resulting in a significant increase in the Na⁺/K⁺ ratio. The Na⁺ content was increased in mungbean plants and roots with increasing salinity level with 0% K level. The highest Na⁺ content was 2.4% for leaves, 9.49% for stems, 2.45% for seeds and 2.89% for roots. In contrast, the K⁺ content decreased 1.98% for leaves, 2.14% for stems, 1.58% for seeds and 0.28% for roots with increasing salinity level with 0% K level. According to Blumwald et al. (2000), the decrease in K⁺ concentration due to NaCl may be attributed to a high external Na⁺ concentration. Wakeel et al.(2011) suggested that the Na⁺ toxicity affects plant growth, increased Na⁺/K⁺ ratio and thus displacement of K⁺ by Na⁺ in the plant cell affects the activity of plasma membrane (PM) H⁺-ATPase. Addition of 150% and 125% K⁺ to the highest salinity stressed plants reduced the Na⁺ (1.26% for leaves, 1.66% for stems, 1.94% for seeds and 1.78% for roots and 1.75% for leaves, 1.93% for stems, 2.13% for seeds and 1.88% for roots respectively) and increased K⁺ (2.56% for leaves, 3.6% for stems, 2.19% for seeds and 0.51% for roots and 2.53% for leaves, 3.45% for stems, 2.18% for seeds and 0.5% for roots respectively) content within plants and roots. Na⁺/K⁺ ratio increased (1.21% for leaves, 4.43% for stems, 1.55% for seeds and 10.32% for roots) with increasing salt doses (12 dS/m) with 0% K level. Therefore, it can be said that, the elevation of KCl concentration in the saline nutrient solution has been proven to be effective in increasing K⁺/Na⁺ ratio in mungbean plants and roots. However, this increased ratio influenced mungbean yield and all other growth parameters.

Table 3. Chemical composition of mungbean leaves and stem as affected by the application of K under saline irrigation water

Treatment s	Leaf nutrient content (%)						Root nutrient content (%)					
	Ca	Mg	K	P	Na	Na:K	Ca	Mg	K	P	Na	Na:K
T ₁	6.89	3.38	3.71	1.2	0.33	0.09	7.44	3.38	8.75	1.33	0.45	0.05
T ₂	3.44	2.31	2.9	0.88	1.18	0.41	3.05	1.68	2.73	0.77	3.13	1.15
T ₃	3.68	2.54	3.17	0.93	1.03	0.32	3.94	2.14	4.55	0.91	2.92	0.64
T ₄	4.77	2.87	3.23	1	0.99	0.31	4.13	2.57	4.61	1	2.39	0.52
T ₅	5.02	3.02	3.41	1.18	0.87	0.26	5.66	3.38	5.05	1.05	2.05	0.41
T ₆	2.08	1.98	2.37	0.61	1.58	0.67	2.44	1.58	2.62	0.64	5.36	2.05
T ₇	3.26	2.06	2.67	0.67	1.31	0.49	3.67	1.67	4.07	0.68	4.03	0.99
T ₈	4.08	2.19	2.81	0.77	1.2	0.43	4.13	1.79	4.07	0.69	3.82	0.94
T ₉	4.38	2.37	2.96	0.82	1.34	0.45	4.7	1.88	4.27	0.86	3.56	0.83
T ₁₀	1.19	1.85	1.98	0.28	2.4	1.21	1.63	0.74	2.14	0.34	9.49	4.43
T ₁₁	2.5	1.91	2.08	0.34	1.88	0.90	2.28	1.04	2.84	0.36	7.54	2.65
T ₁₂	3.03	1.97	2.53	0.43	1.75	0.69	3.13	1.39	3.45	0.59	6.66	1.93
T ₁₃	3.4	2.01	2.56	0.63	1.26	0.49	3.63	1.64	3.6	0.65	5.98	1.66

Table- 4. Chemical composition of mungbean seeds and roots as affected by the application of K under saline irrigation water

Treatments	Seed nutrient content (%)						Stem nutrient content (%)					
	Ca	Mg	K	P	Na	Na:K	Ca	Mg	K	P	Na	Na:K
T ₁	3.41	1.55	3.13	0.87	0.28	0.09	3.29	1.49	2.03	1.03	0.61	0.30
T ₂	2.21	1.01	2.01	0.62	1.27	0.63	1.8	1	1.13	0.46	2.14	1.89
T ₃	2.23	1.23	2.78	0.8	1.09	0.39	1.94	1.12	1.14	0.71	1.97	1.73
T ₄	2.71	1.23	2.79	0.83	1.09	0.39	2.71	1.13	1.17	0.76	1.46	1.25
T ₅	3.34	1.32	2.89	0.85	0.98	0.34	2.18	1.23	1.34	0.85	1.38	1.03
T ₆	1.7	0.69	1.71	0.5	1.97	1.15	2.21	0.88	0.47	0.28	2.4	5.11
T ₇	2.01	1.2	2.19	0.75	1.66	0.76	2.38	0.97	0.61	0.41	2.31	3.79
T ₈	2.64	1.22	2.51	0.76	1.39	0.55	3.29	0.99	0.84	0.41	1.88	2.24
T ₉	2.69	1.23	2.56	0.77	1.2	0.47	4.47	1.04	1.05	0.62	1.62	1.54
T ₁₀	1.25	0.57	1.58	0.47	2.45	1.55	0.67	0.31	0.28	0.15	2.89	10.32
T ₁₁	1.51	0.69	2.06	0.68	2.27	1.10	1.3	0.59	0.39	0.29	1.31	3.36
T ₁₂	1.51	0.77	2.18	0.68	2.13	0.98	2.14	0.82	0.5	0.31	0.94	1.88
T ₁₃	1.97	0.89	2.19	0.71	1.94	0.89	2.5	0.94	0.51	0.36	0.91	1.78

Table- 5. Chemical characteristics of the experimental soil after harvesting of the mungbean

Treatments	EC		pH	Ca	Mg	K	P	S	B	Zn	Na	Na:K	Ca:K
	dSm												
	5 cm	15 cm		meq/100ml			µg/ml						
T ₁	0.54	0.16	6.4	4.28	2.58	0.18	257	197.3	1.3	11.6	0.44	2.44	23.78
T ₂	5.04	3.98	6.4	2.63	1.65	0.23	193	79.9	1.1	10.1	1.01	4.39	11.43
T ₃	5.61	4.14	6.5	3.2	2.08	0.28	257	111.7	1.1	11.1	0.88	3.14	11.43
T ₄	5.29	2.59	6.3	3.64	2.22	0.37	241	187.2	1.2	11.3	0.81	2.19	9.84
T ₅	5.06	2.59	6.5	3.87	2.43	0.46	257	187	1.2	11.5	0.67	1.46	8.41
T ₆	5.86	3.85	6.2	2.48	1.85	0.24	205	111.5	0.98	10.3	1.49	6.21	10.33
T ₇	5.74	4.77	6.3	2.78	2.11	0.37	239	153	0.99	11.1	1.11	3.00	7.51
T ₈	6.13	3.43	6.4	3.41	2.27	0.4	249	159.9	1.1	11	0.94	2.35	8.53
T ₉	6.44	4.7	6.4	3.45	2.3	0.42	238	182	1.1	11.3	0.89	2.12	8.21
T ₁₀	8.44	3.52	6.2	2.28	0.95	0.22	188	69.3	0.92	9.8	2.27	10.32	10.36
T ₁₁	8.12	6.52	6.3	3.11	1.1	0.25	199	141.9	9.7	10.3	2.05	8.20	12.44
T ₁₂	9.71	5.29	6.4	3	2.07	0.34	206	132.6	0.99	10.6	1.88	5.53	8.82
T ₁₃	8.16	3.44	6.5	3.33	2.08	0.44	249	141.9	1.2	10.8	1.71	3.89	7.57

Results showed that the saline irrigation increased the EC value. The highest EC value (9.67 at 5 cm depth and 6.52 at 15 cm depth) was obtained from the highest salinity with 0% K level. The application of K affected Na, K, Ca, Mg, P, S, B, Z and ratios of Na:K and Ca:K. The addition of K fertilizers under saline influenced the salts and nutrients dynamics in the soils. A significant decrease in the values of EC, Na, Ca, K, SAR, and increase in pH was observed (Table 5) as compared to control values. The overall higher values of pH in the post-harvest soil might attribute the release of HCO₃ and CO₃ in the soil. The K in soil solution increased with the addition of K fertilizers (Tables 3). Addition of 150% K increased K in soil from 0.23 to 0.46 at 4 dS/m salinity level, 0.24 to 0.42 at 8 dS/m salinity level and 0.22 to 0.44 at 12 dS/m salinity level. Increases in the soluble K in soil

promoted K uptake which could interfere the uptake of other cations (Na, Ca and Mg). These phenomena can reduce adverse effects of the salinity (Abd El-Hadi et al., 2001).

The saline irrigation water had effect on the Na in soil which increased with saline irrigation and decreased with K treatment (Tables 3). The effect of the addition of KCl was decreased Na in soil solution. Correspondingly, the ratios of Na:K, and Ca:K of soil solution also decreased significantly ($P < 0.001$) with K treatments.

Conclusion

Potassium fertilization can eliminate the deleterious effects of salinity on mung bean yield to some extent. Increasing potassium levels caused an increase in plant fresh weight and dry weight and chlorophyll content, except plant height, root length, number of leaves. Additional K application with saline irrigation water had a positive role on nutrient (Ca, Mg, P and K) uptake, except Na uptake which decreased in response to increasing potassium levels. However, this is only a single year data; therefore, no discreet conclusion can be drawn unless the research runs for few more years.

References

- Abd El-Hadi, A.H., Khader, M.S. El-Kholy, M.H., Zahran, F.A., Negm. A.Y. 2001. Phosphorus and potash effects. *Soils, Water and Environ. Res. Inst., ARC, Egypt* Al-Harbi, A.R., 1995. Growth and nutrient composition of tomato and cucumber seedlings as affected by sodium chloride salinity and supplemental calcium. *Journal of plant nutrition*, 18(7), pp.1403-1416.
- Blanco, F.F., Folegatti, M.V. and Henriques Neto, D., 2008. Doses de N e K no tomateiro sob estresse salino: I. Concentração de nutrientes no solo e na planta. *Revista Brasileira de Engenharia Agrícola e Ambiental*, 12(1), pp.26-33.
- Blumwald, E., Aharon, G.S. and Apse, M.P., 2000. Sodium transport in plant cells. *Biochimica et Biophysica Acta (BBA)-Biomembranes*, 1465(1-2), pp.140-151.
- Flowers, T.J. and Yeo, A.R., 1986. Ion relations of plants under drought and salinity. *Functional Plant Biology*, 13(1), pp.75-91.
- Gurgel, M.T., Uyeda, C.A., Gheyi, H.R., de Oliveira, F.H., Fernandes, P.D. and Silva, F.V.D., 2010. Crescimento de meloeiro sob estresse salino e doses de potássio. *Revista Brasileira de Engenharia Agrícola e Ambiental*, 14(1), pp.3-10.
- Haque, S.A., 2006. Salinity problems and crop production in coastal regions of Bangladesh. *Pakistan Journal of Botany*, 38(5), pp.1359-1365.
- Islam, A.M.I.N.U.L., Chandrabiswas, J.A.T.I.S.H., Karim, A.J.M.S., Salmapervin, M. and Saleque, M.A., 2015. Effects of potassium fertilization on growth and yield of wetland rice in grey terrace soils of Bangladesh. *Res. Crop Ecophysiol. J*, 10(2), pp.64-82.
- Kabir, M.E., Karim, M.A. and Azad, M.A.K., 2004. Effect of potassium on salinity tolerance of mungbean (*Vigna radiata* L. Wilczek). *Journal of Biological Sciences*, 4(2), pp.103-110.
- Langer, K., Levchenko, V., Fromm, J., Geiger, D., Steinmeyer, R., Lautner, S., Ache, P. and Hedrich, R., 2004. The poplar K⁺ channel KPT1 is associated with K⁺ uptake during stomatal opening and bud development. *The Plant Journal*, 37(6), pp.828-838.
- Michael, A.M., 1978. *Irrigation: theory and practice*. Vikas
- Negrão, S., Schmöckel, S.M. and Tester, M., 2017. Evaluating physiological responses of plants to salinity stress. *Annals of botany*, 119(1), pp.1-11.
- Qadir, M., Ghafoor, A. and Murtaza, G., 2000. Amelioration strategies for saline soils: a review. *Land Degradation & Development*, 11(6), pp.501-521.
- Salim, M. and Pitman, M.G., 1988. Salinity tolerance of mungbean (*Vigna radiata* L.): seed production. *Biologia plantarum*, 30(1), p.53.
- Shannon, M.C. and Grieve, C.M., 1998. Tolerance of vegetable crops to salinity. *Scientia horticulturae*, 78(1-4), pp.5-38.
- Shimazaki, K.I., Doi, M., Assmann, S.M. and Kinoshita, T., 2007. Light regulation of stomatal movement. *Annual review of plant biology*, 58(1), pp.219-247.
- Wakeel, A., Sümer, A., Hanstein, S., Yan, F. and Schubert, S., 2011. In vitro effect of different Na⁺/K⁺ ratios on plasma membrane H⁺-ATPase activity in maize and sugar beet shoot. *Plant Physiology and Biochemistry*, 49(3), pp.341-345.

PROJECT (ACIAR-KGF):

MITIGATING RISK AND SCALING-OUT PROFITABLE CROPPING SYSTEM INTENSIFICATION PRACTICES IN THE SALT AFFECTED COASTAL ZONES OF THE GANGES DELTA

CONJUNCTIVE USE OF FRESH- AND SALINE WATER FOR MAIZE AND SUNFLOWER CULTIVATION IN COASTAL AREAS OF BANGLADESH

M. A. HOSSAIN¹, S. K. BISWAS², D. K. ROY² AND S.S.A. KAMAR³

Abstract

The experiment was conducted at the two project sites Dacope, (Khulna) and Amtali, (Borguna) during the Rabi season of 2020-21 to make the farmers aware of this proven technology and to promote the use of fresh- and saline water conjunctively for cultivation of two promising crops: maize and sunflower, in saline coastal area of Bangladesh. Two crops (Maize and Sunflower) were used for promoting the technology. BARI Hybrid Maize-9 and BARI Surjomukhi-3 were used as the promoting variety for maize and sunflower, respectively. Two treatments T₁ (Farmers' practice (only two with FW- at 25-30 DAS and at 55-60 DAS)) and T₂ (Conjunctive use of fresh- and saline water (Three- 1 with FW at 25 DAS, and 2 with SW at 50 DAS and 70 DAS)) were applied with three replications to fulfill the targeted objectives. From table 1a, it was observed that all parameters gave given highest result at conjunctive use treatment in both locations. From table 1b, it was observed that all parameters gave highest result at conjunctive use treatment in Amtali, Barguna. For Dacope, Khulna all parameters except grain/cob were obtained highest result at conjunctive use treatment. It was observed from table 2a and 2b that, the irrigation water productivity was found higher in conjunctive use treatments than farmer practice. The water salinity of the canal at Dacope was observed greater compared to Amtali canal due to low and high tide and river water salinity entrance to the canal before protecting the canal for rainwater storage. The soil salinity results showed that slightly higher salt accumulation occurred among the treatments within the top soil layer in 0-15 cm depth than lower depth of soil profiles.

Introduction

In coastal area of Bangladesh, availability of freshwater is reasonably scarce. Pond, groundwater in deeper layer and canal water to some extent are the only source of fresh water. Though groundwater can provide an opportunity for the farmers of some areas to supplement their irrigation requirements and cope with the shortage of the surface fresh water supplies, withdrawal of useable groundwater from deeper layer is costly and strictly restricted to avoid intrusion of saline sea water. In the winter season, when variety of rabi crops are grown and successful growth of these crops are fully dependent on irrigation, availability of these fresh water further decreased as most of the ponds and canals are dried up. So, applying full irrigation for successful growth of rabi crops is not possible only with freshwater. There are substantial sources of saline water, which could be utilized for irrigation if suitable soil, crop and water management are practiced. In most cases, saline water reduces the yield, but with the careful and strategic use of saline water can benefit the farmers by minimize the adverse effect on crop yield. Generally, plants can tolerate salinity as it grows older. That is, at the early growth stages, most of the crops are very sensitive to water salinity. At the later stages, crops have better resisting ability to salinity. This unique characteristic has led the farmers to use of fresh of low saline water at early growth stage and moderate saline water at later growth stage conjunctively to irrigate crops. Conjunctive use of fresh and saline water has already been proved as a good option for growing different rabi crops including maize and sunflower in coastal saline areas of Bangladesh. At present, few farmers of coastal area are being practicing this proven technology. There are some sources of saline water like as canal water, pond water in saline prone areas of Bangladesh that can be used for irrigation. Recently, the cultivation of a wide range of crops such as maize, sunflower, watermelon, wheat, mustard and vegetables following T.Aman harvest has been expanding around

¹CSO (in-charge), IWM Division, BARI, Gazipur

²SSO, IWM Division, BARI, Gazipur

³SO, IWM Division, BARI, Gazipur

surface water sources and shallow wells with low salinity water (Akanda et al., 2015). In most cases, saline water reduces the yield, but with the careful and appropriate soil-water-plant management practices could be used for crop production in saline areas of Bangladesh (Majid and Hossain, 2013). Most of the coastal areas have many surface water bodies filled with moderately saline to high saline water, whereas some of the areas have limited fresh groundwater sources (Hasan et al., 2013). Some areas also have access to non-saline water river through the dry season. Accumulation of salts in the root zone affects the plants at different growth stages (Saqib et al., 2004). Appropriate irrigation scheduling and method are very important for saline water irrigation. Therefore, irrigation scheduling technique is needed to minimize yield reductions and better utilization of surface and ground water sources in coastal regions of Bangladesh. Therefore, this study has been undertaken to identify the salt sensitive stages and better understanding of how crops respond to salinity by applying the conjunctive use of fresh and saline water for irrigation at different growth stages. Therefore, the objectives of this demo was to make more farmers aware of this proven technology and to promote the use of fresh- and saline water conjunctively for cultivation of two promising crops: maize and sunflower, in saline coastal area of Bangladesh.

Materials and Methods

Crops: Sunflower and Maize

Variety: BARI Surjomukhi-3 and BARI Hybrid Maize-9

Treatment:

T₁: Farmers' practice (only two with FW- at 25-30 DAS and at 55-60 DAS)

T₂: Conjunctive use of fresh- and saline water (Three- 1 with FW at 25 DAS, and 2 with SW at 50 DAS and 70 DAS)

Farmer: Dilip Halder

Location: Dacope, Khulna

Farmer: Nasir Pyada

Location: Amtali, Barguna

		Sunflower	Maize
Dacope:	Sowing:	25/12/20	25/12/20
	Harvesting:	12/04/21	12/04/21
	Irrigation:	13/01/21	13/01/21
		26/01/21	26/01/21
		22/02/21	22/02/21
Amtali:	Sowing:	27/12/20	28/12/20
	Harvesting:	05/04/21	08/05/21
	Irrigation:	15/01/21	15/01/21
		28/01/21	28/01/21
		24/02/21	24/02/21

Results and Discussion

Effect of irrigation with fresh- and saline water on yield contributing parameters and yield of sunflower and maize during 2020-2021 was shown in Table 1a and Table 1b. From table 1a, it was observed that all parameters were given highest result at conjunctive use treatment in both locations. The higher yield of sunflower was found 1.84 t/ha and 2.50 t/ha from conjunctive use treatment compared to farmers practice (1.31 t/ha and 2.04 t/ha) in Dacope, Khulna and Amtali, Barguna, respectively.

From table 1b, it was also observed that all parameters were given highest result at conjunctive use treatment in Amtali, Barguna. For Dacope, Khulna all parameters except grain/cob were obtained highest result at conjunctive use treatment. The higher yield of maize was found 7.87 t/ha and 8.84 t/ha from conjunctive use treatment compared to farmers practice (6.68 t/ha and 7.22 t/ha) in Dacope, Khulna and Amtali, Barguna, respectively.

Table 1a. Effect of irrigation with fresh- and saline water on yield contributing parameters and yield of sunflower during 2020-2021

Treatment	Plant height (cm)	Head dia, cm	Seed/head, no	Seed wt/head (g)	100-seed wt., g	Seed yield (t/ha)
Dacope, Khulna						
T1(FP)	68	14.3	453	26.10	5.68	1.31
T2(CU)	77	15.4	514	30.20	6.35	1.84
SD	6.32	0.75	42.10	2.84	0.43	0.372
Barguna						
T1(FP)	85	29	280	27.2	7.33	2.04
T2(CU)	101	35	339	31.6	7.80	2.50
SD	10.31	4.32	40.72	3.11	0.33	0.33

Table 1b. Effect of irrigation with fresh- and saline water on yield contributing parameters and yield of maize during 2020-2021

Treatment	Plant height (cm)	Cob length (cm)	Cob perimeter (cm)	Grain/cob (no.)	1000-grain wt., (g)	Yield (t/ha)
Dacope, Khulna						
T1(FP)	169	17.6	11.6	427.3	22.24	6.68
T2(CU)	176	18.2	13.9	442.7	24.36	7.87
SD	7.95	0.46	2.68	10.89	1.50	0.63
Amtali, Barguna						
T1(FP)	186	17.75	11.5	436.8	22.88	7.22
T2(CU)	195	18.75	13.7	454.7	25.12	8.84
SD	6.36	0.71	1.56	12.66	1.58	0.95

Water productivity

Irrigation water productivity of sunflower and maize during 2020-2021 was shown in Table 2a and Table 2b. It was observed that, the irrigation water productivity was found higher in conjunctive use treatments than farmer practice. The number of irrigation and irrigation water applied were also higher in conjunctive use treatments than the farmer practice. Though the irrigation water applied in Conjunctive use treatments but the yield was found highest at this treatment. So it can be stated that the effective water use in conjunctive use treatment were higher than farmer practice treatment.

Table 2a. Irrigation water productivity of sunflower

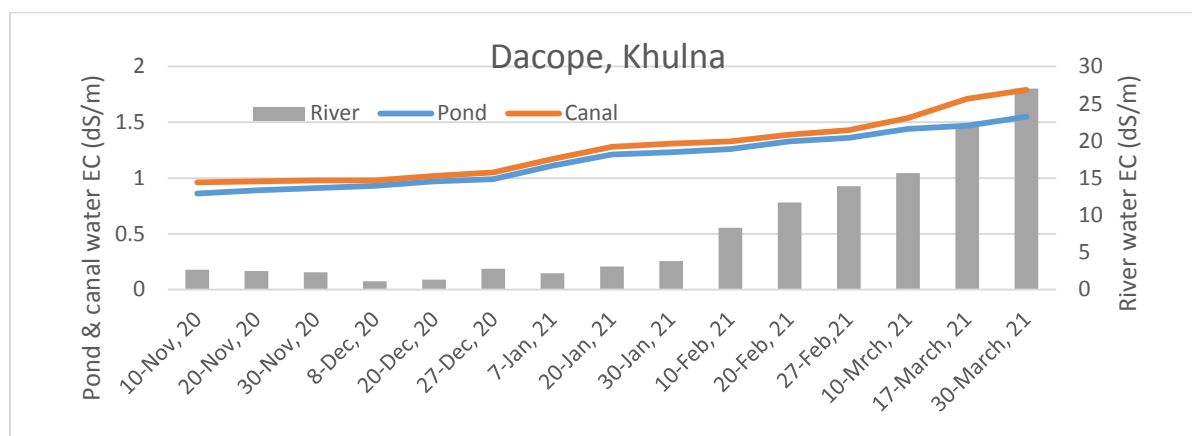
Treatment	No. of irrigation	Irrigation water applied, mm	Yield (t/ha)	Irrigation water productivity (kg/m ³)
Dacope				
T1(FP)-FI	2	111	1.31	1.18
T2(CU)-AFI	3	132	1.84	1.39
Amtali				
T1(FP)	2	116	2.04	1.76
T2(CU)	3	141	2.50	1.77

Table 2b. Irrigation water productivity of maize

Treatment	No. of irrigation	Irrigation water applied, mm	Yield (t/ha)	Irrigation water productivity (kg/m ³)
Dacope				
T1(FP)-FI	2	132	6.68	5.06
T2(CU)-AFI	3	154	7.87	5.11
Amtali				
T1(FP)	2	138	7.22	5.23
T2(CU)	3	157	8.84	5.63

Water salinity

Water salinity of pond, canal and river were recorded at 10 days interval during the crop growing season (November, 2020 – April, 2021) for both locations are shown in Fig. 1. The water salinity of the pond ranged from around 1.5 (November 2020) to 3.5 dS/m (April 2021) at with an average of 2.7 dS/m at Tildanga, Dacope. The water salinity of the canal ranged from around 2 to 3.8 with an average of 2.9 dS/m at Tildanga, Dacope. The average water salinity of the tubewell was 1.23 dS/m throughout the crop growing season at Amtali, Barguna. River water salinity ranged from around 7(Novemembr 2018) to 11 dS/m (April 2019) with an average of 9.5 dS/m at Amtali and 5 (November 2018) to 20 dS/m (April 2019) with an average of 13 dS/m at Tildanga, Dacope. The water salinity of the canal at Dacope was observed greater compared to Amtali canal due to low and high tide and river water salinity entrance to the canal before protecting the canal for rainwater storage. The water was not available to the canal of Sikhandarkhali, Amtali from mid-February to March during 2019 which hampered to the crop production at the project sites. After protecting the canal, water salinity was observed similar trend in pond water due to protect the low and high tide and protect the entrance water salinity to the canal and increase the rainwater storage in the canal during rain.



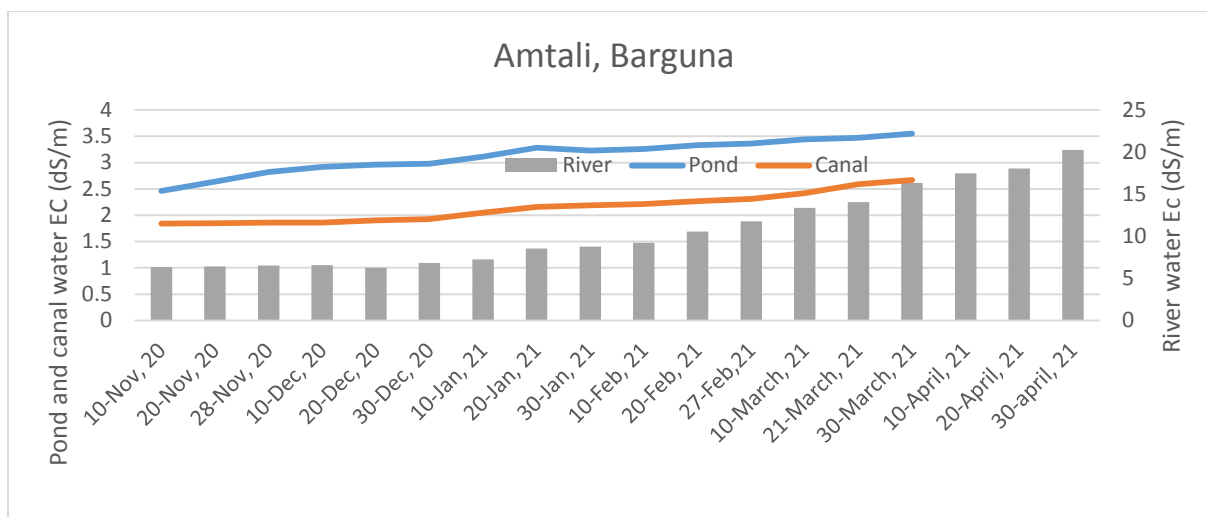
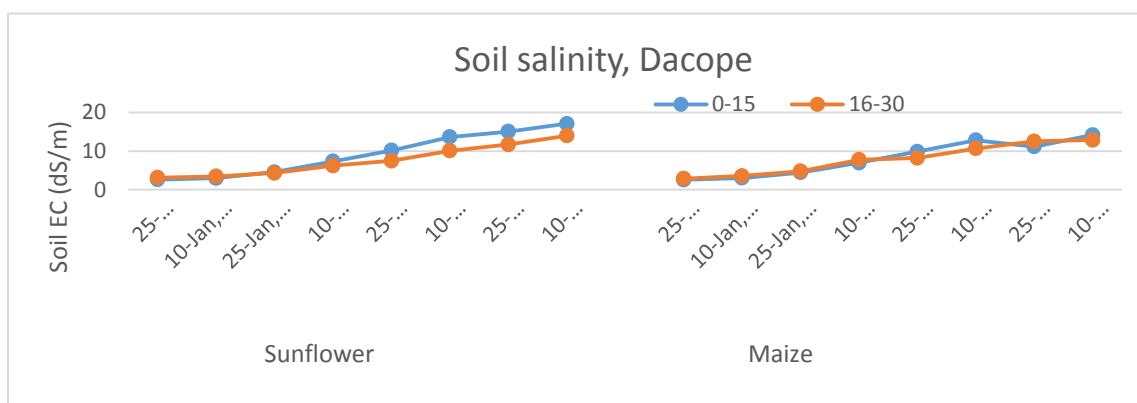


Fig. 1 Pond, canal, and river water salinity at Dacope, Khulna and Amtali, Barguna

Soil salinity

Salinity of field soil water (EC_w) during the growing season for various treatments is shown in Fig. 2. On average, the changes in salinity of field soil water varied from around 4 dS/m (December 2020) to 25 dS/m (February 2019) in 0-60 cm soil profiles with 15 cm increments at Tildanga, Dacope, Khulna and 4-15 dS/m at Amtali, Barguna. The exact soil salinity (EC_e) varied from around 2 to 13 dS/m at Tildanga and 2 to 7 dS/m at Amtali during the crop-growing season. The highest salt accumulation was occurred in mid to end of the February 2019 in all treatments in soil profiles. The salinity results showed that slightly higher salt accumulation occurred among the treatments within the top soil layer in 0-15 cm depth than lower depth of soil profiles. Due to water uptake and soil evaporation, salt accumulation was generally higher in the soil surface. In treatment T_3 , T_4 , salt accumulation was slightly higher than the treatment of T_1 due to consequence use of alternative medium saline water (2 to 3.5 dS/m) irrigation from canal to crop. In this study, the figures indicate that the soil salinity was not substantially greater salt accumulation in soil profiles among the treatments due to medium saline water (2 to 3 dS/m) irrigation and salinity may tolerable for wheat/barley germination to crop yield production in the coastal areas of Bangladesh. Consequently, barley cultivation would be practiced and optioned for intensifying cropping system with salinity and available water scarcity problem in the coastal areas of Bangladesh.



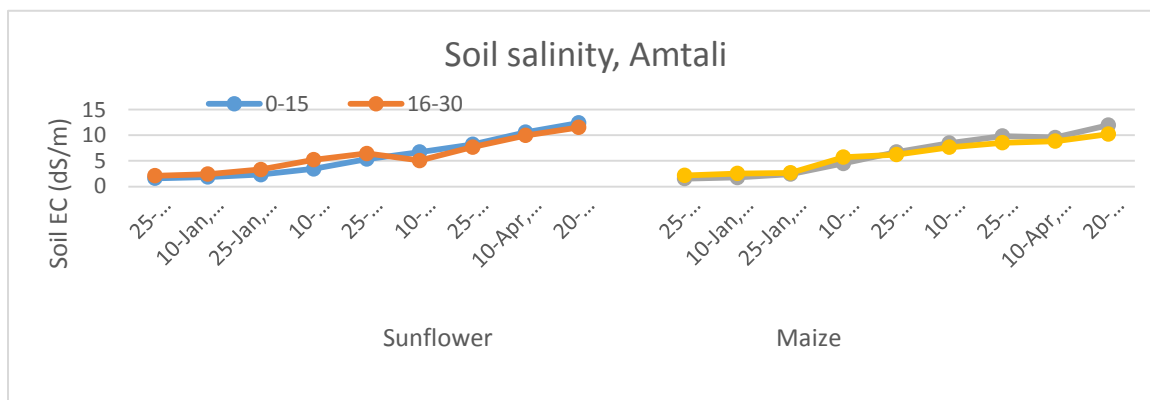


Fig. 2 Soil salinity at Dacope, Khulna and Amtali, Barguna

Conclusion

It could be stated that sunflower and maize were gave highest yield at conjunctive use treatment in both locations. The irrigation water productivity was found higher in the conjunctive use treatment than farmer practice. The water salinity of the canal at Dacope was observed greater compared to Amtali canal due to low and high tide and river water salinity entrance to the canal before protecting the canal for rainwater storage. The soil salinity results showed that slightly higher salt accumulation occurred among the treatments within the top soil layer in 0-15 cm depth than lower depth of soil profiles.

Reference

- Akanda, A.R., Biswas, S.K., Sarker, K. K., Mondal, M.S., Saleh, A.F. Rahman, M.M. and Mosleuddin, A.Z.M. (2015).Response of wheat, mustard and watermelon to irrigation in saline soils. The paper was presented in 'Productive, profitable and resilient agriculture and aquaculture systems', a project of the CGIAR Challenge Program on Water and Food (CPWF) and the CSISA Bangladesh project, funded by USAID. Pp.492-503.
- Hasan MR, Shamsuddin M, Hossain AFMA (2013) Salinity status in groundwater: a study of selected upazilas of southwestern coastal region in Bangladesh. *Glob Sci Technol J* 1(1):112–122
- Mojid, M. A. and Hossain, A. B. M. Z. 2013. Conjunctive Use of Saline and Fresh Water for Irrigating Wheat (*Triticum aestivum* L.) at Different Growth Stages. *The Agriculturists*, 11(1): 15-23
- Saqib, M., Akhtar, J. and Qureshi, R. H. 2004. Pot study on wheat growth in saline and water logged compact soil. *Soil and Tillage Research*, 77:169-177.

LOW COST DRIP IRRIGATION FOR TOMATO AND CHILI CULTIVATION IN SALINE COASTAL AREAS OF BANGLADESH

M.A. HOSSAIN¹, S.K. BISWAS², D.K. ROY² AND S.S.A. KAMAR³

Abstract

The experiment was conducted at the two project sites of Dacope, (Khulna) and Amtali, (Borguna) during the Rabi season of 2020-21 to promote the drip irrigation system and to increase the crop productivity and improve livelihood of small farmers for cultivation of two high value crops: tomato and chili, in saline coastal area of Bangladesh. BARI Tomato-3 and local chili variety were used for cultivation. Two treatments T₁ (Farmers' practice) and T₂ (Drip irrigation at 3-day interval) were applied with three replications to fulfill the targeted objectives. From table 1a and 1b, it was observed that all parameters were gave highest result at T₂ treatment in both locations. It can be stated from table 2a and 2b that the effective water use in T₂ treatment were higher than farmer practice treatment. The soil salinity was observed higher at flood irrigation treatments than drip irrigation treatment.

Introduction

The agricultural development in the coastal saline area of Bangladesh is constrained by the scarcity of fresh water for dry season irrigation. In winter, cultivation of rabi crops are very limited due to inadequate availability of good quality water for crop irrigation. Ponds and canals water are lowly saline that can be used for irrigation, but the quantity is not enough. Therefore, the presently available pond and canal water needs to be used strategically for high value crops. Drip irrigation systems are a promising water saving technology for the coastal zone (Mahanta et al., 2019; Samui et al., 2020). Mahanta et al. (2019) and Samui et al. (2020) demonstrated that drip irrigation is highly profitable for high value vegetables (though the initial cost is high) such as tomato, chilli, brinjal, cucumber, okra, etc. The system has proved its superiority over other conventional methods of irrigation. This is especially so for irrigating fruit and vegetable crops owing to its precise and direct application of water in the root zone with a considerable saving in fertilizer and water. It also has the potential to increase the yield of crops even at reduced irrigation water application (Yohannes and Tadesse, 1998). Some fertigation studies with tomato, brinjal, okra, pumpkin, watermelon, etc. gave encouraging results in terms of growth, yield, and economic return in coastal area of Bangladesh. Recently, it has created interest among the farmers of coastal area because of increased crop productivity with less water and fertilizer requirement. Considering the shortage of fresh water storage, water-saving irrigation by drip technology should be an attractive option and could be demonstrated among farmers to popularize this technology among the farmers of coastal area for growing high value horticulture crops. Therefore, two field demonstrations were set up with the objectives of making more farmers aware of this proven technology and promoting the use of fresh- and saline water conjunctively for cultivation of two high value crops: tomato and chili, in saline coastal area of Bangladesh.

Objectives:

- To promote the drip irrigation system for cultivation of different rabi crops in saline coastal area
- To increase the crop productivity and improve livelihood of small farmers

Materials and Methods

Crops: Tomato and Chili

Variety: BARI Tomato-3 and Local

Treatment:

T₁: Farmers' practice

T₂: Drip irrigation at 3 day interval

¹ CSO (in-charge), IWM Division, BARI, Gazipur

² SSO, IWM Division, BARI, Gazipur

³ SO, IWM Division, BARI, Gazipur

Farmer: Prodyut Halder

Location: Dacope, Khulna

Farmer: Jahir Talukder

Location: Amtali, Barguna

Dacope	Tomato	Chilli
Date of sowing	25/12/20	25/12/20
Date of harvesting	From 21/02/21 to 13/04/21	From 25/02/21 to 23/04/21
Amtali	Tomato	Chilli
Date of sowing	26/02/20	27/02/20
Date of harvesting	From 18/02/21 to 30/03/21	From 10/03/21 to 04/04/21

Results and Discussion

Effect of drip irrigation on yield and yield contributing parameters of tomato and chilli during 2020-2021 was shown in Table 1a and Table 1b. From table 1a, it was observed that all parameters were given highest result at drip irrigation treatment of tomato in both locations. The higher yield of tomato was found 60.56 t/ha and 55.47 t/ha from drip irrigation treatment compared to farmers practice (45.34 t/ha and 43.78 t/ha) in Dacope, Khulna and Amtali, Barguna, respectively. From table 1b, it was also found that all parameters were given highest result at drip irrigation treatment of chilli in both locations. The higher yield of chilli was found 1.92 t/ha and 1.44 t/ha from drip irrigation treatment compared to farmers practice (1.20 t/ha and 1.14 t/ha) in Dacope, Khulna and Amtali, Barguna, respectively.

Table 1a. Effect of drip irrigation on yield and yield contributing parameters of tomato during 2020-2021

Treatment	Plant height	Branch/pl	Wt. of fruit/plant (no.)	Wt. of fruit/plant (kg)	Yield (t/ha)
Dacope, Khulna					
T1-FI	64.6	5.8	25.4	2.4	45.34
T2-Drip irrigation	68.8	7.2	30.8	3.2	60.56
Amtali, Barguna					
T1-FI	59	6.8	24.8	2.2	43.78
T2-Drip irrigation	66.4	7.6	31.4	2.56	55.47

From table 1b, it was observed that all parameters were given highest result at T₂ treatment in both locations.

Table 1b. Effect of drip irrigation on yield and yield contributing parameters of chilli during 2020-2021

Treatment	Plant height	Branch/plant	No of fruit/pl	100- chili, g	Yield (t/ha)
Dacope, Khulna					
T1-FI	56	4.8	25.4	193	1.20
T2-Drip irrigation	67	5.6	32.8	231	1.92
Amtali, Barguna					
T1-FI	59.1	4.4	27.5	173	1.14
T2-Drip irrigation	63.4	5.0	30.6	187.2	1.44

Water productivity

Irrigation water productivity of tomato and chili during rabi season of 2020- 2021 was summarized in Table 2a and Table 2b. It was observed from table 2a and 2b that, the irrigation water productivity

was found higher in T₂ treatments than farmer practice. The number of irrigation and irrigation water applied were also higher in T₂ treatments than the farmer practice. Though the irrigation water applied in T₂ treatments but the yield was found highest at this treatment. So it can be stated that the effective water use in T₂ treatment were higher than farmer practice treatment.

Table 2a. Irrigation water productivity of tomato during rabi season of 2020- 2021

Treatment	Irrigation water applied, mm	Yield (t/ha)	Irrigation water productivity (kg/m ³)
Dacope			
T1-FI	302	45.34	15.01
T2-Drip	223	60.56	27.15
Amtali			
T1-FI	297	43.78	14.74
T2-Drip	229	55.47	24.22

Table 2b. Irrigation water productivity of chilli during rabi season of 2020- 2021

Treatment	Irrigation water applied, mm	Yield (t/ha)	Irrigation water productivity (kg/m ³)
Dacope			
T1-FI	324	1.20	0.370
T2-Drip	267	1.92	0.719
Amtali			
T1-FI	318	1.14	0.358
T2-Drip	255	1.44	0.564

Soil salinity

Soil salinity of top soil were recorded at 15 days interval during the crop growing season (December, 2020 – April, 2021) are shown in Fig. 1 and Fig 2 for both locations. The soil salinity ranged from 2.0 to 15 dS/m at tomato cultivation at Tildanga, Dacope. The soil salinity was observed high at flood irrigation treatments. The soil salinity ranged from 2.5 to 15.5 dS/m at tomato cultivation at Tildanga, Dacope. The salinity of the canal at Dacope was observed greater compared to Amtali due to low and high tide and river water salinity entrance to the canal before protecting the canal for rainwater storage. The water was not available to the canal of Sikhandarkhali, Amtali from mid-February to March during 2020 which hampered to the crop production at the project sites. After protecting the canal, water salinity was observed similar trend in pond water due to protect the low and high tide and protect the entrance water salinity to the canal and increase the rainwater storage in the canal during rain.

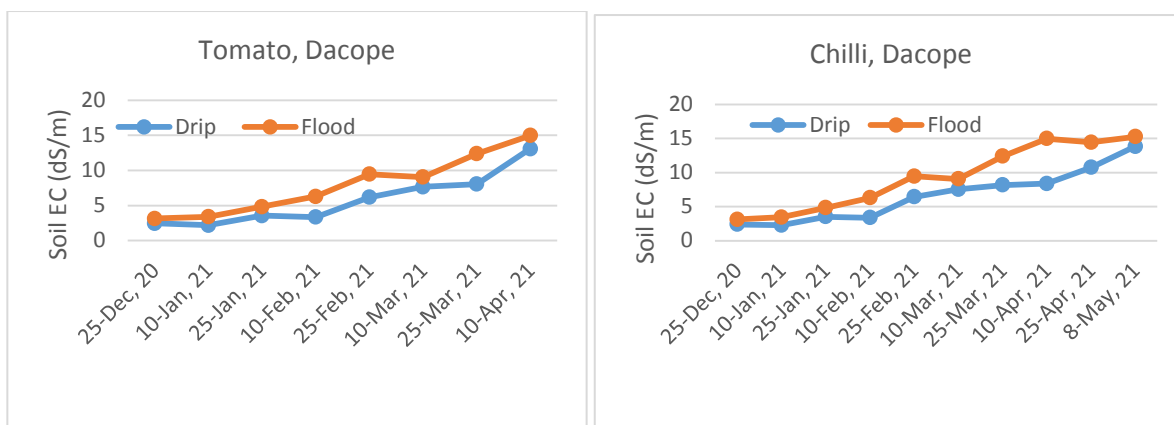


Fig. 1 Salinity of top soil (0 -15 cm) under drip and flood irrigation system for tomato and chili cultivation at Dacope, Khulna.

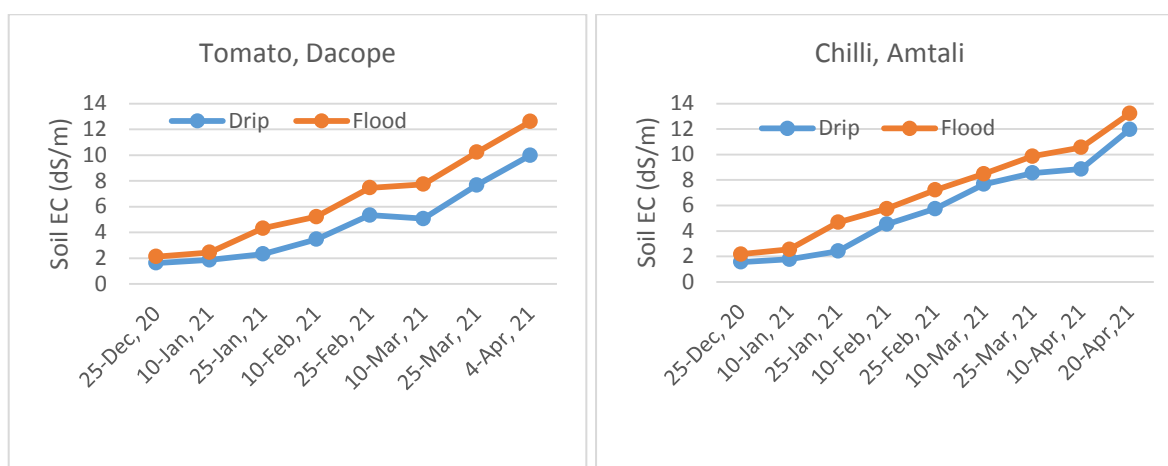


Fig. 2 Salinity of top soil (0 -15 cm) under drip and flood irrigation system for tomato and chili cultivation at Amtali, Barguna.

Conclusion

It was observed (table 1a and 1b,) that yield and yield parameters were given highest result at drip irrigation treatment in both locations. It can be stated (table 2a and 2b) that the effective water use in drip treatment were higher than flood irrigation treatment. The soil salinity was observed higher at flood irrigation treatment than drip irrigation treatment.

Reference

- Mahanta, K.K., Burman, D., Sarangi, S.K., Mandal, U.K., Maji, B., Mandal, S., Digar, S., Mainuddin, M. (2019). Drip irrigation for reducing soil salinity and increasing cropping intensity: case studies in Indian Sundarbans. *Journal of the Indian Society of the Coastal Agricultural Research*, 37(2): 64-71.
- Samui, I., Skalicky, M., Sarkar, S., Brahmachari, K., Sau, S., Ray, K., Hossain, A., Ghosh, A., Nanda, M.K., Bell, R.W., Mainuddin, M., Brestic, M., Liu, L., Saneoka, H., Raza, M.A., Erman, M., Sabagh, A.E.L., (2020). Yield response, nutritional quality and water productivity of tomato (*Solanum lycopersicum* L.) are influenced by drip irrigation and straw mulch in the coastal saline ecosystem of Ganges Delta, India. *Sustainability*, 12, 6779; doi:10.3390/su12176779.
- Yohannes F., Tadesse T. (1998): Effect of drip and furrow irrigation and plant spacing on yield of tomato at Dire Dawa, Ethiopia. *Agricultural Water Management*, 35: 201–207.

GROWTH AND YIELD OF SPINACH AS AFFECTED BY DIFFERENT LEVELS OF IRRIGATION IN COASTAL SALINE AREA OF BANGLADESH

M. A. HOSSAIN¹, S. K. BISWAS², D. K. ROY² AND S.S.A. KAMAR³

Abstract

Water resources are being put under increasing pressure across the globe including Bangladesh. Though most of the vegetable crop, including spinach, requires enough moisture to maintain good yield and quality, improving water productivity is even more important in water scarce situation. With this view, field experiments were conducted in farmers' field of coastal area during 2020 – 2021 to evaluate the effects of different irrigation levels (100%, 80% and 60% ETo) on growth, yield of spinach as well as soil salinity. The experiment was laid out in completely randomized block design with three irrigation regimes (100% ETo, 80% ETo and 60% ETo) replicated three times. Both the yield and yield contributing parameters were found highest under full irrigated treatment, while the highest water productivity was obtained under mild stress treatment of 80% ETo. Mild stress treatment (80% ETo) produced the spinach yield that was at par with full irrigated treatment. Though the most stressed irrigation treatment (60% ETo) produced the lowest yield, water productivity was found even more than full irrigated treatment. Soil salinity recorded in deficit irrigation treatments were slightly higher than that of full irrigated treatment indicated that deficit irrigation in saline coastal area helped accumulating more salt in the soil. Employing deficit irrigation strategies will enable a reduction in requirement of irrigation water which will, in turn, reduce the scarcity of irrigation water in coastal saline area of Bangladesh

Introduction

The agriculture in coastal Bangladesh is facing problems due to inadequate availability of freshwater resources, and ever-growing demand for more efficient food production for the expanding populations. The shortage of water resources of good quality calls for use of marginal quality water such as saline water for crop irrigation as an alternative to fresh water. There are substantial sources of saline water, which could be utilized for irrigation if suitable soil, crop and water management are practiced. In most cases, saline water reduces the yield, but with the careful and strategic use of saline water can benefit the farmers by minimizing its adverse effect on crop yield. Generally, plants can tolerate salinity as it grows older. That is, at the early growth stages, most of the crops are very sensitive to water salinity, while at the later stages, crops gain better tolerance to salinity. This unique characteristic has led the farmers to use fresh or low saline water at early growth stage and moderate saline water at later growth stage conjunctively to irrigate crops. Conjunctive use of fresh and saline water has already been proved as a good option for growing different rabi crops including maize and sunflower in coastal saline areas of Bangladesh. At present, few farmers of coastal area are being practicing this proven technology. But this technology has not yet been tested for growing vegetable crops like spinach, amaranth, etc. Therefore, the objectives of this study was to find out the effects of different irrigation levels on spinach yield and water productivity under conjunctive use of fresh and saline water in salinity affected areas of Bangladesh.

Objectives:

- To find out the effects of different irrigation levels on spinach yield and water productivity under conjunctive use of fresh and saline water
- To make the farmers aware of the use of fresh and saline water conjunctively for spinach cultivation

Materials and Methods

Crop: Spinach

Farmer: Raboti Halder

Variety: BARI Palong-1

Location: Dacope, Khulna

¹ CSO (in-charge), IWM Division, BARI, Gazipur

² SSO, IWM Division, BARI, Gazipur

³ SO, IWM Division, BARI, Gazipur

A field experiment with spinach (variety: BARI Palong-1) was conducted at the farmer's field of Tiladanga village of Dacope, Khulna and Amtali, Barguna during 2020 – 2021 with the aim to determine the growth, yield and irrigation water use efficiency of spinach under different levels of irrigation. The soil was a silty clay loam having a bulk density of 1.44 gm/cc and field capacity of 29.57%. The experiment was designed in a randomized complete block with three treatments and four replications to identify effect of wastewater on the growth and yield of spinach, a popular leafy vegetable in winter season of Bangladesh, including coastal area. The treatments were as follows:

T₁= Irrigation at 100% ETo

T₂= Irrigation at 80% ETo

T₃= Irrigation at 60% ETo

The standard dose of fertilizers was calculated with the help of Fertilizer Recommendation Guide (FRG, 2012) considering soil nutrient status as 84, 8, 37, and 7 kg/ha for N, P, K, and S, respectively. The entire doses of these fertilizers, except nitrogen, were applied and incorporated into soil at the time of final land preparation. Nitrogen was applied in three equal splits: one-third each at final land preparation, and at 25 and 45 DAP as top dressed. Seeds of spinach were sown on 25 and 30 December 2020, respectively, at Dacope and Amtali with spacing of 30 cm x 15 cm in an elementary plot of 6 m x 3 m. Each elementary plots were separated by a 1.0 m buffer to avoid any lateral movement of water from adjacent plots.

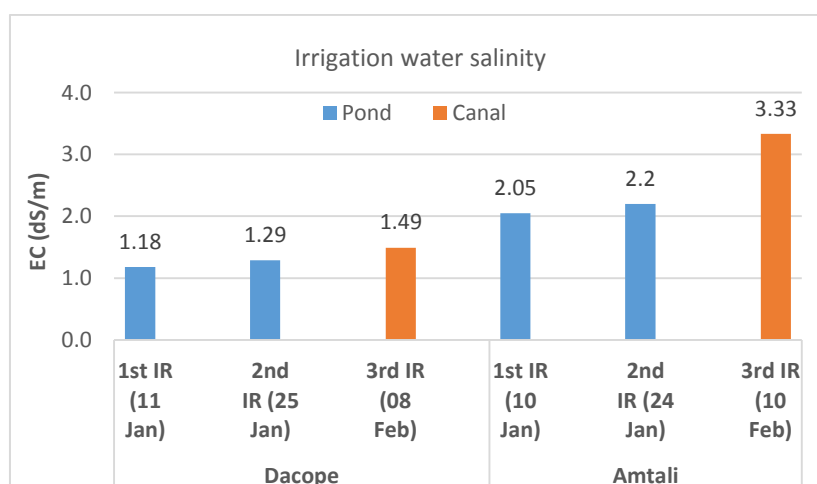


Fig.1. Salinity of pond and canal water used for irrigating spinach crop at Dacope and Amtali areas during 2020 – 2021.

Irrigation water was applied based on the pan evaporation method at different crop growth stages. The calculated amount of irrigation water was supplied to the experimental plots using a polyethylene hose pipe. A light irrigation amounting 20 mm was applied just after sowing to ensure proper germination of seed. Thereafter, irrigation water was applied on weekly basis and stopped one week before harvest. A total of three irrigations was applied: first two irrigations with almost fresh pond water (about 2.0 dS/m) and third irrigation with lowly saline (>3.0 dS/m at Amtali) water (Fig. 1). Crop was harvested on 16 February, 2021 at Dacope and 20 February 2021 at Amtali. At harvest data on plant height, leaves per plant, leaf width and length, fresh yield were collected. Data on soil salinity was also collected to see the salinity dynamics in the growing season. Analysis of variance was done using MSTAT-C package to test the statistical significance ($P \leq 0.05$) of the effects of irrigation on spinach.

Results and Discussion

Growth and yield of spinach

The growth parameters and yield of spinach as obtained under different irrigation regimes are summarized in Table 2. Irrigation regimes had significant impact on plant height, leaves per plant, leaf size, and yield of spinach. On the other hand, deficit irrigation at 60%ETo water regime produced the most inferior crop attributes due to less water availability for plant to grow. In both locations, the tallest plant recorded in the plots treated with 100% ETo and it was 20.5% taller than that receiving water at 60% fertilizer (T₂). This treatment also produced the highest breath (12.53cm) and length of leaves. While treatment T₁ produced the highest leaf length and breadth and the control treatment demonstrated the lowest leaf breadth. Similarly, number of leaves per plant was found maximum in treatment T₁, followed by treatment T₂ and T₃. Number of leaves per plant under treatment T₂ and T₃ was comparable. However, a positive correlation between plant height and leaves per plant was observed. The taller plant had higher number of leaves per plant and vice versa. All these attributes found maximum in 100% ETo water regime which collectively realized the highest yield under this water regime. The yield of spinach under T₂ and T₃ treatments were 21.8 and 39.0% lower than that obtained under T₁ treatment, respectively. The result of this study indicated that spinach should be irrigated with higher water amounts for obtaining higher yield. The change between the yields with applied seasonal irrigation water amounts was significantly linear. Many researchers also found that spinach yield was reduced significantly with the decreased irrigation quantities (Imtiyaz et al., 2000; Leskovar and Piccinni, 2005; Leskovar et al., 2005, 2008).

Table 1. Effect of different irrigation regimes on yield contributing parameters and yield of spinach during 2020-2021

Treatment	Plant population (no./m)	Plant ht.,cm	Leaves/plant	Leaf length,cm	Leaf width, cm	Fresh yield (g/m)	Fresh yield (t/ha)
Dacope							
T1	25	25.22	9.00	19.22	8.88	445.47	17.22
T2	25	23.99	7.66	17.99	7.99	467.11	14.38
T3	30	22.55	6.77	17.33	7.33	561.88	11.42
LSD _{0.05}	5.24	4.12	3.47	3.02	1.86	2.18	4.16
CV(%)	4.46	6.72	5.68	7.23	4.06	6.52	6.39
Barguna						kg	
T1	36.10	22.33	6.55	15.33	10.22	1.505	16.83
T2	31.77	22.33	6.08	14.82	9.52	1.683	13.05
T3	36.88	21.0	5.88	13.87	8.99	1.49	10.90
LSD _{0.05}	6.07	3.35	2.37	2.78	2.76	2.88	4.54
CV(%)	6.62	3.44	6.02	8.03	6.15	7.18	7.14

Water productivity

High crop water productivity values are preferred in water-scarce situation (Geerts and Raes, 2009). Therefore, determining the optimal water amounts applied to plants for obtaining high water productivity is necessary. Irrigation water productivity (IWP) of Indian spinach was increased slightly with the decreasing irrigation quantities at 80% ETo; thereafter it decreased with further decreasing of irrigation regime in both locations (Table 2). IWPs under full irrigated treatment were estimated as 13.04 and 12.4 kg/m³ for Dacope and Amtali site, respectively, which were very close to the values (13.15 and 12.40 kg/m³) obtained under 60%ETo. Even the highest values of WPs that obtained under 80%ETo water regime were not remarkably higher than those obtained under other two treatments. Total irrigation water applied recorded for ETo water regimes were 132 mm for Dacope and 137 mm for Amtali. Amount of irrigation water was linearly decreased from 100%ETo to 60%ETo treatments. But the WP increased when amount of water decreased from 100ETo to 80%ETo regime. Decrease in WP with further decrease in irrigation water quantity at 60%ETo regime indicated that plant felt stress at deficit irrigated treatment 60%ETo. This experiment demonstrated that a reasonably good yield of

spinach can be achieved with higher water productivity and 20% water saving in coastal saline area of Bangladesh. Although treatment 100% ETo received higher amount of water than other treatments, it failed to produce higher WP in both the locations. This may be due to the fact that increased in yield was not proportionate with increased water supply up to a certain limit. Treatment 80% ETo had the highest irrigation water productivity of 13.61kg/m³ at Dacope and 12.91 at Amtali which were identical with other two treatments of 100% and 60% ETo. This result indicated that the highest values of WP were found for the water stressed treatment of 80% ETo, while the overall crop productivity was found the highest in full irrigated treatment. Even the most stressed treatment of 40% ETo produced higher water productivity than full irrigated treatment 100% ETo. Nishihara et al., (2001) also reported highest WP of spinach for the water deficit treatment grown in a greenhouse.

Table 2. Effect of different irrigation regimes on irrigation water productivity of spinach

Location	Irrigation treatment	Irrigation water applied (mm)	Yield(t/ha)	IWP (kg/m ³)
Dacope	100% ETo	132	17.22	13.04
	80% ETo	105.6	14.38	13.61
	60% ETo	79.2	10.42	13.15
Amtali	100% ETo	137	16.83	12.28
	80% ETo	109.6	14.15	12.91
	60% ETo	82.2	10.23	12.44

Soil salinity

Salinity of field soil during the growing season of spinach under different irrigation treatments is shown in Fig. 2. Irrespective of treatments, soil salinity increased gradually from 2.33 dS/m at the time of sowing (last week of December, 2020) to 9.40 dS/m after harvest (February 2021) in top 15 cm soil profile at Tildanga, Dacope, Khulna. While the field soil salinity ranged from 2.02 to 6.70 dS/m at Amtali, Barguna. As soil salinity at sowing time was less than 2.5 dS/m, so it had not any detrimental effect on seed germination. In general, most of the crops' seed do not germinates when soil salinity goes beyond 4.0 dS/m. Though the differences in soil salinity between treatments were minimal, slightly higher salt accumulation occurred in the soil with deficit irrigated treatments (60% and 80% ETo) than that in full irrigated treatment (100% Eto). Deficit irrigation with 60% ETo increased soil salinity by about 7.0% as compared to full irrigated treatment at harvest. In general, soil salinity increases if crop evapotranspiration is higher than irrigation application. Many researchers (Ding, et al., 2020, Alamran, et al., 2013) reported that soil salinity in general increased with decreasing level of applied water. Even though amount of salt added to soil through irrigation water was higher in full irrigated treatment, salt accumulation was not higher in this treatment. This is due to the fact that salt accumulation through capillary rise restricted by irrigation was higher in full irrigated treatment than deficit irrigation treatments.

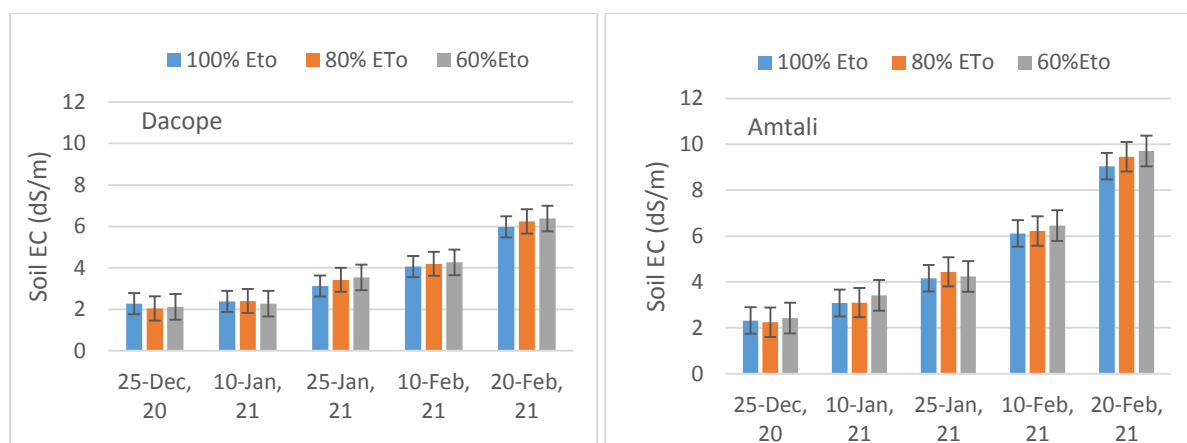


Fig. 2. Soil salinity of spinach field under different irrigation regimes during crop growing season of 2020 – 2021.

Conclusions

Spinach growth and yield was significantly affected by amount of irrigation water applied. Yield increased gradually as amount of irrigation water applied was increased. Spinach yield was found the highest under full irrigated treatment while yield started to decrease when deficit irrigation strategies were employed. Yield under deficit irrigation treatment of 80%ETo was at par with the yield under full irrigated treatment. The water productivity was found the highest with about 20% water saving, while on the other hand, the overall water productivity was slightly decreased. As for water regime, deficit irrigation slightly increased soil salinity as compared to full irrigated treatment. Therefore, considering the spinach yield, water productivity as well as soil salinity, mild deficit irrigation strategies could be practiced in order to save water in water scarce coastal area of Bangladesh.

References

- Imtiyaz, M., N. P. Mgalla, B. Chepete, and S.K. Manase. 1999. Response of six vegetable crops to irrigation schedules. *Agric. Water Manage.*, 45: 331 – 342.
- Nishihara, E., M. Inoue, K. Kondo, K. Takahashi and N. Nakata. 2001. Spinach yield and nutritional quality affected by controlled soil water matric head. *Agric. Water Manage.*, 51: 217 – 229.
- Geerts, S., and D. Raes. 2009. Deficit irrigation as an on-farm strategy to maximize crop water productivity in dry areas. *Agricultural Water Management*, 96 (9), 1275-1284.
- Leskovar, D. I. and G. Piccinni. 2005. Yield and leaf quality of processing spinach under deficit irrigation. *Hortscience*, 40 (6), 1868-1870.
- Leskovar, D. I., G. Piccinni, S. Agehara and K. S. Yoo. 2008. Deficit irrigation and plant population impact on yield, quality and phytochemicals in spinach. Abstracts of the International Spinach Conference. San Antonio, Texas, 30 November–2 December 2008, Texas: A&M AgriLife Extension Service.
- Leskovar, D. I., G. Piccinni and D. Moore. 2005. Deficit irrigation and plant population effects on leaf quality and yield of spinach. *Hortscience*, 40 (4), 1095.
- Alomran, A., I.I. Louki, A. Aly and M.E.A. Nadim. 2013. Impact of deficit irrigation on soil salinity and cucumber yield under greenhouse condition in an arid environment. *J. Agric. Sci and Tech.* 15 (6): 1247 – 1259.
- Ding, Z., A.M.S. Kheir, M.G.A. Ali, O.A.M. Ali, A.I.N. Abdelaal, X. Lin, Z. Zhou, B. Wang, B. Liu and Z. He. 2020. The integrated effect of salinity, organic amendments, phosphorus fractionation and wheat productivity. *Scientific Reports* 10, 2736.

CROP CAFETERIA WITH SOME PROMISING CROPS IN SALT-AFFECTED COASTAL AREAS OF BANGLADESH

M. A. HOSSAIN¹, S. K. BISWAS², D. K. ROY² AND S.S.A. KAMAR³

Abstract

The crop cafeteria was demonstrated at the project site Dacope, (Khulna) during the Rabi season of 2020-21 to make the farmers aware of the cultivation and production technologies of the crops and to motivate farmers to cultivate the demonstrated crops using the adopted technologies. Brinjal, Okra, Chili, Onion, Quinoa were demonstrated with the plot size 20 square meter. **The yield was satisfactory.** Due to scarcity of irrigation water, it was not possible to cultivate vegetables round the year. Vegetable cultivation is very much profitable in this saline area.

Introduction

Soil salinity is one of the serious abiotic stresses that reduce plant growth, development and productivity. The coastal areas of Bangladesh cover about 20% of the country and comprise more than 30% of the cultivable lands of the country. About 30% of the lands of the coastal areas of Bangladesh are affected by salinity. Agricultural land in these areas is under-utilized and cropping intensity in coastal zone of Bangladesh (173%) is significantly below the country's average cropping intensity of 199% (Haque, 2006; BBS, 2011). The factors which contribute to the development of saline soil are tidal flooding during the wet season (June-October), direct inundation by saline water, daily tides and the upward capillary movement of saline ground water during the dry season (November to May) driven by soil evaporation, resulting in surface deposition. The severity of the salinity problem in Bangladesh increases with the desiccation of the soil. The effects of salinity depend on its magnitude at critical stages of crop growth, but in severe cases reduces yield to zero. The dominant crop grown in the saline areas is transplanted Aman (T.Aman) rice which is grown during the kharif-2 season (June-September) using traditional long-duration low-yielding varieties. The primary cropping pattern followed in the coastal areas is Fallow-Fallow-T. Aman. Cropping intensity in the coastal zone of Bangladesh is low and large areas of agricultural land remains fallow during the dry season. But recently, the cultivation of a wide range of crops such as maize, sunflower, watermelon, wheat, mustard and vegetables following T.Aman harvest has been expanding around surface water sources and shallow wells with low salinity water (Akanda *et al.*, 2015). Cropping intensity can be increased in slightly saline areas by adopting proper soil and water management practices and by the introduction of salt-tolerant crop varieties. Bhattacharya *et al.* (2015) reported that a rice-rice-rabi system produced around 18 t/ha/yr of rice equivalent yield (REY) in low salinity regions of the coastal zone of Bangladesh where drainage was possible during the rainy season. Triple rice cropping with a total system production of around 16 t/ha/yr is possible in the coastal zone of Bangladesh in areas where there is year-round fresh water availability, separation of lands of different elevation, and the ability to drain excess water. In the coastal saline zone, with its short winter season, timely sowing/planting of rabi (winter) crops is essential to avoid problems with drought and high salinity late in the season, but this is restricted by late harvest of T. Aman rice. Prolonged water-logging due to inadequate drainage and faulty operation of sluice-gate facilities restricts potential land use for crop production within the polders. Besides, cropping systems depend on climate, soil type and water availability to achieve the desired optimum production through efficient use of available resources, and the patterns of crops are decided upon through consideration of the interaction of farm resources, farm enterprises and the availability of technologies. The diversified rice-wheat cropping system in non-saline soils involving potato, vegetable, peas, groundnut and clever water management practices increases production, economic return and water use efficiency. Crop diversification is an option to achieve paradigm change from the traditional one crop cultivation to two or more crops per year. The proper selection of crops and salt-tolerant cultivars, management of water supplies and maintenance of soil and a suitable soil environment can be ensured under low saline water irrigation. The introduction of maize, sunflower, wheat or mustard in rice systems is necessary to replace the fallow during the winter season. During the rainy season, if the canal/pond has stored excess water, it may provide irrigation to rabi crops. The feasibility of different cropping patterns based on more efficient water management to produce two or three crops in a year have been demonstrated in the salt

affected areas of coastal region in Bangladesh. Therefore, field experiments were undertaken on diversified cropping patterns with different crops and water management practices, aiming to increase the cropping intensity, the crop production, water productivity, and economic returns for farmers in the salt affected areas of coastal zone in Bangladesh.

Objectives:

- To make the farmers aware of the cultivation and production technologies of the crops
- To motivate farmers to cultivate the demonstration crops using the adopted technologies

Materials and Methods

Crops: Brinjal, Okra, Chili, Onion, Quinoa

Farmer: Bipul Halder

Location: Tildanga, Dacope, Khulna

Date of planting/sowing: 25 December 2020

Crop	Date of sowing/planting	Date of harvest
Onion	02/01/21	08/04/21
Quinoa	25/12/20	27/02/21
Brinjal	25/12/20	From 17/03/21 to 25/04/21
Chilli	25/12/20	From 27/02/21 to 23/04/21
Okra	25/12/20	From 15/02/21 to 17/04/21

Results and Discussion

The crop cafeteria with some promising high value crops were cultivated at the project site Dacope, Khulna. The yield was satisfactory. Due to scarcity of irrigation water, it was not possible to cultivate vegetables round the year. Vegetable cultivation is very much profitable in this saline area.

Crop	Yield/plot, kg
Onion	9.65
Quinoa	16.70
Brinjal	8.0
Chilli	2.70
Okra	3.80

Conclusion

Due to scarcity of irrigation water, it was not possible to cultivate vegetables round the year. Vegetable cultivation is very much profitable in this saline area.

Acknowledgement

This project work is supported by the financial aid from the Australian Centre for International Agricultural Research (ACIAR), Australia and Krishi Gobeshona Foundation (KGF), Bangladesh.

References

Akanda, A.R., Biswas, S.K., Sarker, K. K., Mondal, M.S., Saleh, A.F. Rahman, M.M. and Mosleuddin, A.Z.M. (2015). Response of wheat, mustard and watermelon to irrigation in saline soils. The paper was presented in 'Productive, profitable and resilient agriculture and

- aquaculture systems', a project of the CGIAR Challenge Program on Water and Food (CPWF) and the CSISA Bangladesh project, funded by USAID. Pp.492-503.
- Bhattacharya, B.J., Mondal, M. K., Humphreys, E. Saha, N. K, Rashid, M. H., Paul, P. C and Ritu, S. P. (2015).Rice-rice-*rabi* cropping systems for increasing the productivity of low salinity regions of the coastal zone of Bangladesh. The paper was presented in 'Productive, profitable and resilient agriculture and aquaculture systems', a project of the CGIAR Challenge Program on Water and Food (CPWF) and the CSISA Bangladesh project, funded by USAID. pp. 436-448.
- BBS (Bangladesh Bureau of Statistics) (2011).Statistical year book of Bangladesh. Bangladesh Bureau of statistics, Statistics Division, Ministry of planning. Government of the people's Republic of Bangladesh.
- Haque, A.A. 2006. Salinity Problems and Crop Production in Coastal Regions of Bangladesh. *Pakistan Journal of Botany* 38(5): 1359-1365.

MULTI-STEP AHEAD PREDICTION OF GROUNDWATER LEVEL FLUCTUATIONS USING COUPLED WAVELET TRANSFORM AND LONG SHORT-TERM MEMORY NETWORKS

D.K. ROY¹, S.K. BISWAS¹ AND K.F.I MURAD²

Abstract

Groundwater level prediction is important for sustainable usage of scarce groundwater reserves of an aquifer to ensure the development of a meaningful groundwater abstraction management strategy. This study evaluated the prediction accuracy and estimation capability of a deep learning algorithm, Long-Short Term Memory (LSTM) network, for multi-step forward forecast of groundwater levels at two observation wells in an aquifer system of the Gazipur Sadar Upazilla, Bangladesh. Model independent partial autocorrelation functions-based feature selection approach was used to recognize appropriate input variables for the prediction models. Root Mean Squared Error (RMSE) criterion was used to calculate the training and test performance of the LSTM models to select the appropriate numbers of hidden layers and hidden neurons within each hidden layer. The prediction accuracy of LSTM network was evaluated using five statistical performance evaluation indices: RMSE, Scatter Index, Maximum Absolute Error, Median Absolute Deviation, and a-20 index. Results revealed that the developed LSTM models could predict one-, two-, and three-week ahead groundwater levels at the observation wells GT3330001 and GT3330002. In general, the prediction performances of the LSTM models at GT3330001 were better than those at GT3330002. The overall results indicate that the proposed LSTM models could be successfully employed to predict multi-step ahead groundwater levels using previous lagged groundwater levels as inputs. For improving prediction accuracy, wavelet transform based data pre-processing was adopted. To achieve this, a maximal overlap discrete wavelet packet transform (MODWPT) was used to decompose the input variables into wavelet packets. Results demonstrate that the MODWPT can be used to generate more accurate forecasts.

Introduction

Groundwater aquifers are considered to be the vital sources of world's potable water supplies and takes the part of an essential role in the sustainability of irrigated agriculture; domestic and industrial water supplies in areas where good quality surface water is inadequate. Human pressure due to population growth, increasing water demand to different sectors and a changing climate have created an enhanced pressure to groundwater resources, and as a consequence, groundwater systems are coming across a rapid degradation. Although human intervention such as over-pumping is considered to be the prime indicator of groundwater level declination, climate change as evidenced by the recent projections, have indicated that the situation will become even worst earlier than was anticipated (Wada and Bierkens, 2014). Excessive abstraction of groundwater resources leads to continuous depletion and variable fluctuations of groundwater level causing a variety of problems such as lowering of the suction heads of pumps, reduction of crop yields due to inadequate irrigation water supplies, decrease in potable water supplies to domestic and industrial purposes, and degradation of water quality, among others. Like many areas in the world, groundwater is the most important usable form of water reserves in Bangladesh, where approximately 80% of the total population depends primarily on the groundwater reserves for their water needs (Hoque and Adhikary, 2020). Therefore, proper management and sustainable utilization of the scanty groundwater reserves in the aquifer in an efficient manner are imperative to secure continuous supplies of groundwater for the future generations. Accurate prediction and forecasting the future scenarios of groundwater level fluctuations may aid in developing such a meaningful groundwater management strategy.

Numerical simulation models of groundwater flow processes have traditionally been applied in groundwater hydrology to better understand the underlying system processes while predicting the future scenarios of groundwater levels (Doble et al., 2017; Masterson and Garabedian, 2007; Park and Parker, 2008). However, predicting groundwater levels using these physically-based models requires

¹ SSO, IWM Division, BARI, Gazipur 1701

² SO, IWM Division, BARI, Gazipur 1701

detail understanding of the aquifer properties, as well as expertise and in-depth knowledge of the modeler about the aquifer geometry and modelling techniques. It is often difficult to obtain relevant and good quality data on aquifer properties and on other appropriate prerequisites, i.e. model 'initial and boundary conditions' required for the development of physically-based models. Sometimes unavailable data are substituted by assumptions made on the data based on the prior knowledge of the modeler regarding the model domain. These assumptions and estimations may lead to difficulties in the calibration and validation processes, which are very important in employing the developed model in the prediction purposes. To overcome these unavoidable complexities associated with physically-based numerical modelling approaches, data-driven prediction modelling approaches relying on the machine learning and artificial intelligence have been introduced and applied in hydrology (Fahimi et al., 2017; Govindaraju, 2000a, 2000b; Maier et al., 2010; Sadler et al., 2018; Yang et al., 2017). Data-driven modelling does not require an explicit definition of the parameters of the physical systems being modelled. In data-driven modelling approaches, a direct mapping or correlation between the predictors (inputs) and responses (outputs) of a model is established by way of an iterative learning method of a machine learning algorithm (Solomatine and Ostfeld, 2008). Artificial Neural Networks (ANN)-based data-driven prediction models have been found to be performed as good as or even better than the physically based simulation models in the field of prediction of nonlinear time series data, e.g. groundwater table data (Karandish and Šimůnek, 2016; Mohanty et al., 2013). As such, there have been a growing appreciation that data-driven approaches can be utilized as an alternative modelling approach for capturing nonlinear dynamics of the aquifer responses quite accurately (Adamowski and Chan, 2011; Daliakopoulos et al., 2005; Oberghell et al., 2019; Roshni et al., 2019).

Groundwater level prediction comes into play when it is an indispensable task to evaluate the dynamics of the groundwater system, i.e., how much groundwater is being abstracted from the aquifer system and how much is actually permitted to be abstracted. Adequately precise short- to medium-term groundwater level prediction aids in developing a sustainable and flexible management strategy in areas where climate change induced droughts or human induced over-pumping is a major driving force (Feng et al., 2008; Guzman et al., 2017; Sahoo et al., 2017). Therefore, prediction of groundwater levels has been an interesting topic in hydrological research niche and various data-driven modelling tools are progressively being employed because they require less amount of data and are simple to implement when weighed against traditional hydrogeological modelling approaches (Zhang et al., 2018). A number of approaches has recently been utilized in the research domain of groundwater level predictions. These include machine learning-based prediction modelling (Dong et al., 2018; Guzman et al., 2017; Mohanty et al., 2015; Sahoo et al., 2017), ANNs (Ghorbani et al., 2018; Lee et al., 2019), hybridized wavelet transform – machine learning methods (Adamowski and Chan, 2011; Barzegar et al., 2017; Peng et al., 2017; Raghavendra and Deka, 2015), hybridized ensemble empirical mode decomposition and machine learning-based models (Gong et al., 2018), nonlinear autoregressive with exogenous inputs (NARX) neural networks (Guzman et al., 2017), ARIMA-particle swarm optimization (Boubaker, 2017), ANN – whale algorithm (Banadkooki et al., 2020), integrated linear polynomial and nonlinear system identification models (Makungo and Odiyo, 2017), ANFIS (Nadiri et al., 2019; Nourani and Mousavi, 2016; Raghavendra and Deka, 2015; Wen et al., 2015; Zare and Koch, 2018), wavelet – ANFIS (Moosavi et al., 2013), Support Vector Machine (SVM) (Nadiri et al., 2019; Tang et al., 2019), hybrid SVM-PSO (Wei et al., 2020), Gaussian Process Regression (Raghavendra and Deka, 2015), Facebook's prophet approach of groundwater level forecasting (Aguilera et al., 2019), physics-inspired coupled space-time artificial neural networks (Ghaseminejad and Uddameri, 2020). A detailed review of artificial intelligence-based approaches in modelling groundwater levels is presented in Rajaei et al. (2019). It is clear that a number of different modelling approaches has been employed to predict groundwater level fluctuations with varying degrees of prediction accuracies. It is also evident that it is practically difficult, if not impossible to recommend a particular prediction model for a particular problem for predicting groundwater level fluctuations. Therefore, more advanced approaches of groundwater level prediction are still a requirement for boosting the prediction accuracies of groundwater level fluctuations.

Deep Learning (DL) has recently been recognized as a developed and sophisticated sub-domain of machine learning techniques in the arena of artificial intelligence. The DL-based modelling has gain popularity in the successful application to various domain of science including language

processing (Plappert et al., 2018), image classification (Fan et al., 2019), computer vision (Fang et al., 2019), speech recognition (Cummins et al., 2018), and time series prediction (Tien Bui et al., 2020; Xu et al., 2019; Yang and Chen, 2019). The usage of DL has also been observed in developing prediction models in the research niche of groundwater level forecasting (Bowes et al., 2019; Supreetha et al., 2020), and prediction of short-term water quality variable (Barzegar et al., 2020). Recurrent Neural Network (RNN) models are able to preserve a memory of previous network states, and are better suited for predicting groundwater levels through modelling time series of groundwater table data observed at an observation well. For this reason, numerous recent studies related to groundwater modelling (Chang et al., 2016; Daliakopoulos et al., 2005; Guzman et al., 2017) have focused on the successful application of the RNNs. However, the standard RNN architectures cannot properly grab hold of the long-term reliance between variables (Bengio et al., 1994) due mainly to the occurrences of two problems: vanishing and exploding gradients. These are situations where the network weights either reach to zero or turn out to be enormously large during training of the network.

Long Short-Term Memory (LSTM) networks, a variant of typical RNN architectures, is capable of overcoming the training drawbacks (vanishing and exploding gradient problems) of RNNs through retaining valuable information for model development while avoiding unnecessary or redundant information being passed to the subsequent states in the model development process. LSTM has successfully been applied to the research arena of natural language processing, and financial time series prediction (Fischer and Krauss, 2018), traffic congestion and travelling period predictions (Zhao et al., 2017). In spite of wide applicability in various research domains, LSTM models has only recently been utilized for the forecast of hydrologic time series (Hu et al., 2018; Liang et al., 2018; Tian et al., 2018; Zhang et al., 2018). Recently, Jeong et al. (2020) applied LSTM-based modelling to estimate groundwater level using the corrupted data (with outliers and noise) and found that robust training of an LSTM model using a developed cost function (“least trimmed squares with asymmetric weighting and the Whittaker smoother”) can adequately model noisy groundwater level data. The prediction ability of an LSTM network was found superior than that of a recurrent neural network in predicting hourly groundwater level values in a coastal city (susceptible to periodic flooding) of Norfolk, Virginia, USA (Bowes et al., 2019). Mouatadid et al. (2019) used a coupled “maximum overlap discrete wavelet transformation” and LSTM for achieving precision and robustness in the forecasting of irrigation flow. Zhang et al. (2018) proposed an LSTM network for predicting depths in water table in agrarian areas and obtained an acceptable prediction result by utilizing simply an uncomplicated data pre-processing technique. Based on their findings, one can argue that an LSTM network does not require a massive data smoothing or pre-processing in producing an acceptable prediction accuracy. The integrated use of gated recurrent unit and convolutional neural network (CNN-GRU) can also be found in recent literature (Pan et al., 2020) for developing water level prediction models in which CNN-GRU outperformed an LSTM model with regard to Nash-Sutcliffe (NS) Efficiency Coefficient, Average Relative Error, and Root Mean Squared Error. The prediction accuracy of a lion algorithm optimized LSTM network was found superior than an ordinary LSTM network for the prediction of groundwater level using the historical groundwater level data obtained from an observation well and rainfall data collected from a weather station located in the Udupi district, India (Supreetha et al., 2020). To the best of our knowledge, this study is the first effort of predicting multi-step ahead groundwater levels at the selected observation wells in the Gazipur Sadar Upazilla, Bangladesh.

Therefore, the key motivation and focus of this study are to delve into the potential of maximal overlap discrete wavelet packet transform (MDWPT) as a pre-processing tool to improve forecasting capability of LSTM for predicting multi-step ahead groundwater level in the selected observation wells.

Materials and Methods

Study area and the data

The study area is situated in the Gazipur Sadar Upazilla having an aerial extent of 446.38 km². It is located between 23.88°N and 24.18°N latitudes and between 90.33°E and 92.50°E longitudes. Pumped groundwater appears to be the prime water resource for household usage and crop irrigation. Excessive abstraction of groundwater from the aquifer has been continuing at an increasing rate every year resulting in a gradual declination of groundwater level. To model future scenarios of groundwater table fluctuations in the selected observation wells, especially to provide multi-step ahead forecast of groundwater levels, previous data on groundwater level fluctuations were used in this research. For this, historical weekly data on groundwater level fluctuations were collected from Bangladesh Water Development Board. Collected data at different observation wells were carefully checked and two observation wells, namely GT3330001, and GT3330002 were selected based on the criterion of least amount of missing entries. The observation well GT83330001 is positioned between 23.93°N latitude and 90.42°E longitude. The position of the observation well GT3330002 is between 23.96°N latitude and 90.48°E longitude. The study area and the positions of the observation wells are shown in Figure 1.

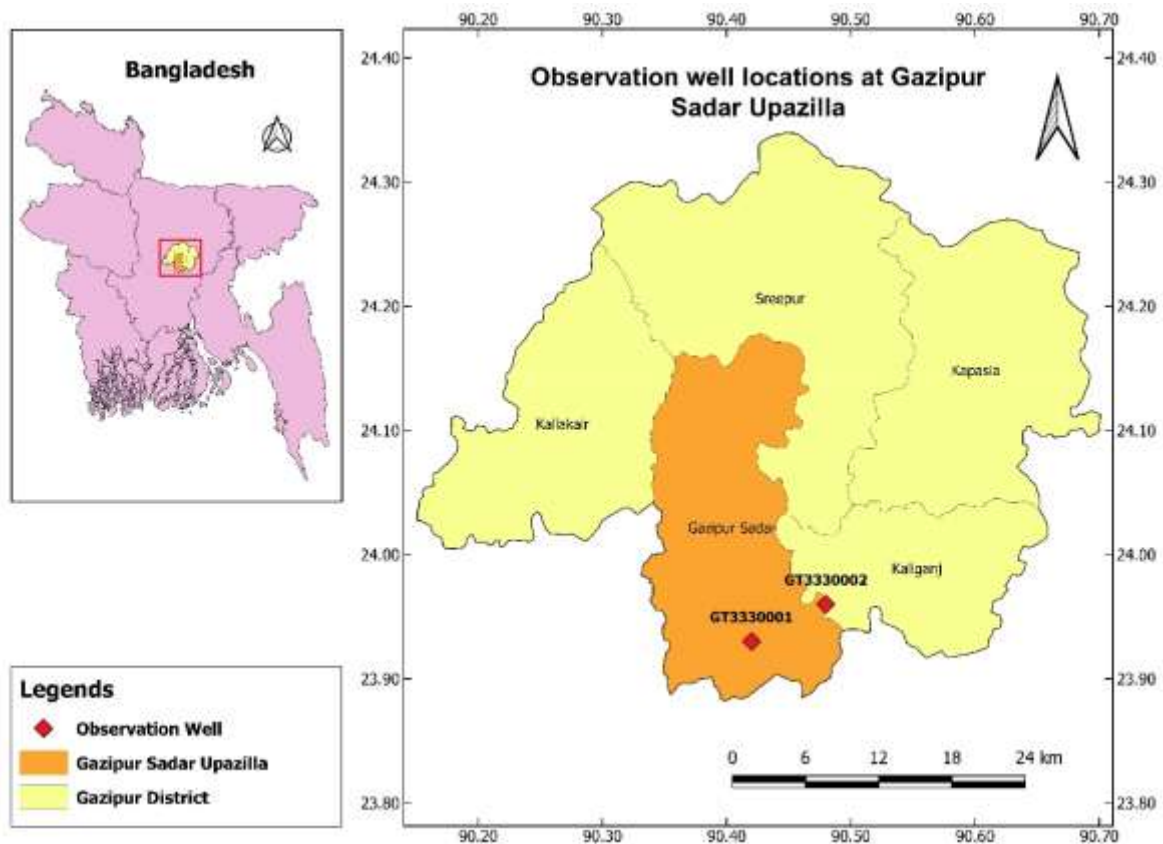


Figure 1. Study area and the locations of the two observation wells.

However, there were some missing values in the groundwater level datasets in the selected observation wells. These missing entries were imputed using the ‘moving median’ approach of data imputation in which a moving median with a specified window length was used to fill missing numeric data. The observation wells GT3330001 and GT3330002 had 2012 (from 07 January 1980 to 17 September 2018) and 1937 (07 January 1980 to 26 December 2016) weekly groundwater level entries after the imputation of missing entries. Timeseries plots of the groundwater levels at the two observation wells are presented in Figure 2.

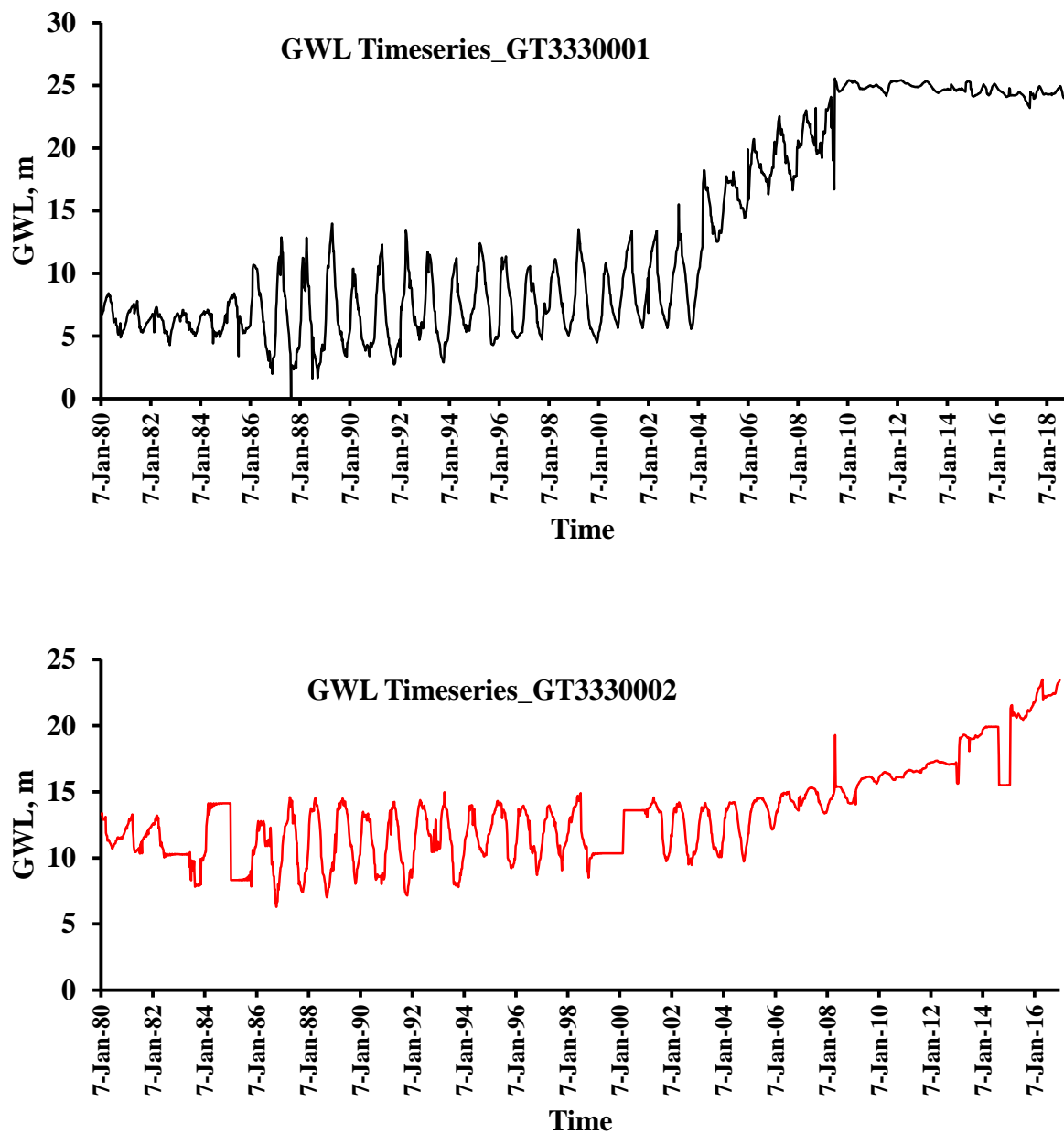


Figure 2. Groundwater level timeseries at the two observation wells GT3330001 and GT3330002.

Table 1 presents few descriptive statistics of the datasets (after imputation of the missing entries) at the selected observation wells. Table 1 reveals that the mean values of groundwater level data range between 12.96 m (at GT3330001) and 13.26 m (at GT3330002) whereas the standard deviation values vary between 3.39 m (at GT3330002) and 7.92 m (at GT3330001).

Table 1. Measures of the statistical parameter values for the groundwater level data (m) at the observation wells

Obs. wells	Min	Max	Mean	Median	STD	Skewness	Kurtosis
GT3330001	0.10	25.57	12.96	9.83	7.92	0.50	-1.39
GT3330002	6.30	23.50	13.26	13.26	3.39	0.74	0.44

The data at both observation wells possess a longer right tail than the left tail in their distribution as evidenced by the positive (right) skewness values (Table 1). The datasets at

observation well GT3330001 showed ‘light-tailed’ distributions because the kurtosis value was negative at this observation well. On the other hand, the datasets at observation well GT3330002 showed ‘heavy-tailed’ distributions because the kurtosis value was positive. The LSTM architecture with multiple hidden units was employed in which the numbers of ‘hidden neurons’ were decided via conducting several trials through varying the number of ‘hidden neurons’ in each trial. The other parameters of the LSTM architecture were selected upon conducting several trials, and the optimum parameter sets are presented in Table-2. These optimum parameter values were used for developing the LSTM models for predicting one-, two-, and three-week ahead GWLs at the two observation wells.

Table-2. Optimum combinations of different training options

Options	Corresponding parameters or values
Optimization solver	'adam'
Maximum epochs	1000
Gradient threshold	1
Initial learning rate	0.001
Minimum batch size	150
Sequence length	1000

The entire dataset was separated into two distinct sets – training and testing samples: 80% of the data records was allocated for the training purpose and the left over 20% was allotted for testing of the developed LSTM models.

Wavelet transform as a pre-processing tool

The target variable at each station was the 1-, 2-, 3- week ahead observed groundwater levels while the explanatory (input) variables were the observed groundwater level in the current week and previous weeks along with their wavelet-decomposed counterparts generated via MODWPT. Proper wavelet decomposition of the explanatory (input) variables, resulting in a set of wavelet and scaling coefficients for each explanatory variable. Each of the lagged groundwater level time series were wavelet-decomposed separately. Random Forest approach was used to identify only those wavelet and scaling coefficients that are useful in generating accurate forecasts of the target variable. The main task of Random Forest approach is to ensure that only those variables relevant to forecasting the target variable are selected while those that are redundant and/or irrelevant are discarded; ideally, resulting in accurate models that are not overly complex or hampered in their forecasting capabilities.

Results and Discussions

The Root Mean Squared Error (RMSE) criterion was used to evaluate the training and testing performance of the developed models. The RMSE values on the training and test dataset for different numbers of neurons in 2019-2020 are given in Table 3. It is observed from Table-3 that at GT3330001, the minimum values of the absolute difference between the training and test RMSE were 0.09 (hidden neurons: 180-150-80), 0.03 (hidden neurons: 150-100-50), and 0.06 (hidden neurons: 150-100-50) for one-, two-, and three-week ahead predictions, respectively. On the other hand, at GT3330002, these values were 3.13 (hidden neurons: 150-120-80-50), 3.22 (hidden neurons: 140-120-60), and 3.14 (hidden neurons: 100-80-50-20) for one-, two-, and three-week ahead predictions, respectively. Therefore, the LSTM models with these hidden neurons were selected as the best performing models over others. A set of several statistical performance evaluation indices were then calculated based on this result. The performance evaluation indices were computed on test datasets using the selected LSTM models for the one-, two-, and three-week ahead predictions of groundwater levels. Other than RMSE, scatter index, MAE, MAD, and a-20 index were calculated to evaluate the performances of the LSTM models at the two observation wells. The results are presented in Table-4. It is observed from Table-4 that the performances of the LSTM models for multi-step ahead predictions at GT3330001 were in general better than the performances of the LSTM models developed at GT3330002. However, at both observation wells, the developed LSTM models provided acceptable results.

Table 3. Train and Test RMSE values for different combinations of hidden layers and hidden neurons in 2019-2020

Hidden neurons	One week ahead prediction		Two weeks ahead prediction		Three weeks ahead prediction	
	Train RMSE, m	Test RMSE, m	Train RMSE, m	Test RMSE, m	Train RMSE, m	Test RMSE, m
GT3330001						
100-50-20	0.454	1.556	0.524	1.257	0.524	1.065
140-120-60	0.620	24.792	1.990	3.651	2.116	24.377
150-100-50	0.666	0.907	0.885	0.910	0.915	0.975
160-120-60	0.524	1.913	0.698	5.347	0.899	1.977
180-150-80	0.737	0.827	0.558	1.220	0.728	1.525
170-140-70	0.403	0.856	0.440	1.536	0.801	22.043
80-60-30	0.784	1.633	0.506	1.012	0.561	0.904
80-60-40-20	0.584	2.295	0.744	2.373	0.626	1.225
100-80-50-20	0.590	1.204	0.669	1.844	0.594	1.546
150-120-80-50	0.594	1.045	0.810	2.167	0.651	18.917
120-100-50-20	0.503	0.707	0.559	1.879	0.636	2.207
GT3330002						
100-50-20	0.339	3.581	0.384	4.115	0.403	13.402
140-120-60	0.913	20.048	0.403	3.623	0.329	4.081
150-100-50	0.405	18.878	0.546	18.326	1.192	20.412
160-120-60	0.503	17.781	0.537	16.172	1.588	17.441
180-150-80	0.918	18.528	0.657	19.094	0.558	20.288
170-140-70	0.371	16.873	0.493	16.909	0.427	16.389
80-60-30	0.392	4.170	0.383	3.897	0.419	3.815
80-60-40-20	0.426	3.871	0.607	4.781	0.522	3.994
100-80-50-20	0.718	3.925	0.489	3.853	0.355	3.493
150-120-80-50	0.337	3.466	0.528	18.194	0.462	19.203
120-100-50-20	0.363	3.480	0.395	3.660	0.434	13.992

The obtained best numbers of hidden layers and hidden neurons in 2019-2020 were used to develop MODWTP based LSTM models (MODWTP-LSTM). The training performance of the developed MODWTP-LSTM models at the two observation wells are presented in Table 4.

Table 4. Training and testing errors for the developed MODWTP-LSTM models during 2020-2021

	Training RMSE, m	Test RMSE, m
GT3330001		
One-week ahead	0.517	0.527
Two-weeks ahead	0.563	0.610
Three-weeks ahead	0.652	0.675
GT3330002		
One-week ahead	0.691	0.739
Two-weeks ahead	0.725	0.856
Three-weeks ahead	0.826	0.876

It is observed from Table 4 that MODWTP as a pre-processing tool significantly improved the training and validation performance of the LSTM model. The findings from the trained and tested LSTM models were used to calculate other statistical performance evaluation indices for assessing the robustness of the proposed MODWTP-LSTM models. The computed performance indices were presented in Table 5.

Table 5. One-, two-, and three-week ahead prediction performance of the developed LSTM model on test dataset

	Performance evaluation indices				
	RMSE, m	Scatter index	MAE, m	MAD, m	a-20 index
2019-2020					
GT3330001					
One-week ahead	0.827	0.034	12.480	0.179	0.997
Two-weeks ahead	0.910	0.037	10.237	0.319	0.997
Three-weeks ahead	0.975	0.040	10.754	0.405	0.997
GT3330002					
One-week ahead	3.466	0.188	7.561	1.200	0.589
Two-weeks ahead	3.623	0.196	7.727	1.326	0.531
Three-weeks ahead	3.493	0.189	7.393	1.327	0.573
2020-2021					
GT3330001					
One-week ahead	0.527	0.024	5.430	0.153	0.999
Two-weeks ahead	0.610	0.027	4.918	0.217	0.997
Three-weeks ahead	0.675	0.030	4.676	0.357	0.998
GT3330002					
One-week ahead	0.739	0.098	4.893	0.867	0.876
Two-weeks ahead	0.856	0.081	4.125	0.894	0.883
Three-weeks ahead	0.876	0.086	3.989	0.905	0.915

Table 5 reveals the superiority of the proposed MODWTP-LSTM over the LSTM models for the selected observation wells as well for the 1-, 2-, and 3-week ahead forecasts. This superior performance was evidenced through all the five statistical performance evaluation indices considered for evaluating the performances of the models in this study.

Conclusions

Precise and robust prediction of groundwater levels can be effectively employed in developing a sustainable and efficient management strategy for groundwater resources. This judicial planning will aid in optimal abstraction and usage of groundwater for agricultural, domestic, and industrial purposes. This study aimed at developing a robust prediction tool for one-, two-, and three-week ahead groundwater level fluctuations using MODWTP-LSTM models. The suitable weekly lag times of groundwater levels as well as their wavelet transformed counterparts were used as inputs to the prediction models while the output from the models was the one-, two-, and three-week ahead groundwater levels. The selection of optimal combination of inputs for the models was executed through a Random Forest based modelling approach. The performance comparison of the proposed models was performed by using several statistical performance evaluation indices. Results of the present study indicated that MODWTP-LSTM models outperformed the LSTM models for all three future time horizons and for the two observation wells considered. Therefore, it can be concluded that MODWTP-LSTM models could be used to predict multi-step ahead groundwater level fluctuations for the study area.

References

- Adamowski, J., Chan, H.F., 2011. A wavelet neural network conjunction model for groundwater level forecasting. *J. Hydrol.* 407, 28–40. <https://doi.org/https://doi.org/10.1016/j.jhydrol.2011.06.013>
- Aguilera, H., Guardiola-Albert, C., Naranjo-Fernández, N., Kohfahl, C., 2019. Towards flexible groundwater-level prediction for adaptive water management: using Facebook’s Prophet

- forecasting approach. *Hydrol. Sci. J.* 64, 1504–1518. <https://doi.org/10.1080/02626667.2019.1651933>
- Banadkooki, F.B., Ehteram, M., Ahmed, A.N., Teo, F.Y., Fai, C.M., Afan, H.A., Sapitang, M., El-Shafie, A., 2020. Enhancement of groundwater-level prediction using an integrated machine learning model optimized by whale algorithm. *Nat. Resour. Res.* <https://doi.org/10.1007/s11053-020-09634-2>
- Barzegar, R., Aalami, M.T., Adamowski, J., 2020. Short-term water quality variable prediction using a hybrid CNN–LSTM deep learning model. *Stoch. Environ. Res. Risk Assess.* 34, 415–433. <https://doi.org/10.1007/s00477-020-01776-2>
- Barzegar, R., Fijani, E., Asghari Moghaddam, A., Tziritis, E., 2017. Forecasting of groundwater level fluctuations using ensemble hybrid multi-wavelet neural network-based models. *Sci. Total Environ.* 599–600, 20–31. <https://doi.org/https://doi.org/10.1016/j.scitotenv.2017.04.189>
- Bengio, Y., Simard, P., Frasconi, P., 1994. Learning long-term dependencies with gradient descent is difficult. *IEEE Trans. Neural Networks Learn. Syst.* 5, 157–166.
- Boubaker, S., 2017. Identification of monthly municipal water demand system based on autoregressive integrated moving average model tuned by particle swarm optimization. *J. Hydroinformatics* 19, 261–281. <https://doi.org/10.2166/hydro.2017.035>
- Bowes, B.D., Sadler, J.M., Morsy, M.M., Behl, M., Goodal, J.L., 2019. Forecasting groundwater table in a flood prone coastal city with long short-term memory and recurrent neural networks. *Water* 11, 1–38.
- Chang, F.-J., Chang, L.-C., Huang, C.-W., Kao, I.-F., 2016. Prediction of monthly regional groundwater levels through hybrid soft-computing techniques. *J. Hydrol.* 541, 965–976. <https://doi.org/https://doi.org/10.1016/j.jhydrol.2016.08.006>
- Cummins, N., Baird, A., Schuller, B.W., 2018. Speech analysis for health: Current state-of-the-art and the increasing impact of deep learning. *Methods* 151, 41–54. <https://doi.org/https://doi.org/10.1016/j.ymeth.2018.07.007>
- Daliakopoulos, I.N., Coulibaly, P., Tsanis, I.K., 2005. Groundwater level forecasting using artificial neural networks. *J. Hydrol.* 309, 229–240. <https://doi.org/https://doi.org/10.1016/j.jhydrol.2004.12.001>
- Deo, R.C., Tiwari, M.K., Adamowski, J.F., Quilty, J.M., 2017. Forecasting effective drought index using a wavelet extreme learning machine (W-ELM) model. *Stoch. Environ. Res. Risk Assess.* 31, 1211–1240. <https://doi.org/10.1007/s00477-016-1265-z>
- Doble, R.C., Pickett, T., Crosbie, R.S., Morgan, L.K., Turnadge, C., Davies, P.J., 2017. Emulation of recharge and evapotranspiration processes in shallow groundwater systems. *J. Hydrol.* 555, 894–908. <https://doi.org/https://doi.org/10.1016/j.jhydrol.2017.10.065>
- Dong, L., Guangxuan, L., Qiang, F., Mo, L., Chunlei, L., Abrar, F.M., Imran, K.M., Tianxiao, L., Song, C., 2018. Application of particle swarm Optimization and extreme learning machine forecasting models for regional groundwater depth using nonlinear prediction models as preprocessor. *J. Hydrol. Eng.* 23, 4018052. [https://doi.org/10.1061/\(ASCE\)HE.1943-5584.0001711](https://doi.org/10.1061/(ASCE)HE.1943-5584.0001711)
- Fahimi, F., Yaseen, Z.M., El-shafie, A., 2017. Application of soft computing based hybrid models in hydrological variables modeling: a comprehensive review. *Theor. Appl. Climatol.* 128, 875–903. <https://doi.org/10.1007/s00704-016-1735-8>
- Fan, L., Zhang, T., Zhao, X., Wang, H., Zheng, M., 2019. Deep topology network: A framework based on feedback adjustment learning rate for image classification. *Adv. Eng. Informatics* 42, 100935. <https://doi.org/https://doi.org/10.1016/j.aei.2019.100935>
- Fang, W., Zhong, B., Zhao, N., Love, P.E.D., Luo, H., Xue, J., Xu, S., 2019. A deep learning-based approach for mitigating falls from height with computer vision: Convolutional neural network. *Adv. Eng. Informatics* 39, 170–177. <https://doi.org/https://doi.org/10.1016/j.aei.2018.12.005>
- Feng, S., Kang, S., Huo, Z., Chen, S., Mao, X., 2008. Neural networks to simulate regional ground water levels affected by human activities. *Ground Water* 46, 80–90. <https://doi.org/10.1111/j.1745-6584.2007.00366.x>
- Fischer, T., Krauss, C., 2018. Deep learning with long short-term memory networks for financial market predictions. *Eur. J. Oper. Res.* 270, 654–669. <https://doi.org/https://doi.org/10.1016/j.ejor.2017.11.054>

- Ghaseminejad, A., Uddameri, V., 2020. Physics-inspired integrated space-time artificial neural networks for regional groundwater flow modeling. *Hydrol. Earth Syst. Sci. Discuss.* 2020, 1–27. <https://doi.org/10.5194/hess-2020-117>
- Ghorbani, M.A., Deo, R.C., Karimi, V., Yaseen, Z.M., Terzi, O., 2018. Implementation of a hybrid MLP-FFA model for water level prediction of Lake Egirdir, Turkey. *Stoch. Environ. Res. Risk Assess.* 32, 1683–1697. <https://doi.org/10.1007/s00477-017-1474-0>
- Gong, Y., Wang, Z., Xu, G., Zhang, Z., 2018. A comparative study of groundwater level forecasting using data-driven models based on ensemble empirical mode decomposition. *Water* 10, 1–20. <https://doi.org/10.3390/w10060730>
- Govindaraju, R.S., 2000a. Artificial neural networks in hydrology. I: Preliminary concepts. *J. Hydrol. Eng.* 5, 115–123. [https://doi.org/10.1061/\(ASCE\)1084-0699\(2000\)5:2\(115\)](https://doi.org/10.1061/(ASCE)1084-0699(2000)5:2(115))
- Govindaraju, R.S., 2000b. Artificial neural networks in hydrology. II: Hydrologic applications. *J. Hydrol. Eng.* 5, 124–137. [https://doi.org/10.1061/\(ASCE\)1084-0699\(2000\)5:2\(124\)](https://doi.org/10.1061/(ASCE)1084-0699(2000)5:2(124))
- Guzman, S.M., Paz, J.O., Tagert, M.L.M., 2017. The use of NARX neural networks to forecast daily groundwater levels. *Water Resour. Manag.* 31, 1591–1603. <https://doi.org/10.1007/s11269-017-1598-5>
- Hochreiter, S., Schmidhuber, J., 1997. Long short-term memory. *Neural Comput.* 9, 1735–1780. <https://doi.org/https://doi.org/10.1162/neco.1997.9.8.1735>
- Hoque, M.A., Adhikary, S.K., 2020. Prediction of groundwater level using artificial neural network and multivariate timeseries models, in: *Proceedings of the 5th International Conference on Civil Engineering for Sustainable Development (ICCESD 2020)*. KUET, Khulna, Bangladesh, pp. 1–8.
- Hu, C., Wu, Q., Li, H., Jian, S., Li, N., Lou, Z., 2018. Deep learning with a long short-term memory networks approach for rainfall-runoff simulation. *Water* 10, 1543.
- Jeong, J., Park, E., Chen, H., Kim, K.-Y., Shik Han, W., Suk, H., 2020. Estimation of groundwater level based on the robust training of recurrent neural networks using corrupted data. *J. Hydrol.* 582, 124512. <https://doi.org/https://doi.org/10.1016/j.jhydrol.2019.124512>
- Karandish, F., Šimůnek, J., 2016. A comparison of numerical and machine-learning modeling of soil water content with limited input data. *J. Hydrol.* 543, 892–909. <https://doi.org/https://doi.org/10.1016/j.jhydrol.2016.11.007>
- Lee, S., Lee, K.-K., Yoon, H., 2019. Using artificial neural network models for groundwater level forecasting and assessment of the relative impacts of influencing factors. *Hydrogeol. J.* 27, 567–579. <https://doi.org/10.1007/s10040-018-1866-3>
- Liang, C., Li, H., Lei, M., Du, Q., 2018. Dongting lake water level forecast and its relationship with the three Gorges dam based on a long short-term memory network. *Water* 10, 1389.
- Maier, H.R., Jain, A., Dandy, G.C., Sudheer, K.P., 2010. Methods used for the development of neural networks for the prediction of water resource variables in river systems: Current status and future directions. *Environ. Model. Softw.* 25, 891–909. <https://doi.org/https://doi.org/10.1016/j.envsoft.2010.02.003>
- Makungo, R., Odiyo, J.O., 2017. Estimating groundwater levels using system identification models in Nzhelele and Luvuvhu areas, Limpopo Province, South Africa. *Phys. Chem. Earth, Parts A/B/C* 100, 44–50. <https://doi.org/https://doi.org/10.1016/j.pce.2017.01.019>
- Masterson, J.P., Garabedian, S.P., 2007. Effects of sea-level rise on ground water flow in a coastal aquifer system. *Ground Water* 45, 209–217.
- Mathworks, 2020a. Technical documentation: zscore [WWW Document]. Stand. z-scores. URL <https://au.mathworks.com/help/stats/zscore.html> (accessed 5.2.20).
- Mathworks, 2020b. Long short-term memory networks [WWW Document]. LSTM Netw. Archit. URL <https://au.mathworks.com/help/deeplearning/ug/long-short-term-memory-networks.html> (accessed 5.2.20).
- Mohanty, S., Jha, M.K., Kumar, A., Panda, D.K., 2013. Comparative evaluation of numerical model and artificial neural network for simulating groundwater flow in Kathajodi–Surua Inter-basin of Odisha, India. *J. Hydrol.* 495, 38–51. <https://doi.org/https://doi.org/10.1016/j.jhydrol.2013.04.041>
- Mohanty, S., Jha, M.K., Raul, S.K., Panda, R.K., Sudheer, K.P., 2015. Using artificial neural network approach for simultaneous forecasting of weekly groundwater levels at multiple sites. *Water*

- Resour. Manag. 29, 5521–5532. <https://doi.org/10.1007/s11269-015-1132-6>
- Moosavi, V., Vafakhah, M., Shirmohammadi, B., Behnia, N., 2013. A wavelet-ANFIS hybrid model for groundwater level forecasting for different prediction periods. *Water Resour. Manag.* 27, 1301–1321. <https://doi.org/10.1007/s11269-012-0239-2>
- Mouatadid, S., Adamowski, J., Tiwari, M.K., Quilty, J.M., 2019. Coupling the maximum overlap discrete wavelet transform and long short-term memory networks for irrigation flow forecasting. *Agric. Water Manag.* 219, 72–85. <https://doi.org/https://doi.org/10.1016/j.agwat.2019.03.045>
- Nadiri, A.A., Naderi, K., Khatibi, R., Gharekhani, M., 2019. Modelling groundwater level variations by learning from multiple models using fuzzy logic. *Hydrol. Sci. J.* 64, 210–226. <https://doi.org/10.1080/02626667.2018.1554940>
- Nourani, V., Mousavi, S., 2016. Spatiotemporal groundwater level modeling using hybrid artificial intelligence-meshless method. *J. Hydrol.* 536, 10–25. <https://doi.org/https://doi.org/10.1016/j.jhydrol.2016.02.030>
- Obergfell, C., Bakker, M., Maas, K., 2019. Identification and explanation of a change in the groundwater regime using time series analysis. *Groundwater* 57, 886–894. <https://doi.org/10.1111/gwat.12891>
- Pan, M., Zhou, H., Cao, J., Liu, Y., Hao, J., Li, S., Chen, C.-H., 2020. Water level prediction model based on GRU and CNN. *IEEE Access* 8, 60090–60100.
- Park, E., Parker, J.C., 2008. A simple model for water table fluctuations in response to precipitation. *J. Hydrol.* 356, 344–349. <https://doi.org/https://doi.org/10.1016/j.jhydrol.2008.04.022>
- Peng, T., Zhou, J., Zhang, C., Fu, W., 2017. Streamflow forecasting using empirical wavelet transform and artificial neural networks. *Water* 9, 406 (1–20). <https://doi.org/https://doi.org/10.3390/w9060406>
- Plappert, M., Mandery, C., Asfour, T., 2018. Learning a bidirectional mapping between human whole-body motion and natural language using deep recurrent neural networks. *Rob. Auton. Syst.* 109, 13–26. <https://doi.org/https://doi.org/10.1016/j.robot.2018.07.006>
- Raghavendra, S.N., Deka, P.C., 2015. Forecasting monthly groundwater level fluctuations in coastal aquifers using hybrid Wavelet packet–Support vector regression. *Cogent Eng.* 2, 999414. <https://doi.org/10.1080/23311916.2014.999414>
- Rajaei, T., Ebrahimi, H., Nourani, V., 2019. A review of the artificial intelligence methods in groundwater level modeling. *J. Hydrol.* 572, 336–351. <https://doi.org/https://doi.org/10.1016/j.jhydrol.2018.12.037>
- Roshni, T., Jha, M.K., Deo, R.C., Vandana, A., 2019. Development and evaluation of hybrid artificial neural network architectures for modeling spatio-temporal groundwater fluctuations in a complex aquifer system. *Water Resour. Manag.* 33, 2381–2397. <https://doi.org/10.1007/s11269-019-02253-4>
- Sadler, J.M., Goodall, J.L., Morsy, M.M., Spencer, K., 2018. Modeling urban coastal flood severity from crowd-sourced flood reports using Poisson regression and Random Forest. *J. Hydrol.* 559, 43–55. <https://doi.org/https://doi.org/10.1016/j.jhydrol.2018.01.044>
- Sahoo, S., Russo, T.A., Elliott, J., Foster, I., 2017. Machine learning algorithms for modeling groundwater level changes in agricultural regions of the U.S. *Water Resour. Res.* 53, 3878–3895. <https://doi.org/10.1002/2016WR019933>
- Solomatine, D.P., Ostfeld, A., 2008. Data-driven modelling: some past experiences and new approaches. *J. Hydroinformatics* 10, 3–22. <https://doi.org/10.2166/hydro.2008.015>
- Supreetha, B.S., Shenoy, N., Nayak, P., 2020. Lion algorithm-optimized long short-term memory network for groundwater level forecasting in Udupi District, India. *Appl. Comput. Intell. Soft Comput.* 2020, 8685724. <https://doi.org/10.1155/2020/8685724>
- Tang, Y., Zang, C., Wei, Y., Jiang, M., 2019. Data-driven modeling of groundwater level with least-square support vector machine and spatial-temporal analysis. *Geotech. Geol. Eng.* 37, 1661–1670. <https://doi.org/10.1007/s10706-018-0713-6>
- Tian, Y., Xu, Y.-P., Yang, Z., Wang, G., Zhu, Q., 2018. Integration of a parsimonious hydrological model with recurrent neural networks for improved streamflow forecasting. *Water* 10, 1655.
- Tien Bui, D., Hoang, N.-D., Martínez-Álvarez, F., Ngo, P.-T.T., Hoa, P.V., Pham, T.D., Samui, P., Costache, R., 2020. A novel deep learning neural network approach for predicting flash flood susceptibility: A case study at a high frequency tropical storm area. *Sci. Total Environ.* 701,

134413. <https://doi.org/https://doi.org/10.1016/j.scitotenv.2019.134413>
- Wada, Y., Bierkens, M.F.P., 2014. Sustainability of global water use: past reconstruction and future projections. *Environ. Res. Lett.* 9, 104003. <https://doi.org/10.1088/1748-9326/9/10/104003>
- Wang, H., Zhao, W., 2009. ARIMA model estimated by particle swarm optimization algorithm for consumer price index forecasting BT - artificial intelligence and computational intelligence, in: Deng, H., Wang, L., Wang, F.L., Lei, J. (Eds.), *International Conference on Artificial Intelligence and Computational Intelligence*. Springer Berlin Heidelberg, Berlin, Heidelberg, pp. 48–58.
- Wei, Z.-L., Wang, D.-F., Sun, H.-Y., Yan, X., 2020. Comparison of a physical model and phenomenological model to forecast groundwater levels in a rainfall-induced deep-seated landslide. *J. Hydrol.* 586, 124894. <https://doi.org/https://doi.org/10.1016/j.jhydrol.2020.124894>
- Wen, X., Feng, Q., Yu, H., Wu, J., Si, J., Chang, Z., Xi, H., 2015. Wavelet and adaptive neuro-fuzzy inference system conjunction model for groundwater level predicting in a coastal aquifer. *Neural Comput. Appl.* 26, 1203–1215. <https://doi.org/10.1007/s00521-014-1794-7>
- Xu, H., Zhou, J., Asteris, P.G., Jahed Armaghani, D., Tahir, M.M., 2019. Supervised machine learning techniques to the prediction of tunnel boring machine penetration rate. *Appl. Sci.* <https://doi.org/10.3390/app9183715>
- Yang, T., Asanjan, A.A., Welles, E., Gao, X., Sorooshian, S., Liu, X., 2017. Developing reservoir monthly inflow forecasts using artificial intelligence and climate phenomenon information. *Water Resour. Res.* 53, 2786–2812. <https://doi.org/10.1002/2017WR020482>
- Yuan, X., Chen, C., Lei, X., Yuan, Y., Muhammad Adnan, R., 2018. Monthly runoff forecasting based on LSTM–ALO model. *Stoch. Environ. Res. Risk Assess.* 32, 2199–2212. <https://doi.org/10.1007/s00477-018-1560-y>
- Zare, M., Koch, M., 2018. Groundwater level fluctuations simulation and prediction by ANFIS- and hybrid Wavelet-ANFIS/Fuzzy C-Means (FCM) clustering models: Application to the Miandarband plain. *J. Hydro-environment Res.* 18, 63–76. <https://doi.org/https://doi.org/10.1016/j.jher.2017.11.004>
- Zhang, J., Zhu, Y., Zhang, X., Ye, M., Yang, J., 2018. Developing a long short-term memory (LSTM) based model for predicting water table depth in agricultural areas. *J. Hydrol.* 561, 918–929. <https://doi.org/https://doi.org/10.1016/j.jhydrol.2018.04.065>
- Zhao, Z., Chen, W., Wu, X., Chen, P.C.Y., Liu, J., 2017. LSTM network: a deep learning approach for short-term traffic forecast. *IET Intell. Transp. Syst.* 11, 68–75. <https://doi.org/10.1049/iet-its.2016.0208>

COASTAL GROUNDWATER MANAGEMENT USING AN UNCERTAINTY-BASED COUPLED SIMULATION-OPTIMIZATION APPROACH

D.K. ROY¹, S.K. BISWAS¹ AND B. DATTA²

Abstract

This study demonstrated the influences of reduced recharge, increased groundwater pumping and climate change induced sea level rise on multi-objective saltwater intrusion management strategies in coastal aquifers. Three meta-models were developed from the solution results of a numerical simulation model that simulated the coupled flow and salt transport processes in a coastal aquifer system. Results revealed that the proposed meta-models can predict density dependent coupled flow and salt transport patterns quite accurately. Based on the comparison result, the best meta-model is selected as a computationally cheap substitute of the simulation model in the coupled simulation-optimization based saltwater intrusion management model. To achieve computational efficiency, the optimization routine of the proposed management model is performed in a parallel computing platform. The performance of the proposed methodology is evaluated for an illustrative multi-layered coastal aquifer system in which the effect of climate change induced sea level rise as well as recharge and pumping scenarios is incorporated for the specified management period. Results show that the proposed saltwater intrusion management model provides acceptable, accurate, and reliable solutions while significantly improving computational efficiency in a coupled simulation-optimization methodology. The developed methodology will be applied in a real-world coastal aquifer system in the southern Bangladesh.

Introduction

Sustainable use of coastal groundwater resources through optimized abstraction can prevent salinization of aquifer resulting from irrational groundwater pumping. To address this management problem as well as to reduce the extent of saltwater intrusion, an optimal saltwater intrusion management strategy needs to be adopted to ensure sustainable and uninterrupted supply of groundwater resources to different sectors. This saltwater intrusion management model can be developed through optimization of groundwater extraction patterns by utilizing a linked simulation-optimization (S/O) approach in which a numerical flow and solute transport simulation model is linked externally to an optimization algorithm to evolve optimal solutions (Bhattacharjya and Datta 2009; Sreekanth and Datta 2010; Sreekanth and Datta 2011a). Besides water abstraction from production bores, a set of barrier extraction wells can also be utilized near the coastline to hydraulically control saltwater intrusion (Sreekanth and Datta 2011b). As water extracted from these barrier extraction wells are no longer usable for beneficial purposes, one of the objectives of the management model should be to minimize the water abstraction from these barrier extraction wells. Another objective of the management model is maximization of water abstraction from the production wells. Therefore, the resulting management model is essentially a multi-objective one, which needs to be solved using a multi-objective optimization algorithm (Datta and Peralta 1986).

However, the use of original simulation model in a linked S/O approach is constrained by huge computational burden because the complex simulation model is called by the optimization algorithm several thousand times to evolve optimal solutions (Dhar and Datta 2009). Replacing the original numerical simulation model by a reasonably accurate meta-model is a promising approach that has been used to achieve computational efficiency in the design and optimization of computationally intensive problems (Goel et al. 2007).

Prediction capability as well as simplicity of any meta-model determines its suitability to replace numerical simulation model in a linked S/O approach. The developed model should also be checked for over-fitting or under-fitting to make sure that properly trained model provides similar results when presented with a new test dataset (Sun et al. 2014). Recently, different meta-models have been used to

¹ Senior Scientific Officer, Irrigation and Water Management Division, BARI, Gazipur 1701

² Professor, College of Science and Engineering, James Cook University, QLD-4814, Australia

approximate density dependent coupled flow and salt transport processes in coastal aquifers. Most common of them includes Artificial Neural Network (ANN) (Bhattacharjya and Datta 2009; Kourakos and Mantoglou 2009; Sreekanth and Datta 2010; Sreekanth and Datta 2011a), Genetic Programming (GP) (Sreekanth and Datta 2010; Sreekanth and Datta 2011a), Evolutionary Polynomial Regression (EPR) (Hussain et al. 2015), Fuzzy Inference System (FIS) (Roy and Datta 2017a), cubic Radial Basis Function (RBF) (Christelis and Mantoglou 2016), and Multivariate Adaptive Regression Spline (MARS) (Roy and Datta 2017c). The generalization capability of any chosen meta-model is an important criterion to determine the ability of the meta-model to produce similar output from a new unseen test data set. Another criterion is the feasibility of its incorporation within a linked S/O approach as a computationally efficient substitute of the coupled flow and solute transport processes. All the mentioned meta-models are suitable for incorporating within a linked S/O approach for developing saltwater intrusion management models. However, many of these meta-models have certain limitations when used as a computationally efficient substitute of the numerical simulation model.

For instance, ANN based meta-models require large computational time for training, and they are susceptible to model over-fitting resulting from premature convergence to local minima (Holman et al. 2014). Moreover, these “Black-Box” models require a large number of datasets for training, e.g. ANN models have stability issue for an insufficient number of training dataset (Hsieh and Tang 1998). GP also requires an extensive training time to obtain the optimal GP model structure (Sreekanth and Datta 2011a). GPs are explicit mathematical formulations (Shiri and Kişi 2011), which produce simple regression models (Sreekanth and Datta 2011a). Further, GPs suffer from being trapped in local minima (Pillay 2004). RBFs, simple in formulation (Sóbester et al. 2014) are quite easy to implement when using certain types of radial functions (Piret 2007). Nevertheless, computational cost and stability are two of the major drawbacks of using the RBF based meta-models (Piret 2007). For higher order polynomial fits, polynomial regression method has stability issues, e.g., different observations within the training dataset may have unexpected influences on far-off parts of the curve in polynomial regression (Green and Silverman 1993). Therefore, to overcome some of the limitations of existing meta-models as well as to search for a more accurate and flexible meta-model for linked S/O approach, the present study evaluates the potential applicability of three different artificial intelligence based meta-models: Adaptive Neuro-fuzzy Inference System (ANFIS), Gaussian Process Regression (GPR), and MARS.

ANFIS is an adaptive fuzzy inference system, which is based on the concepts of fuzzy set theory and neural networks. ANFIS has successfully been applied in multi-dimensional fields (Jang et al. 1997) and is recognized as an effective tool to model non-linear systems due to its capability to capture non-linear relationships between predictors and response variables (Sugeno and Yasukawa 1993; Takagi and Sugeno 1985). Although ANFIS has been successfully applied in different domains of groundwater modeling (Emamgholizadeh et al. 2014; He et al. 2014; Khaki et al. 2015; Khashei-Siuki and Sarbazi 2015; Kurtulus and Razack 2010; Roy and Datta 2017d), it has not been used to approximate density dependent coupled flow and salt transport processes to develop saltwater intrusion management models for coastal aquifers incorporating climate change induced sea level rise phenomena.

MARS is a nonparametric approach of building a functional relationship between the predictors and responses using a set of coefficients and Basis functions (Friedman 1991). It is recognized as a rapid, flexible, and reasonably accurate artificial intelligence based meta-model (Salford-Systems 2013). Previous literature demonstrated the potential applicability of MARS model in different research domains of water resource (Adamowski et al. 2012; Beuchat et al. 2011; Nasserri et al. 2013; Samadi et al. 2015; Sharda et al. 2006; Sharda et al. 2008; Zabihi et al. 2016). Recently, Roy and Datta (2017c) proposed an ensemble of MARS based meta-models to develop a saltwater intrusion management model for a multilayered coastal aquifer system. However, MARS based meta-modelling approach has not been used for approximating saltwater intrusion processes in situations where climate change induced sea level rise and water concentration of tidal river is accounted for.

GPR, which assumes a Gaussian prior distribution of the model variables, is a stochastic approach (Jacobs and Koziel 2015) of performing modelling within a Bayesian framework. GPR

based meta-models are non-linear models that provide probabilistic information of prediction. According to GPR approach, the learning of a machine is formulated in terms of a Bayesian estimation problem, where the parameters of the machine are assumed as random variables drawn from a Gaussian distribution (Bazi et al. 2012). GPR is a nonparametric modelling approach, i.e., no assumption is made about the shape of the function to estimate. GPR provides a “principled, practical, and probabilistic approach to learning in kernel machines” (Rasmussen and Williams 2005). GPR has been successfully applied in many engineering applications as a popular artificial intelligence tool (Forrester et al. 2008). Recently, a GPR based meta-model is proposed to develop a single objective coastal groundwater management model (Rajabi and Ketabchi 2017). However, GPR has not been used as an approximate simulator of the density dependent coupled flow and salt transport processes of a multi-layered coastal aquifer system incorporating the influence of climate change induced sea level rise.

Besides computational accuracy, computational efficiency is another important property of any meta-model that determines its feasibility to link externally within an optimization algorithm for regional scale management of coastal aquifers. Once the right meta-model is selected based on computational accuracy and efficiency, the next possible way of attaining further computational efficiency is to run the optimization model in parallel computing framework. The basic idea behind using the parallel computation facilities is to distribute the objective functions and other linear and non-linear constraints of the optimization formulation among the learner machines. This technique is able to achieve further computational efficiency in meta-model-based management model (Ketabchi and Ataie-Ashtiani 2015). This present study utilizes four physical cores of a standard seven core PC [Intel (R) Core (TM) i7-4790 CPU@3.60 GHz] to evaluate the objective functions and constraints of the multi-objective saltwater intrusion management problem.

Tidal fluctuations have effect on the dynamics of groundwater flow patterns in coastal aquifers, such as fluctuations of groundwater table, and groundwater discharge to the sea (Liu et al. 2012). For an unconfined coastal aquifer system, tidal oscillations significantly reduce the overall extent of the seawater intrusion due to an increase in the total discharge of water towards the sea from the aquifer (Kuan et al. 2012). Chen and Hsu (2004) demonstrated that the saltwater intrusive profile varies only in vertical direction in an unconfined aquifer due to the influence of tidal fluctuations. Any further horizontal movement of the saltwater intrusion profile was not observed because tidal oscillation induced variation in groundwater table is progressively reduced with horizontal distance from the beach. Heiss and Michael (2014) also demonstrated that the variation of salinity in the intertidal zone during the tidal fluctuations were minimal. Narayan et al. (2007) showed that the effect of tidal fluctuations on groundwater levels is limited to the areas close to the coast, and therefore, tidal influence on saltwater intrusion can be neglected when compared with the effects due to groundwater pumping. In addition, nonphysical instabilities may arise from an increase in flow velocities due to the tide induced oscillating boundary condition in the sea face side of the model domain (Brovelli et al. 2007). This phenomenon, in combination with non-linear nature of the saltwater intrusion processes of coastal aquifers poses a significant computational burden for 3D simulation of the coastal aquifers. Based on the above discussions, the effect of tidal fluctuation is not incorporated in the simulation model of the present study.

Relative sea level rise, providing an additional saline water head at the seaside (Yang et al. 2015), has a significant impact on an increase in the salinization process of the coastal aquifers around the globe (Shrivastava 1998). Therefore, sea level rise can accelerate saltwater intrusion processes in aquifer systems, and several centuries would be required to equilibrate this sea level rise induced saltwater intrusion even if the sea level has fallen back to its original position (Webb and Howard 2011). However, the effect of this sea level rise induced increase in hydraulic heads of groundwater system is confined within few kilometers of the coastline and main rivers (Essink et al. 2010). Although excessive groundwater withdrawal is considered as the major cause of saltwater intrusion (Narayan et al. 2007), relative sea level rise in combination with the effect of excessive groundwater pumping can exacerbate the already vulnerable coastal aquifers (Langevin and Zygnerski 2013). Numerous studies have demonstrated the effect of relative sea level rise on the salinization process of the aquifer. For instance, an additional saltwater intrusion length of 9.0 km was observed in the Nile

Delta aquifer as a result of 50 cm rise in water heads in the Mediterranean Sea (Sherif and Singh 1999). Evidence of saltwater intrusion was also reported in the Noord-Holland province of the Netherlands for the same 50 cm relative sea level rise per century (Essink 2001). Relative sea level rise induced saltwater intrusion was also reported in Broward County, Florida, USA for a sea water level in excess of 48 cm per century (Dausman and Langevin 2005). For an unconfined aquifer, 800 m inland movement of the mixing zone was caused by a relative sea level rise of 47.5 cm per century (Giambastiani et al. 2007). A simulation study considering 25 cm sea level rise for a period of 105 years demonstrated the saltwater intrusion length of about 1 km for a shallow coastal aquifer in southern Florida, USA (Langevin and Zygnerski 2013). An inland movement of 1250 m of the seawater-freshwater interface was reported for a sea level rise of 100 cm per century (Yang et al. 2015). Long term changes in the mean sea level rises and decreased recharge due to inadequate rainfall and increased evapotranspiration are responsible for an average increase in salinity (Comte et al. 2014). However, the effect of relative sea level rise has not been incorporated in a saltwater intrusion management model for a multi-layered coastal aquifer system under the influence of transient pumping stress applied to the aquifer. The present study intends to incorporate the effects of relative sea level on the optimized groundwater extraction values for a management period of 5 years.

Therefore, this research proposes a saltwater intrusion management model by incorporating the effects of relative sea level rise, increased groundwater extraction and reduced recharge for the duration of the proposed management time frame by utilizing a linked S/O approach. Contribution of the present study consists of providing a comparison of the simulation model results with and without considering relative sea level rise, proposing a computationally efficient and accurate meta-model to approximate saltwater intrusion processes, and suggesting water managers to choose appropriate management alternatives from a set of alternate feasible solutions. Present study does not consider tidal fluctuations as it is well established that tidal fluctuation induced head variation has very little influence on saltwater intrusion processes and that tidal fluctuation induced saltwater intrusion has setback mechanism. However, present study considers variation of water concentrations of the tidal river, and seasonal fluctuation of head at the upstream end of river. This study adopts a multi-layered anisotropic coastal aquifer system in which each individual layer represents different materials characterized by varying hydraulic conductivity values in these layers. The flow and transport process considered are also transient and density dependent.

Materials and Methods

Numerical simulation model

Aquifer processes are simulated using a density dependent finite element-based 3D coupled flow and salt transport numerical simulation model, FEMWATER (Lin et al. 1997). The simulation model generates salinity concentrations at designated monitoring locations using randomized groundwater extraction values as inputs obtained from the Latin Hypercube Sampling (LHS) technique (Pebesma and Heuvelink 1999). The governing equations of the combined flow and salt transport processes are expressed as (Lin et al. 1997):

$$\frac{\rho}{\rho_0} F \frac{\partial h}{\partial t} = \nabla \cdot \left[\mathbf{K} \cdot \left(\nabla h + \frac{\rho}{\rho_0} \nabla z \right) \right] + \frac{\rho}{\rho^*} q \quad (1)$$

$$F = \alpha' \frac{\theta}{n} + \beta' \theta + n \frac{dS}{dh} \quad (2)$$

where, F = storage coefficient, h = pressure head, t = time, K = hydraulic conductivity tensor, z = potential head, q = either a source or a sink, ρ = water density at chemical concentration C , ρ_0 = referenced water density at zero chemical concentration, ρ^* = density of injection fluid or that of the withdrawn water, θ = moisture content, α' = modified compressibility of water, β' = modified compressibility of the medium, n = porosity, S = saturation.

The hydraulic conductivity tensor, K is represented by

$$K = \frac{\rho g}{\mu} k = \frac{(\rho/\rho_o)}{\mu/\mu_o} \frac{\rho_o g}{\mu_o} k_s k_r = \frac{\rho/\rho_o}{\mu/\mu_o} K_{so} k_r \quad (3)$$

where, μ = dynamic viscosity of water chemical concentration C , μ_o = reference dynamic viscosity at zero chemical concentration, k_s = saturated permeability tensor, k_r = relative permeability or relative hydraulic conductivity, k_{so} = referenced saturated conductivity tensor.

The 3D solute transport is expressed as

$$\begin{aligned} & \theta \frac{\partial C}{\partial t} + \rho_b \frac{\partial S}{\partial t} + V \cdot \nabla C - \nabla \cdot (\theta D \cdot \nabla C) \\ & = - \left(\alpha' \frac{\partial h}{\partial t} + \lambda \right) (\theta C + \rho_b S) - (\theta K_w C + \rho_b K_s S) \\ & + m - \frac{\rho^*}{\rho} q C + \left(F \frac{\partial h}{\partial t} + \frac{\rho_o}{\rho} V \cdot \nabla \left(\frac{\rho}{\rho_o} \right) - \frac{\partial C}{\partial t} \right) C \end{aligned} \quad (4)$$

where, ρ_b = bulk density of the medium, C = for material concentration in aqueous phase, S = material concentration in adsorbed phase, V = discharge, ∇ = del operator, D = Dispersion coefficient tensor, λ = decay constant, $M = qC_m \rightarrow$ artificial mass rate, C_m = material concentration in the source, K_w = first order biodegradation rate constant through dissolved phase, K_s = first order biodegradation rate through adsorbed phase, K_d = distribution coefficient.

The dispersion coefficient tensor D in equation (4) is expressed as

$$\theta D = a_T |V| \delta + (a_L - a_T) \frac{VV}{|V|} + a_m \theta \tau \delta \quad (5)$$

Where, $|V|$ = magnitude of V , δ = Kronecker delta tensor, a_T = lateral dispersivity, a_L = longitudinal dispersivity, a_m = molecular diffusion coefficient, and τ = is tortuosity.

Input-output training pattern

Meta-models learn from the input-output training patterns generated by simulating the aquifer processes multiple times using a set of different transient groundwater extraction values obtained through LHS. Groundwater extraction patterns from a combination of production bores and barrier extraction wells in space and time (transient) are considered. These groundwater extraction patterns ranging from 0–1300 m³/day are used as inputs to the numerical simulation model to obtain saltwater concentration values at specified OPs as output. A set of such input-output patterns is used train and validate the proposed meta-models.

Meta-models

Three different artificial intelligence based meta-models are evaluated and compared in order to identify an accurate, reliable, and computationally efficient substitute of the density reliant coupled flow and salt transport processes of a multi-layered coastal aquifer system. Brief accounts of all of these meta-models are presented in the following sub-sections.

ANFIS

A Sugeno type ANFIS structure is adopted because of its simplicity and good learning capabilities compared to other types of ANFIS structures (Jang et al. 1997). To obtain the final ANFIS structure, an initial FIS structure is developed whose parameters are tuned using a hybrid algorithm. Fuzzy C-mean Clustering Approach (FCM) (Bezdek et al. 1984) is applied to generate this initial FIS structure.

FCM is a useful tool in compressing the dataset by dividing them into a group of similar cluster members that greatly reduces modifiable parameters (linear and non-linear) of a FIS. Number of fuzzy if-then rules also depends on the choice of number of clusters. Optimum number of clusters is selected by conducting several trials using different number of clusters and observing the resulting Root Mean Square Error (RMSE) of prediction. Numbers of clusters that produce minimum RMSE as well as yield least variance in RMSE values between learning and testing sets of data are chosen as adequate.

A Sugeno-type FIS, also known as Takagi-Sugeno-Kang model introduced in 1985 (Sugeno 1985) is ideal for developing primary FIS structures to be trained using suitable training algorithm to obtain the desired ANFIS structure. FISs are suitable for non-linear mapping of input and output spaces by utilizing fuzzy if-then rules. If-then rules set for a first-order Sugeno FIS for two inputs (α and β), one output (γ), and two fuzzy rules are given by:

$$\text{Rule 1: If } \alpha \text{ is } P_1 \text{ and } \beta \text{ is } Q_1 \text{ then } f_1 = p_1\alpha + q_1\beta + r_1, \quad (6)$$

$$\text{Rule 2: If } \alpha \text{ is } P_2 \text{ and } \beta \text{ is } Q_2, \text{ then } f_2 = p_2\alpha + q_2\beta + r_2 \quad (7)$$

The proposed Sugeno ANFIS has five layers, namely a fuzzy layer, a product layer, a normalized layer, a defuzzification layer, and a total output layer. Description of each of these layers are not repeated here; interested readers are directed towards a detailed description of these layers in Jang et al. (1997). A combination of the least squares and backpropagation gradient descent methods, known as ‘hybrid algorithm’ is used to tune the parameters of the proposed Sugeno type FIS.

GPR

GPR (Rasmussen and Williams 2005) is a flexible, nonparametric, probability based approach in which the output variable, Y is a function of input variables, $X(k)$ such that $Y = f(X(k)) + \varepsilon$, where ε is a Gaussian noise with variance σ_n^2 (Bishop 2006). The GPR approach of meta-modelling is based on the Gaussian process theory developed by Rasmussen and Williams (2005). Rasmussen and Williams (2005) defined Gaussian process (GP) as “*A Gaussian process is a collection of random variables, any finite number of which has a joint Gaussian distribution*”. The definition inevitably suggests a prerequisite of ‘consistency’, also known as marginalization property. This marginalization property implies that if the GP e.g. specifies $(y_1, y_2) \sim N(\mu, \Sigma)$, then it must also specify $y_1 \sim N(\mu_1, \Sigma_{11})$ where the relevant sub-matrix of Σ is Σ_{11} .

A Gaussian process is entirely indicated by its mean and covariance functions. The mean function provides a description of the expected value of the function at any particular point within the input space, and is given by

$$\text{Mean function: } m(x_i) = E[f(x_i)], \quad (8)$$

On the other hand, the covariance function, considered as the most influential and important element of a GPR model, defines proximity (nearness) or resemblance (similarity) between the predictor values x_i and response (target) value y_i (Rasmussen and Williams 2005). Covariance between the two latent variables $f(x_i)$ and $f(x_j)$ is specified by the covariance function, i.e. how response at one point x_i is affected by responses at other points x_j , $i \neq j, i = 1, 2, \dots, n$ is also determined by the covariance function. The covariance function is expressed as

$$\text{Covariance function: } k(x_i, x_j) = E[(f(x_i) - m(x_i))(f(x_j) - m(x_j))] \quad (9)$$

Finally, the Gaussian process can be written as

$$f(x) \sim gp(m(x_i), k(x_i, x_j)) \quad (10)$$

The parameters associated with mean and covariance functions, commonly known as free parameters or hyperparameters, define the properties of predictive probability distribution. The

values of the hyperparameters are obtained through maximizing log-likelihood function of the training data (Rasmussen and Williams 2005), and is given by

$$\log p(Y|X) = -\frac{1}{2} Y^T (K + \sigma_n^2 I)^{-1} Y - \frac{1}{2} \log \left(|K + \sigma_n^2 I| \right) - \frac{n}{2} \log(2\pi), \quad (11)$$

where n is the number of training samples.

MARS

MARS is a non-parametric, rapid, and flexible adaptive regression technique (Friedman 1991), which is capable of building regression models by dividing the entire solution space into various intervals of input variables, and builds a regression model by fitting individual Splines or Basis functions to each interval (Bera et al. 2006). MARS based meta-models are able to predict future responses through predictor-response mapping by integrating both a forward and a backward stepwise procedure. To avoid the development of unnecessarily complex model, and to prevent model over-fitting, MARS incorporates the backward stepwise procedure that eliminates irrelevant input variables in determining the output variable (Salford-Systems 2013). Maximum numbers of Basis functions are set as 200 to allow MARS to build a relatively complex model during the forward pass (100 forward steps). Minimum number of observations between the knots is selected by conducting numerical experiments by changing this parameter to a reasonable number of times. No penalty is added to the variables, enabling MARS to give equal priority to all input variables in the forward-stepping process of model development. However, in the backward stepping process MARS sparingly selects the most relevant input variables required to predict the output variables. This backward step keeps the developed model as simple as possible, with less possibility of model over-fitting. A commercial software package, Salford Predictive Modeller® (Salford-Systems 2016) is used to build the MARS models.

For all considered meta-models, training dataset consists 80% of the total input-output patterns generated by utilizing the numerical simulation model, FEMWATER. Remaining 20% of the generated patterns are used for validation of the meta-models. Once training and validation steps are completed, the meta-models thus developed are presented with a totally different realization of test dataset to check the prediction capability. This new realization of test dataset is presented to all developed meta-models to maintain consistency and a fair comparison.

Management model

The proposed management model utilizes a linked S/O approach in which a properly trained and validated meta-model is used as an approximate simulator of the aquifer processes. Two conflicting objectives of groundwater extraction strategy are considered: (1) maximum withdrawal of groundwater for beneficial purposes, (2) minimum extraction of water from barrier pumping wells to control saltwater intrusion by establishing a hydraulic head barrier near the coastal boundary. The multi-objective management model provides a tradeoff between these two conflicting objectives in terms of a Pareto optimal front, which consists of several feasible alternative groundwater extraction strategies that meet the pre-specified allowable saltwater concentration limits at specified locations.

Mathematical formulation

Two conflicting objectives as well as the constraints of the optimization formulation of the proposed management model can be expressed as (Roy and Datta (2017b))

$$\text{Maximize : } f_1(Q_{PW}) = \sum_{m=1}^M \sum_{t=1}^T Q_{PW_m}^t \quad (12)$$

$$\text{Minimize : } f_2(Q_{BW}) = \sum_{n=1}^N \sum_{t=1}^T Q_{BW_n}^t \quad (13)$$

$$\text{s. t. } C_i = \xi(Q_{PW}, Q_{BW}) \quad (14)$$

$$C_i \leq C_{\max} \quad \forall_i \quad (15)$$

$$Q_{PW \min} \leq Q_{PW_m}^t \leq Q_{PW \max} \quad (16)$$

$$Q_{BW \min} \leq Q_{BW_n}^t \leq Q_{BW \max} \quad (17)$$

where $Q_{PW_m}^t$ represents water extraction from the m^{th} pumping well throughout t^{th} time phase; $Q_{BW_n}^t$ stands for water extraction from n^{th} barrier extraction well throughout t^{th} time phase; $Q_{PW \min}$ and $Q_{BW \min}$ denote the minimum permissible amount of groundwater extraction from the production and barrier extraction wells respectively; $Q_{PW \max}$ and $Q_{BW \max}$ represent the maximum amount of groundwater extraction permissible from the production and barrier wells respectively; C_i symbolizes saltwater concentrations at i^{th} OPs at the closure of the management period; $\xi(\)$ denotes the density reliant coupled flow and salt transport simulation model, and constraint (14) indicates linking of the simulation model within the optimization framework, either using a numerical simulation model, or a trained and tested Meta-model; constraint (15) specifies the maximum allowable salt concentration at specified OPs; equations (20) and (17) outline the lower and upper limits on the water extraction rate from the pumping wells and barrier extraction wells, respectively; subscripts $_{PW}$ and $_{BW}$ stand for production bores and barrier extraction wells, respectively; M, N, and T stands for the entire pumping wells, barrier extraction wells, and time periods, respectively. The first objective of maximization of groundwater extraction from the pumping wells for beneficial use is represented by Equation (12), and the second objective of minimizing the water extraction from barrier pumping wells is given by Equation (13).

Optimization algorithm: CEMGA

Multi-objective optimization of the proposed management model is executed by utilizing a population based search algorithm, Controlled Elitist Multi-objective Genetic Algorithm (CEMGA) (Deb and Goel 2001). The key feature of CEMGA lies in its ability to prefer an individual, who despite having a low fitness value, helps increasing diversity of the population. The diversity is preserved by regulating the populations' elite members during the progress of the algorithm, making new population more diverse. More specifically, this regulated elitist tactic allows a particular fraction of the population (dominated populations) to be part of the current preeminent non-dominated solutions. This inclusion of a particular portion of dominated solutions in the non-dominated solutions greatly reduces the effect of elitism. 'Pareto Fraction' and 'Distance Function' are the two parameters that control the extent of elitism. First parameter restricts the number of individuals (elite members) on Pareto front, whereas the second one is intended to preserve diversity on the Pareto front by giving preference to individuals who are reasonably far-off on the front (Deb and Goel 2001).

Performance evaluation criteria

RMSE, Coefficient of Correlation (R), Mean Absolute Percentage Relative Error (MAPRE), Nash-Sutcliffe Efficiency Coefficient (NS), and Threshold Statistics (TS) are used to evaluate the prediction capability of ANFIS, GPR, and MARS based meta-models. On the other hand, the proposed management models' performance is validated by checking the constraint violation, and by confirming whether the constraints are satisfied at their upper limits. Finally, the optimized pumping values are used with the simulation model to obtain the corresponding saltwater concentration values. These concentration values are compared with those obtained by the meta-model within the optimization framework.

Root Mean Square Error (RMSE) is calculated using

$$RMSE = \sqrt{\frac{1}{n} \sum_{i=1}^n (C_{i,o} - C_{i,p})^2} \quad (18)$$

Correlation Coefficient (R) is expressed as

$$R = \frac{\sum_{i=1}^n (C_{i,o} - \bar{C}_o)(C_{i,o} - \bar{C}_p)}{\sqrt{\sum_{i=1}^n (C_{i,o} - \bar{C}_o)^2} \sqrt{\sum_{i=1}^n (C_{i,p} - \bar{C}_p)^2}} \quad (19)$$

Mean Absolute Percentage Relative Error (MAPRE) is calculated as

$$PMARE = \frac{1}{n} \sum_{i=1}^n \left| \frac{C_{i,o} - C_{i,p}}{C_{i,o}} \right| \times 100 \quad (20)$$

Nash-Sutcliffe Efficiency Coefficient (NS) is given by

$$NS = 1 - \frac{\sum_{i=1}^n (C_{i,o} - C_{i,p})^2}{\sum_{i=1}^n (C_{i,o} - \bar{C}_o)^2} \quad (21)$$

where, $C_{i,o}$ and $C_{i,p}$ are the observed and predicted saltwater concentrations; \bar{C}_o and \bar{C}_p denotes the mean of the observed and predicted saltwater concentrations; and n represents the number of data points.

Parallel computing

In order to achieve further computational efficiency of the meta-model based linked S/O approach, entire optimization problem is distributed among multiple workers (computational engines for parallel computing) in a parallel pool. In parallel computing, parameters are spontaneously distributed to worker machines throughout the implementation phases of parallel computations. Two conflicting objective functions and all binding constraints of the proposed optimization formulation are solved by utilizing a parallel pool of workers (physical cores of a CPU) by utilizing parallel computing toolbox of MATLAB (MathWorks 2017a-b).

Application of the proposed methodology for an illustrative study area

An illustrative study area is used to evaluate the performance of the proposed saltwater intrusion simulation model. The study area is similar to one developed in Roy and Datta (2017a) except that the present study considered an average sea level rise of 1.8 mm/year, seasonal variation of river water stage, and varying saltwater concentration of river water near the sea. However, the present study does not consider the variation of head due to tidal fluctuations because several previous studies demonstrated the negligible effects of tidal fluctuation on salinization of coastal aquifers (Chen and Hsu 2004; Heiss and Michael 2014; Kuan et al. 2012; Narayan et al. 2007). Initial head of the seaside boundary was assumed to be 0 m and allowed to increase incrementally during the simulation period of 50 years whereas the seaside head is varied based on the imposed sea level rise scenarios. Two stress periods of 6 months each are considered. Time-varying specified heads are assigned to both ends of the seaside boundary. The upstream end of the river is also assigned a time-varying specified head considering a variation of head during the wet and dry seasons (1 and 0.85 m, respectively). These time-varying specified heads varies linearly along the stream until they reached the assigned specified heads at the seaside boundary. The seaside boundary is assigned with a constant concentration of 35,000 mg/L, whereas the river boundary has varying concentrations. In the first 194-m length of the river from the sea, river water concentration is assigned as 12,000 mg/L and assumed to gradually decrease until it reaches 0 mg/L at the upstream end of the river. The assigned river water concentrations are given in Table 1.

Table 1. River water concentration

Distance from the seaside boundary (m)	Concentration (mg/L)
0 – 194	12000
194 – 388	5000
388 – 582	1000
582 – 1356	100
1356 – 1744	0
1744 – 2907	0

Figure 1 is a 3D view of the aquifer system of the study area. The study area has an aerial extent of 4.35 km² with an evenly spread pumping well field having a well density of 3.68 wells/km² (16 wells/4.35 km²). The unconfined aquifer has a total thickness of 80 m divided into four distinct layers of aquifer materials; each layer was assumed to be homogeneous. An anisotropy ratio (k_x/k_y) = 2.0 was used, where k_x = horizontal hydraulic conductivity in the x-direction, k_y = horizontal hydraulic conductivity in the y-direction, k_z = vertical hydraulic conductivity in the z-direction. The value of k_z is taken as one tenth of the hydraulic conductivity values in the x-direction. Table 2 lists hydraulic conductivity values, along with other aquifer parameters.

Table 2. Aquifer parameters

Parameter	Value			
	Top layer	Second layer	Third layer	Bottom layer
Hydraulic conductivity in x-direction (m/d)	5	10	15	3
Hydraulic conductivity in y-direction (m/d)	2.5	5	7.5	1.5
Hydraulic conductivity in z-direction (m/d)	0.5	1	1.5	0.3
Molecular diffusion coefficient (m ² /d)	0.69	0.69	0.69	0.69
Longitudinal dispersivity (m)	80	80	80	80
Lateral dispersivity (m)	35	35	35	35
Soil porosity	0.2	0.3	0.3	0.06
Compressibility (md ² /kg)	1.34×10 ⁻¹⁵	1.34×10 ⁻¹⁷	1.34×10 ⁻¹⁷	1.34×10 ⁻¹⁶
Bulk density (kg/m ³)	1650	1600	1550	1700

The illustrative multi-layered coastal aquifer study area considers 11 potential production wells that allow water extraction for beneficial purposes (denoted by PW1–PW11 in Figure 1). The study also considers 5 barrier extraction wells to create a hydraulic barrier near the seaside boundary for controlling saltwater intrusion (denoted by BW1–BW5 in Figure 1). Water is extracted from the 2nd and 3rd layer of the aquifer. Aquifer processes are simulated for a period of 5 years divided into 5 uniform time steps of 1 year each, where rate of extraction of water from both the production and barrier wells are considered constant. Therefore, considering the spatial and temporal variation of water extraction, present study considers 80 input variables (16 wells × 5 years) with lower and upper limits set as 0 and 1300 m³/day, respectively. The resulting saltwater concentration due to water abstraction from the wells at the end of management period of 5 years is monitored at 5 OPs. The proposed management model is developed by optimizing water extraction from the production and barrier wells while keeping salinity concentrations at the specified OPs within maximum allowable limits. Consequently, present study considers multi-objective type problem setting for developing the management model. OPs are located at three different salinity zones: OP1 is located in the low salinity zone, OP2 and OP3 are placed at the moderate salinity zone, OP4 and OP5 are located in high salinity zones. OPs are placed at different salinity zones with a view to use the extracted water from different regions of the aquifer for different purposes.

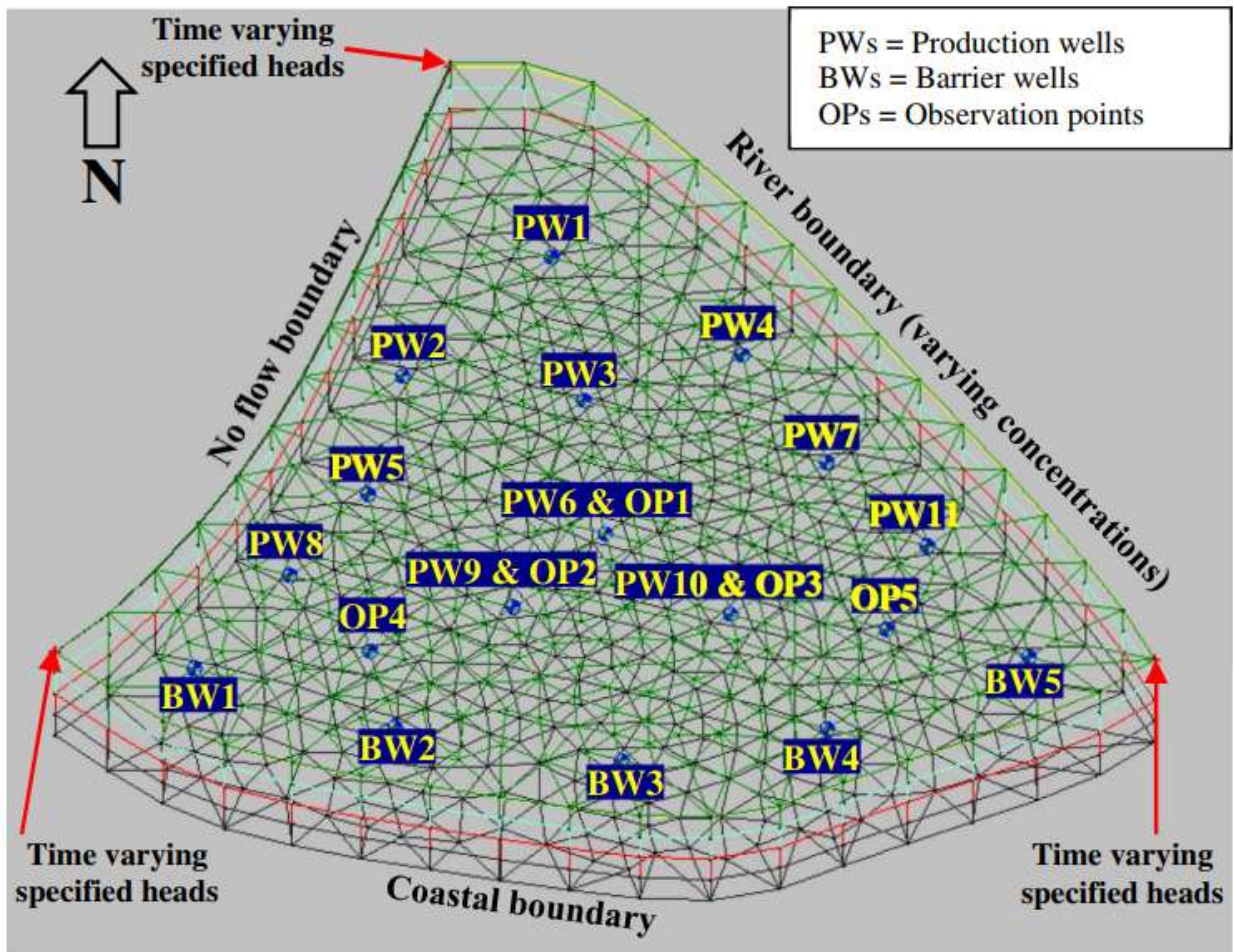
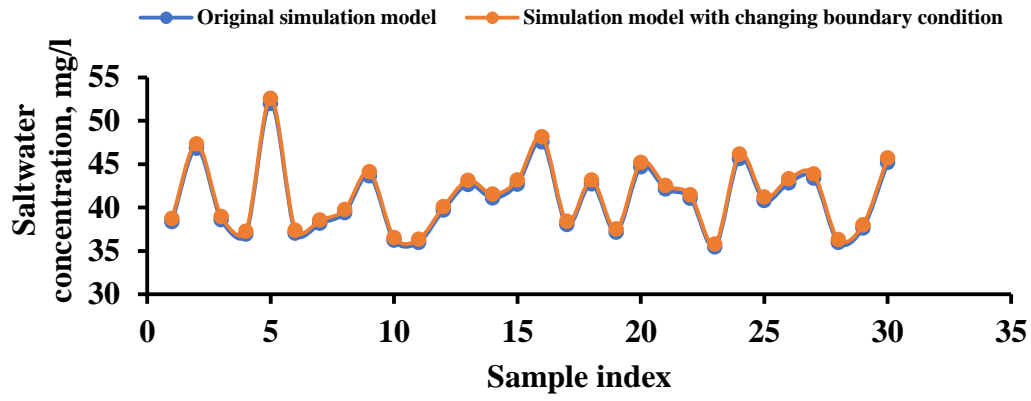


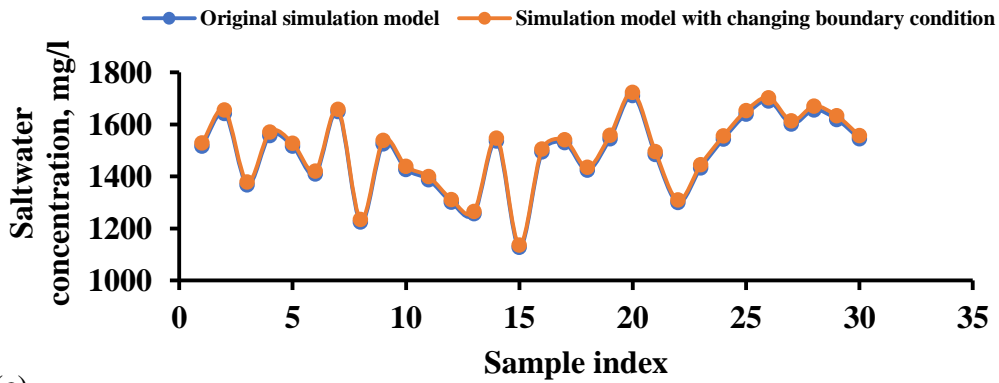
Figure. 1 Illustrative study area.

To demonstrate the effects of sea level rise, river water concentration, and seasonal variation of river water stage on the migration of salt plume, a comparison of the simulation results is performed with and without these boundary conditions. However, individual effects of these parameters are not considered in the present study. The Mean Absolute Percentage Relative Difference (MAPRD) in saltwater concentration values with respect to the original simulation model (without the effects of sea level rise, river water concentration, and seasonal variation of river water stage) at observation points OP1, OP2, OP3, OP4, and OP5 are 0.99%, 0.81%, 0.92%, 0.47%, and 0.82% respectively. These MAPRD values are compared with the MAPRE values obtained through proposed meta-models to make sure that the meta-models can accurately capture differences in saltwater concentration values at different OPs. Figure 2 illustrates the difference in concentration values with and without these changing boundary conditions at five OPs. For brevity of presentation, only first 30 observations are presented in Figure 2.

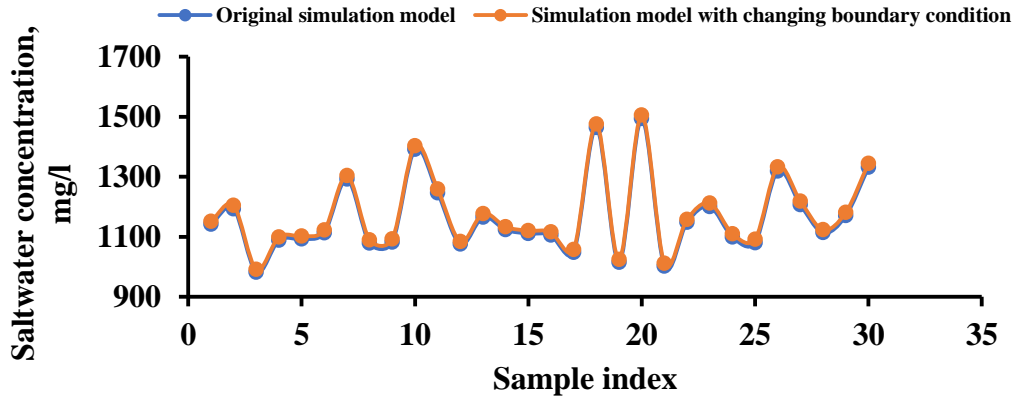
(a)



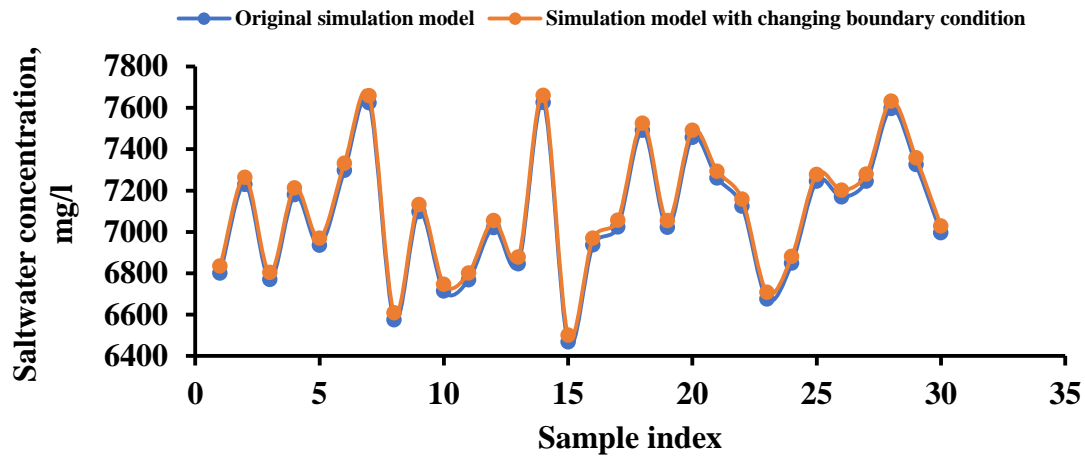
(b)



(c)



(d)



(e)

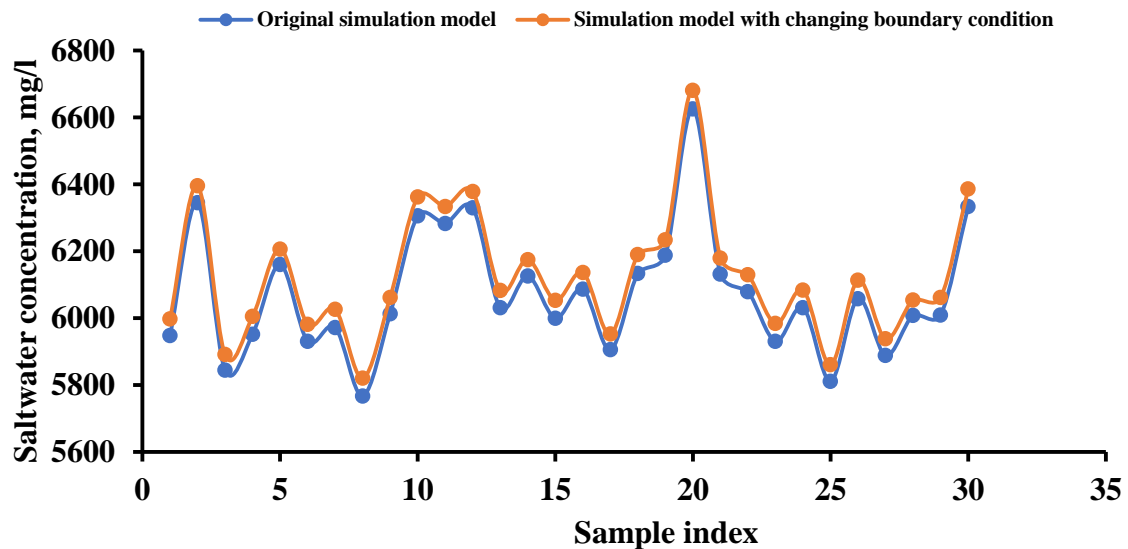


Figure 2. Comparison of numerical simulation results with and without sea level rise for the 30 sets of pumping values: a) Observation point OP1, (b) Observation point OP2, (c) Observation point OP3, (d) Observation point OP4, (e) Observation point OP5.

Modeling of groundwater flow and solute transport processes in real life coastal aquifers are influenced by uncertain model parameters (Sreekanth and Datta 2014b). In groundwater modeling system, the major sources of uncertainties arise from the associated aquifer characteristics such as hydraulic conductivity, compressibility, and bulk density (Ababou and Al-Bitar 2004). Aquifer recharge is another source of uncertainty. To determine the effect of uncertain model parameter estimates on groundwater flow and saltwater intrusion processes in coastal aquifers, 30 different randomized realizations of hydraulic conductivity, compressibility, bulk density, and aquifer recharge are utilized in the present study. These uncertain model parameters are assumed homogeneous within a geological material layer, but heterogeneous within respect to each material layer. Different realizations of a representative set of hydraulic conductivity values are obtained from a lognormal distribution with a specified mean and standard deviation of the associated distribution. Aquifer recharge and compressibility realizations are generated from LHS (Pebesma and Heuvelink 1999) uniform distributions within the parameter space with specific lower and upper bounds. Realizations of bulk density are obtained from LHS technique from a p-dimensional multivariate normal distribution with specific mean and covariance. Groundwater flow and transport processes are

simulated using these randomized set of uncertain model parameters for a fixed set of transient groundwater extraction values from both the production and barrier extraction wells. This procedure ensures a fair comparison between the resulting salinity concentrations from different randomized realizations of uncertain model parameters.

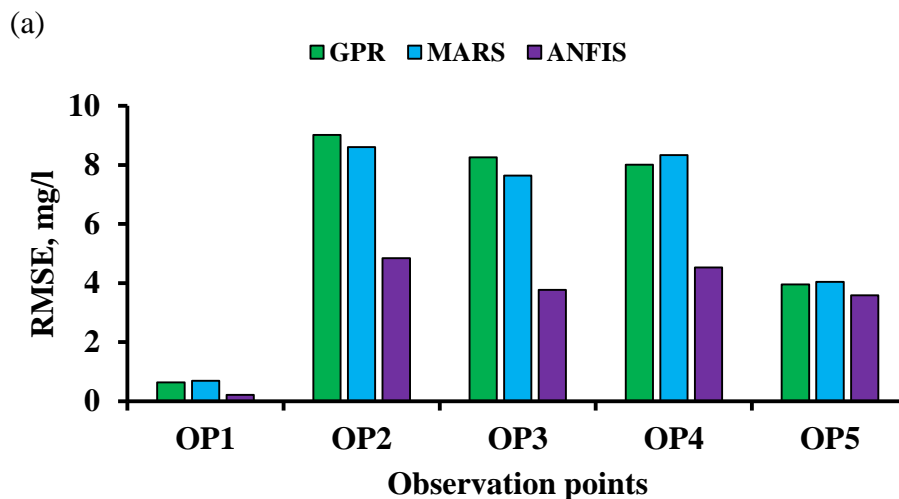
Salinity concentrations at different OPs obtained from these realizations of uncertain parameters are compared with those obtained when the mean values of these uncertain model parameters are used. MAPRD of salinity concentration values at different OPs are calculated for both cases, e.g. considering both with and without sea level rise scenarios. The MAPRD values are less than 6% for both cases and at different OPs. The MAPRD values at OP1, OP2, OP3, OP4, and OP5 are 2.43%, 5.0%, 5.43%, 4.18%, and 3.0% respectively when the sea level rise scenario is not considered. With sea level rise scenario, the corresponding values of MAPRD are 2.51%, 5.15%, 5.63%, 4.22%, and 3.24% respectively at different OPs. It is also noted that more than 80% of the observations are below 9% relative difference for both sea level rise and no sea level rise scenarios. Therefore, incorporation this type of model parameter uncertainties is important when developing regional scale saltwater intrusion management model for real world case studies. However, in this limited evaluation study, the effects of the uncertainties arising from uncertain model parameters are not incorporated as the MAPRD values of salinity concentrations at all OPs are less than 6% for both with and without sea level rise scenarios. However, these issues of model parameter uncertainties along with randomized multidimensional heterogeneity in terms of model parameters need to be incorporated in a rigorous real world regional scale saltwater intrusion management model.

In the next year, the developed and verified methodologies will be applied in a real-life coastal aquifer system of the southern Bangladesh.

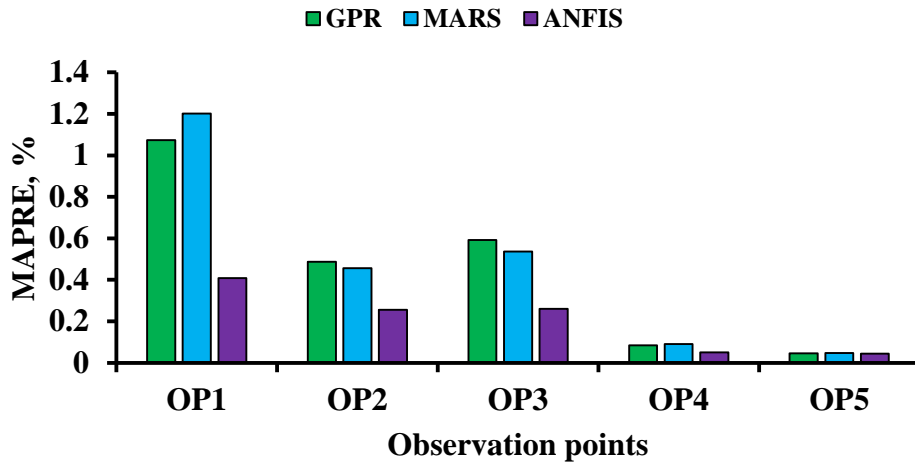
Results and Discussion

Comparison of the performance of ANFIS, GPR, and MARS based meta-models

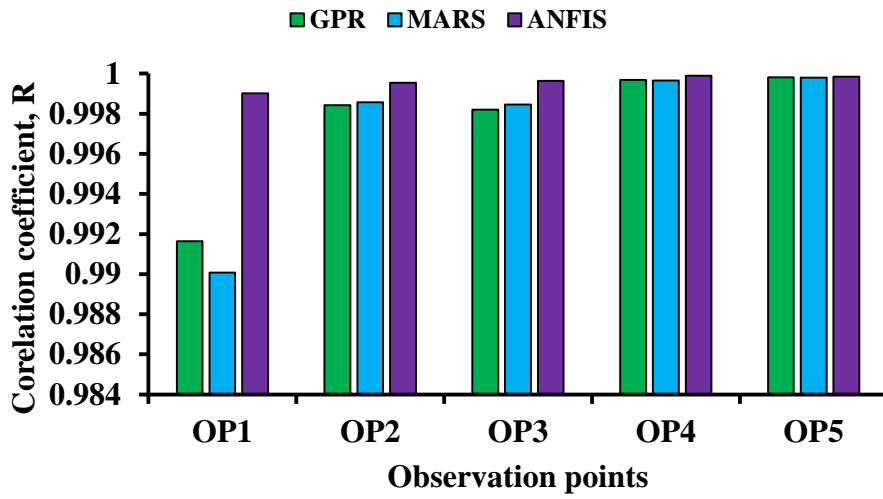
Performance of the ANFIS, GPR, and MARS based meta-models to approximate density dependent coupled flow and salt transport processes in a multi-layered coastal aquifer are evaluated. Each developed meta-model is utilized to predict salinity concentration at specified OPs with respect to transient pumping stress applied to the aquifer. Performance of ANFIS, GPR, and MARS based meta-models are compared based on their performances on a new realization of test dataset. Results are summarized in Figures 3–4 and Tables 3–4.



(b)



(c)



(d)

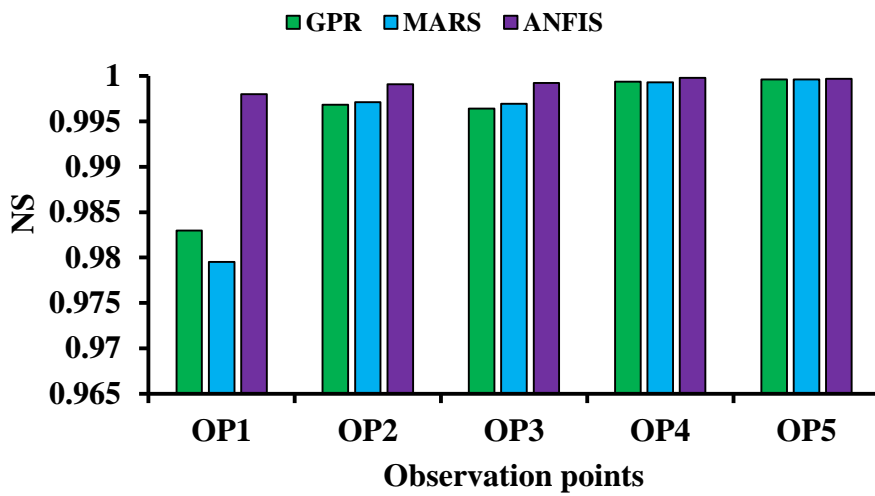


Figure 3. Comparison of prediction performance based on different statistical indices: (a) RMSE, (b) MAPRE, (c) R, (d) NS.

Figure 3 illustrates performance of the proposed meta-models at different OPs based on RMSE, MAPRE, R, and NS criteria, calculated from the actual and predicted saltwater concentration values. However, for this performance evaluation purpose only, actual concentrations are those synthetically obtained as solution of the numerical simulation model in response to water abstraction from the aquifer. Predicted concentrations denote the concentrations predicted by the meta-models. It is seen from Fig. 6 [Fig. 6] that all meta-models produce lower values of RMSE (Figure 3a) and MAPRE (Figure 3b) as well as higher values of R (Figure 3c) and NS (Figure 3d). Although both ANFIS, GPR, and MARS based meta-models are sufficiently accurate in predicting the responses, ANFIS exhibits relatively better performance than GPR and MARS models at all OPs based on all the performance measures. Therefore, it is concluded that ANFIS models' prediction accuracy in terms of capturing the trends of responses at different regions is quite satisfactory. The prediction accuracy of GPR and MARS is different at different OPs: GPR produces better results at OP1, OP4, and OP5 whereas MARS provides better prediction at OP2 and OP3 for all statistical performance measures as shown in Figure 3.

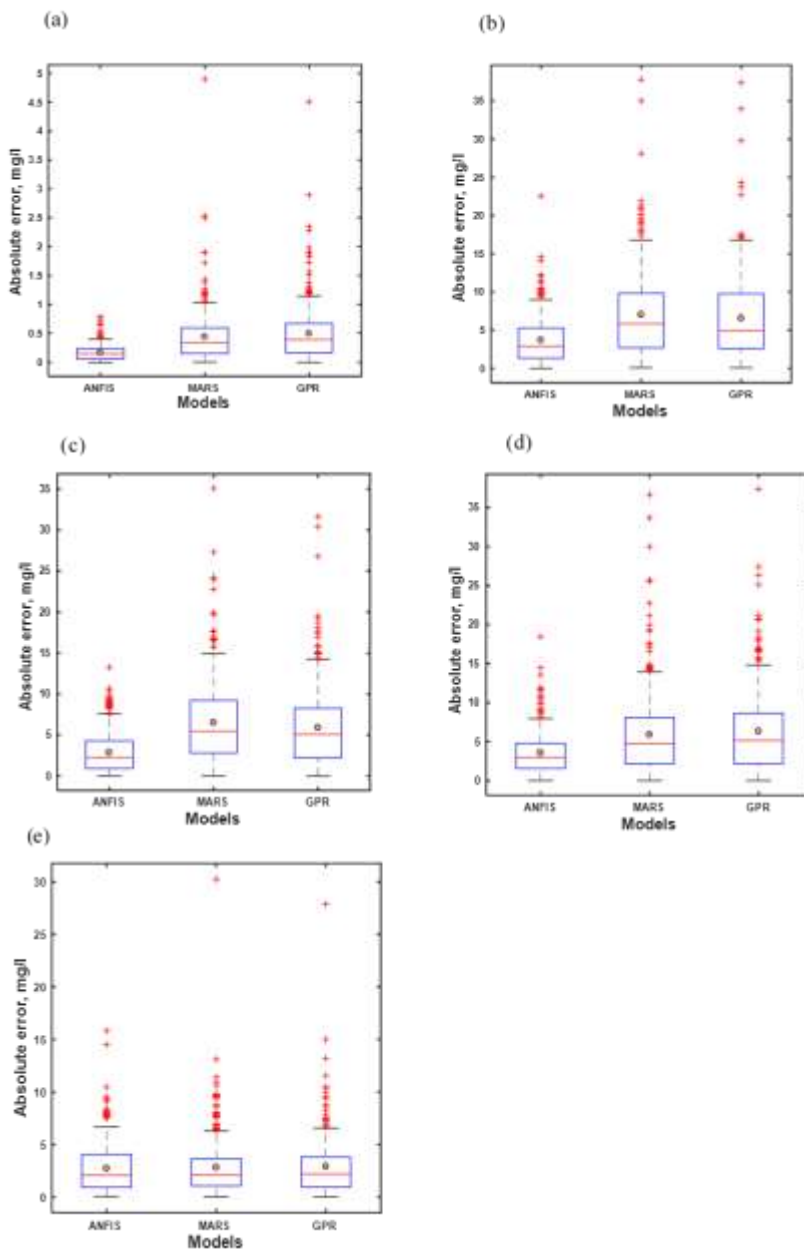


Figure 4. Absolute prediction error boxplots at (a) observation point OP1, (b) observation point OP2, (c) observation point OP3, (d) observation point OP4, (e) observation point OP5.

Figure 4 illustrates boxplots of absolute errors between the actual and predicted saltwater concentration values obtained by ANFIS, GPR, and MARS meta-models at different OPs. In Figure 4, red horizontal line indicates median of absolute errors whereas mean of the absolute errors is represented by small circles. Figure 4 also demonstrates the superiority of ANFIS model over GPR and MARS models at all OPs.

Table 3. Threshold statistics between actual and predicted concentration values predicted by ANFIS, GPR, and MARS meta-models for observation points OP1–OP5

OPs	Selected thresholds								
	<1%			<2%			<5%		
	ANFIS	GPR	MARS	ANFIS	GPR	MARS	ANFIS	GPR	MARS
OP1	94.33	56.33	52	100	87.33	84.33	100	99	98.67
OP2	99.67	92	91	100	99.33	99.33	100	100	100
OP3	99	84.33	88	100	98.33	98.67	100	100	100
OP4	100	100	100	100	100	100	100	100	100
OP5	100	100	100	100	100	100	100	100	100

*OPs = Observation points

The TS values provide distribution of errors, and give an estimation of the percentage of sample indices whose Relative Error (RE) values are smaller than the pre-defined threshold values. Three threshold values (<1%, <2%, and <5%) are chosen in the present study so that predictive RE values obtained from all meta-models fall within the selected threshold values. It is apparent from Table 3 that ANFIS outperforms both GPR and MARS meta-models in terms of TS criteria.

Table 4. Training time requirement (sec) to train different meta-models

Models	OP1	OP2	OP3	OP4	OP5
ANFIS	94	86	85	84	85
GPR	131	139	137	132	142
MARS	58	55	54	50	55

*OPs = Observation points

Another important criterion that should be considered in the selection process of any meta-model for linked S/O methodology is the computational time required to train the model. Table 4 presents the computational time required to develop ANFIS, GPR, and MARS meta-models at all OPs. It is noted that the difference in time requirement is not very substantial among different OPs for any specific meta-model. However, for all OPs, MARS requires the least training time followed by ANFIS and GPR meta-models. All developed models are computationally efficient, and can be suitable for linking within an optimization framework. However, considering both the prediction accuracy and computational efficiency criteria, the performance of ANFIS meta-model is considered superior. Therefore, it can be concluded that ANFIS is the most dependable prediction model to be used in a linked S/O methodology based saltwater intrusion management model at least based on the limited evaluations performed in this study.

Performance of the proposed management model using the best performing meta-model (ANFIS)

Prediction accuracy, computational efficiency, and feasibility of incorporation within a linked S/O approach determine the suitability of any meta-model for the development of regional scale saltwater intrusion management model. Based on the above criteria, ANFIS is selected as a good candidate for replacing and approximating the numerical simulation model within a linked S/O approach to determine Pareto optimal groundwater extraction strategies. Five ANFIS meta-models predicting saltwater concentrations at five different OPs are individually linked to CEMGA, and the optimization routine is run in a parallel computing platform. Several trials are conducted to choose the optimal parameter values of the optimization routine by using different combinations of these parameters. A population size of 2000, crossover fraction of 0.9, migration fraction of 0.2, and a Pareto front

population fraction of 0.7 is found optimal for producing a reliable Pareto optimal front of the management problem. The value of function tolerance is set as $1e-05$ whereas constraint tolerance is set to $1e-04$. The optimization algorithm evaluates 4496001 different groundwater extraction patterns in 2247 iterations to determine the global optimal solution of groundwater extraction patterns. The Pareto optimal front of the proposed saltwater intrusion management model is presented in Figure 5. The Pareto front provides 1400 non-dominated feasible groundwater extraction patterns in which any one of the extraction patterns can be used without exceeding the maximum allowable saltwater concentrations at specified OPs. The optimization routine takes about 6.87 hours to find the global optimal solution.

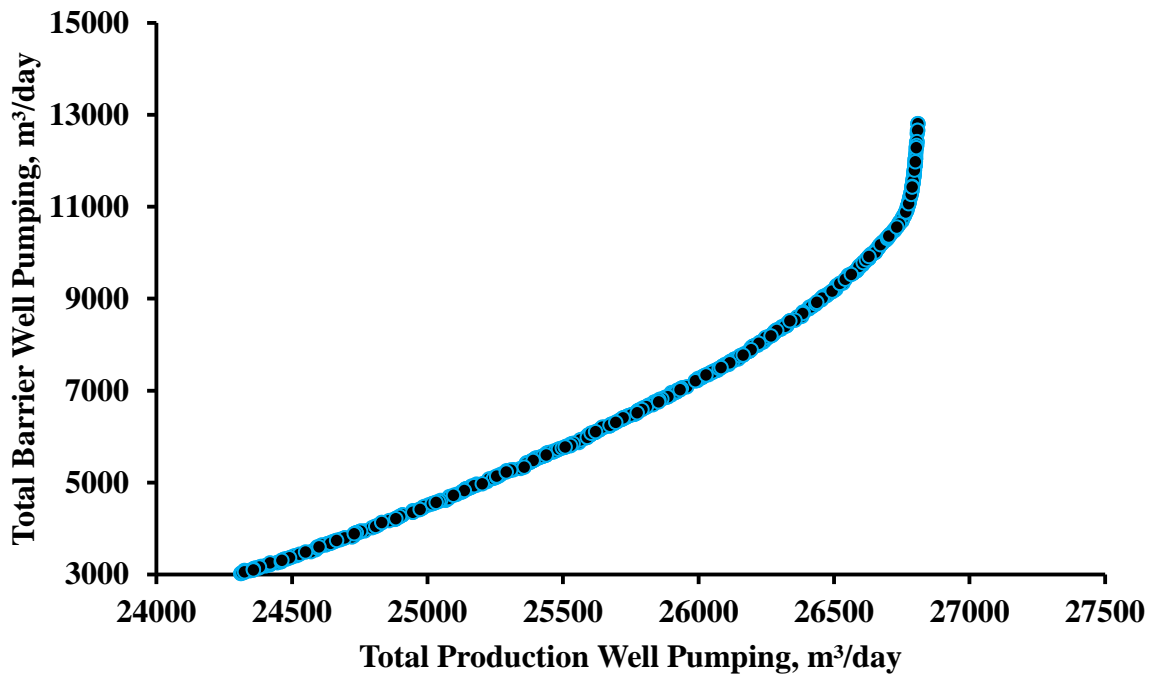


Figure 5. Pareto optimal front of the management model.

The Pareto optimal solutions shown in Figure 5 illustrate the conflicting nature of the two objectives, a necessary condition for a multiple objective optimal management. It can be seen from Figure 5 that an increased abstraction from production wells is associated with an increasing amount of barrier well extraction, which cannot be used for beneficial purposes due to high salinity. Therefore, water withdrawal from barrier extraction wells can be adjusted based on the demand for beneficial water use without compromising the pre-set maximum allowable salt concentrations at different OPs.

Verification of the management model

The proposed linked S/O based optimization scheme is evaluated based on two essential criteria: constraint violation, and closeness to the imposed constraints. The first criterion ensures the correctness of the optimization procedure whereas the second criterion allows maximum possible groundwater extraction within the imposed constraints. For all solutions in the Pareto optimal front, saltwater concentrations (computed by ANFIS within the optimization framework) are smaller than the pre-specified maximum allowable limits at all OPs. This confirms the satisfaction of all the imposed constraints as per solution prediction, and as per actual concentrations. Moreover, for the prescribed groundwater extraction patterns, ANFIS meta-models (within the optimization framework) provide saltwater concentration values very close to the pre-specified limits. This implies that the optimization model converges to the upper limit of constraints. In addition, the prescribed management strategy in terms of optimized groundwater extraction provided by the ANFIS meta-model based optimization routine is verified with the results obtained from the original numerical

simulation model. For this, 20 randomly selected groundwater extraction patterns obtained from different regions of the Pareto front are used to compare the ANFIS predicted, and numerical model simulated saltwater concentration values. Table 5 presents comparison of concentration values as well as the Percentage Relative Error (PRE) between the concentration values. It is obvious from Table 5 that numerical model simulation results are very close to the ANFIS predictions within the optimization model. PRE values are very small for all selected solutions at all OPs indicating the reliability of the proposed linked S/O based saltwater intrusion management model. At OP1, the PRE is less than 2% whereas the PRE values at OP2, OP3, OP4, and OP5 are close to 1%, less than 1%, less than 0.5%, and less than 0.1% respectively. Therefore, the proposed ANFIS-CEMGA based saltwater intrusion management model is capable of obtaining accurate solutions for optimal groundwater extraction from a set of beneficial pumping wells and barrier extraction wells for a multi-layered coastal aquifer.

Table 5. Validation of the optimization model through running the original simulation model using the optimized pumping values

Obs.	OP1			OP2			OP3			OP4			OP5		
	Conc., mg/l		RE, %	Conc., mg/l		RE, %	Conc., mg/l		RE, %	Conc., mg/l		RE, %	Conc., mg/l		RE, %
	ANFIS	SM		ANFIS	SM		ANFIS	SM		ANFIS	SM		ANFIS	SM	
1	39.97	39.27	1.79	999.7	1010.0	1.02	798.1	793.5	0.57	6386.2	6379.0	0.11	5494.8	5490.8	0.07
2	40.00	39.32	1.73	998.5	1008.5	0.99	799.3	797.2	0.26	6380.7	6371.6	0.14	5496.0	5492.6	0.06
3	39.99	39.25	1.89	999.5	1009.1	0.96	799.1	792.8	0.79	6395.3	6395.9	0.01	5485.5	5481.8	0.07
4	39.99	39.32	1.69	1000.0	1010.0	0.99	799.3	798.0	0.16	6381.0	6371.3	0.15	5497.8	5494.8	0.05
5	39.94	39.29	1.65	999.5	1009.4	0.98	799.8	798.7	0.13	6383.7	6374.1	0.15	5497.9	5495.1	0.05
6	39.99	39.27	1.84	998.7	1008.4	0.96	798.9	793.6	0.67	6389.8	6386.0	0.06	5487.9	5484.3	0.06
7	39.95	39.21	1.90	999.9	1009.4	0.95	798.6	792.2	0.80	6396.8	6398.3	0.02	5484.3	5480.4	0.07
8	39.95	39.24	1.80	999.0	1009.2	1.01	799.7	795.3	0.55	6385.3	6378.4	0.11	5495.5	5491.9	0.07
9	40.00	39.31	1.76	999.7	1009.7	0.99	799.1	795.8	0.40	6389.1	6382.1	0.11	5498.5	5494.8	0.07
10	40.00	39.28	1.83	999.6	1009.4	0.98	797.9	792.8	0.64	6390.2	6387.0	0.05	5493.4	5489.4	0.07
11	39.99	39.22	1.97	1000.0	1009.3	0.93	799.9	792.7	0.91	6399.8	6403.9	0.06	5481.2	5477.0	0.08
12	39.98	39.23	1.93	999.0	1008.6	0.95	799.5	792.9	0.83	6399.4	6401.3	0.03	5484.5	5480.5	0.07
13	39.96	39.21	1.92	999.6	1009.3	0.96	799.5	793.1	0.81	6399.8	6401.6	0.03	5485.5	5481.5	0.07
14	39.93	39.21	1.83	999.9	1009.5	0.96	799.6	794.3	0.67	6392.7	6389.7	0.05	5493.9	5489.9	0.07
15	39.96	39.22	1.90	999.7	1009.4	0.95	800.0	793.9	0.76	6398.7	6399.1	0.01	5490.6	5486.4	0.08
16	39.99	39.25	1.88	999.3	1008.8	0.94	799.3	793.3	0.76	6396.3	6395.3	0.02	5492.0	5487.9	0.08
17	39.94	39.19	1.91	999.9	1009.3	0.93	799.4	793.5	0.74	6399.5	6399.6	0.00	5487.3	5483.8	0.06
18	39.98	39.30	1.72	999.6	1009.5	0.99	798.7	796.3	0.31	6385.4	6377.1	0.13	5496.8	5493.7	0.06
19	39.99	39.27	1.84	999.2	1009.0	0.97	798.6	793.5	0.65	6390.6	6387.3	0.05	5492.7	5488.8	0.07
20	39.98	39.22	1.94	999.6	1009.0	0.94	799.1	792.4	0.85	6395.7	6396.7	0.02	5483.4	5479.3	0.07

Conclusion

In this study, a linked S/O based saltwater intrusion management model is proposed for a multi-layered coastal aquifer system. The proposed methodology considers seasonal variation of river water stage, river water concentration near the sea, and climate change induced sea level rise for the specified management period. ANFIS, GPR, and MARS based meta-models are developed as a computationally cheap substitute of the density reliant coupled flow and salt transport processes in the proposed saltwater intrusion management model. These meta-models are trained from datasets of predictor-response arrays of groundwater withdrawal and resultant saltwater concentrations obtained through a density dependent 3D coupled flow and salt transport numerical simulation model. The meta-models are compared based on their prediction accuracy, reliability, and computational efficiency. Results demonstrated that both models are capable of capturing the trend of coupled flow and salt transport processes of a multi-layered coastal aquifer system. However, based on a closer look at the prediction accuracy, and computational efficiency, ANFIS based meta-model is selected as a computationally cheap and feasible soft computing tool for incorporating into the linked S/O approach. The proposed methodology is employed to derive solution of the multiple objective optimization formulation consisting of two conflicting objectives of groundwater extraction. Parallel computing platform of MATLAB is used to implement the proposed methodology to achieve further computational efficiency. For assessing the proposed methodology, an illustrative multi-layered coastal aquifer system has been selected as a synthetic case study. Optimal solution obtained utilizing

meta-model is verified using the actual simulation model whereas optimal pumping values derived from optimal solution serves as inputs to the simulation model. It is demonstrated for an illustrative coastal aquifer study area that extraction of water according to the prescribed management strategy can limit the salt concentrations at OPs to pre-specified limits.

To incorporate realistic error scenarios or uncertainties in modeling within the scope of synthetic modeling, the effect of uncertainties in hydrogeological parameters on the predicted concentration values at designated OPs is investigated. Hydraulic conductivity, aquifer recharge, bulk density and compressibility are included in ascertaining the resulting effect on predicted spatial salinities. Both scenarios, with and without sea level rise are incorporated in these simulations. These effects are not substantial, and are not incorporated for solving the management strategies in this limited study. However, these issues are important and need to be addressed adequately in many real-life study areas.

Adaptive meta-models can be useful and efficient, especially when the initial data used for training the meta-models is small and the range is extensive. This option also needs going back to the numerical simulation model for retraining in a modified data range, which may not be computationally very efficient. In addition, the training can be restricted to subdomains, and not the entire decision space. Therefore, this approach may be largely dependent on the candidate or suboptimal solutions and may not result in a global optimal solution.

The present study considers a stratified coastal aquifer having four distinct layers of aquifer materials in which materials within each layer are considered homogeneous. The issue of heterogeneity is also important, and the degree of heterogeneity may determine how this issue can be addressed in a real-life study area. While the performance evaluation results presented here are based on spatial or layered heterogeneity, randomized heterogeneity assuming the heterogeneity is a random field has not been addressed in this study. Future research can be directed towards extending the application of this methodology to heterogeneous coastal aquifer systems incorporating random fields of different aquifer parameters. In addition, present study considers parallel pool of worker machines within the local clusters of a PC for efficiently executing the optimization routine. For more complex optimization settings, a parallel pool consisting of more PCs or any other high performance-computing platform can be considered.

Reference

- Ababou, R., and Al-Bitar, A. (2004). "Salt water intrusion with heterogeneity and uncertainty: mathematical modeling and analyses." *Devol. Water Sci.*, 55, 1559-1571.
- Adamowski, J., Chan, H. F., Prasher, S. O., and Sharda, V. N. (2012). "Comparison of multivariate adaptive regression splines with coupled wavelet transform artificial neural networks for runoff forecasting in Himalayan micro-watersheds with limited data." *J. Hydroinform.*, 14(3), 731-744.
- Bazi, Y., Alajlan, N., and Melgani, F. (2012). "Improved estimation of water chlorophyll concentration with semisupervised gaussian process regression." *IEEE Geosci. Remote Sens. Lett.*, 50(7), 2733-2743.
- Bera, P., Prasher, S. O., Patel, R. M., Madani, A., Lacroix, R., Gaynor, J. D., Tan, C. S., and Kim, S. H. (2006). "Application of MARS in simulating pesticide concentrations in soil." *T. Asabe*, 49(1), 297-307.
- Beuchat, X., Schaefli, B., Soutter, M., and Mermoud, A. (2011). "Toward a robust method for subdaily rainfall downscaling from daily data." *Water Resour. Res.*, 47(9), W09524.
- Bezdek, J. C., Ehrlich, R., and Full, W. (1984). "FCM: The fuzzy c-means clustering algorithm." *Comput. Geosci.*, 10(2), 191-203.
- Bhattacharjya, R. K., and Datta, B. (2009). "ANN-GA-based model for multiple objective management of coastal aquifers." *J. Water. Resour. Plan. Manage.*, 135(5), 314-322.
- Bishop, C. (2006). "Pattern recognition and machine learning." Springer-Verlag, New York.
- Brovelli, A., Mao, X., and Barry, D. A. (2007). "Numerical modeling of tidal influence on density-dependent contaminant transport." *Water Resour. Res.*, 43(10), W10426.

- Chen, B.-F., and Hsu, S.-M. (2004). "Numerical study of tidal effects on seawater intrusion in confined and unconfined aquifers by time-independent finite-difference method." *J. Waterw. Port. Coast. Ocean. Eng.*, 130(4), 191-206.
- Christelis, V., and Mantoglou, A. (2016). "Pumping optimization of coastal aquifers assisted by adaptive metamodelling methods and radial basis functions." *Water Resour. Manage.*, 30(15), 5845-5859.
- Comte, J.-C., Join, J.-L., Banton, O., and Nicolini, E. (2014). "Modelling the response of fresh groundwater to climate and vegetation changes in coral islands." *Hydrogeol. J.*, 22(8), 1905-1920.
- Datta, B., and Peralta, R. C. (1986). "Interactive computer graphics-based multiobjective decision-making for regional groundwater management." *Agric. Water Manage.*, 11(2), 91-116.
- Dausman, A. M., and Langevin, C. D. (2005). "Movement of the saltwater interface in the surficial aquifer system in response to hydrologic stresses and water-management practices, Broward County, Florida." US Geological Survey Scientific Investigations Report 2004-5256.
- Deb, K., and Goel, T. (2001). "Controlled elitist non-dominated sorting genetic algorithms for better convergence." *Evolutionary multi-criterion optimization: first international conference, EMO 2001 Zurich, Switzerland, March 7-9, 2001 proceedings*, E. Zitzler, L. Thiele, K. Deb, C. A. Coello Coello, and D. Corne, eds., Springer Berlin Heidelberg, Berlin, Heidelberg, 67-81.
- Dhar, A., and Datta, B. (2009). "Saltwater intrusion management of coastal aquifers. I: linked simulation-optimization." *J. Hydrol. Eng.*, 14(12), 1263-1272.
- Emamgholizadeh, S., Moslemi, K., and Karami, G. (2014). "Prediction the groundwater level of Bastam Plain (Iran) by artificial neural network (ANN) and adaptive neuro-fuzzy inference system (ANFIS)." *Water Resour. Manage.*, 28(15), 5433-5446.
- Essink, G. H. P. O. (2001). "Salt water intrusion in a three-dimensional groundwater system in the Netherlands: A numerical study." *Transport Porous. Med.*, 43(1), 137-158.
- Essink, G. H. P. O., van Baaren, E. S., and de Louw, P. G. B. (2010). "Effects of climate change on coastal groundwater systems: A modeling study in the Netherlands." *Water Resour. Res.*, 46(10), W00F04.
- Forrester, A. I. J., Sóbester, A., and Keane, A. J. (2008). "Constructing a surrogate." *Engineering Design via Surrogate Modelling*, John Wiley & Sons, Ltd, 33-76.
- Friedman, J. H. (1991). "Multivariate adaptive regression splines (with Discussion)." *Ann. Stat.*, 19(1), 1-67.
- Giambastiani, B. M. S., Antonellini, M., Essink, G. H. P. O., and Stuurman, R. J. (2007). "Saltwater intrusion in the unconfined coastal aquifer of Ravenna (Italy): A numerical model." *J. Hydrol.*, 340(1-2), 91-104.
- Goel, T., Haftka, R. T., Shyy, W., and Queipo, N. V. (2007). "Ensemble of surrogates." *Struct. Multidiscip. O.*, 33(3), 199-216.
- Green, P. J., and Silverman, B. W. (1993). "Nonparametric regression and generalized linear models: A roughness penalty approach." Taylor & Francis, Abingdon U.K.
- He, Z., Wen, X., Liu, H., and Du, J. (2014). "A comparative study of artificial neural network, adaptive neuro fuzzy inference system and support vector machine for forecasting river flow in the semiarid mountain region." *J. Hydrol.*, 509, 379-386.
- Heiss, J. W., and Michael, H. A. (2014). "Saltwater-freshwater mixing dynamics in a sandy beach aquifer over tidal, spring-neap, and seasonal cycles." *Water Resour. Res.*, 50(8), 6747-6766.
- Holman, D., Sridharan, M., Gowda, P., Porter, D., Marek, T., Howell, T., and Moorhead, J. (2014). "Gaussian process models for reference ET estimation from alternative meteorological data sources." *J. Hydrol.*, 517, 28-35.
- Hsieh, W. W., and Tang, B. (1998). "Applying neural network models to prediction and data analysis in meteorology and oceanography." *Bull. Am. Meteorol. Soc.*, 79(9), 1855-1870.
- Hussain, M. S., Javadi, A. A., Ahangar-Asr, A., and Farmani, R. (2015). "A surrogate model for simulation-optimization of aquifer systems subjected to seawater intrusion." *J. Hydrol.*, 523, 542-554.
- Jacobs, J. P., and Koziel, S. (2015). "Reduced-cost microwave filter modeling using a two-stage Gaussian process regression approach." *Int. J. RF. Microw. C. E.*, 25(5), 453-462.

- Jang, J.-S. R., Sun, C. T., and Mizutani, E. (1997). *Neuro-fuzzy and soft computing: A computational approach to learning and machine intelligence*, Prentice Hall.
- Ketabchi, H., and Ataie-Ashtiani, B. (2015). "Review: Coastal groundwater optimization—advances, challenges, and practical solutions." *Hydrogeol. J.*, 23(6), 1129-1154.
- Khaki, M., Yusoff, I., and Islami, N. (2015). "Application of the artificial neural network and neuro-fuzzy system for assessment of groundwater quality." *CLEAN – Soil, Air, Water*, 43(4), 551-560.
- Khashei-Siuki, A., and Sarbazi, M. (2015). "Evaluation of ANFIS, ANN, and geostatistical models to spatial distribution of groundwater quality (case study: Mashhad plain in Iran)." *Arab. J. Geosci.*, 8(2), 903-912.
- Kourakos, G., and Mantoglou, A. (2009). "Pumping optimization of coastal aquifers based on evolutionary algorithms and surrogate modular neural network models." *Adv. Water Resour.*, 32(4), 507-521.
- Kuan, W. K., Jin, G., Xin, P., Robinson, C., Gibbes, B., and Li, L. (2012). "Tidal influence on seawater intrusion in unconfined coastal aquifers." *Water Resour. Res.*, 48(2), W02502.
- Kurtulus, B., and Razack, M. (2010). "Modeling daily discharge responses of a large karstic aquifer using soft computing methods: Artificial neural network and neuro-fuzzy." *J. Hydrol.*, 381(1–2), 101-111.
- Langevin, C. D., and Zygnerski, M. (2013). "Effect of sea-level rise on salt water intrusion near a coastal well field in Southeastern Florida." *Groundwater*, 51(5), 781-803.
- Lin, H. J., Rechar, D. R., Talbot, C. A., Yeh, G. T., Cheng, J. R., Cheng, H. P., and Jones, N. L. (1997). "A three-dimensional finite element computer model for simulating density-dependent flow and transport in variable saturated media: Version 3.0." US Army Engineering Research and Development Center, Vicksburg, Miss.
- Liu, Y., Shang, S.-H., and Mao, X.-M. (2012). "Tidal effects on groundwater dynamics in coastal aquifer under different beach slopes." *J. Hydrodynam.*, 24(1), 97-106.
- MathWorks (2017a-a). "Fuzzy logic toolbox: MATLAB version 2017a " The Mathworks Inc, Mathworks, Natick.
- MathWorks (2017a-b). "Parallel computing toolbox: MATLAB version R2017a " The Mathworks Inc, Mathworks, Natick.
- Mohammadi, K., Shamshirband, S., Petković, D., Yee, P. L., and Mansor, Z. (2016). "Using ANFIS for selection of more relevant parameters to predict dew point temperature." *Appl. Therm. Eng.*, 96, 311-319.
- Narayan, K. A., Schleeberger, C., and Bristow, K. L. (2007). "Modelling seawater intrusion in the Burdekin Delta Irrigation Area, North Queensland, Australia." *Agric. Water Manage.*, 89(3), 217-228.
- Nasseri, M., Tavakol-Davani, H., and Zahraie, B. (2013). "Performance assessment of different data mining methods in statistical downscaling of daily precipitation." *J. Hydrol.*, 492, 1-14.
- Papadopoulou, M. P., Nikolos, I. K., and Karatzas, G. P. (2010). "Computational benefits using artificial intelligent methodologies for the solution of an environmental design problem: saltwater intrusion." *Water Sci. Technol.*, 62(7), 1479–1490.
- Pebesma, E. J., and Heuvelink, G. B. M. (1999). "Latin hypercube sampling of gaussian random fields." *Technometrics*, 41(4), 303-312.
- Pillay, N. (2004). "An investigation into the use of genetic programming for the induction of noviceprocedural programming solution algorithms in intelligent programming tutors." Dissertation, University of KwaZulu-Natal, Durban.
- Piret, C. (2007). "Analytical and numerical advances in radial basis functions." Ph.D. dissertation, Univ. of Colorado, Boulder, CO.
- Rajabi, M. M., and Ketabchi, H. (2017). "Uncertainty-based simulation-optimization using Gaussian process emulation: Application to coastal groundwater management." *J. Hydrol.*, 555(Supplement C), 518-534.
- Rasmussen, C. E., and Williams, C. K. I. (2005). *Gaussian processes for machine learning*, The MIT Press.
- Roy, D. K., and Datta, B. (2017a). "Fuzzy c-mean clustering based inference system for saltwater intrusion processes prediction in coastal aquifers." *Water Resour. Manage.*, 31(1), 355-376.
- Roy, D. K., and Datta, B. (2017b). "Genetic algorithm tuned fuzzy inference system to evolve optimal groundwater extraction strategies to control saltwater intrusion in multi-layered coastal aquifers under parameter uncertainty." *Model. Earth Syst. Environ.*, <https://doi.org/10.1007/s40808-017-0398-5>, 1-19.
- Roy, D. K., and Datta, B. (2017c). "Multivariate adaptive regression spline ensembles for management of multilayered coastal aquifers." *J. Hydrol. Eng.*, 22(9), 04017031.

- Roy, D. K., and Datta, B. (2017d). "Optimal management of groundwater extraction to control saltwater intrusion in multi-layered coastal aquifers using ensembles of adaptive neuro-fuzzy inference system." World Environmental and Water Resources Congress 2017, American society of civil engineers, May 21–25, 2017, Sacramento, California, USA, 139-150.
- Salford-Systems (2013). "SPM Users Guide: Introducing MARS." Salford Systems, San Diego, CA.
- Salford-Systems (2016). "MARS® (Version 8.0 Ultra), Multivariate Adaptive Regression Spline." Salford Systems, San Diego, CA.
- Samadi, M., Jabbari, E., Azamathulla, H. M., and Mojallal, M. (2015). "Estimation of scour depth below free overfall spillways using multivariate adaptive regression splines and artificial neural networks." *Eng. Appl. Comp. Fluid*, 9(1), 291-300.
- Sharda, V. N., Patel, R. M., Prasher, S. O., Ojasvi, P. R., and Prakash, C. (2006). "Modeling runoff from middle Himalayan watersheds employing artificial intelligence techniques." *Agric. Water Manage.*, 83(3), 233-242.
- Sharda, V. N., Prasher, S. O., Patel, R. M., Ojasvi, P. R., and Prakash, C. (2008). "Performance of Multivariate Adaptive Regression Splines (MARS) in predicting runoff in mid-Himalayan micro-watersheds with limited data." *Hydrol. Sci. J.*, 53(6), 1165-1175.
- Sherif, M. M., and Singh, V. P. (1999). "Effect of climate change on sea water intrusion in coastal aquifers." *Hydrolog. Process.*, 13(8), 1277-1287.
- Shiri, J., and Kişi, Ö. (2011). "Comparison of genetic programming with neuro-fuzzy systems for predicting short-term water table depth fluctuations." *Comput. Geosci.*, 37(10), 1692-1701.
- Shrivastava, G. S. (1998). "Impact of sea level rise on seawater intrusion into coastal aquifer." *J. Hydrol. Eng.*, 3(1), 74-78.
- Sóbestor, A., Forrester, A. I. J., Toal, D. J. J., Tresidder, E., and Tucker, S. (2014). "Engineering design applications of surrogate-assisted optimization techniques." *Optim. Eng.*, 15(1), 243-265.
- Sreekanth, J., and Datta, B. (2010). "Multi-objective management of saltwater intrusion in coastal aquifers using genetic programming and modular neural network based surrogate models." *J. Hydrol.*, 393(3–4), 245-256.
- Sreekanth, J., and Datta, B. (2011a). "Comparative evaluation of genetic programming and neural network as potential surrogate models for coastal aquifer management." *Water Resour. Manage.*, 25(13), 3201-3218.
- Sreekanth, J., and Datta, B. (2011b). "Optimal combined operation of production and barrier wells for the control of saltwater intrusion in coastal groundwater well fields." *Desalin. Water Treat.*, 32(1-3), 72-78.
- Sreekanth, J., and Datta, B. (2014a). "Design of an optimal compliance monitoring network and feedback information for adaptive management of saltwater intrusion in coastal aquifers." *J. Water. Resour. Plan. Manage.*, 140(10), 04014026.
- Sreekanth, J., and Datta, B. (2014b). "Stochastic and robust multi-objective optimal management of pumping from coastal aquifers under parameter uncertainty." *Water Resour. Manage.*, 28(7), 2005-2019.
- Sugeno, M. (1985). *Industrial applications of fuzzy control*, Elsevier Science Inc.
- Sugeno, M., and Yasukawa, T. (1993). "A fuzzy-logic-based approach to qualitative modeling." *IEEE Trans. Fuzzy Syst.*, 1(1), 7.
- Sun, A. Y., Wang, D., and Xu, X. (2014). "Monthly streamflow forecasting using Gaussian process regression." *J. Hydrol.*, 511, 72-81.
- Takagi, T., and Sugeno, M. (1985). "Fuzzy identification of systems and its applications to modeling and control." *IEEE Trans. Syst. Man Cybern.*, SMC-15(1), 116-132.
- Webb, M. D., and Howard, K. W. F. (2011). "Modeling the transient response of saline intrusion to rising sea-levels." *Ground Water*, 49(4), 560-569.
- Yang, J., Graf, T., and Ptak, T. (2015). "Sea level rise and storm surge effects in a coastal heterogeneous aquifer: a 2D modelling study in northern Germany." *Grundwasser*, 20(1), 39-51.
- Zabihi, M., Pourghasemi, H. R., Pourtaghi, Z. S., and Behzadfar, M. (2016). "GIS-based multivariate adaptive regression spline and random forest models for groundwater potential mapping in Iran." *Environ. Earth Sci.*, 75(8), 665.

PREDICTION OF SALTWATER INTRUSION FOR DIFFERENT SCENARIOS OF AQUIFER RECHARGE AND GROUNDWATER EXTRACTION UNDER CHANGING CLIMATE

D.K. ROY¹, S.K. BISWAS¹, AND M.A. HOSSAIN²

Abstract

The present study intended to evaluate the effects of climate change induced sea level rise and reduced recharge scenarios as well as anthropogenic activity of enhanced groundwater extraction on the inland progression of saltwater wedge in a coastal aquifer study area. The methodology is demonstrated in an illustrative coastal aquifer system resembling a real coastal aquifer study area. The reason why an illustrative coastal aquifer is chosen is that any methodology needs to be evaluated first for a hypothetical study area before applying in a real-life coastal aquifer study area. Simulation is performed with the combination of different scenarios for a period of 50 years. Results demonstrate that there is a significant influence of the future scenarios on the salinity intrusion process and that salinity intrusion in designated monitoring locations increases with the simulation period. The developed methodology will be tested in a real-life coastal aquifer study area in the southern Bangladesh.

Introduction

Groundwater is an important source of freshwater supplies to the coastal regions of the world including Bangladesh. An increasing trend in human settlements near the coastal regions inevitably requires more freshwater supplies to meet the demand for agricultural, industrial, and domestic requirements. This growing need of freshwater supplies results in overexploitation of the valuable groundwater resources in coastal areas. On top of that, the effects of ongoing climate change are likely to influence the hydrological cycle that will negatively impact the availability of freshwater resources worldwide. Global warming has already triggered drought induced water scarcity in Bangladesh significantly affecting the quantity and quality of groundwater resources, especially in the coastal regions. In fact, over-pumping and climate change induced drought are responsible for accelerating saltwater intrusion processes around the globe including Bangladesh. Therefore, measures should be taken to ensure sustainable management of coastal aquifers for providing safe abstraction of groundwater without causing harm to the aquifer. Assessing the consequences of this anthropogenic activity and its effects on the complex subsurface largely rely on the accurate characterization and simulation of the aquifer processes, and in particular prediction capabilities of future scenarios by the appropriate simulation models. Therefore, this study intends to assess the effects of various scenarios of aquifer recharge and groundwater abstraction on the saltwater intrusion into the aquifer.

In addition, relative sea level rise, providing an additional saline water head at the seaside (Yang et al. 2015), has a significant impact in increasing the salinization of the coastal aquifers around the globe (Shrivastava 1998). Therefore, sea level rise can accelerate saltwater intrusion processes in aquifer systems, and several centuries would be required to equilibrate this sea level rise-induced saltwater intrusion even if the sea level has fallen back to its original position (Webb and Howard 2011). However, the effect of this sea level rise-induced increase in hydraulic heads of the groundwater system is confined within a few kilometers of the coastline and main rivers (Oude Essink et al. 2010). Although excessive groundwater withdrawal is considered the major cause of saltwater intrusion (Narayan et al. 2007), relative sea level rise in combination with the effect of excessive groundwater pumping can exacerbate the already vulnerable coastal aquifers (Langevin and Zygnerski 2013). This study does not consider tidal fluctuations because it is well established that tidal fluctuation-induced head variation has truly little influence on saltwater intrusion processes, and that tidal fluctuation-induced saltwater intrusion has a setback mechanism. However, the present study considers variation of water concentrations in the tidal river, and seasonal fluctuation of head at the

¹ SSO, IWM Division, BARI, Gazipur

² CSO(in-charge), IWM Division, BARI, Gazipur

upstream end of river. This study adopts a multilayered anisotropic coastal aquifer system in which each individual layer represents different materials characterized by varying hydraulic conductivity values in these layers. The flow and transport process considered are also transient and density dependent.

In sum, this study synthetically generates different groundwater pumping and recharge scenarios based on projected population growth and climate change scenarios. Climate change induced relative sea level rise has also been included in the simulation process to evaluate the aquifer's response with the pumping stress applied to the aquifer in changing climatic scenarios. The resulting effect of these natural and anthropogenic factors on the saltwater intrusion processes is monitored at designated monitoring locations.

Materials and Methods

Aquifer processes are simulated using a density dependent finite element-based 3D coupled flow and salt transport numerical simulation model, FEMWATER (Lin et al. 1997). The simulation model generates salinity concentrations at designated monitoring locations using randomized groundwater extraction values as inputs obtained from the Latin Hypercube Sampling (LHS) technique (Pebesma and Heuvelink 1999). The governing equations of the combined flow and salt transport processes are expressed as (Lin et al. 1997):

$$\frac{\rho}{\rho_0} F \frac{\partial h}{\partial t} = \nabla \cdot \left[\mathbf{K} \cdot \left(\nabla h + \frac{\rho}{\rho_0} \nabla z \right) \right] + \frac{\rho}{\rho^*} q \quad (1)$$

$$F = \alpha' \frac{\theta}{n} + \beta' \theta + n \frac{dS}{dh} \quad (2)$$

where, F = storage coefficient, h = pressure head, t = time, K = hydraulic conductivity tensor, z = potential head, q = either a source or a sink, ρ = water density at chemical concentration C , ρ_0 = referenced water density at zero chemical concentration, ρ^* = density of injection fluid or that of the withdrawn water, θ = moisture content, α' = modified compressibility of water, β' = modified compressibility of the medium, n = porosity, S = saturation.

The hydraulic conductivity tensor, K is represented by

$$K = \frac{\rho g}{\mu} k = \frac{(\rho/\rho_0) \rho_0 g}{\mu/\mu_0 \mu_0} k_s k_r = \frac{\rho/\rho_0}{\mu/\mu_0} K_{so} k_r \quad (3)$$

where, μ = dynamic viscosity of water chemical concentration C , μ_0 = reference dynamic viscosity at zero chemical concentration, k_s = saturated permeability tensor, k_r = relative permeability or relative hydraulic conductivity, k_{so} = referenced saturated conductivity tensor.

The 3D solute transport is expressed as

$$\begin{aligned} & \theta \frac{\partial C}{\partial t} + \rho_b \frac{\partial S}{\partial t} + V \cdot \nabla C - \nabla \cdot (\theta D \cdot \nabla C) \\ & = - \left(\alpha' \frac{\partial h}{\partial t} + \lambda \right) (\theta C + \rho_b S) - (\theta K_w C + \rho_b K_s S) \\ & + m - \frac{\rho^*}{\rho} q C + \left(F \frac{\partial h}{\partial t} + \frac{\rho_0}{\rho} V \cdot \nabla \left(\frac{\rho}{\rho_0} \right) - \frac{\partial C}{\partial t} \right) C \end{aligned} \quad (4)$$

where, ρ_b = bulk density of the medium, C = for material concentration in aqueous phase, S = material concentration in adsorbed phase, V = discharge, ∇ = del operator, D = Dispersion coefficient tensor, λ = decay constant, $M = qC_m \rightarrow$ artificial mass rate, C_m = material concentration in the source, K_w = first order biodegradation rate constant through dissolved phase, K_s = first order biodegradation rate through adsorbed phase, K_d = distribution coefficient.

The dispersion coefficient tensor D in equation (4) is expressed as

$$\theta D = a_T |V| \delta + (a_L - a_T) \frac{VV}{|V|} + a_m \theta \tau \delta \quad (5)$$

Where, $|V|$ = magnitude of V , δ = Kronecker delta tensor, a_T = lateral dispersivity, a_L = longitudinal dispersivity, a_m = molecular diffusion coefficient, and τ = is tortuosity.

An illustrative study area is used to evaluate the performance of the proposed saltwater intrusion simulation model. The study area is similar to one developed in Roy and Datta (2017) except that the present study considered an average sea level rise of 1.8 mm/year, seasonal variation of river water stage, and varying saltwater concentration of river water near the sea. However, the present study does not consider the variation of head due to tidal fluctuations because several previous studies demonstrated the negligible effects of tidal fluctuation on salinization of coastal aquifers (Chen and Hsu 2004; Heiss and Michael 2014; Kuan et al. 2012; Narayan et al. 2007). Initial head of the seaside boundary was assumed to be 0 m and allowed to increase incrementally during the simulation period of 50 years whereas the seaside head is varied based on the imposed sea level rise scenarios. Two stress periods of 6 months each are considered. Time-varying specified heads are assigned to both ends of the seaside boundary. The upstream end of the river is also assigned a time-varying specified head considering a variation of head during the wet and dry seasons (1 and 0.85 m, respectively). These time-varying specified heads varies linearly along the stream until they reached the assigned specified heads at the seaside boundary. The seaside boundary is assigned with a constant concentration of 35,000 mg/L, whereas the river boundary has varying concentrations. In the first 194-m length of the river from the sea, river water concentration is assigned as 12,000 mg/L and assumed to gradually decrease until it reaches 0 mg/L at the upstream end of the river. The assigned river water concentrations are given in Table 1.

Table 1. River water concentration

Distance from the seaside boundary (m)	Concentration (mg/L)
0 – 194	12000
194 – 388	5000
388 – 582	1000
582 – 1356	100
1356 – 1744	0
1744 – 2907	0

Figure 1 is a 3D view of the aquifer system of the study area. The study area has an aerial extent of 4.35 km² with an evenly spread pumping well field having a well density of 3.68 wells/km² (16 wells/4.35 km²). The unconfined aquifer has a total thickness of 80 m divided into four distinct layers of aquifer materials; each layer was assumed to be homogeneous. An anisotropy ratio (k_x/k_y) = 2.0 was used, where k_x = horizontal hydraulic conductivity in the x-direction. k_y = horizontal hydraulic conductivity in the y-direction. k_z = vertical hydraulic conductivity in the z-direction. The value of k_z is taken as one tenth of the hydraulic conductivity values in the x-direction. Table 2 lists hydraulic conductivity values, along with other aquifer parameters.

Table 2. Aquifer parameters

Parameter	Value			
	Top layer	Second layer	Third layer	Bottom layer
Hydraulic conductivity in x-direction (m/d)	5	10	15	3
Hydraulic conductivity in y-direction (m/d)	2.5	5	7.5	1.5
Hydraulic conductivity in z-direction (m/d)	0.5	1	1.5	0.3
Molecular diffusion coefficient (m ² /d)	0.69	0.69	0.69	0.69
Longitudinal dispersivity (m)	80	80	80	80
Lateral dispersivity (m)	35	35	35	35
Soil porosity	0.2	0.3	0.3	0.06
Compressibility (md ² /kg)	1.34×10^{-15}	1.34×10^{-17}	1.34×10^{-17}	1.34×10^{-16}
Bulk density (kg/m ³)	1650	1600	1550	1700

The illustrative multilayered coastal aquifer study area considered 11 potential production wells that allow water extraction for beneficial purposes (denoted by PW1–PW11 in Figure 1). It also considers additional 5 pumping wells placed relatively close to the seaside boundary (denoted by BW1 – BW5 in Figure 1). The salinity concentration is monitored at 5 monitoring locations denoted by OP1 – OP5. It is noted that pumping wells PW6, PW9, and PW10 are used for both pumping and monitoring purposes.

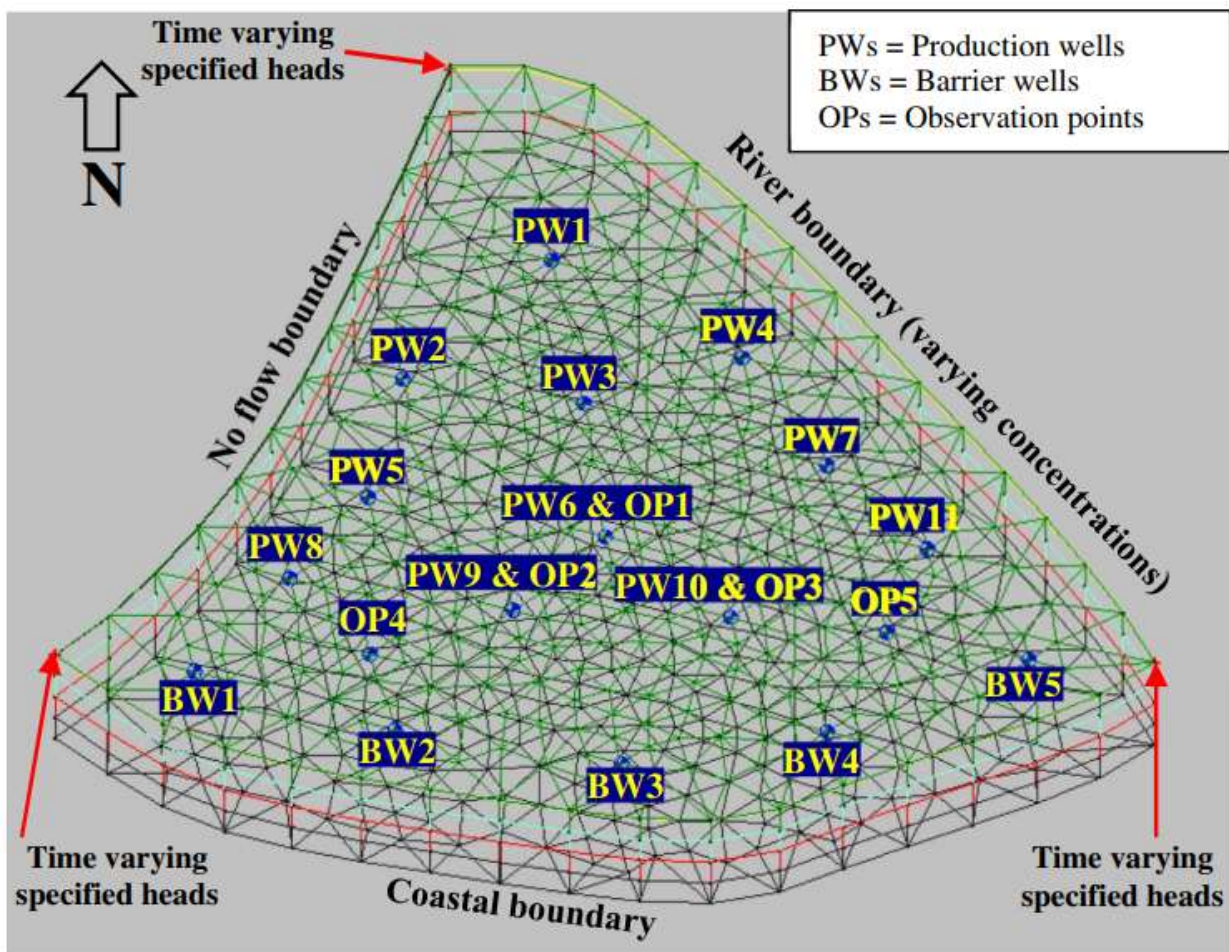


Figure 1. Illustrative study area.

Figure 2 illustrates the assigned groundwater extraction patterns totaling from 16 pumping wells during the simulation periods of 50 years. During these periods, groundwater extraction is assumed to be increased to meet the increasing water demands in different sectors, with agriculture

being considered as the highest water users. Although Figure 2 apparently shows a linear increasing trend, groundwater pumping patterns are not linear. These pumping values are the summed-up pumping values from the 16 well for a 5-year period. Instead, a spatiotemporal pumping is applied in which the pumping varies spatially (among various wells) and temporally (during the simulation period).

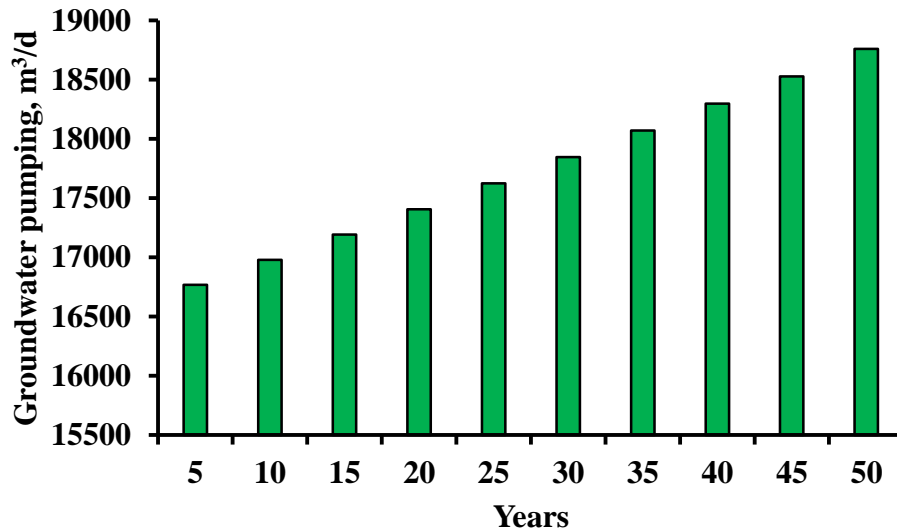


Figure 2. Assigned groundwater pumping values during successive simulation periods.

Figure 3 illustrates the used recharge values which are applied uniformly over the top aquifer layer. The recharge values are obtained from random sampling using LHS approach. As opposed to groundwater pumping values, the recharge values are randomly selected to accommodate the variability and uncertainty in climatic parameters.

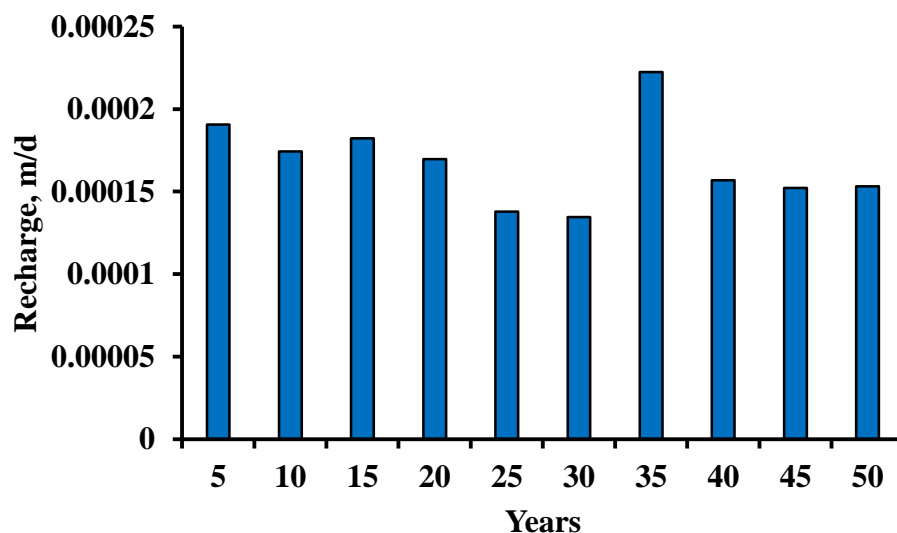


Figure 3. Varying groundwater recharge due to climatic variabilities during successive simulation periods.

Figure 4 shows the projected sea level rise scenarios during the simulation period. An average sea level rise of 1.8 mm/year is assumed. The seaside head is then calculated and assigned to both ends of the seaside boundary of the study area.

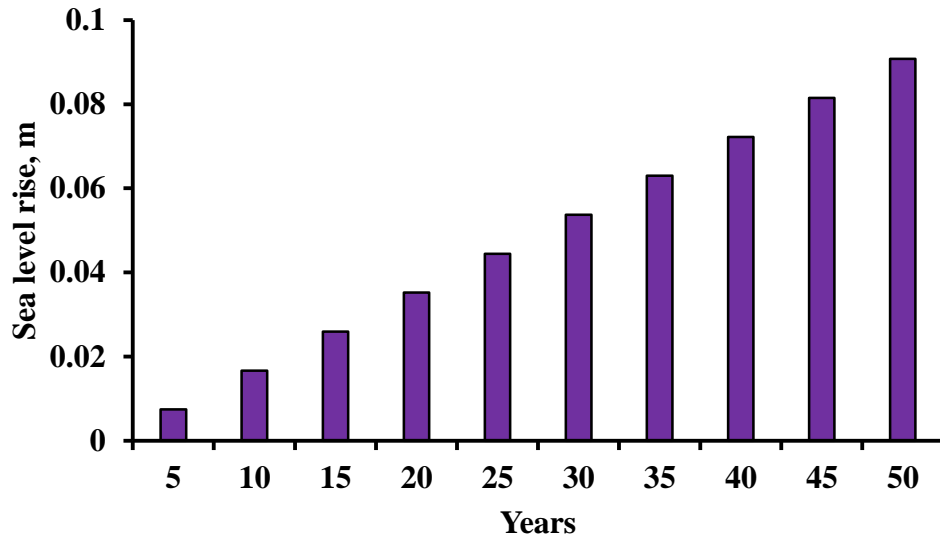


Figure 4. Progressive relative sea level rise assigned on the seaside boundary during successive simulation periods.

Results and Discussion

To demonstrate the effects of increased groundwater extraction, reduced recharge, sea level rise, river water concentration, and seasonal variation of river water stage on the migration of salt plume, a continuous simulation for a period of 50 years is performed. Figures 5 and 6 demonstrate the inland movements of saltwater plume over time. Compared to the simulation results after 5 years (Figure 5 a), a significant increase in saltwater wedge movement is observed in the result of simulation for a period of 25 years (Figure 5 b). Saltwater intrusion is observed to be more pronounced when performed a 50 year simulation with varies recharge, increased groundwater abstraction, and enhanced sea level rise scenarios (Figure 6 a). Figure 6 b presents a 3D view of the saltwater intrusion processes under changing groundwater parameters.

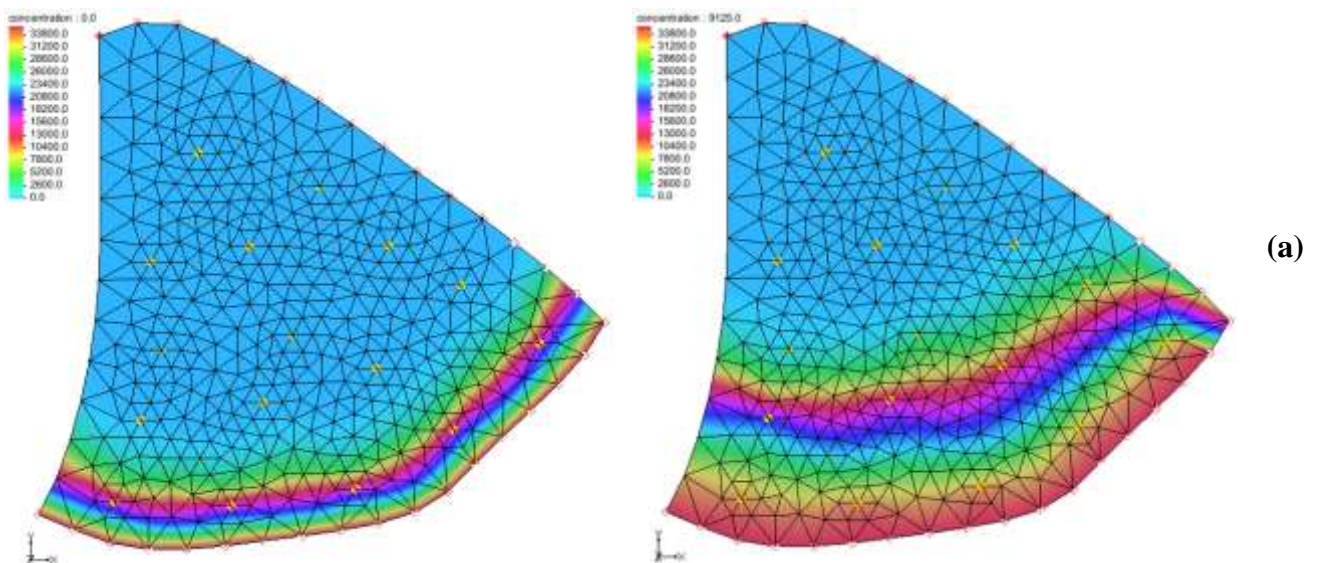


Figure 5. Resulting saltwater concentrations in the aquifer after (a) 5 and (b) 25 years.

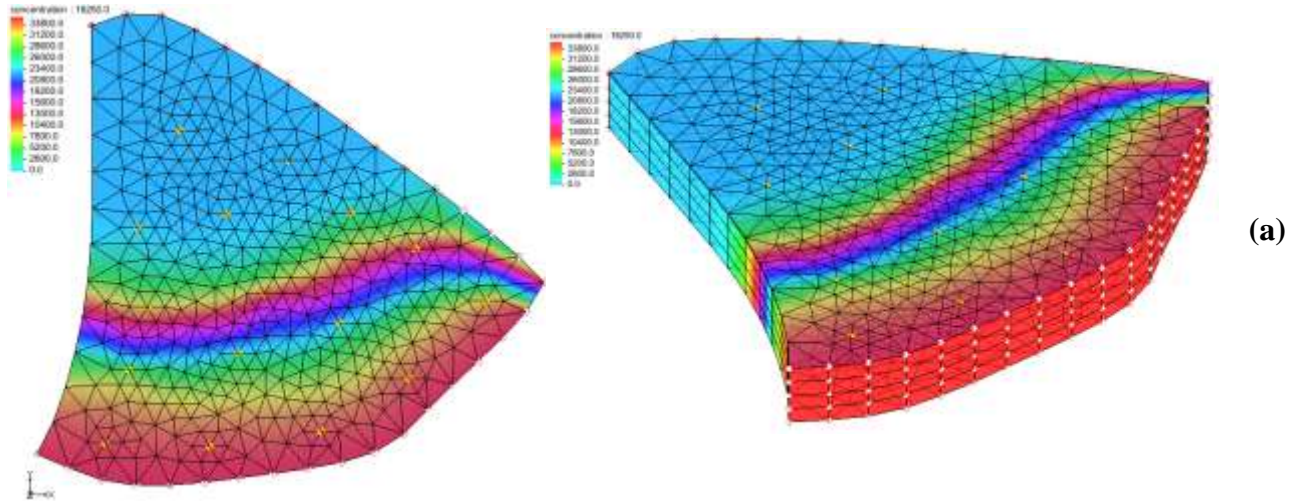


Figure 6. Salinity intrusion in the aquifer after 50 years (a) plain view (b) three-dimensional view.

Figure 7 presents the salinity concentrations at individual monitoring locations during successive simulation periods. It is observed from Figure 7 that salinity concentrations increase with the increased pumping stress applied to the aquifer although the magnitude varies. It is also observed that salinity concentrations are more evident at monitoring locations ML2, LM3, ML4, and ML5 when compared to the monitoring location ML1. This is because the monitoring location ML1 is located further inland from the seaside boundary whereas the monitoring locations ML4 and ML5 are placed relatively close to the seaside boundary. Nevertheless, increased groundwater extraction in combination with increased sea level rise and varying recharge scenarios inevitably increase the extent of salinity intrusion in the aquifer as monitored in various monitoring locations placed at different parts of the aquifer.

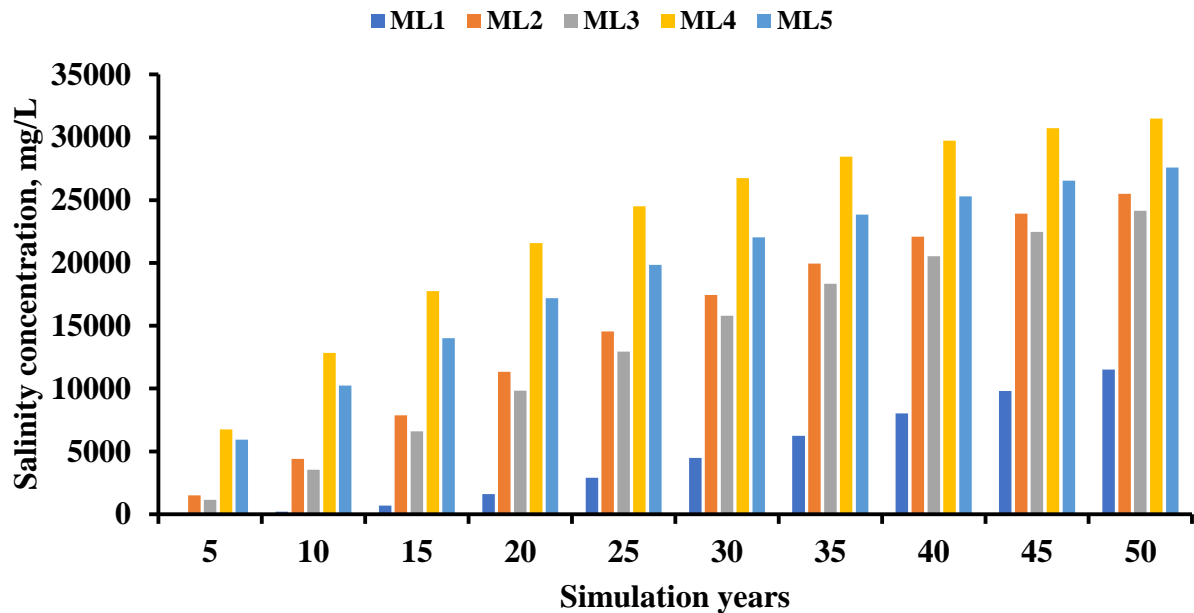


Figure 7. Observed salinity concentrations at the monitoring locations during the simulation period of 50 years

Conclusion

Coastal aquifers are susceptible to saltwater intrusion arising from a multitude of factors including overpumping of groundwater resources, climate change induced sea level rise and reduced recharge. This study demonstrated the potential impact of these natural and anthropogenic factors in the salinity intrusion processes of a coastal aquifer system. Results reveal the significant impact of these future scenarios on the saltwater intrusion phenomena as evidenced by the increased salinity concentrations at the designated monitoring locations over the simulation period. The findings of this study is of great importance to developing a meaningful saltwater intrusion management strategy. The study will be continued for the second year for validation of the developed methodologies in a real-life coastal aquifer system in the southern Bangladesh.

References

- Chen, B.-F., and S.-M. Hsu. 2004. "Numerical study of tidal effects on seawater intrusion in confined and unconfined aquifers by timeindependent finite-difference method." *J. Waterway Port Coastal Ocean Eng.* 130 (4): 191–206. [https://doi.org/10.1061/\(ASCE\)0733-950X\(2004\)130:4\(191\)](https://doi.org/10.1061/(ASCE)0733-950X(2004)130:4(191)).
- Heiss, J. W., and H. A. Michael. 2014. "Saltwater-freshwater mixing dynamics in a sandy beach aquifer over tidal, spring-neap, and seasonal cycles." *Water Resour. Res.* 50 (8): 6747–6766. <https://doi.org/10.1002/2014WR015574>.
- Kuan, W. K., G. Jin, P. Xin, C. Robinson, B. Gibbes, and L. Li. 2012. "Tidal influence on seawater intrusion in unconfined coastal aquifers." *Water Resour. Res.* 48 (2): W02502. <https://doi.org/10.1029/2011WR010678>.
- Langevin, C. D., and M. Zygnerski. 2013. "Effect of sea-level rise on salt water intrusion near a coastal well field in southeastern Florida." *Groundwater* 51 (5): 781–803. <https://doi.org/10.1111/j.1745-6584.2012.01008.x>.
- Lin, H.-C. J., D. R. Richards, C. A. Talbot, G.-T. Yeh, J.-R. Cheng, H.-P. Cheng, and N. L. Jones. 1997. *A three-dimensional finite element computer model for simulating density-dependent flow and transport in variable saturated media: Version 3.0*. Vicksburg, MS: US Army Engineering Research and Development Center.
- Narayan, K. A., C. Schleeberger, and K. L. Bristow. 2007. "Modelling seawater intrusion in the Burdekin Delta irrigation area, North Queensland, Australia." *Agric. Water Manage.* 89 (3): 217–228. <https://doi.org/10.1016/j.agwat.2007.01.008>.
- Oude Essink, G. H. P., E. S. van Baaren, and P. G. B. de Louw. 2010. "Effects of climate change on coastal groundwater systems: A modeling study in the Netherlands." *Water Resour. Res.* 46 (10): W00F04. <https://doi.org/10.1029/2009WR008719>.
- Pebesma, E. J., and G. B. M. Heuvelink. 1999. "Latin hypercube sampling of Gaussian random fields." *Technometrics* 41 (4): 303–312. <https://doi.org/10.1080/00401706.1999.10485930>.
- Roy, D. K., and B. Datta. 2017. "Fuzzy c-mean clustering based inference system for saltwater intrusion processes prediction in coastal aquifers." *Water Resour. Manage.* 31 (1): 355–376. <https://doi.org/10.1007/s11269-016-1531-3>.
- Shrivastava, G. S. 1998. "Impact of sea level rise on seawater intrusion into coastal aquifer." *J. Hydrol. Eng.* 3 (1): 74–78. [https://doi.org/10.1061/\(ASCE\)1084-0699\(1998\)3:1\(74\)](https://doi.org/10.1061/(ASCE)1084-0699(1998)3:1(74)).
- Webb, M. D., and K. W. F. Howard. 2011. "Modeling the transient response of saline intrusion to rising sea-levels." *Ground Water* 49 (4): 560–569. <https://doi.org/10.1111/j.1745-6584.2010.00758.x>.
- Yang, J., T. Graf, and T. Ptak. 2015. "Sea level rise and storm surge effects in a coastal heterogeneous aquifer: A 2D modelling study in northern Germany." *Grundwasser* 20 (1): 39–51. <https://doi.org/10.1007/s00767-014-0279-z>.

MONITORING OF GROUND WATER LEVEL AT DIFFERENT BARI STATIONS

M. A. HOSSAIN¹, S.K. BISWAS², D.K. ROY², K.F.I. MURAD³, S.S.A. KAMAR³, F. AKTER³, M. MORSHED⁴, AND M.A. RAHMAN

Abstract

This study was conducted at the research fields of Irrigation and water Management Division (IWM), RARS, Rahmatpur, Barisasl, and RARS Ishurdi, Pabna of Bangladesh Agricultural Research Institute (BARI) during 2019-2020 and 2020-2021. Two observation wells were installed at IWM Division, BARI, Bazipur and RARS Rahmatpur, Barishal for regular monitoring of groundwater level fluctuations. On the other hand, an existing well was used to monitor groundwater level fluctuations at RARS, Ishurdi, Pabna. In IWM Division research field, a boring depth of 210 ft. with a strainer length 20 ft. was found sufficient for the purpose of groundwater level monitoring. At RARS, Rahmatpur, Barishal, the boring depth was 860 ft with a strainer length of 20 ft. The existing well at RARS Ishurdi station had a boring depth of 120 ft with a strainer length of 20 ft. It is noted that the boring depth and the strainer length depends on the underlying water bearing strata. The installation of observation wells at other stations is ongoing. The monitoring of groundwater level fluctuations in the installed observation well at IWM Division and RARS, Eahmatpr, Barishal as well as the in the existing well at RARS Ishurdi has been continuing.

Introduction

Variations in water storage, including surface water, snow and ice, soil moisture, and groundwater, are essential for understanding a wide range of hydrologic, climatic, and ecologic processes and are important for water resources and agricultural management. Water scarcity is a global concern, with an estimated 1.1 billion people lacking access to clean water (Salman, 2005). Increasing demand for water requires more accurate information needed on water resources. While monitoring networks for precipitation and rivers exist in most regions, monitoring of subsurface water reservoirs (soil moisture and groundwater) is inadequate. However, groundwater represents a much larger fraction (~30%) of global fresh water resources than rivers (~0.006%) (Dingman, 2002). In addition, depletion of groundwater resources has increased substantially in the last several decades, particularly in places where groundwater- based irrigation has expanded (Scanlon et al., 2007). However, monitoring of groundwater storage in Bangladesh is extremely limited. Lack of information on groundwater storage changes inhibits development and execution of effective water management plans. Many countries with severe groundwater depletion problems have limited information on spatial and temporal variability in groundwater storage (Strassberg et al., 2009), as monitoring networks are generally limited and it is difficult to regionalize point- based measurements. To improve water resources management, it is critical to develop monitoring systems that provide accurate and timely information on the status of water reservoirs, including water in soil and aquifers. Therefore, an experiment was proposed with a view to meet the following objectives:

- 1) Installation of observation well at different BARI stations
- 2) Regular monitoring of groundwater level at 7 days' interval
- 3) To determine the depletion of groundwater level

Materials and Methods

The evaluation of groundwater issues and the implementation of management solutions require hydrogeological data that are in part 'baseline' and in part 'time-variant'. The collection of the 'time-variant component' (groundwater level monitoring, groundwater quality monitoring, water well abstraction monitoring (direct or indirect), well groundwater level variations, river flow gauging, meteorological observations and satellite land-use surveys) is what is usually considered 'groundwater

¹ CSO(in-charge), IWM Division, BARI, Gazipur

² SSO, IWM Division, BARI, Gazipur

³ SO, IWM Division, BARI, Gazipur

⁴ SO, RARS, BARI, Ishurdi

monitoring'. Groundwater monitoring thus comprises the collection, analysis and storage of a range of data on a regular basis according to specific objectives. The type and volume of data required will vary considerably with the management issue being addressed, but is also inevitably dependent upon available financial resources. At the heart of all groundwater investigation and monitoring are wells, of the two basic types indicated below. They represent keyholes to aquifers, which allow groundwater pressure and quality measurements to be made and thus furnish information from which the health of the aquifer system can be judged. When water wells are drilled, they provide one-off unique in-situ data on the groundwater resource and its variation with depth and data acquired during drilling (borehole logging) and initial test pumping form key baseline reference information on groundwater quantity and quality, in addition to their value for the determination of abstraction well potential. However, data collected from water wells once operational are normally more difficult to interpret, because groundwater levels are affected by the drawdown-recovery cycle and pumped-sample quality reflects the variable mixing of groundwater from a wide range of aquifer depths and residence times. The observation wells are dedicated monitoring stations, sited and designed to detect potential changes in groundwater flow and quality design parameters include selection of depth for the intake screen, frequency of measurement (if not continuous) and selection of quality parameters. To overcome the widespread presence of depth variation in hydraulic head and/or groundwater quality, nested piezometers or well clusters can be used. Piezometer nests are more cost effective than observation well clusters, but should only be used if proper sealing can be achieved to prevent vertical flow between their screens.

As part of the continuing work, one observation well was installed at the research field of IWM Division, BARI, Gazipur. Another one was installed at the research field of the RARS, Rahmatpur, Barishal. At RARS Ishurdi, Pabna, an existing well, recently abandoned for water extraction, have been using for the monitoring of groundwater level fluctuations. Ground water level fluctuation data at 7 days' interval have been measuring since the installation of the observation wells.

Results

Installation of an observation well at IWM Division, Gazipur

An observation well was installed at the IWM experimental field, Joydebpur, Gazipur-1701 on January 08, 2020. The observation well is located between 23.99°N latitude and 90.41°E longitude. Aerial map of the study area with the location of the observation well is shown in Figure 1.

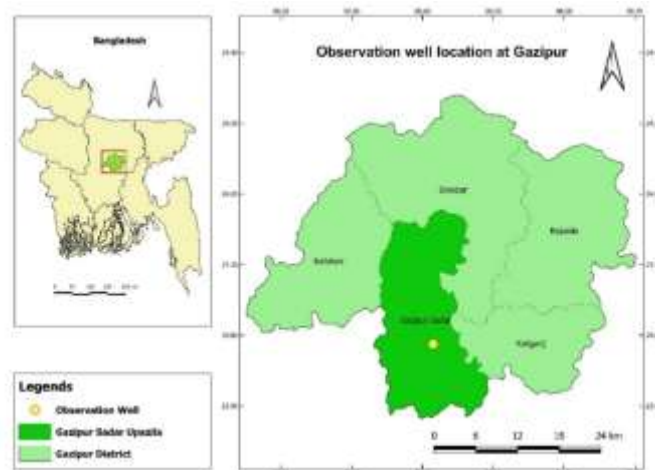


Figure 1. Aerial map and location of the observation well.

The position of the observation well within the IWM research field is presented in Figure 2.



Figure 2. Position of the observation well in the IWM research field.

The installation depth was decided upon careful examination of the water bearing strata during the installation. As such, the depth of boring was 210 ft. including the blind pipe beneath the strainer (5 ft.). The strainer length was 20 ft. A schematic representation of the groundwater observation well is presented in Figure 3.

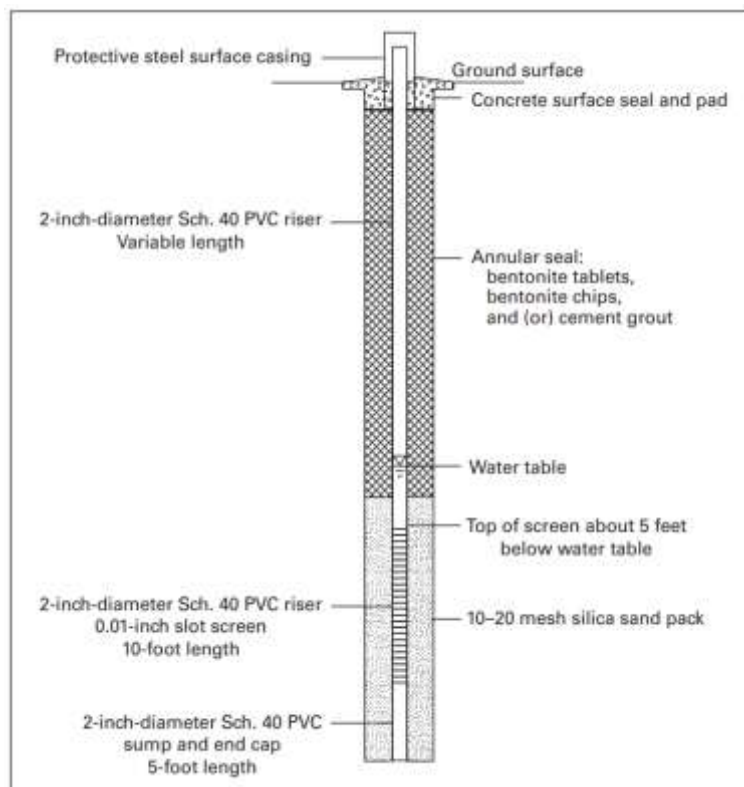


Figure 3. Schematic diagram of groundwater observation well.

After installation, regular monitoring of groundwater level fluctuations at 7 days' interval have been performing. The groundwater level fluctuations at IWM Division, BARI, Gazipur collected during 2019-2020 and 2020-2021 are presented in Figures 4 and 5. It is observed from Figures 4 and 5 that GWL reached the lowest (-134 ft) on 12 July 2020 during 2019-2020, whereas, it reached to -137 ft on 18 July 2021 during 2020-2021.

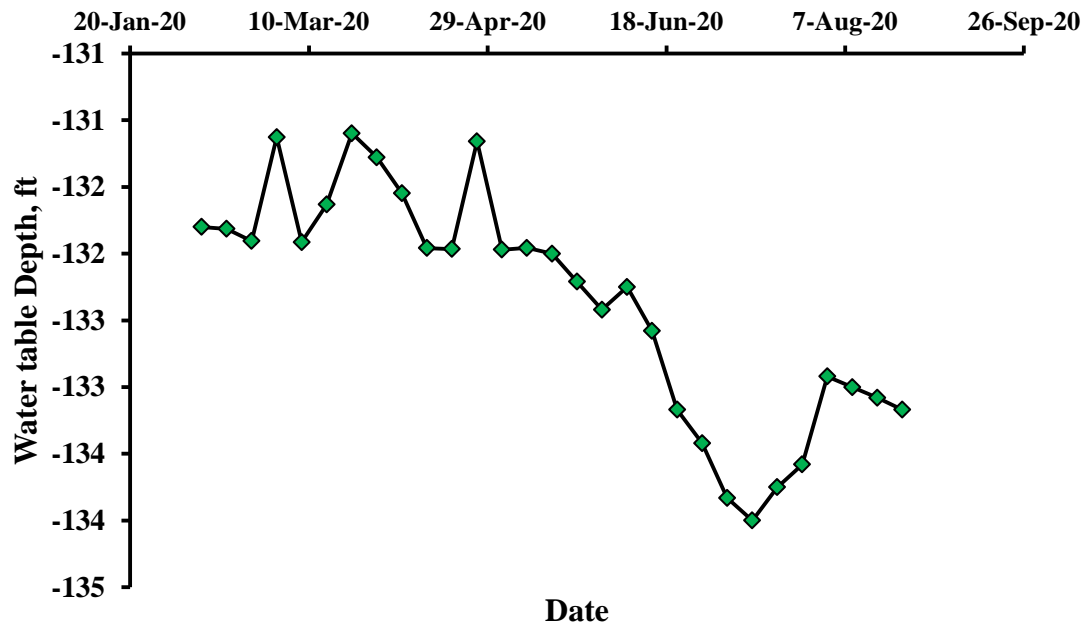
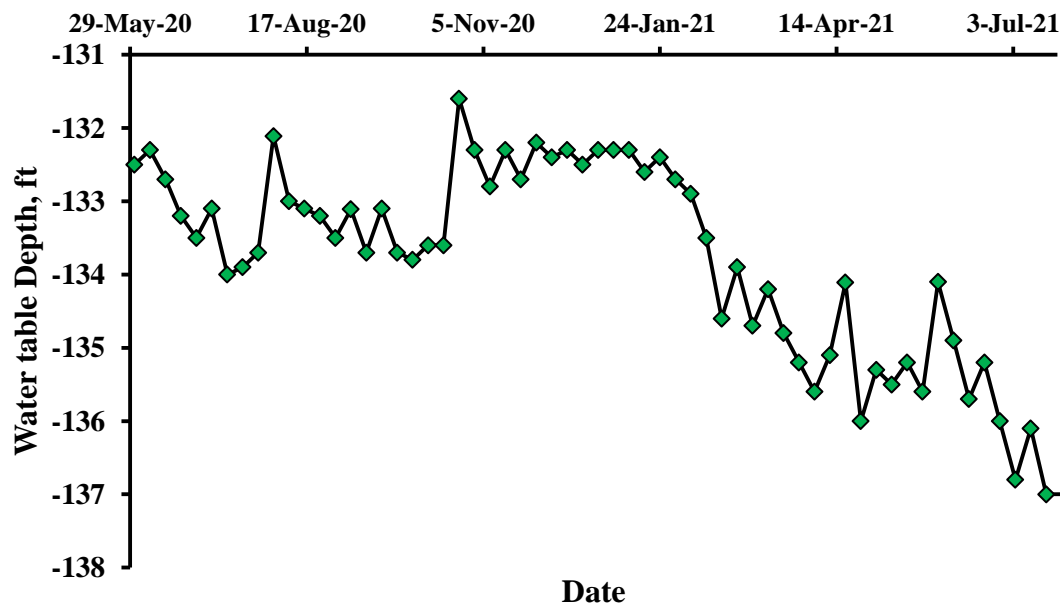


Figure 4. Weekly groundwater level fluctuations during the monitoring period of 2019-2020 at IWM Division, Gazipur.



Installation of an observation well at RARS, Rahmatpur, Barishal

Another observation well was installed at the RARS, Rahmatpur, Barishal on February 25, 2020. The observation well is located between 22.79°N latitude and 90.29°E longitude. The installation depth was decided upon careful examination of the water bearing strata during the installation. As such, the depth of boring was 860 ft. including the blind pipe beneath the strainer (5 ft.). The strainer length was 20 ft. The measured water level fluctuations during 2019-2020 and 2020-2021 are presented in Figures 6 and 7. It is observed from Figure 6 that during 2019-2020, the lowest level of GWL (-22 ft) was found on 20 June 2020 and on 25 July 2020. On the other hand, Figure 7 reveals that the GWL reached its lowest value (-25.5 ft) on 06 May 2021 during 2020-2021.

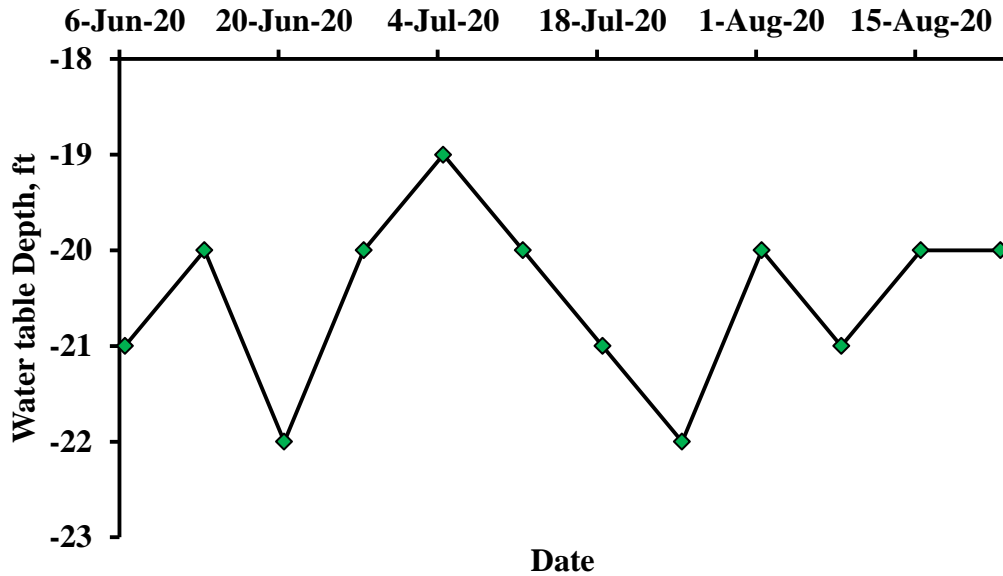


Figure 6. Weekly groundwater level fluctuations during the monitoring period of 2019-2020 at RARS, Rahmatpur, Barishal.

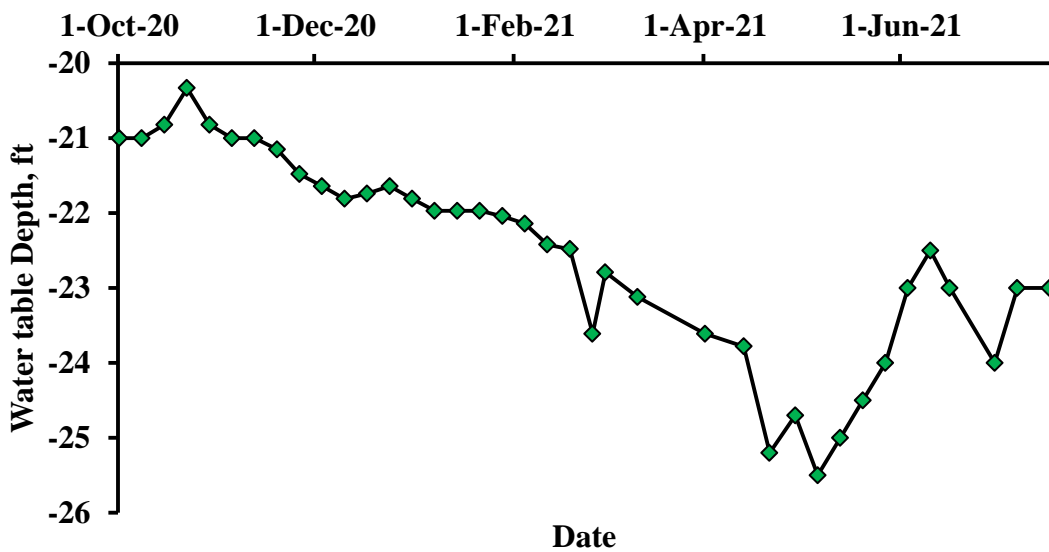


Figure 7. Weekly groundwater level fluctuations during the monitoring period of 2020-2021 at RARS, Rahmatpur, Barishal.

Monitoring of groundwater levels via an existing groundwater well at Ishurdi, Pabna

The selected observation well is located between 21.12°N latitude and 89.08°E longitude. The depth was 120 ft with a strainer length of 20 ft. The measured water level fluctuations during 2020-2021 are presented in Figure 8. Figure 8 showed that GWL reached to the lowest level of -29.50m on 21 April 2021 during the monitoring period of 2020-2021 at RARS, Ishurdi.

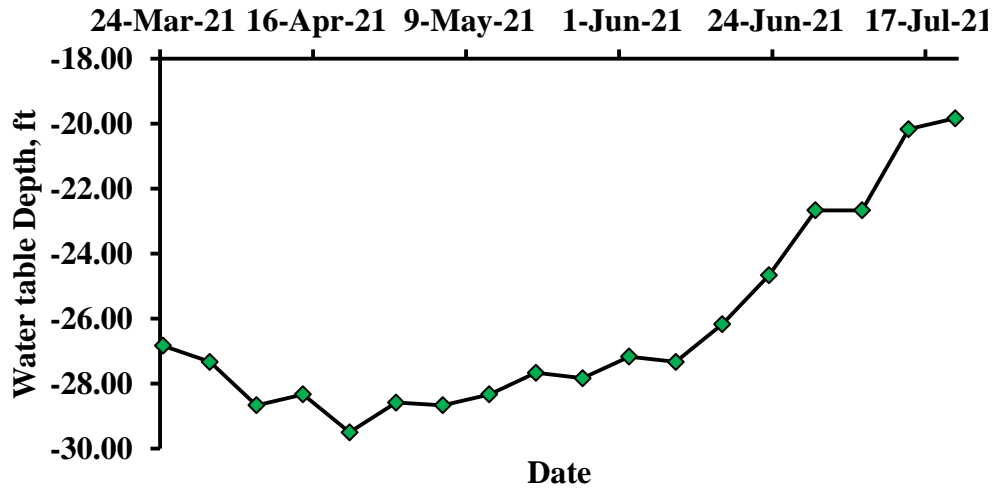


Figure 8. Weekly groundwater level fluctuations during the monitoring period of 2020-2021 at RARS, Ishurdi, Pabna

Conclusions

Two observation wells, one at IWM Division, BARI, Gazipur while another one at RARS, Rahmatpur, Barishal were installed thus far. At RARS Ishurdi, Pabna, an existing groundwater well was selected for the monitoring purpose. Therefore, the results presented in this report were based on the installed observation wells for the monitoring period of 2019-2020 and 2020-2021 as well as the selected observation well at Ishurdi during 2020-2021. The study should be continued for performing the installation of other observation wells at other BARI stations.

References

- Dingman, S. L. (2015). *Physical hydrology*. Waveland press.
- Salman, S. M. (2005). United Nations General Assembly Resolution: International Decade for Action, Water for Life, 2005–2015: A Water Forum Contribution. *Water international*, 30(3), 415-418.
- Scanlon, B. R., Jolly, I., Sophocleous, M., & Zhang, L. (2007). Global impacts of conversions from natural to agricultural ecosystems on water resources: Quantity versus quality. *Water resources research*, 43(3).
- Strassberg, G., Scanlon, B. R., & Chambers, D. (2009). Evaluation of groundwater storage monitoring with the GRACE satellite: Case study of the High Plains aquifer, central United States. *Water Resources Research*, 45(5).

PROJECT (NATP-2, PBRG):

GROUNDWATER RESOURCES MANAGEMENT FOR SUSTAINABLE CROP PRODUCTION IN NORTH WEST HYDROLOGICAL REGION OF BANGLADESH

S.K. BISWAS¹, D.K. ROY¹, AND K.F.I. MURAD²

Executive Summary

Groundwater aquifers are one of the most vital sources of the freshwater supplies for the beneficial purposes in the northern part of Bangladesh. Recently, over-pumping of groundwater resources leads to continuous depletion of groundwater level causing a variety of problems such as lowering of the suction heads of pumps, reduction of crop yields due to inadequate irrigation water supplies, decrease in potable water supplies to domestic and industrial purposes, and degradation of water quality, among others. Therefore, proper management and sustainable utilization of the scanty groundwater reserves in an efficient manner are imperative to secure continuous supplies of groundwater for the future generations. With these perspective, a coordinated project entitled "Groundwater resources management for sustainable crop production in northwest hydrological region of Bangladesh" was implemented by the different NARS institutes like BARI, BRRI and BINA with BARC as coordinate component with a view to sustainable management of groundwater resources of northwest region through optimizing water demand and supply. The objectives of this study were i) To assess groundwater availability and recharge pattern in different districts of northwest hydrological region of Bangladesh, ii) To optimize groundwater abstraction for irrigation, and iii) To suggest plan for sustainable use of groundwater for crop production. The specified selected locations where this study was conducted were Godagari and Tanore upazila of Rajshahi and Joypurhat sadar and Kalai upazila of Joypurhat district.

Based on an extensive investigation, a few location specific promising cropping patterns based field trials with rice and non-rice crops (T.Aman rice, potato, tomato, mustard, wheat, boro) were conducted with adoption of water saving irrigation technologies in respect of the project aim. Long-term (1980-2018) historical groundwater level data were collected and prediction model was developed by using discrete Space-state modeling approach for future forecasting of groundwater level. Irrigation, domestic and municipal water requirement were assessed to predict long term yearly groundwater abstraction pattern. A hydrologic model MODFLOW was used to optimize of groundwater abstraction. Groundwater samples were collected from both STWs and DTWs before starting (November/December) and at the end (February/March) of dry season irrigation to examine its suitability for irrigation over the season.

Rice equivalent yield (REY) and water productivity (WP) were found higher in cropping patterns where high yielding rabi crops like tomato, potato and maize were included and water saving irrigation technologies were adopted. Among the cropping patterns, the highest REY and WP were obtained from Tomato-Boro-T.Aus followed by Potato-Boro-T.Aman pattern while the lowest was from Mustard-Boro-T.Aman pattern. Use of water saving irrigation technologies increased REY by 8-24% and saved about 20-25% water over existing farmers' practice. From this study, it was observed that groundwater level declination was more in Tanore upazila than other three upazilas and will be almost double by the year 2040 in Tanore years if the present rate of abstraction continues. In Godagari, Joypurhat sadar, and Kalai upazila, the future trends of groundwater level fluctuations as predicted by the model are quite interesting. While the groundwater level declination was found obvious in most of the observation wells, the groundwater levels showed increasing trends in few observation wells at Joypurhat and Godagari. Groundwater abstraction pattern due to irrigation, domestic and municipal uses has been assessed and it is apparent that total abstraction will increase by 33-35% in Joypurhat area and by 40-45% in Rajshahi area in the next 20 years. The groundwater quality in the study areas has been evaluated for agricultural use. The water quality indices such as SAR, SSP, RSC, KR and WQI were calculated to find out its suitability for irrigation. In respect of all evaluating criteria, groundwater of the study area was found suitable and can safely be used for irrigation purpose.

Sustainable beneficial water abstraction from the aquifer can be ensured by optimizing water abstraction on the basis of the existing and future scenarios of the climatic variability, e.g. recharge through rainfall. In this report, the effects of three scenarios of recharge on the observed head at the

¹ SSO, IWM Division, BARI, Gazipur

² SO, IWM Division, BARI, Gazipur

designated observation wells at four upazillas in Rajshahi (Tanore and Godagari upazilla) and Joypurhat (Joypurhat sadar and Kalai upazilla) districts was investigated. The three recharge scenarios considered was: (i) actual recharge, (ii) 90% of the actual recharge, and (iii) 110% of the actual recharge. The aquifer processes were simulated using a calibrated 3D finite difference based numerical simulation code MODFLOW. The results revealed that the computed groundwater heads at the three observation wells varied noticeably as a result of the changes in the recharge scenarios. In the business-as-usual case, the MODFLOW computed heads at the three observation wells GT 8194046, GT8194048, and GT8194049 at Tanore upazilla on 24 September 2018 (data obtained from the BWDB) were 16.388m, 18.133m, and 22.215m, respectively. When the recharge was reduced to 90%, the computed heads dropped significantly, and the values were 7.970m, 11.150m, and 18.106m, respectively at the three observation wells. On the other hand, if the recharge would be increased to 110%, the computed heads were found as 20.707m, 21.745m, and 24.413m, respectively which indicates a substantial increase in the quantity of head development. At Godagari upazilla, the MODFLOW computed heads for the business-as-usual case were 9.389m, 11.046m, 6.170m, and 6.112m at the observation wells GT 8134017, GT 8134020, GT 8134021, and GT 8134022, respectively. When the recharge was reduced to 90%, the computed heads dropped, and the values were 6.577m, 5.670m, - 0.475m, and 1.447m, respectively at the four observation wells. On the other hand, if the recharge would be increased to 110%, the MODFLOW computed heads at the observations were found as 12.155m, 16.325m, 12.660m, and 10.682m, respectively which indicates a substantial increase in the quantity of head development. In Joypurhat sadar upazilla, the computed heads for the business-as-usual case were 11.05231m and 3.980m at the observation wells GT 3847001 and GT 3847003, respectively. When the recharge was reduced to 90%, the computed heads dropped, and the values were 9.406m, and 3.335m, respectively at the two observation wells. On the other hand, if the recharge would be increased to 110%, the MODFLOW computed heads at the observations were found as 12.688m, and 4.620m, respectively. In Kalai upazilla, the observed and computed heads were monitored at two observation wells (GT3847001 and GT 3847003). In this upazilla, the MODFLOW computed heads for the business-as-usual case were 11.05231m and 3.980m at the observation wells GT 3861004 and GT 3861005, respectively. When the recharge was reduced to 90%, the computed heads dropped, and the values were 6.306m, and 5.533m, respectively at the two observation wells. On the other hand, if the recharge would be increased to 110%, the MODFLOW computed heads at the observations were found as 7.592m, and 6.943m, respectively. The increased and decreased recharge scenarios were computed using the existing groundwater pumping values in the year 2018. Therefore, it is concluded that groundwater recharge has a significant effect on the head development in the groundwater aquifers of the Tanore and Godagari upazilla, Rajshahi and Joypurhat sadar and Kalai upazilla, Joypurhat.

The sustainable use and management of groundwater is now a great challenge in the northwest region of Bangladesh. Due to cultivation of water intensive crops, irrational irrigation management, indiscriminate installation of pumps and non-availability of modern technologies, the use of groundwater is much higher in this region compared to other parts of the country leading to declination of groundwater table at an alarming rate. Because of this threat, it is important to exploiting groundwater annually not exceeding the replenished amount from annual seasonal rainfall. Therefore, the key challenges are now to increase agricultural productivity without deteriorating the groundwater resources. Safe abstraction of groundwater resources is only possible if the irrigation water is utilized judiciously by implementing apposite irrigation methods, and practicing water saving technologies with low water consuming cropping patterns simultaneously and by optimizing water abstraction on the basis of the existing and future scenarios of the climatic variability, e.g. recharge through rainfall. Policy intervention is also needed to create awareness among the farmers and other stakeholders about the consequences of indiscriminate use of groundwater. Thus, sustainable groundwater resources management will sustain agricultural production in this region.

Keywords: Groundwater, abstraction, recharge, cropping pattern, water quality, water saving technology

1. Background

The increase of food production with less irrigation water use has been the main policy target in farm management over the recent years, particularly in countries with limited water and land resources (FAO 2002). It has been estimated that if sustainable irrigation water management strategies are not implemented, there will be an estimated loss of agricultural production of 7.8% by 2080 (Cline 2007). Bangladesh is one of the world's most densely populated countries, where food security has been a continuous challenge since its liberation. The expansion of irrigated crop land has probably been the most dramatic development in Bangladesh agriculture during the last 25 years mainly through groundwater irrigation. In Bangladesh, agriculture is responsible for more than 65 percent of total fresh water withdrawal (Shamsudduha *et al.* 2011), where nearly 80 percent of this irrigation water comes from groundwater resources due to uncertainty of year-round surface water availability (Rahman & Mahbub 2012). Clearly, the availability of groundwater for irrigation has contributed to manifold increase in crop productivity. Studies found that the contribution of groundwater has increased from 41% in 1982-83 to 77% in 2006-07. The ratio of groundwater to surface water use is much higher in north-western districts of Bangladesh compared to other parts of the country. Climatically, this area belongs to dry humid zone with annual average rainfall vary between 1,400 and 1,900 mm. The seasonal distribution of this amount of rainfall shows that almost 92.7% rainfall occurs during May to October and less than 6% rainfall occurs during the dry season irrigation period of cultivating rice (November to April). All the rivers and canals become dry during the dry season and make the people completely dependent on groundwater (Shahid 2008; Shahid and Behrawan 2008) to meet up the demand of cultivating crops, especially for boro rice.

Though the groundwater dominates the total irrigated area, its sustainability is at risk in terms of quantity in the northwest region (Simonovic 1997; Shahid 2011) through over extraction of this resources. Researchers have revealed that over extraction of groundwater for irrigation due to lack of proper knowledge, cultivation of water intensive crops, irrational irrigation management, indiscriminate installation of pumps and non-availability of modern technologies are the major reasons behind the current crisis (Adhikary *et al.* 2013; Ali *et al.* 2012; Shahid & Hazarika 2010). In addition, global climate change effects and reduced water flow in major rivers due to upstream water diversion by India has made the situation worse (Adhikary *et al.* 2013). Different studies have documented that groundwater table has been declined by at least 10 meters during the last 14 years (Ali *et al.* 2012; Shahid & Hazarika 2010) in some areas of the Barind tract of northwest region. Decline of groundwater [strong declining trends (0.5 – 1.0 meter/year) in the central part of the country, moderately declining trend (0.1 – 0.5 meter/year) in western, north-western and north-eastern areas during dry season] is a threat of water resources for future if annually not replenished from annual seasonal rainfall. This substantial declination of groundwater level during the last decade causing threat to the sustainability of water use for irrigation in this region and impacting upon other sectors as well (Jahan *et al.* 2010). Frequent shortage of water has had impacts that can be ranged as economic, social and environmental (Islam *et al.* 2014). If this over-utilization continues, it may result in its exhaustion after few years that may have serious impact on the agriculture-based economy of the country. So, emphasis should be given on the sustainability of these valuable resources.

Although maximizing crop production through greater expansion of irrigated lands is a basic requirement, sustainable utilization of country's limited water resources is also a major concern. The key challenges are now to increase agricultural productivity without deteriorating the groundwater resources (Shahid & Hazarika 2010). This is possible only if safe extraction of groundwater resources, the irrigation water is utilized judiciously by implementing apposite irrigation methods, and practicing water saving cropping patterns simultaneously. Policy level interventions are also needed to achieve sustainable use of groundwater for irrigation through adaptation of effective measures by the farmers aiming to achieve food security and ecological balance.

General objective(s):

- To assess groundwater availability and recharge pattern in different districts of northwest hydrological region of Bangladesh
- To optimize groundwater abstraction for irrigation

- To suggest plan for sustainable use of groundwater for crop production

Specific objectives (component wise):

- To determine aquifer recharge and groundwater utilization pattern
- To assess available groundwater resources, To develop various scenarios for sustainable crop production using groundwater models
- To find out optimum management techniques and suitable cropping patterns for sustainable groundwater use

2. Methodology

2.1. Selection of site and farmers

Selection of project sites were made based on two major criteria: an agricultural intensive area with crop irrigation largely depend on groundwater resources; high barind and low barind area in the north-west region of Bangladesh. Thus, the site selected for this project was Godagari and Tanore upazilas of Rajshahi district in the high barind area, and Kalai and Joypurhat sadar of Joypurhat district in the low-barind area. In both areas, farmers who are cultivating major crops of that area and had easy access to irrigation facilities and showed should their interest to adopt modern irrigation technologies were selected to conduct field trials with different crops and water saving technologies.

2.2. Cropping pattern based field trials with rice and non-rice crop

The study was initiated during the rabi season of 2018-2019 after harvesting of T.Aman rice in both Joypurhat and Barind area of Rajshahi. The soil of the study area is loam - clay loam with an average field water-holding capacity of 28.5- 30.5 % and wilting point of 14.12-15.2%. Soil bulk density in the 0 to 60 cm depth ranges from 1.31 to 1.43 g/cc, with a weighted average of 1.39 g/cc. A typical dry climate with comparatively high temperature prevails in Barind area. Temperature ranges from a minimum of 8°C in the winter to a maximum of 44°C in the summer. More than 85% of the total rainfall occurs from mid June to October and the magnitude of annual rainfall varies from 1300-1500 mm in Rajshahi and 1800 - 2000 mm in Joypurhat. Based on an extensive investigation on the existing cropping patterns in the study areas, two/three promising cropping patterns from each study area were selected for project works and the field experiments were conducted following the major cropping patterns of the respective study area. Three/four different cropping patterns with four/five principal crops of that region were selected as rotation crops, including T.Aman, boro, wheat, mustard, and potato. Mungbean, a popular fallow crop, was included in T.Aman-Wheat-Fallow pattern after wheat cultivation. Irrigation schedule of different crops with their sowing/transplanting and harvesting date are presented in Table 1. All crops were grown in the following sequences starting with rabi crops as: T.Aman-Potato-Boro, T.Aman-Mustard-Boro, T.Aman-Wheat-Fallow. Another pattern Boro-Fallow-T.Aman was tested as control treatment.

For each crop, recommended doses of fertilizers were used and standard cultural practices were followed. Crops were sown immediately after harvesting of T. Aman with a view to save water for irrigation with effective utilization of profile soil moisture. Each crop was grown on a 100 m² plot with three replications. The growing period for wheat crop was Nov-March, for potato Nov-February, for mustard Oct/Nov-January/Feb and for boro rice December-April. At maturity, all crops were harvested manually to determine grain yield and aboveground biomass. Soil water content was monitored at 20 cm incremental depth up to 60 cm depth for wheat and mustard, and up to 40 cm depth for potato before and after irrigation. Soil moisture content at sowing and at harvest was monitored to find out the amount of profile soil moisture contributing to crops. All cultural practices were done as per recommendations. Important agronomic data and parameters were collected during the cropping season and harvest time.

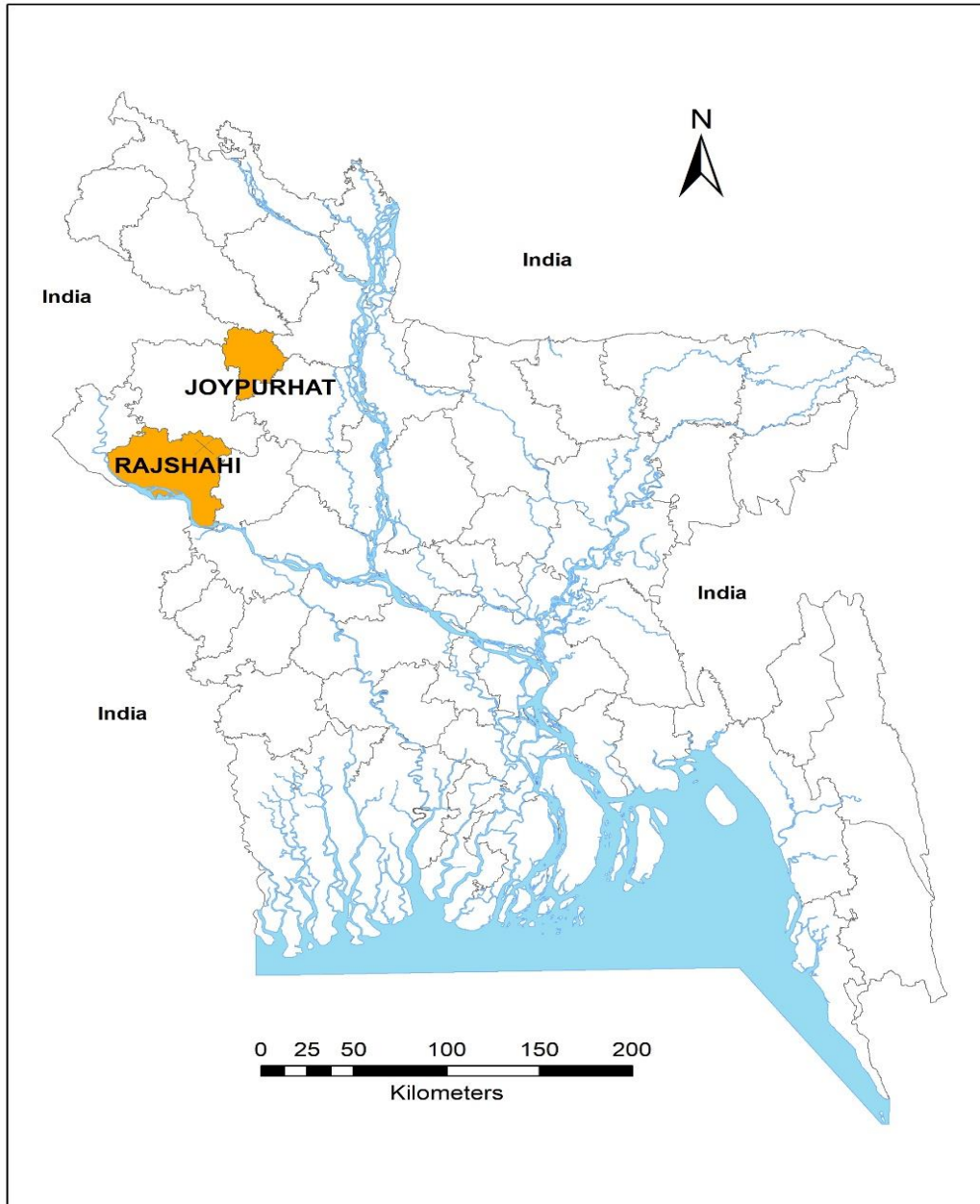


Figure 1. Geographical map showing the study locations.

Yield was estimated by collected sample from one square meter area of each replication. Harvest wheat/rice was threshed, cleaned and weighed and finally the yield was calculated at 14% moisture content. All weather data of the cropping period influencing crop water use were also collected. Depth of irrigation water applied in each irrigation was duly recorded. Total water use by the wheat, potato and other non-rice crops during the entire cropping period (sowing to harvest) was calculated by using the field water balance equation as:

$$TWU = I + P + - D - R \pm \Delta SWS$$

Where, TWU is the total water use (mm), P is the effective rainfall (mm), I is the irrigation water applied (mm), D is the deep percolation (mm), R the run-off and ΔSWS is the change in water storage in the soil profile. Deep percolation (D) was assumed negligible, since water was applied only to replenish soil moisture in the root zone. Run-off due to irrigation or rainfall was taken to be zero as irrigation/rainfall water was protected by 15 cm height levees.

Table 1. Irrigation schedule of different crops with their sowing/transplanting and harvesting dates

Crops	Treatments	Sowing/ transplanting date	Harvesting date
Wheat (BARI Gom- 30)	T ₁ = Irrigation at CRI and pre-flowering stages T ₂ = Irrigation at CRI and grain formation stages T ₃ = Irrigation at CRI, pre-flowering and grain formation stages (20, 55 and 75 DAS)	20-22/11/2018	13-15/03/2019
Mustard (BARI Sarisha- 14)	T ₁ = One irrigation at vegetative stage T ₂ = One irrigation at pre-flowering stage T ₃ = Two irrigation at vegetative and pod formation stages	18-21/11/2018	11-13/02/2019
Potato (Diamant)	T ₁ = Farmers' practice (FP) T ₂ = Irrigation at stolonization, tuberization and bulking stages in furrow system (FI) T ₃ = Irrigation at stolonization, tuberization and bulking stages in alternate furrow system (AFI)	10-17/11/2018	11-15/02/2019
Boro (BRRIdhan- 28)	T ₁ = Farmers' practice (ponding up to 3-5 cm) T ₂ = Irrigation on 3rd day after disappearing of standing water T ₃ = Irrigation when water level fall 15 cm below ground surface	03-07/01/2018	27-30/04/2019
T.aman (BRRIdhan- 56)	T ₁ = Farmers' practice T ₂ = AWD with 20 cm depth T ₃ = AWD with 25 cm depth	21-28 July 2018	24-29 Oct 2019
T.Aus	T ₁ = Farmers' practice T ₂ = AWD with 20 cm depth T ₃ = AWD with 25 cm depth	03-09/06/19	11-13/08/19
Maize	T ₁ = Irrigation at vegetative and flowering stages (FP) T ₂ = Irrigation at seedling, vegetative and silking stages by furrow irrigation (FI) T ₃ = Irrigation at seedling, vegetative and silking stages by alternate furrow irrigation (AFI)	01/12/18	05/05/19
Tomato	T ₁ = Furrow irrigation T ₂ = Drip irrigation T ₃ = Alternate furrow irrigation	13-15/09/19	14/11/19- 18/12/19

Water productivity was determined as the ratio of yield to total water used by the crop as:

$$WP= Y/TWU$$

Where, WP is the water productivity (kg m^{-3}), Y is the crop yield (kg ha^{-1}) and TWU the total water use ($\text{m}^3 \text{ha}^{-1}$).

Total water use by rice crop during the entire cropping period (planting to harvest) was calculated by using the following equation:

$$TWU= I + P - R - (S \& P)$$

Where, TWU is the total water use (mm), I is the irrigation water applied (mm), P is the effective rainfall (mm), R the run-off (mm) and S& P is the seepage and percolation (mm). Run-off was taken to be zero as irrigation water was protected by 30 cm height levees.

Water requirement (WR) for boro rice was determined as irrigation water applied (mm) plus effective rainfall (mm) during the cropping season.

Unlike non-rice crop, water productivity was determined as the ratio of water requirement to the yield as:

$$WP = WR/Y$$

Where, WP is the water productivity (m³/kg) and Y is the crop yield (kg/ha) and WR the water requirement (m³/ha).

Water use efficiency (WUE) was calculated by dividing the total water use by water requirement during the cropping season as:

$$WUE = TWU/WR$$

Where, WUE is the water use efficiency (%), TWU the total water use (mm) and WR is the water requirement (mm)

2.3. Long-term yearly groundwater abstraction pattern

2.3.1. Irrigation Water Requirement:

The people of the study area are dependent on groundwater for irrigation and domestic uses. Thus a large portion of groundwater is abstracted to meet up irrigation water requirement while a small portion is abstracted for domestic and municipal water requirements. Irrigation in the study area is provided either by DTWs or STWs or LLPs. Under the present situation, DTWs are of different capacities while STWs are mainly of same capacity. Most of the DTWs (80%) are of 2 cusec and some are of 1 cusec (about 20%), STWs and LLPs are of 0.50 cusec capacity. Abstraction due to irrigation was estimated by the field irrigation water requirement (FIWR) for each crop. FIWR was calculated utilizing evapotranspiration (*ET₀*), effective rainfall, crop coefficient, crops and cropping patterns of the study areas. Thus, total irrigation water requirement for the entire area is FIWR of crops and area under each crop. Crop coverage under each crop for entire area was estimated from the Upazila wise area weighted average crop coverage.

2.3.2. Domestic and Municipal Water Requirement:

In Bangladesh, about 97% of total potable water is met up from groundwater sources. It is understood from the field survey that domestic and municipal water source of the study area is solely based on groundwater. Therefore, assessment of domestic and municipal water requirement is important to see the abstraction effect on groundwater table. Estimation of the present population and projected population is necessary for assessing the present and future domestic and municipal water demand. The Per Capita water demand is the annual average water consumption of one person daily. Thus average daily demand over a year means the annual average daily demand. The total quantity of water required by the community can be computed using the following equation.

$$Q = P \times q$$

Where, Q is the present or projected quantity of water required by the community per day, P is the present or projected population and q is the rate of water consumption per capita per day.

The projected population is estimated by the Geometric Progression method (Ahmed et al, 2003):

$$P_p = P_b (1 + r)^n$$

Where, P_p = projected population in the year n

P_b = Base population

r = rate of natural increase of population per year

n = number of years being considered.

On the basis of population projection by geometric progression method and per capita water demand, the domestic and municipal water requirement was estimated. According to the NWMP report, per capita gross water demand for municipal town and rural areas are 166 lpcd and 30 lpcd respectively. The gross water demand of municipal town includes 119 lpcd net domestic water demand, 20% of it as a system loss, 10% as gross commercial demand and 15% as industrial demand. On the other hand it has 50% returned flow from the commercial demand and 75% returned flow, thus the net water demand for municipal town becomes 76 lpcd. The gross water demand for rural areas doesn't include any loss and commercial and industrial demand. Thus the net water demand for rural areas is same as the gross water demand.

2.4. Trend of groundwater level fluctuation in the study area

Secondary data of weekly groundwater level fluctuations at selected observation wells of the study areas were collected from Bangladesh Water Development Board. For Tanore upazila, historical weekly groundwater level data from January 1980 to September 2018 for the selected observation wells of Bangladesh Water Development Board were used. Collected data were used to predict the trend of change of groundwater level by using discrete Space-state and MAKSENS modeling approach. Observation well GT 8194046 is located at 24.68⁰N latitude and 88.53⁰E longitude. Observation well GT 8194048 is situated at 24.57⁰N latitude and 88.55⁰E longitude whereas the observation well GT 8194049 is located at 24.63⁰N latitude and 88.58⁰E longitude. For Godagari upazila, four observation wells were selected based on the availability and quality of the observed data. Observation well GT 8134017 is located at 24.4⁰N latitude and 88.43⁰E longitude. Observation well GT 8134020 is located at 24.52⁰N latitude and 88.38⁰E longitude. Observation well GT 8134021 is located at 24.49⁰N latitude and 88.46⁰E longitude. Observation well GT 8134022 is located at 24.43⁰N latitude and 88.46⁰E longitude. In Joypurhat sadar, two observation wells were selected based on the availability and quality of the observed data. Observation well GT 3847001 is located at 25.13⁰N latitude and 89.06⁰E longitude. Observation well 3847003 is located at 25.12⁰N latitude and 89.12⁰E longitude. In Kalai upazila, two observation wells (GT 3861004 and GT 3861005) were selected based on the availability and quality of the observed data. Observation well GT 3861004 is located at 25.02⁰N latitude and 89.15⁰E longitude. Observation well GT 3861005 is located at 24.98⁰N latitude and 89.12⁰E longitude.

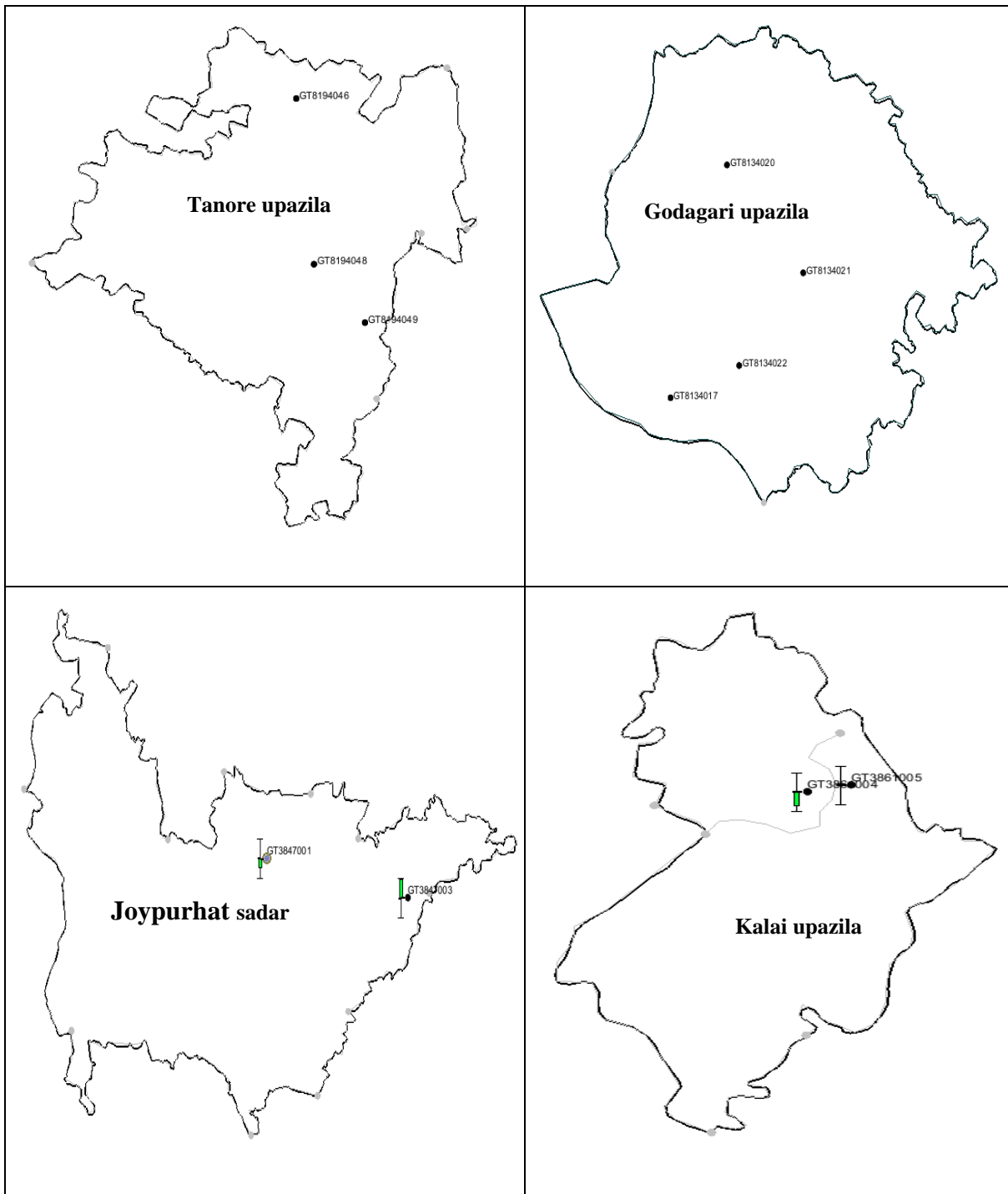


Figure 2. Locations of the observation wells in the study area.

Time series of water level data of the selected observation wells of the study areas are illustrated in Figure 3 below.

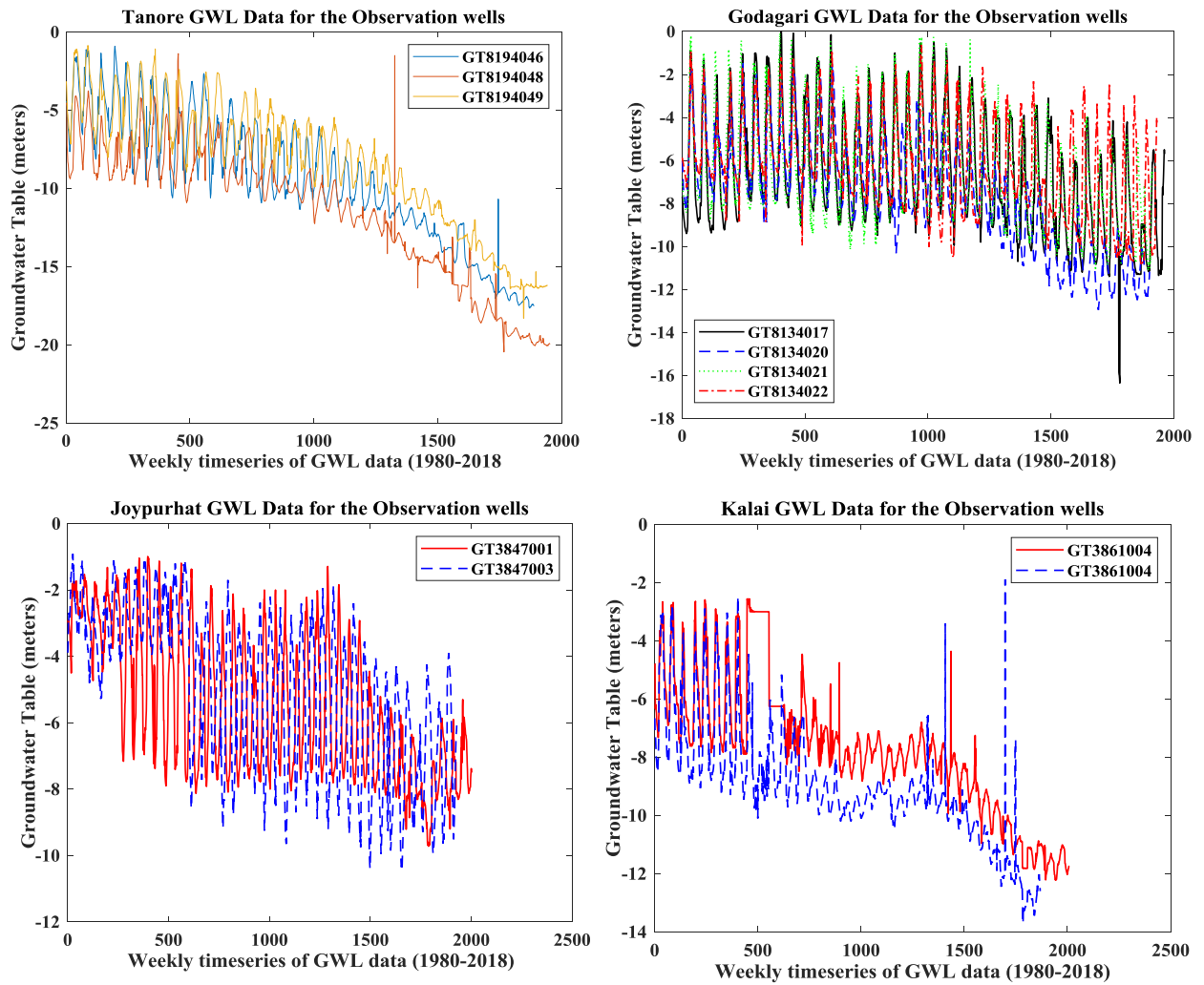


Figure 3. Groundwater level time series data for the selected observation wells of study areas.

Observation well GT 8194046 is located at 24.68°N latitude and 88.53°E longitude. Observation well GT 8194048 is situated at 24.57°N latitude and 88.55°E longitude whereas the observation well GT 8194049 is located at 24.063°N latitude and 88.58°E longitude.

2.4.1. Discrete Space-State model:

2.4.1.1. Modelling technique

This study utilizes a discrete Space-State model as a prediction tool for future scenarios of groundwater level forecasting. The groundwater table can be modelled as a state-space system with noise input and measured water table date as output. The measured water table is proportional to the system state, i.e.

$$x_{n+1} = Ax_n + Ke_n \quad (1)$$

$$y_n = Cx_n + e_n \quad (2)$$

Where, x_n is the state vector, contains the weekly water table values; y_n is the output from the model; e_n is the noise and A, C, K are to be identified.

In Space-State modelling approach, a model is identified to accurately compute a dynamic system with response to an input. Two different approaches exist to generate an identified model response: (a) Simulation that computes model response using input data and initial conditions, and (b) Prediction that computes the model response at some specified amount of time in the future using the current and past values of measured input and output values, as well as initial conditions. The present study utilizes the prediction focused approach of the system identification process in which the overall goal is to create a realistic dynamic system model that can be used or handed off for an application goal. During the model identification process, a one-step prediction focus is used as it generally produces the best results. By using both input and output measurements, one-step prediction accounts for the nature of the disturbances. Accounting for disturbances provides the most statistically optimal results.

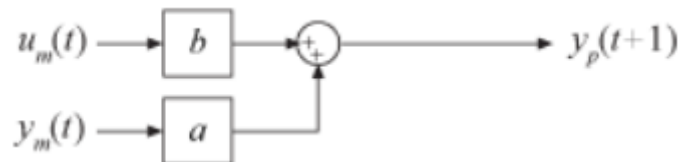
Prediction focused approach:

Prediction means projecting the model response k steps ahead into the future using the current and past values of measured input and output values. k is called the prediction horizon, and corresponds to predicting output at time kT_s , where T_s is the sample time. In other words, given measured inputs $u_m(t_1, \dots, t_{N+K})$ and measured outputs $y_m(t_1, \dots, t_N)$, the prediction generates the final output $y_p(t_{N+K})$.

For example, if the input and output signals of a physical system are $u_m(t)$ and $y_m(t)$, respectively, then the first order equation of this system can be represented by

$$y_p(t + 1) = ay_m(t) + bu_m(t) \tag{3}$$

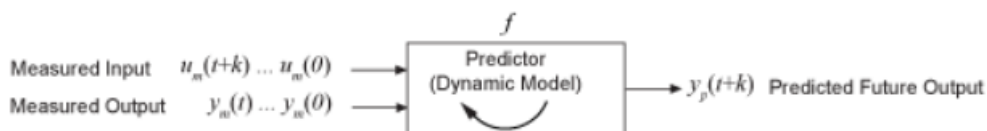
where y is the output and u is the input. The system can be represented by the following block diagram



In general, to predict the model response k steps into the future ($k \geq 1$) from the current time t , one must know the inputs up to time $t + k$ and outputs up to time t such that:

$$y_p(t + k) = f(u_m(t + K), u_m(t + k - 1), \dots, u_m(t), u_m(t - 1), \dots, u_m(0), y_m(t), y_m(t - 1), y_m(t - 2), \dots, y_m(0)) \tag{4}$$

Where, $u_m(0)$ and $y_m(0)$ are the initial states. $f(\cdot)$ represents the predictor, which is a dynamic model whose form depends on the model structure.



A MATLAB command is used to identify a discrete state-space model from the measured data. Historical weekly time series of water table data for 38 years is used for developing the time series model, which is used for future water level predictions for a period of the next 22 years (up to 2040).

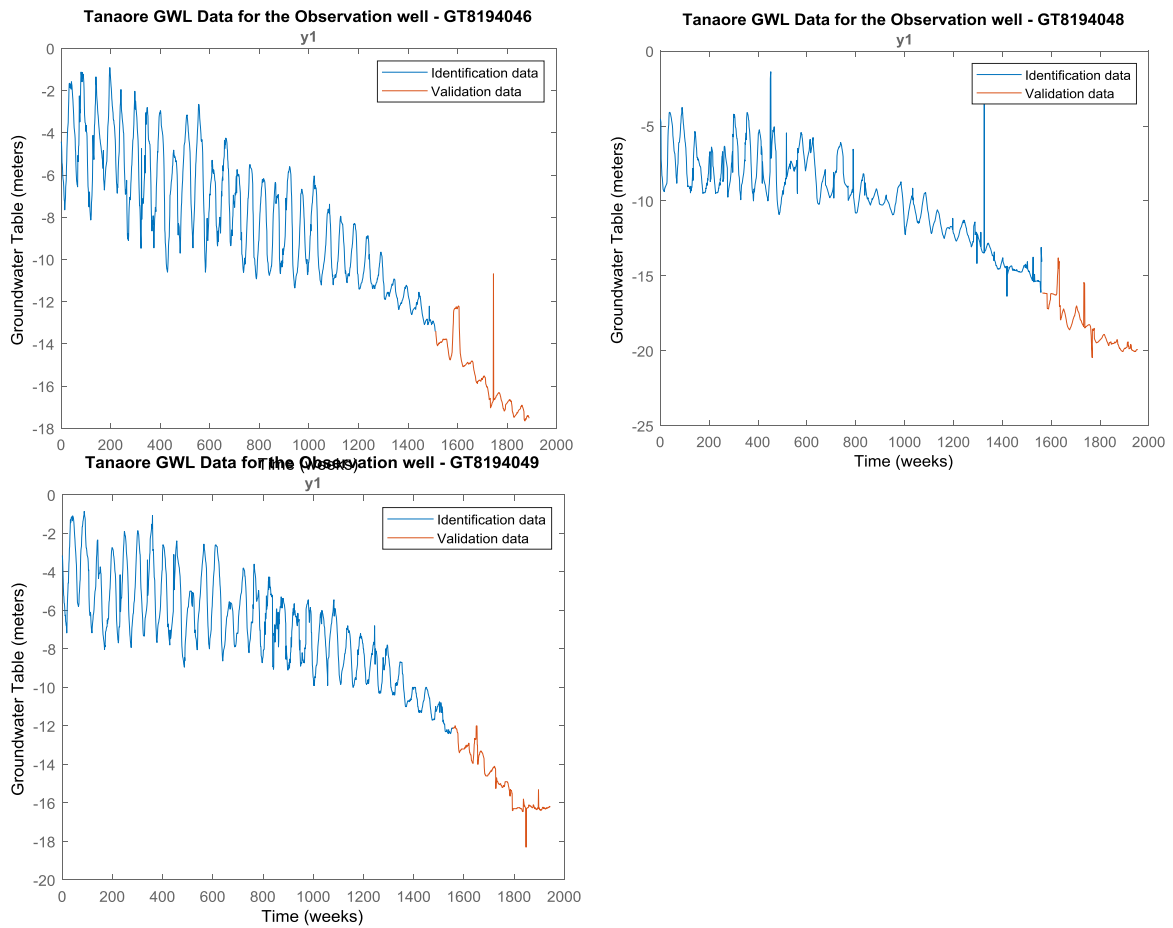


Figure 4. Partitioning of the data into identification and validation datasets at Tanore upazila.

The original time series of groundwater table data was divided into identification (training) and validation data. Eighty percent of the entire time series data was used to train the model whereas the rest 20% was used to validate the developed model. After satisfactory training of the models, the trained and validated models were used for future predictions. Figures 3, 4, 5, and 6 present the partitioning of the time series dataset into training and validation dataset for the three selected observation wells in Tanore, Godagari, Joypurhat sadar, and Kalai upazilas, respectively.

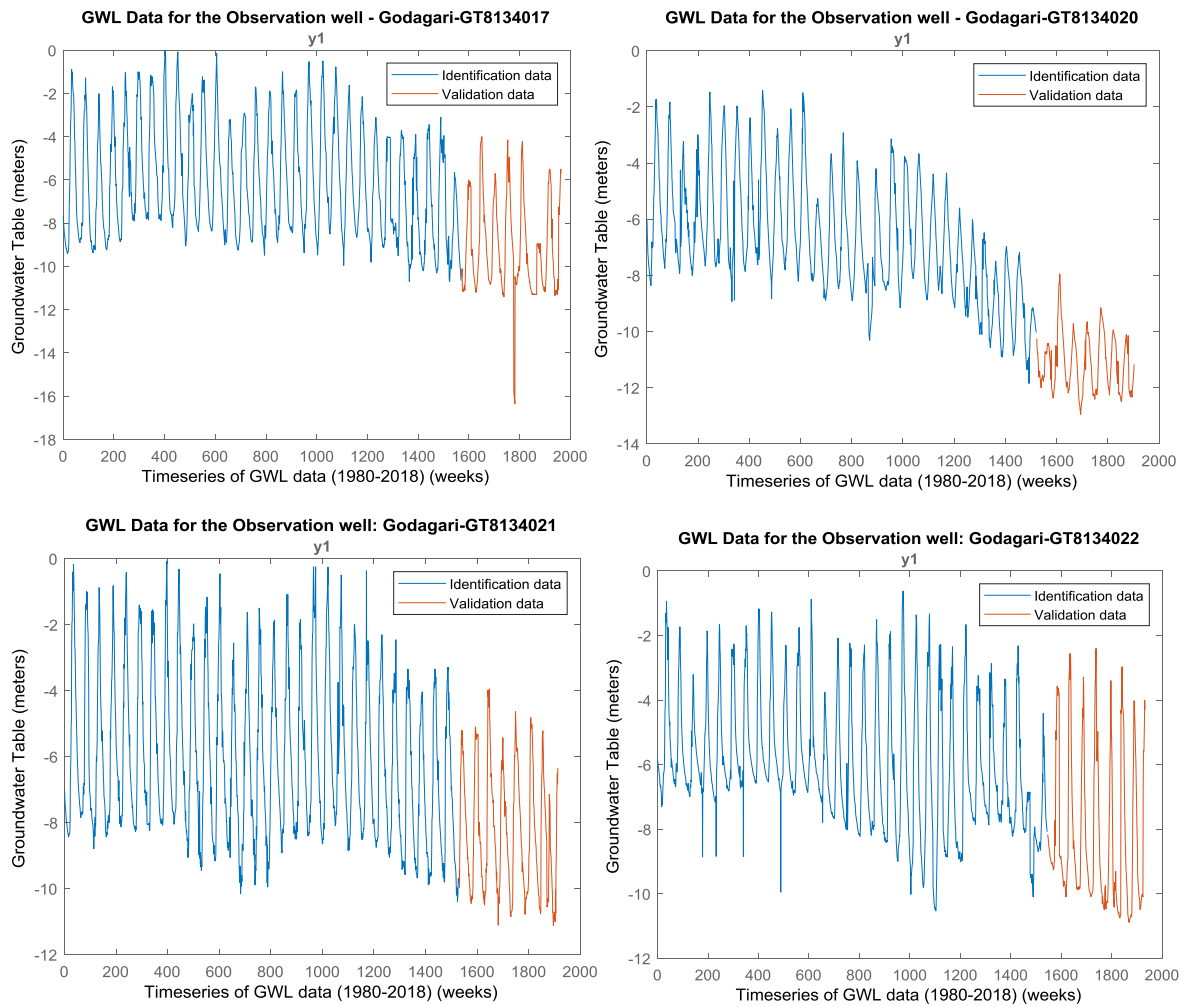


Figure 5. Partitioning of the data into identification and validation datasets at Godagari upazila.

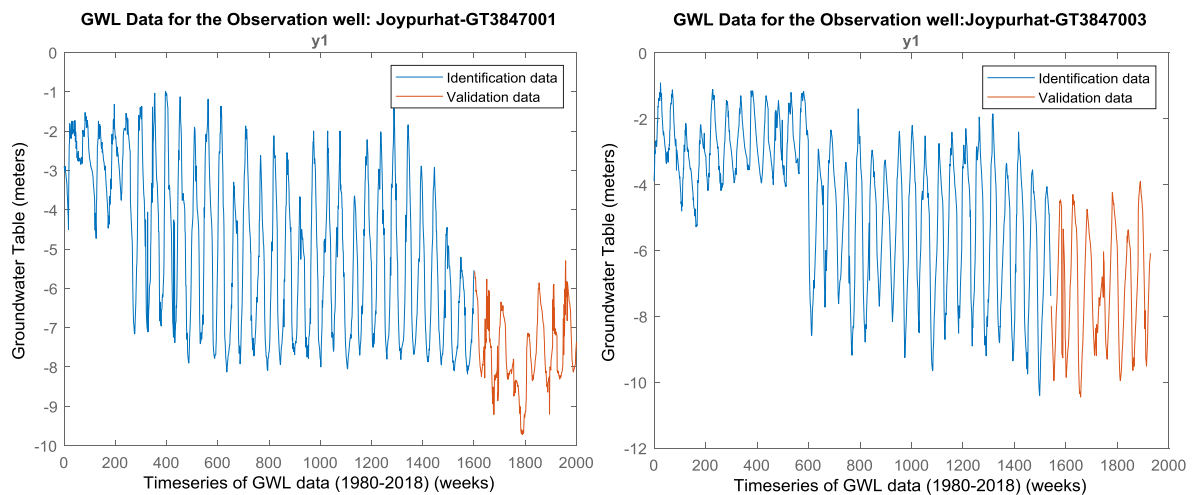


Figure 6. Partitioning of the data into identification and validation datasets at Joypurhat Sadar upazila.

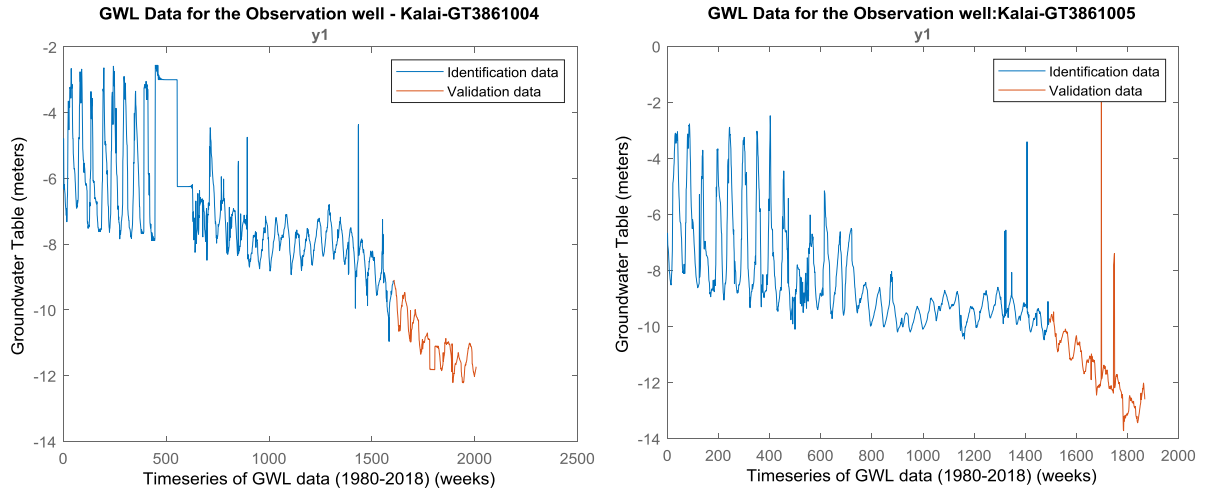


Figure 7. Partitioning of the data into identification and validation datasets at Kalai upazila.

2.4.1.2. Performance criteria:

Akaike's Final Prediction Error (FPE):

FPE criterion provides a measure of model quality by simulating the situation where the model is tested on a different data set. According to Akaike's theory, the most accurate model has the smallest FPE. Akaike's Final Prediction Error (FPE) is defined by the following equation:

$$FPE = \det \left(\frac{1}{N} \sum_1^N e(t, \hat{\theta}_N) (e(t, \hat{\theta}_N))^T \right) \left(\frac{1 + d/N}{1 - d/N} \right) \quad (5)$$

Where, N is the number of values in the estimation data set, $e(t)$ is a ny -by- 1 vector of prediction errors, θ_N represents the estimated parameters, d is the number of estimated parameters. If number of parameters exceeds the number of samples, FPE is not computed when model estimation is performed.

Mean Squared Error (MSE):

$$MSE = \frac{1}{N} \sum_{i=1}^N (Actual_i - Prdicted_i)^2 \quad (6)$$

2.4.1.3. Model development:

As the first step of the model development, a 1-step ahead prediction was performed for the selected observation well locations for all the study areas. For instance, in observation well GT8194046 of the Tanore upazila, the system identified 440 numbers of free coefficients to develop a Space-State model for which estimation data fit was found to be 91.35% (prediction focus). The FPE and MSE values of 0.07358 and 0.06796, respectively were found, which indicate a very good prediction model. The corresponding values of free coefficients, FPE and MSE values of observation wells GT8194048 and GT8194049 were presented in Table 2. The modelling approaches for the other three upazilas were performed using the similar procedures, and the obtained results indicated the good modelling performance on the basis of prediction focus, FPE, and MSE values.

Table 2. Prediction performance of the developed models at observation wells GT8194048 and GT8194049 at Tanore upazila

Observation Well	Free coefficients	Fit to estimation data (prediction focus), %	FPE	MSE
GT8194048	440	81.42	0.292	0.2704
GT8194049	440	89.98	0.07411	0.06861

The identified models minimized the 1-step ahead prediction. Now, the model was validated using a 10-step ahead predictor, i.e., given y_0, \dots, y_n , the model was used to predict y_{n+10} . Note that the measured and predicted values, $y_0 - \hat{y}_0, \dots, y_n - \hat{y}_n$, were used to make the y_{n+10} prediction. The 10-step ahead prediction results for the identification and the validation data for observation wells of Tanore, Godagari, Joypurhat sadar, and Kalai upazilas are presented in Figures 7, 8, 9, and 10, respectively.

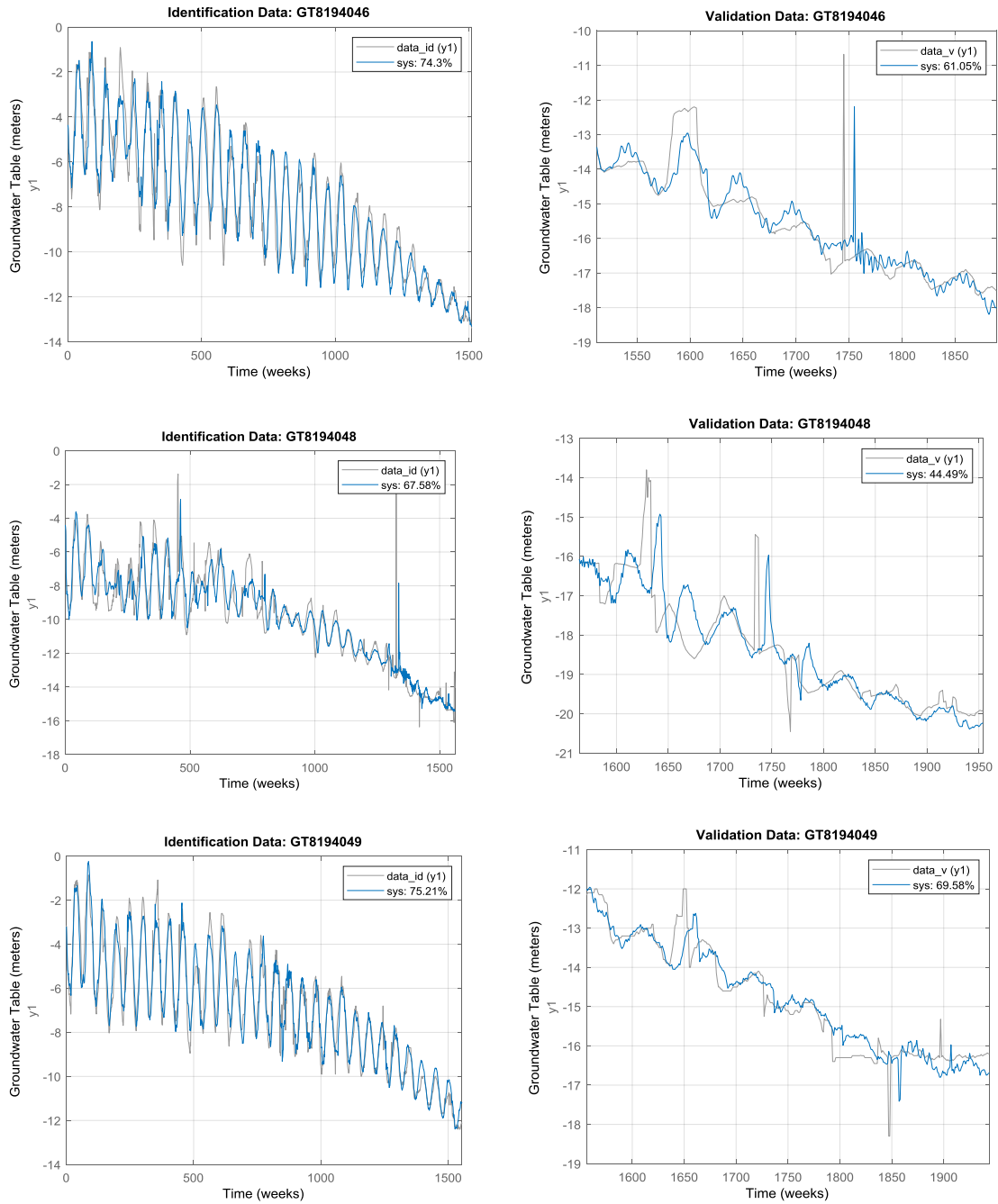


Figure 8. 10-step ahead prediction results for the identification and validation data at observation wells GT8194046, GT8194048, and GT8194049 for Tanore upazila.

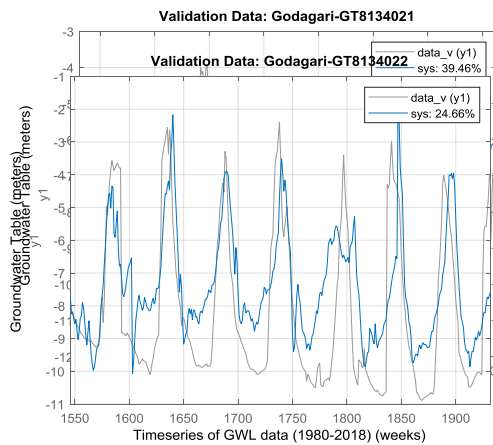
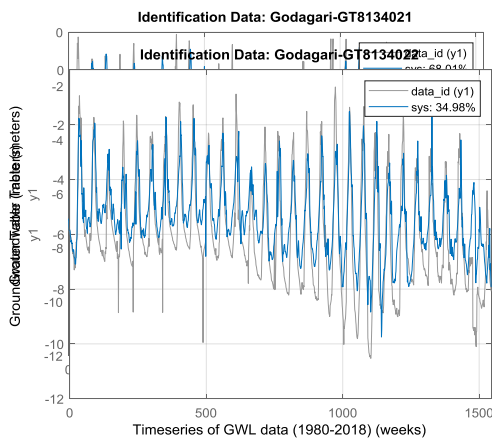
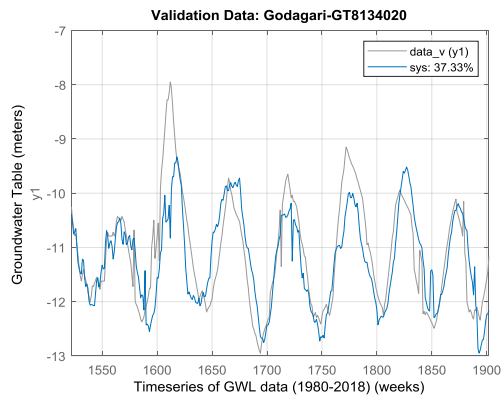
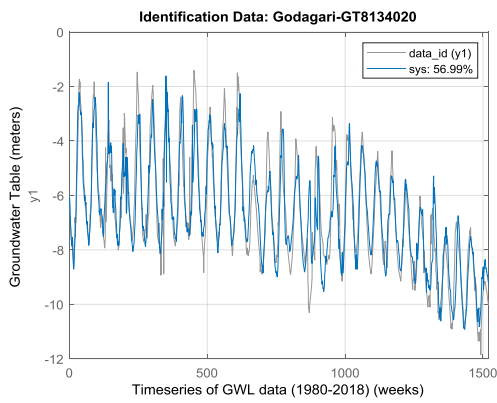
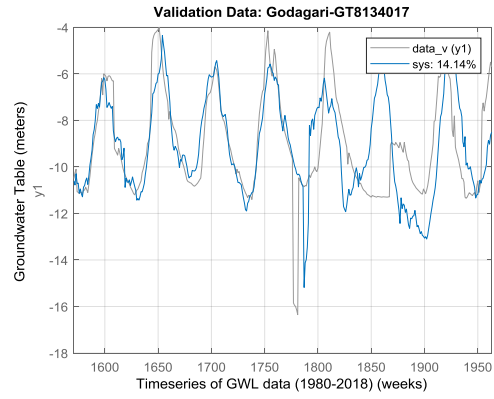
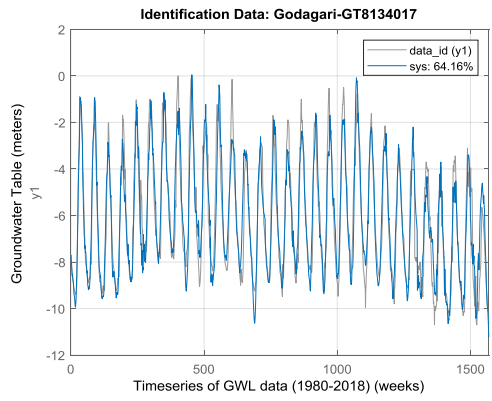


Figure 9. 10-step ahead prediction results for the identification and validation data at observation wells GT8134017, GT8134020, GT8134021, GT8134022 for Godagari upazila.

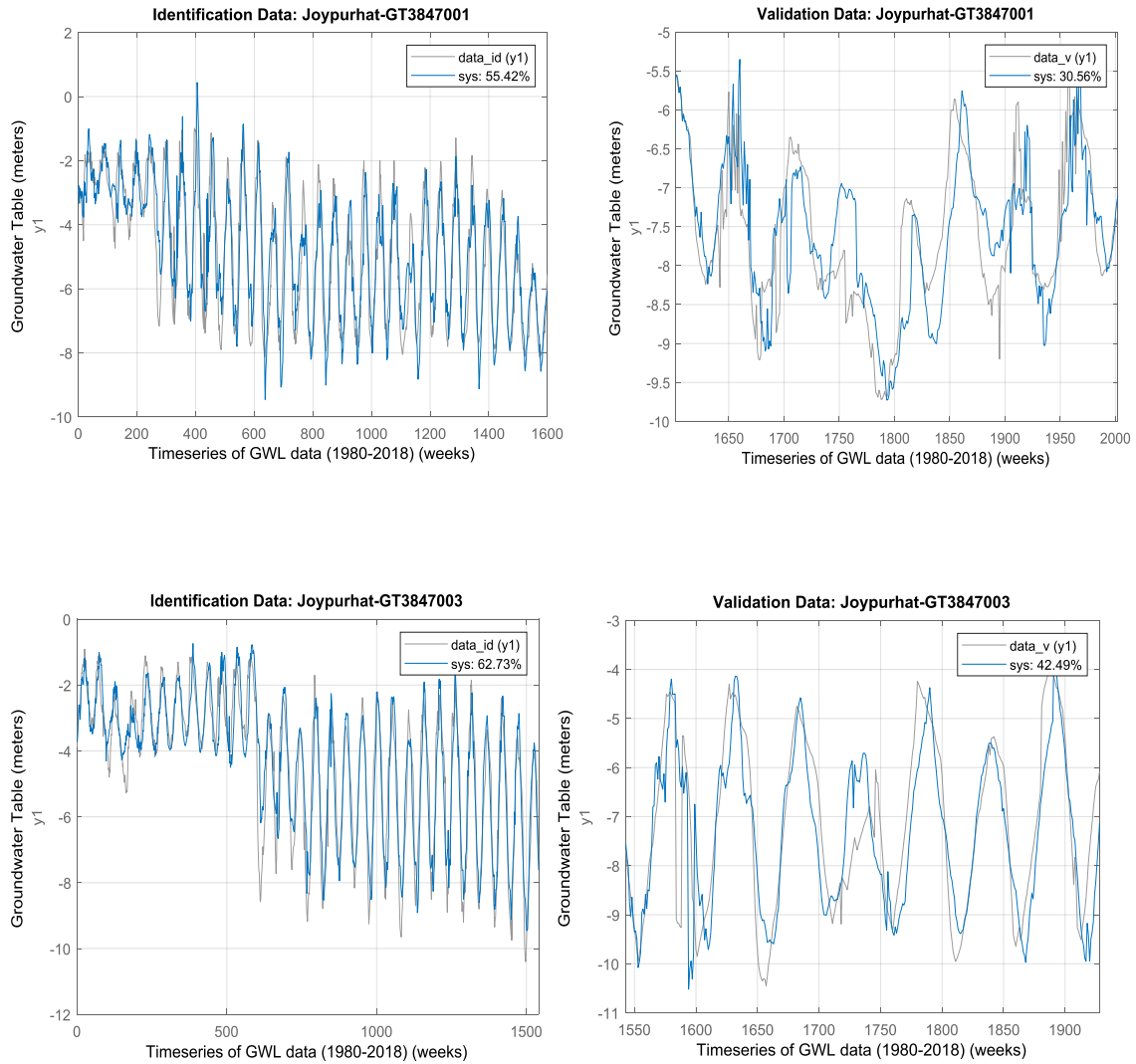


Figure 10. 10-step ahead prediction results for the identification and validation data at observation wells GT3847001 and GT3847003 for Joypurhat sadar upazila.

It is observed from Figures 7, 8, 9, and 10 that both identification and validation datasets at the observation wells of the four upazilas showed that the predictor matched well with the measured data. Then to further verify the developed prediction model, forecasting within the range of the validation data was performed. Forecasting used the measured data record $y_0, y_1, \dots, y_n - \hat{y}_n$ to compute the model state at time step n . This value was used as initial condition for forecasting the model response for a future time span. We forecasted the model response over the time span of the validation data and then compared the two.

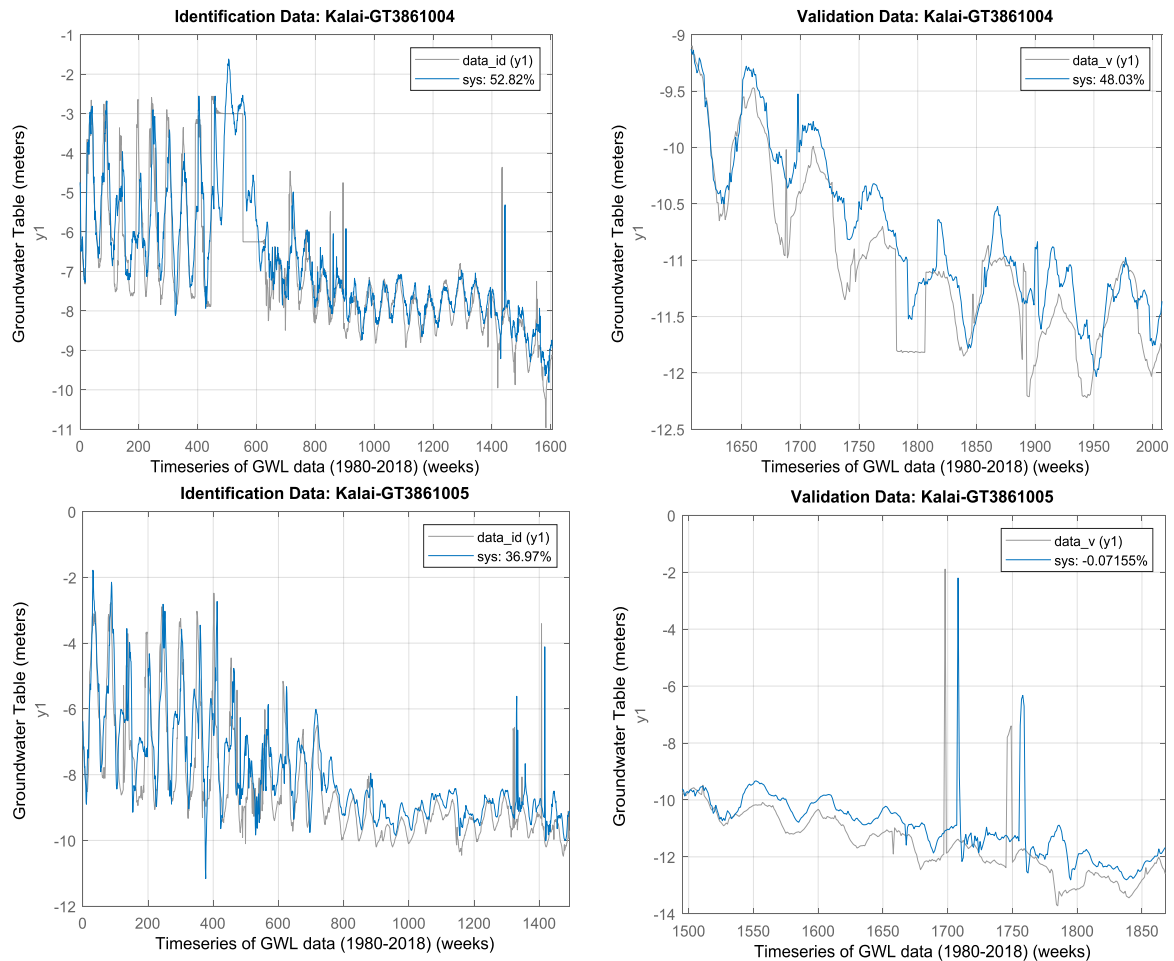


Figure 11. 10-step ahead prediction results for the identification and validation data at observation wells GT3861004 and GT3861005 for Kalai upazila

2.4.2. MAKESENS modeling approach:

- MAKESENSE performs two types of statistical analyses.
- First, the presence of a monotonic increasing or decreasing trend is tested with the nonparametric Mann-Kendall test, and
- Secondly, the slope of a linear trend is estimated with the nonparametric Sen's method.
- The Sen's method uses a linear model to estimate the slope of the trend and the variance of the residuals should be constant in time.
- Annual data needs to be used.

Secondary data of weekly groundwater level fluctuations at selected observation wells were collected from Bangladesh Water Development Board. Historical weekly groundwater level data from January 1980 to September 2018 of three observation wells of Bangladesh Water Development Board were used. Along with this, a few observation wells were selected in the study areas for collecting groundwater level data directly. Collected data were used to predict the trend of change of groundwater level by using discrete Space-state and MAKSENS modeling approach

Historical weekly groundwater level data of thirty five years (1984 - 2018) were collected from three observation wells of Bangladesh Water Development Board. (BWDB). The sites differed in hydrologic, climatic and agricultural peculiarities. The collected GWL data were arranged in month wise and then reduced to mean value. The trend of computed monthly GWL was detected and estimated

by MAKESENS trend model. It is a computer model, which was developed using Microsoft Excel 97 and the macros were coded with Microsoft Visual Basic (Salami et al., 2002). MAKESENS implements statistical analyses in two ways. Firstly, the presence of a monotonic increasing or decreasing trend was tested with the non-parametric Mann-Kendal test and, secondly, the slope of a linear trend was estimated with the non-parametric Sen's Method (Gilbert, 1987). The model was used to analyse the trend of change of arranged climatic parameters. The testing was done at the significance level of 0.001, 0.01, 0.05 and 0.10. The changes of groundwater levels were computed based on the trend analysis results as: Groundwater level = B+Q (2018-1984).

where,

B = the intercept,

Q = the slope of the trend line

2.5. Optimization of groundwater abstraction by Hydrologic Model

Previous studies in the Bengal Delta modelled a very large area (Faneca Sanchez et al., 2015; Michael and Voss, 2009) by assuming groundwater abstraction per unit area of the model domain. The withdrawals were dispersed based on estimations done for each administrative unit. Of note, it is difficult to show point pumping in the model domain as individual bores because of the large number of unreported wells and the large scale of the study area. Therefore, the exact location of the point pumping was approximated in the present study on the basis of the land-use pattern of the study area. In conformance with the total water abstraction and for simplicity in the model, total water abstraction was distributed among the individual wells during the calibration process. Groundwater abstractions for domestic, industrial, and agricultural water use were discussed earlier in Section 10.3. Total irrigated area in the study area was obtained from the district statistics for Tanore upazila (Bangladesh Bureau of Statistics (BBS), 2013). The total irrigated area was multiplied by an abstraction rate of 1 m/pumping season/m² of irrigated area (Harvey et al., 2006).

The entire model domains of all four upazilas were discretized into finite difference grids with a cell size of 300m×300m. The type and thickness of aquifer material layers were chosen in accordance with the lithological data of the study area. As most of the physical processes are occurred in the first few meters of the aquifer, the aquifer thicknesses of 95 m, 80m, 65m, and 70 m were chosen for Tanore, Godagari, Joypurhat sadar, and Kalai upazilas, respectively. The total thickness of the aquifer was divided into three layers of materials for all upazilas. In Tanore upazila, first layer below the ground surface belongs to silty clay with a thickness of 45 m, followed by a layer of fine to medium sand with 25 m thickness, followed by a soil type of medium to coarse sand with a thickness of 25 m. In Godagari upazila, first layer below the ground surface belongs to silt with a thickness of 25 m, followed by a layer of medium sand with 30 m thickness, followed by a soil type of coarse sand with a thickness of 25 m. In Joypurhat sadar upazila, first layer below the ground surface belongs to sandy clay with a thickness of 20 m, followed by a layer of medium sand with 25 m thickness, followed by a soil type of medium to coarse sand with a thickness of 20 m. In Kalai upazila, first layer below the ground surface belongs to silty clay with a thickness of 20 m, followed by a layer of fine to medium sand with 25 m thickness, followed by a soil type of very coarse sand with a thickness of 25 m. An average estimate of hydraulic conductivity was assigned to each model layer. The aquifer material within each model layer was assumed homogeneous, only vertical heterogeneity in terms of hydraulic conductivity was considered. The hydraulic conductivity values used in this study were in accordance with previous studies conducted in the Bengal Delta (Faneca Sanchez et al., 2015; Michael and Voss, 2009). A vertical anisotropy of 4 was chosen (GMS user's manual). The 3-D view of the model domains with finite difference grids is shown in Fig. 12.

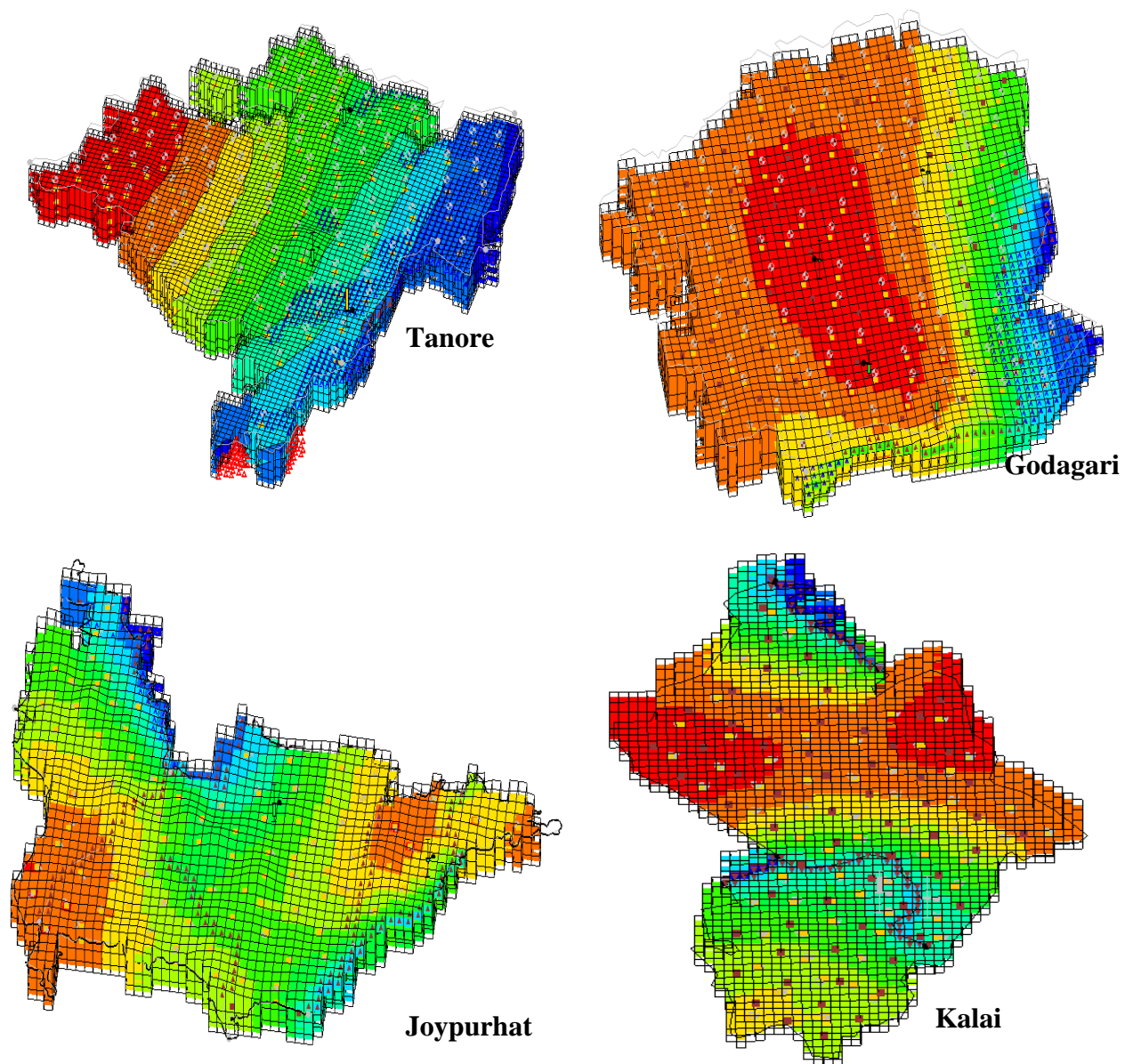


Figure 12 Three dimensional view of the study areas.

The calibration process was initiated from a steady state condition of the hydraulic heads in the finite difference grids of the model domain. To achieve this condition, the simulation model was run for 80 years. The simulation was performed in stages with an interval of 10 years. An average value of pumping was used during this simulation period. Outputs at the end of the 10th year's simulation were used as initial conditions for the succeeding intervals of 10 years' period. The process was continued until a stable condition with respect to hydraulic head was achieved. These hydraulic head estimates at various grids of the model area were used as initial conditions of the calibration process. At this stage, the actual groundwater abstraction from the study area was used. The calibration was performed for the observed hydraulic heads on September 2018, and the hydraulic heads were monitored at the designated monitoring locations. Recharge and hydraulic conductivity estimates were fine-tuned to achieve the hydraulic heads closer to the actual hydraulic heads in the observation wells. Table 3 presents major parameter values used in the calibrated groundwater simulation models.

Table 3. Parameter values of the calibrated model

Parameters	Values	Units
<u>Tanore upazila</u>		
Hydraulic conductivity in X-direction for soil layer 1	2.5	m/day
Hydraulic conductivity in X-direction for soil layer 2	18	m/day
Hydraulic conductivity in X-direction for soil layer 3	25	m/day
Vertical anisotropy for the soil layers	4	-
Aquifer recharge applied on the top soil layer	0.0004	m/day
Conductance of the specified head boundaries	1.0	(m ² /day)/m
Specific yield of Aquifer layer 1	0.01	-
Specific yield of Aquifer layer 2	0.01	-
Specific yield of Aquifer layer 3	0.01	-
<u>Godagari upazila</u>		
Hydraulic conductivity in X-direction for soil layer 1	3.5	m/day
Hydraulic conductivity in X-direction for soil layer 2	15	m/day
Hydraulic conductivity in X-direction for soil layer 3	22	m/day
Vertical anisotropy for the soil layers	4	-
Aquifer recharge applied on the top soil layer	0.00038	m/day
Conductance of the specified head boundaries	1.0	(m ² /day)/m
Specific yield of Aquifer layer 1	0.01	-
Specific yield of Aquifer layer 2	0.01	-
Specific yield of Aquifer layer 3	0.01	-
<u>Joypurhat sadar upazila</u>		
Hydraulic conductivity in X-direction for soil layer 1	4.5	m/day
Hydraulic conductivity in X-direction for soil layer 2	18.8	m/day
Hydraulic conductivity in X-direction for soil layer 3	23	m/day
Vertical anisotropy for the soil layers	4	-
Aquifer recharge applied on the top soil layer	0.0007	m/day
Conductance of the specified head boundaries	1.0	(m ² /day)/m
Specific yield of Aquifer layer 1	0.01	-
Specific yield of Aquifer layer 2	0.01	-
Specific yield of Aquifer layer 3	0.01	-
<u>Kalai upazila</u>		
Hydraulic conductivity in X-direction for soil layer 1	2.5	m/day
Hydraulic conductivity in X-direction for soil layer 2	18	m/day
Hydraulic conductivity in X-direction for soil layer 3	23	m/day
Vertical anisotropy for the soil layers	4	-
Aquifer recharge applied on the top soil layer	0.00033	m/day
Conductance of the specified head boundaries	1.0	(m ² /day)/m
Specific yield of Aquifer layer 1	0.01	-
Specific yield of Aquifer layer 2	0.01	-
Specific yield of Aquifer layer 3	0.01	-

2.6. Collection and analysis of water samples

Groundwater samples were collected before starting (November/December, 2018) and at the end (February/March, 2019) of dry season irrigation to examine its suitability for irrigation over the season. The samples were collected from different sources like STWs and DTWs of the study areas. The water samples were collected in white plastic bottles filling up to the brim and immediately sealed to avoid exposure to air. Then the samples were labeled and brought to the laboratory for chemical analysis. The samples were analyzed for different water quality parameters such as pH, EC, PO₄²⁻, NO₃²⁻, Cl⁻, HCO₃⁻, Na⁺, K⁺, Ca²⁺ and Mg²⁺. The analysis was done in the laboratories of BRAC, Gazipur and Soil Science Division, BARI, Gazipur.

Groundwater suitability for irrigation purpose in this study area was assessed using SAR (Sodium Adsorption Ratio), RSC (Residual Sodium carbonate), SSP (Soluble Sodium percentage) and KR (Kelly's ratio). All determined groundwater concentrations used in assessing these indices were in meq/l.

SAR (Sodium Adsorption Ratio) is a measure of suitability of water for irrigation with respect to the sodium hazard. The SAR values were calculated using the following equation:

$$SAR = \frac{Na^+}{(\sqrt{Ca^{+2} + Mg^{+2}})/2}$$

The residual sodium carbonate is a measure of the hazard involved in the use of high carbonate waters. RSC is calculated as follows:

$$RSC = (CO_3^{2-} + HCO_3^-) - (Ca^{+2} + Mg^{+2})$$

Kelly (1940) and Paliwal (1967) introduced another factor to assess quality and classification of water for irrigation purposes based on the concentration of Na^+ against Ca^{2+} and Mg^{2+} . It can be calculated using the following equation:

$$KR = \frac{Na^+}{Ca^{2+} + Mg^{2+}}$$

$KR > 1$ indicates an excess level of Na^+ in waters. Therefore, water with a $KI \leq 1$ has been recommended for irrigation, while water with $KI \geq 1$ is not recommended for irrigation due to alkali hazards (Ramesh and Elango 2012; Karanth 1987).

To get a comprehensive picture of overall quality of groundwater, the WQI was used. WQI is defined as a rating reflecting the composite influence of different water quality parameters on the overall quality of water. The FAO standard specified for irrigation water was used for the calculation of WQI. The WQI was computed through three steps. First, each of the measured parameters (pH, EC, TDS, Na, Ca, Mg, K, CO_3 , HCO_3 , Cl, SO_4 , NO_3 , PO_4 , Fe, Zn and B) was assigned a weight (w_i) according to its relative importance in the overall quality of water for irrigation purposes. The maximum weight 5 was assigned to parameters like pH, EC, TDS, Na^+ , Cl^- , and SO_4^{2-} due to their importance in water quality assessments. A minimum weight of 1 was assigned to zinc because of its insignificant role. Other parameters were assigned weights between 1 and 5 based on their relative importance in the evaluation of water quality.

In the second step, the relative weight (W_i) of the chemical parameter was computed using the following equation:

$$W_i = w_i / \sum_{i=1}^n w_i$$

where W_i is the relative weight, w_i is the weight of each parameter, and n is the number of parameters.

In the third step, a quality rating scale (q_i) for each parameter is assigned by dividing its concentration in each water sample by its respective standard according to the guidelines given by FAO, 1997 and the result is multiplied by 100:

$$q_i = (C_i/S_i) \times 100$$

where q_i is the quality rating, C_i is the concentration of each chemical parameter in each water sample in mg/L, and S_i is the irrigation water standard for each chemical parameter in mg/L.

For computing WQI, the sub index (SI) is first determined for each chemical parameter, as given below:

$$SI = W_i \times q_i$$

$$WQI = \sum SI_i/n$$

where SI_i is the sub index of i^{th} parameter; W_i is relative weight of i^{th} parameter; q_i is the rating based on concentration of i^{th} parameter, and n is the number of chemical parameters. The computed WQI

values are classified into five categories: excellent water (WQI < 50); good water (WQI = 50–100); poor water (WQI = 100–200); very poor water (WQI = 200–300); and water unsuitable for irrigation (WQI > 300).

3. Results and discussion

3.1. Yield, water requirement and water productivity of crops

3.1.1. T. Aman:

Yield, water requirement and water productivity of T.Aman rice obtained from the separate experimental fields at four locations during 2018-2019 are presented in Table 4a and 4b. Over the locations, yield varied from 3.41 to 4.17 t/ha in 2018 with minimum in farmers' practice treatment T₁ and maximum in T₂ where AWD with 20 cm depth was used for determining irrigation timing. In Rajshahi, grain yield was significantly lowest in T₁ compared to both AWD treatments T₂ and T₃. In Joypurhat too, highest yield was obtained from T₂ and it was insignificant compared to both T₁ and T₃. This happened because treatment T₂ and T₃ received almost same number and amount of irrigation water. Even treatment T₁ received ample amount of water from rainfall that almost satisfied the water requirement of T. Aman rice. But in Rajshahi, as number and amount of irrigation were different among treatments, so difference in grain yields were found a significant. In 2019 too, highest yields were obtained from T₂. But yields obtained from T₁ and T₂ were almost same as these treatments received same amount of water from irrigation as well as from rainfall. In 2018, however, WPs were found highest in T₃, except Godagari where highest WP was obtained from T₁. Over the other three locations, WP varied from 1.58 m³/kg for T₁ to 1.83 m³/kg for T₃. That is, 1580 to 1830 liters of water was required to produce one kilogram of rice whereas in 2019, 1180 to 1500 litres of water was needed. As yield was found higher in 2019, so does the water productivity. Water requirement was varied from 528 mm to as much as 729 mm in 2018 whereas in 2019 it varied from 537 to 686 mm with minimum in T₁ and maximum in T₂.

Table 4a. Yield, water requirement and water productivity of T. Aman rice during 2018

Treat-ment	Applied water (mm)	Eff. rainfall (mm)	WR (mm)	Yield (t/ha)	Water productivity (m ³ /kg)	Yield increased (%)
Godagari (cv. BRR1 dhan 51)						
T ₁	200	328	528	2.65	1.99	
T ₂	412	328	740	4.17	1.77	57.36
T ₃	384	328	712	3.96	1.80	49.43
Tanore (cv. BRR1 dhan 62)						
T ₁	210	306	516	2.90	1.78	
T ₂	423	306	729	3.98	1.83	37.24
T ₃	346	306	652	3.56	1.83	22.76
Kalai (cv: Swarna)						
T ₁	207	362	569	3.61	1.58	
T ₂	287	362	649	3.77	1.72	4.43
T ₃	296	362	658	3.79	1.74	4.99
Joypurhat sadar (cv: Guti Swarna)						
T ₁	204	354	558	3.41	1.64	
T ₂	294	354	648	3.66	1.77	7.33
T ₃	294	354	648	3.63	1.79	6.45

Table 4b. Yield, water requirement and water productivity of T. Aman rice during 2019

Treat-ment	Applied water (mm)	Eff. rainfall (mm)	WR (mm)	Yield (t/ha)	Water productivity (m ³ /kg)	Yield increased (%)
Godagari (cv. BRRI dhan 51)						
T ₁	155	421	576	4.17	1.29	
T ₂	237	421	658	4.77	1.30	13.42
T ₃	155	421	576	4.13	1.30	-0.89
Tanore (cv. Sumon Swarna)						
T ₁	162	375	537	4.26	1.18	
T ₂	241	375	616	4.86	1.19	13.16
T ₃	162	375	537	4.32	1.16	1.32
Kalai (cv: Swarna)						
T ₁	130	494	624	3.91	1.48	
T ₂	192	494	686	4.35	1.48	10.45
T ₃	130	494	624	3.87	1.50	-0.95
Joypurhat sadar (cv: Guti Swarna)						
T ₁	120	431	551	4.05	1.27	
T ₂	178	431	609	4.24	1.34	4.37
T ₃	120	431	551	4.03	1.27	-0.46

3.1.2. Boro:

The effects of different irrigation treatments on yield, water requirement and water productivity of boro rice grown in four different upazilas are presented in Table 5. Two different rice varieties: BRRI dhan 28 and BRRI dhan 29 were used as test crops. BRRI dhan 29 performed better in terms of yield, but in terms of water requirement and water productivity BRRI dhan performed better under all irrigation regimes. Irrespective of variety, treatment T₁ and/or T₂ produced the highest and identical yield of rice. AWD method with 15 cm depth (T₂) yielded more or less similar yield that obtained by farmers' practice. In some plots, AWD with 15 cm depth performed better while some other plots farmers' practice produced the highest yield. While AWD with 25 cm depth (T₃) produced about 3% less yield than farmers practice treatment T₁. However, water requirement was obviously higher in treatment T₁ as this treatment received irrigation more frequently than AWD treatments. Water productivity was found highest (less water required to produce 1.0 kg of rice) in AWD method with 25 cm depth as this treatment produced the highest yield with more efficient water use. Water required to produce highest yield was ranged from 1017 to 1096 mm for AWD with 15 cm depth and from 1139 to 1176 mm for farmers' practice with minimum values for BRRI dhan 28 and Maximum values for BRRI dhan 29. The difference in water requirement between these two varieties was due to difference in their growing period.

Table 5. Yield, water requirement and water productivity of boro rice during 2019

Treatment	WR (mm)	Yield (t/ha)	Water productivity (m ³ /kg)	Yield reduction (%)	Water saved (%)	TWU (mm)	WUE (%)
Godagari (cv. BRRI dhan 28)							
T ₁	1128	5.31	2.12	-		727	64.45
T ₂	1017	5.27	1.93	0.75	9.84	662	65.09
T ₃	912	5.06	1.80	2.82	19.15	635	69.63
Tanore (cv. BRRI dhan 29)							
T ₁	1176	5.80	2.03	-		746	63.44
T ₂	1096	5.78	1.90	0.34	6.80	684	62.41
T ₃	952	5.56	1.71	3.62	19.05	658	69.12
Kalai (cv. BRRI dhan 29)							
T ₁	1149	5.63	2.04	-		739	64.32
T ₂	1044	5.78	1.81	-2.66	9.14	676	64.75
T ₃	958	5.49	1.74	0.71	16.62	662	69.10
Joypurhat sadar (cv. BRRI dhan 28)							
T ₁	1139	5.19	2.19			718	63.04
T ₂	1027	5.16	1.99	0.58	9.83	658	64.07
T ₃	908	5.03	1.81	3.08	20.28	636	70.04

3.1.3. Wheat:

Yield, water requirement and water productivity of wheat obtained from the two separate experimental fields at two locations are presented in Table 6. Highest yields (4.73 t/ha at Godagari and 4.36 t/ha at Tanore) were obtained from T₃ treatment that received three irrigations at CRI, booting and grain filling stage up to field capacity at both locations. Only 3-4% decrease in yields were recorded in treatment T₂ (two irrigation at CRI and booting stages) which were at par with T₃. The result revealed that less frequent irrigation can reduce the yield of wheat, but the amount of reduction can significantly be minimized by changing the timing of irrigation application. Therefore, where water is scarce, two irrigations at CRI and grain filling stage (T₂) can be suggested rather than irrigation at CRI and booting stage (T₁). A reasonably good yield, though the lowest, was obtained from treatment T₁ received irrigation only at CRI stage. Total water use was highest in irrigation treatment T₃ as it received three number of irrigation. Although the number of irrigation was same for T₁ and T₂, T₂ received slightly more water, because irrigation interval in this treatment was higher and the soil was more dried to receive more amount of irrigation water. WPs were also found highest (2.34-2.63 kg/m³) in this treatment T₂ with a water saving of about 24% over treatment T₃. So, considering water saving, water productivity and grain yield, two irrigations at CRI and booting stages can be suggested for growing wheat crop in this drought prone and water scarce area.

Table 6. Yield, water requirement and water productivity of wheat

Treatment	WR (mm)	Yield (t/ha)	Water productivity (kg/m ³)	Yield increased (%)	Yield decreased (%)	Water saved over T ₃ (%)
Godagari (cv. BARI Gom 30)						
T ₁	161	4.08	2.53	-	13.74	29.69
T ₂	174	4.57	2.63	12.0	3.38	24.01
T ₃	229	4.73	2.08	15.93	-	-
Tanore (cv. BARI Gom 30)						
T ₁	166	3.90	2.35	-	10.55	30.25
T ₂	179	4.18	2.34	7.18	4.12	24.07
T ₃	238	4.36	1.83	11.79		-

3.1.4. Potato:

Variation in tuber yield, water requirement and water productivity of potato under three different irrigation treatments are presented in Table 7a and 7b. The yield of potato was significantly higher in furrow irrigation compared to the farmers practice in all study areas except in Joypurhat where treatment with farmers' practice and furrow irrigation produced almost same yield while alternate furrow irrigation produced the lowest.

Table 7a. Yield, water requirement and water productivity of potato during 2018-19

Treatment	WR (mm)	Yield (t/ha)	Water productivity (kg/m ³)	Water saved (%)	Yield increased over T ₁ (%)
Godagari (cv. BARI Alu 7)					
T ₁	336	28.65	8.53	-	-
T ₂	285	31.28	10.98	15.17	9.18
T ₃	196	30.07	15.34	41.66	4.96
Tanore (cv. BARI Alu 7)					
T ₁	342	35.56	10.40	-	-
T ₂	281	37.18	13.23	17.83	4.56
T ₃	203	35.90	17.68	40.64	0.96
Kalai (cv. BARI Alu 8)					
T ₁	307	31.76	10.35	-	-
T ₂	276	34.47	12.49	15.18	8.53
T ₃	186	33.98	18.27	41.67	6.99
Joypurhat sadar (cv. BARI Alu 26)					
T ₁	298	26.64	8.94	-	-
T ₂	268	26.86	10.02	17.84	0.83
T ₃	193	24.33	12.61	40.64	-8.67

In other locations, however, alternate furrow irrigation produced the second highest yields those were at par with furrow irrigation. Compared to farmers' practice, the average yield increased in furrow irrigation and alternate furrow irrigation system was 7.42% and 4.30%, respectively. From the result it is clear that both furrow and alternate furrow irrigation can significantly improve the growth and yield of potato, where the difference in yield between furrow and alternate furrow is marginal. From Table 6, it is seen that significantly higher irrigation water was applied in farmers' practice compared to furrow irrigation and alternate furrow irrigation. Therefore, the total water use was also highest in the farmers' practice, whereas the lowest water use was in alternate furrow irrigation treatments. About 40% water was saved in alternate furrow irrigation treatment compared to the farmers' practice, whereas it was about 15% in furrow irrigation treatments. Water productivity was considerably higher in alternate furrow irrigation and furrow irrigation treatments than that of farmers' practice due to higher yield obtained in these treatments with comparatively lower irrigation water use. Highest water productivity (12.49 – 17.68 kg/m³) was observed in alternate furrow irrigation followed by furrow irrigation treatment (10.02–13.23 kg/m³), whereas the lowest (8.53–10.40 kg/m³) was always in farmers practice. Water productivity was around 65% higher in alternate furrow and around 22% higher in every furrow irrigation compared to the traditional irrigation practice.

Table 7b. Yield, water requirement and water productivity of potato during 2019-20

Treatment	WR (mm)	Yield (t/ha)	Water productivity (kg/m ³)	Water saved (%)	Yield increased over T ₁ (%)
Godagari (cv. BARI Alu 7)					
T ₁	333	30.76	9.24		
T ₂	288	32.58	11.31	13.51	5.92
T ₃	201	29.80	14.83	39.64	-3.22
Tanore (cv. BARI Alu 7)					
T ₁	326	37.2	11.41		
T ₂	284	46.6	15.56	12.88	20.17
T ₃	206	44.2	22.62	36.81	18.28
Kalai (cv. BARI Alu 8)					
T ₁	315	33.45	10.62		
T ₂	279	35.32	12.66	11.43	5.59
T ₃	197	33.38	16.94	37.46	-0.21
Joypurhat sadar (cv. BARI Alu 26)					
T ₁	292	27.66	9.47		
T ₂	257	28.09	10.93	11.99	1.55
T ₃	189	26.55	14.05	35.27	-4.18

3.1.4. Mustard:

Yield of mustard differed significantly by the number and timing of irrigation (Table 8a & 8b). Grain yield of mustard increased considerably when number of irrigation increased from one to two. But it showed an insignificant yield variation when yield under one irrigation either at vegetative or pre-flowering stage were compared. Though treatments T₁ and T₂ both received one irrigation, yield variation was observed between them due to variation in timing of water application with marginally higher yield in T₂ where water was applied at pre-flowering stage. This result indicate that pre-flowering stage is more responsive than vegetative stage. However, the highest yield (1.56-1.61 t/ha) was obtained

from treatment T₃ that received two irrigations at vegetative and pod formation stages. The lowest yield (1.39-1.43 t/ha) was obtained from T₁ when irrigation was applied at vegetative stage. Around 10-15% higher yield was noticed in T₃ compared to T₁, while yield difference between T₁ and T₂ was registered as 2 - 4%. Though treatment T₁ and T₂ both received one irrigation, amount of water requirement was slightly higher in T₂ due to timing of application. Treatment T₂ received irrigation about 10 days later than T₁ when plants were taller with drier field soil, hence more water was needed to fulfill the crop demand. Obviously treatment T₃ that received two irrigations at vegetative and pod formation stages gave the highest yield with low water productivity. As increase in yield was not proportionate to water use, so water productivity was slightly lower in treatment T₃ than other two treatments. A reasonably good yield and water productivity was obtained from treatment T₂ with one irrigation only at pre-flowering stage is preferred to irrigation at vegetative stage, even it is preferred to two irrigations at vegetative and pod formation stages in water scarce situation.

Table 8a. Yield, water requirement and water productivity of mustard during 2018-19

Treatment	WR (mm)	Yield (t/ha)	Water productivity (kg/m ³)	Yield increased (%)	Water saved over T ₃ (%)
Godagari (cv. BARI Sarisha 14)					
T ₁	139	1.43	1.03		19.19
T ₂	142	1.47	1.04	2.16	17.44
T ₃	172	1.56	0.91	9.09	-
Tanore (cv. BARI Sarisha 14)					
T ₁	143	1.39	0.97		19.66
T ₂	149	1.48	0.99	4.20	16.29
T ₃	178	1.61	0.90	15.83	-

Table 8b. Yield, water requirement and water productivity of mustard during 2019-20

Treatment	WR (mm)	Yield (t/ha)	Water productivity (kg/m ³)	Yield increased (%)	Water saved over T ₃ (%)
Godagari (cv. BARI Sarisha 14)					
T ₁	133	1.15	0.91	-	21.30
T ₂	145	1.19	0.85	1.65	14.20
T ₃	169	1.49	0.80	12.40	-
Tanore (cv. BARI Sarisha 17)					
T ₁	136	1.21	0.94	-	21.39
T ₂	147	1.25	0.88	1.56	15.03
T ₃	173	1.57	0.82	10.16	-

3.2. Effect of irrigation on the yield of rabi crops and rice equivalent yields

Individual crop yield under different cropping sequences are presented in Table 9a. It is seen that irrigation had significant effects on the yield of rabi crops wheat, mustard, tomato and potato. Yield of mustard differed significantly when number of irrigation increased from one to two. But it showed an insignificant yield variation when irrigation was applied either at vegetative stage or at flowering stage. Similarly, yield of wheat increased slightly when number of irrigation increased from two to three. The highest yield of wheat was obtained from treatment T₃ that received three irrigations at CRI, booting

and flowering stages, non-significantly followed by treatment T₂ that received two irrigations at CRI and grain filling stages.

Table 9a. Rice equivalent yield (REY) of different cropping patterns of study areas

Pattern	Irrigation treatment	Crop yield (t/ha)				Rice equivalent yield (t/ha)	
		Rabi	Boro	T. aus	T. aman	Rabi	Total
Location: Godagari							
Mustard-Boro-T.Aman	T ₁	1.29	5.31	-	2.65	2.30	10.26
	T ₂	1.32	5.27	-	4.17	2.35	11.79
	T ₃	1.56	5.06	-	3.96	2.78	11.80
Tomato-Boro-T. aus	T ₁	48.03	4.8	3.84	-	20.56	29.20
	T ₂	52.29	4.06	4.21	-	22.38	30.65
	T ₃	45.04	4.51	4.13	-	19.28	27.92
Potato-Boro-T.Aman	T ₁	29.7	5.53	-	3.56	10.60	19.69
	T ₂	31.93	5.48	-	4.62	11.40	21.50
	T ₃	29.93	5.13	-	4.2	10.69	20.02
Maize-T. aus-T. aman	T ₁	7.82	4.93	-	2.77	5.02	16.38
	T ₂	9.96	5.01	-	3.77	6.39	19.84
	T ₃	9.28	4.41	-	3.51	5.96	18.22
Location: Tanore							
Wheat-T.Aus-T.Aman	T ₁	4.08	-	3.93	2.71	3.79	10.43
	T ₂	4.57	-	4.17	3.48	4.24	11.89
	T ₃	4.73	-	4.26	3.57	4.39	12.22
Potato-Boro-T.Aman	T ₁	35.56	5.8	-	2.9	12.69	21.39
	T ₂	37.18	5.78	-	3.98	13.27	23.03
	T ₃	35.9	5.56	-	3.56	12.82	21.94
Potato-T.Aus-T.Aman	T ₁	34.64	-	3.62	2.79	12.37	18.78
	T ₂	36.49	-	3.87	3.54	13.03	20.44
	T ₃	35.2	-	3.36	3.32	12.57	19.25
Location: Kalai							
Potato-Boro-T.Aman	T ₁	32.60	5.63	-	3.49	11.64	20.76
	T ₂	34.89	5.78	-	3.63	12.46	21.87
	T ₃	33.68	5.49	-	3.6	12.02	21.11
Mustard-Boro-T.Aman	T ₁	1.1	5.41	-	3.61	1.96	10.98
	T ₂	1.11	5.56	-	3.77	1.98	11.31
	T ₃	1.39	5.29	-	3.79	2.47	11.55
Location: Joypurhat sadar							
Potato-Boro-T.Aman	T ₁	27.15	5.19	-	3.41	9.69	18.29
	T ₂	27.47	5.16	-	3.66	9.81	18.63
	T ₃	25.44	5.03	-	3.63	9.08	17.74
Mustard-Boro-T.Aman	T ₁	1.02	5.41	-	3.56	1.82	10.79
	T ₂	1.08	5.56	-	3.71	1.92	11.19
	T ₃	1.31	5.29	-	3.65	2.33	11.27

The yield under T₁ was significantly lowest compared to T₃. Though both the treatments, T₁ (farmers' practice) and T₂ received two irrigations, a variation in yield was observed due to difference in timing of irrigation with slightly higher yield was found in treatment T₂. The result revealed that less frequent irrigation can reduce the yield of wheat, but the amount of reduction can significantly be minimized by changing the timing of irrigation application. Therefore, where water is scarce, two

irrigations at CRI and grain filling stage (T_2) could be suggested rather than irrigation at CRI and booting stage (T_1). In case of mustard, yield variation was insignificant between treatments T_1 (vegetative) and T_2 (irrigation at pre-flowering stage). A significantly higher yield was obtained from treatment T_3 that received two irrigations at pre-flowering and pod formation stages. This yield under treatment T_1 and T_2 was at par with slightly higher yield was found when irrigation was applied at pre-flowering stage. So, if only one irrigation is applied, pre-flowering stage is preferred to irrigation at vegetative stage, even it is preferred to two irrigations at vegetative and pod formation stages in water scarce situation.

The yield of potato was significantly higher in every furrow irrigation compared to the farmers' practice (every furrow with different irrigation schedule) in all study areas except in Joypurhat where treatment with farmers' practice and every furrow irrigation produced almost same yield while alternate furrow irrigation produced the marginally lowest. In other locations, however, alternate furrow irrigation produced the second highest yields those were at par with every furrow irrigation. On average over the locations, the yield of potato was significantly higher in both every furrow irrigation and alternate furrow irrigation compared to the farmers practice. The average yield increased in furrow irrigation and alternate furrow irrigation than that of the farmers practice was 7.42% and 4.30%, respectively. From the result it is clear that both furrow and alternate furrow irrigation can significantly improve the growth and yield of potato, where the difference in yield between furrow and alternate furrow is marginal.

The yield of tomato was significantly influenced by the different irrigation methods. The highest fruit yields of 52.29 t/ha was obtained from the treatment T_2 which received drip irrigation at 3 days interval. This was at par with the yield that obtained under traditional furrow irrigation (T_1) at 10 days interval. Alternate furrow irrigation at 10 days interval produced slightly lower yield than traditional furrow irrigation with a greater saving (about 35%) of irrigation water. Drip fertigation not only produced the highest yield, but also offered a greater saving of water (45%) and fertilizer.

The grain yield of maize was found a bit higher in every furrow irrigation than that of the alternate furrow irrigation while farmers' practice treatment had the significantly lowest yield. The difference in yield between the treatment T_2 (furrow) and T_3 (alternate furrow) was insignificant, but the total water use was significantly lower in alternate furrow irrigation treatment (T_3) compared to the every furrow irrigation treatment (T_2), as it received less amount of irrigation water. Thus, alternate furrow irrigation can be a judicious option for maize cultivation in water scarce areas.

As yield of different crops in a particular cropping sequence varied, rice equivalent yield (REY) also varied with different irrigation treatments (Table 9a). Among the tested crops, tomato had the highest rice equivalent yield (REY) under T_2 water management practice followed by REY of potato. The highest yield of potato under this water regime contributed much to be the highest REY. These two crops have high yield potential to give the higher REY compared to other crops like mustard and wheat. However, the lowest yield of mustard resulted in the lowest REY which was even lower than that of boro rice. Though wheat also gave the lower REY, it was higher compared to the yield of boro rice. Thus, most of the rabi crops had the higher REY than boro rice.

3.3. Total rice equivalent yield, total water use and water productivity of different cropping patterns

Total rice equivalent yield (TREY) in a given pattern was varied with the different crops in a crop sequence and irrigation practices (Table 9a) while total water use and water productivity of different crops under different cropping sequences in a particular irrigation treatment are presented in Table 9b.. Here, in most cases, rice equivalent yield was found the higher under T_2 irrigation regime where BARI recommended standard practices were followed for non-rice crops and BRRI recommended practices were followed for rice crop. In Tomato-Boro-T.Aman pattern, REY was found the highest in treatment T_2 where the tomato crop yielded the highest under drip irrigation. A drastic improvement of REY was happened due to inclusion of very high yielding crop- tomato in the pattern. Next to tomato, potato is another high yielding crop. So inclusion of this crop in Potato-Boro-T.Aman cropping pattern gave the second highest REY with higher value under T_2 water regime followed by Maize-T.Aus-T.Aman cropping pattern. In this regime, all rice and non-rice crops of the patterns such as potato, maize, Boro, T.Aus and T.Aman performed better and helped increasing the TREY. However, the lowest REYs were

obtained in farmers' practice irrigation management T₁, except in Potato-Boro-T.Aman at Joypurhat sadar where the lowest REY was obtained from T₃ due to lower yield of potato and boro under this water regime. As mustard is a crop with low yield potential, the Mustard-Boro-T.Aman pattern had the lowest REY compared to other patterns tested.

Table 9b. Cropping pattern based water productivity

Pattern	Irrigation treatment	Water use (mm)				WP (kg/m ³)		
		Rabi	Boro	T. aus	T. aman	TWU	REY	WP
Location: Godagari								
Mustard-Boro-T.Aman	T ₁	139	1128	-	528	1795	10.26	0.57
	T ₂	142	1017	-	724	1883	11.79	0.63
	T ₃	172	912	-	678	1762	11.80	0.67
Tomato-Boro-T. aus	T ₁	358	1136	538	-	2032	29.20	1.43
	T ₂	266	1019	740	-	2025	30.65	1.51
	T ₃	293	917	723	-	1933	27.92	1.44
Potato-Boro-T.Aman	T ₁	333	1108	-	552	1993	19.69	0.99
	T ₂	288	991	-	699	1978	21.50	1.09
	T ₃	201	885	-	644	1730	20.02	1.16
Maize-T. Aus-T.Aman	T ₁	296	-	538	533	1367	16.38	1.20
	T ₂	348	-	740	728	1816	19.84	1.09
	T ₃	266	-	723	714	1703	18.22	1.07
Location: Tanore								
Wheat-T. Aus-T.Aman	T ₁	161	-	538	528	1227	10.43	0.85
	T ₂	174	-	728	713	1615	11.89	0.74
	T ₃	229	-	711	682	1622	12.22	0.75
Potato-Boro-T.Aman	T ₁	336	1176		516	2028	21.39	1.05
	T ₂	285	1096		729	2110	23.03	1.09
	T ₃	196	952		652	1800	21.94	1.22
Potato-T. Aus-T.Aman	T ₁	342		542	512	1396	18.78	1.35
	T ₂	281		737	721	1739	20.44	1.18
	T ₃	203		713	661	1577	19.25	1.22
Location: Kalai								
Potato-Boro-T.Aman	T ₁	307	1149		569	2025	20.76	1.03
	T ₂	276	1044		649	1969	21.87	1.11
	T ₃	186	958		628	1772	21.11	1.19
Mustard-Boro-T.Aman	T ₁	110	1146		564	1820	10.98	0.60
	T ₂	119	1041		652	1812	11.31	0.62
	T ₃	156	953		626	1735	11.55	0.67
Location: Joypurhat sadar								
Potato-Boro-T.Aman	T ₁	298	1139		558	1995	18.29	0.92
	T ₂	268	1027		648	1943	18.63	0.96
	T ₃	193	908		628	1729	17.74	1.03
Mustard-Boro-T.Aman	T ₁	107	1129		558	1794	10.79	0.60
	T ₂	113	1015		648	1776	11.19	0.63
	T ₃	152	902		628	1682	11.27	0.67

Total water use and water productivity of different cropping patterns under different management options are shown in Table 9b. Water used and water productivity was widely varied by cropping pattern and irrigation regimes. Total water use was found highest in Tomato-Boro-T.Aus cropping pattern followed by Potato-Boro-T.Aman and Mustard-Boro-T.Aman patterns and the lowest

was recorded by Potato-T.Aus-T.Aman closely followed by Wheat-T.Aus-T.Aman and Maize-T.Aus-T.Aman cropping patterns. Though all were three- crop based patterns, TWU by the previous patterns were higher than latter patterns due to inclusion of more water intensive boro rice. Even tomato consumed the more water than other rabi crops. So, the highest water consumed pattern was Tomato-Boro-T.Aus and the TWU by this pattern varied from 1906 mm to 2052 mm with minimum in treatment T₃ and maximum in treatment T₂. In Potato-Boro-T.Aman pattern, TWU varied from 1730 mm for T₃ to 1993 mm for T₁ in Godagari. In other locations, it varied from 1729 mm in T₃ to as high as 2025 mm either in farmers practice T₁ or standard practice T₂. In Tanore, water used by T.Aman under farmers' practice treatment T₁ was much lower than T₂ as farmer applied less number of irrigation. The difference in TWU between these two management options arose from difference in water use by T.Aman. In Kalai and Joypurhat sadar, TWU by Potato-Boro-T.Aman patterns were higher than that by Mustard-Boro-T.Aman patterns. The difference in TWU between these two patterns arose from difference in water use by mustard and potato. On average, TWU was lower in non-rice rabi crops, except maize, than rice and vegetables crops.

Crop water productivity (WP) or water use efficiency (WUE) expressed in kg/m³ is an efficiency term, expressing the amount of marketable product (e.g. kilograms of grain) in relation to the amount of input needed to produce that output (cubic meters of water). Among the cropping patterns, Tomato-Boro-T.Aus had the highest WP ranged from 1.43 to 1.51 kg/m³ followed by Potato-T.Aus-T.Aman and Potato-Boro-T.Aman patterns in which WP ranged from 1.18 to 1.35 kg/m³ and 0.99 to 1.16 kg/m³, respectively, with maximum in water management practice where water saving technologies (drip, AWD, AFI) were adopted. Both the crops potato and tomato have the high yield potential and their inclusion in any pattern perceptibly will increase the TREY and WP as well. Over the locations, WP varied from 0.99 to 1.15 kg/m³ for Potato-Boro-T.Aman with minimum in T₁ and maximum in T₃ water management option. The pattern Mustard-Boro-T.Aman had the lowest WP ranging from 0.57 to 0.67 kg/m³ for Rajshahi and from 0.60 to 0.67 kg/m³ for Joypurhat. In this pattern too, WP was found highest under T₃ management option. In general, WP was found higher in water management options where water saving technology was included as a treatment.

3.4. Groundwater abstraction pattern

3.4.1. Abstraction due to irrigation, domestic and municipal water demand:

Groundwater abstraction due to irrigation, domestic and municipal requirement are presented in Figure 13, 14, 15 and 16. While future prediction of groundwater abstraction for irrigation, domestic and municipal use in study areas are presented in Figure 17. From figures, it is apparent that abstraction due to domestic uses increasing almost steadily over the years for all study areas. This is because of gradual increase of population and their demand for domestic uses. Whereas abstraction due to irrigation varied over the year with less abstraction in wet (rainfall) year and high in dry year. In dry year, water demand by crops was fully satisfied by groundwater pumping while rainfall partially satisfied the crop water demand in wet year. On average over the year, increasing trend of groundwater abstraction for irrigation was evident and so does the total water abstraction. It is apparent from Figure 17 that groundwater abstraction will continue to increase if the present rate of abstraction continues. As the increasing demand of water is triggering more in Rajshahi than in Joypurhat, so more groundwater need to be abstracted in future from Barind area of Rajshahi. Abstraction will be increasing by 33-35% in Joypurhat study areas while it will be increasing by 40-45% in Rajshahi in the next 20 years. So, appropriate measures should be taken to ensure judicious use of water in all sectors especially in agriculture to protect the groundwater resources from being further depleted.

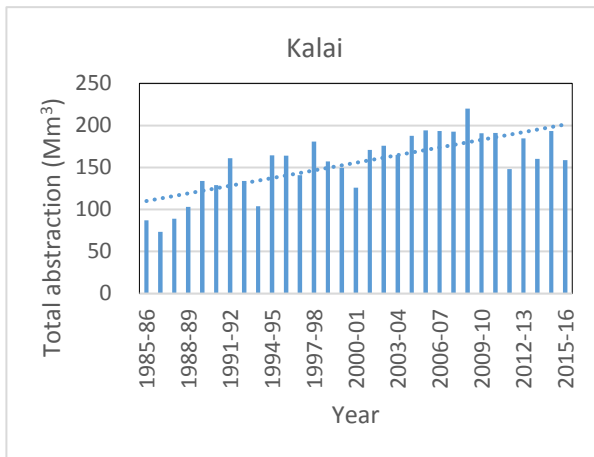
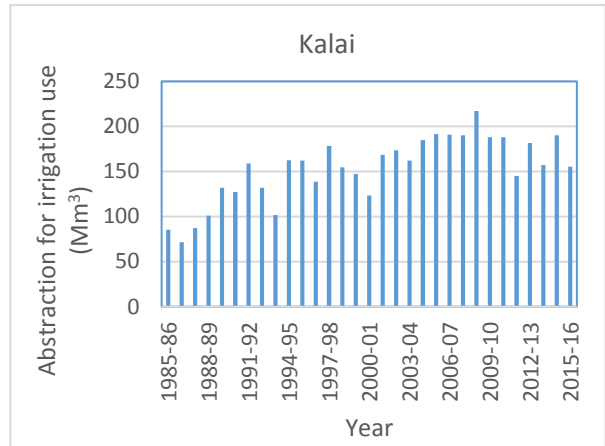
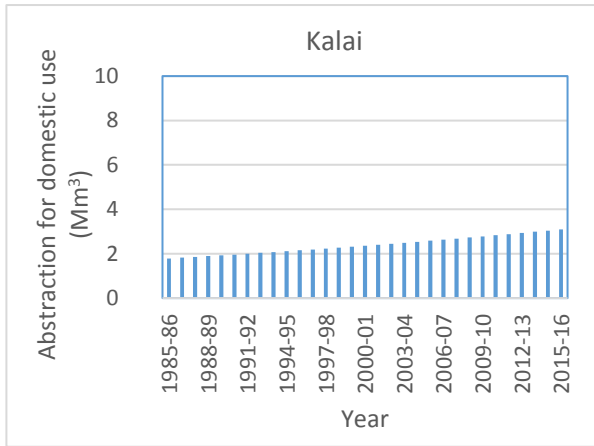
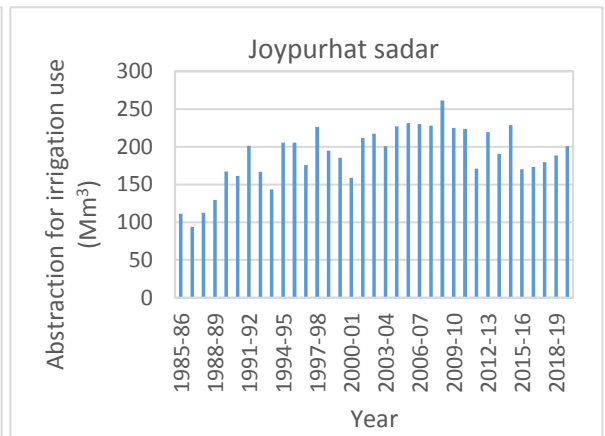
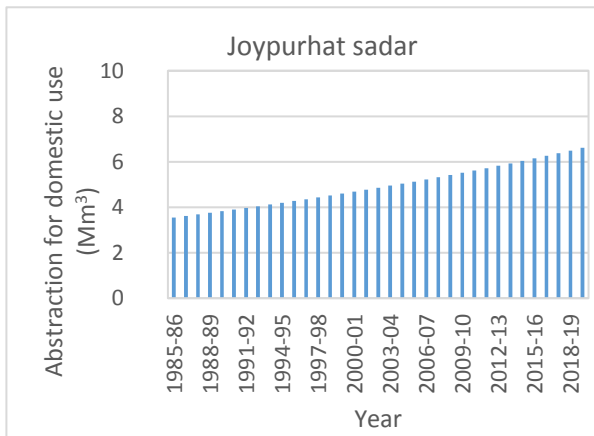


Figure 13. Groundwater abstraction pattern in Kalai upazila.



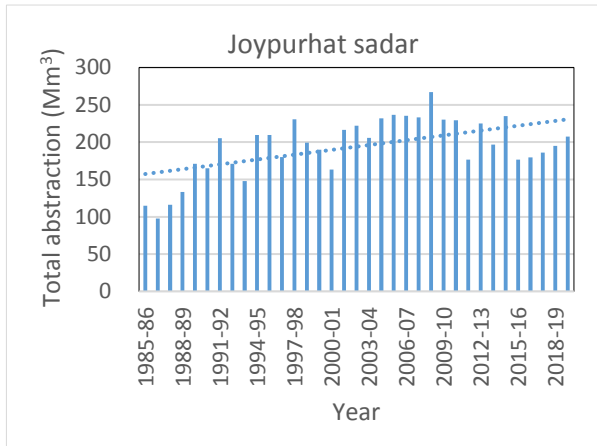


Figure 14. Groundwater abstraction pattern in Joypurhat sadar upazila.

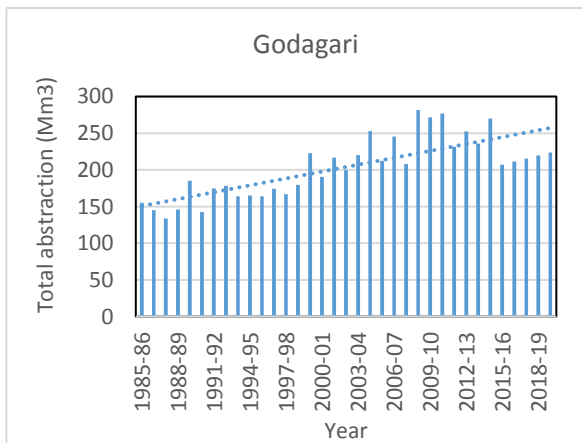
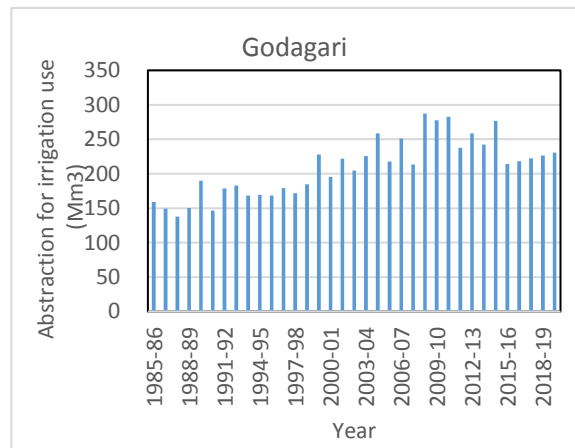
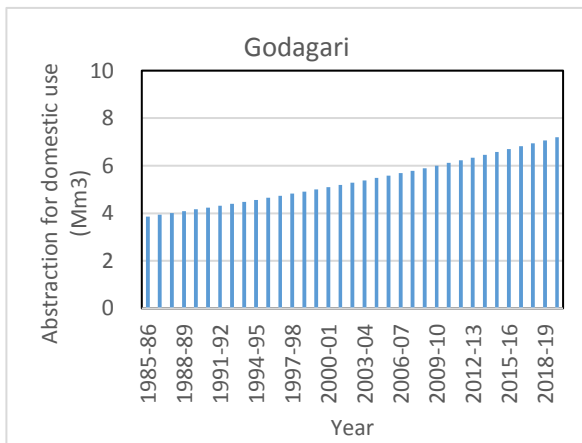


Figure 15. Groundwater abstraction pattern in Godagari upazila.

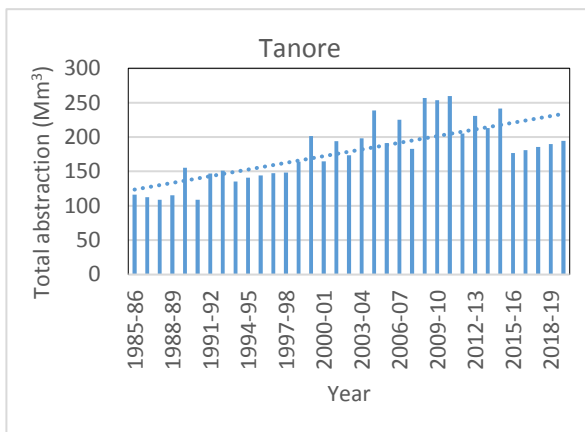
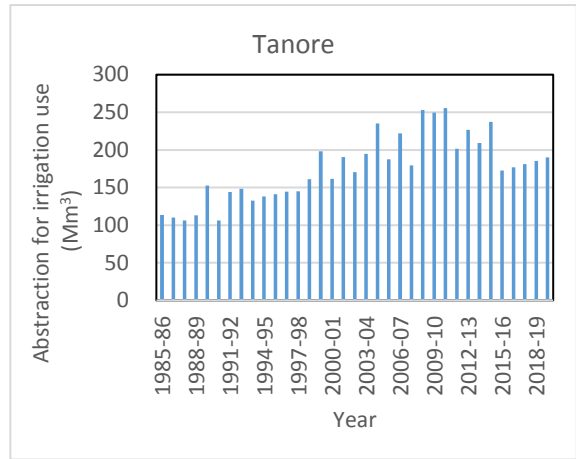
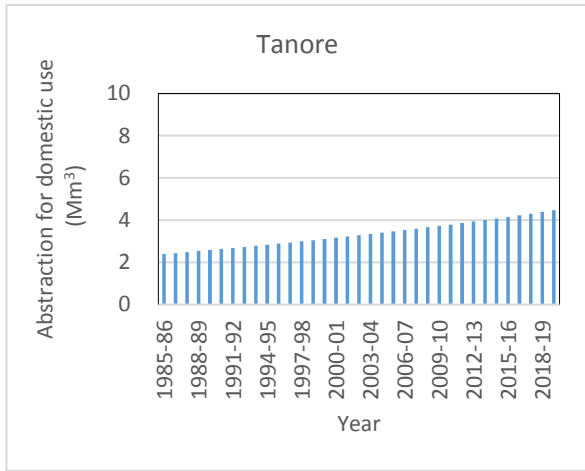


Figure 16. Groundwater abstraction pattern in Tanore upazila.

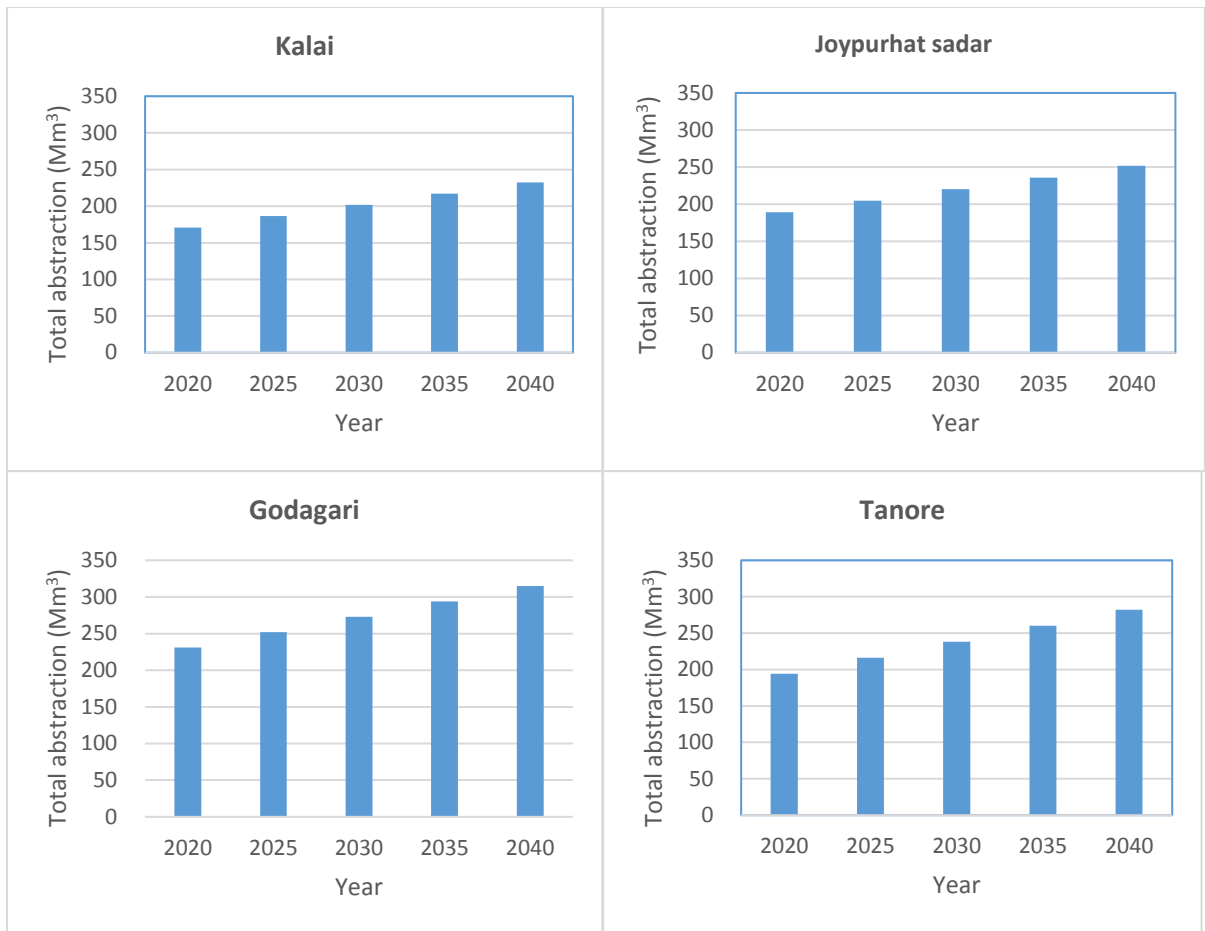


Figure 17. Predicted groundwater abstraction for irrigation, domestic and municipal use in study areas

3.5. Trends of groundwater levels fluctuation

Predicted response over the validation data's time span at the observation wells of Tanore, Godagari, Joypurhat sadar, and Kalai upazilas are illustrated in Figures 11, 12, 13, and 14, respectively.

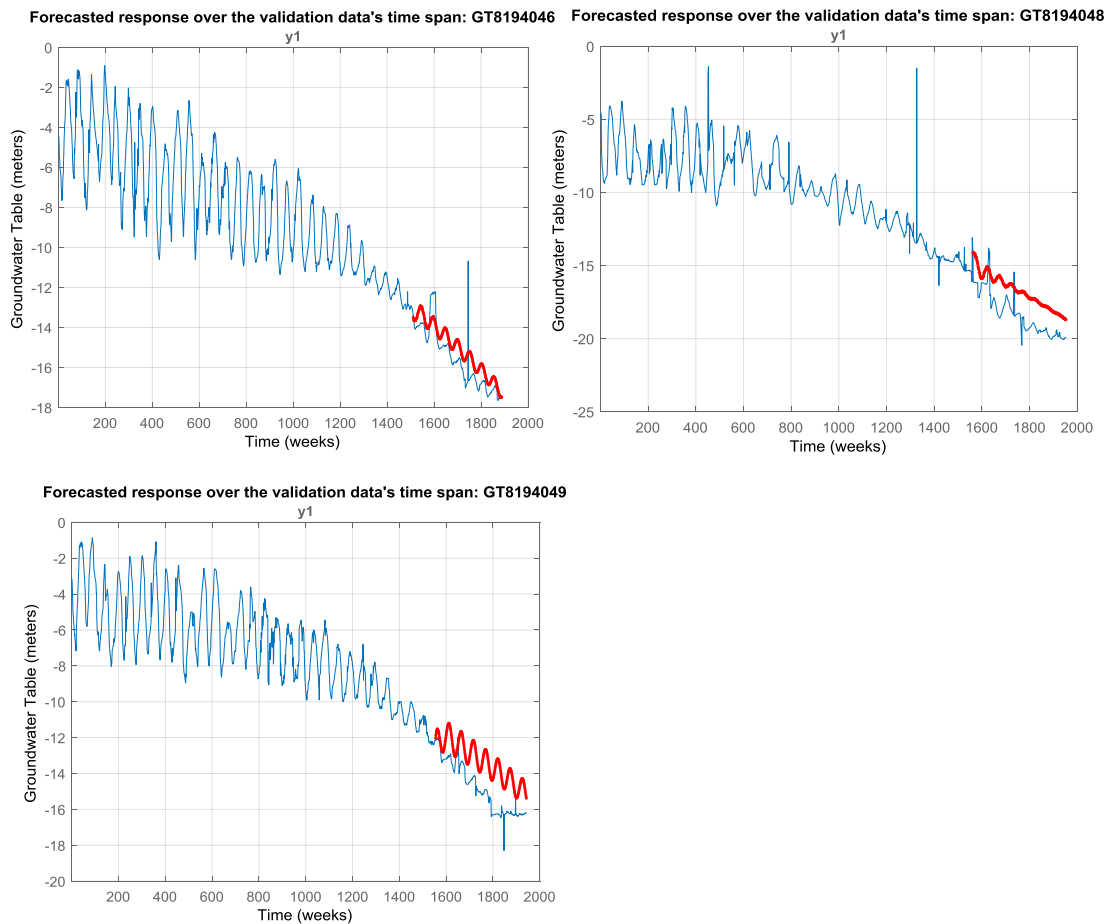


Figure 18. Predicted response over the validation data's time span at observation wells GT8194046, GT8194048, and GT8194049 for Tanore upazila.

The plot shows that the model response overlaps the measured value for the validation data. The combined prediction and forecasting results indicate that the model represents the measured water level data. Figures 18, 19, 20, and 21 show that there are relatively good agreements between the simulated and observed groundwater levels for all the developed models at the selected observation wells in the four upazilas. Thus, it is practically possible to develop groundwater forecasting models using this data-driven approach. However, there are discrepancies in matching some of the peak events, where the events may be under predicted or over predicted values.

The forecasting results also show that over large horizons the model variance is large and for practical purposes future forecasts should be limited to short horizons. For the water level prediction model, a horizon of 22 years is appropriate given the previous data available is only for 38 years.

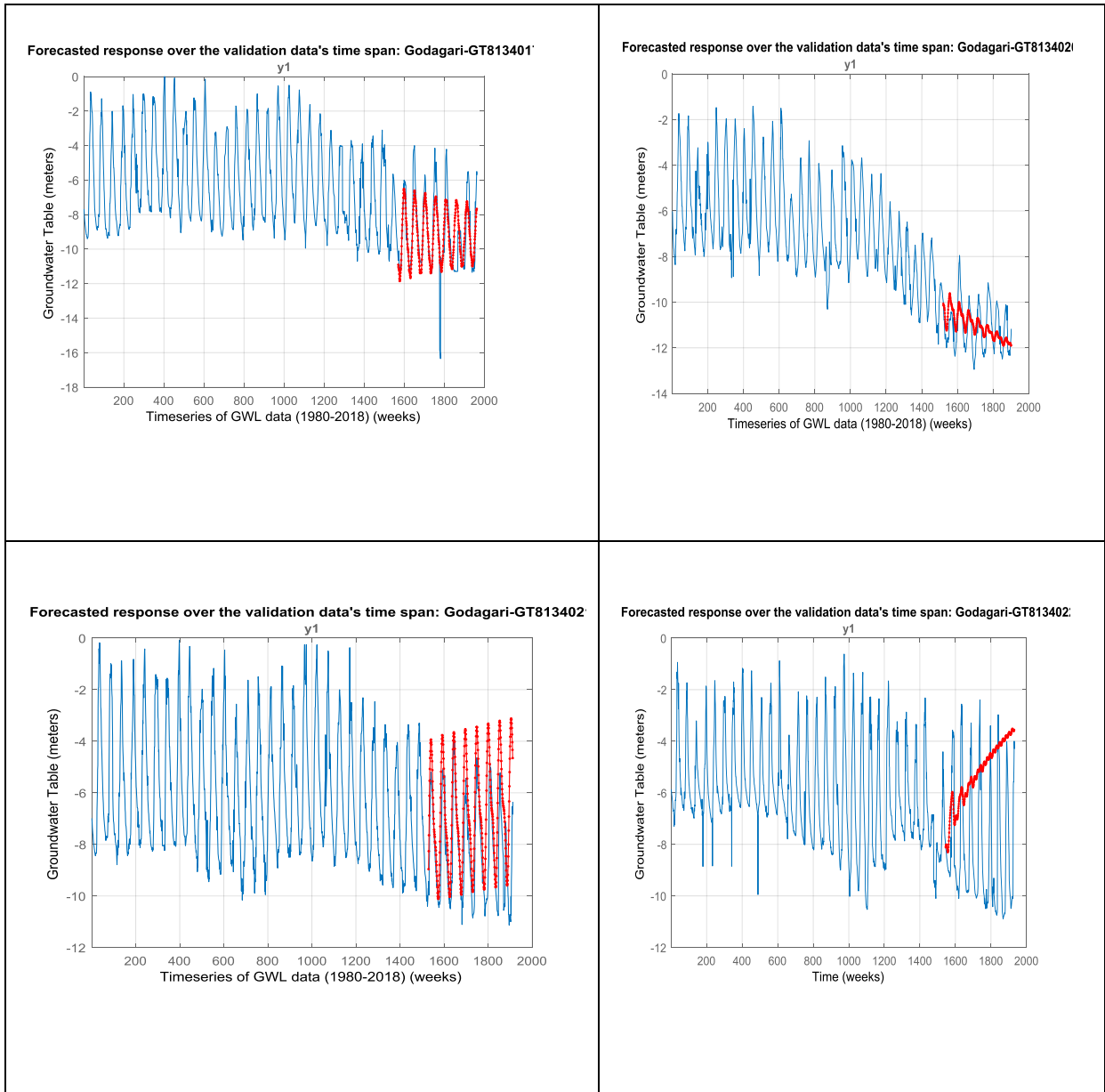


Figure 19. Predicted response over the validation data's time span at observation wells GT8134017, GT8134020, GT8134021, GT8134022 for Godagari upazila.

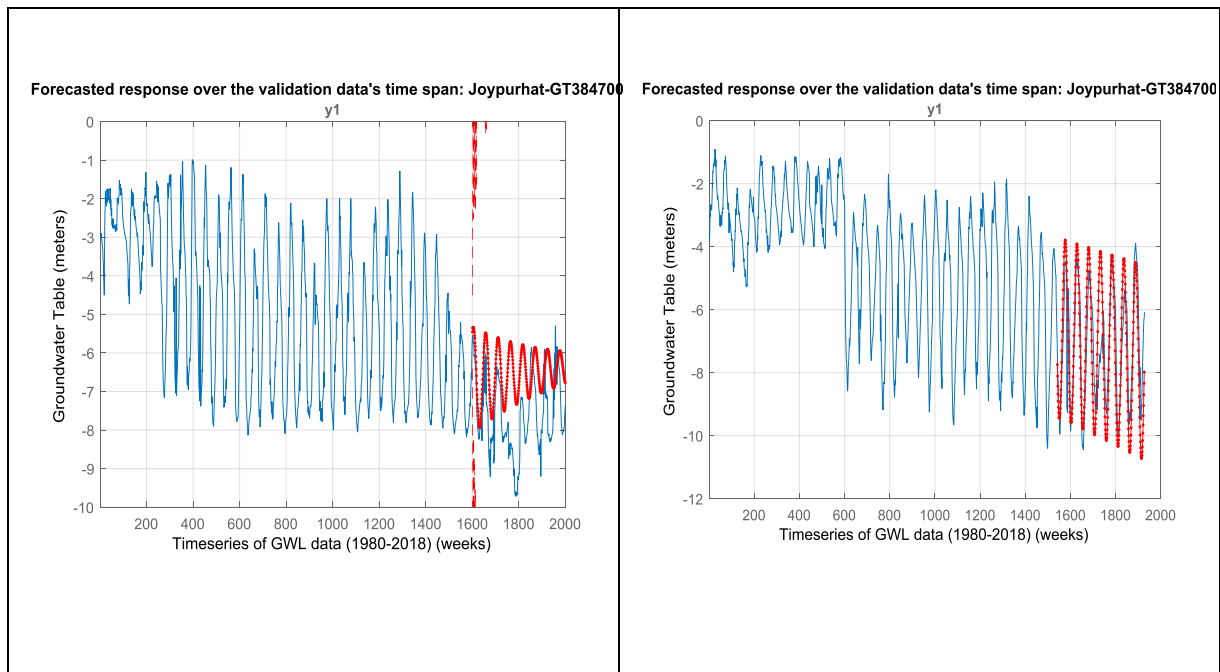


Figure 20. Predicted response over the validation data's time span at observation wells GT3847001 and GT3847003 for Joypurhat sadar upazila.

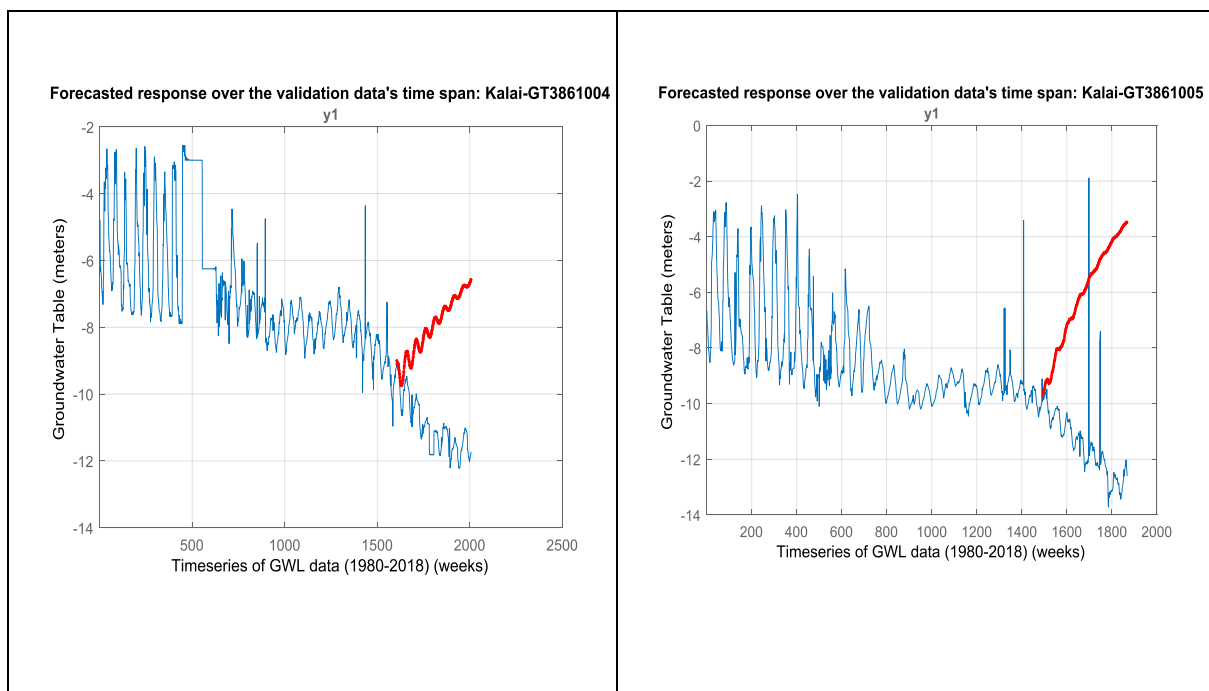


Figure 21. Predicted response over the validation data's time span at observation wells GT3861004 and GT3861005 for Kalai upazila.

The properly trained and validated models were then used to forecast the response 1105 steps into future for the time span of 22 years (From 25/09/2018 to 24/09/2040). The forecasted results are presented in Figures 22, 23, 24, and 25, respectively for Tanore, Godagari, Joypurhat sadar, and Kalai upazilas. In these figures, the green curve shows the measured identification data whereas the blue curve shows the measured validation data that spans over 1-1900 weeks. The red curve is the forecasted response for 1105 weeks beyond the measured data's time range.

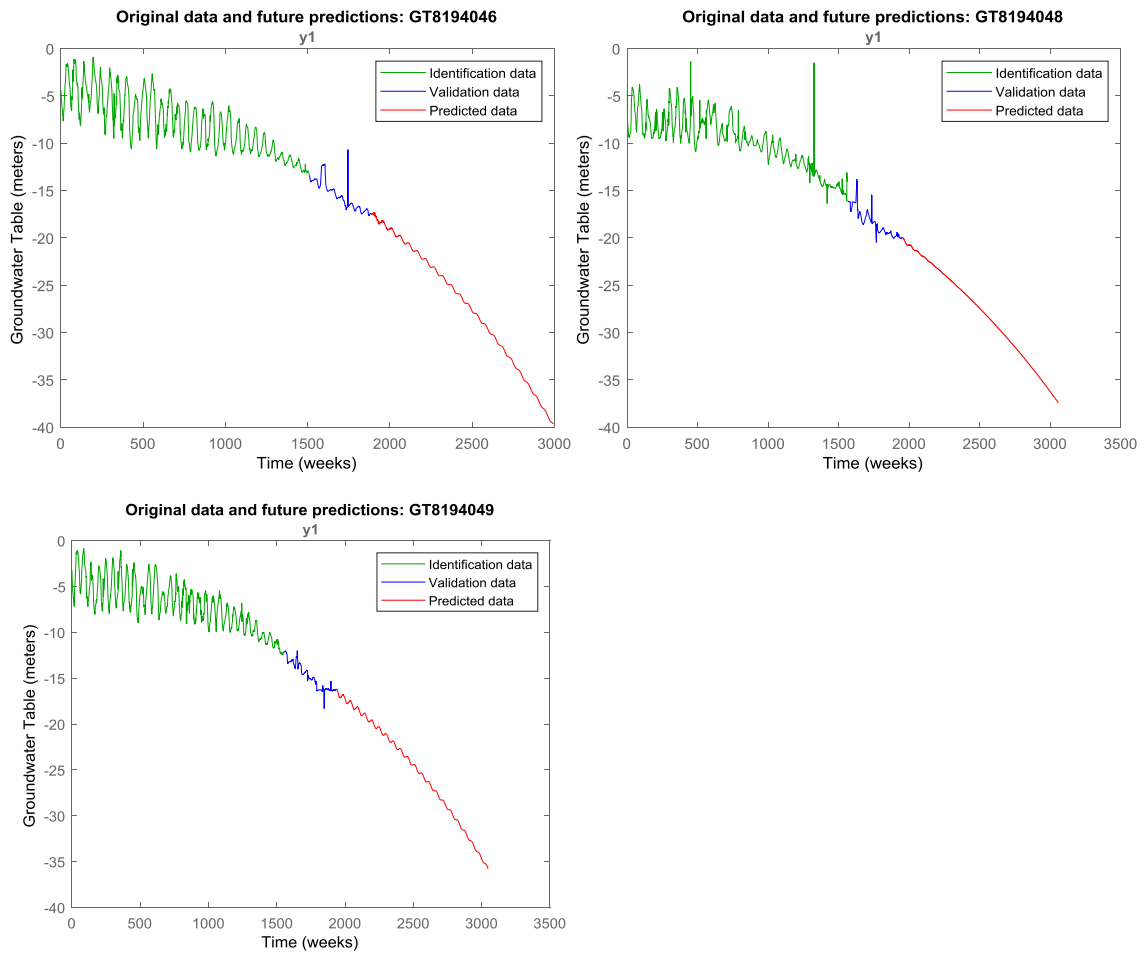


Figure 22. Original and future predicted data at observation wells GT8194046, GT8194048, and GT8194049 for Tanore upazila.

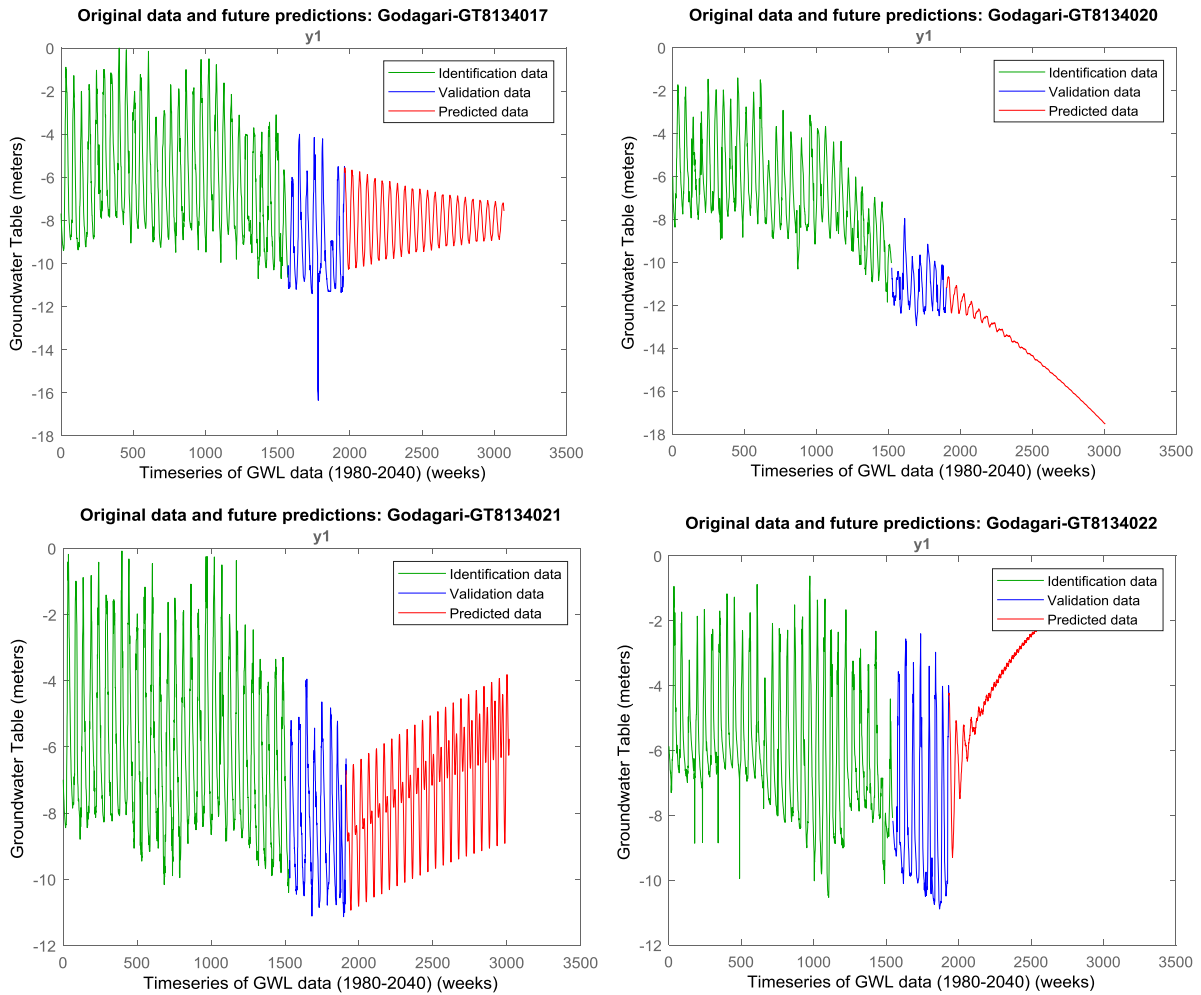


Figure 23. Original and future predicted data at observation wells GT8134017, GT8134020, GT8134021, GT8134022 for Godagari upazila.

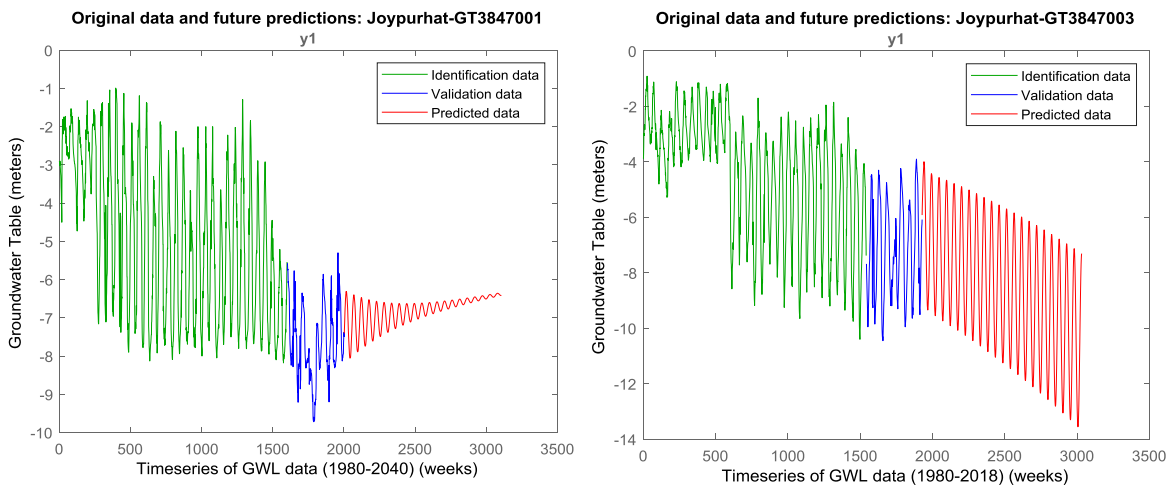


Figure 24. Original and future predicted data at observation wells GT3847001 and GT3847003 for Joypurhat sadar upazila.

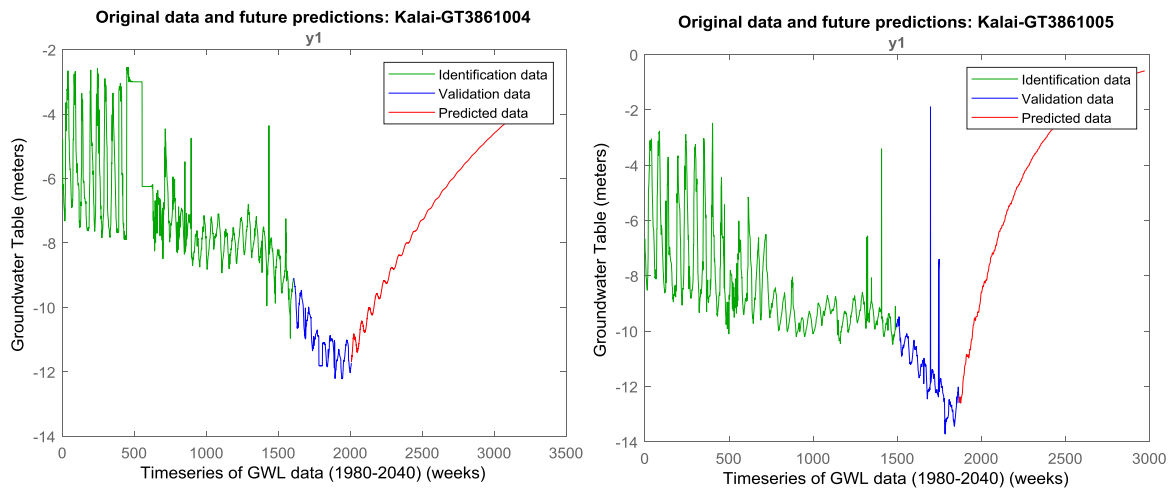


Figure 25. Original and future predicted data at observation wells GT3861004 and GT3861005 for Kalai upazila.

Figures 26, 27, 28, and 29 illustrate groundwater level at the selected observation wells on 24/09/2018 and the projected (model predictions) groundwater table on 24/09/2040. It is perceived from Figure 19 that groundwater level declination almost doubled at all the three observation wells at Tanore upazila for the next 22 years if the present rate of abstraction continues. In Godagari, Joypurhat sadar, and Kalai upazila, the future trends of groundwater level fluctuations were quite interesting as obtained by the modelling results. While the groundwater level declination was found obvious in few observation wells, the groundwater levels showed increasing trends in some observation wells. The increasing trend in groundwater levels in some observation wells indicated the recent initiatives adopted by the authority in imposing the constraints of the maximum withdrawal limits. It is concluded that the proposed modeling framework can serve as an alternative approach to simulating groundwater level change and water availability, especially in regions where subsurface properties are unknown.

Of note, the forecasting results are entirely based on the historical groundwater level data based on the previous abstraction and recharge rates. As the increasing demand of water is triggering more and more groundwater abstraction from the aquifer and the recharge rate is decreasing due to scanty rainfall in that area, the groundwater level declination might be even more dangerous than the projected ones if corrective measures are not taken. Moreover, the sticky clay subsurface of the study area slows down the natural recharge to the aquifer. Therefore, groundwater abstraction should be judiciously optimized in the study area to protect the already vulnerable groundwater resources.

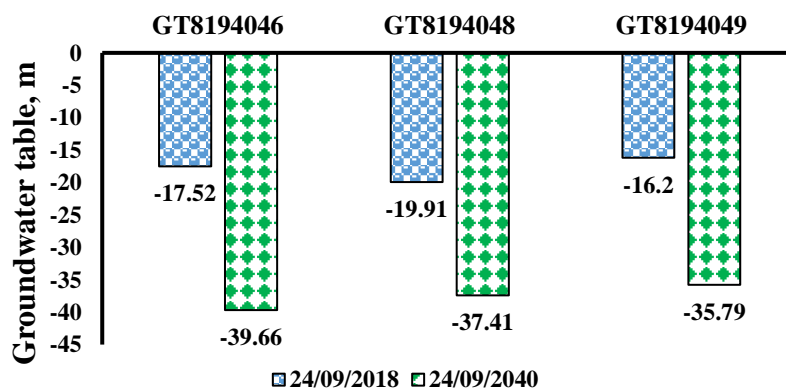


Figure 26. Present and future scenarios of groundwater table at three observation wells for Tanore upazila.

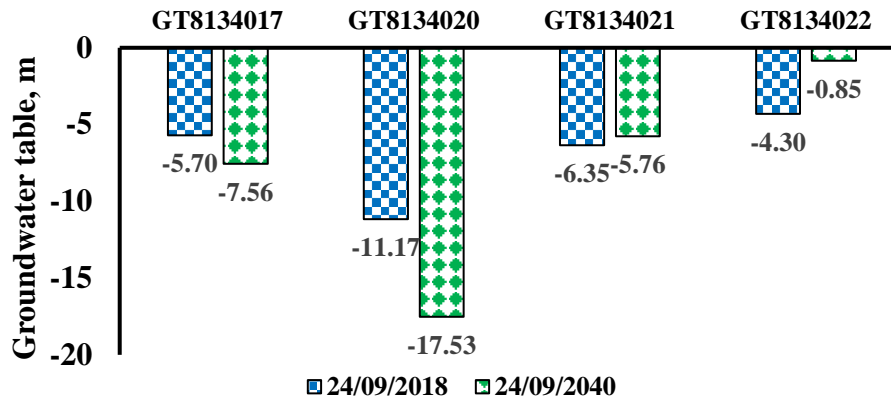


Figure 27. Present and future scenarios of groundwater table at three observation wells for Godagari upazila.

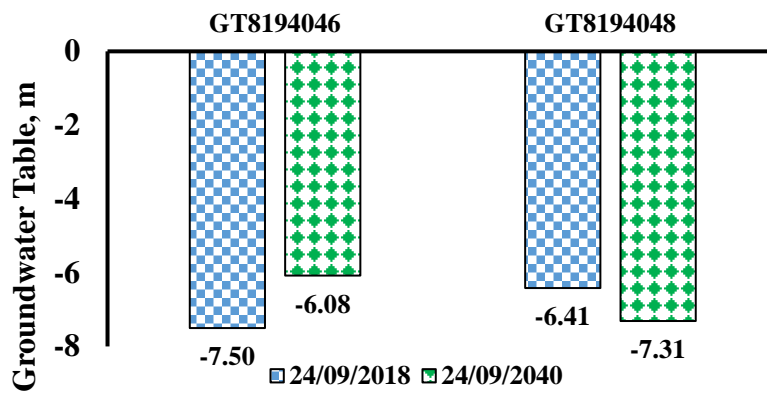


Figure 28. Present and future scenarios of groundwater table at three observation wells for Joypurhat Sadar upazila.

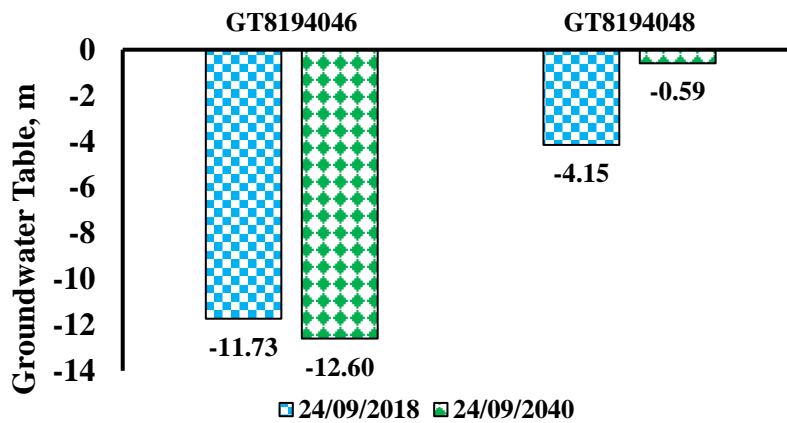


Figure 29. Present and future scenarios of groundwater table at three observation wells for Kalai upazila.

3.5.1. Conclusions:

The present study investigated the accuracy of the discrete Space-State modelling approach for forecasting weekly groundwater levels. The core idea was to develop a dynamic prediction model using the prediction focused approach to accurately forecast future groundwater levels at specified observation wells. The models were developed using the historical groundwater level data of the study area. The combined training, validation and forecasting results indicated that the model represented the measured water level data quite accurately. Therefore, the modelling approach presented in this report can be used as an alternative to the complex numerical simulation models in data scarce situations. A univariate time series of groundwater level has been performed and presented in this report. Future studies may aim to consider a multivariate time series analysis that considers the effects of other hydrogeological parameters for groundwater level predictions.

3.6. Trend in GWL fluctuation (MAKESENS Model)

Table 10. Rate of change of maximum water table depth (myear⁻¹) and prediction of maximum water table depth (m) at Tanore of Rajshahi

Observation well	Rate of change of maximum water table (myear ⁻¹)	Maximum WT change from 1980 to 2018	Maximum WT in 2018	Prediction of maximum water table (WT) depth in different year			
				2025	2030	2035	2040
GT8194046	0.300 ***	11.400	17.250	19.350	20.850	22.350	23.85
GT8194048	0.390 ***	14.820	20.830	22.930	24.880	26.830	28.78
GT8194049	0.298 ***	11.324	16.544	18.644	20.134	21.624	23.114

- $0.3 \times 38 = 11.4$, $17.25 + (7 \times 0.3) = 19.35$, $17.25 + (12 \times 0.3) = 20.85$ and so on...
- Linear interpolation based on the rate of change of maximum water table
- Real systems are not that much straightforward
- Cannot act as an alternative to Numerical simulation in data scarce situations

3.7. Optimization of groundwater abstraction

A numerical simulation model, MODFLOW was employed to determine the groundwater heads as well as to optimize groundwater abstraction at different observation wells in study areas under three groundwater recharge scenarios. The model was calibrated using the available hydrogeological data of the study areas. The modelling works of the four upazilas in Rajshahi and Joypurhat districts are presented in this section of the report. The study areas of Tanore, Godagari, Joypurhat sadar, and kalai upazila have the aerial extents of 297.2463 km², 446.53 km², 244.03 km², and 156.99 km², respectively. The aerial map of the study areas is presented in Fig 30.

In order to optimize groundwater abstraction, the following three scenarios were considered:

- Scenario 1: abstraction < recharge; i.e. < 90% (more sustainable)
- Scenario 2: abstraction = recharge; i.e. = 100% (less sustainable)

Scenario 3: abstraction > recharge; i.e. > 110% (business-as-usual)

The aquifer processes of study areas were simulated using a calibrated 3D finite difference based numerical simulation code MODFLOW. The modelling and the scenario development were performed based on the very limited quantity of available hydrogeological data.

Actual and simulated groundwater levels at the observation wells during the calibration process are presented in Table 11.

Table 11. Actual and simulated groundwater levels at the observation wells during the calibration process

Observation wells	Actual, m	Simulated, m	Residual, m
<u>Tanore upazila</u>			
GT8194046	17.52	16.388	1.13155
GT8194048	19.191	18.133	1.07832
GT8194049	20.20	22.215	-2.01514
<u>Godagari upazila</u>			
GT8134017	8.70	9.39	-0.68889
GT8134020	11.17	11.05	0.12381
GT8134021	6.35	6.17	0.18004
GT8134022	6.90	6.11	0.78809
<u>Joypurhat sadar upazila</u>			
GT3847001	11.73	11.052	0.67769
GT3847003	4.149	3.9779	0.17103
<u>Kalai upazila</u>			
GT3861004	7.50	7.137	0.36222
GT3861005	6.41	6.445	-0.03516

The calibration targets at different observation wells for the study areas are presented in Fig. 30. The components of a calibration target are illustrated in Fig. 31. The center of the target corresponds to the observed value. The top of the target corresponds to the observed value plus the interval and the bottom corresponds to the observed value minus the interval. The colored bar represents the error. If the bar lies entirely within the target, the color bar is drawn in green. If the bar is outside the target but the error is less than 200%, the bar is drawn in yellow. If the error is greater than 200%, the bar is drawn in red.

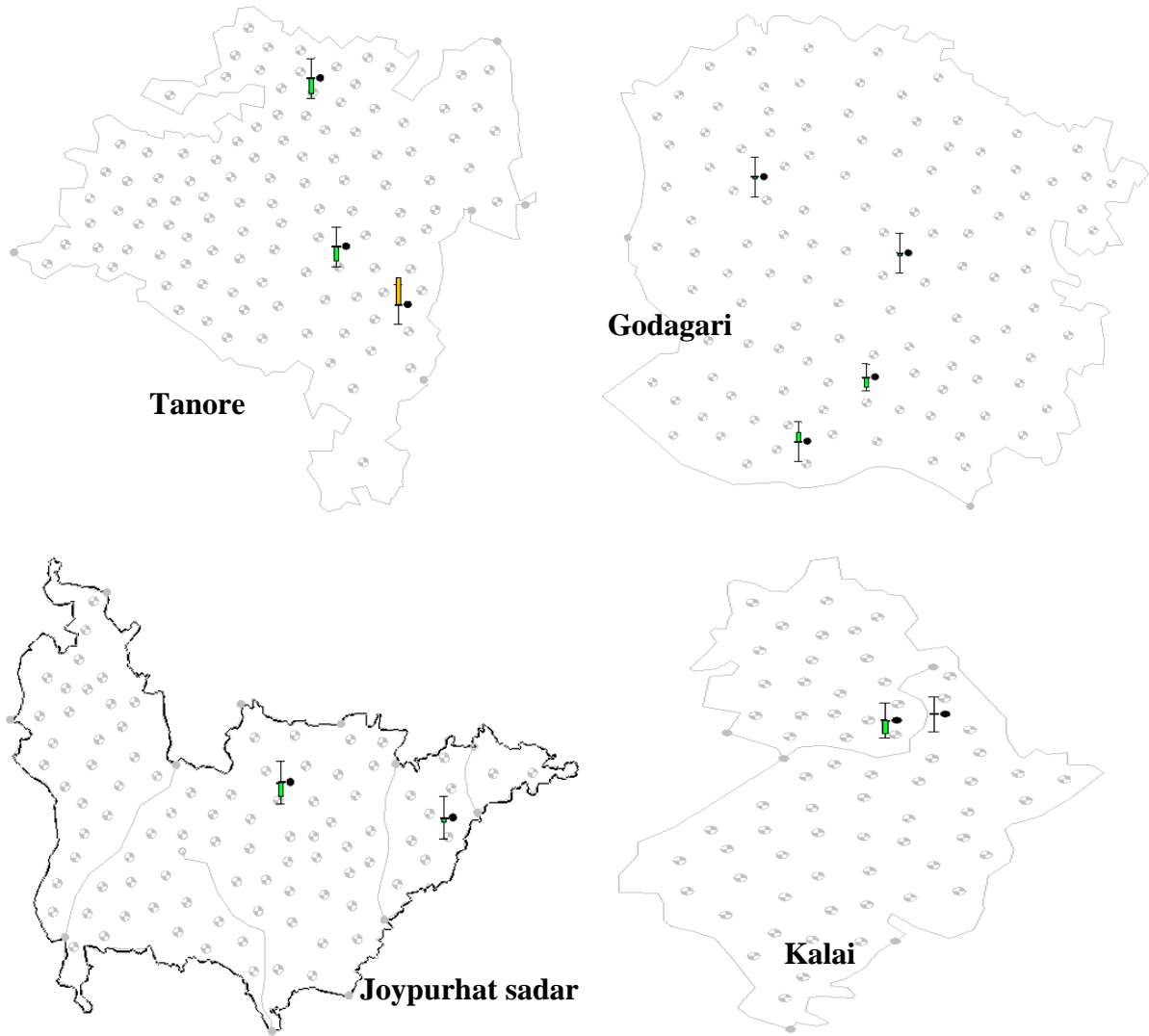


Figure. 30 Calibration target error bars at three observation wells.

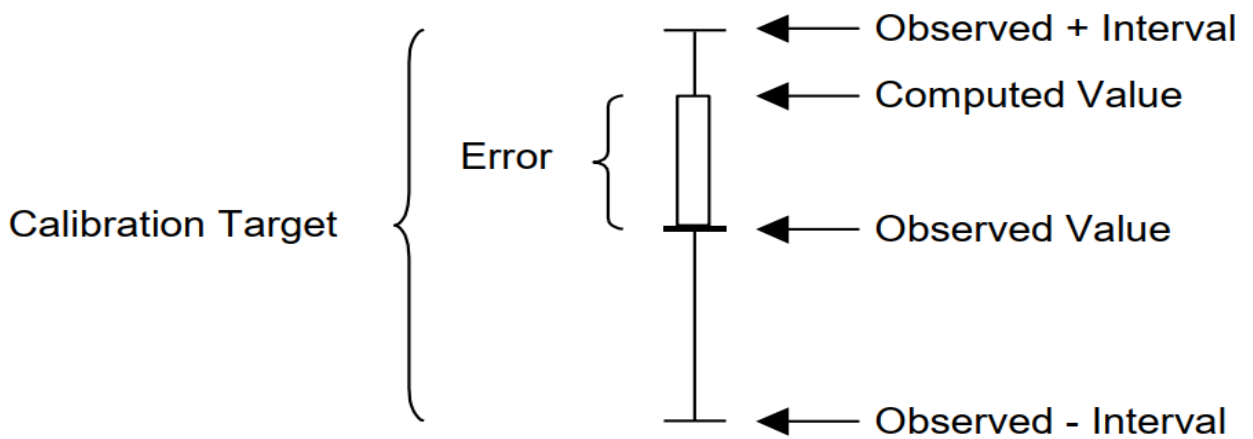


Figure. 31 Components of the calibration target.

Contour plot of the simulated groundwater heads for the calibrated model is presented in Fig. 32. While contour plots of the groundwater heads with respect to the 10% decreased and increased recharge are shown in Fig. 33 and 34, respectively.

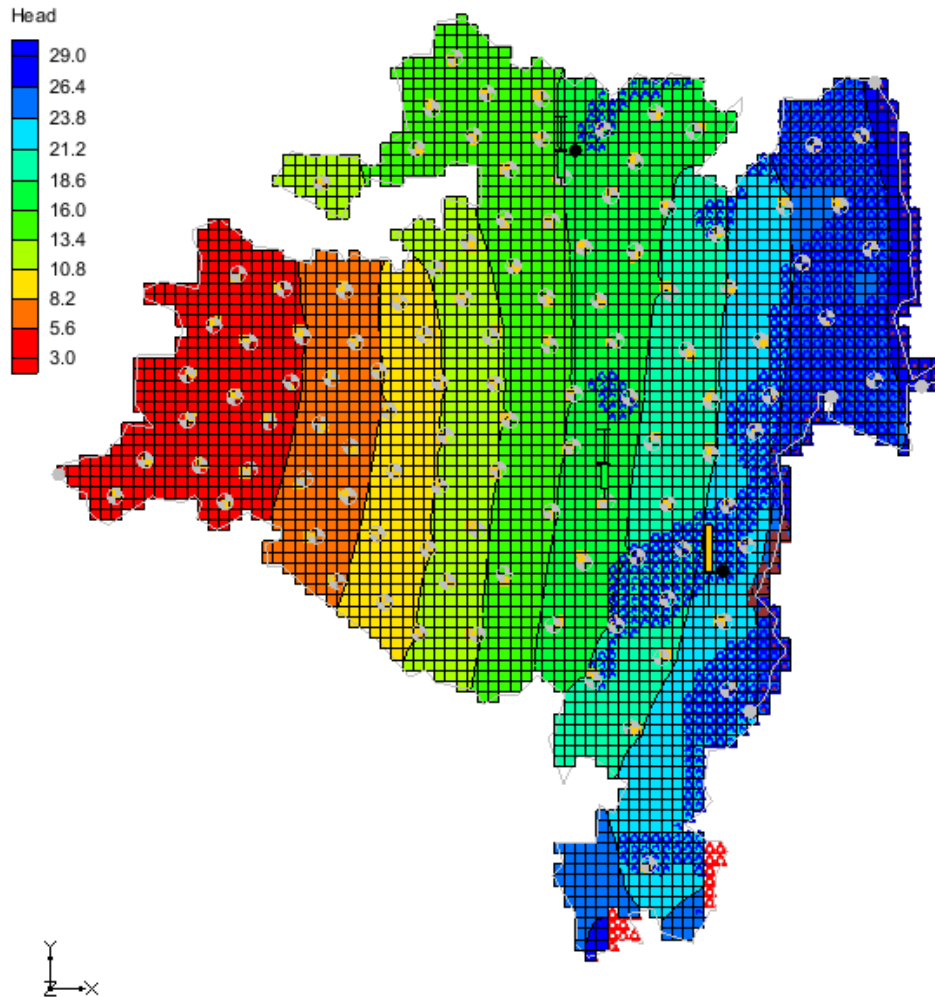


Figure. 32 Contour plot of the groundwater heads in the calibrated model.

Computed groundwater levels for the two scenarios at the observation wells are presented in Table 12.

Table 12. Computed groundwater levels for 90% and 110% of the actual recharge

Observation wells	Actual, m	Computed, m	
		90% of actual recharge	110% of actual recharge
<i>Tanore upazila</i>			
GT8194046	17.52	7.970	20.707
GT8194048	19.191	11.150	21.745
GT8194049	20.20	18.106	24.413
<i>Godagari upazila</i>			
GT8134017	8.70	6.577	12.155
GT8134020	11.17	5.670	16.325
GT8134021	6.35	-0.475	12.659
GT8134022	6.90	1.447	10.682
<i>Joypurhat sadar upazila</i>			
GT3847001	11.73	9.406	12.688
GT3847003	4.149	3.335	4.6199
<i>Kalai upazila</i>			
GT3861004	7.50	6.306	7.592
GT3861005	6.41	5.533	6.943

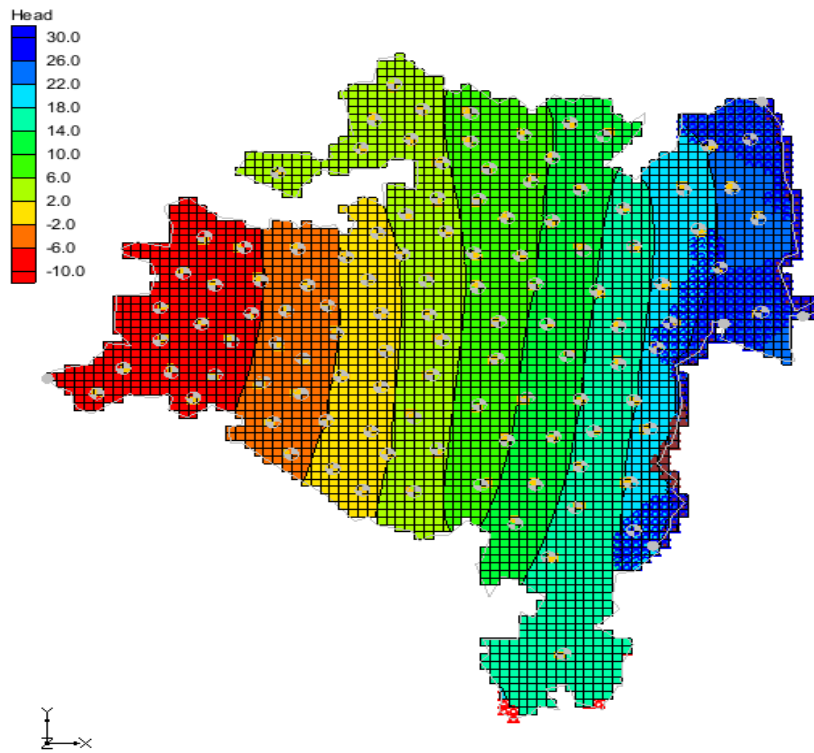


Figure. 33. Contour plot of the groundwater heads with respect to the decreased recharge (90% of the actual).

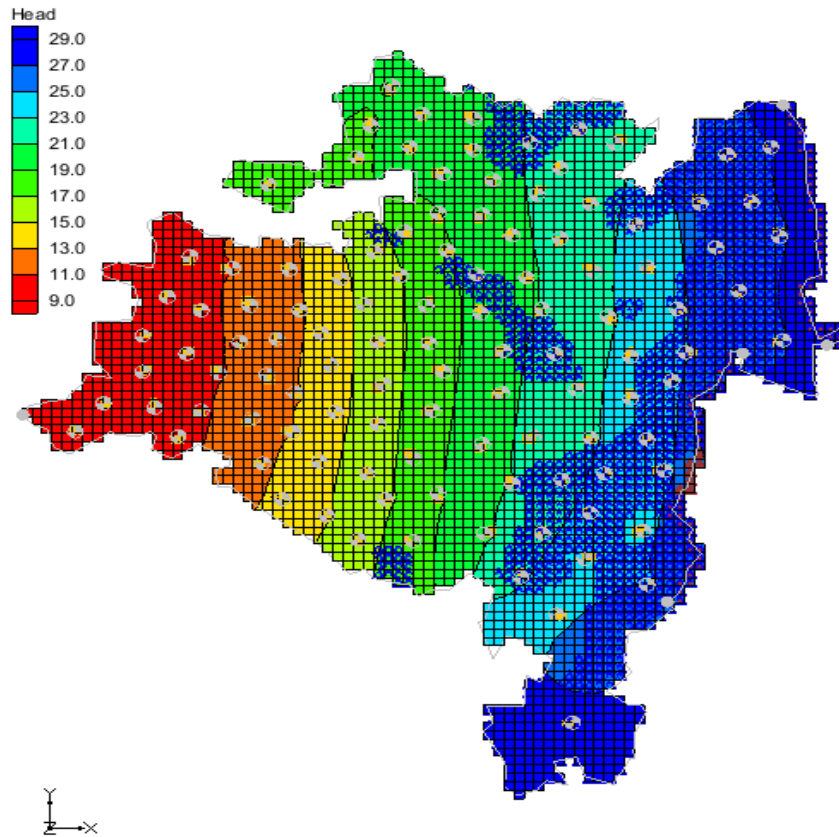


Figure. 34. Contour plot of the groundwater heads with respect to the increased recharge (110% of the actual).

The results revealed that the computed groundwater heads at the observation wells varied noticeably as a result of the changes in the recharge scenarios. In the business-as-usual case, the MODFLOW computed heads at the three observation wells GT 8194046, GT8194048, and GT8194049 at Tanore upazila on 24 September 2018 (based on the available groundwater head data obtained from the BWDB) were 16.388m, 18.133m, and 22.215m, respectively. When the recharge was reduced to 90%, the computed heads dropped significantly, and the values were 7.970m, 11.150m, and 18.106m, respectively at the three observation wells. On the other hand, if the recharge would be increased to 110%, the MODFLOW computed heads at the observations were found as 20.707m, 21.745m, and 24.413m, respectively which indicates a substantial increase in the quantity of head development. At Godagari upazila, the observed and computed heads were monitored at four observation wells (GT 8134017, GT 8134020, GT 8134021, and GT 8134022). In this upazila, the MODFLOW computed heads for the business-as-usual case were 9.389m, 11.046m, 6.170m, and 6.112m at the observation wells GT 8134017, GT 8134020, GT 8134021, and GT 8134022, respectively. When the recharge was reduced to 90%, the computed heads dropped, and the values were 6.577m, 5.670m, - 0.475m, and 1.447m, respectively at the four observation wells. On the other hand, if the recharge would be increased to 110%, the MODFLOW computed heads at the observations were found as 12.155m, 16.325m, 12.660m, and 10.682m, respectively which indicates a substantial increase in the quantity of head development. In Joypurhat sadar upazila, the observed and computed heads were monitored at two observation wells (GT 3847001 and GT 3847003). In this upazila, the MODFLOW computed heads for the business-as-usual case were 11.05231m and 3.980m at the observation wells GT 3847001 and GT 3847003, respectively. When the recharge was reduced to 90%, the computed heads dropped, and the values were 9.406m, and 3.335m, respectively at the two observation wells. On the other hand, if the recharge would be increased to 110%, the MODFLOW computed heads at the observations were found as 12.688m, and 4.620m, respectively. In Kalai upazila, the observed and computed heads were monitored at two observation wells (GT 3847001 and GT 3847003). In this upazila, the MODFLOW computed heads for the business-as-usual case were 11.05231m and 3.980m at the observation wells GT 3861004 and GT 3861005, respectively. When the recharge was reduced to 90%, the computed

heads dropped, and the values were 6.306m, and 5.533m, respectively at the two observation wells. On the other hand, if the recharge would be increased to 110%, the MODFLOW computed heads at the observations were found as 7.592m, and 6.943m, respectively. The increased and decreased recharge scenarios were computed using the existing groundwater pumping values in the year 2018. Therefore, it is concluded that groundwater recharge has a significant effect on the head development in the groundwater aquifers of the Tanore and Godagari upazila, Rajshahi and Joypurhat sadar and Kalai upazila, Joypurhat.

3.7.1. Conclusions:

The optimal groundwater abstraction strategy has been considered an effective measure of maintaining groundwater levels in aquifers for the safe and beneficial abstraction. In this research, a finite difference based 3-D flow based numerical code, MODFLOW, was utilized to simulate the groundwater heads with respect to different recharge scenarios in the Tanore and Godagari upazila of Rajshahi district and Joypurhat sadar and Kalai upazila of Joypurhat district in the northern Bangladesh. Input data for the selected study areas were collected from different sources. Scarcity and reliability of available data is a challenging issue in implementing regional scale saltwater intrusion models in this location. Therefore, the best possible subjective judgment was used in choosing the data for simulating the aquifer processes. The limited assessment results demonstrate that, groundwater recharge has an influential effect on the groundwater level fluctuations, and using a carefully planned groundwater abstraction strategy, it is possible to modify the groundwater storage that will help in preserving the precious groundwater storage in the study area.

3.8. Suitability of groundwater for irrigation

The chemical compositions of the collected groundwater samples in pre-irrigation and post-irrigation season are presented in Table 13a and 13b, respectively. The pH value was found slightly higher in post-irrigation season than pre-irrigation season. The pH values of groundwater samples in the study area ranged from 7.11 to 7.36, and 7.22–7.54 for pre- and post-season irrigation periods respectively. The high pH value indicated the slight alkalinity of water, possibly due to the presence of appreciable amounts of sodium, calcium, magnesium, and carbonate ions (Rao *et al.*, 1982). All the samples conform to FAO standard of 6.5 – 8.4 for irrigation use. The range of electrical conductivity (EC) was 0.36 – 0.58 dS/m in pre-irrigation season and 0.48 – 0.66 dS/m in post-irrigation season. Over the seasons, EC value of groundwater of the study area ranged from 0.36 to 0.66 dS/m with an average value range 0.47 – 0.57 dS/m, which according to Wilcox (1955) falls within the irrigation water quality classification stand ‘excellent to good’. In terms of the ‘degree of restriction on use’, EC value of < 700 $\mu\text{S}/\text{cm}$ refers the water to ‘none’; 700-3000 $\mu\text{S}/\text{cm}$ ‘slight to moderate’ and 3000 $\mu\text{S}/\text{cm}$ ‘severe’ (UCCC, 1974). It is easily presumable from the EC values in Table 2a and 2b, all water samples of the study area are suitable for irrigation purpose as it falls under category ‘none’ (UCCC, 1974).

The concentrations of Na^+ , Ca^{++} , Mg^{++} , and K^+ in water samples varied in the ranges of 10.42-17.81, 18.34-21.27, 2.10-3.20 and 2.02-2.62 mg/L in pre-irrigation season and in the ranges of 11.02-18.86, 18.34-21.27, 3.46-5.52 and 2.22-2.74 mg/L respectively in post-irrigation season. Recommended maximum concentrations of Na^+ , Ca^{++} , Mg^{++} and K^+ for long-term irrigation use on all soils are 200, 200, 100 and 10 mg/L, respectively (Ayers and Westcot, 1985). Therefore, all the samples in the study area can be used safely for long-term irrigation.

One of the toxic major ions in irrigation water is chloride (Bouderbala 2015). Chlorides are not absorbed or held back by soils, therefore, it moves readily with the soil-water, and is taken up by the crops, moves in the transpiration stream and accumulates in the leaves. If the chloride concentration in the leaves exceeds the tolerance of the crop, injury symptoms develop, such as leaf burn or drying of the leaf tissue, yellowing of leaf and spotting on the leaf. High content of Cl^- in water also limits its use in sprinkler irrigation. In the present study, chloride concentration varied from 1.32-1.67 in pre-irrigation season and 1.58-1.81 mg/L in post-irrigation irrigation, respectively which fall under excellent category according Ayre and Westcot (1985). The upper limit of NO_3^- , SO_4^{--} and HCO_3^- was 0.84, 9.94 and 222.06 mg/L respectively which is far below their corresponding recommended levels of 50, 250 and 400 mg/L. So, these parameters might not be problematic for irrigation use.

Table 13a. Mean quality parameters of groundwater at different study sites during November - December 2018

Location	Parameters, mg/L except pH											
	Source	pH	EC (dS/m)	PO ₄ ⁻	K	NO ₃ ⁻	Cl ⁻	Na	Ca	Mg	HCO ₃ ⁻	SO ₄ ⁻
Godagari	DTW (n=6)	7.24	0.42	0.72	2.20	0.64	1.57	14.14	31.27	2.12	191.23	7.48
	STW (n=4)	7.33	0.46	0.80	2.34	0.68	1.38	16.12	34.78	3.20	202.54	8.12
Tanore	DTW (n=5)	7.11	0.36	0.63	2.14	0.76	1.47	15.06	36.42	2.66	205.39	7.66
	STW (n=3)	7.22	0.48	0.82	2.16	0.72	1.49	17.67	19.36	2.72	229.56	7.92
Kalai	DTW (n=8)	7.15	0.54	0.54	2.54	0.68	1.63	11.32	37.07	2.54	200.56	8.07
	STW (n=2)	7.23	0.58	0.62	2.70	0.66	1.67	13.46	28.68	2.58	205.39	8.84
Joypurhat sadar	DTW (n=6)	7.17	0.49	0.65	2.12	0.74	1.42	9.44	39.34	2.10	198.66	9.28
	STW (n=2)	7.36	0.48	0.74	2.32	0.82	1.32	10.36	32.64	2.88	222.38	9.74
Range		7.11 - 7.36	0.36 - 0.58	0.54 - 0.82	2.12 - 2.54	0.64 - 0.82	1.32 - 1.67	9.44 - 17.67	18.34 - 21.27	2.10 - 3.20	191.23 - 229.56	7.66 - 9.74
Average		7.23	0.48	0.69	2.32	0.71	1.49	13.45	32.45	2.60	206.96	8.39

Table 13b. Mean quality parameters of groundwater at different study sites during March – April 2019

Location	Parameters, mg/L except pH											
	Source	pH	EC (dS/m)	PO ₄ ⁻	K	NO ₃ ⁻	Cl ⁻	Na	Ca	Mg	HCO ₃ ⁻	SO ₄ ⁻
Godagari	DTW (n=6)	7.32	0.54	0.80	2.28	0.72	1.76	14.68	21.27	3.46	208.62	6.98
	STW (n=4)	7.43	0.66	0.82	2.40	0.78	1.60	17.22	20.78	4.12	222.06	7.58
Tanore	DTW (n=5)	7.22	0.48	0.72	2.46	0.82	1.62	15.86	19.42	4.62	203.86	8.04
	STW (n=3)	7.42	0.57	0.88	2.54	0.76	1.72	18.12	19.36	4.84	216.66	8.18
Kalai	DTW (n=8)	7.28	0.62	0.62	2.62	0.70	1.81	13.81	21.07	5.52	196.86	8.36
	STW (n=2)	7.36	0.64	0.68	2.74	0.74	1.85	15.52	20.68	4.58	211.94	8.56
Joypurhat sadar	DTW (n=6)	7.25	0.52	0.74	2.22	0.78	1.66	11.02	18.34	3.54	178.16	9.52
	STW (n=2)	7.44	0.58	0.76	2.40	0.86	1.58	13.32	18.44	3.82	202.08	9.94
Range		7.22 - 7.54	0.48 - 0.66	0.62 - 0.88	2.22 - 2.62	0.70 - 0.84	1.58 - 1.81	11.02 - 18.86	18.34 - 21.27	3.46 - 5.52	178.16 - 222.06	7.58 - 9.94
Average		7.35	0.58	0.75	2.46	0.77	1.49	14.94	19.92	4.31	205.03	8.40

The suitability of groundwater for irrigation is dependent on the effects of the mineral constituents of the water on both the plant and the soil. In this study, SAR, SSP, RSC and KR were used to carry out the assessment of the suitability of water for irrigation purposes (Table 13). Irrigation water that has high sodium (Na⁺) content can bring about a displacement of exchangeable cations Ca²⁺ and Mg²⁺ from the clay minerals of the soil, followed by the replacement of the cations by sodium. SAR (Sodium Adsorption Ratio) is a measure of suitability of water for irrigation with respect to the sodium hazard. As higher deposition of sodium may cause damage to soil, soil irrigation with high sodium depositing waters are not suitable. SAR is directly related to adsorption of sodium by soil, therefore it is a better measure of sodium (alkali) hazard in irrigation water. High SAR in any irrigation water implies hazard of sodium (Alkali) replacing Ca and Mg of the soil through cation exchange process, a situation eventually damaging to soil structure, namely permeability which ultimately affects the fertility status of the soil and reduce crop yield (Gupta, 2005). SAR gives the clear idea about the adsorption of sodium by soil. Based on the grading criteria of water for irrigation, SAR is classified into excellent (<10), good (10-18), permissible (18-26), unsuitable (>26) (Khodapanah et al. 2009). The assessment results with these methods are listed in Table 53b. As per SAR value all samples collected either from STW or from DTW in both seasons fall into excellent category. During pre-irrigation season

the values of SAR of the collected water samples ranged from 0.40 to 0.99 with an average value of 0.62 and it ranged from 0.69 to 0.95 during post-irrigation season with an average value of 0.79.

The residual sodium carbonate (RSC) is a measure of the hazard involved in the use of high carbonate waters. Water quality for irrigation is influenced when concentration of carbonates and bicarbonates is higher than calcium and Magnesium. Waters containing high concentrations of these ions, calcium and possibly magnesium (Mg^{+2}) may precipitate as carbonates when water is concentrated by transpiration and evaporation. With the removal of calcium and magnesium from soil solution, the relative proportion of sodium is increased with attendant increase in alkali hazard. A high range of RSC in irrigation water means an increase in the adsorption of sodium on the soil. Water having $RSC > 5$ has not been recommended for irrigation because of damaging effects on plant growth. According to USDA (United State Department of Agriculture) any source of water in which RSC is higher than 2.5 is not considered suitable for agriculture purpose, and water < 1.25 is recommended as safe for irrigation purpose. A negative value of RSC reveals that concentration of Ca^{2+} and Mg^{2+} is in excess. A positive RSC denotes that Na^+ existences in the soil are possible. RSC calculation is also important in context to calculate the required amount of gypsum or sulfuric acid per acre-foot in irrigation water to neutralize residual carbonates effect. RSC values for pre-irrigation season varied from 1.11 to 2.54 with an average value of 1.55 while for post-irrigation season SRC values varied from 1.71 to 2.18 with an average value of 2.01. In both the seasons, KR values were found less than 1, indicating that all groundwater samples are suitable for irrigation use.

Table 14. Water quality indices for suitability assessment of different water sources for irrigation

Location	Source	Pre-irrigation season				Post-irrigation season			
		SAR	RSC	SSP (%)	KR	SAR	RSC	SSP (%)	KR
Godagari	DTW	0.66	1.39	25.50	0.353	0.78	2.07	31.16	0.472
	STW	0.70	1.31	25.33	0.349	0.90	2.26	34.15	0.542
Tanore	DTW	0.65	1.32	23.79	0.321	0.84	1.99	32.70	0.509
	STW	0.99	2.57	38.06	0.643	0.95	2.18	35.42	0.574
Kalai	DTW	0.48	1.22	18.77	0.238	0.69	1.71	27.53	0.397
	STW	0.64	1.72	25.41	0.355	0.80	2.06	31.23	0.477
Joypurhat sadar	DTW	0.40	1.11	15.74	0.192	0.62	1.71	27.41	0.395
	STW	0.47	1.77	18.91	0.241	0.74	2.07	30.79	0.467
Average		0.62	1.55	23.94	0.34	0.79	2.01	31.30	0.48
Range	DTW	0.40-0.66	1.11-1.39	15.74-25.50	0.192-0.353	0.62-0.84	1.71-2.07	27.41-32.70	0.39-0.509
	STW	0.47-0.99	1.31-1.77	18.77-38.06	0.241-0.643	0.74-0.95	2.07-2.26	30.79-35.42	0.467-0.574

Soluble Sodium Percent (SSP) is also used to evaluate sodium hazard. Water with a SSP greater than 60% may result in sodium accumulations that will cause a breakdown in the soil's physical properties (Khodapanah et al. 2009). The values for the soluble sodium percent (SSP) in the study areas were found to vary from 15.74 to 38.06% with an average value of 23.94 % in pre-irrigation season and from 27.41 to 35.42 with an average value of 31.30 in post-irrigation season (Table 13b). This result corroborates the findings of Khan *et al.* (1989) who found SSP ranging from 14.50 to 37.55 in the North-West region of Bangladesh. Based on the classification after Wilcox (1955) for SSP, all samples fall under excellent and good class, so can be used safely for irrigation.

In the study area, the assessment of groundwater quality for irrigation was also carried out through the estimation of Water Quality Index (WQI) to identify its suitability for irrigation purpose (Fig. 35). This index is an important parameter for assessing groundwater quality and its suitability (Avvannavar and Shrihari, 2008). The advantage of water quality index is based on the relative importance of essential parameters with respect to standards of irrigation purposes.

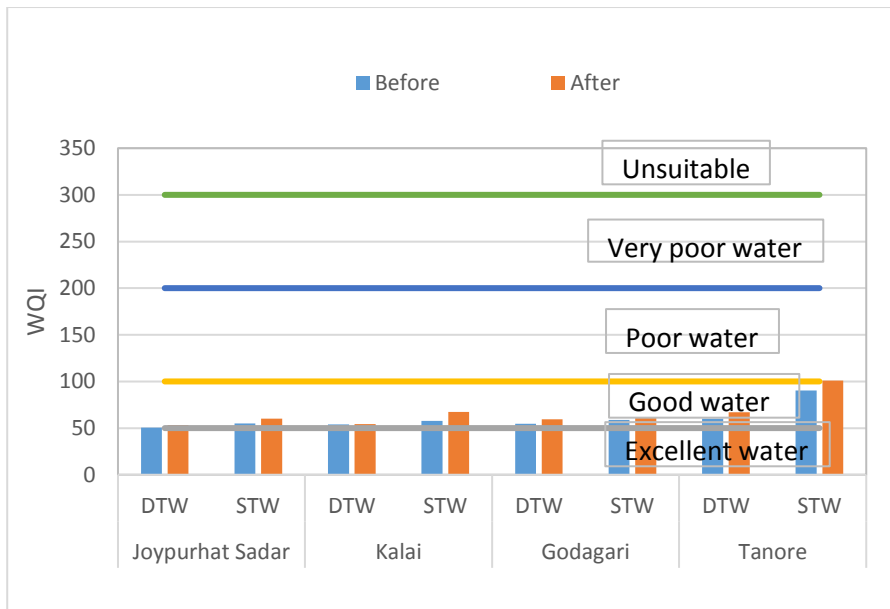


Figure. 35. Water quality index (WQI) of groundwater at different location of the study area (solid line represents the range of different categories of water quality).

The WQI ranged from 50.45 to 60.1 for DTW and from 55.15 to 90.24 for STW in pre-irrigation season while it ranged from 53.26 to 67.21 and 60.04 to 101.12 for STW and DTW water, respectively, in post-irrigation season. According to the WQI values, all the samples were found to be “good” in pre-irrigation season whereas in post-irrigation season, all samples were found also “good” except STW’s water of Tanore was found poor with WQI value of 101.12. Dissolved ions such as Na^+ , K^+ , Mg^{++} , HCO_3^- , Cl^- , NO_3^- , and SO_4^- , during post-monsoon period affected WQI values. High iron concentration in groundwater caused high WQI values; high chloride concentrations also contributed to high WQI values typically during the post-monsoon period.

Table 15: Classification of groundwater quality in the study area

Quality index	Categories	Ranges	Sources of water	
			Pre-irrigation	Post-irrigation
SAR	Excellent	<10	STW, DTW	STW, DTW
	Good	10 – 18		
	Permissible	18 – 26		
	Unsuitable	>26		
SRC	Excellent	<1.25	STW, DTW	-
	Permissible	1.25-2.5	-	STW, DTW
	Unsuitable	>2.5	STW (Tanore)	-
SSP	Excellent	0 – 20	DTW(K), STW/DTW(Joyp)	-
	Good	20 – 40	STW, DTW	STW, DTW
	Permissible	40 – 60	-	-
	Doubtful	60 – 80	-	-
	Unsuitable	>80	-	-
KR	Suitable	<1	STW, DTW	STW, DTW
	Unsuitable	≥ 1	-	-
WQI	Excellent	<50	DTW (Joypur)	-
	Good	50 – 100	STW, DTW	STW, DTW
	Poor	100 – 200	-	STW (Tanore)
	Very poor	200 – 300	-	-
	Unsuitable	>300	-	-

3.8.1. Conclusions:

The groundwater quality in two districts (Rajshahi and Joypurhat) of north-west region has been evaluated for agricultural use. The water quality indices such as SAR, SSP, RSC and KR were calculated to find out its suitability for irrigation. The results based on these indices indicate that quality of groundwater samples fall into excellent and good categories for irrigation use. The water quality index (WQI) has been determined to better assess suitability of groundwater for irrigation and it is observed that all the samples were “good” except few were found “poor” in post-irrigation season. Therefore, in respect of all evaluating criteria, groundwater of the study area was found suitable and can safely be used for irrigation purpose.

4. Key findings of the project

Groundwater level declination was found more in Tanore upazila than other three upazilas. It will be almost double by the year 2040 in Tanore. In Godagari, Joypurhat sadar, and Kalai upazila, the future trends of groundwater level fluctuations as predicted by the model are quite interesting. While the groundwater level declination was found obvious in most of the observation wells, the groundwater levels showed increasing trends in few observation wells at Joypurhat and Godagari.

Groundwater abstraction as predicted will be increasing by 33-35% in Joypurhat study areas while it will be increasing by 40-45% in Rajshahi in the next 20 years.

Groundwater levels at the observation wells of the study areas varied noticeably as a result of the changes in the recharge scenarios. In the business-as-usual case, the MODFLOW computed heads at the three observation wells GT 8194046, GT8194048, and GT8194049 in Tanore were 16.388m, 18.133m, and 22.215m, respectively, in 2018. When the abstraction was reduced to 90%, the computed heads rose significantly to 7.970m, 11.150m, and 18.106m, respectively. On the other hand, if the abstraction would be increased to 110%, the MODFLOW computed heads at the observations were found as 20.707m, 21.745m, and 24.413m, respectively which indicates a substantial increase (drop) in the quantity of head development.

The water quality indices such as SAR, SSP, RSC and KR indicate that quality of groundwater samples fall into excellent and good categories for irrigation use. As per water quality index (WQI), a combined water quality index to better assess suitability of groundwater for irrigation, all the samples were “good” except few were found “poor” in post-irrigation season. In respect of all evaluating criteria, groundwater of the study area was found suitable and can safely be used for irrigation purpose.

Rice equivalent yield (REY) and water productivity (WP) were found higher in cropping patterns where high yielding rabi crops like tomato, potato and maize were included and water saving irrigation technologies were adopted. Among the cropping patterns, the highest REY and WP were obtained from Tomato-Boro-T.Aus followed by Potato-Boro-T.Aman pattern while the lowest was from Mustard-Boro-T.Aman pattern. Use of water saving irrigation technologies increased REY by 8-24% and saved about 20-25% water over existing farmers’ practice.

Challenges

- Adoption of apposite irrigation technology by the farmers;
- Policy intervention to create awareness among the farmers and other stakeholders about the consequences of indiscriminate use of groundwater.

Suggestions for Future Planning

- The groundwater system of the study area are complex and dynamics linked with surface water availability in the region. So, surface water availability need to be determined and a groundwater surface water management plan is required for the study area.
- An appropriate methodology for estimation of potential recharge of the study area need to be established.
- A relationship of recharge with space variant parameters like thickness, soil properties, etc. can be developed.

Acknowledgement

This project work is funded by the Program Based Research Grant (PBRG), National Agricultural Technology Program (NATP): Phase II Project, Bangladesh Agricultural Research Council, Bangladesh.

5. References

- Bangladesh Bureau of Statistics (BBS). (2013). District statistics 2011: Rajshahi district. Bangladesh Bureau of Statistics. Statistics and informatics division. Ministry of planning. Government of the People's Republic of Bangladesh Retrieved from www.bbs.gov.bd
- Doble, R.C., Pickett, T., Crosbie, R.S., Morgan, L.K., Turnadge, C., Davies, P.J., 2017. Emulation of recharge and evapotranspiration processes in shallow groundwater systems. *J. Hydrol.* 555, 894–908. <https://doi.org/https://doi.org/10.1016/j.jhydrol.2017.10.065>
- Faneca Sanchez, M. et al. (2015). SWIBANGLA: Managing saltwater intrusion impacts in coastal groundwater systems of Bangladesh Final Report. Deltares report number: 1207671-000-BGS-0016 doi:10.13140/2.1.2447.0721
- Ferrant, S., Caballero, Y., Perrin, J., Gascoin, S., Dewandel, B., Aulong, S., Dazin, F., Ahmed, S., Maréchal, J.-C., 2014. Projected impacts of climate change on farmers' extraction of groundwater from crystalline aquifers in South India. *Sci. Rep.* 4, 3697. <https://doi.org/10.1038/srep03697>
- Harvey, C.F. et al., 2006. Groundwater dynamics and arsenic contamination in Bangladesh. *Chem. Geol.*, 228(1): 112-136. DOI: 10.1016/j.chemgeo.2005.11.025
- Hoque, M.A., Adhikary, S.K., 2020. Prediction of groundwater level using artificial neural network and multivariate timeseries models, in: Proceedings of the 5th International Conference on Civil Engineering for Sustainable Development (ICCESD 2020). KUET, Khulna, Bangladesh, pp. 1–8.
- Masterson, J.P., Garabedian, S.P., 2007. Effects of sea-level rise on ground water flow in a coastal aquifer system. *Ground Water* 45, 209–217.
- Masterson, J.P., Pope, J.P., Fienen, M.N., Monti, J.J., Nardi, M.R., Finkelstein, J.S., 2016. Assessment of groundwater availability in the northern atlantic coastal plain aquifer system from long island, New York, to North Carolina, Professional Paper. Reston, VA, USA. <https://doi.org/10.3133/pp1829>
- Michael, H.A., Voss, C.I., 2009. Controls on groundwater flow in the Bengal Basin of India and Bangladesh: regional modeling analysis. *Hydrogeol. J.*, 17(7): 1561. DOI:10.1007/s10040-008-0429-4
- Park, E., Parker, J.C., 2008. A simple model for water table fluctuations in response to precipitation. *J. Hydrol.* 356, 344–349. <https://doi.org/https://doi.org/10.1016/j.jhydrol.2008.04.022>
- Pauw, P.S., Oude Essink, G.H.P., Leijnse, A., Vandenbohede, A., Groen, J., van der Zee, S.E.A.T.M., 2014. Regional scale impact of tidal forcing on groundwater flow in unconfined coastal aquifers. *J. Hydrol.* 517, 269–283. <https://doi.org/https://doi.org/10.1016/j.jhydrol.2014.05.042>
- Wada, Y., Bierkens, M.F.P., 2014. Sustainability of global water use: past reconstruction and future projections. *Environ. Res. Lett.* 9, 104003. <https://doi.org/10.1088/1748-9326/9/10/104003>
- Woo, C.S., Katherine, N., Latif, K., Prabhakar, C.T., 2016. Impacts of climate change and urbanization on groundwater resources in a barrier island. *J. Environ. Eng.* 142, D4016001. [https://doi.org/10.1061/\(ASCE\)EE.1943-7870.0001123](https://doi.org/10.1061/(ASCE)EE.1943-7870.0001123)

EFFECTS OF FLOATING AGRICULTURE PRACTICE ON THE WATER BODY OF POND

S.S.A. KAMAR¹, M.A. HOSSAIN², S.K. BISWAS³, D.K. ROY³, K.F.I. MURAD¹, M.M.R. TALUKDER⁴

Abstract

This experiment was conducted at RARS, Rahmatpur, Barishal to determine the change of water quality of canals for cultivating fish and household uses and to determine the change of water quality of ponds for cultivating fish and household uses. The water samples were collected from three selected ponds of RARS, Rahmatpur, Barishal. The selected ponds were mentioned as; FL-1 (Floating Agriculture practiced since 2015), FL-2 (Floating Agriculture practiced since 2018) and F (Fresh Pond). The water quality parameters were analyzed from TCL and Soil Lab, BRAC, Gazipur. It was not possible to collect water samples in the months of March, April and May of 2020 due to Covid-19 lockdown. For all three ponds the water temperature was observed below 34⁰C in all months which was good for fish cultivation. The pH level was ranged from 6.66-7.73 at all three selected ponds. It was observed (figure 3) that the (UIA) Un Ionized Ammonia level at all selected ponds were suitable for channel catfish. The total dissolved solids (TDS) were in desirable limit but in case of floating agriculture practice ponds (FL-1 and FL-2) the TDS level was found higher than fresh pond (F). The Ca levels were in affordable range for only channel fish cultivation (Figure 5). The P values (Figure 6) were good for plankton/shrimp production but the P value was crossed the limit in floating agriculture practiced ponds for other fish production. According to table-7, it was observed that the nitrate values at all months were in tolerable limit.

Introduction

The southern part of the country consists of coastal lowland and mangrove areas formed by the delta of large river systems. Bangladesh suffers from flooding almost every year to a small or large extent, and in the case of the years with small-scale flooding, the losses have not been assessed properly, but for those years with large-scale flooding, different institutes try to assess the loss from their perspective (Mirza and Ahmad 2005). In some parts of Bangladesh, most affected by flood and where water remains for a prolonged period, farmers are using their submerged lands for crop production by adopting traditional methods which are similar to hydroponic agriculture practices, i.e. floating agriculture, whereby plants can be grown on the water in a bio-land or floating bed of water hyacinth, algae or other plant residues. The procedure of making the floating bed is usually the same, however the size, shape and local materials vary from region to region (Islam and Atkins 2007; APEIS 2004).

The most commonly used material is water hyacinth, but topapana, son ghash, nollghash, wood ash, and dissected coconut fibers are also used (Islam and Atkins 2007: 131). Water hyacinth is utilized not only for the foundation of production system as floating beds during the monsoon season but also for compost especially during the winter cultivation on the ground. Because crops could absorb prime nutrients such as nitrogen, potassium and phosphorus from the floating beds and below water, there is almost no need for fertilizer input. This technique brings many ecological benefits, such as the good use of an invasive species like water hyacinth – a very effective way to control this notorious weed; platform residues can be used as organic fertilizer (this practice cuts pollution from chemical fertilizers). The water quality of the canals and ponds used for floating cultivation were going down day by day for decomposition of water hyacinth, topapana, son ghash, nollghash, wood ash and coconut fiber in large scale. So it is needed to analyze the water quality of that canals and ponds for fish cultivation and household use. Objective of the experiment were given below

- i) To determine the change of water quality of ponds for cultivating fish and household uses.

¹ SO, IWM Division, BARI, Gazipur

² CSO (in-charge), IWM Division, BARI, Gazipur

³ SSO, IWM Division, BARI, Gazipur

⁴ PSO, RARS, BARI, Rahmatpur, Barishal

Materials and Methods

The experimental water samples were collected from Regional Agricultural Research Station, Rahmatpur, Barishal. Three water samples were collected from three selected ponds of Regional Agricultural Research Station, Rahmatpur, Barishal. The two samples were collected from floating agriculture practice ponds and one sample was collected from a fresh pond. The treatments of the experiment were given below:

FL-1 = Floating Agriculture Practice as well as fish culture since 2015

FL-2 = Floating Agriculture Practice as well as fish culture since 2018

F = Fresh Pond

The water quality parameters of the collected samples were analyzed at TLC and soil lab of BARDC, Gazipur. The water quality parameters were given below

- | | | | | |
|-----------------|-------------------|--------------------------------|-------------------------------|--------|
| 1. Temperature | 2. pH | 3. Ammonium (NH ₄) | 4. Nitrate (NO ₃) | 5. TDS |
| 6. Calcium (Ca) | 7. Phosphorus (P) | 8. Nitrogen (N) | 9. DO | |

Results and Discussion

Fish do not like any kind of changes in their environment. Anita Bhatnagar and Pooja Devi (2013) stated that any changes add stress to the fish and the larger and faster the changes, the greater the stress. So the maintenance of all the factors becomes very essential for getting maximum yield in a fish pond. Adequate oxygen, proper temperature, transparency, limited levels of metabolites and other environmental factors affecting fish culture characterize good water quality. The initial studies of water quality of a fish pond in India were probably conducted by Sewell (1927) and Pruthi (1932). After that many workers have studied the physico-chemical condition of inland waters either in relation to fish mortality or as part of general hydrological survey (Alikunhi *et al.*, 1952; Upadhyaya, 1964). Workers (Mumtazuddin *et al.*, 1982; Delince, 1992; Garg and Bhatnagar, 1999; Bhatnagar, 2008) also have studied the details of various pond ecosystems. Bhatnagar and Singh (2010) studied the pond fish culture in relation to water quality in Haryana. However, this experiment would provide the basic guidelines, parameter wise for the fish farmers who are interested in floating agriculture practice as well as fish culture in a single pond via maintaining water quality of their ponds.

Temperature is defined as the degree of hotness or coldness in the body of a living organism either in water or on land (Lucinda and Martin, 1999). As fish is a cold blooded animal, its body temperature changes according to that of environment affecting its metabolism and physiology and ultimately affecting the production. Higher temperature increases the rate of bio-chemical activity of the micro biota, plant respiratory rate, and so increase in oxygen demand. It further cause decreased solubility of oxygen and also increased level of ammonia in water. According to Delince (1992) 30-35⁰ C is tolerable to fish. Bhatnagar *et al.* (2004) suggested that the levels of temperature as 28-32⁰C good for tropical major carps, 25-30⁰C – ideal for *Penaeous monodon* culture; < 20⁰C – sub lethal for growth and survival for fishes; <12⁰C – lethal but good for cold water species and > 35⁰C- lethal to maximum number of fish species. According to Santhosh and Singh (2007) suitable water temperature for carp culture is between 24 and 30⁰C. According to figure 1 the average temperature was found within 26.70⁰C to 33.60⁰C in all selected ponds. it could be stated that the temperature of all selected ponds was found good for fish cultivation.

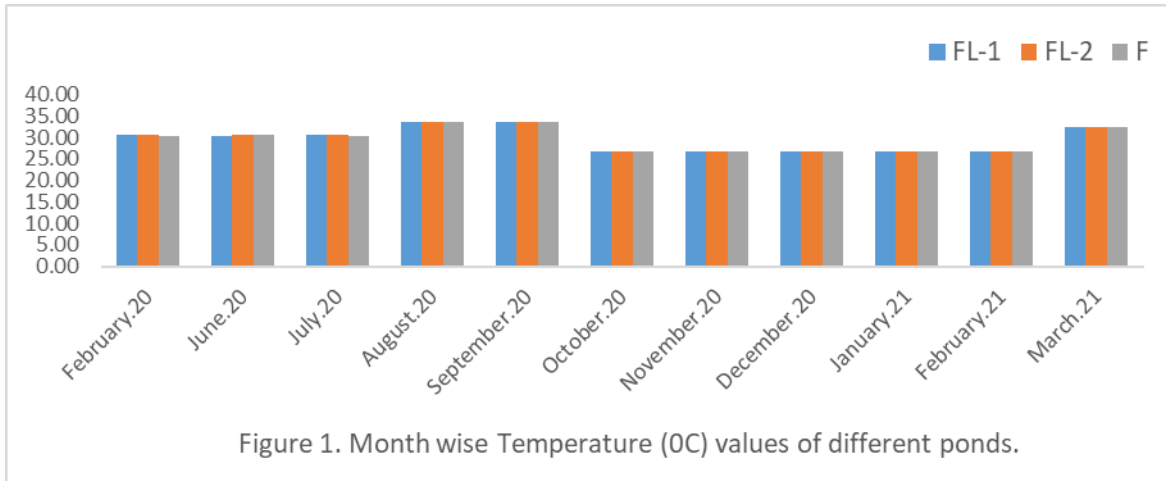


Figure 1. Month wise Temperature (°C) values of different ponds.

pH is measured mathematically by, the negative logarithm of hydrogen ions concentration. The pH of natural water is greatly influenced by the concentration of carbon dioxide which is an acidic gas (Boyd, 1979). Fish have an average blood pH of 7.4, a little deviation from this value, generally between 7.0 to 8.5 is more optimum and conducive to fish life. pH between 7 to 8.5 is ideal for biological productivity, fishes can become stressed in water with a pH ranging from 4.0 to 6.5 and 9.0 to 11.0 and death is almost certain at a pH of less than 4.0 or greater than 11.0 (Ekubo and Abowei, 2011). According to Santhosh and Singh (2007) the suitable pH range for fish culture is between 6.7 and 9.5 and ideal pH level is between 7.5 and 8.5 and above and below this is stressful to the fishes. Ideally, an aquaculture pond should have a pH between 6.5 and 9 (Wurts and Durborow, 1992; Bhatnagar *et al.*, 2004). From figure 2, it could be stated that the pH range was within the limit of 6.5 to 9 in all ponds. A pH value higher than 8.5 indicates that a significant amount of sodium bicarbonate may be present in the water. So pH level higher than 8.5 and lower than 5 is harmful for household uses.

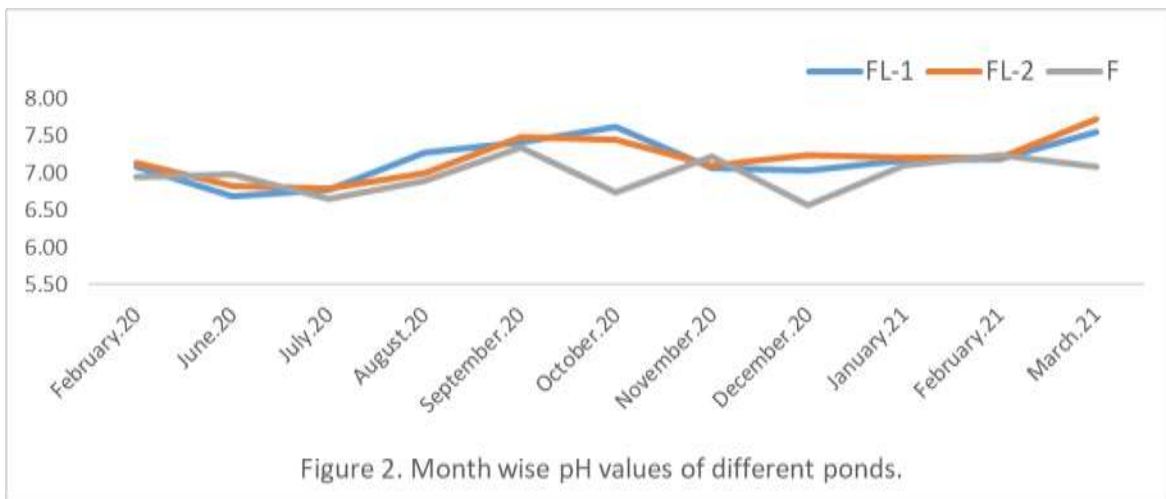
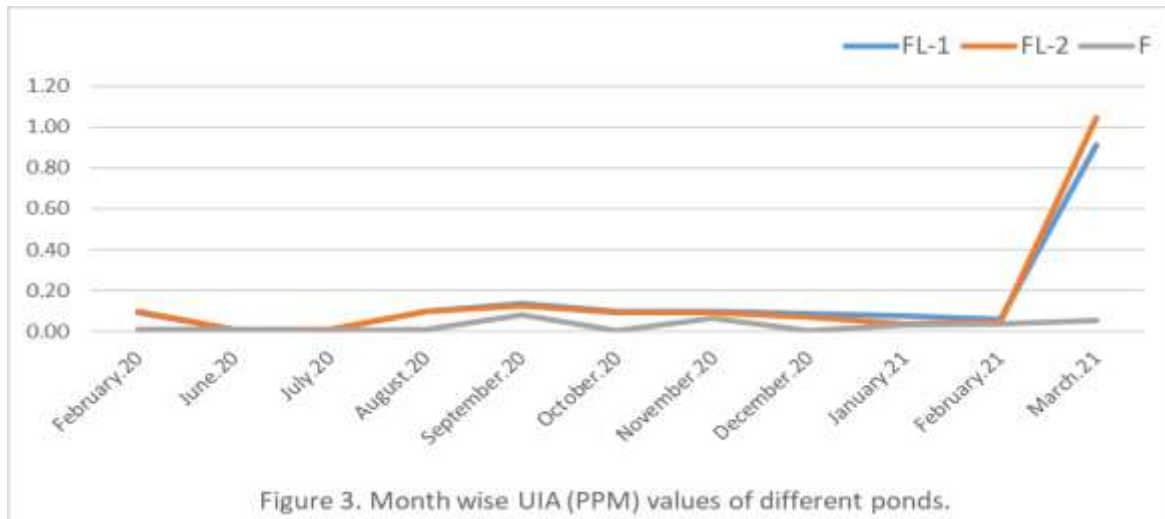


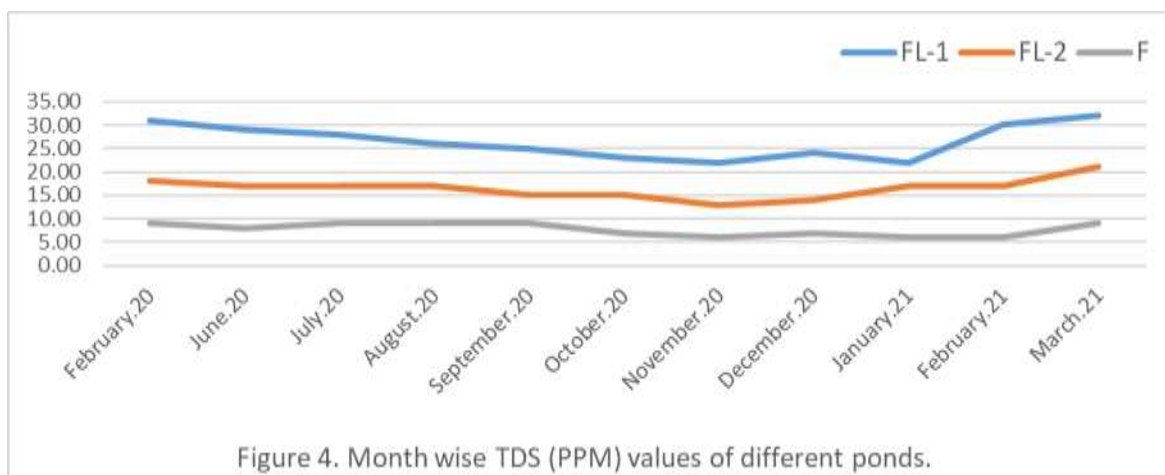
Figure 2. Month wise pH values of different ponds.

Animals produce ammonia as a byproduct of protein metabolism. What is measured by chemical analysis (Nessler method) for ammonia is called total ammonia nitrogen (TAN) because it includes two forms of ammonia: ammonia (NH₃), the unionized form, and the ammonium ion (NH₄⁺). The unionized ammonia (UIA) is toxic to fish. The temperature and pH of water affects the ratio of (NH₄⁺):(NH₃) in water. For salmonid fishes, it is recommended that the concentration of UIA not exceed 0.0125 to 0.02 mg/L to maintain health of the fish, however, the toxic concentrations of UIA (NH₃) for trout are about 0.32 mg/L for rainbow trout, but 1.50-3.10 for channel catfish (Ruffier *et al.* 1981, cited by Boyd 1990a). Thus, a UIA of 1.7 mg/L, would be a expected to cause mortality of most fish, and it would be stressful for channel catfish. From figure 3 it was observed that the unionized ammonia level is suitable for channel catfish but not suitable for salmonid and craps in some cases. Bhatnagar *et al.* (2004) suggested 0.01-0.5 ppm is desirable for shrimp; >0.4 ppm is lethal to many

fishes & prawn species; 0.05-0.4 ppm has sublethal effect and <0.05 ppm is safe for many tropical fish species and prawns. Bhatnagar and Singh (2010) recommended the level of ammonia (<0.2 mg L⁻¹) suitable for pond fishery.



The *total dissolved solids*, or *TDS*, includes ionized and non ionized matter but only the former is reflected in the conductivity. Where TDS are high the water may be "saline" and the applicable parameter "Salinity". Salinity is defined as the total concentration of electrically charged ions (cations – Ca⁺⁺, Mg⁺⁺, K⁺, Na⁺ ; anions – CO₃⁻, HCO₃⁻, SO₄⁻, Cl⁻ and other components such as NO₃⁻, NH₄⁺ and PO₄⁻). Salinity is a major driving factor that affects the density and growth of aquatic organism's population (Jamabo, 2008). Garg and Bhatnagar (1996) have given desirable range 2 ppt for common carp; however, Bhatnagar *et al.* (2004) gave different ideal levels of salinity as 10-20 ppt for *P. monodon*; 10-25 ppt for euryhaline species and 25-28 ppt for *P. indicus*. Barman *et al.* (2005) gave a level of 10 ppt suitable for *Mugil cephalus* and Garg *et al.* (2003) suggested 25 ppt for *Chanos chanos* (Forsskal). From figure 4, it was observed that the total dissolved solids were in desirable limit but in case of floating agriculture practice ponds the TDS was found more than fresh pond. Values of less than 500 ppm (mg/L) are satisfactory and up to 1,000 ppm (mg/L) could be tolerated with little effect in household uses.



Calcium is generally present in soil as carbonate and most important environmental, divalent salt in fish culture water. Fish can absorb calcium either from the water or from food. Wurts and Durborow (1992) recommended range for free calcium in culture waters is 25 to 100 ppm (63 to 250 ppm CaCO₃ hardness) and according to them Channel catfish can tolerate minimum level of mineral calcium in their feed but may grow slowly under such conditions. According to figure 5, the Ca values were in affordable range for channel fish cultivation.

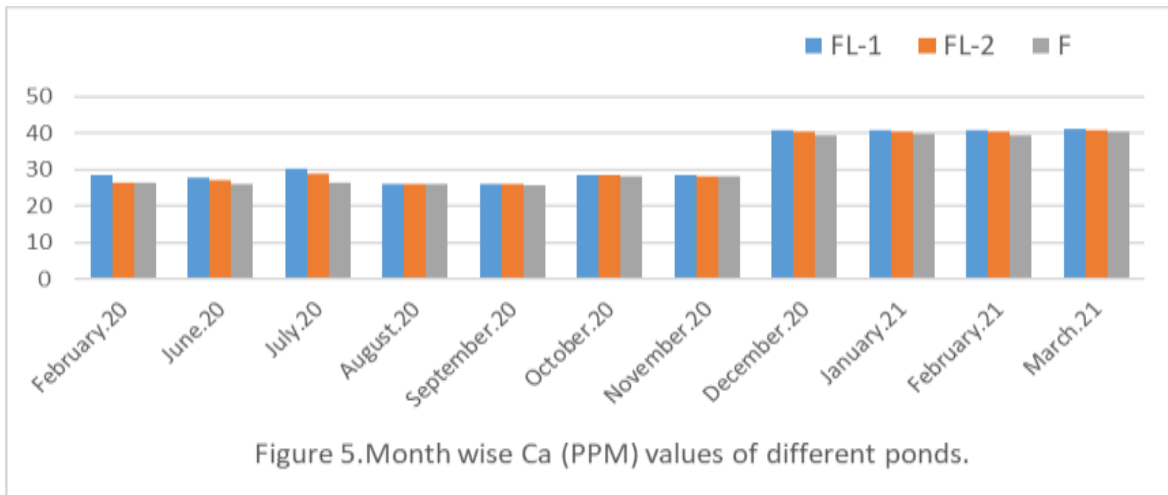


Figure 5. Month wise Ca (PPM) values of different ponds.

Almost all of the phosphorus (P) present in water is in the form of phosphate (PO₄) and in surface water mainly present as bound to living or dead particulate matter and in the soil is found as insoluble Ca₃(P₀₄)₂ and adsorbed phosphates on colloids except under highly acid conditions. It is an essential plant nutrient as it is often in limited supply and stimulates plant (algae) growth and its role for increasing the aquatic productivity is well recognized. According to Stone and Thomforde (2004) the phosphate level of 0.06 ppm is desirable for fish culture. Bhatnagar *et al.* (2004) suggested 0.05-0.07 ppm is optimum and productive; 1.0 ppm is good for plankton/shrimp production. From figure 6 it was observed that the P values were good for plankton/shrimp production but were above limit for other fish production.

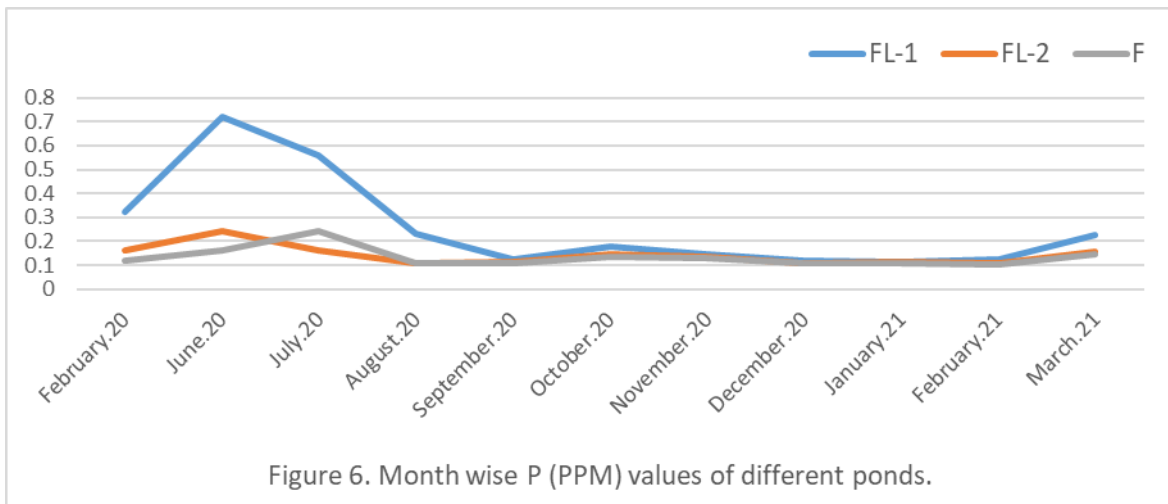


Figure 6. Month wise P (PPM) values of different ponds.

Where ammonia and nitrite were toxic to the fish, Nitrate is harmless and is produced by the autotrophic *Nitrobacter* bacteria combining oxygen and nitrite. Nitrate levels are normally stabilized in the 50-100 ppm range. According to Stone and Thomforde (2004) nitrate is relatively nontoxic to fish and not cause any health hazard except at exceedingly high levels (above 90 ppm). However, OATA (2008) recommends that nitrate levels in marine systems never exceed 100 ppm. According to figure 7, it was observed that the nitrate values in the all months were in tolerable limit. Nitrate in excess of 45 mg/L (or in excess of 10 mg/L if reported as nitrate-nitrogen) is of health significance to pregnant women and infants under six months.

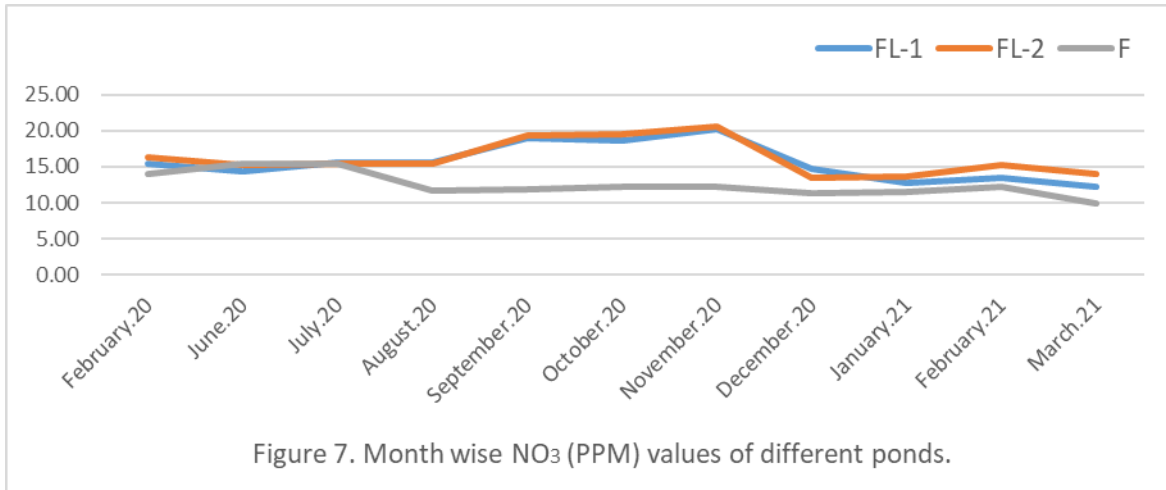


Figure 7. Month wise NO₃ (PPM) values of different ponds.

Oxygen is the first limiting factor for growth and well-being of fish. Fish require oxygen for respiration, which physiologists express as mg of oxygen consumed per kilogram of fish per hour (mgO₂/kg/h). The respiratory rate increases with increasing temperature, activity, and following feeding, but decreases with increasing mean weight. In ponds, the major source of oxygen is from algal photosynthesis and from wind mixing the air and water. *Robert C. Summerfelt* stated that at temperatures optimum for growth, fish are stressed at oxygen concentrations less than 5 mg/L. If the condition is chronic, fish stop feeding, growth slows down, stress-related disease begins. For rainbow trout, mortality may begin at 3 mg/L, but channel catfish tolerate less than 2 mg/L before mortality commences. However, if the gills of fish are damaged by parasites (hamburger gill disease is a good example of a severe protozoan disease of the gills of channel catfish), the fish may die when oxygen concentrations drop only slightly below 5 mg/L. From figure 8, it could be stated that the DO levels of all three selected ponds were suitable for all kinds of fish culture. According to Bhatnagar and Singh (2010) and Bhatnagar *et al.* (2004) DO level >5ppm is essential to support good fish production.

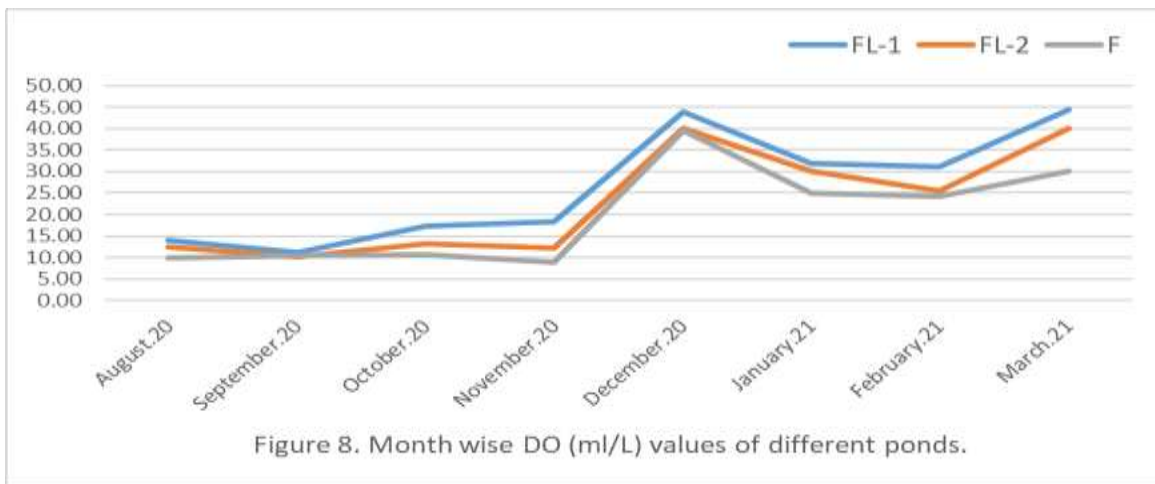


Figure 8. Month wise DO (ml/L) values of different ponds.

Conclusion

This is the second year experiment. It is needed to continue for next year for confirming the trend.

Reference

- Alikunhi, K. H., Ramachandra, V. and Chaudhuri, H., (1952), Mortality of carp fry under supersaturation of dissolved oxygen in water, Proceedings of the national institute of sciences of India, 17 (4), pp 261-264.
- Bhatnagar, A. and Devi, P., (2013), Water quality guidelines for the management of pond fish culture. International journal of environmental sciences, 3(6), pp 1980-2009

- Bhatnagar, A., Jana, S.N., Garg, S.K. Patra, B.C., Singh, G. and Barman, U.K., (2004), Water quality management in aquaculture, In: Course Manual of summerschool on development of sustainable aquaculture technology in fresh and saline waters, CCS Haryana Agricultural, Hisar (India), pp 203- 210.
- Barman, U. K., Jana, S.N., Garg, S. K., Bhatnagar, A. and Arasu, A.R.T., (2005), Effect of inland water salinity on growth feed conversion efficiency and intestinal enzyme activity in growing grey mullet, *Mugil cephalus* (Lin.): Field and laboratory studies, *Aquaculture international*, 13(3), pp 241-256.
- Bhatnagar, A. and Singh, G., (2010), Culture fisheries in village ponds: a multi-location study in Haryana, India. *Agriculture and Biology Journal of North America*, 1(5), pp 961-968.
- Delince, G., (1992), *The ecology of the fish pond ecosystem*, Kluwer Acadmic Publisers London, pp 230.
- Ekubo, A. A. and Abowei, J. F. N., (2011), Review of some water quality management principles in culture fisheries, *Research Journal of Applied Sciences, Engineering and Technology*, 3(2), pp 1342-1357.
- Garg, S. K. and Bhatnagar, A., (1996). Effect of varying doses of organic and inorganic fertilizers on plankton production and fish biomass in brackish water ponds, *Aquaculture Research (The Netherlands)*, 27, pp 157-166.
- Garg, S.K., Jana, S.N. and Bhatnagar, A., (2003), Effect of inland groundwater salinity on digestibility and other aspects of nutrition physiology in *Mugil cephalus* and *Chanos chanos* (Forsskal), In: *Fish production using brackish water in arid ecosystem* (eds. Garg, S.K. and Arasu, A.R.T.), Ankush Printers, Hisar, pp 53-59.
- Islam, T. and Atkins, P., 2007. Indigenous floating cultivation: a sustainable agricultural practice in the wetlands of Bangladesh. *Development in Practice* 17 (1): 130-136.
- Jamabo, N.A., (2008), *Ecology of Tympanotonus fuscatus* (Linnaeus, 1758) in the Mangrove Swamps of the Upper Bonny River, Niger Delta, Nigeria. Ph.D. Thesis, Rivers State University of Science and Technology, Port Harcourt, Nigeria, pp 231.
- Lucinda, C. and Martin, N., (1999), *Oxford English Mini- Dictionary* Oxford University Press Inc, New York, pp 200-535.
- Mumtazuddin, M., Rahman, M. S. and Mostafa, G., (1982), Limnological studies of four selected rearing ponds at the aquaculture experiment station, Mymensingh. *Bangladesh Journal of Fisheries Research*, 2-5 (1-2), pp 83-90.
- Ornamental Aquatic Trade Association (OATA), (2008), *Water Quality Criteria-ornamental fish*. Company Limited by Guarantee and Registered in England No 2738119 Registered Office Wessex House, 40 Station Road, Westbury, Wiltshire, BA13 3JN, UK.
- Pruthi, H.S., (1932), Investigations regarding a recent epidemic of fish mortality in the tank in the Indian museum compound with remarks on the causation of such epidemics in general. *Review of Hydrobiology Hydrographic*, 26, pp 242-257.
- Sewell, R.B.S., (1927), On mortality of fishes, *Journal of the Asiatic Society of Bengal*, 22, pp 177-204.
- Stone, N. M. and Thomforde H. K., (2004), *Understanding Your Fish Pond Water Analysis Report*. Cooperative Extension Program, University of Arkansas at Pine Bluff Aquaculture / Fisheries
- Santhosh, B. and Singh, N.P., (2007), *Guidelines for water quality management for fish culture in Tripura*, ICAR Research Complex for NEH Region, Tripura Center, Publication no.29
- Upadhyaya, M.P., (1964), *Seminar on inland fisheries development in U. P.*, pp 127-135.
- Wurts, W.A. and Durborow, R. M., (1992), Interactions of pH, Carbon Dioxide, Alkalinity and Hardness in Fish Ponds Southern Regional Aquaculture Center, SRAC Publication No. 464.

PROJECT (SACP-IWM PART):
**DISSEMINATION OF WATER SAVING TECHNOLOGIES FOR NON-RICE
CROPS IN SALINE PRONE AREAS OF BANGLADESH**

M.A. HOSSAIN¹, D.K. ROY², S.K. BISWAS², K.F.I. MURAD³, S.S.A. KAMAR³

Abstract

Demonstrations of solar powered water saving irrigation technologies on crop production were executed at five upazillas under five districts. In 2019-2020, demonstrations were conducted at three upazilas under three districts of the southern saline prone areas of Bangladesh. In 2020-2021, field demonstrations were extended to two more upazillas in the districts of Bhola and Noakhali. In 2019-2020, twelve demonstrations were conducted at the selected areas whereas in 2020-2021, four additional demonstrations were performed. Two water saving irrigation technologies (AFI and drip irrigation) were compared with the traditional farmer practice. Alternet furrow irrigation (AFI) was used for maize and sunflower cultivation and drip irrigation system was used for tomato and watermelon cultivation. Solar power was also used for mitigating the pumping cost in drip irrigation system. In general, the AFI technology showed superior performance over the traditional farmers' practices for maize and sunflower cultivation in the study areas for both growing seasons of 2019-2020 and 2020-2021. This higher performance was evidenced by the better numeric values of the yield and yield attributing characters of both sunflower and maize crops in AFI adopted plots when compared to the traditional irrigation practice used by the farmers in the study areas. Likewise, statistically significant yield difference was observed among the treatments (solar powered drip irrigation system and farmer's practice) for watermelon and tomato cultivation in the study areas in both 2019-2020 and 2020-2021 growing seasons. AFI and solar powered drip irrigation treatments provided highest BCR for all crops and for the two growing seasons. The farmers were benefited and interested in using this promising water saving irrigation technologies.

Introduction

Bangladesh is an agro-based country where agriculture has enormous contribution to the national economy and to livelihood of the people (Murshed-E-Jahan and Pems, 2011). Agricultural growth of Bangladesh has accelerated after independence, where irrigation expansion happened during mid 80's (Hoque, 2001). But the agricultural growth has been impeded due to natural disasters and fluctuations in food prices. This natural disaster mainly occurs due to unfavorable weather which is now severe (Harun-ur-Rashid and Islam, 2007). Salinity and drought are the main stress environments in Bangladesh (Athar and Ashraf, 2009; Harun-ur-Rashid and Islam, 2007). The nature and extent of these environments vary with season, topography and location (Athar and Ashraf, 2009).

Soil salinity is a major problem in the coastal region during the dry period. Soil salinity starts increasing from last week of December and reaches to its peak level in the month of March and April (≈ 25 dS/m), and minimum salinity (< 2 dS/m) occurs in the months of July and August after the onset of the monsoon rains (Haque, 2006). Coastal soils vary widely in nature of salinity, depth and fluctuation of groundwater along with the seasonal variation in the salinity of surface water (Yan et al., 2015). Farmers mostly grow T.Aman during July-December and the lands remain fallow due to salinity development and scarcity of irrigation water during rest periods of the year.

To minimize water application losses and increase water use efficiencies (WUE) in the saline, drought prone and hilly regions of Bangladesh, modern irrigation technologies developed by Bangladesh Agricultural Research Institute (BARI) that are suitable for non-rice crops should be disseminated in the farmers' field. The promising water management technologies are: (i) drip fertigation that are recommended for high value vegetable and fruit crops, (ii) alternate furrow irrigation method suitable for both field crops and vegetables planted in rows, and (iii) deficit irrigation, mostly suitable for field crops like wheat, maize, mustard, sunflower, etc. Fertigation (Drip

¹ CSO(in-charge), IWM Division, BARI, Gazipur

² SSO, IWM Division, BARI, Gazipur

³ SO, IWM Division, BARI, Gazipur

irrigation with fertilizer) can be used for growing high value vegetable and fruit crops like tomato, brinjal, cauliflower, strawberry, guava, etc. for higher yield, water productivity and economic return. Drip irrigation can increase yield of these crops and water use efficiency (WUE) by 10-19% and 16-23%, respectively as compared to furrow irrigation with a considerable amount of fertilizer (40%) and water saving (48%). This method can be demonstrated intensively in saline prone areas where freshwater availability is very scarce for irrigation. Besides, alternate furrow irrigation (AFI) technology, also suitable for the row field crops, can save irrigation water by about 35% with no loss of yield. In the areas under draught and saline stress to bring more area under cultivation. Dissemination of these technologies to the farmers will help them to harvest the benefits of water irrigation while minimizing the risk of its use for crop production and to increase the crop-water productivity and reduce irrigation water use in saline areas of Bangladesh.

Materials and Method

The experiments were conducted at different locations of Southern districts named Patuakhali, Borguna, Bhola, Noakhali, and khulna. In Patuakhali district, there were 6 AFI experiments and 3 drip irrigation experiments in 2019-2020 whereas 7 AFI experiments and 3 drip irrigation experiments were carried out in 2020-2021. At Borguna district there were one drip irrigation experiments for both 2019-2020 and 2020-2021 growing seasons. Although two drip irrigation experiments were conducted in khulna district for 2019-2020, there were no drip irrigation experiments in Khulna district in 2020-2021. In Bhola district, 3 solar powered drip irrigation experiments were conducted during 2020-2021 growing season. One solar powered drip irrigation experiment was also conducted in Noakhali district. In addition, 6 solar powered irrigation pumps and 6 solar panels were provided to 30 farmers of the Kaliganj upazilla, Satkhira district in order to facilitate irrigation in the Gher boundaries. The location wise experiments and crops details for the 2019-2020 and 2020-2021 growing seasons are presented in Tables 1 and 2.

Table 1. Location wise Experiments and Crop/Variety details in 2019-2020 growing season

District	Upazila	Village	Crop	Variety	Technology used
Patuakhali	Kalapara	Noyapara	Maize	BHM-9	AFI
	Kalapara	Noyapara, Nobinpur, Diarankhola, Maithvanga	Sunflower	BARI Surzomukhi-2	AFI
	Kalapara	Azimpur	Watermelon	Jaguar Jumbo	Drip
Borguna	Amtali	Ghotkhali	Brinjal	Hybrid	Drip
Khulna	Koyra	3 no koyra	Tomato	BARI tomato-21 BARI hybrid tomato-5	Drip
	Koyra	3 no koyra	Watermelon	Jaguar Jambo	Drip

Location wise crop, sowing/planting and harvesting dates along with the treatments are shown in Tables 3 and 4 for the growing seasons 2019-2020 and 2020-2021, respectively. The fertilizers were applied as per BARI recommended dose. The following data were collected from the selected plant samples from each plot.

- Plant population
- Plant height/ Vine length (cm)
- Cob per plant/ Number of fruit per plant
- Individual fruit weight (gm)
- Cob length/fruit length (cm)
- Fruit diameter (cm)
- Number of seeds per cob/ Number of seeds per head
- 1000 seed weight/100 seed weight (gm)

- Plot yield (t/ha)
- Salinity data (ds/m)

Table 2. Location wise Experiemnts and Crop/Variety details in 2020-2021 growing season

Farmer's name	Location	Area covered, decimal	Crop	Variety	Technology used
Md. Mosharaf Gazi	Azimpur, Kuakata, Patuakhali	33	Watermelon	Big family	Drip
Md. Delowar Mridha	Azimpur, Kuakata, Patuakhali	33	Watermelon	Big family	Drip
Md. Mohibul Musulli	Azimpur, Kuakata, Patuakhali	33	Watermelon	Big family	Drip
Md. Sarowar hossain	Kalapara, Kuakata, Patuakhali	33	Maize	BHM-9	AFI
Md. Amir Hossain	Tulatoli, Kuakata, Patuakhali	33	Maize	BHM-9	AFI
Md. Abdur Rashid	Noyapara, Kuakata, Patuakhali	33	Maize	BHM-9	AFI
Babul Miah	Fasipara, Kuakata, Patuakhali	33	Maize	BHM-9	AFI
Jolil Miah & Halim Miah	Fasipara, Kuakata, Patuakhali	66	Maize	BHM-9	AFI
Abu Saleh	Fasipara, Kuakata, Patuakhali	66	Sunflower	BAR Surjomukhi - 2	AFI
Bahadur Miah	Fasipara, Kuakata, Patuakhali	66	Sunflower	BAR Surjomukhi - 2	AFI
Jalal Mridha	Fasipara, Kuakata, Patuakhali	66	Sunflower	BAR Surjomukhi - 3	AFI
Md. Liton Shikder	Ghotkhali, Amtoli, Barguna	28	Brinjal	BARI Bt. Brinjal - 4	Drip
Md. Rasel Miah	Halimabad, charfashion, Bhola	24	Brinjal	BARI Bt. Brinjal - 4	Drip
Md. Akhtar Hossain	Halimabad, charfashion, Bhola	28	Sweet Gourd	BARI Mistikumra - 2	Drip
Md. Idris Miah	Halimabad, charfashion, Bhola	24	Tomato	BARI Tomato -15	Drip
Md Saiful Islam	Banglabazar, Dharmapur, Noakhali Sadar	62	Watermelon	Jaguar Jumbo	Drip

Table 3. Location wise sowing, harvesting dates and the treatments of different crops in 2019-2020

Upazila	Crop	Date of Sowing/ Planting	Date of Harvesting	Treatments
Kalapara	Maize	30.12.2019	25.05.2020	T ₁ = Alternet Farrow Irrigaion (AFI) T ₂ = Farmer Practice (FP)
Kalapara	Sunflower	24.12.2019	08.04.2020	T ₁ = AFI T ₂ = FP
Kalapara	Watermelon	10.01.2020	05.04.2020	T ₁ = Solar Powered Drip Irrigation T ₂ = FP
Amtali	Brinjal	10.12.2020	19.05.2020	T ₁ = Solar Powered Drip Irrigation T ₂ = FP
Koyra	Tomato	27.11.2019	27.03.2020	T ₁ = Solar Powered Drip Irrigation T ₂ = FP
Koyra	Watermelon	12.01.2020	03.04.2020	T ₁ = Solar Powered Drip Irrigation T ₂ = FP

Table 4. Location wise sowing, harvesting dates and the treatments of different crops in 2019-2020

Location	Crop	Date of Sowing/ Planting	Date of Harvesting	Treatments
Azimpur	Watermelon	12.12.2020	Multiple	T ₁ = Solar Powered Drip Irrigation (SPDI) T ₂ = Farmers' Practice (FP)
	Do	25.12.2020	Multiple	T ₁ = SPDI T ₂ = FP
	Do	28.12.2020	Multiple	T ₁ = SPDI T ₂ = FP
Kalapara	Maize	15.12.2020	15.05.2021	T ₁ = Alternet Farrow Irrigaion (AFI) T ₂ = FP
Tulatoli	Do	17.12.2020	20.05.2021	T ₁ = AFI T ₂ = FP
Noyapara	Do	20.12.2020	25.05.2021	T ₁ = AFI T ₂ = FP
Fasipara	Do	20.12.2020	24.05.2021	T ₁ = AFI T ₂ = FP
	Do	20.12.2020	23.05.2021	T ₁ = AFI T ₂ = FP
	Do	22.12.2020	26.05.2021	T ₁ = AFI T ₂ = FP
	Sunflower	24.12.2020	09.04.2021	T ₁ = AFI T ₂ = FP
	Do	05.01.2021	22.05.2021	T ₁ = AFI T ₂ = FP
	Do	27.12.2020	11.04.2021	T ₁ = AFI T ₂ = FP
Amtoli	Brinjal	30.11.2020	Multiple	T ₁ = SPDI T ₂ = FP
Bhola	Brinjal	12.01.2021	Multiple	T ₁ = SPDI T ₂ = FP
	Sweet gourd	23.01.2021	Multiple	T ₁ = SPDI T ₂ = FP
	Tomato	26.12.2020	Multiple	T ₁ = SPDI T ₂ = FP
Noakhali	Watermelon	12.12.2020	Multiple	T ₁ = SPDI T ₂ = FP

Solar Irrigation System

In this project, IWM division used solar powered drip irrigation system. Solar power is free of cost. The installation cost was little higher, but it was less than an LLP installation cost. Farmers can use this portable solar panel for charging their home system. At the coastal region solar powered home system is available at every house. So, farmers can use this portable solar panel for multiple purposes. The specification and cost of solar irrigation system was given below.

Item	Specification	Amount	Unit Price (BDT)	Total Cost BDT)
Solar Panel	300 watts	1	32	9600
Pump	180 watts	1	4500	4500
Accessories	-	-	-	500
Total-				14600

Results and Discussion

The results obtained in the experiment have been presented in this section under relevant headings and sub-headings with necessary tables. The effects of different irrigation practices on different crops have been elaborated. Findings on crop yield and yield attributing characters of the growing season 2019-2020 are presented in Tables 5 through 10. Results of 2020-2021 are presented following the results of 2019-2020.

Table 5 shows the yield and yield components of maize at Kalapara upzilla under Patuakhali district. The plant population, plant height, cob length, number of seeds per cob, 100 seed weight and yield were found highest (7.50, 255.45 cm, 19.95 cm, 474.30, 25.63 g and 9.01 t/ha) in treatment T₁. AFI gave the highest result in all farmer fields. The yield of maize was statistically significant among the treatments.

Table 5. Yield and yield components of maize at Kalapara upazila under Patuakhali district during 2019-2020

Treatment	Plant Population/m ²	Plant Height (cm)	Number of Cob/Plant	Cob Length (cm)	Number of Seed/ Cob	100 Seed Weight (gm)	Yield (t/ha)
T ₁	7.50a	255.45a	1.00	19.95a	474.30a	25.63a	9.01a
T ₂	7.25a	246.98a	1.00	18.40a	461.80a	25.18a	8.42b
CV (%)	4.79	6.36	-	6.63	4.92	2.23	1.71
LSD	-	-	-	-	-	-	0.34

Table 6 shows the yield and yield components of sunflower at Kalapara upzilla under Patuakhali district. The plant population, plant height, head diameter, number of seeds per head, 1000 seed weight and yield were found comparatively high (7.00, 143.57 cm, 59.47 cm, 464.67, 88 g and 1.99 t/ha) at treatment T₁. AFI performed better than conventional irrigation in all farmer fields. The head diameter, number of seed per head, 1000 seed weight and yield were statistically significant.

Table 6. Yield and yield components of sunflower at Kalapara upazila under Patuakhali district during 2019-2020

Treatment	Plant Population/m ²	Plant Height (cm)	Head Diameter (cm)	Number of Seed/ Head	1000 Seed Weight (gm)	Yield (t/ha)
T ₁	7.00	143.57a	59.47a	464.67a	88.00a	1.99a
T ₂	6.67	139.90a	50.35b	420.00b	77.67b	1.73b
CV (%)	-	4.62	5.11	0.74	5.81	2.09
LSD	-	-	9.85	11.47	16.91	0.14

Table 7 shows the yield and yield components of watermelon at Kalapara upzilla under Patuakhali district. The vine length, number of fruits per plant, individual fruit weight and yield were found comparatively high (292.47 cm, 1.83, 6.18 kg and 35.51 t/ha) at treatment T₁. Drip irrigation performed better than conventional irrigation in all farmer fields. The vine length, and yield of watermelon were found statistically significant among the treatments.

Table 7. Yield and yield components of watermelon at kalapara upazila under patuakhali district during 2019-2020

Treatment	Vine Length (cm)	Number of Fruits/ Plant	Individual Fruit Weight (kg)	Yield (t/ha)
T ₁	292.47a	1.83a	6.18a	35.51a
T ₂	280.17b	1.40a	5.41a	29.91b
CV (%)	0.57	12.62	7.14	2.78
LSD	5.73	-	-	3.20

Table 8 shows the yield and yield components of BARI hybrid tomato-5 at Koyra upzilla under Khulna district. The number of fruits per plant, individual fruit weight, fruit length, fruit diameter and yield were found comparatively high (31.67, 92.33 g, 4.23 cm, 3.90 cm and 94.27 t/ha) at treatment T₁. Drip irrigation performed better than conventional irrigation in all farmer fields. The number of fruits per plant, fruit length, fruit diameter and yield were observed statistically significant among the treatments.

Table 8. Yield and yield components of BARI Hybrid tomato-5 at Koyra upazila under Khulna district during 2019-2020

Treatment	Number of plant per plot	Number of fruits per plant	Individual Fruit Weight (gm)	Fruit Length (cm)	Fruit Diameter (cm)	Yield (t/ha)
T ₁	6	31.67a	92.33a	4.23a	3.90a	94.27a
T ₂	6	18.00b	86.00a	4.18b	3.76b	64.19b
CV (%)	-	8.69	4.84	0.26	0.38	6.43
LSD	-	7.58	-	0.04	0.05	17.89

Table 9 showed the yield and yield components of BARI tomato-21 at koyra upzilla under khulna district.

Table 9. Yield and yield components of BARI tomato-21 at koyra upazila under khulna district during 2019-2020

Treatment	Number of plant per plot	Number of fruits per plant	Individual Fruit Weight (gm)	Fruit Length (cm)	Fruit Diameter (cm)	Yield (t/ha)
T ₁	6	48.33a	58.33a	4.26a	2.51a	66.72a
T ₂	6	35.67b	53.67b	4.18a	2.49a	52.37b
CV (%)	-	1.94	1.92	0.61	0.28	1.12
LSD	-	2.87	3.79	-	-	2.34

The number of fruits per plant, individual fruit weight, fruit length, fruit diameter and yield were found comparatively high (48.33, 58.33 gm, 4.26 cm, 2.51 cm and 66.72 t/ha) at treatment T₁. Drip irrigation performed better than conventional irrigation in all farmer fields. The number of fruits per plant, individual fruit weight and yield were statistically significant among the treatments.

Table 10 shows the yield and yield components of watermelon at Koyra upzilla under Khulna district. The vine length, weight of fruit per plant, individual fruit weight and yield were found comparatively high (242.80, 10.02 kg, 5.01 kg and 44.48 t/ha) at treatment T₁. Drip irrigation performed better than conventional irrigation in all farmer fields. The vine length, weight of fruit per plant, individual fruit weight and yield were statistically significant among the treatments.

Table 10. Yield and yield components of watermelon at Koyra upazila under Khulna district during 2019-2020

Treatment	Vine Length (cm)	Number of Fruit per Plant	Weight of Fruit per Plant (kg)	Individual Fruit Weight (kg)	Yield (t/ha)
T ₁	242.80a	2	10.02a	5.01a	44.48a
T ₂	214.78b	2	7.12b	3.56b	32.35b
CV (%)	0.32	-	0.83	0.83	0.43
LSD	2.58	-	0.25	0.13	0.58

Findings from the demonstrations on watermelon, maize, sunflower, brinjal, sweet gourd and tomato under water saving and traditional irrigation practices carried out in various locations of the southern Bangladesh during 2020-2021 growing season are presented in brief in the subsequent paragraphs. Unlike 2019-2020, all the statistical analysis were carried out in MATLAB environment

(MATLAB 2019b). The statistical inference was made through comparing the variation between groups to the variation within groups. If the ratio of between-group variation to within-group variation is significantly high, then it can be concluded that the group means are significantly different from each other. This was measured using a test statistic that has an F -distribution with $(k-1, N-k)$ degrees of freedom:

$$F = \frac{SSR/k - 1}{SSE/N - k} = \frac{MSR}{MSE} \sim F_{k-1, N-k}$$

where MSR is the mean squared treatment, MSE is the mean squared error, k is the number of groups, and N is the total number of observations. If the p -value for the F -statistic is smaller than the significance level, then the test rejects the null hypothesis that all group means are equal and concludes that at least one of the group means is different from the others. The significance level was taken as 0.05.

In Tables 11 through 18, ' F ' indicates the F -statistic, which is the ratio of the mean squares; and ' $Prob.>F$ ' indicates the p -value, which is the probability that the F -statistic can take a value larger than the computed test-statistic value.

Table 11 presents the yield and yield attributing characters of watermelon at Azimpur under Patuakhali district. It is observed from Table 11 that the yield and other parameters have higher numeric values in solar powered drip irrigation treatments when compared to traditional irrigation practices. This trend indicates a superior performance of the water saving drip irrigation systems over traditional irrigation practices for watermelon production in the salinity prone southern Bangladesh. From Table 11, it is observed that number of fruits per plant (p -value = 0.0097 < 0.05) and yield (p -value = 0.00049 < 0.05) were statistically significant between the treatments.

Table 11. Yield and yield components of watermelon at Azimpur under Patuakhali district during 2020-2021

Treatments	Vine Length (cm)	Number of Fruits/ Plant	Individual Fruit Weight (kg)	Yield (t/ha)
T ₁	287.33	1.96	6.23	36.63
T ₂	281.67	1.64	5.89	28.98
F	4.66	21.53	1.71	346.1
Prob.>F	0.097	0.0097	0.2616	0.00049

Yield and yield attributing characters of maize at Fasipara, Patuakhali are shown in Table 12, which indicates a better performance of AFI over the traditional irrigation systems. Plant height, cob length, and number of seeds per cob were statistically significant between the treatments as indicated by the lower p -values than the assigned significance level. Although not statistically significant between the treatments, the yield of maize was obtained higher (8.95 t/ha) in AFI than its counterpart (8.39 t/ha).

Table 12. Yield and yield components of maize at Fasipara under Patuakhali district during 2020-2021

Treatments	Plant Population/m ²	Plant Height (cm)	Number of Cob/Plant	Cob Length (cm)	Number of Seed/ Cob	100 Seed Weight (gm)	Yield (t/ha)
T ₁	7.35	252.32	1	20.12	470.23	25.71	8.95
T ₂	7.12	247.61	1	18.87	465.17	25.53	8.39
F	5.42	65.1	-	12.7	14.24	0.34	2.68
Prob.>F	0.0804	0.0013	-	0.0235	0.0196	0.5925	0.177

Demonstration on sunflower at Fasipara under Patuakhali district based on AFI and traditional irrigation practice is shown in Table 13. Although the yield of sunflower was not statically significant between the treatments, the AFI approach provided higher yield of sunflower (2.31 t/ha) that the farmers' practice-based irrigation approach (2.12 t/ha). Parameters like plant height, head diameter, number of seed per head, and 1000 seed weight were found statistically significant between the treatments.

Table 13. Yield and yield components of sunflower at Fasipara under Patuakhali district during 2020-2021

Treatments	Plant Population/m ²	Plant Height (cm)	Head Diameter (cm)	Number of Seed/ Head	1000 Seed Weight (gm)	Yield (t/ha)
T ₁	6.85	145.61	60.12	471.24	89.56	2.31
T ₂	6.38	139.85	53.98	455.32	81.02	2.12
F	3.44	230.6	153.01	229.85	114.24	3.09
Prob.>F	0.1374	0.0001	0.0002	0.0001	0.0004	0.1536

Table 14 shows the yield and yield components of brinjal at Amtali under Barguna district. It is perceived from Table 14 that all parameters were statistically significant between the treatments as indicated by the *p*-values lower than the threshold *p*-value of 0.05. Treatment T₁ (solar powered drip irrigation) produced higher value of brinjal yield (31.64 t/ha) compared to treatment T₂ (Farmers' practice), which produced 29.37 t/ha of brinjal yield.

Table 14. Yield and yield components of brinjal at Amtali under Barguna district during 2020-2021

Treatments	Length of fruit, cm	Diameter of fruit, cm	Unit weight of fruit, g	Yield, t/ha
T ₁	8.59	7.12	450	31.64
T ₂	7.12	6.35	425	29.37
F	116.11	15.87	12.98	52.84
Prob.>F	0.001	0.0163	0.0227	0.0023

Yield and yield contributing parameters of brinjal at Charfashion under Bhola district are presented in Table 15, which shows a statistically significant brinjal yield between the treatments. Treatment T₁ and T₂ produced brinjal yields of 30.64 t/ha and 27.37 t/ha, respectively. Other parameters like length of fruit and unit weight of fruit were found significantly different between the treatments.

Table 15. Yield and yield components of brinjal at Charfashion under Bhola district during 2020-2021

Treatments	Length of fruit, cm	Diameter of fruit, cm	Unit weight of fruit, g	Yield, t/ha
T ₁	7.53	6.52	435	30.64
T ₂	6.98	6.19	412	27.37
F	41.63	5.32	10.73	84.85
Prob.>F	0.003	0.0823	0.0306	0.0008

Parameters regarding yield and yield contributing characteristics of tomato at Charfashion under Bhola district are shown in Table 16, which indicates a relatively better performance of solar powered drip irrigation system (T₁) than the Farmers' practice (T₂) in tomato cultivation. Number of fruits per plant, individual fruit weight, and yield were found to be statistically significant between the treatments. Treatment T₁ produced higher tomato yield of 72.07 t/ha than treatment T₂ (59.45 t/ha).

Table 16. Yield and yield components of tomato at Charfashion under Bhola district during 2020-2021

Treatment	Number of plants/plots	Number of fruits/plants	Individual Fruit Weight (gm)	Fruit Length (cm)	Fruit Diameter (cm)	Yield (t/ha)
T ₁	6	50.23	57.39	4.25	2.48	72.07
T ₂	6	43.67	54.45	4.19	2.45	59.45
F	-	52.74	74.45	0.39	0.18	77.72
Prob.>F	-	0.0015	0.002	0.566	0.6966	0.0019

Table 17 presents yield and yield components of sweet gourd at Charfashion under Bhola district. It is observed from Table 17 that the sweet gourd production was significantly higher in treatment T₁ (35.83 t/ha) when compared to treatment T₂ (27.85 t/ha). The yields between the treatments were statistically significant. In addition, number of fruits per plant and individual fruit weights were also found statistically significant between the treatments.

Table 17. Yield and yield components of sweet gourd at Charfashion under Bhola district during 2020-2021

Treatments	Number of fruits/plants	Individual fruit weight, kg	Yield, t/ha
T ₁	4.13	4.82	35.83
T ₂	3.58	3.89	27.85
F	61.54	23.96	178.69
Prob.>F	0.0014	0.0081	0.0002

Yield and yield components of watermelon at Banglabazar under Noakhali district during 2020-2021 are presented in Table 18, which indicates that all parameters except the number of fruits per plant were statistically significant between the treatments. Treatment T₁ produced watermelon yield of 32.83 t/ha, which is significantly higher than the watermelon yield of 22.59 t/ha in treatment T₂.

Table 18. Yield and yield components of watermelon at Banglabazar under Noakhali district during 2020-2021

Treatments	Vine Length (cm)	Number of Fruits/ Plant	Individual Fruit Weight (kg)	Yield (t/ha)
T ₁	279.67	1.83	5.98	32.83
T ₂	258.85	1.78	4.23	22.59
F	14.76	0.83	57.93	124.8
Prob.>F	0.0184	0.4131	0.0016	0.0004

Water requirement and water productivity

Table 19 represents the total water use during the whole season and the water productivity that represents the productivity of water in producing crop yields for the growing season 2019-2020. The water productivity for maize production was higher (1.05 kg/m³) in AFI treatment than farmer practice (0.73 kg/m³). The water productivity for sunflower production was higher (1.02 kg/m³) in AFI treatment than farmer practice (0.51 kg/m³). The water productivity for watermelon production was higher (10.30 kg/m³) in drip irrigation treatment than farmer practice (7.67 kg/m³). The water productivity for BARI Hybrid tomato-5 production was higher (9.58 kg/m³) in drip irrigation treatment than farmer practice (5.89 kg/m³). The water productivity for BARI tomato-21 production was higher (6.788 kg/m³) in drip irrigation treatment than farmer practice (4.81 kg/m³). Water productivity decreases with increasing quantity of water applied.

Table 19. Total water use and water productivity of different crops during 2019-2020

Crop	Treatment	Total water use (cm)	Yield (t/ha)	Water productivity (kg/m ³)
Maize	T ₁	86.01	9.01	1.05
	T ₂	115.4	8.42	0.73
Sunflower	T ₁	19.56	1.99	1.02
	T ₂	34.20	1.73	0.51
Watermelon	T ₁	58.82	40.00	6.79
	T ₂	70.62	31.13	4.41
BARI Hybrid tomato-5	T ₁	98.38	94.27	9.58
	T ₂	128.84	64.19	4.98
BARI tomato-21	T ₁	98.38	66.72	6.78
	T ₂	128.84	52.37	4.06

Table 20 represents the total water use during the whole season and the water productivity that represents the productivity of water in producing crop yields for the growing season 2020-2021. It is perceived from Table 20 that water productivity, in general, was observed higher in water saving irrigation treatments when compared to the Farmers' practice treatments for all cultivated crops in different locations. This attributed to the capability of producing higher yields with lower water requirements by the water saving irrigation treatments. Numeric values of the water productivity for different crops are shown in Table 20 and are not repeated in the texts. Although varied numerically, a similar trend of crop water use, yield, and hence water productivity was observed between the two growing seasons.

Table 20. Total water use and water productivity of different crops during 2020-2021

Crop	Treatment	Total water use (cm)	Yield (t/ha)	Water productivity (kg/m ³)
Maize	T1	87.73	8.95	1.02
	T2	117.71	8.39	0.71
Sunflower	T1	19.95	2.31	1.16
	T2	34.88	2.12	0.61
Watermelon	T1	60.00	36.63	6.11
	T2	72.03	28.98	4.02
Tomato	T1	100.35	72.07	7.18
	T2	131.42	59.45	4.52
Sweet gourd	T1	57.36	35.83	6.25
	T2	68.63	27.85	4.06
Brinjal	T1	43.692	31.64	7.24
	T2	49.555	29.37	5.93

Economic Analysis

Table 21 shows the cost components and total cost of different crops and treatments of the project sites during the growing season 2019-2020. It was observed from the cost analysis that the total cost was high at farmer practice for all crops. In case of watermelon, BARI hybrid tomato-5 and BARI tomato-21 solar irrigation system were used for drip irrigation. So, the cost shown at the irrigation component for watermelon, BARI hybrid tomato-5 and BARI tomato-21 was actually the installation cost of solar irrigation system. For maize and sunflower diesel engine operated LLP was used for irrigation.

Table 21. Cost analysis of different crops and treatments of the project sites during 2019-2020

Crop Treatment	Land preparation (tk/ha)	Seed (tk/ha)	Fertilizer (tk/ha)	Pesticide (tk/ha)	Irrigation (tk/ha)	Labor (tk/ha)	Total Cost (tk/ha)
Maize							
T ₁	9375	8000	28800	0	16000	38800	100975
T ₂	9375	8000	28800	0	32000	55000	133175
Sunflower							
T ₁	9375	3000	23400	0	24000	18800	78575
T ₂	9375	3000	23400	0	28000	20000	83775
Watermelon							
T ₁	11250	16875	32400	30000	14600	75000	180125
T ₂	11250	16875	32400	30000	28000	95000	213525
BARI Hybrid tomato-5							
T ₁	12870	4000	14790	5000	14600	51400	102660
T ₂	12870	4000	14790	5000	14600	66800	118060
BARI tomato-21							
T ₁	12870	1200	14790	5000	14600	51400	99860
T ₂	12870	1200	14790	5000	14600	66800	115260

The total cultivation cost as well as a breakdown of individual cost items for the growing season 2020-2021 is presented in table 22. As demonstrations were performed in some new locations, the total cost reflects the inclusion of installation costs as well. The price difference was due to the variable costs of materials and labor not only between the seasons but also between the locations.

Table 22. Cost analysis of different crops and treatments of the project sites during 2020-2021

Crop Treatment	Land preparation (tk/ha)	Seed (tk/ha)	Fertilizer (tk/ha)	Pesticide (tk/ha)	Irrigation (tk/ha)	Labor (tk/ha)	Total Cost (tk/ha)
Maize							
T1	9563	8160	29376	3060	16320	39576	106055
T2	9563	8160	29376	3060	32640	56100	138899
Sunflower							
T1	9563	3060	23868	2040	24480	19176	82187
T2	9563	3060	23868	2040	28560	20400	87491
Watermelon							
T1	11475	17213	33048	30600	14892	76500	183728
T2	11475	17213	33048	30600	28560	96900	217796
Tomato							
T1	13127	2040	15086	5100	15606	52428	103387
T2	13127	2040	15086	5100	27132	68136	130621
Sweet gourd							
T1	11475	1224	16106	4590	13872	56100	103367

T2	11475	1224	16106	4590	24837	68034	126266
Brinjal							
T1	10455	2550	17228	5610	17850	54876	108569
T2	10455	2550	17228	5610	25296	66096	127235

Table 23 shows the BCR of different crops of the project sites for the growing season 2019-2020. It was observed from table 23 that the BCR of AFI and drip irrigation system was high for all crops and the BCR for farmer practice treatment was comparatively less than the water saving technologies.

Table 23. Benefit Cost Ratio of different crops and treatments of the project sites during 2019-2020

Crop Treatment	Total Cost (tk/ha)	Total Return (tk/ha)	BCR
Maize			
T ₁	100975	180200	1.78
T ₂	133175	168400	1.26
Sunflower			
T ₁	78575	99500	1.27
T ₂	83775	86500	1.03
Watermelon			
T ₁	180125	400000	2.22
T ₂	213525	311300	1.46
BARI Hybrid tomato-5			
T ₁	102660	282810	2.75
T ₂	118060	192570	1.63
BARI tomato-21			
T ₁	99860	200160	2.00
T ₂	115260	157110	1.36

Table 24 presents the BCR of different crops of the project sites for the growing season 2020-2021. As indicated by Tables 23 and 24, the BCR followed the similar trend between the two growing seasons despite a difference in numeric values.

Table 24. Benefit Cost Ratio of different crops and treatments of the project sites during 2020-2021

Crop Treatment	Total Cost (tk/ha)	Total Return (tk/ha)	BCR
Maize			
T1	106055	185606	1.75
T2	138899	173452	1.25
Sunflower			
T1	82187	102485	1.25
T2	87491	89095	1.02
Watermelon			
T1	183728	412000	2.24
T2	217796	320639	1.47
Tomato			
T1	103387	291294	2.82
T2	130621	198347	1.52
Sweet gourd			
T1	103367	206165	1.99
T2	126266	161823	1.28
Brinjal			
T1	108569	309165	2.85
T2	127235	264823	2.08

Conclusion

The experiments were conducted through Small Holder Agricultural Competitiveness Project (SACP) jointly funded by IFAD and GoB. The project sites were at the coastal region of Bangladesh. Two water saving irrigation technologies (Alternate Farrow Irrigation and Solar Powered Drip Irrigation) were demonstrated at the farmers' field. The farmers were benefited and interested to use these types of water saving technologies. Farrow Irrigation and Solar Powered Drip Irrigation has given better result than farmer practice and the BCR of those water saving technologies were remain high than the existing farmer practice. As we know that the southern districts of Bangladesh are suffering from shortage of water and fresh irrigation water at the Rabi season to grow winter crops. So, we need to disseminate these two promising water saving irrigation technologies covering a range of locations within the salt affected southern parts of Bangladesh. The findings not only provide a valuable insight regarding crop production under water scarcity but also motivate the farmers of the project site in using water saving irrigation technologies to achieve higher yields.

Acknowledgement

This project work (Smallholder Agricultural Competitiveness Project) is funded by the International Fund for Agricultural Development (IFAD) and Government of Bangladesh (GoB).

Reference

- Athar, H. R., & Ashraf, M. (2009). Strategies for crop improvement against salinity and drought stress: An overview. In *Salinity and water stress* (pp. 1-16). Springer, Dordrecht.
- Haque, S. A. (2006). Salinity problems and crop production in coastal regions of Bangladesh. *Pakistan Journal of Botany*, 38(5), 1359-1365.
- Harun-ur-Rashid, M., & Islam, M. S. (2007). Adaptation to climate change for sustainable development of Bangladesh agriculture. *Bangladesh Agriculture Research Institute*.
- Hoque, M. E. (2001). Crop diversification in Bangladesh. *Crop Diversification in the Asia-Pacific Region*, 5-23.
- Murshed-E-Jahan, K., & Pemsil, D. E. (2011). The impact of integrated aquaculture–agriculture on small-scale farm sustainability and farmers' livelihoods: experience from Bangladesh. *Agricultural Systems*, 104(5), 392-402.
- Yan, S. F., Yu, S. E., Wu, Y. B., Pan, D. F., She, D. L., & Ji, J. (2015). Seasonal variations in groundwater level and salinity in coastal plain of eastern China influenced by climate. *Journal of Chemistry*, 2015.

Internal Review Workshop 2021

Irrigation and Water Management Division

BARI, Gazipur

Chairman : Dr. Md. Shirazul Islam, Former Director (Res.), BARI, Gazipur

Expert Member : 1. Dr. Md. Abdur Rashid, Ex. Chief Scientific Officer & Head
Irrigation and Water Management Division, BRRI, Gazipur
2. Dr. Abeda Khatun, Director, HRC, BARI, Gazipur

Rapporteurs

1. Dr. Dilip Kumar Roy, SSO, IWM Division, BARI, Gazipur
2. Md. Shamshul Alam Kamer, SO, IWM Division, BARI, Gazipur

Rapporteur's Report

1. Modelling results of nitrogen leaching experiment should be included in the next year report.
2. Irrigation treatments should be redesigned for mango fruit cracking experiment.
3. Future experiments should be directed towards the application of solar powered drip and sprinkler irrigation systems.
4. More demonstrations should be executed in future on the developed water saving irrigation technologies.
5. Present status of groundwater quantity as well as aquifer properties need to be monitored.
6. Popular horticultural fruits such as BARI aam-4, BARI aam-11, and BARI malta-1 should be brought under future investigations using advanced irrigation technologies.
7. Experiments on irrigation management practices in Polder areas of southern coastal belt could be implemented.
8. Studies on precision irrigation should be conducted.

At a Glance
Irrigation and Water Management Division, BARI, Gazipur

Establishment

Irrigation and Water Management Division is one of the 17 research divisions of BARI. It has been created as a full flazed division after dividing Agricultural Engineering Division in 1990. Presently, the division is headed by a Chief Scientific Officer along with 07 scientists of agricultural engineering disciplines. It is devoted to contribute in increasing the yield and production of agricultural crops through the promotion of irrigation and the improvement of water resources management for sustainable agriculture. By this time, this division has developed about 51 irrigation and water management technologies of which most of them are being used at the field level.

Scientific Personnel

Designation	Existing Number
Chief Scientific Officer :	01 (In-charge)
Senior Scientific Officer :	02
Scientific Officer :	05 (2 in daputation)
Total :	08

Scientific Staff

Designation	Existing Number
Scientific Assistant :	03
Total :	03

List of the Scientists and Scientific Staffs Involved in IWM Research Program during 2020-2021

SL. No.	Name	Designation
1	Dr. Md. Anower Hossain	Chief Scientific Officer (in-charge) & Head
2	Dr. Sujit Kumar Biswas	Senior Scientific Officer
3	Dr. Dilip Kumar Roy	Senior Scientific Officer
4	Farzana Akter	Scientific Officer
5	Khandakar Faisal Ibn Murad	Scientific Officer
6	SK. Shamshul Alam Kamar	Scientific Officer
7	Md. Jubair Hasan	Assistant Agricultural Engineer
8	Md. Kamal Hossain	Scientific Assistant
9	Md. Enayet Sharif	Scientific Assistant
10	Mostafa Kamal	Scientific Assistant
11	Mohammad Samim Miah	Office Assistant Cum-computer Operator
12	Md. Abul Kalam	Office Assistant Cum-computer Operator
13	Md. Jahirul Islam	Surveyor
14	Md. Monayem Kabir	Laboratory Attendant

Rainfall Data in mm (From July 2020 to June 2021)

Date	July/ 2020	August/ 2020	September/ 2020	October/ 2020	November/ 2020	December/ 2020	January/ 2021	February/ 2021	March/ 2021	April/ 2021	May/ 2021	June/ 2021
1	0	8	13	8	23	0	0	0	0	0	0	170
2	0	0	0	16	0	0	0	0	0	0	0	0
3	4	0	0	2	0	0	0	0	0	0	6	0
4	10	0	0	0	0	0	0	0	0	0	0	0
5	3	9	0	2	0	0	0	0	0	12	0	31
6	1	0	0	9	0	0	0	0	0	0	0	15
7	4	4	5	42	0	0	0	0	0	0	0	5
8	2	0	11	9	0	0	0	0	0	0	1	2
9	3	0	0	0	0	0	0	0	0	3	3	5
10	19	6	967	0	0	0	0	0	0	0	0	0
11	68	3	4	0	0	0	0	0	0	0	28	34
12	25	0	0	10	0	0	0	0	0	0	0	1
13	18	0	2	0	0	0	0	0	1	0	0	6
14	0	0	4	0	0	0	0	0	0	0	0	12
15	2	3	0	0	0	0	0	0	0	0	0	24
16	0	20	4	0	0	0	0	0	0	0	1	4
17	1	1	0	0	0	0	0	0	0	19	0	0
18	1	12	0	0	0	0	0	0	0	0	22	55
19	0	0	07	1	0	0	0	0	0	0	0	21
20	31	1	4	01	0	0	1	0	0	0	0	26
21	50	5	12	15	0	0	0	0	0	0	0	46
22	23	5	30	35	0	0	0	0	0	7	0	19
23	2	3	8	7	0	0	0	0	0	0	0	0
24	8	0	2	0	0	0	0	0	0	0	0	1
25	5	3	2	0	0	0	0	0	0	0	21	1
26	0	0	0	0	0	0	0	0	0	0	0	2
27	11	1	0	0	0	0	0	0	0	0	1	0
28	48	0	0	0	0	0	0	0	0	0	3	0
29	17	96	-	0	0	0	0	-	0	7	0	71
30	0	0	-	0	0	0	0	-	0	0	0	0
31	0	0	-	-	-	0	0	-	0	-	7	-